SSC-SDE-1
SDC-89-00001

SSC-SDC
SOLENOIDAL DETECTOR NOTES

FIRST DAY PRESENTATIONS
DALLAS SOLENOIDAL DETECTOR MEETING
JUNE 26-29, 1989

G. Gilchriese, R. Cahn, H. Williams, S. Mori, H. Ogren, H. Sadrozinski,
H. Gordon, M. Pripstein, D. Bintinger, A. Lankford, S. Errede

June 26, 1989

Schedule of Presentations

Introduction (G. Gilchriese)	9:00 - 9:20 a.m.
Physics Goals (R. Cahn)	9:20- 10:05
Motivation for Solenoidal Detector (H. Williams)	10:05 - 10:45
Break	10:45 - 11:15
Review of Large and Small Solenoids (S. Mori)	11:15 - 11:55
Tracking Systems	
Wire Chambers (H. Ogren)	11:55 - 12:25 p.m.
Silicon Systems (H. Sadrozinski)	12:25 - 12:55
Lunch	1:00 - 2:30
Calorimetry	
Liquid argon (H. Gordon)	2:30 - 3:05
Room Temperature (M. Pripstein)	3:05 - 3:40
Scintillator (D. Bintinger)	3:40 - 4:15
Break	4:15 - 4:45
Trigger and DAQ (A. Lankford)	4:45 - 5:25
Organization of Remaining Meeting Time (G. Trilling)	5:25 - 5:45

*Note Presentation on Muon Systems postponed until June 27.

HOT ROD
HIGH SPEED SERIAL LINK

- High-speed, 40-bit, 1000 Mbit/sec data link
- Applications
  - CPU-to-CPU or peripheral
  - CPU-to-graphics terminal
  - Backplane extender
- Parallel 40-bit TTL bus interface
  - All bits are user definable
- Asynchronous input using STRB/ACK
- On-chip PLL, Crystal Oscillator
- Single +5V supply operation
- 68-pin PLCC or LCC

Point-to-Point Communications

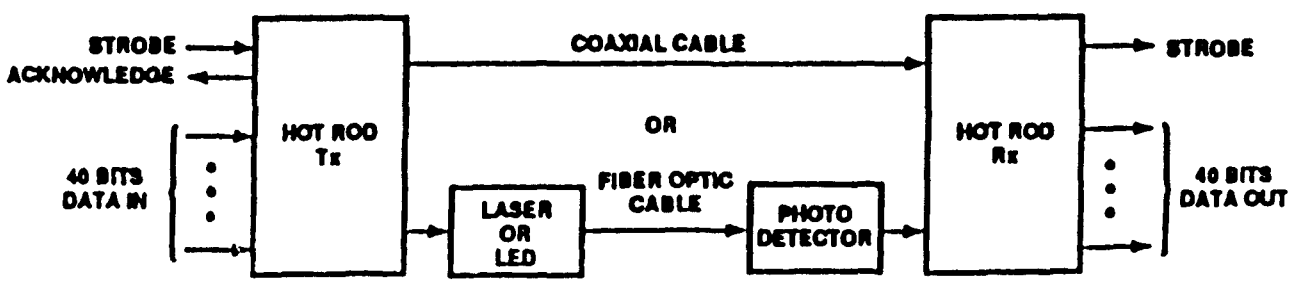

PARALLEL EVENT BUILDER

PURPOSE: ELIMINATE BOTTLENECK

of ALL DATA thru ONE PATH.

INPUT PATHS # PARALLEL OUTPUT PATHS

≠ necessarily, but naturally same for same b/w

SEVERAL SCHEMES

MULTI-DROP INTO PROCESSOR MEMORIES (DØ)

MATRIX BUFFER/ROUTER NODES (similar, but feed row of ⊼:

GENERALIZED CROSS-POINT SWITCH

A SIMPLER SWITCHING NETWORK

BARREL SHIFTER Bowden + Barsotti (FNAL)

⇒ simple control

cyclicly connect each input to each output

SIMILARITIES, esp: NEEDS

EXTENSIVE BUFFERING (smooth event-to-event fluct; otherwise limited by longest event fragment.

BALANCE AVG. DATA RATES (otherwise limited by slowest data path)

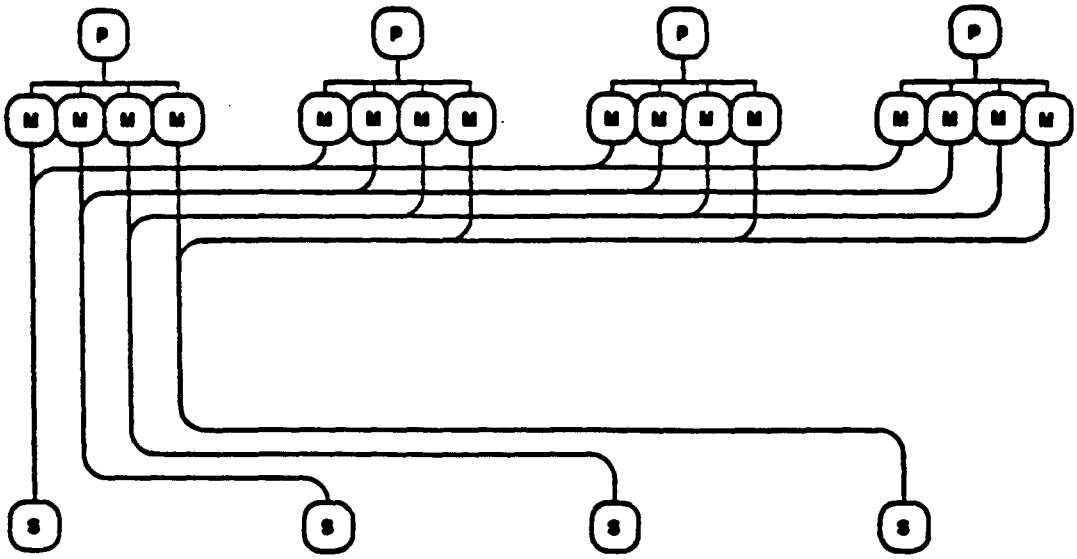
P
M
S

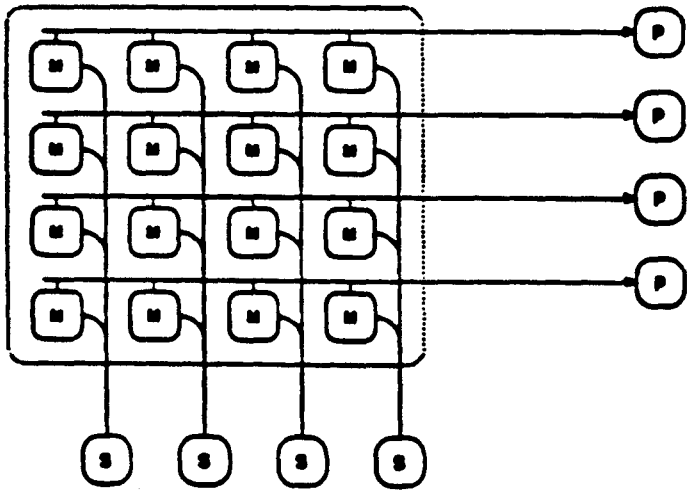
M
P
S

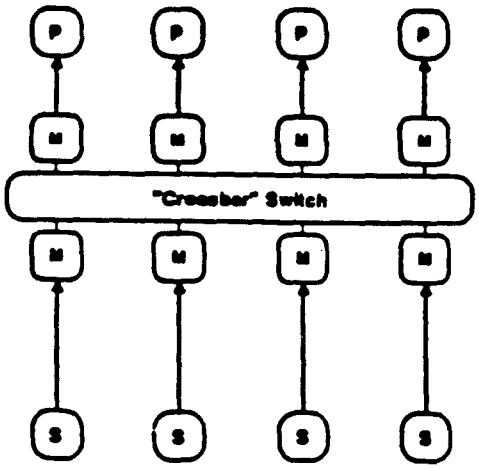
P
M
"Crossbar" Switch
S

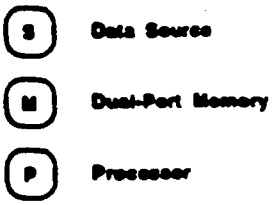
S
Data Source
M
Dual-Port Memory
P
Processor

BARREL SHIFTER EXAMPLE

4 × 4 : 4 INPUTS 4 OUTPUTS

4 DATA STREAMS OF EQUAL-SIZE EVENT FRAGMENTS
EACH STREAM DELAYED BY ONE ADDITIONAL TIME SLOT

STEP - THRU

GENERALIZE TO N×N

NEED EVENT FRAGMENTS TO SPAN DATA PACKETS
or multiple event fragments per packet

ACCOMPLISH BY ~~[illegible]~~ DEFINING

"LOGICAL FIFO's"

IN EACH BUFFER.

THESE MAP DIRECTLY TO A
LOGICAL FIFO IN RECEIVER

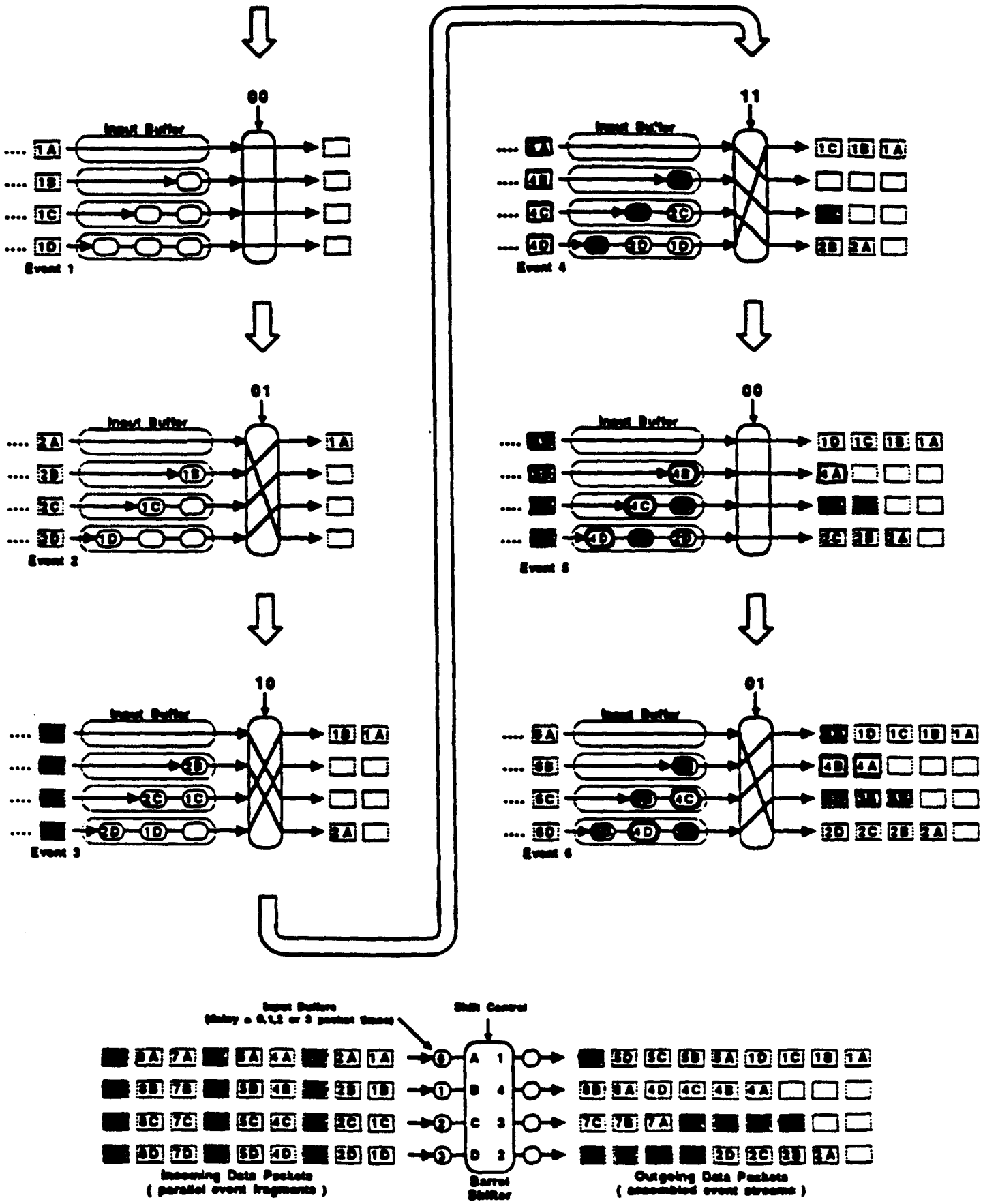

Barrel Shift Event Builder (for fixed length event data)

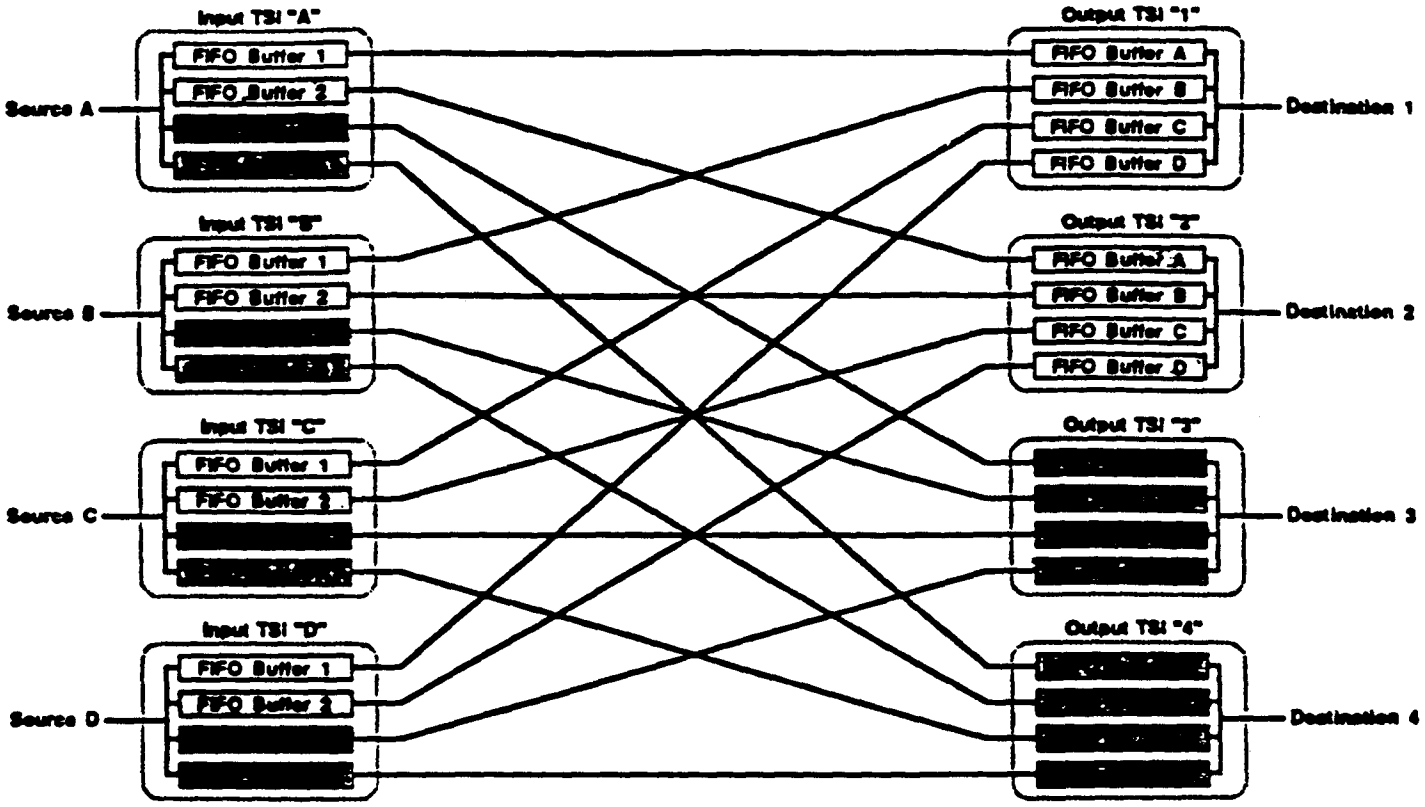

Logical Switch Operation

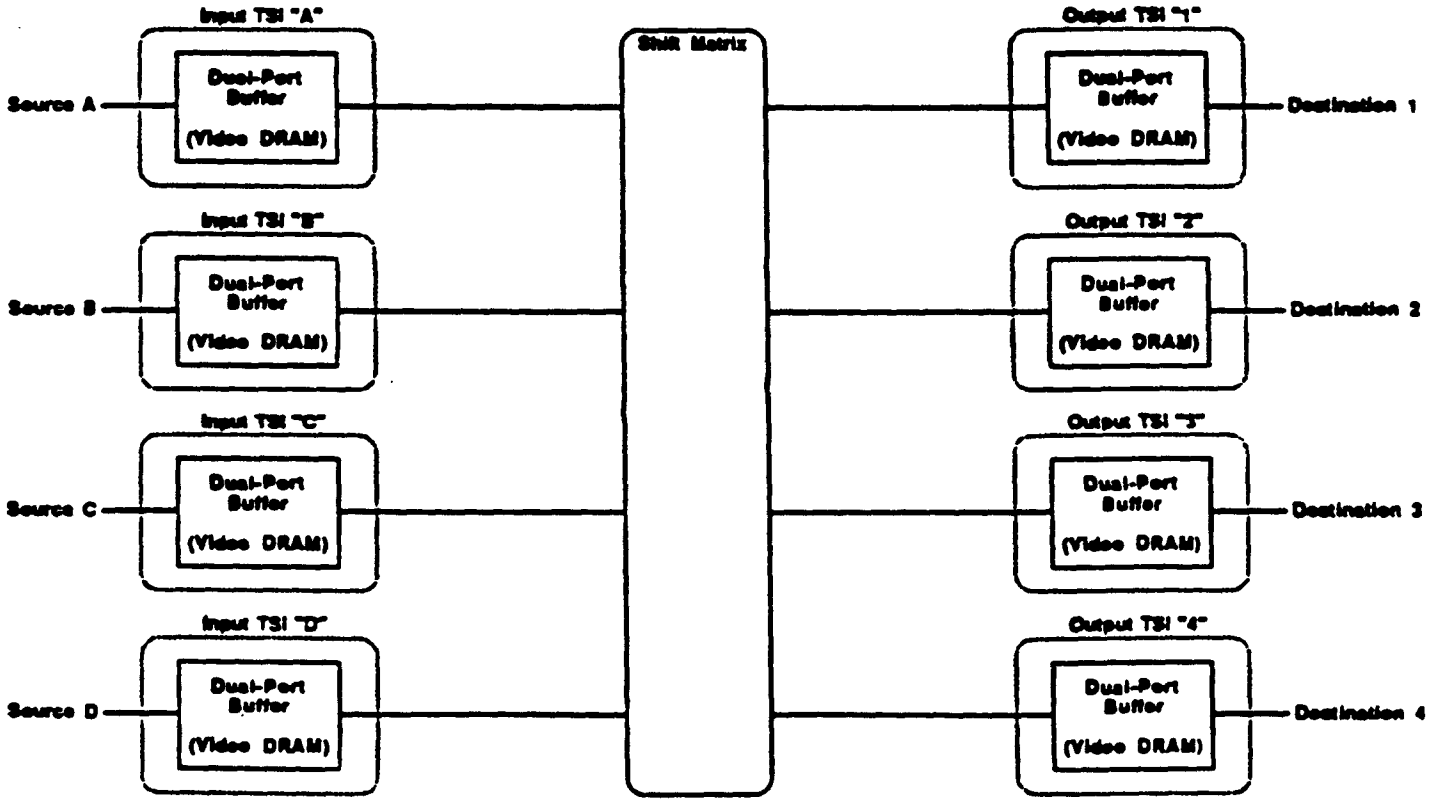

Physical Switch Operation

Processing Farms: The Problem

- 10^4-10^5 events/sec
- 1 MByte/event
- 10-100 VAX 11/780 seconds/event
- Rich Programming Environment

General Purpose Processors

- Developments in RISC processors
- Example: ACP MIPS VME board
- "Conservative" Projection

  50-100 VAX equivalents per processor
  4 processors/board (200-400 VAX/board)
  15 boards/crate (3000-6000 VAX/crate)
  30-50 crates (10^5-3 10^5 per system)

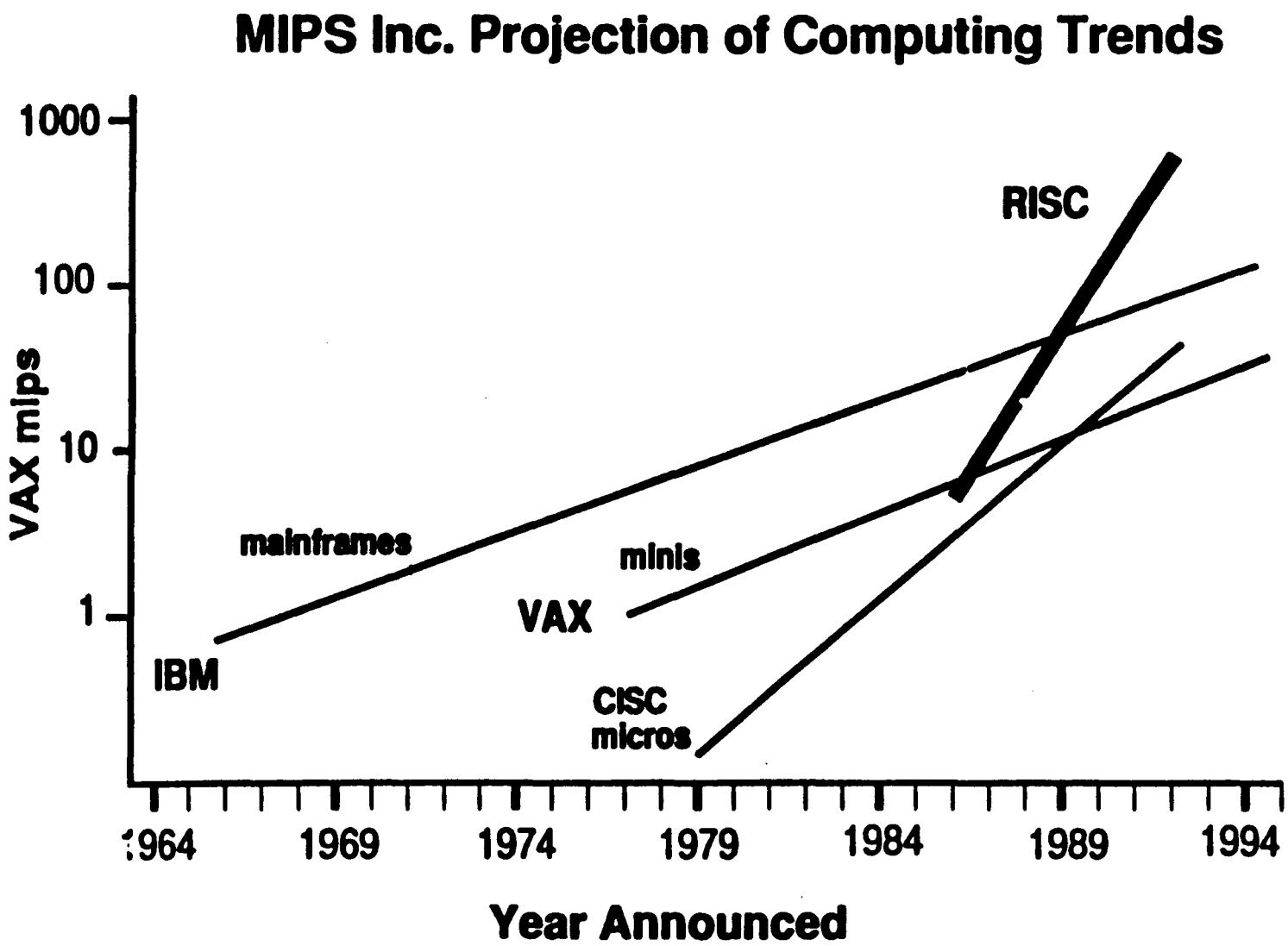
MIPS Inc. Projection of Computing Trends
1000
100
10
1
VAX mips
RISC
mainframes
minis
VAX
IBM
CISC
micros
1964
1969
1974
1979
1984
1989
1994
Year Announced

Processing time depends on three components:

Execution Time = Instructions/Task

* Cycles/Instruction

* Time/Cycle

RISC (Reduced Instruction Set Computers) seek to minimize the second and third component.

Cycles/Instruction = 10.6 for VAX 11/780
6.3 for Motorola 68020
1.25 for MIPS R3000

Simpler architecture allows higher clock speeds and implementation in faster technologies (ECL, GaAs)

PROCESSOR FARMS

LARGE AGGREGATE CPU (10^5-10^6 VAX)

=> LARGE NUMBER PROCESSORS (1000 - 5000)

(10 - 100 "VAX-SECONDS"/EVENT AVERAGE)

EXAMPLE:

4 RISC PROCESSORS/BOARD
BUS : FUTUREBUS +
DATA INPUT via HIGH-SPEED EXTERNAL BUS
PROCESSOR CRATE includes BOOT NODE and MASS STORAGE

INDUSTRY INTEREST IN MASSIVE PARALLEL COMPUTING
on a similar scale
$O(10^3$-$10^4)$ NODES FOR SCIENTIFIC COMPUTING
loosely-coupled RISC w/ MESSAGE PASSING

OTHER (IMPORTANT) ISSUES

MANAGING DATA FLOW + PROCESSING
CONTINUOUS OPERATION DURING CONFIGURATION CHANGES
IN SITU DEBUGGING OF PRODUCTION CODE
DEVELOPMENT ENVIRONMENT FOR NEW CODE
FACILITIES FOR VERIFICATION

i.e.: COMFORTABLE ENVIRONMENT w/ OPERATING SYSTEM TOOLS

i860: A 64-bit Microprocessor

Single-chip numeric microprocessor

- 64-bit internal data paths
- 64-bit data bus to memory

"RISC" architecture

Multiple pipelined functional units

- separate integer, floating point, and graphic units
- separate 4 Kbyte code cache and 8 Kbyte data cache

1.02 million transistors

33/40 MHz operation on CHMOS IV

i860 Multi-Function Organization

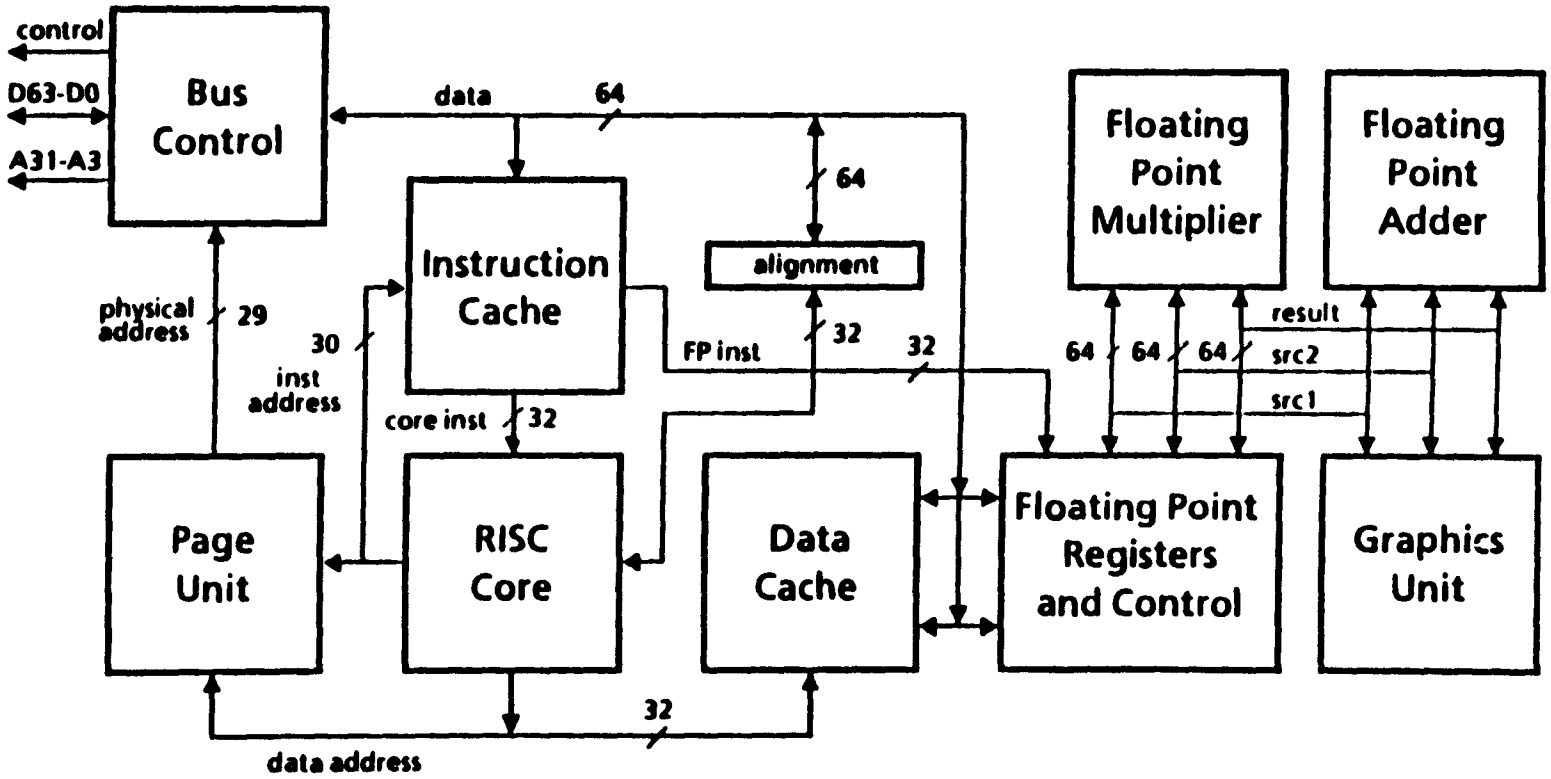

TEXAS INSTRUMENTS HAS DEMONSTRATED GaAs VHSIC SCALE INTEGRATION IN THE MIPS PROCESSOR BEING DEVELOPED FOR DARPA AND IS UTILIZING GaAs GATE ARRAYS IN ITS NEW MILITARY SYSTEMS

Press Release

TEXAS INSTRUMENTS DEMONSTRATES WORLD'S FIRST 100 MHz 32-BIT RISC CPU

DALLAS (NOVEMBER 1, 1988) —

Texas Instruments has demonstrated the world's first 32-bit reduced instruction set computer (RISC), single-chip microprocessor operating with a clock rate in excess of 100 million cycles per second. Built with TI's unique heterojunction bipolar (HBT) process, this 12,900 gate microprocessor is also the largest functional logic device built to date using gallium arsenide (GaAs) material.

The microprocessor is developed by TI's Defense Systems and Electronics Group (DSEG) with support from Control Data Corporation (CDC) under a contract with the Defense Advanced Research Projects Agency (DARPA). This 32-bit RISC processor uses the DARPA MIPS CORE Instruction Set Architecture (ISA). A 32-bit RISC architecture is favored by DoD for the next generation DoD standard processor.

Intel-DARPA Touchstone Project

Building the Technology for Supercomputers in the '90s

- A $27.5 million development contract
- The goal: a practical ultra high performance supercomputer technology
  - 200 GFLOPS (2,000 node) prototype by late 1991
  - Ease of use comparable to today's workstations
- Specific research focus on...

Interconnect technology	Software environments
Node architectures	High performance graphics

- Touchstone will be the technology driver for future iPSC systems

Touchstone Interconnect

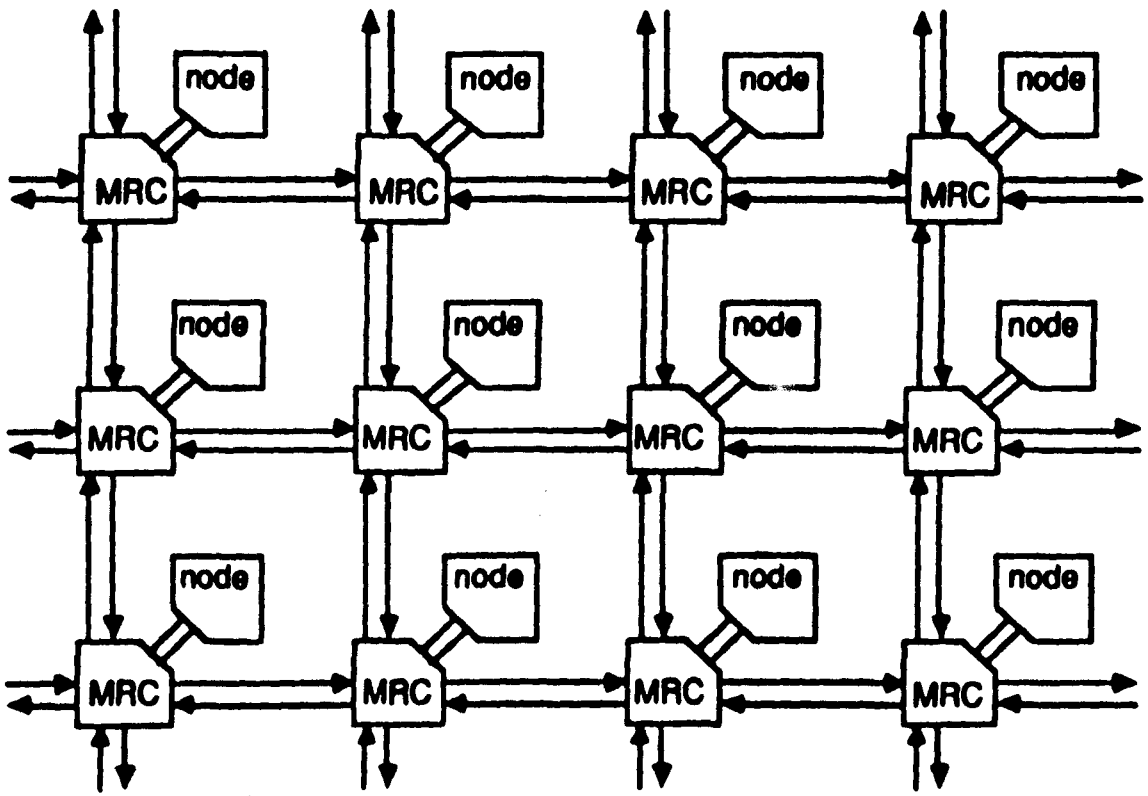

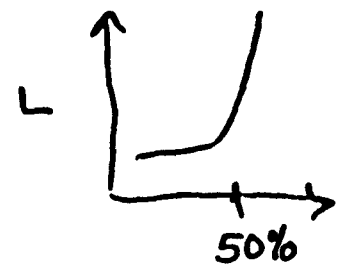

- 32 x 64 mesh
- 8,000 Mbytes/sec bi-section bandwidth
- Scalable to 4000 nodes
- Wormhole Routing

High Speed Mesh Router

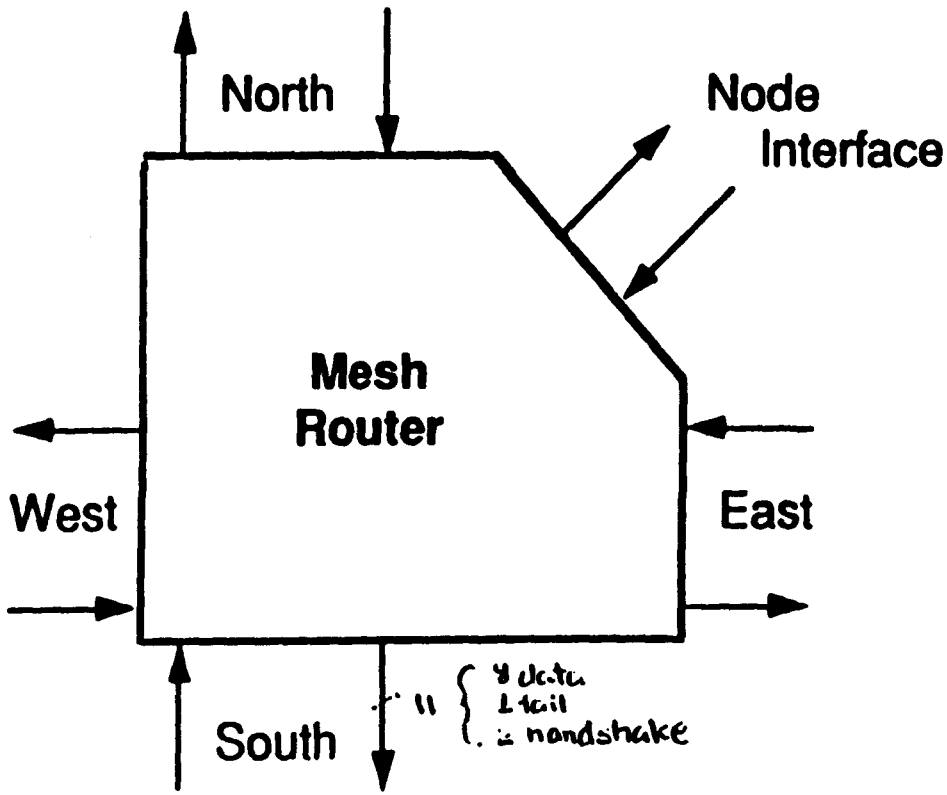

- Single VLSI chip
- Byte-wide channels
  - unidirectional
  - 128 Mbytes/sec
- Low latency
  (40ns/hop)
- Self-timed design

Special Purpose Processors

- General purpose processors may not be sufficient
- Specialized devices have traditionally been up to 1000 times as powerful for specific tasks
- Specialized devices can be used both before event event building (on sub events) or after (on full events)
- Modern DSPs have high level languages and operating systems

Special Purpose Processors

- Traditionally hard-wired microcoded devices
- Still have a role despite increasingly powerful general purpose processors
    - Jet finding, track finding, ...
    - Current specialized processors provide 5000 VAX equivalents for these tasks
    - Neural networks
- Digital Signal Processors (DSPs) now have high level languages and full operating systems supporting program development
- ASIC (Application Specific Intergrated Circuits) with RISC and DSP cores becoming available

ON LINE MASS STORAGE

10 - 100 events/sec × 1 MByte/event ≤ 100 MBytes/sec

EVEN AFTER FARM, DATA RATE IS HIGH.

NEED A PLACE TO PUT THE DATA.

SOLUTION:

PARALLEL RECORDING MEDIA (even without leaps in technology)

THRU SWITCH ?

EX: E - Systems

CURRENT SYSTEM (NOT UNLIKE OUR PROBLEM)

NEAR FUTURE SYSTEM

(DRIVEN BY TV INDUSTRY)

DATA VOLUME + MEDIA COST

FAVOR VIDEO CASSETTES

ROBOTICS / FILE SERVERS

⇒ READY / AUTOMATED ACCESS

PROJECTION

SYSTEM COST DEPENDS ON ACCESS TIME

CIRCA 1988 SYSTEM

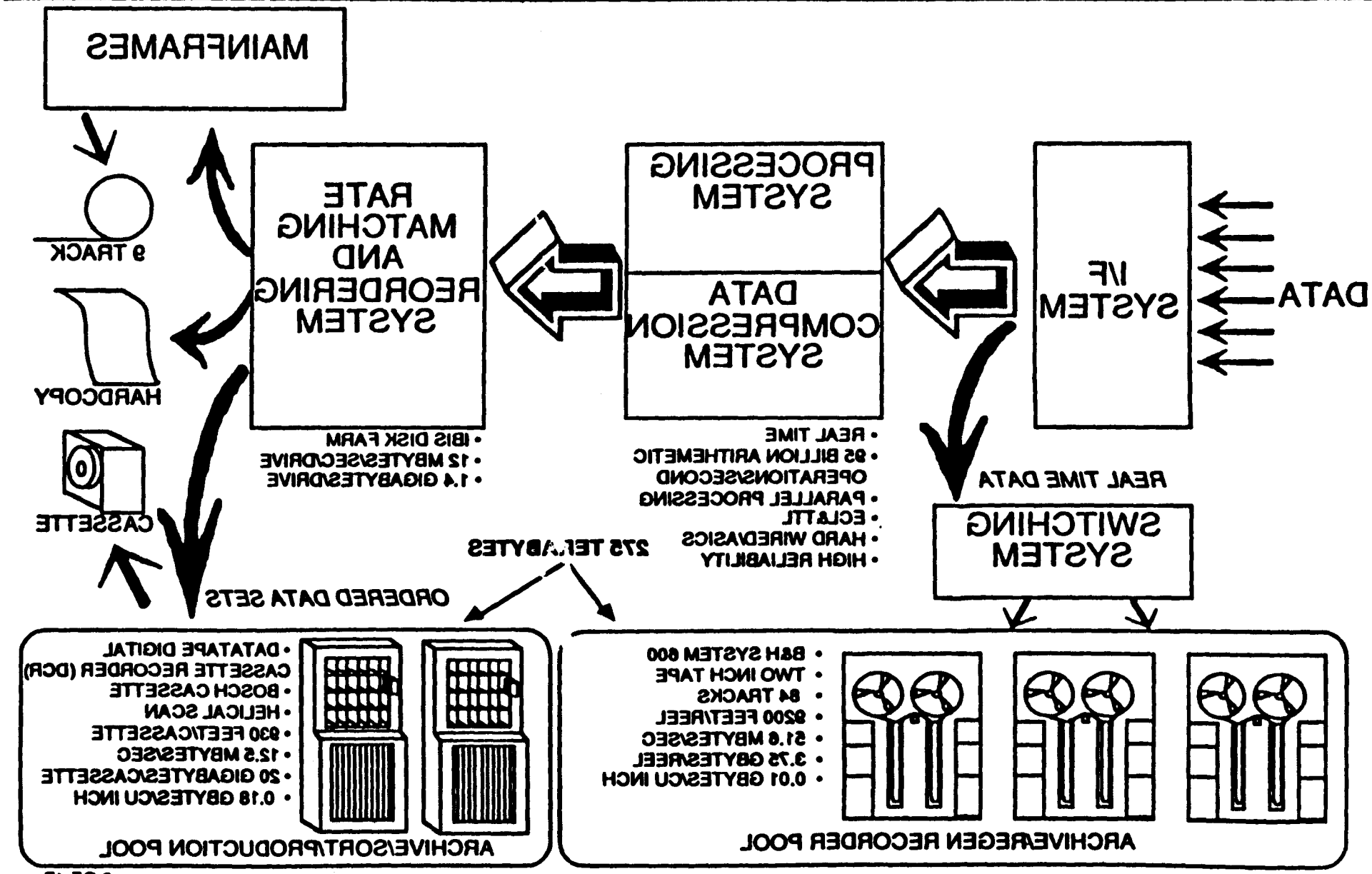

E-SYSTEMS
GARLAND DIVISION

CIRCA 1993 SYSTEM

SSC DATA ACQUISITION
TASK GROUP WORKSHOP
MAY 3-5, 1989

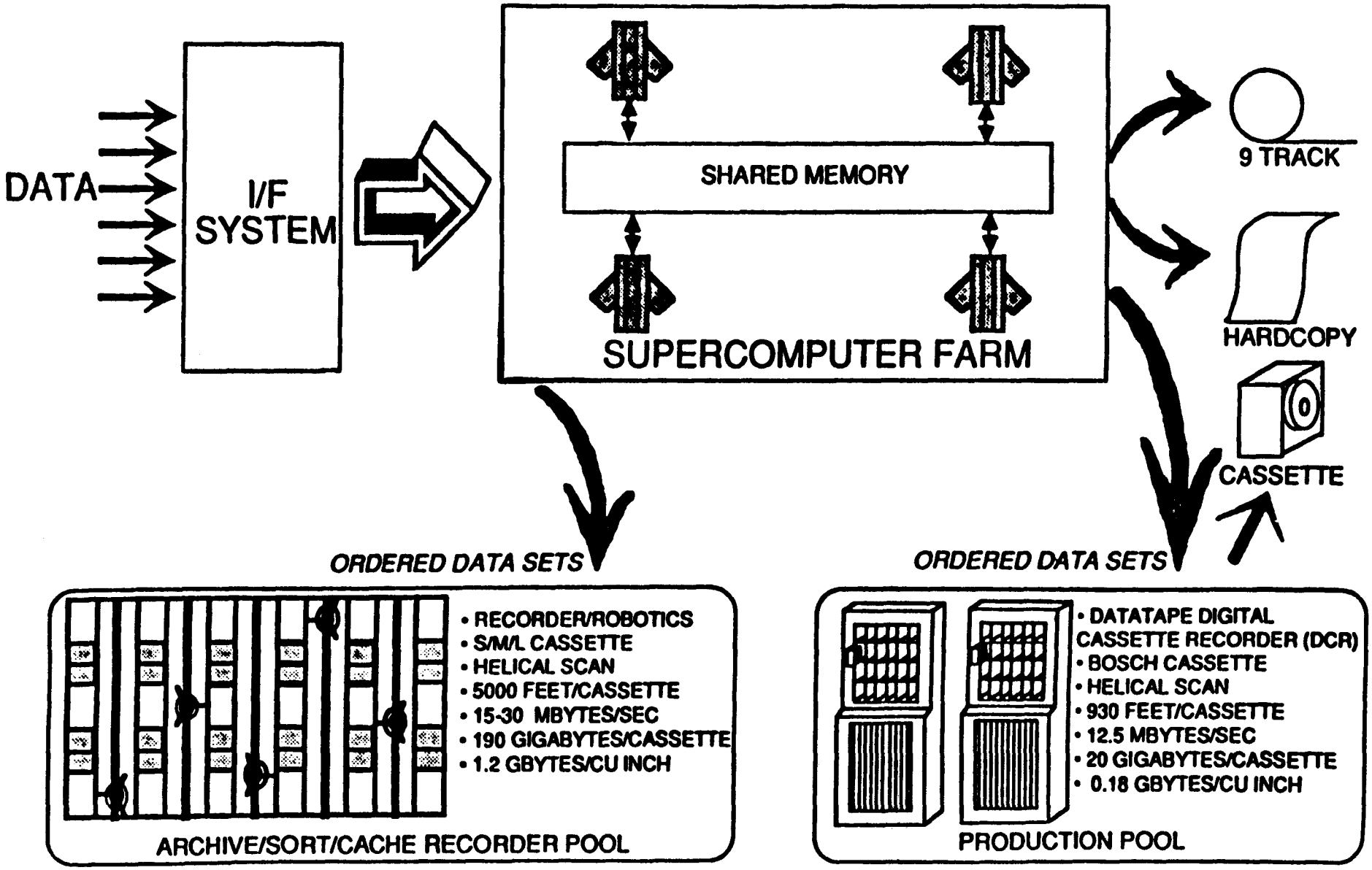

VOLUME

- EVEN THE HIGHEST DENSITY STORAGE TECHNIQUES WILL REQUIRE SUBSTANTIAL STORAGE VOLUMES...

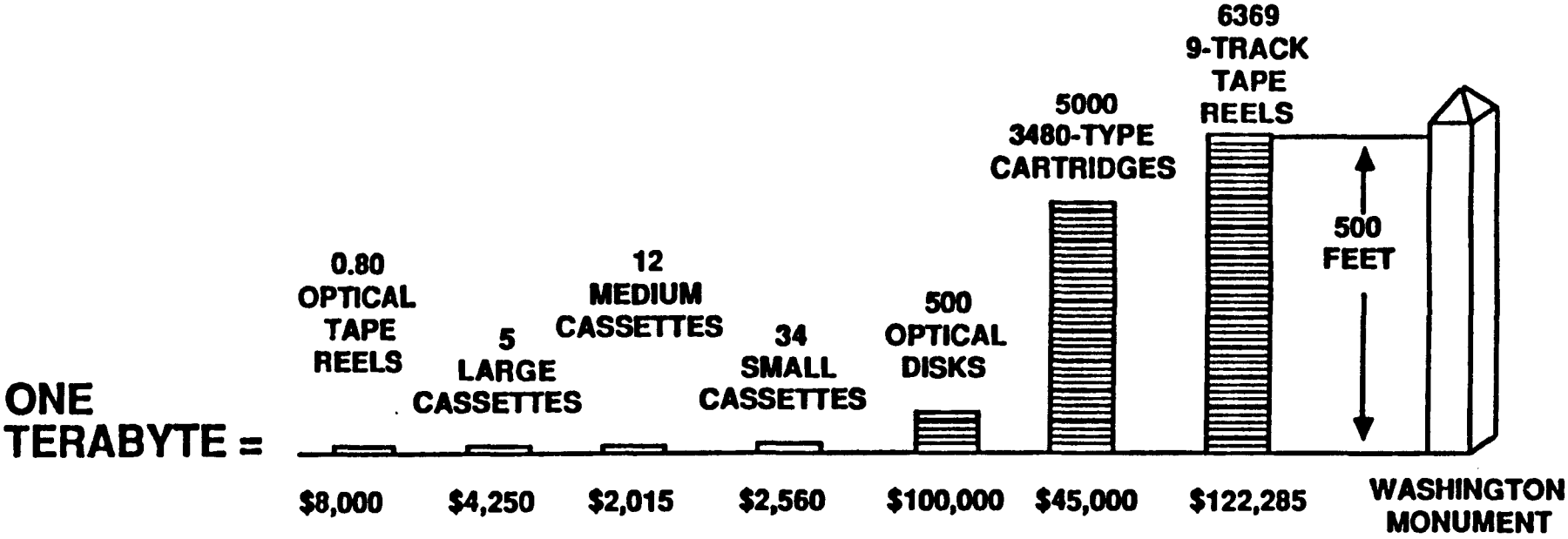

1 SMALL CASSETTE CONTAINS 29,500 MEGABYTES or 187 REELS OF TAPE

1 MEDIUM CASSETTE CONTAINS 86,625 MEGABYTES or 551 REELS OF TAPE

1 LARGE CASSETTE CONTAINS 189,875 MEGABYTES or 1,185 REELS OF TAPE

...BUT ROBOTICS CAN MINIMIZE ACCESS TIMES

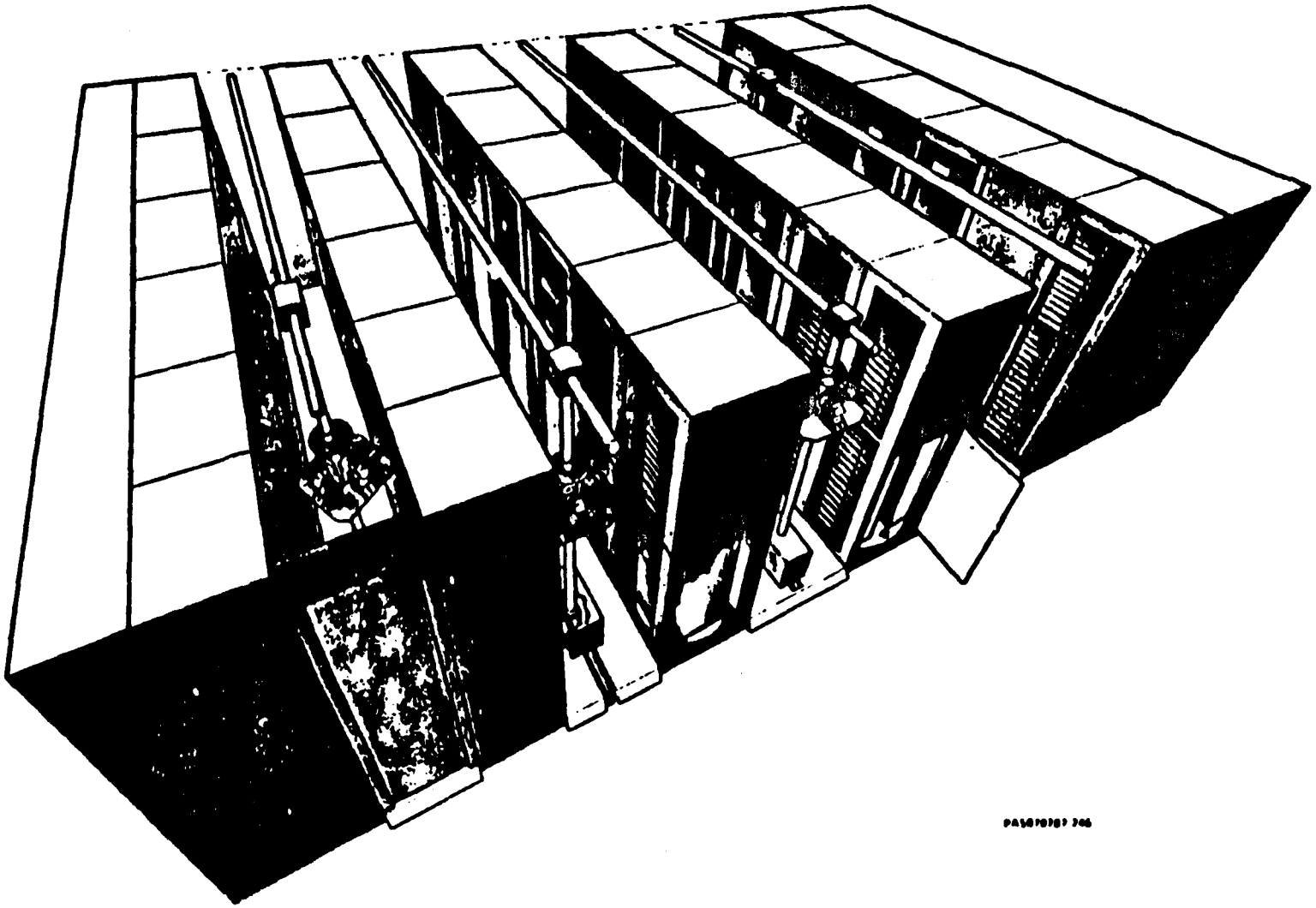

AS8901-348

MID 1990'S MASS STORAGE SYSTEMS

- SYSTEM I/O RATE → SYSTEM DEPENDENT
- SYSTEM STORAGE → 50 PENTABYTES
- STORAGE SYSTEM COST → $5/GIGABYTE
- MEDIA COST → $2/GIGABYTE
- RECORDER I/O RATE → 30+ MBYTES/SECOND

➡ THE MASS STORAGE ARCHITECTURE MUST FIT INTO THE FRAMEWORK OF THE SYSTEM ARCHITECTURE TO TAKE FULL ADVANTAGE OF THIS TECHNOLOGY

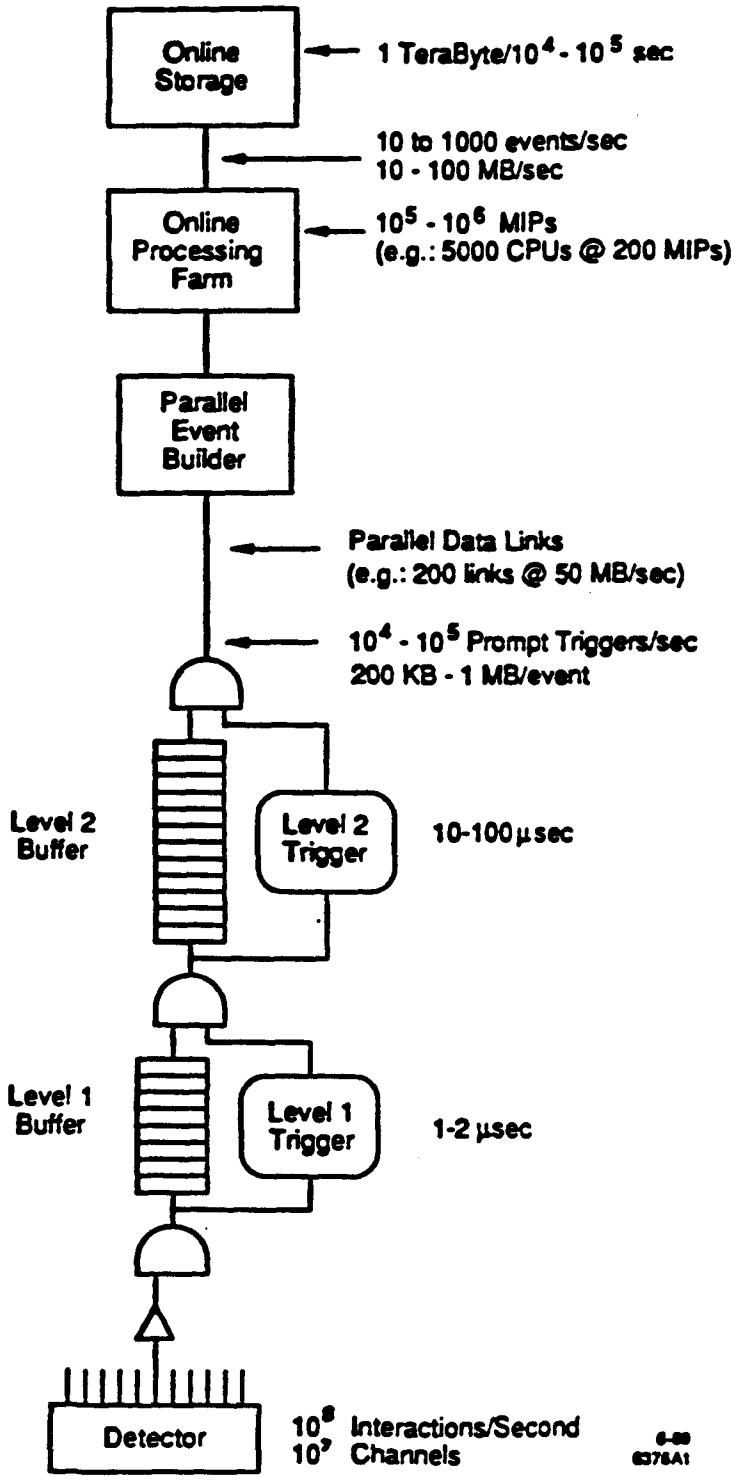
Online Storage
1 TeraByte/10^4 - 10^5 sec
10 to 1000 events/sec
10 - 100 MB/sec
Online Processing Farm
10^5 - 10^6 MIPs
(e.g.: 5000 CPUs @ 200 MIPs)
Parallel Event Builder
Parallel Data Links
(e.g.: 200 links @ 50 MB/sec)
10^4 - 10^5 Prompt Triggers/sec
200 KB - 1 MB/event
Level 2 Buffer
Level 2 Trigger
10-100 μsec
Level 1 Buffer
Level 1 Trigger
1-2 μsec
Detector
10^8 Interactions/Second
10^7 Channels

SUMMARY

EMPHASIS HAS BEEN ON HIGH-SPEED DATA FLOW.

capability allows flexibility in TRIG/DAQ performance.

NOTE:

SEPARATE DATA FLOW + CONTROL

SIMPLE CONTROL OF FLOW

EXTENSIVE USE OF PARALLELISM
(data flow, switch, farm, mass storage)

SCALING TO REQUIRED PERFORMANCE

NEED A MODULAR IMPLEMENTATION
TO ALLOW US TO EXPLOIT ADVANCES
IN TECHNOLOGY.

SSC DATA ACQUISITION SEEMS FEASIBLE.

DIRECTIONS, not yet DESIGNS

BUT ...

SOFTWARE !

GENERALIZED FRONT END ELECTRONICS

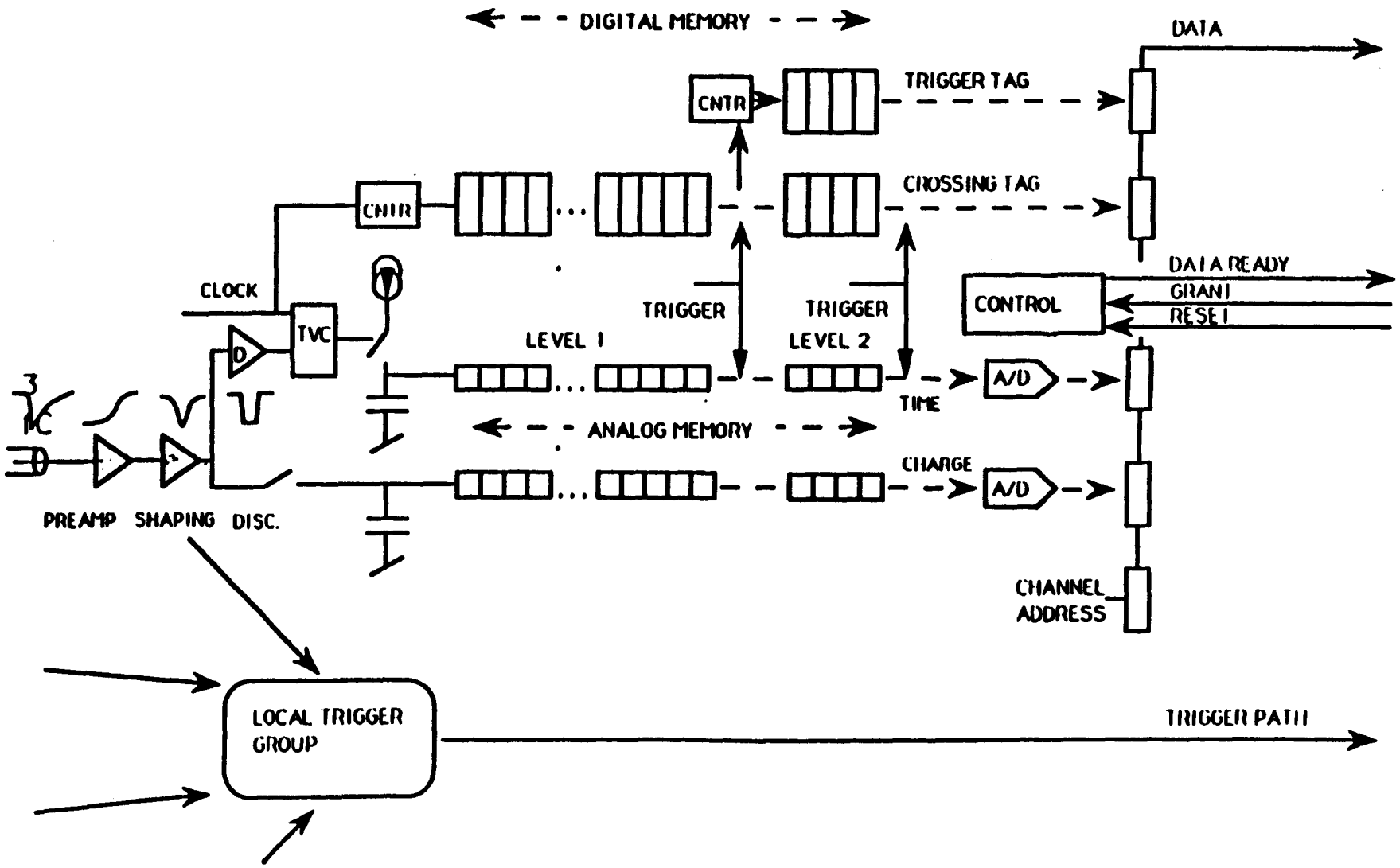

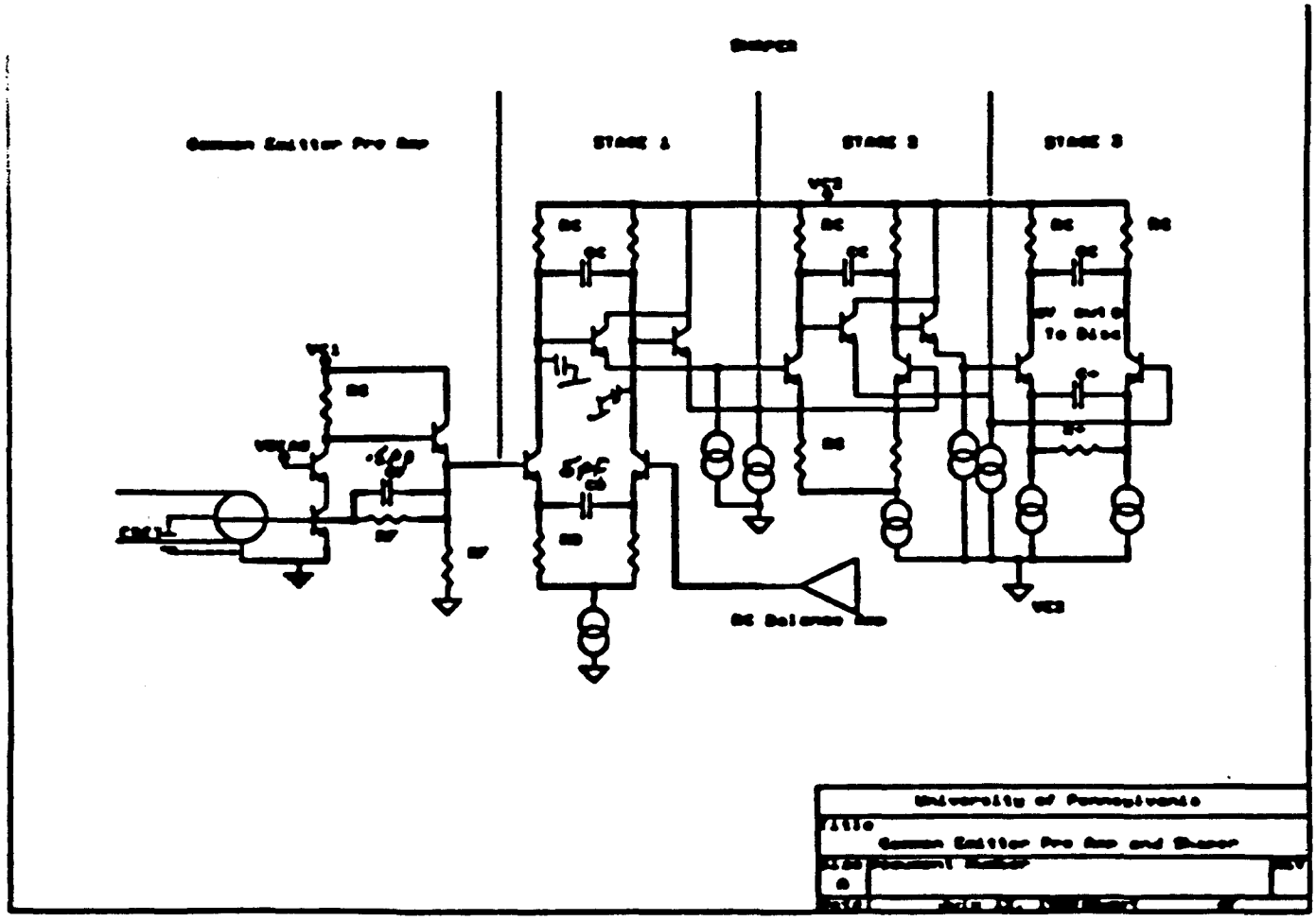
STAGE 1
STAGE 2
STAGE 3
To Dials
DC Balance Amp
University of Pennsylvania

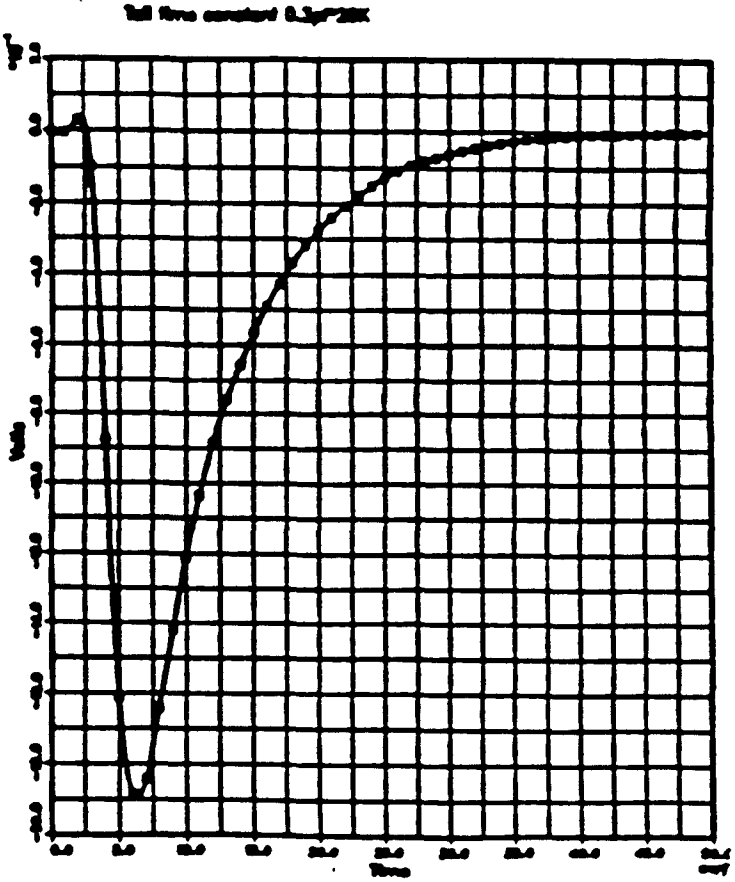
Volts
Time

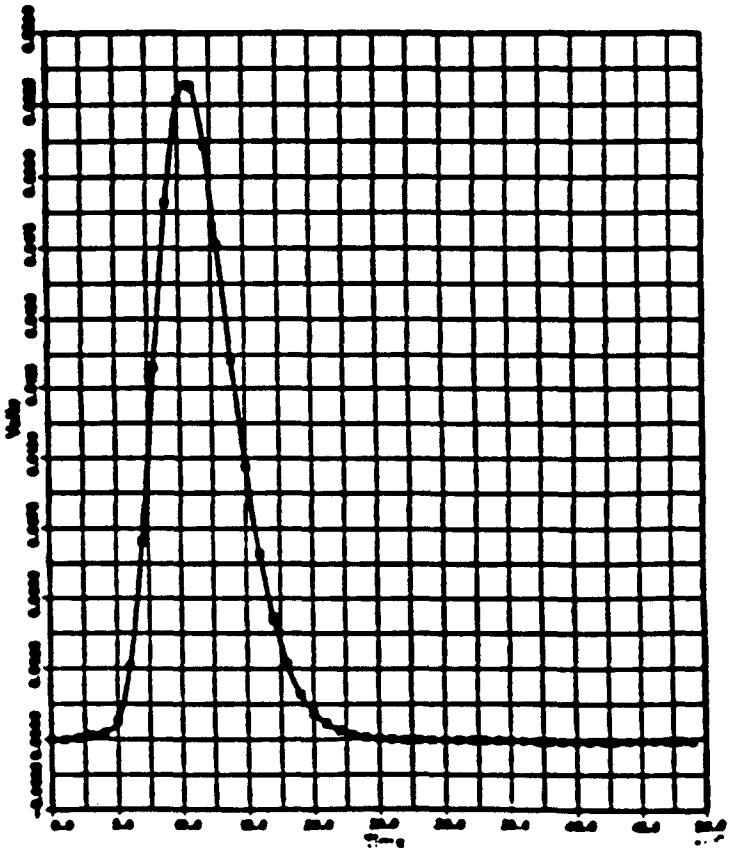
Volts

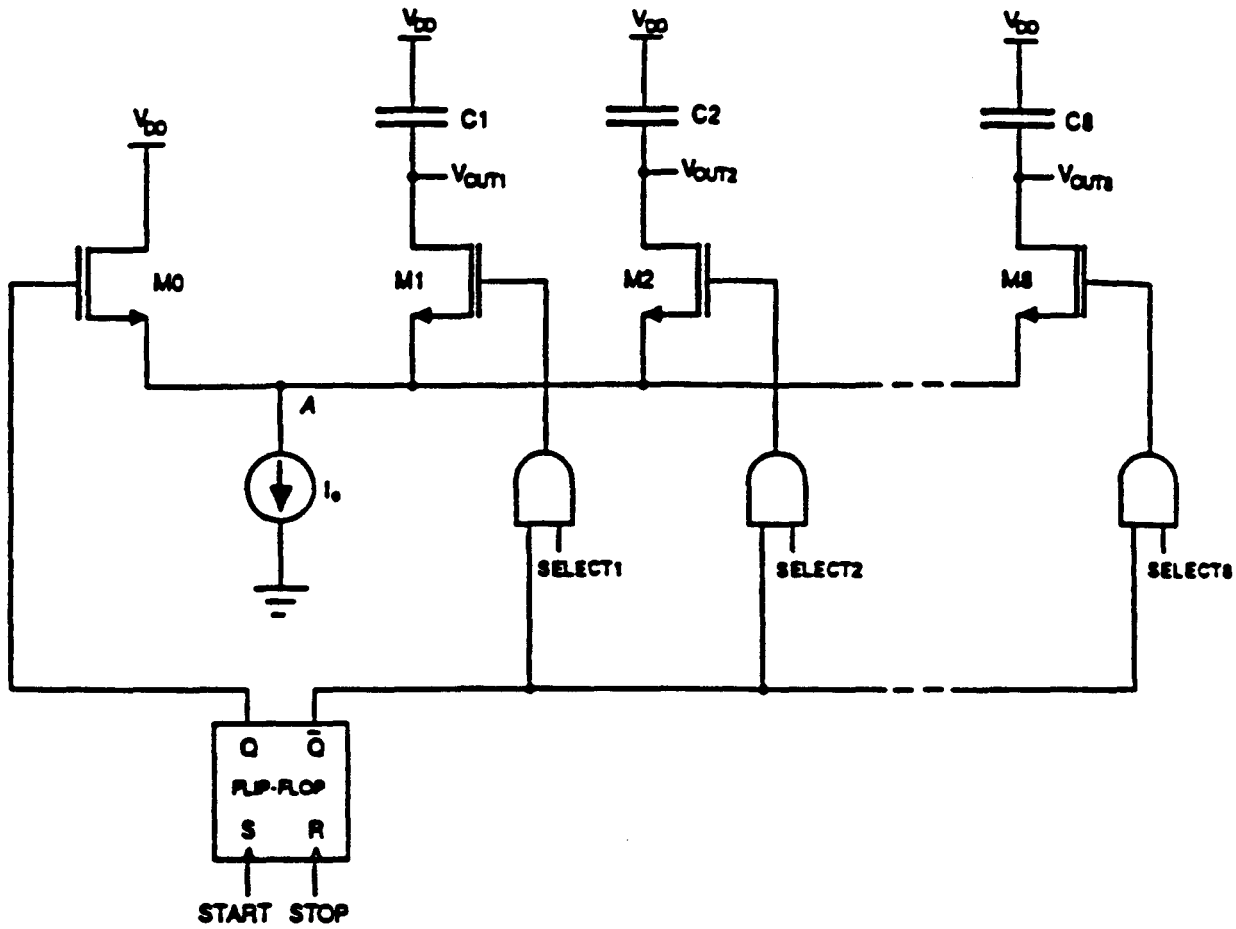
V_{DD}
V_{DD}
V_{DD}
V_{DD}
C1
C2
C8
V_{OUT1}
V_{OUT2}
V_{OUT8}
M0
M1
M2
M8
A
I_o
SELECT1
SELECT2
SELECT8
Q
$\bar{Q}$
FLIP-FLOP
S
R
START
STOP

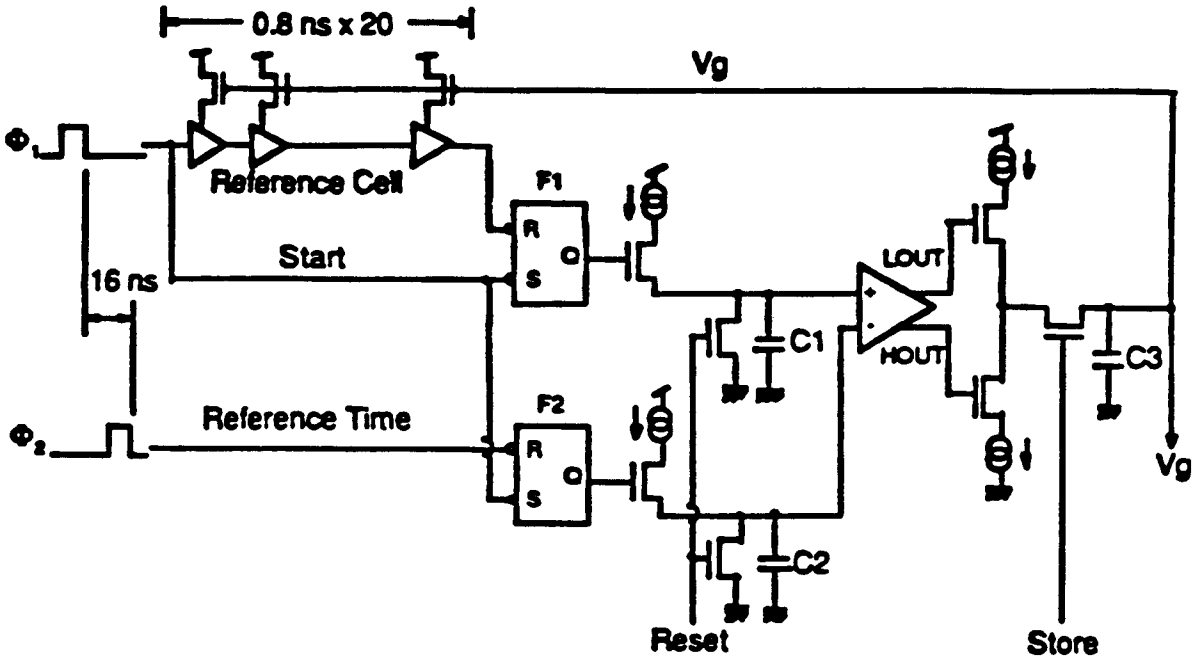

Fig. 5 TMC Feedback Circuit.

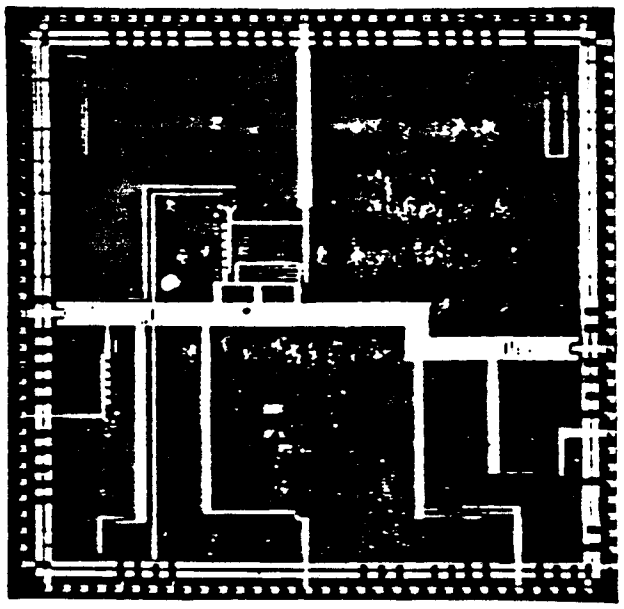

Fig. 6 Microphotograph of the TMC chip.

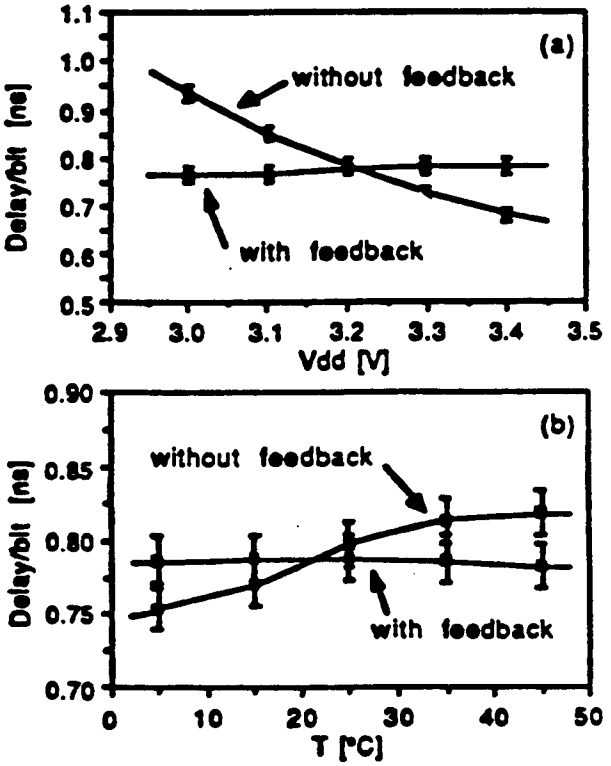

Fig. 7 (a) Supply voltage dependence of the delay element. (b) Temperature dependence of the delay element.

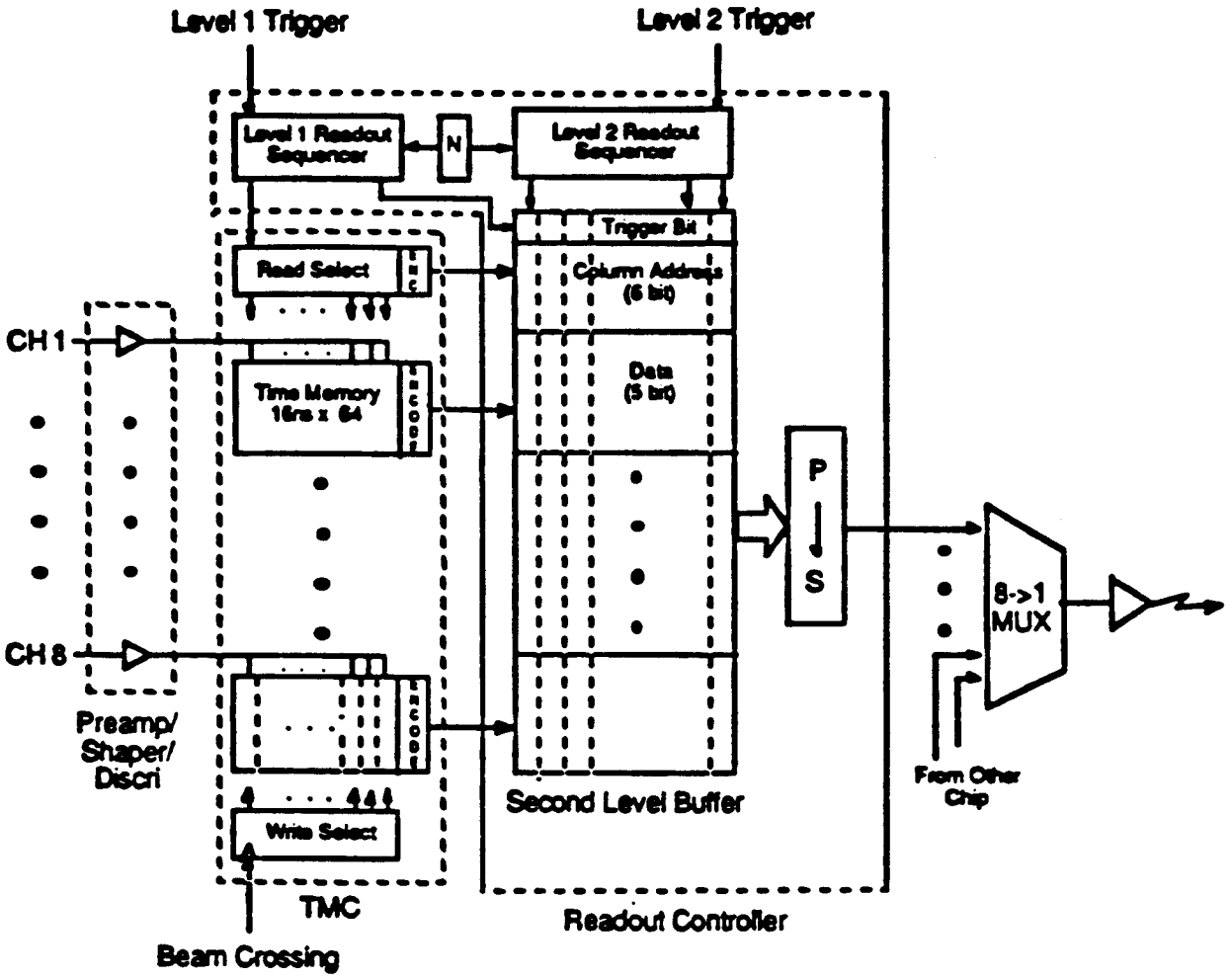

Fig. 8 Readout scheme of the time measurement system.

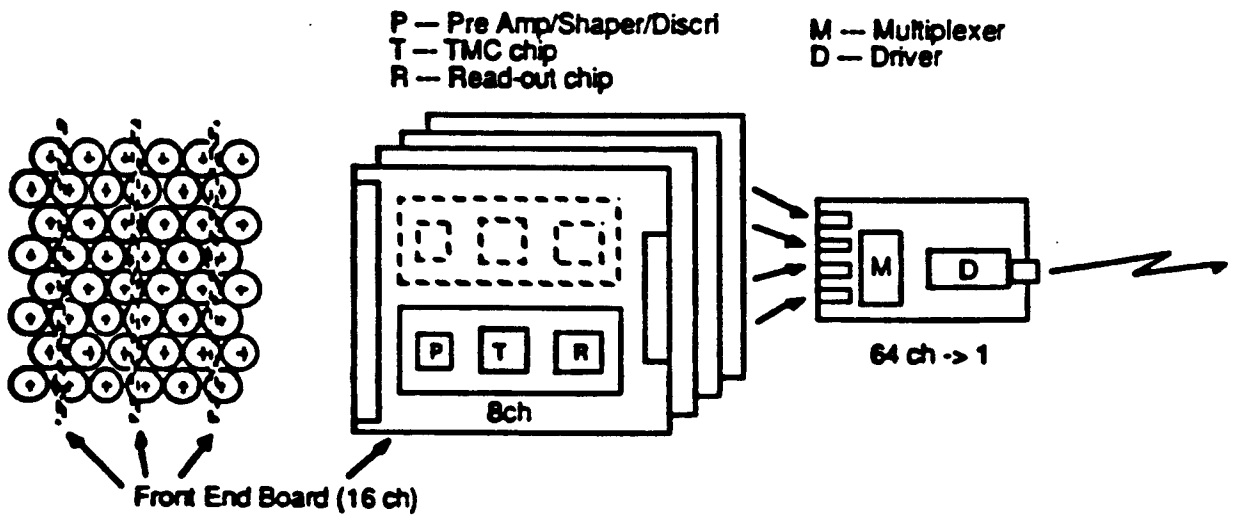

Fig. 9 Mounting of the front-end electronics to the 8 layer straw tube.

Si μ STRIP SYSTEM

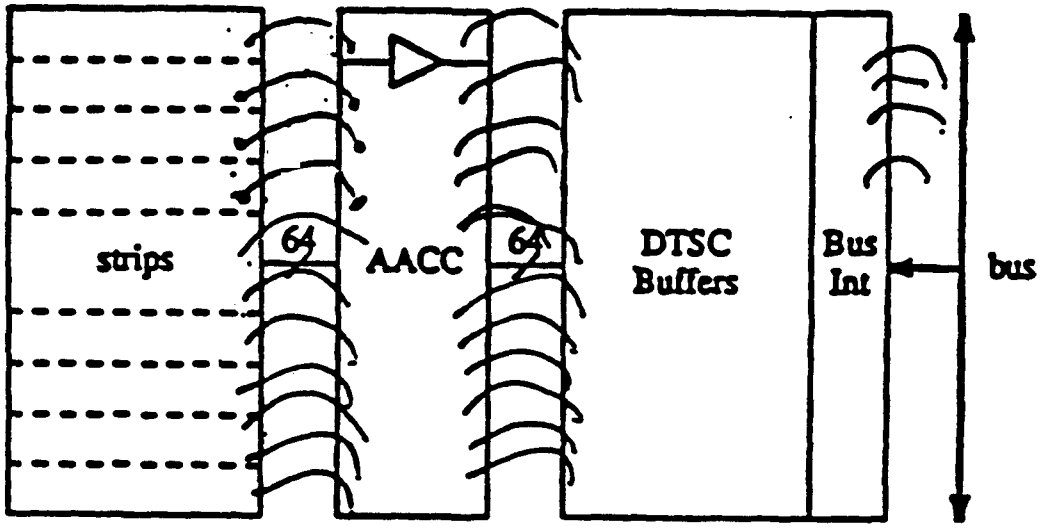

Fig. 17

DTSC

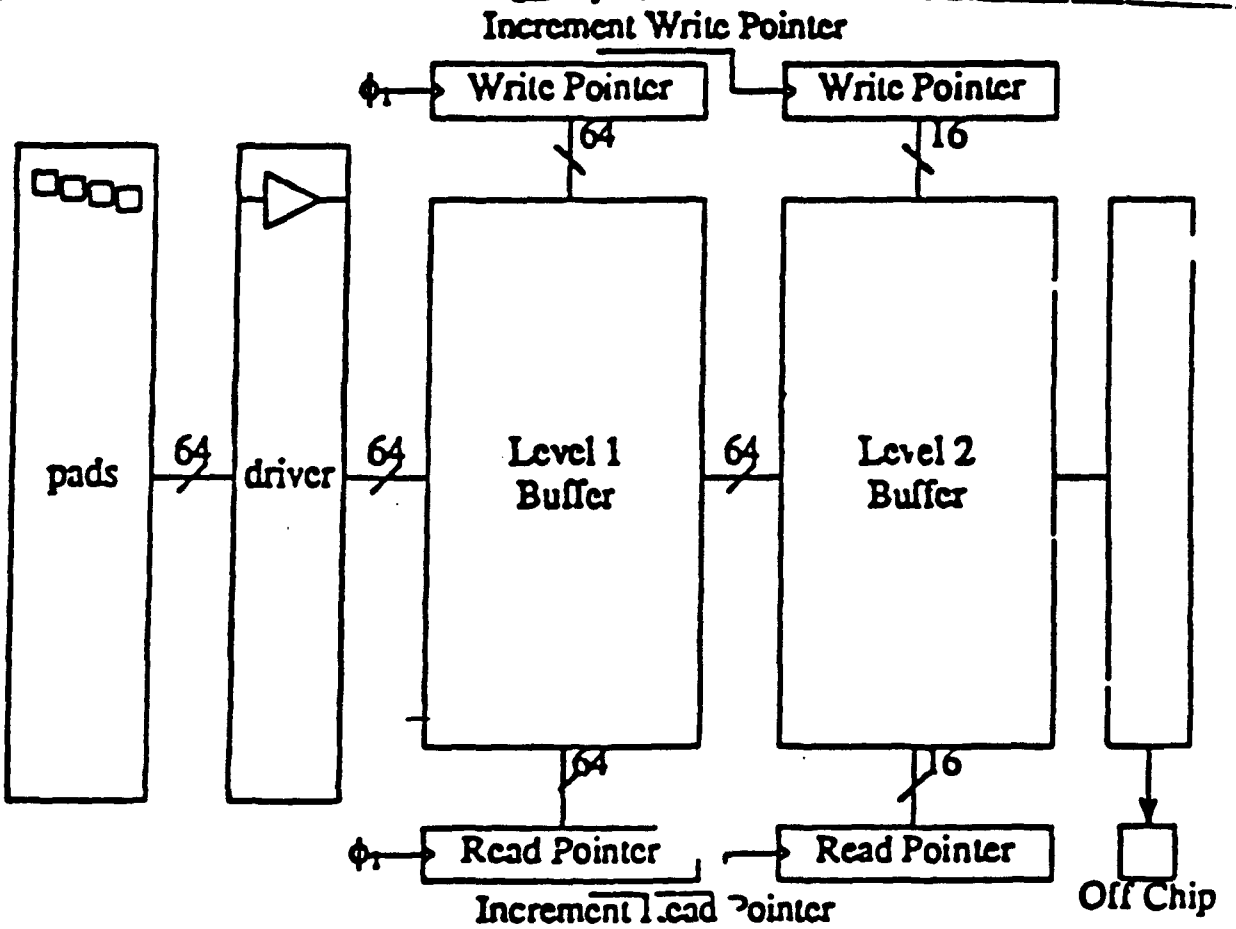

Fig. 18

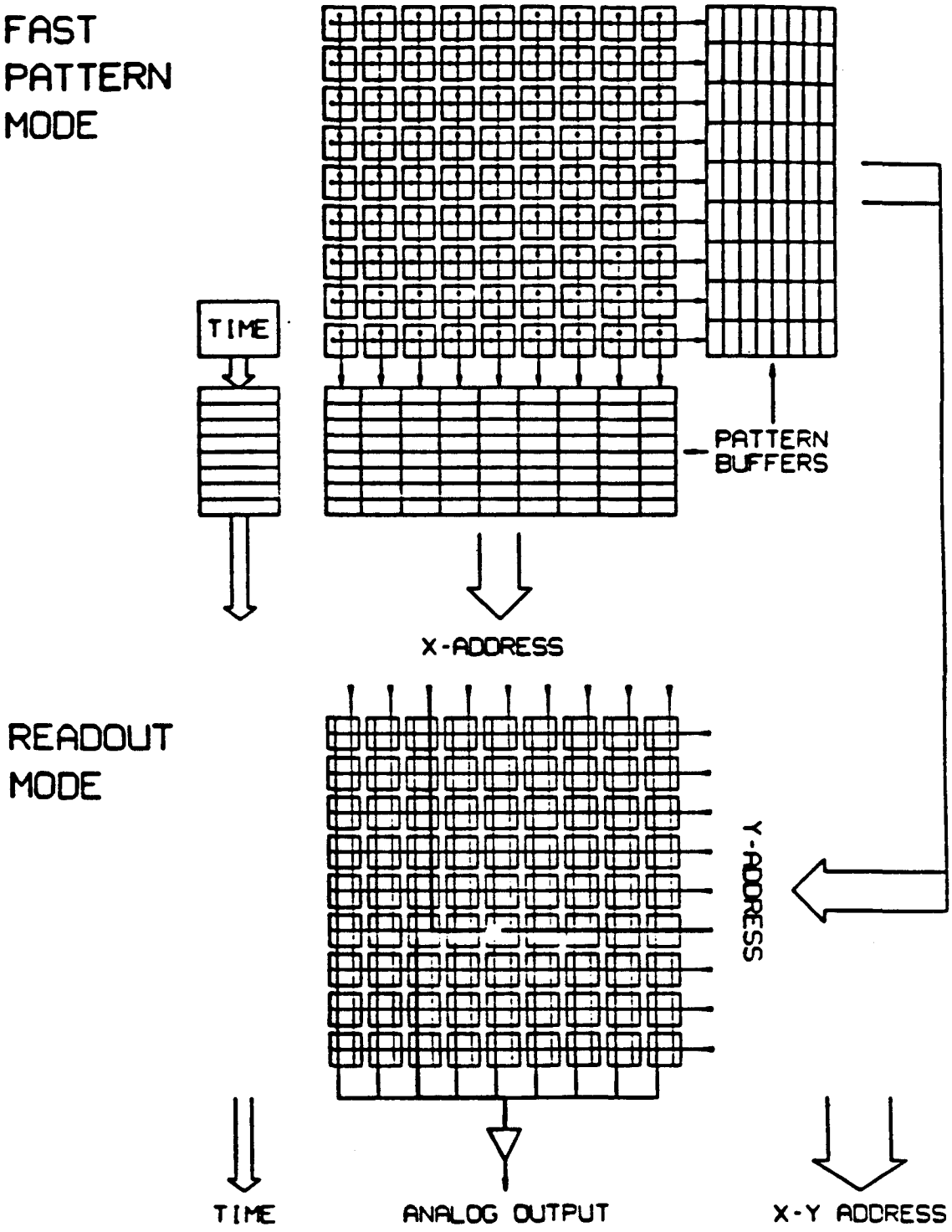
FAST
PATTERN
MODE
TIME
PATTERN
BUFFERS
X-ADDRESS
READOUT
MODE
Y-ADDRESS
TIME
ANALOG OUTPUT
X-Y ADDRESS

HYBRID APPROACH OPTIMIZES PERFORMANCE, MINIMIZES COST

HUGHES

7729-SP9 MC18

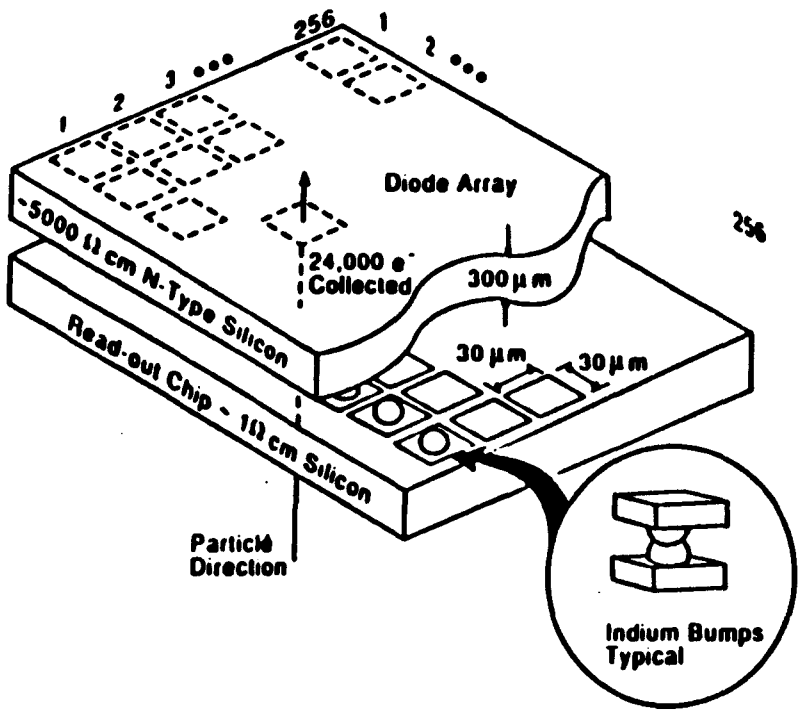

- EACH ELEMENT OF THE HYBRID CAN BE SEPARATELY OPTIMIZED
- CHANGES IN ONE OR THE OTHER ELEMENT e.g. DETECTOR OR READOUT CHIP CAN BE ACCOMODATED QUICKLY AT LOWER RISK AND COST
- YIELD LOSSES IN DETECTOR AND READOUT PROCESSING NOT COMPOUNDED

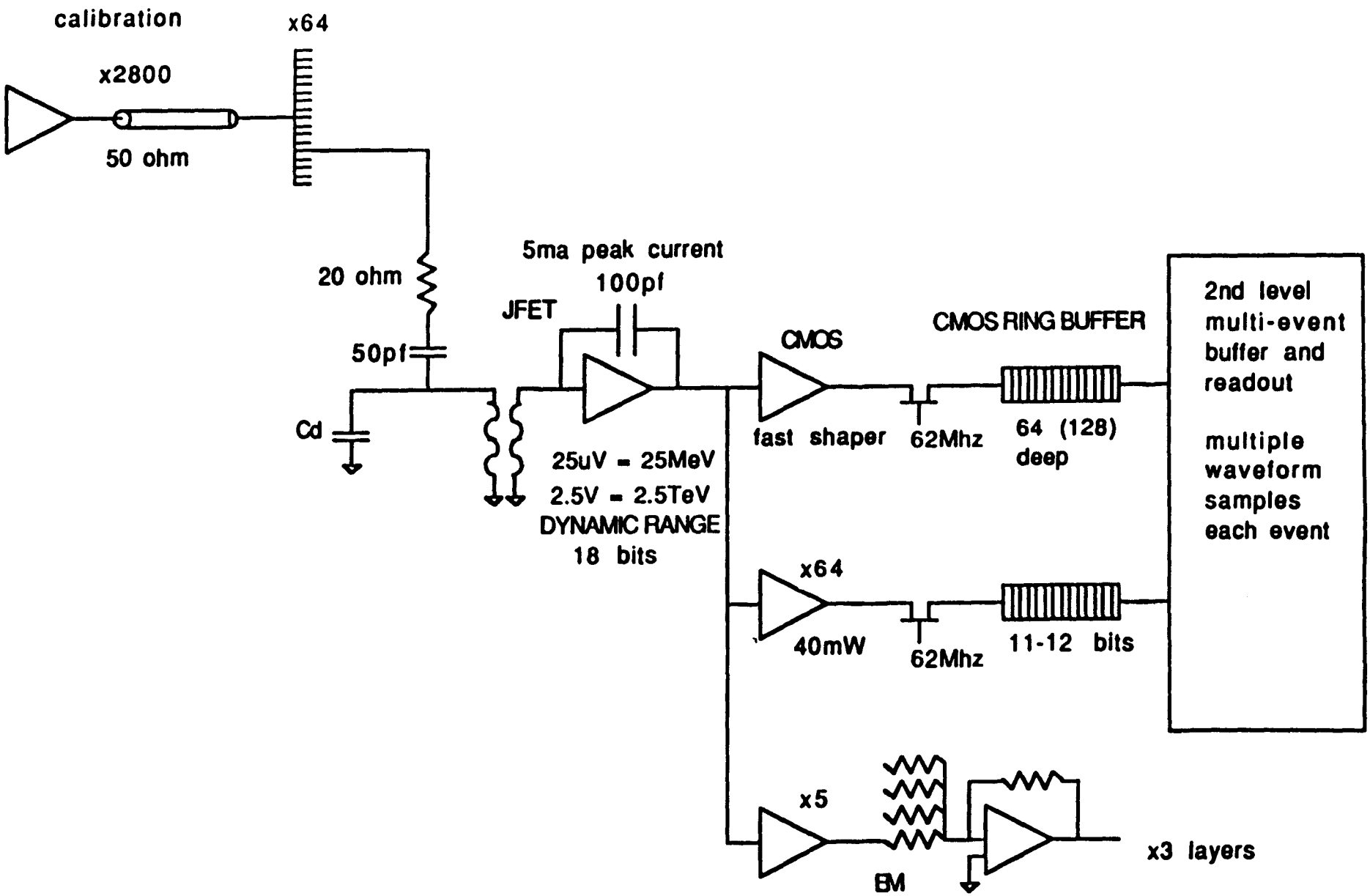
calibration
x64
x2800
50 ohm
20 ohm
50pf
Cd
5ma peak current
100pf
JFET
25uV = 25MeV
2.5V = 2.5TeV
DYNAMIC RANGE
18 bits
CMOS
fast shaper
62Mhz
CMOS RING BUFFER
64 (128)
deep
2nd level
multi-event
buffer and
readout
multiple
waveform
samples
each event
x64
40mW
62Mhz
11-12 bits
x5
BM
x3 layers

EM:3mm U HAD:3mm U trigger tower

.08x.08 EM .32x.32 HAD

CAL	noise match MeV	noise unmat	noise 3:1	pileup	noise match	noise unmat	noise 3:1	pileup
EM	165	400		110	660	1600		480
HD	570	4030	450	280	2300	16100	1800	1170
		TIME				TIME		
10	1ns	2ns			12ns	80	12	
25					5	32	5	
50					2	16	3	
100					1	8	1	
GeV								

LEVI-5

CAL	dø x dn	Pad width	Cpad pF	#plates 3mm U	#plates 6mm U	# chnls
EM1	0.04x0.04	7cm	34	6		80x160
EM2	0.02x0.02	3.5	9	8		160x320
EM3	0.04x0.04	7	34	11		80x160
HD1	0.04x0.04	8.4	49	30	15	80x160
HD1'	0.04x0.04	8.4	49	30	15	80x160
HD2	0.04x0.04	9.9	68	30	15	80x160
HD2'	0.04x0.04	9.9	68	30	15	80x160
HD3	0.04x0.04	12.1	102	30	15	80x160
HD3'	0.04x0.04	12.1	102	30	15	80x160
HD4	0.04x0.04	13.9	135	30	15	80x160
HD4'	0.04x0.04	13.9	135	30	15	80x160

CAL	dø x dn	Pad width	Cpad pF	#plates 3mm U	#plates 6mm U	# chnls
EM1	0.04x0.04	7cm	34	6		80x160
EM2	0.02x0.02	3.5	9	8		160x320
EM3	0.04x0.04	7	34	11		80x160
HD1	0.04x0.04	8.4	49	30	15	80x160
HD1'	0.04x0.04	8.4	49	30	15	80x160
HD2	0.04x0.04	9.9	68	30	15	80x160
HD2'	0.04x0.04	9.9	68	30	15	80x160
HD3	0.04x0.04	12.1	102	30	15	80x160
HD3'	0.04x0.04	12.1	102	30	15	80x160
HD4	0.04x0.04	13.9	135	30	15	80x160
HD4'	0.04x0.04	13.9	135	30	15	80x160

	EM:3mm U HAD:3mm U		EM:3mm U HAD:6mm U	
CAL	Cd+Cstray+Cconn+Cf	pf	Cd+Cstray+Cconn+Cf	pf
EM1	(200+90+60+100)	450	(200+90+60+100)	450
EM2	(70+60+80+100)	310	(70+60+80+100)	310
EM3	(370+150+110+100)	730	(370+150+110+100)	730
		nf		nf
HD1	(1470+500+300+100)	2.3	(740+250+150+100)	1.2
HD1'				
HD2	(2040+600+300+100)	3.0	(1020+300+150+100)	1.6
HD2'				
HD3	(3060+730+300+100)	4.1	(1530+470+150+100)	2.3
HD3'				
HD4	(4050+830+300+100)	5.2	(2030+420+150+100)	2.7
HD4'				

CAL	EM:3mm U noise match	EM:3mm U noise unmat	HAD:3mm U noise 3:1	EM:3mm U noise match	EM:3mm U noise unmat	HAD:6mm U noise 3:1
EM1	35	85		35	85	
EM2	30	60		30	60	
EM3	45	135		45	135	
HD1	80	430	50	110	430	45
HD2	90	560	60	125	560	60
HD3	110	770	85	150	770	85
HD4	120	970	110	160	950	105

T=300K Rs=30ohm e/mu=0.5 Ca=20pf tpeak=50ns

EM:3mm U HAD:3mm U

CAL	C(nf) 1:1	max resist	max length	C(nf) 1:3	max resist	max length
EM1	0.45	55	3.7m		55	3.7m
EM2	0.31	80	3.7m		80	3.7m
EM3	0.73	34	3.7m		34	3.7m
HD1	2.3	11 ohm	3.7m	0.26	96 ohm	3.7m
HD2	3.0	8	3.7m	0.33	76	3.7m
HD3	4.1	6	3.7m	0.46	55	3.7m
HD4	5.2	5	3.7m	0.58	43	3.7m

cable = 50 ohm (135pf/m) RC<25nsec L->doubles capacitance

LEVI - 4

CALORIMETER SIGNAL DECONVOLUTION

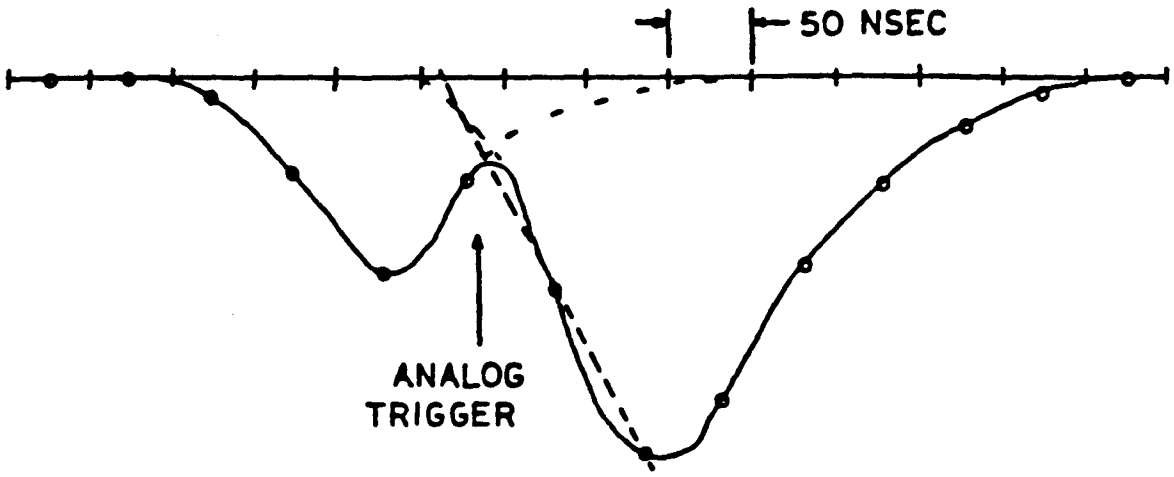

CONSIDERATIONS FOR SCINTILATION CALORIMETERS

READOUT TECHNIQUE: PMT'S VS. ALTERNATIVES
- INSIDE VS. OUTSIDE MAGNETIC FIELD
- DYNAMIC RANGE
- SPEED OF RESPONSE & SIGNAL-TO-NOISE

SIGNAL PROCESSING FOR UNIFORM RESPONSE
- ARRIVAL TIME OF LIGHT VARIES BY ABOUT 30 nsec

SIGNAL PROCESSING FOR LONGITUDINAL DEPOSITION
- TO DISTINGUISH EM AND. HAD COMPONENTS

SIGNAL PROCESSING FOR BUNCH IDENTIFICATION

CALIBRATION, incl. OF DEGRADATION OF $\lambda_{ATTENUATION}$

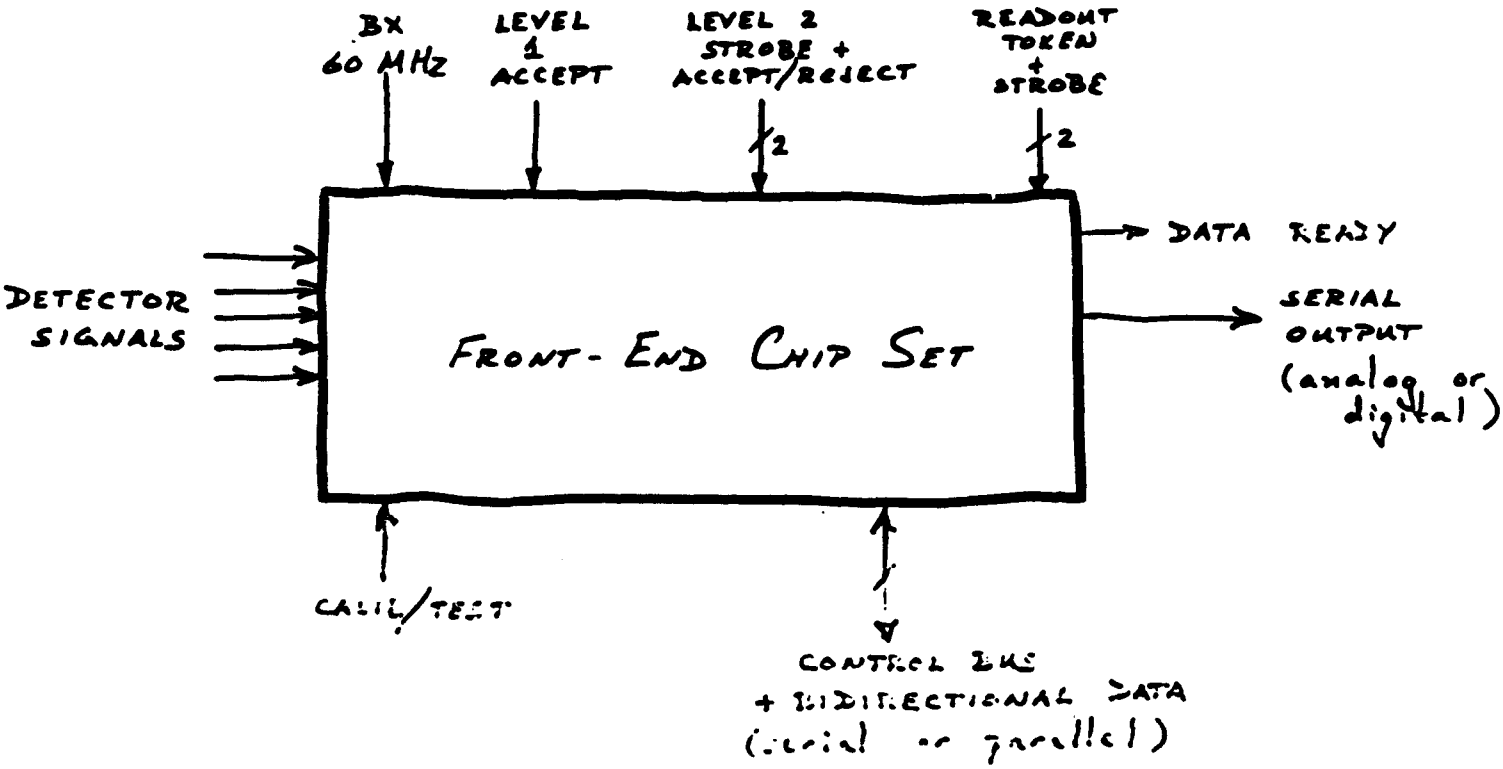

A LOGICAL "GROUP" OF CHANNELS WILL BE CONTROLLED BY CUSTOM VLSI.

THE GROUP MAY LOOK VERY MUCH THE SAME AS THIS TO THE HIGHER LEVEL OF CONTROL.

NOTE THAT THERE IS A NON-NEGLIGIBLE AMOUNT OF POWER IN CLOCK DRIVERS.

SLAC
LAC PREAMP
SLAC
LAC PREAMP
SLAC
LAC PREAMP

Cooling Costs

Power Density (w/in^2) Av.	Max.	Cooling Method	Cost	Repair or Design
.2	.4	convection	$0	easy
.4	.8	forced air	$250 + $200/kw	↓
1.0	1.5	forced air w/ H.S.	add $2 per pkg	↓
4.0	5.0	custom forced air	$750 + $500/kw	↓
4.0+	5.0+	liquid	$2000 + $1500/kw	difficult

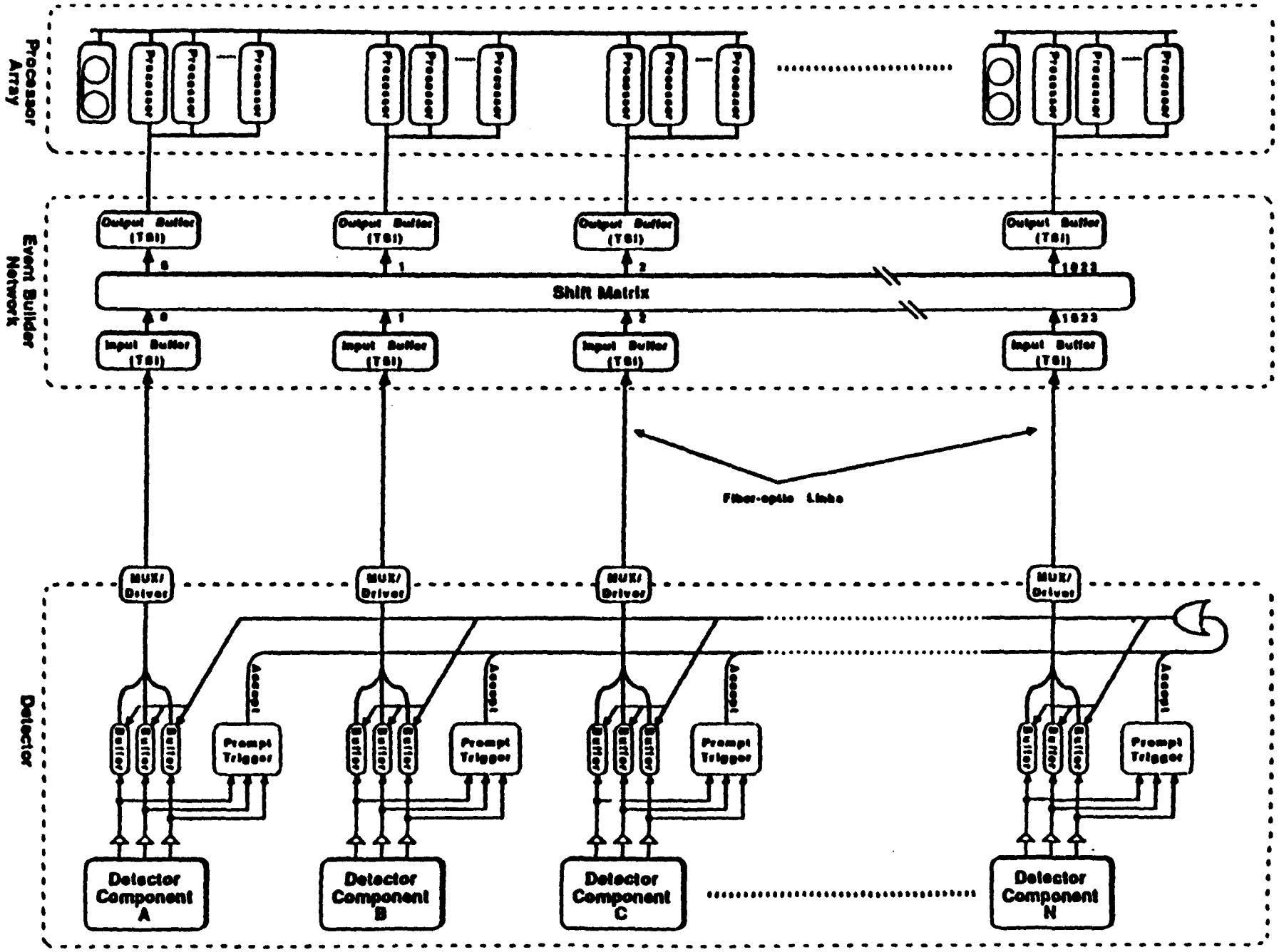

Generalized System Architecture

DATA COLLECTION

SEVERAL HUNDRED THOUSAND f.e. IC'S PROVIDING DATA
(100's - KHz each)

MULTIPLEXED ONTO A MANAGEABLE NUMBER (100 - 1000)

HIGH-SPEED DATA CHANNELS

w/ AGGREGATE DATA RATE few - 100 GBps

HIERARCHICAL SOLUTION

NEARBY DATA CHANNELS

↓

LARGE GROUPINGS (e.g. REGION of SOLID ANGLE)

ALL ON THE DETECTOR

DATA DRIVEN

DATA SOURCE PUSHES DATA INTO INTERMEDIATE BUFFER

DATA COLLECTORS GATHER DATA AT HIGHEST POSSIBLE RATE AND PUSH IT ACROSS LINK TO NEXT STAGE OF BUFFERS.

Possible Data Path From The Detector

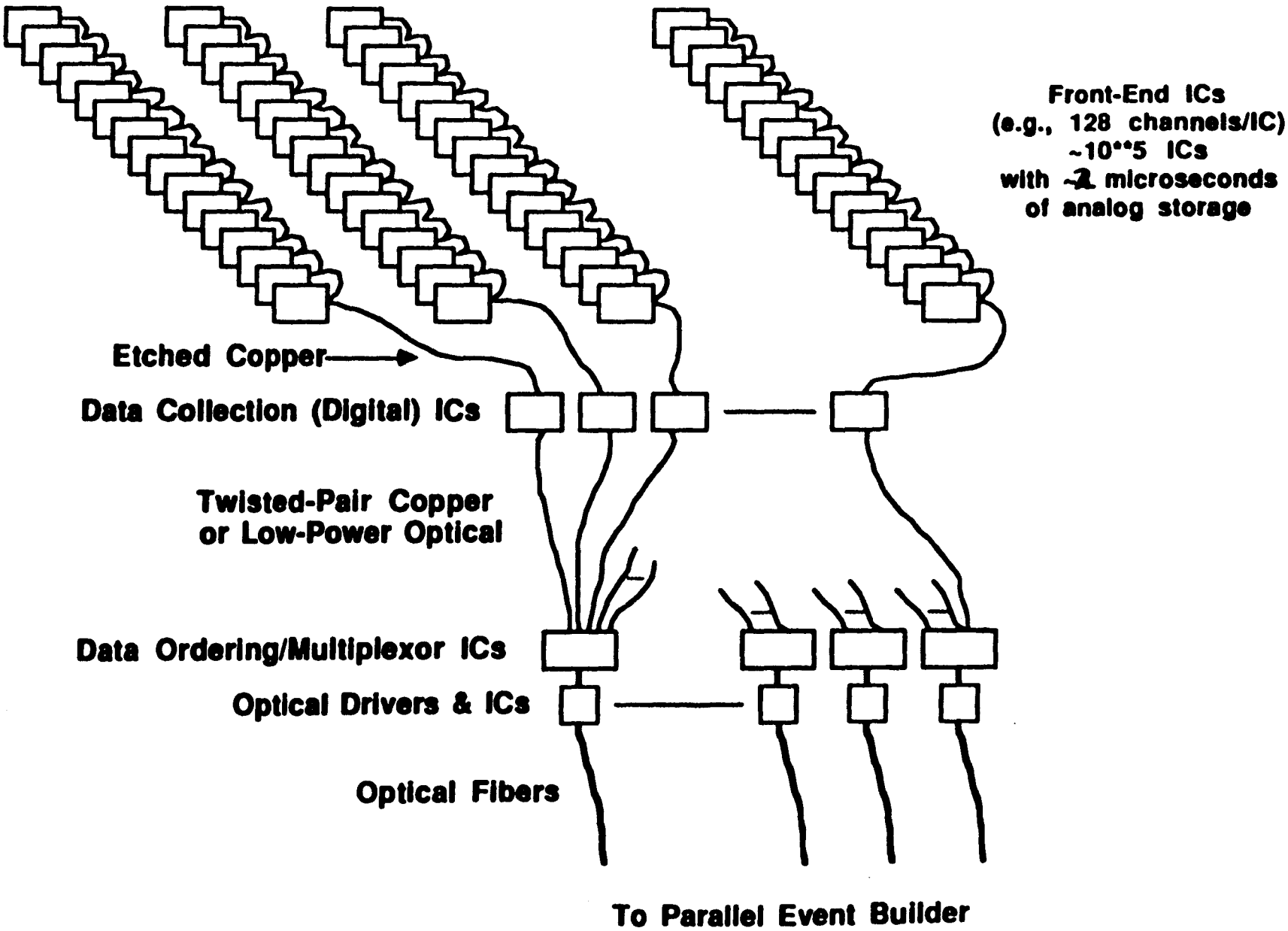

DATA-DRIVEN DATA COLLECTION

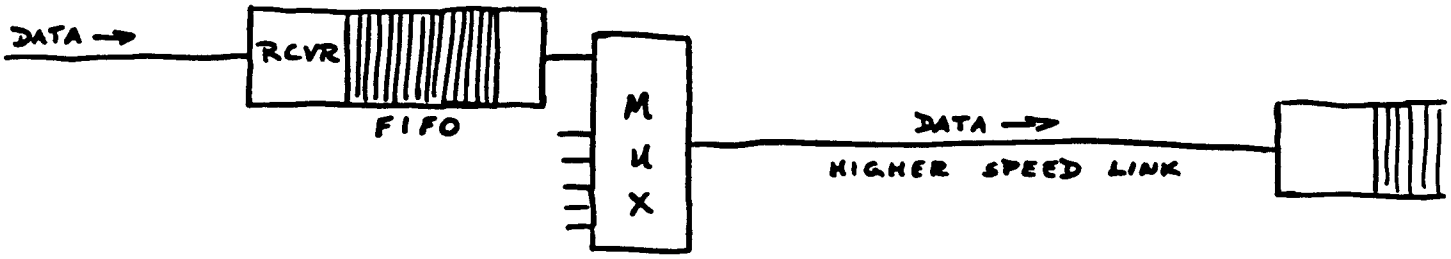

BANDWIDTH OF EACH LINK USED TO FULL EFFICIENCY.

DATA TAGGED BY EVENT + CHANNEL.

DATA PACKET ≠ EVENT.

EVENT BUILDING DECOUPLED FROM COLLECTION/XMISSION

CONTROL IS MINIMIZED.

STRAIGHT-FORWARD VERIFICATION AND DIAGNOSIS OF COMMUNICATION LINKS.

AMENABLE TO EXPERT SYSTEMS

DATA TRANSMISSION

BACK TO COLLECTION Xparency

TECHNOLOGY APPROPRIATE TO REQUIRED BANDWIDTH AT EACH LEVEL.

COPPER BUSSES ON PC NEAR DETECTOR
HIGH-SPEED FIBRE OPTICS TO EVENT BUILDER
TRANSITION: HIGH-SPEED Cu → MODEST SPEED F/O

ADVANTAGES OF FIBER

esp: bandwidth

small volume and mass within detector

rad hard (MegaRad, self annealed)
Gallium Arsenide

NEEDS OF COMPUTER INDUSTRY DRIVING COSTS DOWN
for links of the sort needed
AND PERFORMANCE UP

COST

PERFORMANCE NOW
→ 100 M~~Bits~~ bits/sec link (TAXI)

CABLE SIZE: NOW + THEN BOTH SMALL

MORE THAN JUST THE F/O LINK

ENCODERS - DECODERS TAXI (AMD)

GaAs DEVELOPMENTS INTEGRATED PHOTODIODES RECEIVERS DESERIALIZATION SERIALIZATION DRIVERS HYBRID LASERS MULTI-CHANN SWI

⇒ 1-2 Gigabit/sec for SSC

OPTICAL FIBER DATA TRANSMISSION

MAJOR ADVANTAGES:

- IMMUNITY TO ELECTROMAGNETIC INTERFERENCE
- LOW TRANSMISSION LOSSES FOR VERY HIGH DATA RATES
- THINNER AND LIGHTER CABLES
- CAPABILITIES EXTENDING TO GIGAHERTZ REGION

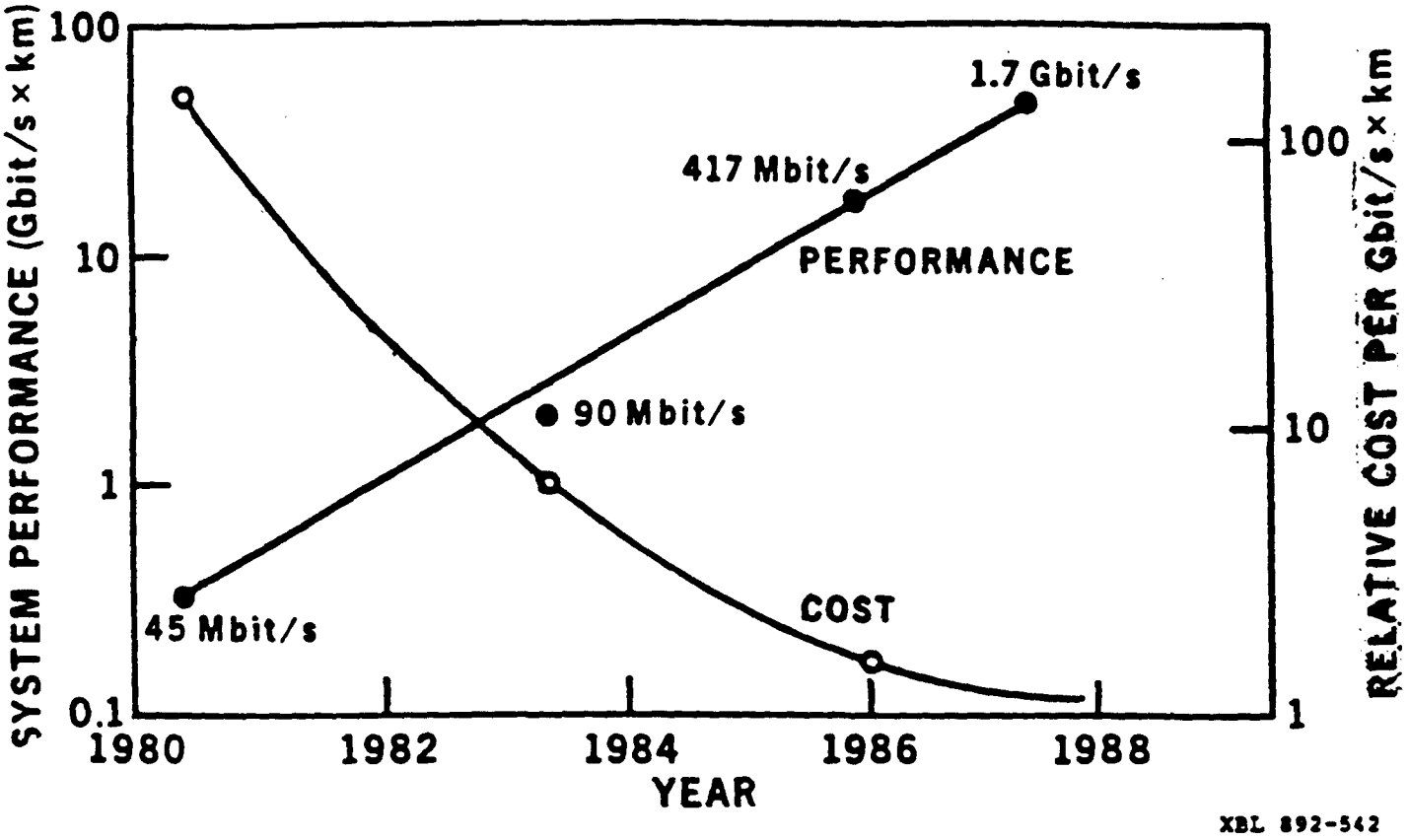

PERFORMANCE AND COST OF FIBER OPTICS DATA TRANSMISSION SYSTEMS

$/Mb/Sec as a Function of Data Rate

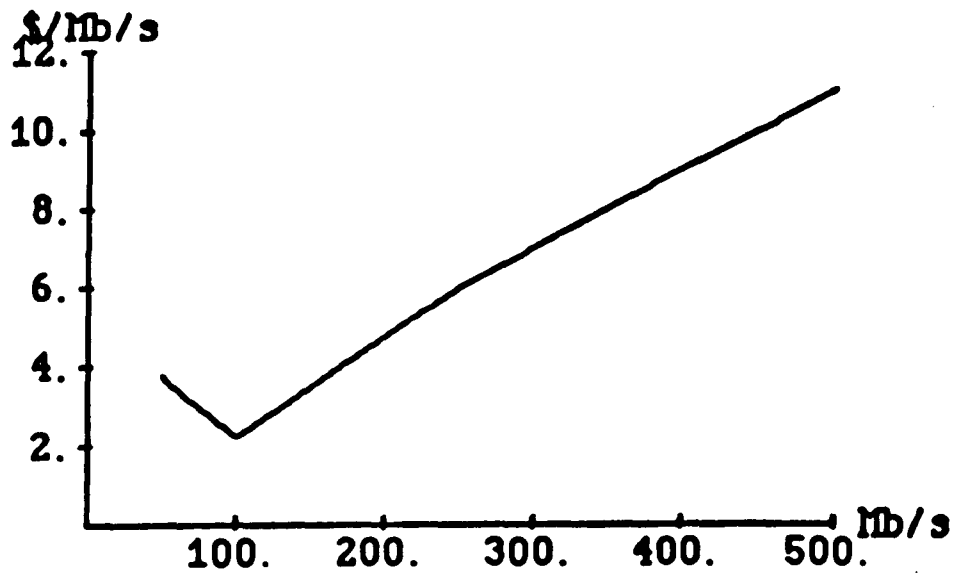

CABLE BUNDLES SHOWN 1/2 ACTUAL SIZE

SSC

5×10^7 CHANNELS
128 CHANNELS/FEIC
16 FEIC/DCC

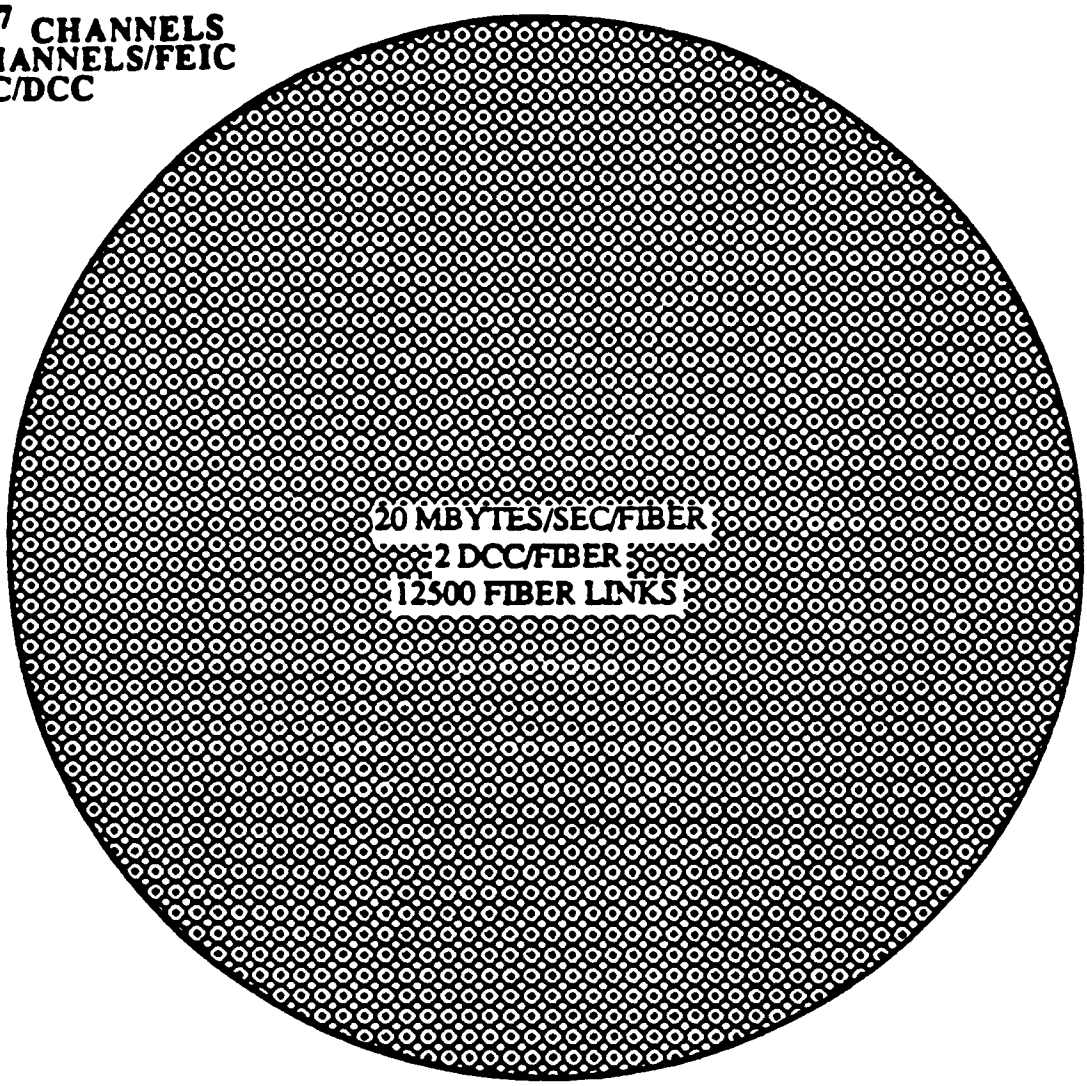

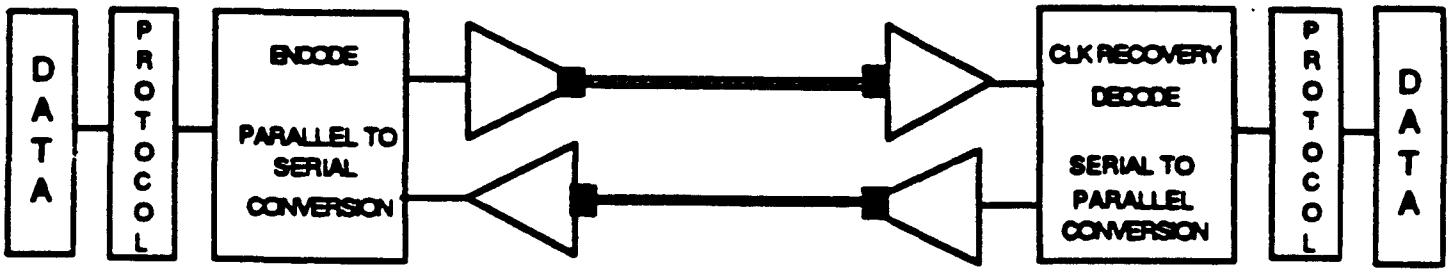
DATA
PROTOCOL
ENCODE
PARALLEL TO SERIAL CONVERSION
CLK RECOVERY
DECODE
SERIAL TO PARALLEL CONVERSION
PROTOCOL
DATA

Design Tradeoffs for 4π Detectors

H. H. Williams
University of Pennsylvania

To B or not to B, that is the question.
Whether to suffer the slings & arrows
Of outrageous field strength
Or to take arms against a sea of troubles
And by opposing end them.

Some Benchmark Experiments

- Heavy t quark (~140 GeV) or 4th generation quark
- Heavy Higgs with $H \rightarrow ZZ \rightarrow \ell^+\ell^-\ell^+\ell^-$
- Heavy Higgs with $H \rightarrow ZZ \rightarrow \ell^+\ell^-\nu\bar{\nu}$
- Heavy Higgs with $H \rightarrow ZZ \rightarrow \ell^+\ell^-q\bar{q}$
- Isolated photons
- Heavy quarks (b,t) $\rightarrow$ leptons

  (as a study of backgrounds to other processes)
- W', Z'
- Compositeness
- Strongly Interacting Bosons W^+W^+, W^-W
- Dynamical Symm Breaking (Techniquarks?)
- Supersymmetry

Primary Goal : Detect and Identify

* electrons
* muons
* neutrinos (missing E_t)
* quarks
* gluons
* W, Z bosons

What about detecting the "Unexpected"?

Presumably new particles couple to those which we already know about

Detector Requirements

Rapidity Coverage

* Electrons $|y| < 3$ (± 0.5)
* Muons $|y| < 3$
* Calorimeter $|y| < 4.5-5.5$ (missing E_t)
* Jets $|y| < 3-4$ (for signal)

Tracking (some tracking is required)

* Electron ID
* Separation of multiple interactions
* Matching electrons, muons, jets to vertex
* Rejection of photon conversions

Detector Requirements

* Rapidity Coverage
* Tracking
* Lepton Identification
* Energy Resolution

Lepton Identification

Goal: Inclusive lepton triggers $P_t > 15-20$ GeV should have little bgnd

UA1, CDF, UA2 already achieve this

e.g. CDF identifies B's, $p_t > 12$ GeV/c w little bgnd

Gluons are important in production process

For $P_t > 20$ GeV, lepton rate is predominantly W, Z (whether jets required or not)

Brash Claim:

magnetic · nonmagnetic

Energy Resolution

* Jets

  Compensated, hermetic, & adequately segmented calorimeter for good $\sigma(E_t)$ & $\sigma(\not{E}_t)$

  $50\%/\sqrt{E} \Rightarrow$ [illegible]

* Muons – Large $\int B dl$ required

  Iron toroids $\Rightarrow$ [illegible] good enough?

  Air core outside calor. $\Rightarrow$ $\sigma_{p/p} \approx (0.04 - 0.15) \times p$ [illegible]

  Field inside calor. $\Rightarrow$ $\sigma_{p/p} \approx 0.26 \times p$ [illegible]

* Electrons

  Calorim. energy resolution 1–2%

  Need field for charge meas.

Simultaneously achieving excellent energy resolution for e, μ, jet is hardest problem

Compromises necessary $\Rightarrow$ physics priorities

Options on the Table

) Precision Muon Detector

Compact calorim with large, external, air core magne

excellent muon resolution

compromised calorimetry ?

no electron charge

few additional options

"Non-magnetic" detector

Med-large calorimeter + good external muon system

moderate muon resolution

excellent calorimetry

no electron charge

limited additional options

"Magnetic" detector

Med-large calorimeter, reasonable ext muon system, field surrounding intersection region

moderate muon resolution

good calorimetry

electron charge

many additional options

(1) & (2) accomplish most of "Primary Goals"

But is that enough?

poor reasons

"nonmagnetic det. will have good c[illegible] few cracks"

good reasons

effectiveness not predictable

strong reasons

Why Include a Magnetic Field?

* Electron Identification (E/p)
* Correction for Cracks
* Calorimeter calibration

* Secondary Vertices
* Tau's
* Invariant Mass
* P_t of tracks, fragmentation

* Electron charge
* Improved muon momentum resolution
* Redundant energy measurement
* Credibility, Flexibility, for New Physics

Credibility, Flexibility for New Physics

Is it sufficient to "just" measure leptons & jet energies?

Probably NOT.

consider UA2, CDF, D0, UA1 – will find top but...
To identify Top <u>cleanly</u> want
better calorimetry & tagging of b

What If?

One produces charged particles with $\sigma_{inel} \approx 1$ mb?
Calorimeter then of little use for energy meas

Why Not Have a Magnetic Field?

What does it Cost?

* Dollars (Swiss Francs, Yen, etc) not so important
* Primarily it conflicts with Calorimeter
* Number of other headaches which are probably manageable (i.e increased drift time in chambers)

Can excellent calorimetry and sufficient BL^2 coexist?

what is "excellent calorimetry"

what is "sufficient BL^2"

note that many of the benefits of magnetic field e.g.

E/p, secondary vertices, charge to 100-200 GeV/c

follow from relatively low fields

Reactions which Drive Momentum Resolution

* $H \rightarrow Z\,Z \rightarrow ee\;ee$

  $ee\;\mu\mu$

  $\mu\mu\;\mu\mu$

* $Z' \rightarrow \mu\mu$

* Charge Determination

  Strongly Interacting Bosons W^+W^+, W^-W^-

  New Heavy Quarks

  ⋮

Effect of Resolution on $H \to ZZ \to \ell^+\ell^- \ell^+\ell^-$

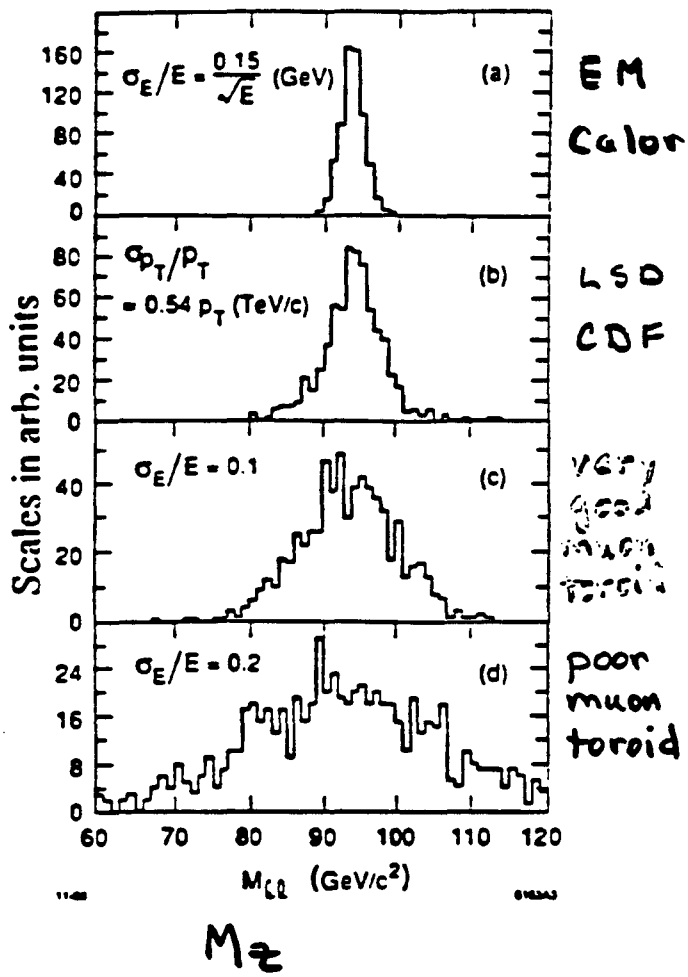

FIG 7 Di-lepton invariant mass distributions for various energy or momentum resolutions for leptons from Higgs bosons of 400 GeV/c^2 mass decaying into $ZZ \to 4\ell^\pm$.

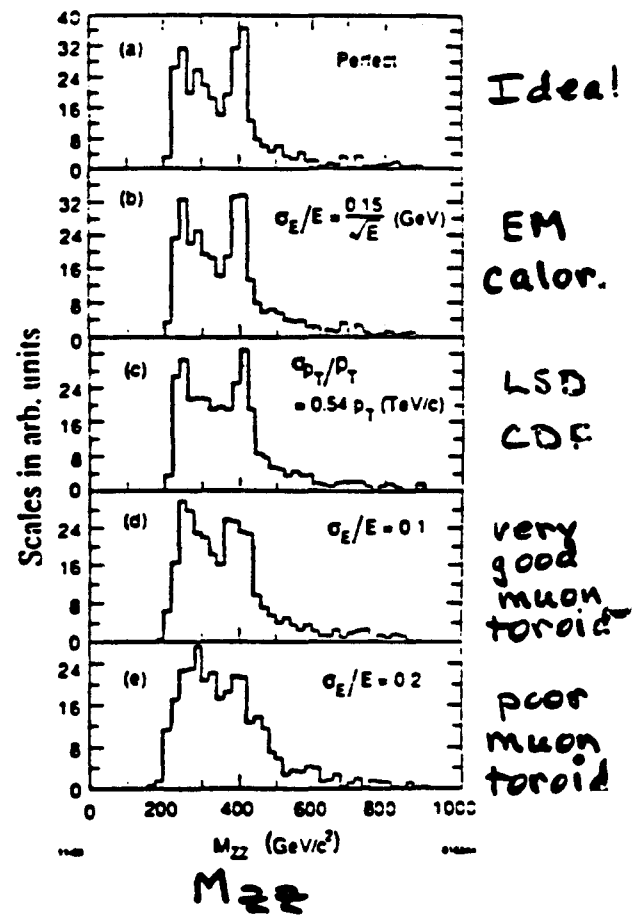

FIG 8 Z-pair mass distributions for various energy or momentum resolutions for $H \to ZZ \to 4\ell^\pm$ for $M_H = 400$ GeV/c^2, along with the background from continuum ZZ production

WANG + HANSON

SNOWMASS 88

NB:

For ee ee, ee $\mu\mu$ ∞ little or no pairing and Z mass constraint should help

The central and intermediate tracking systems are shown in Fig. 8. The momentum resolution as a function of polar angle and rapidity is shown in Fig. 9.

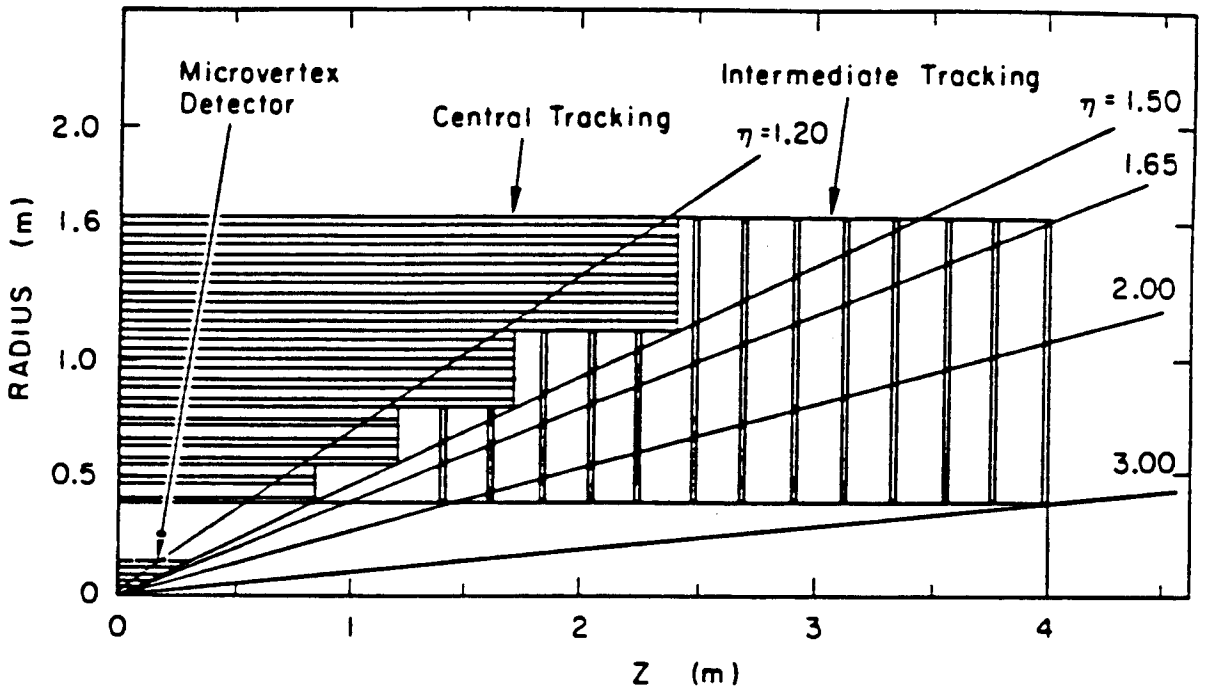

Fig. 8. Schematic view of central and intermediate tracking systems in the Large Solenoid Detector.

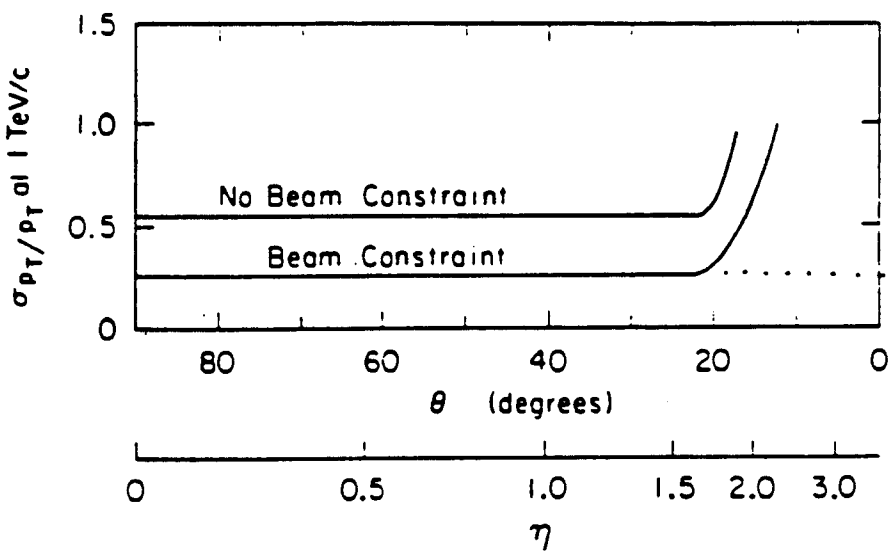

this with 1 Tesla gives performance on previous page

Fig. 9. Momentum resolution as a function of polar angle and rapidity in the Large Solenoid Detector for the 13 superlayers at radii > 50 cm in the central tracking system and intermediate tracking Option A.

p_t distribution for e, μ from $H \to ZZ$

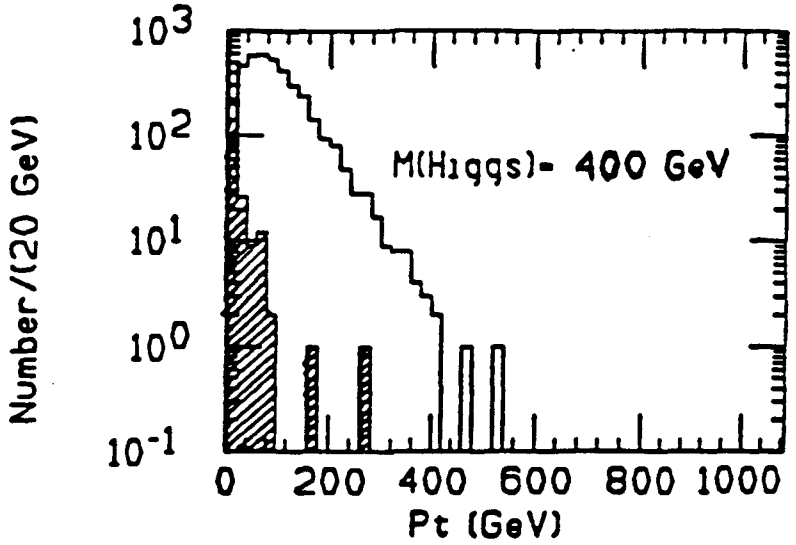

8.2 The P_T distribution of electrons in Higgs events for $M_H = 400$ GeV. The hatched bins indicate the contribution from non-Z sources in Higgs events.

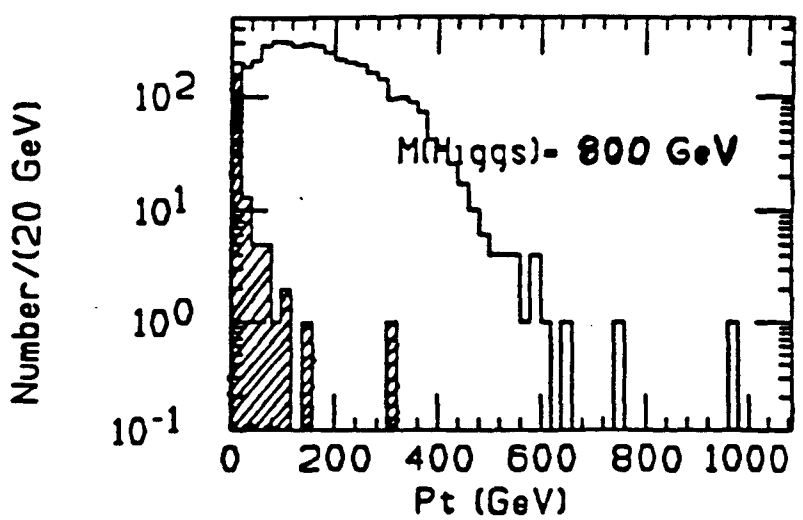

note log scale
p_t's relatively low.

8.3 Same as 8.2 but for $M_H = 800$ GeV.

FROM CAHN ET AL

BERKELEY 87

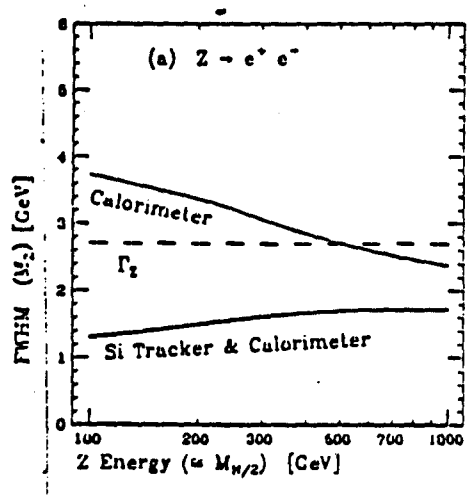

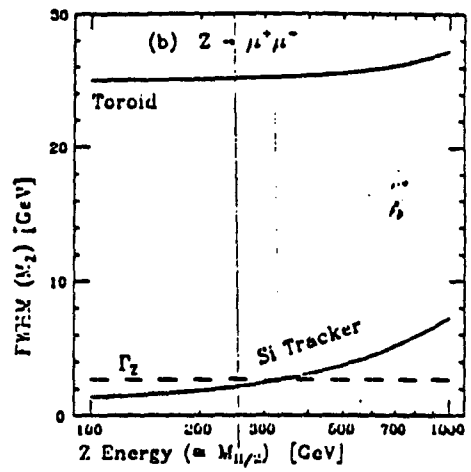

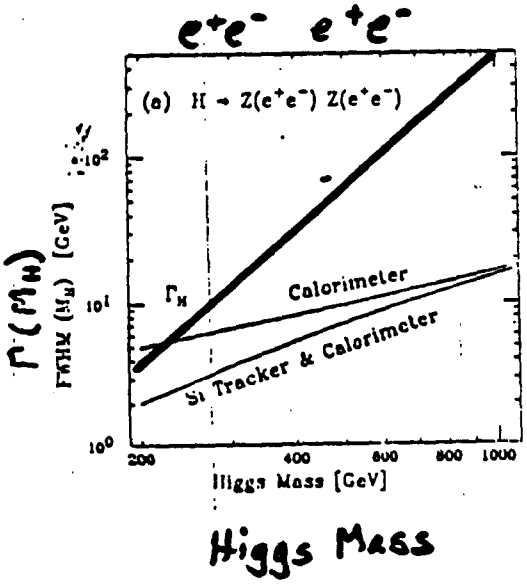

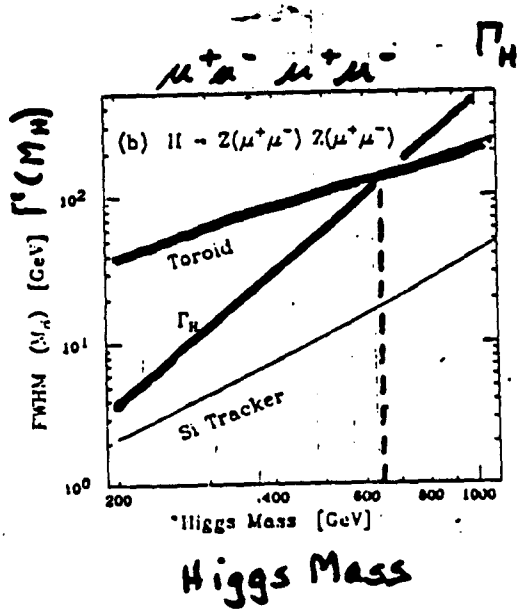

toroid resolution

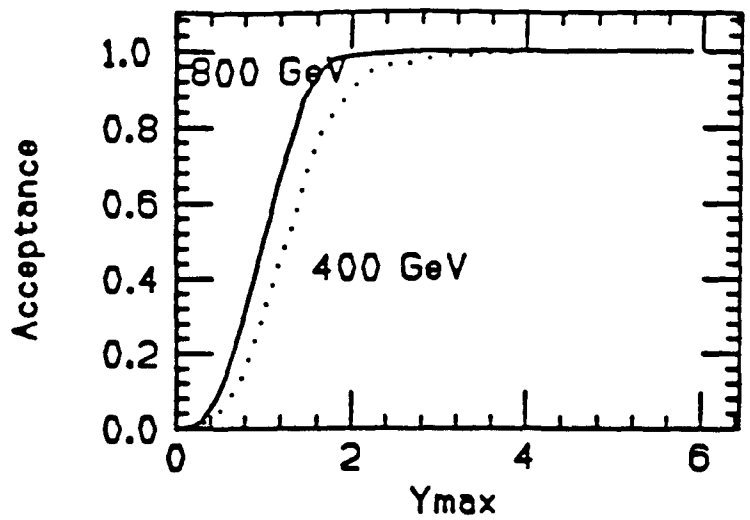

4 lepton accept. vs rapidity coverage

8.1 The four-lepton acceptance vs lepton rapidity coverage.

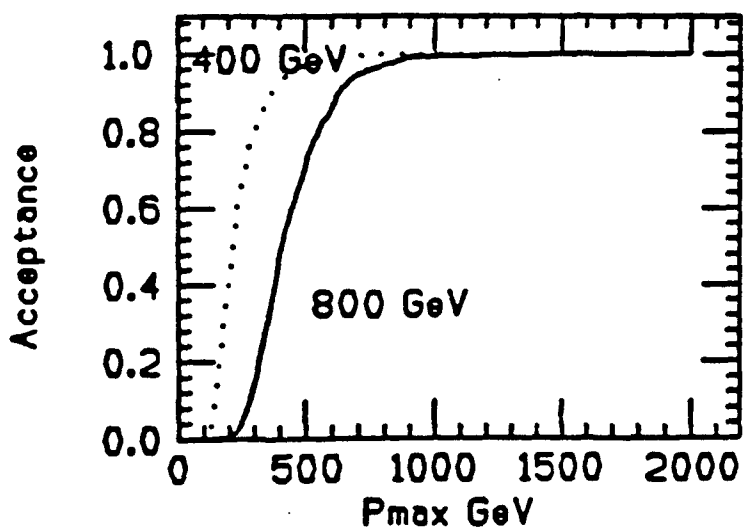

4 lepton accept. vs. total p of most energetic lepton

8.4 The four-lepton acceptance vs the total momentum of the most energetic lepton.

FROM CAHN ET AL.

BERKELEY 87

Summary for $H \to ZZ$

1/4 $ee\,ee$ - no problem, resolution excellent

1/4 $ee\,\mu\mu$ - good toroid system ($\sigma_{p/p} \sim 0.1-0.15$) or LSD tracking should give sufficient resolution

1/4 $\mu\mu\,\mu\mu$ - will degrade the fastest because of pairing ambiguities as well as resolution
could consider "giving up" on this channel

$Z' \to \ell^+\ell^-$

* electrons have inherently much better resolution than muons
* signature (mass bump) is clean, robust, & unambiguous
* including μ's adds at most $\times 2$ in rate, less in significance

$\Rightarrow$ just rely on electrons ?

Strong symmetry breaking

will see enhancement in WW

Presence of W^+W^+, W^-W^- as well as W^+W^-

Potentially very important channel

Note that events will be $1/4$ ee
$2/4$ $e\mu$
$1/4$ $\mu\mu$

This plus cleanliness of $e\mu$
$\Rightarrow$ electron charge very important

W^+W^+ final state

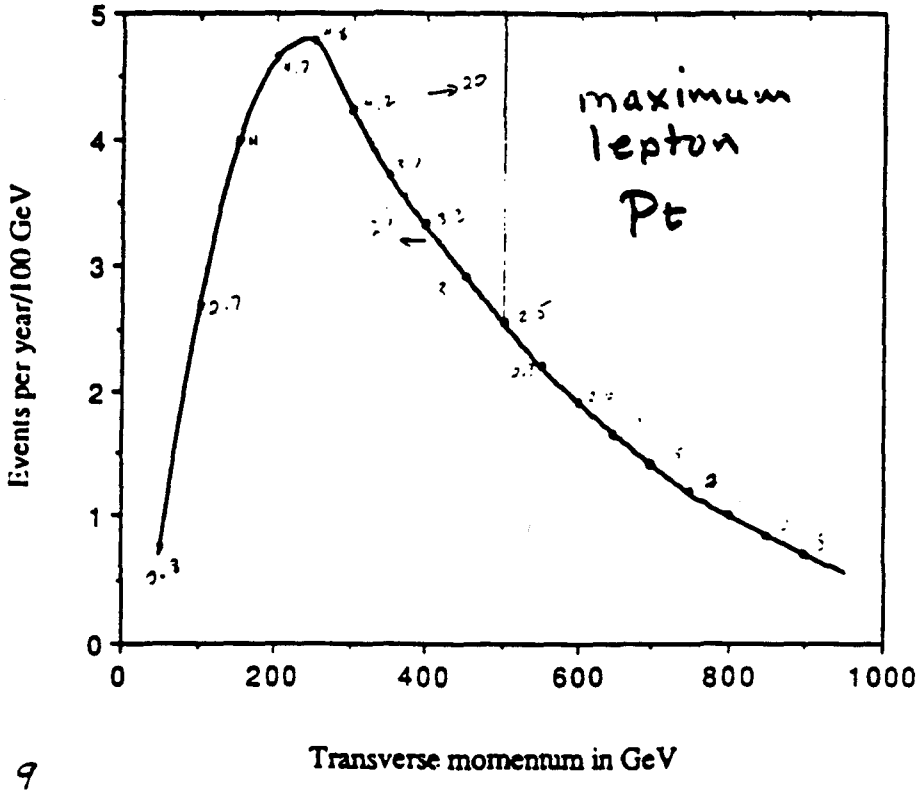

Fig 9

The P_T distribution of the lepton with the larger P_T from W^+W^+ events for $|y_W| < 1.5$ and $m_{WW} > 0.5$ TeV as predicted by the model of Chanowitz and Gaillard (Ref. 4).

Lepton P_t Spectra for some other channels.

Leptons from gluino decay

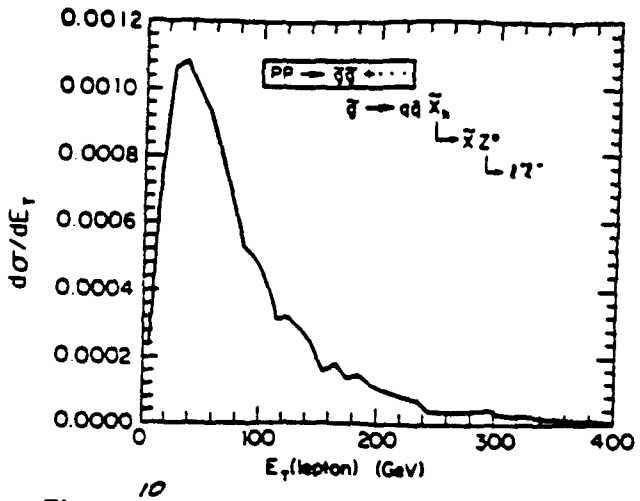

Figure 10 The E_T spectrum of leptons in gluino decay

$Q\bar{Q}$ 500 GeV

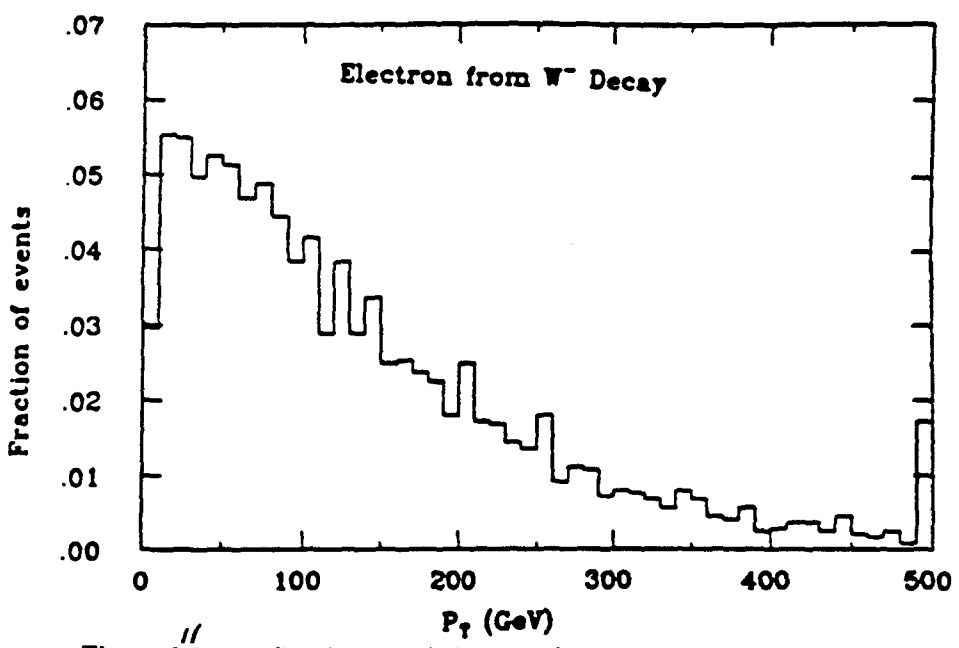

Figure 11. P_T distribution of electrons from $W^- \to e^-\bar{\nu}$ in decays of the D quark at $\sqrt{s}$ = 40 TeV for M_t = 70 GeV and M_D = 500 GeV from ISAJET.

nearly hopeless ?

hermeticity !

Reactions Which Drive Calorimeter Resolution

* $H \to W\,W$, $W \to q\bar{q}$, $W \to \ell\nu$ (probably swamped by $t\bar{t}$)

* $H \to Z\,Z$, $Z \to q\bar{q}$, $Z \to \ell^+\ell^-$

* $t\,\bar{t}$, $\bar{t} \to \bar{b}\,W$, $W \to q\bar{q}$, $t \to b\,W$, $W \to \ell\nu$

* Z', $W' \to q\bar{q}$

* Missing E_T

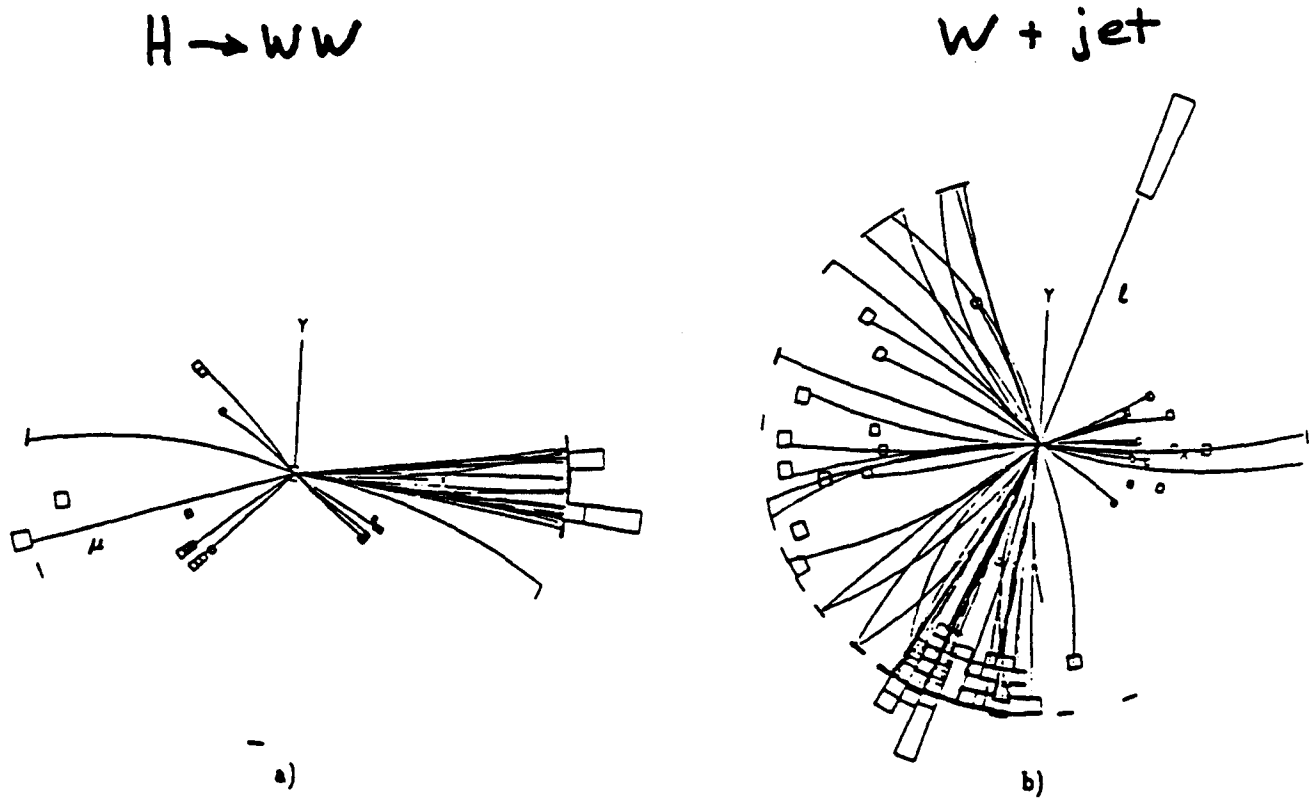

Fig. 1. Event display which shows charged tracks with $p_t \geq 0.5$ GeV and calorimeter cells with $E_t > 0.5$ GeV in $|Y| < 2.5$ together with the isolated lepton from the W decay. *a)* Higgs $\rightarrow W^+W^+$ event with $M_{WW} = 1230$ GeV, $N_{ch} = 33$ and $m_{jet} = 73$ GeV. *b)* Mixed EW-QCD event with invariant mass $M_{W_{jet}} = 1280$ GeV, $N_{ch} = 73$ and $m_{jet} = 82$ GeV.

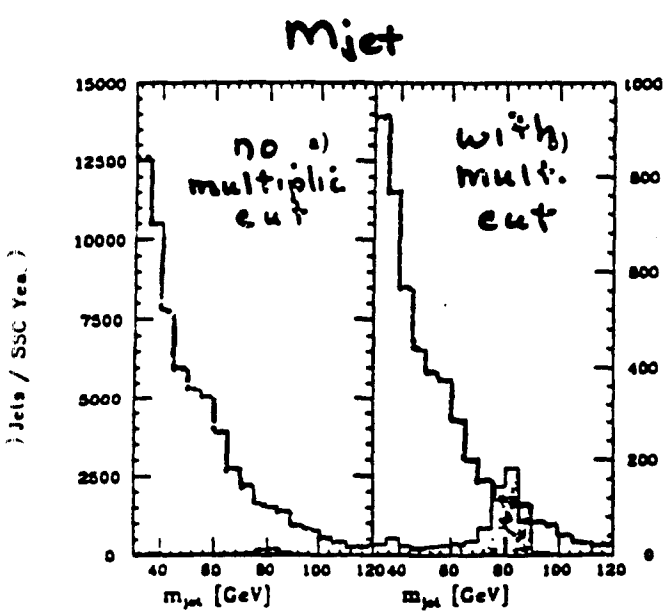

Fig. 2. Mass of jets m_{jet} with $R = 0.5$ and $E_t > 100$ GeV for Higgs (solid line) and $W+$ jet (dotted line) production: *a)* before multiplicity cut, *b)* after multiplicity cut.

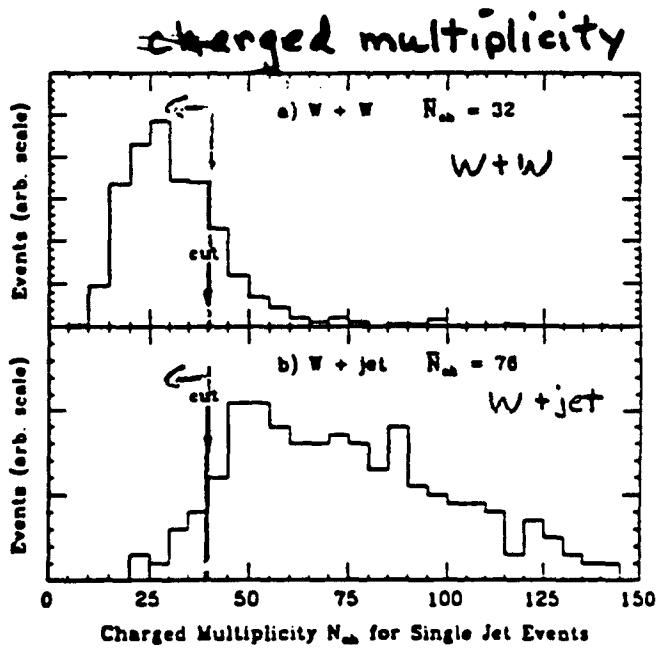

Fig. 3. Charged event multiplicity N_{ch} for tracks with $|Y| < 2.5$ and $p_t \leq 0.5$ GeV: *a)* Higgs $\rightarrow WW$, *b)* $W+$ jet.

SADROZINSKI ET AL.

More sophisticated anal.
finding 2 jets

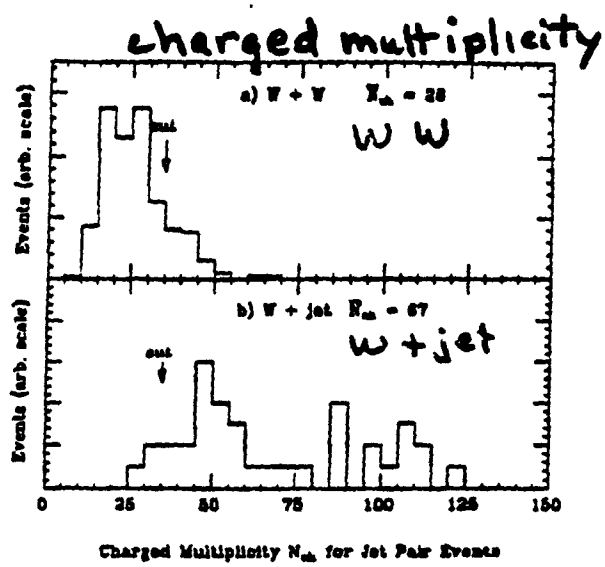

Fig. 6. Charged event multiplicity N_{ch} for events with a jet pair looking like a $W(m_{jet} \approx m_{jet,jet} \approx m_W)$: *a)* Higgs, *b)* mixed E.W.

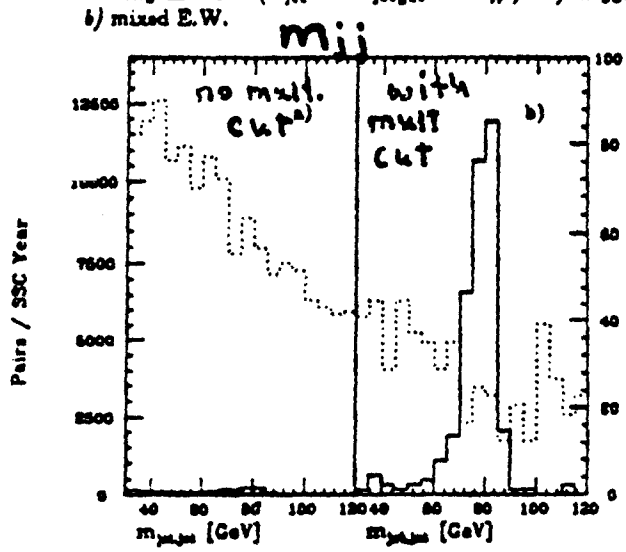

Fig. 7. Jet pair mass $m_{jet,jet}$ for the Higgs $\rightarrow WW$ decay (solid line) and mixed E.W. decay (dotted line). *a)* before cuts, *b)* after cuts (Table 2.).

$H \to WW \to \ell \nu q \bar{q}$ (problem of $t\bar{t}$?)

* considerable grounds for optimism
* more studies need (incl W + 2 jet)
* tracking plays very important role
* can imagine more sophisticated cuts on tracking

$H \to ZZ \to \ell^+ \ell^- q \bar{q}$

similar results as for WW
not swamped by $t\bar{t}$ background

← Heavy Quark $t\bar{t} \to bW\,\bar{b}W \to b\ell\nu\; b q\bar{q}$

$Q\bar{Q} \to tW\,\bar{t}W \to bWW\,\bar{b}WW$

signal to noise inherently much better

should be good chance for $W \to q\bar{q}$

— $\sigma = 8$ GeV
gaussian

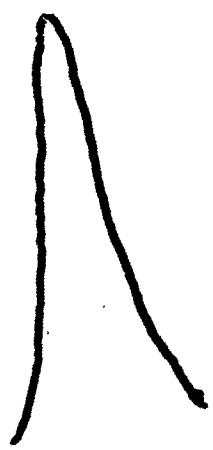

— 90 GeV ±I MC
±50% norm unc.
W width not quite right

$e + \geq 2$ jets $\quad E_t(e) > 20,\ \not{E}_t > 20,\ E_j > 10\,\mathrm{GeV}$
$M_t > 40\,\mathrm{GeV}$

Preliminary

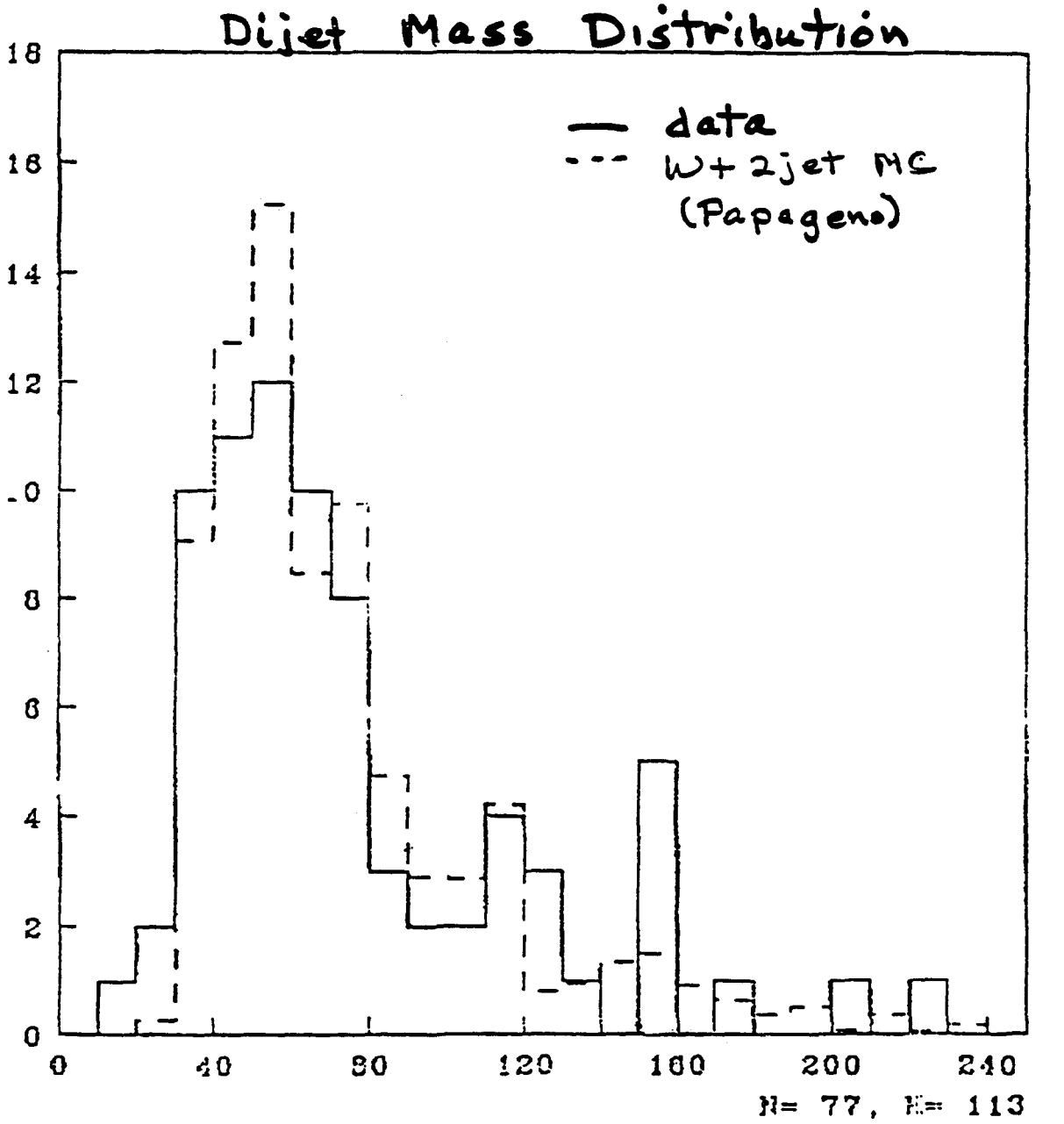

$M_{jet\,jet}$

$\sigma(M_W)$ for high p_T W's

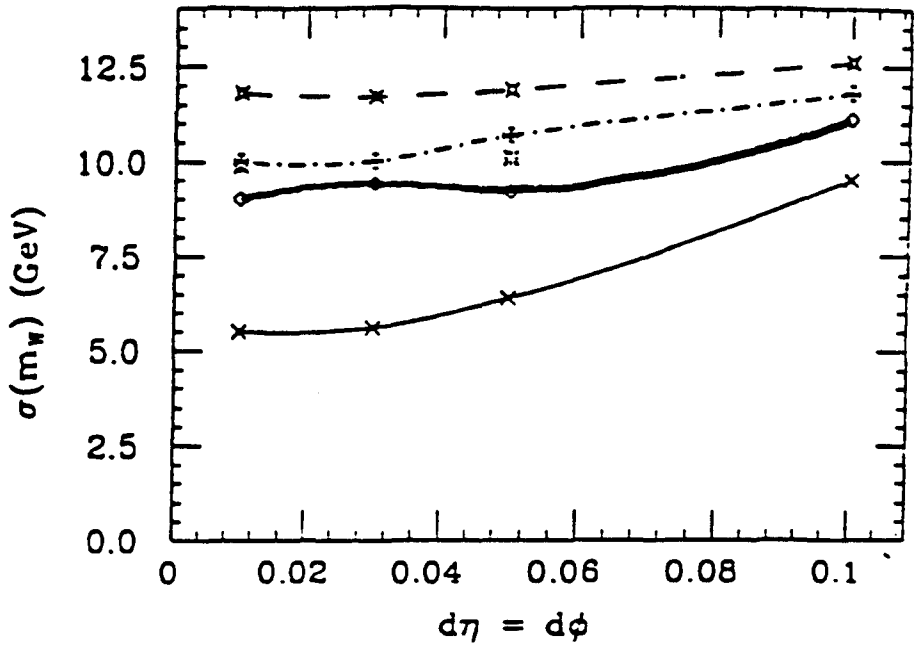

FIG. 16. The W mass resolution for different inner calorimeter radii and absorption lengths. For comparison, Case 1 is shown as solid, Case 3 as dots, Case 5 as dashes, Case 6 as dot-dashes and Case 7 as starburst points.

—— IDEAL DETECTOR

▬▬ $X_0 = 0.8$ cm $\lambda = 22$ cm
$R_{INNER} = 160$ cm

- - - - - SAME, BUT $R_{INNER} = 80$ cm

—·—·— $X_0 = 0.4$ cm, $\lambda = 12$ cm $R_{INNER} = 80$ cm

✳ 2 T FIELD ADDED TO .....

FROM BAY ET AL.

Warning to non-magnetic detector proponents...

Hamlet's solution to his quandary did not provide for a long future.

Summary $t\bar{t} \rightarrow bW\bar{b}W \rightarrow b\ell\nu\bar{b}q\bar{q}$

good calorimeter resolution +
tagging of b quark
(+ mult cuts for high p_T W's)

$\Downarrow$

clean ident. of $t\bar{t}$

Similar results should hold for heavier quarks.

Compact Solenoid Detector

B = 4T
L = 2m

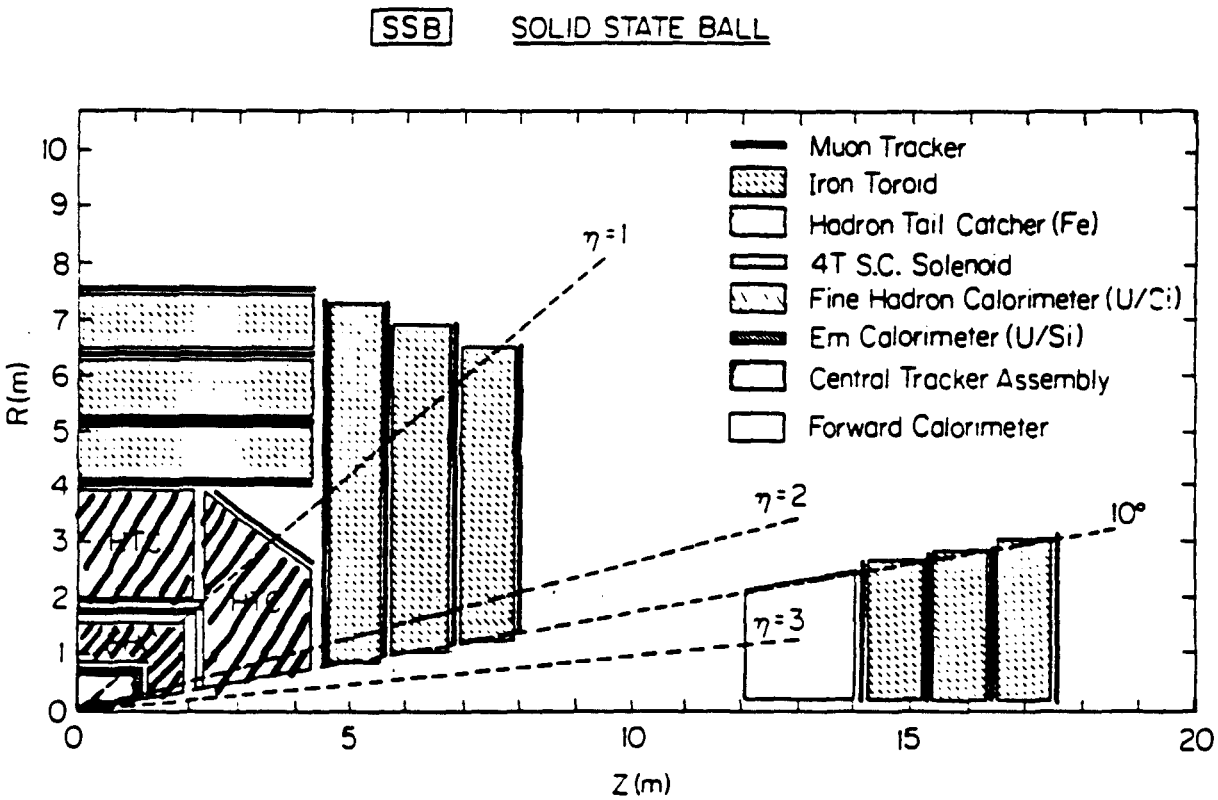

Figure 3.2 The SSB Compact Detector

SMART Solenoid Detector

B = 6T
L = 1 m

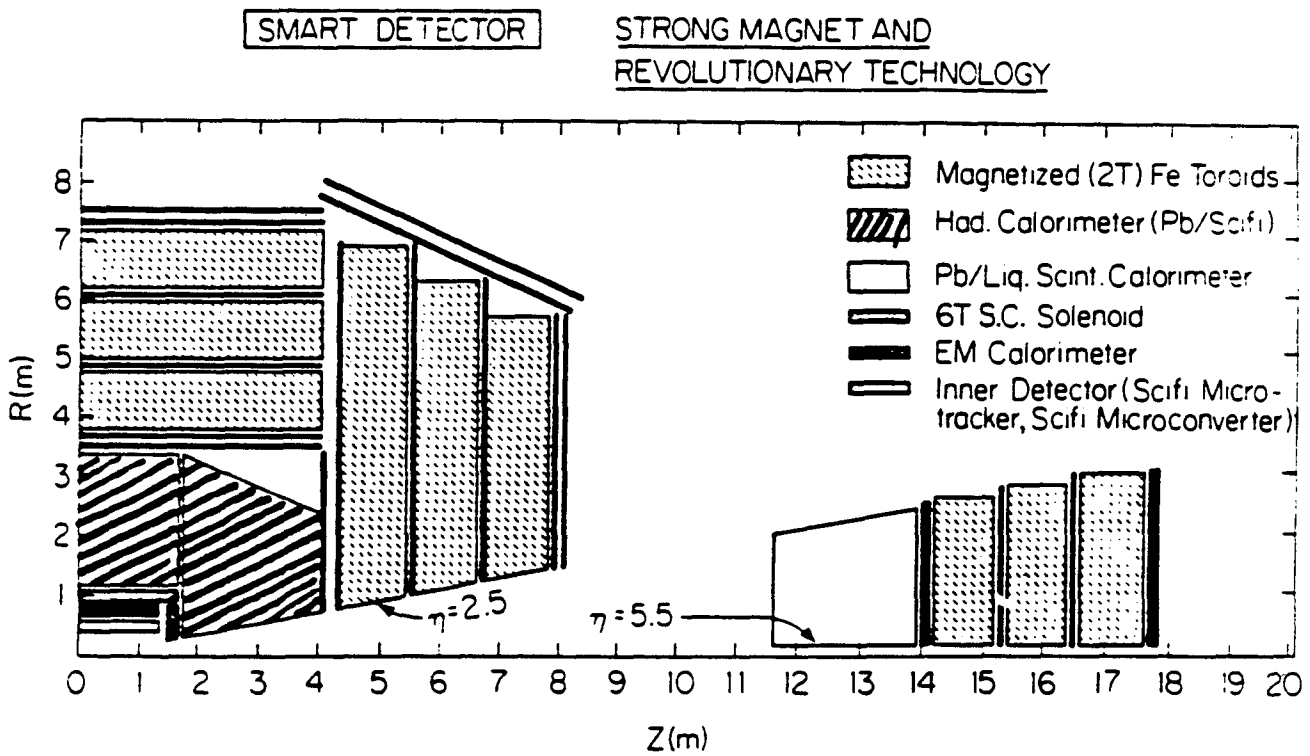

Figure 3.3 The SMART Compact Detector

B = 2 T
L = 4.5 m

LSD

[LARGE SOLENOID GEOMETRY]

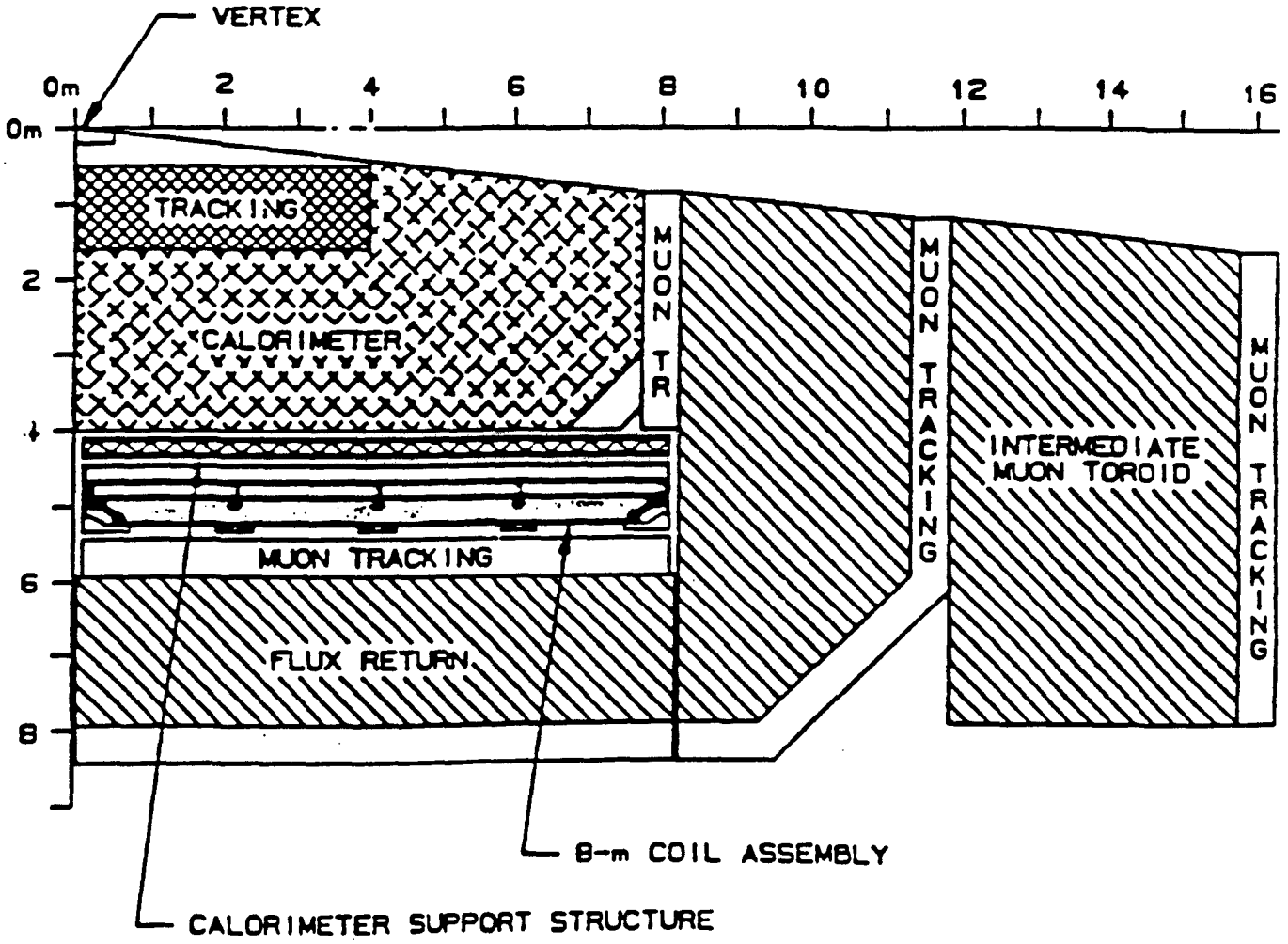

Fig. 1 SSC detector with large superconducting solenoid.

"Non-magnetic" Detector (with weak field?)

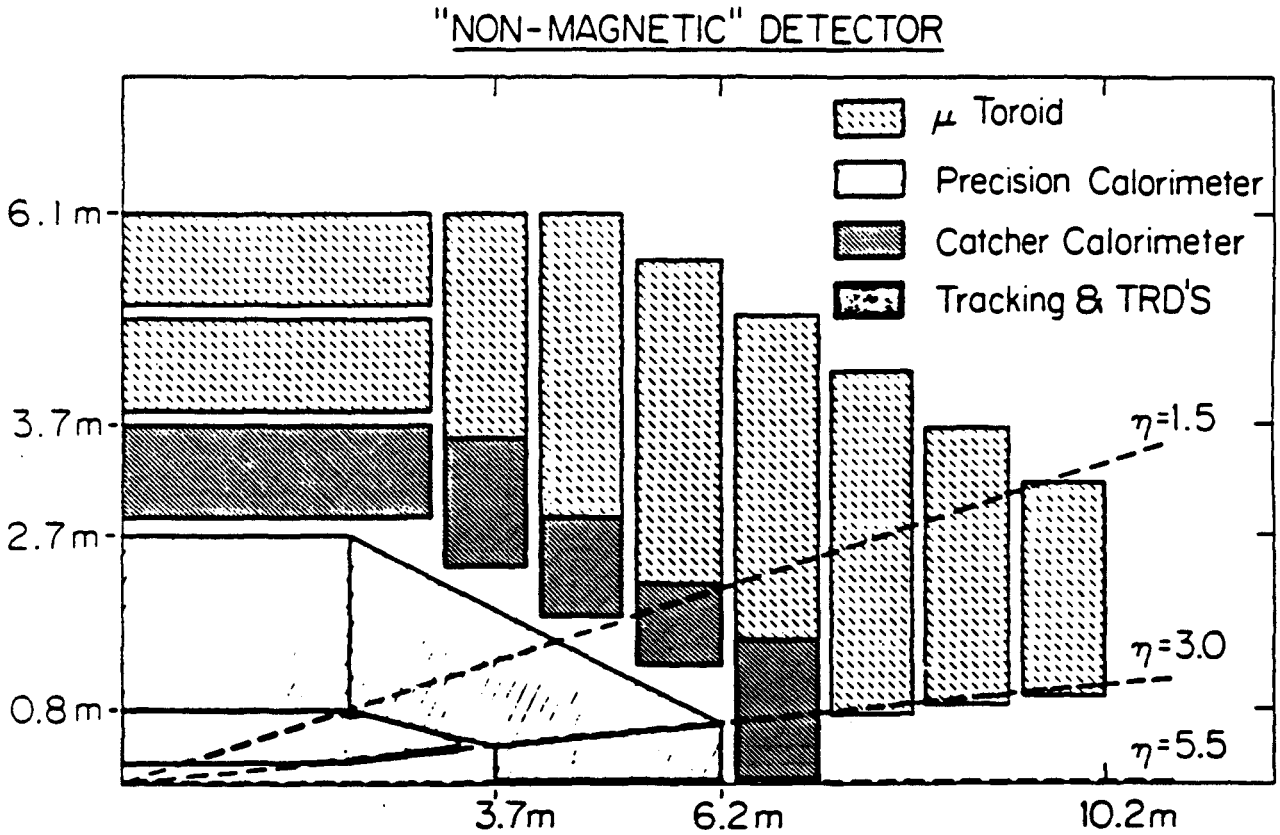

Figure 3.4 The Non-Magnetic Detector

JAPANESE DESIGN (T. KONDO)

[SMALL SOLENOID GEOMETRY]

B = 2 Tesla

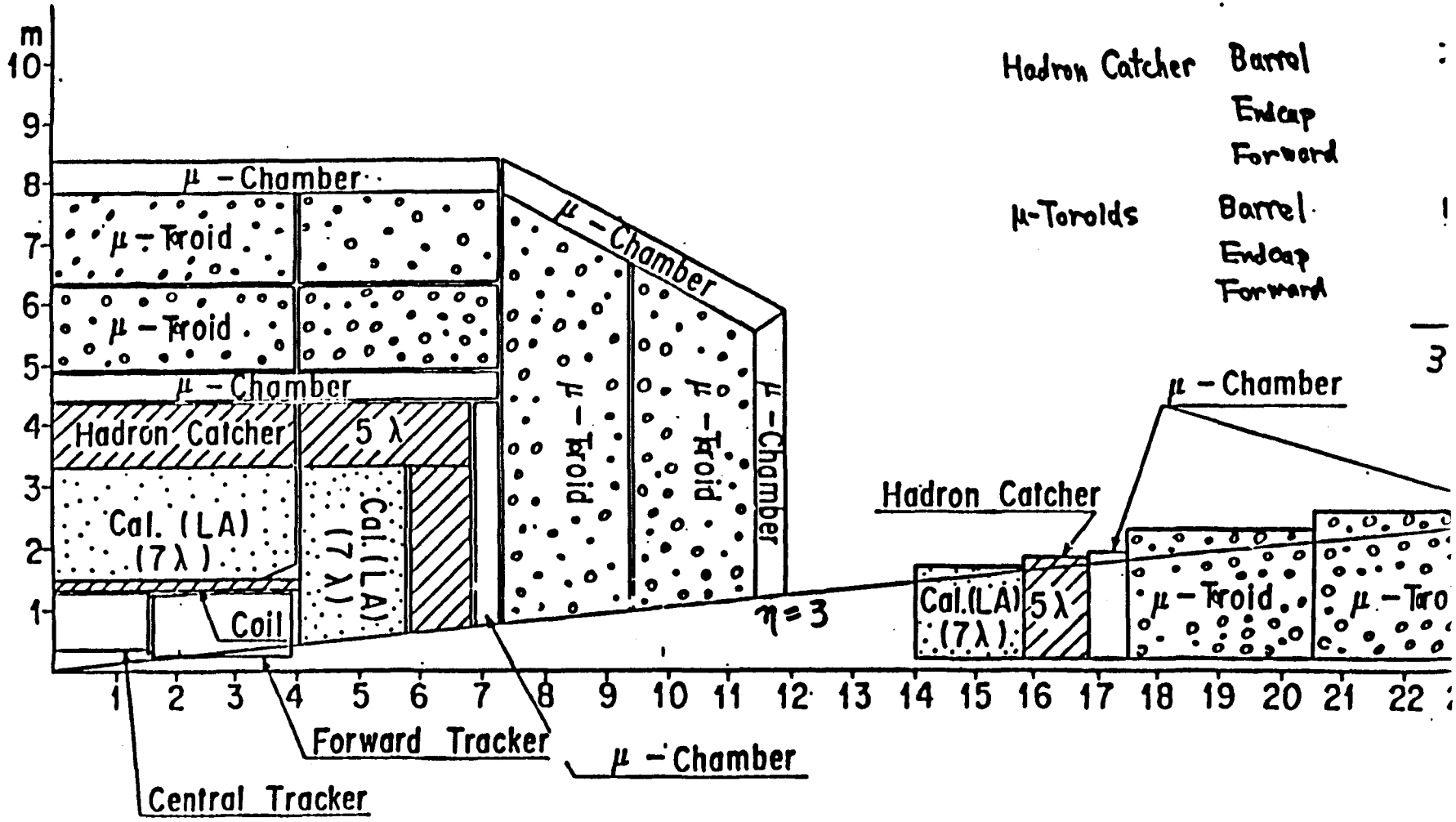

Calorimeter	Barrel	
	Endcap	
	Forward	
Hadron Catcher	Barrel	
	Endcap	
	Forward	
μ-Toroids	Barrel	
	Endcap	
	Forward	

Shigeki Mori

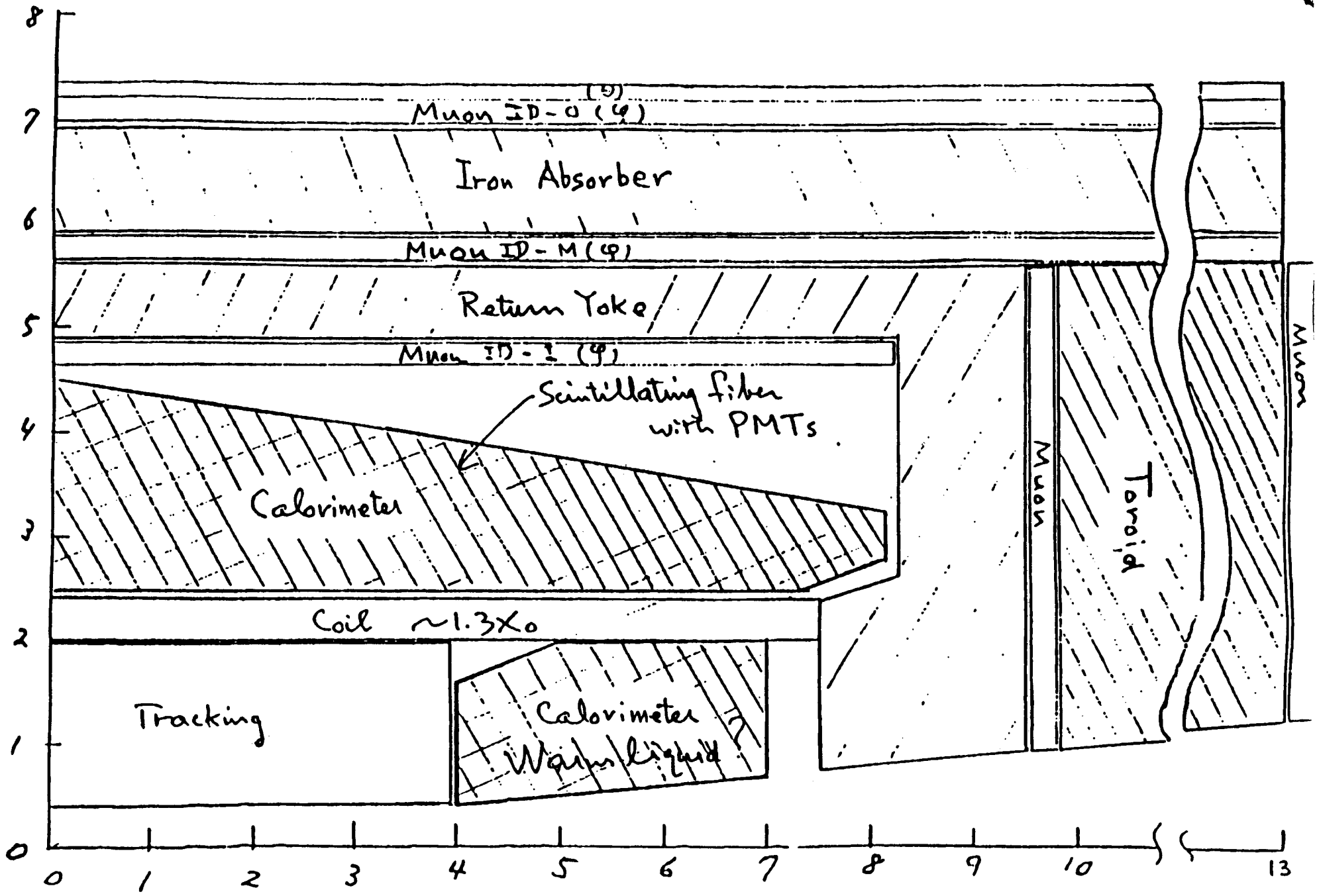

Three options for coil design

* Coil Outside Calorimeter

  Hermeticity excellent

  Significant improvement in σ_p/p (muons)

  Calorimeter signal to noise? No transformers? Electrostat. Tran.

  what is "penalty" in signal to noise?

  Scintillator Readout:

  PM's don't work? Will work in smaller B

  Substitute for PM's?

* Coil Inside Calorimeter

  Calorimeter Readout free of constraints

  Hermeticity problem from famous 30° crack?

  Is iron required in Endplug calorimeter?

  Is endplug calorim in field free region?

* Coil after 1-2 λ

  Hermeticity much better?

  Is $e/\pi = 1.0$ spoiled?

Effect of coil on e/h (after EM calorim)

this may be OK →

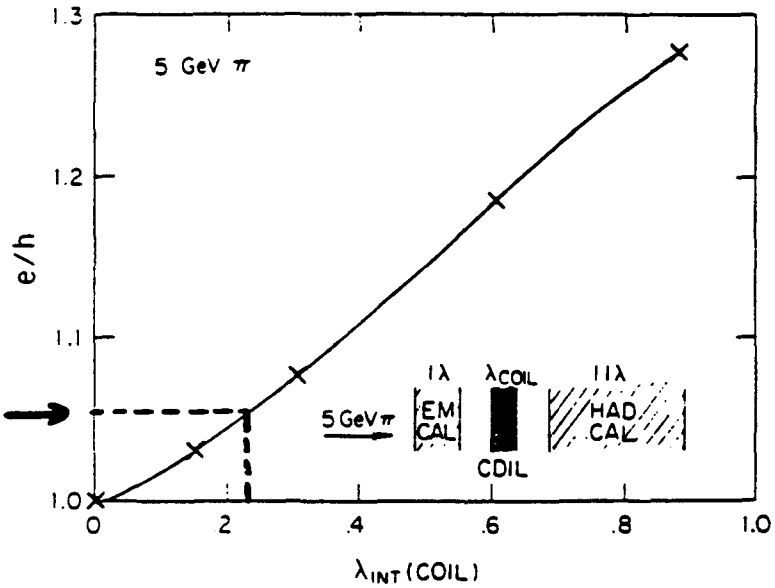

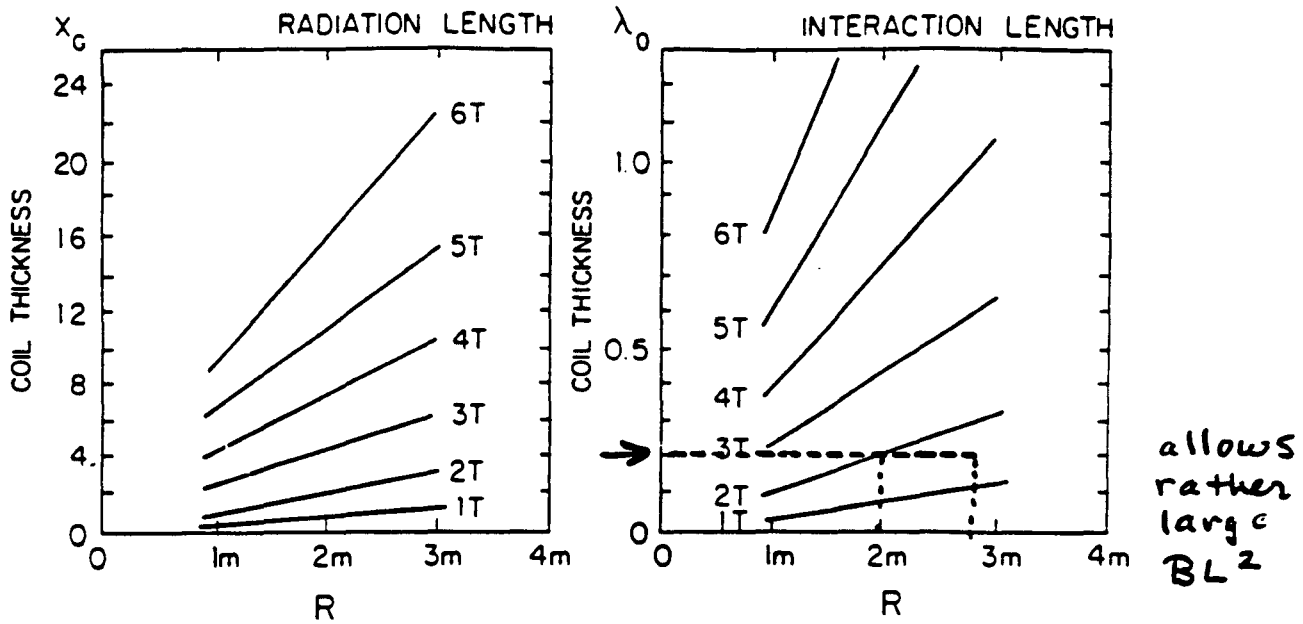

Figure 4.9 Thickness of high field superconducting magnets.

Summary

* Magnetic Field provides many benefits

  Clear & fundamental

  electron charge, improved σ_p/p

  Clear but secondary importance

  calorim. calib, underst. bgnds,

  Potentially important but intangible

  redundant p measurement
  secondary vertices
  utility of p_t, invariant mass cuts

  Options for future

  tracking upgrades 15 yrs from now (trans)

* Excellent calorimetry is very high priority

  missing E_t resolution

  dijet mass resolution

Primary Design Tradeoff

Excellent Calorim vs Sufficient BL^2
σ_E/E vs σ_p/p

Use high priority physics topics to quantify

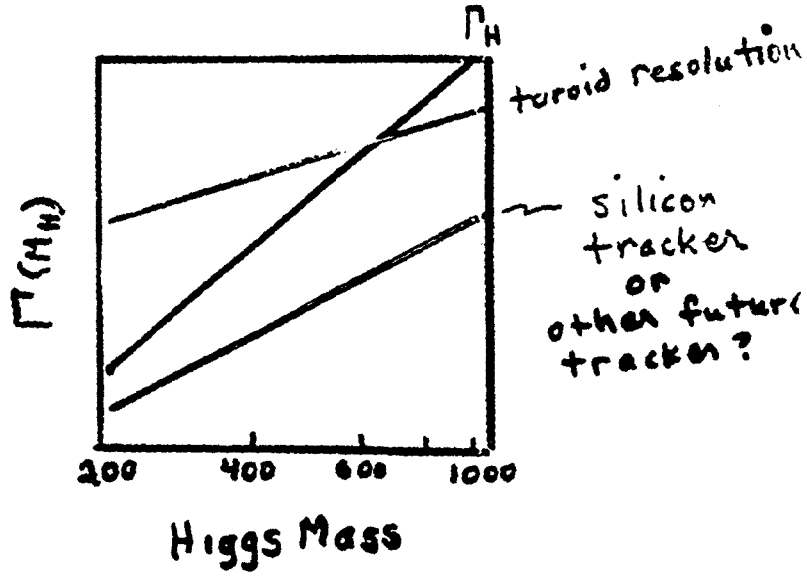
Γ_H
toroid resolution
silicon tracker or other future tracker?
$\Gamma(M_H)$
200
400
600
1000
Higgs Mass

A goal for the Workshop:
refined understanding of
compatibility of calorimeter & BL^2
for three different coil configurations

Longer Term Studies

$H \to ZZ \to ee\,ee$

is sign information needed?
is sign in central region only sufficient

$H \to ZZ \to ee\,\mu\mu$

σ_p/p for muons so that $\Gamma_{Resol} < \Gamma_{Higgs}$
include Z mass constraint

$H \to ZZ \to \mu\mu\,\mu\mu$

σ_p/p so $\Gamma_{Resol} \approx \Gamma_{Higgs}$; include pairing ambiguities

$H \to ZZ \to \ell^+\ell^-\,q\bar{q}$

$\sigma(M_W)$ as ftn of σ_E; include clustering combinatoric effects

Measure mult. for 200-300 GeV jets from CDF

$H \to W^+W^+$

effic for sign determ for $\mu\mu$, ee, μe

$t\bar{t} \to bW\,\bar{b}W \to b\ell\nu\,\bar{b}\,q\bar{q}$

$\sigma(M_W)$ as ftn of σ_E include clustering effects, combinatorics

$Q\bar{Q} \to tW\bar{t}W \to bWW\,\bar{b}WW$

Effic for ident $W \to Q\bar{Q}$ as ftn of $\# W \to \ell\nu$

Construction of a LARGE system

a) 2T design

b) 0.7T design

Longer Term Studies

$H \to ZZ \to ee\,ee$

is sign information needed?
is sign in central region only sufficient

$H \to ZZ \to ee\,\mu\mu$

σ_p/p for muons so that $\Gamma_{Resol} < \Gamma_{Higgs}$
include Z mass constraint

$H \to ZZ \to \mu\mu\,\mu\mu$

σ_p/p so $\Gamma_{Resol} \approx \Gamma_{Higgs}$; include pairing ambiguities

$H \to ZZ \to \ell^+\ell^-\,q\bar{q}$

$\sigma(M_W)$ as ftn of σ_E; include clustering combinatoric effects

Measure mult. for 200-300 GeV jets from CDF

$H \to W^+W^+$

effic for sign determ for $\mu\mu$, ee, μe

$t\bar{t} \to bW\,\bar{b}W \to b\ell\nu\,\bar{b}\,q\bar{q}$

$\sigma(M_W)$ as ftn of σ_E include clustering effects, combinatorics

$q\bar{q} \to tW\,\bar{t}W \to bWW\,\bar{b}WW$

effic for sign determ as fn of # $W \to \ell\nu$

Construction of a LARGE system

a) 2T design

b) 0.7T design

SSC-SD-1
b.

S. Mori Dallas

6-26-1989

Large and Small Solenoids

1. Introduction
2. Large, SCDF, and Small
   VLS
3. Thin Solenoids without Return Yokes
4. Conclusions

Large Solenoids

$B \lesssim 0.5$ T : conventional or superconducting

$B \gtrsim 0.7$ T : superconducting

Conventional (Al, Cu)

Power, cost

No serious technical limitations? ($\lesssim 2$T

Superconducting

Quench protection

large stored energy

Cryostat arrangement

mechanical support

Magnetic field dependence (* dimensions)

$B \lesssim 2$ T : Al-stabilized NbTi/Cu*

Indirect cooling

Thin (X_0, λ)

$B \gtrsim 2$ T : Heavily structured conductor**

Pool boiling (direct)

Thick

* Proved Technology only for $B \lesssim 1.5$ T.

** AMY

The Most Important Requirements for Detector Magnets

Stable operation

No disturbance during physics runs

Comfortable safety margin in design

Almost impossible to repair at a large SSC detector

Easy maintenance arrangement

Intrinsically safe against quenches

Quite Important Considerations

Compactness

Material thickness

Radiation and absorption

e/hadron separation

Energy resolution

Costs

Schedule

etc.

Main Parameters of Detector Solenoids

• thin (Al stabilizer)

Detector	Lab.	Compl.year	ID(m)	L(m)	B_0(T)	E(MJ)	T(rl)	Cool.	
• CELLO	DESY	1979	1.5	3.5	1.5	7.0	0.5	FF	1st gen.
• TPC	SLAC	-	2.0	3.4	1.5	10.7	0.4	FF	1st gen.
• CLEO	Cornell	1982	1.9	3.4	1.5	9.4	0.7	FF	1st gen.
• CDF	FNAL	1984	2.9	5.1	1.5	30	0.8	FF	2nd gen.
• TOPAZ	KEK	1984	2.7	5.4	1.2	20	0.7	FF	2nd gen.
• VENUS	KEK	1985	3.4	5.6	0.75	12	0.5	FF	2nd gen.
AMY	KEK	1986	2.5	2.1	3.0	40	-	PB	
• ALEPH	CERN	1987	5.2	7.0	1.5	137	1.6	TS	3rd gen.
DELPHI	CERN	1988	5.0	7.4	1.2	108	4	FF	3rd gen.
CLEO-II	Cornell	1988	2.9	3.8	1.5	25	-	TS	3rd gen.
• ZEUS	DESY	1988	1.9	2.8	1.8	18	0.9	FF	
Large	SSC		8.6	16	2	1500	-	PB	
• SCDF	SSC		4.0	15	2	300	1.3	FF	
• Small	SSC		3.0	8	2	99	0.8	FF	
• VLS	SSC		6	21	1.7	700	~1.5	FF	

FF: forced flow, PB:pool boiling, TS:thermo syphon

1st generation

Inner bobbin

2nd generation

Extruded aluminum stabilizer for monolithic superconductor

No inner bobbin (shrink-fit or inner winding)

3rd generation

Modular, superconducting cables (longer unit length and higher reliablity)

Main Parameters of Solenoids for SSC

Items	Large*	SCDF	Small
	Tsukuba/ Hitachi	thin	thin
Vacuum vessel			
Diameter:outer/inner(M)	9.6/8.6	4.8/4.0	3.5/3 ~~6/3.5~~
Length(m)	16	15	8
Material	SUS304	A5083Al	Al-all.
Thickness:outer/inner(mm)	40/25	40/10	6/4
Central field(T)	2	2	2
Material thickness(rl)	large	1.3	0.76
Total weight(t)	540	69	
Cold mass(t)	390	39	10
Coil			
Number of modules	8	2	1
Stored energy(MJ)	1500	300	99
Current(A)	6400	8000	10000
Inductance(H)	73	9.4	2.0
Number of layers	6	1	1
Conductor			
NbTi:Cu:Al ratio	AMY-type	1:1:26	1:0.8:58
Dimensions(mm^2)	14wx12	4.8x35	5.6x35
Short sample current(kA)	11.6;4.4T	16.0;2T	
Purity of Al stabil.(RRR)	>1000	>1000	
LHe cryogenics			
Method	PB	FF	FF
Vessel			
Material	SUS304LN	A5083Al	Al-all.
Thickness:outer/inner(mm)	28/37	35/0	12.3/0

* Tsukuba/Hitachi, FNAL:
Two designs are very consistent although optimization of some parameters is significantly different.

Main Characteristics of Solenoids for SSC

Items	Large	SCDF	Small
Stored energy (MJ)	1500	300	99
Estimated cost (10^8¥)*	75	34	'15'
	(50M$)	(23M$)	(10M$)
(without including auxiliary equipment, tests, transport, and on-site assembly)			
Model solenoid	AMY	CDF	ZEUS?
Stored energy (MJ)	40	30	
Cost (10^8¥)	5	6	
A maker suggests that the cost is approximately proportional to the three quarter power of the ratio of the stored energies of two solenoids of the same type. The CDF solenoid was used for cost estimate of 'Small' because no appropriate model solenoid is available.			
Magnetic field (T)			
Barrel calorimeter	2.0 uniform	<0.01 app. null	<0.5 varying
Tracking chambers	uniform	uniform	non-uniform
Potential difficulties	large size, transportation, high cost	straight-forward	axial compressive forces
Barrel muon system	simple, no toroid	simple, no toroid	massive toroids

* 3CD Snowmass 84
1.5T, 7mφ x 11m, 360MJ
$19M (p.633)

hoop stress $= \frac{B^2}{2\mu}$

1st generation :

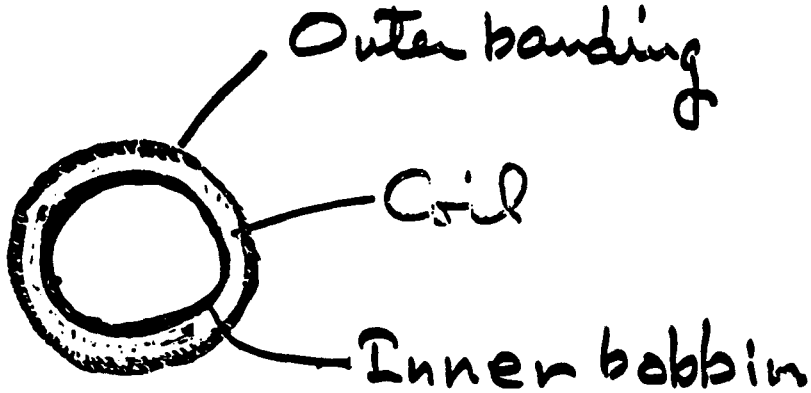

2nd generation :
(3rd .....)

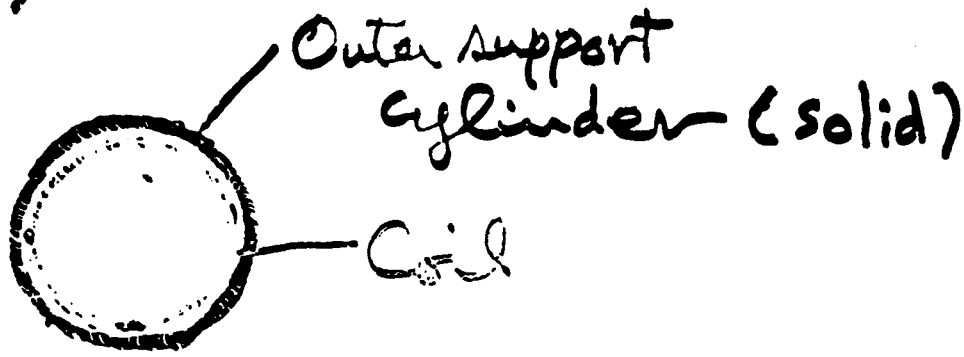

(Bobbinless)

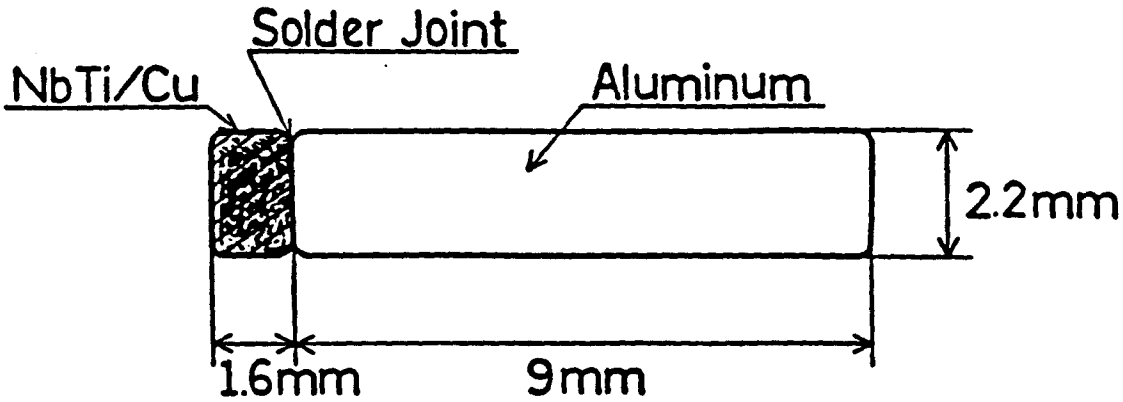

(a) CELLO

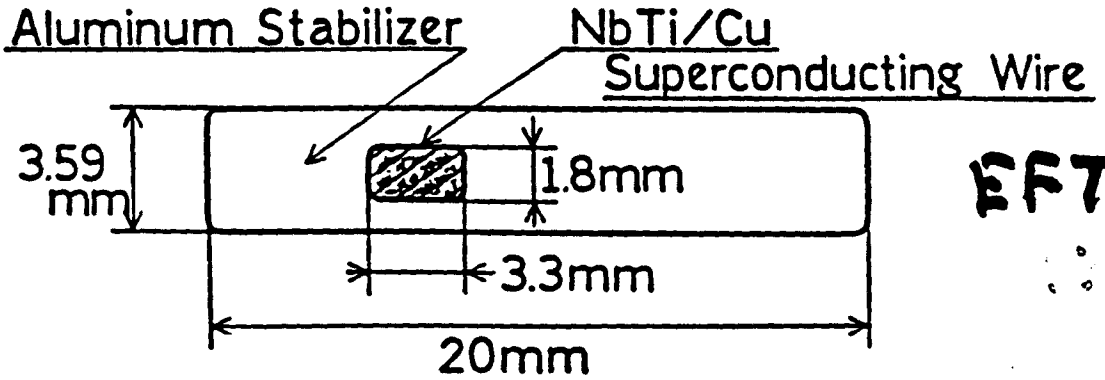

EFT conducto

Superconducting Wire; 50μm$^{\Phi}$×1400(2.75mm^2)
Material Ratio; Al:Cu:NbTi=24:1:1
Aluminum Purity; 99.99 %

(b) CDF R/D

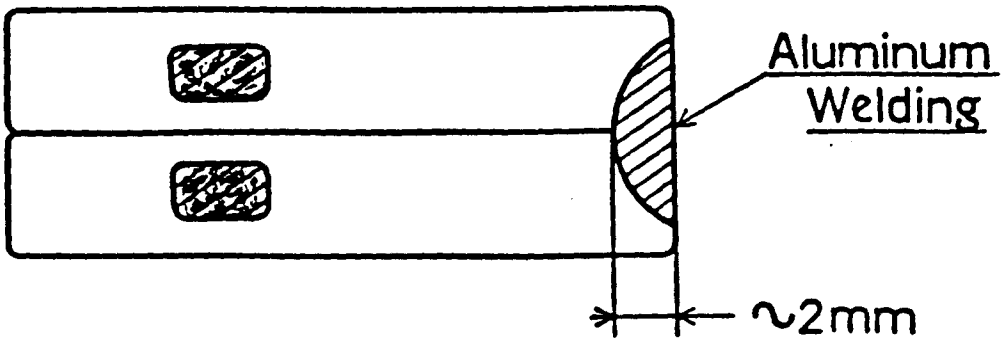

(c) JOINT, CDF R/D

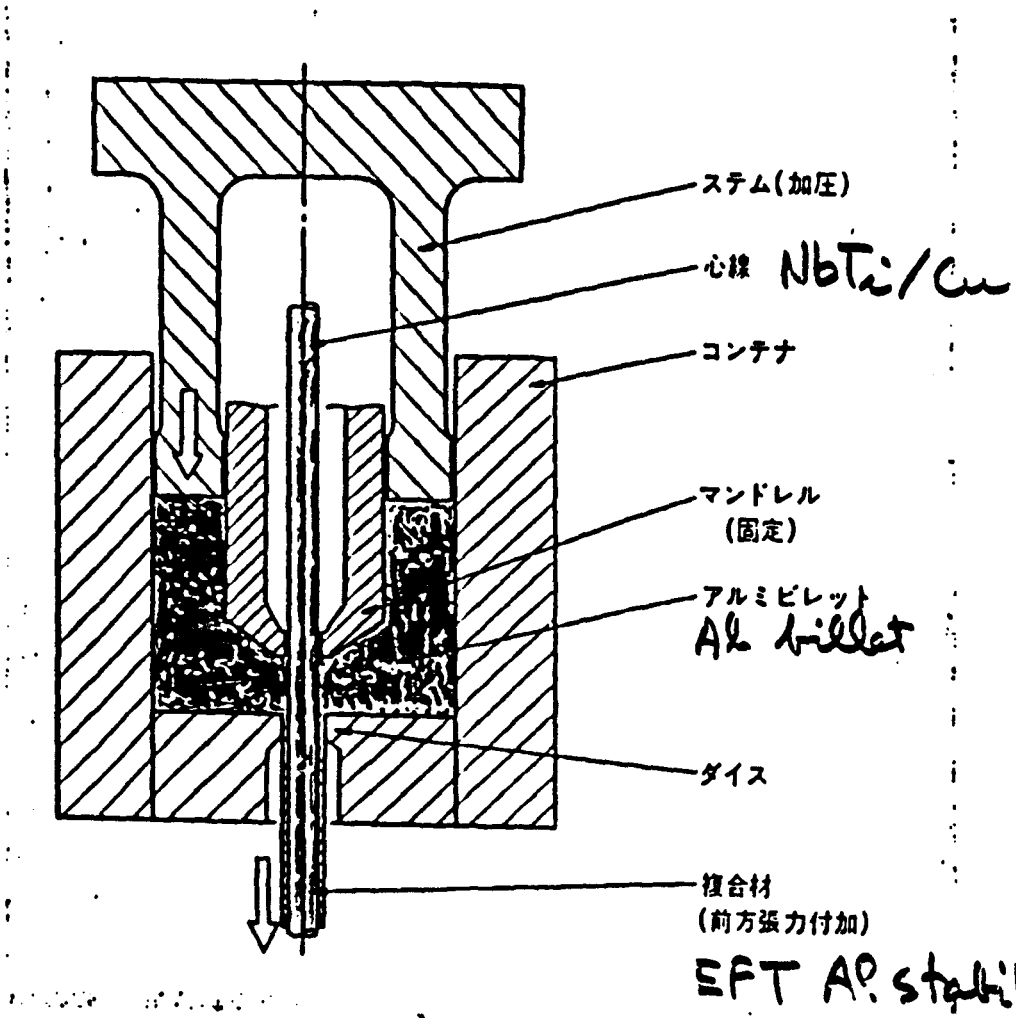

図5　EFT法の原理　前方張力を付加することにより，押出比の大きい複合材押出しが可能となり，しかも押出速度が速く，変形抵抗の差が大きい素材による複合線材の製法に適した加工法である。

- Temperature
- Pressure
- Speed.

Shearing strength
~ 3 kg/mm²

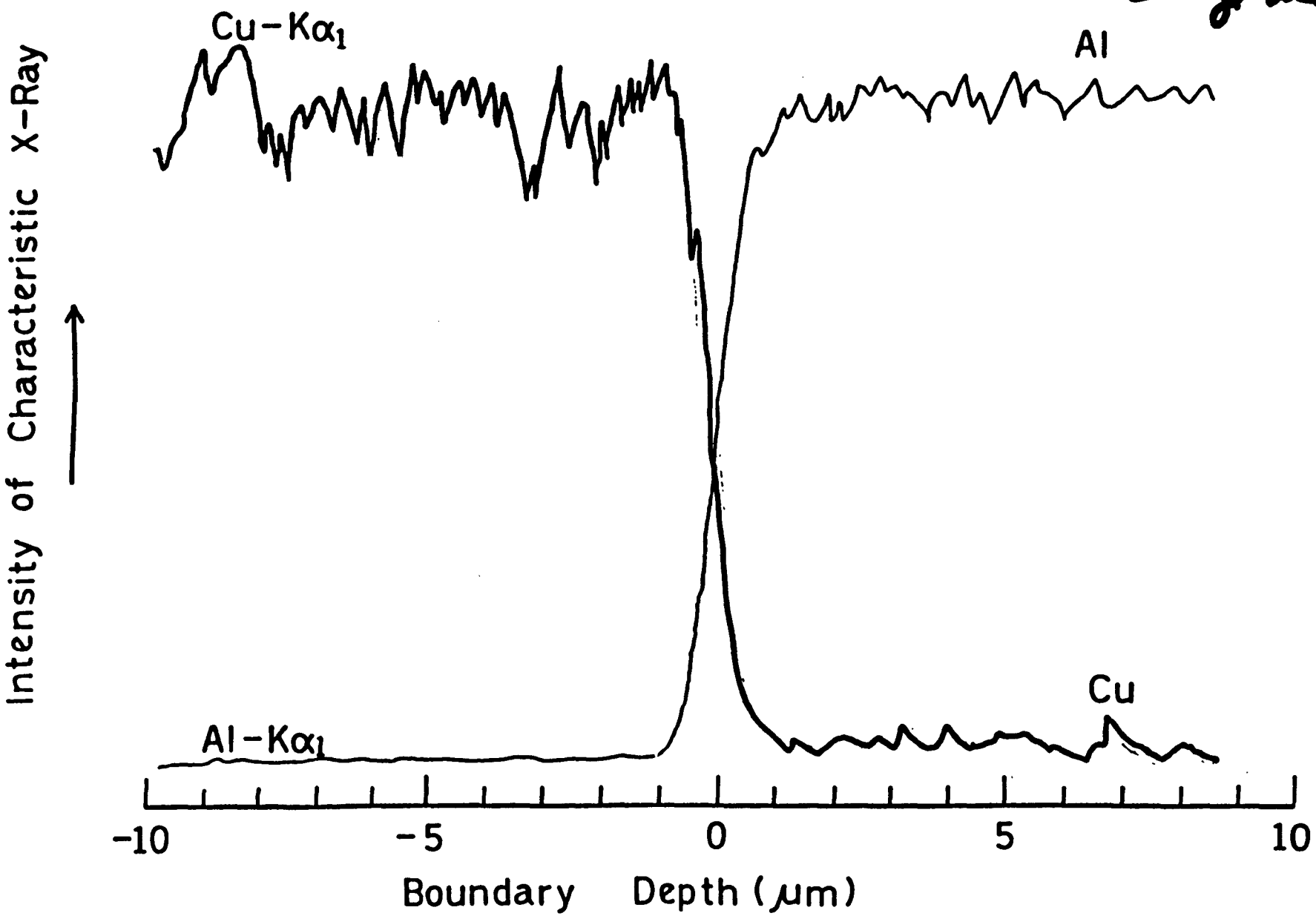

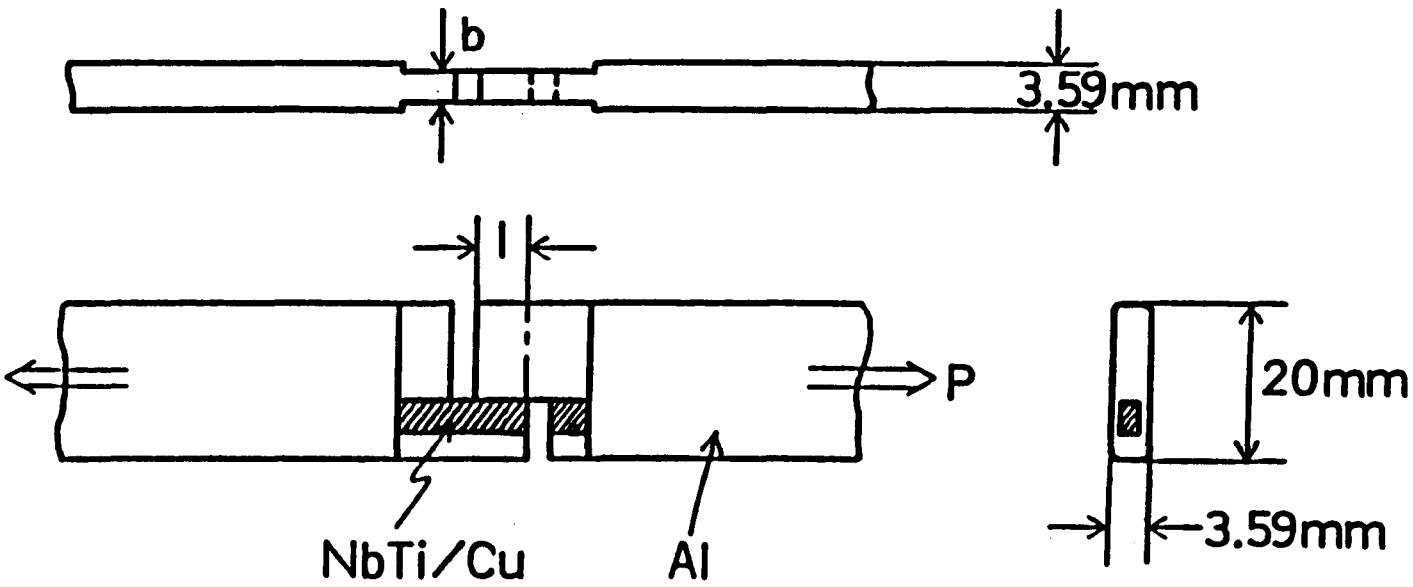

Shearing Force of Binding $\tau = P/(b \cdot l)$

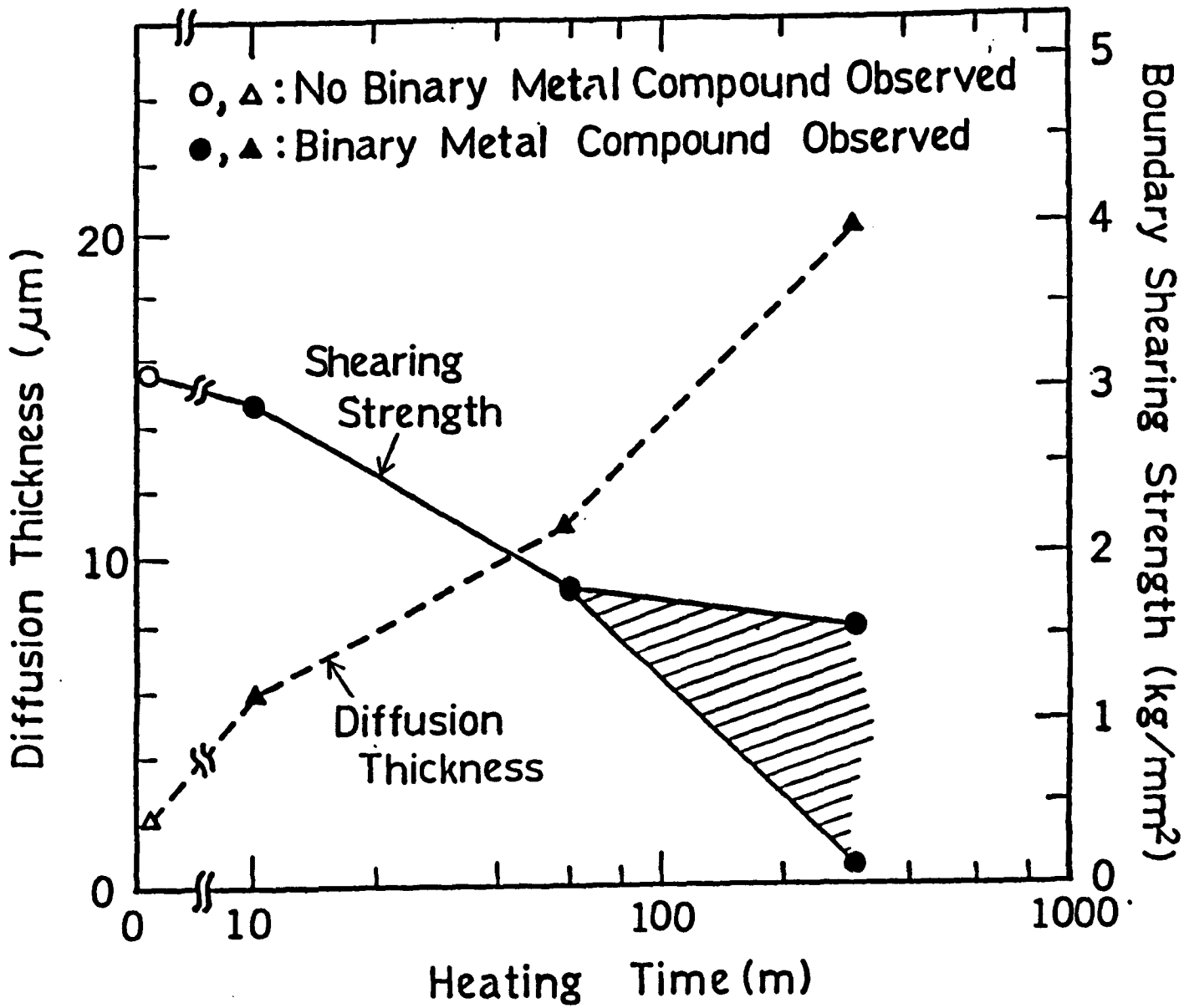
○, △ : No Binary Metal Compound Observed
●, ▲ : Binary Metal Compound Observed
Shearing Strength
Diffusion Thickness
Diffusion Thickness (μm)
Boundary Shearing Strength (kg/mm²)
Heating Time (m)
0
10
20
0
1
2
3
4
5
0
10
100
1000

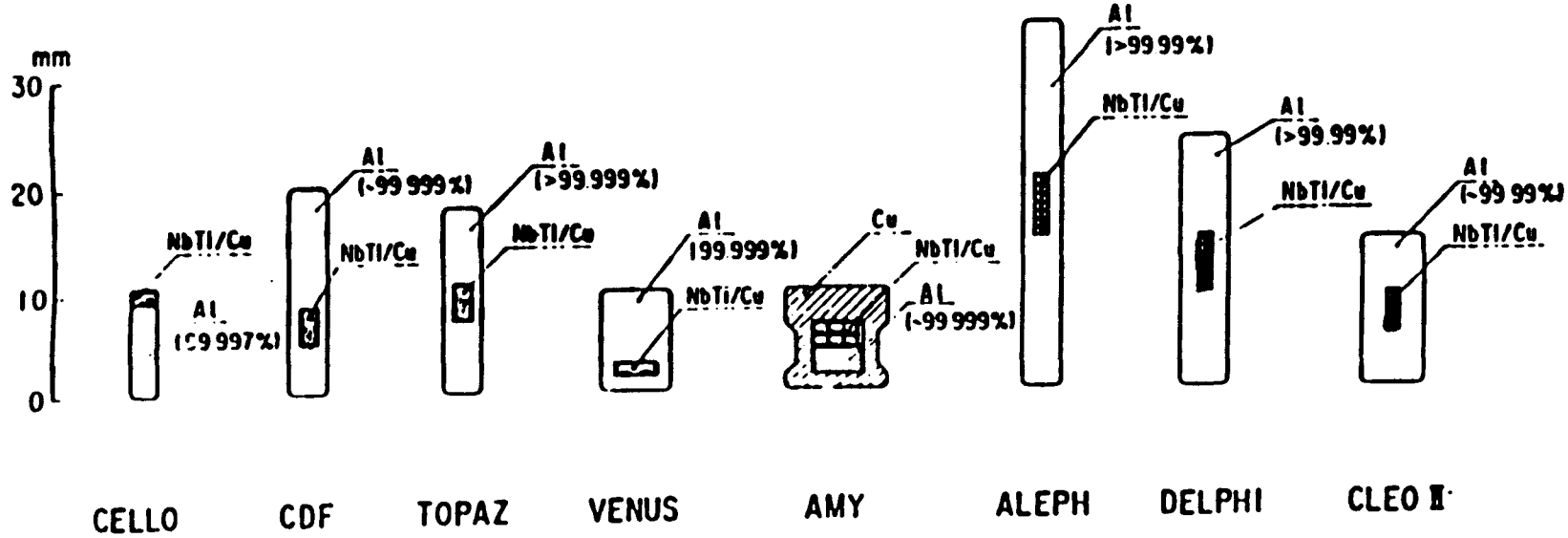

monolithic

cable

Why pure aluminum for stabilizer?

Quench protection

Temperature rise : $\Delta T \lesssim 100\,K$

Maximum voltage to grd $\lesssim 1000\,V$

$$\Gamma \equiv \gamma \int^{T_{max}} \frac{C}{\rho}\, dT = \frac{I_0^2 \tau}{2A^2}$$

$$= \frac{E_0 J_0^2}{V_{max} I_0}$$

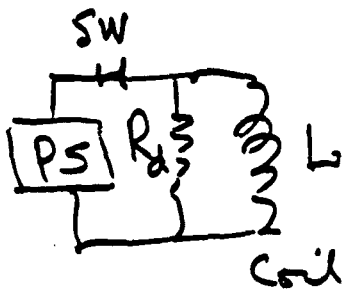

(Coil resistance: negligible)

γ: density
ρ: resistivity
C: specific heat
$\tau = L/R_d$
$J_0 = I_0/A$
$E_0 = LI_0^2/2$, $V_{max} = I_0 R_d$

For a given T_{max}, Γ is determined by the conductor (composition, not dimension)

E_0, I_0, Γ : fixed

$$V_{max} \propto J_0^2$$

or E_0, Γ : fixed

$$V_{max} \propto \frac{J_0^2}{I_0}$$

large C, small ρ : desirable.

$\Delta L/L \sim 2.2\times10^{-5}\ T^{-1}$

$\Delta L/L\big|_{4K}^{300K} \sim 0.43\%$

A. THERMAL EXPANSION OF SOLIDS

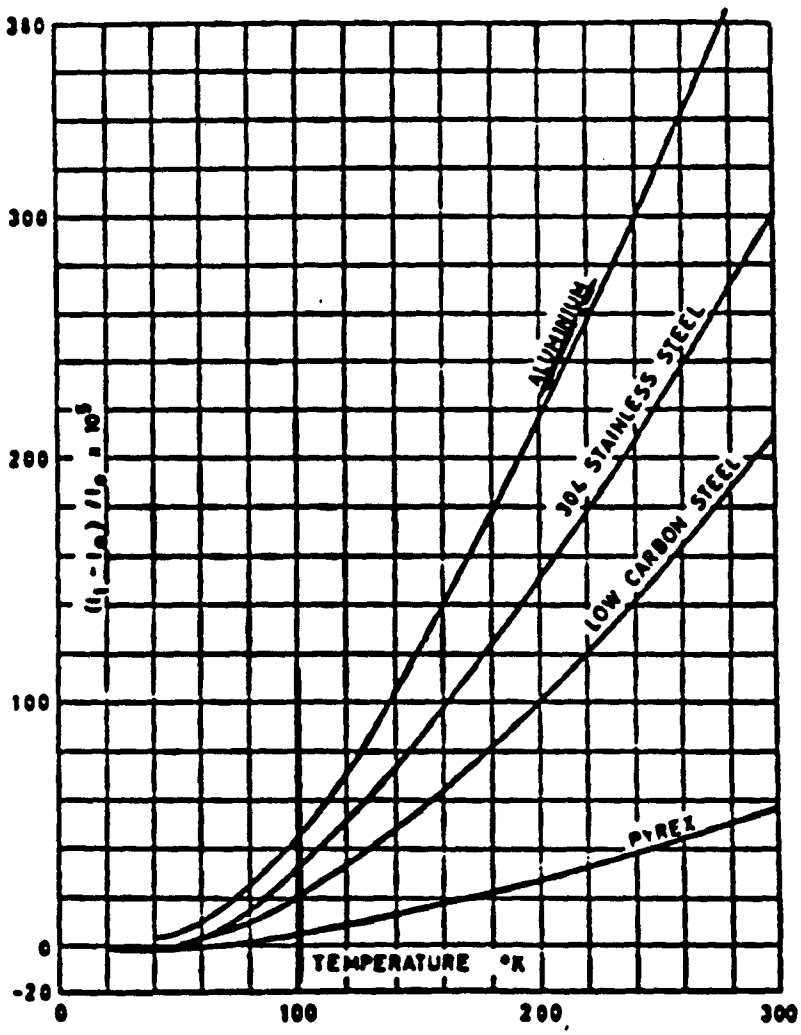

Fig. 12.1. Thermal expansion of aluminium, steel, stainless steel and pyrex.

Cryostable parameter α

$$\alpha = \frac{\rho I^2}{P A q \beta}$$

$$= \frac{I^2}{P q \beta \sum_i \frac{A_i}{\rho_i}}$$

$\alpha < 1$: Complete cryogenic stability
Stekly et al.

P : conductor perimeter

$q \cdot \beta$: thermal flux from the conductor to LHe
($q \beta = 0.13 \pm$ W/cm^2)
AMY.

ρ : small
pure aluminum stabilizer

$$RRR \equiv \frac{\rho_{300K}}{\rho_{4.2K}}$$

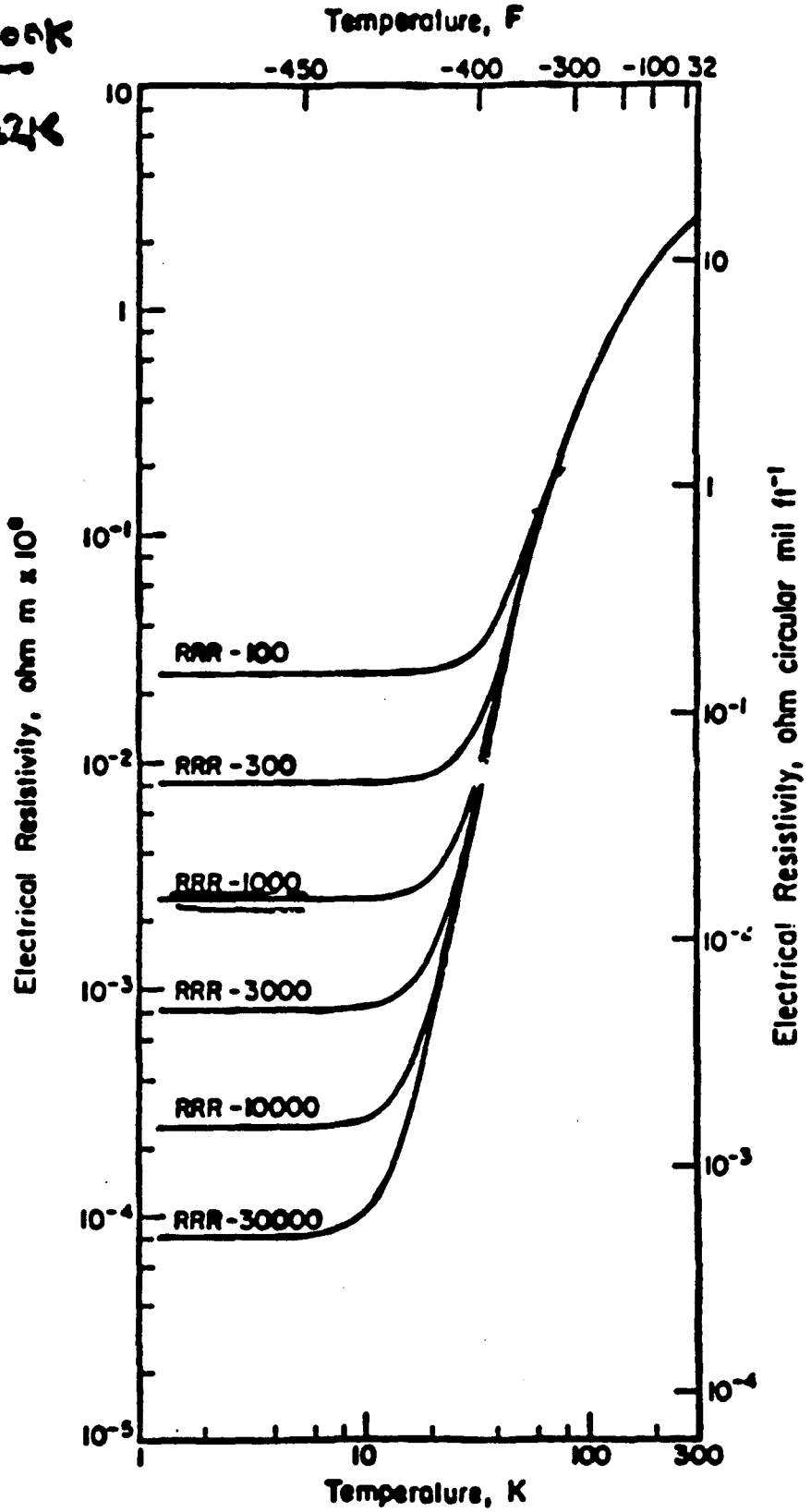

FIGURE 4.1.1-R1. ELECTRICAL RESISTIVITY VERSUS TEMPERATURE FOR ALUMINUM

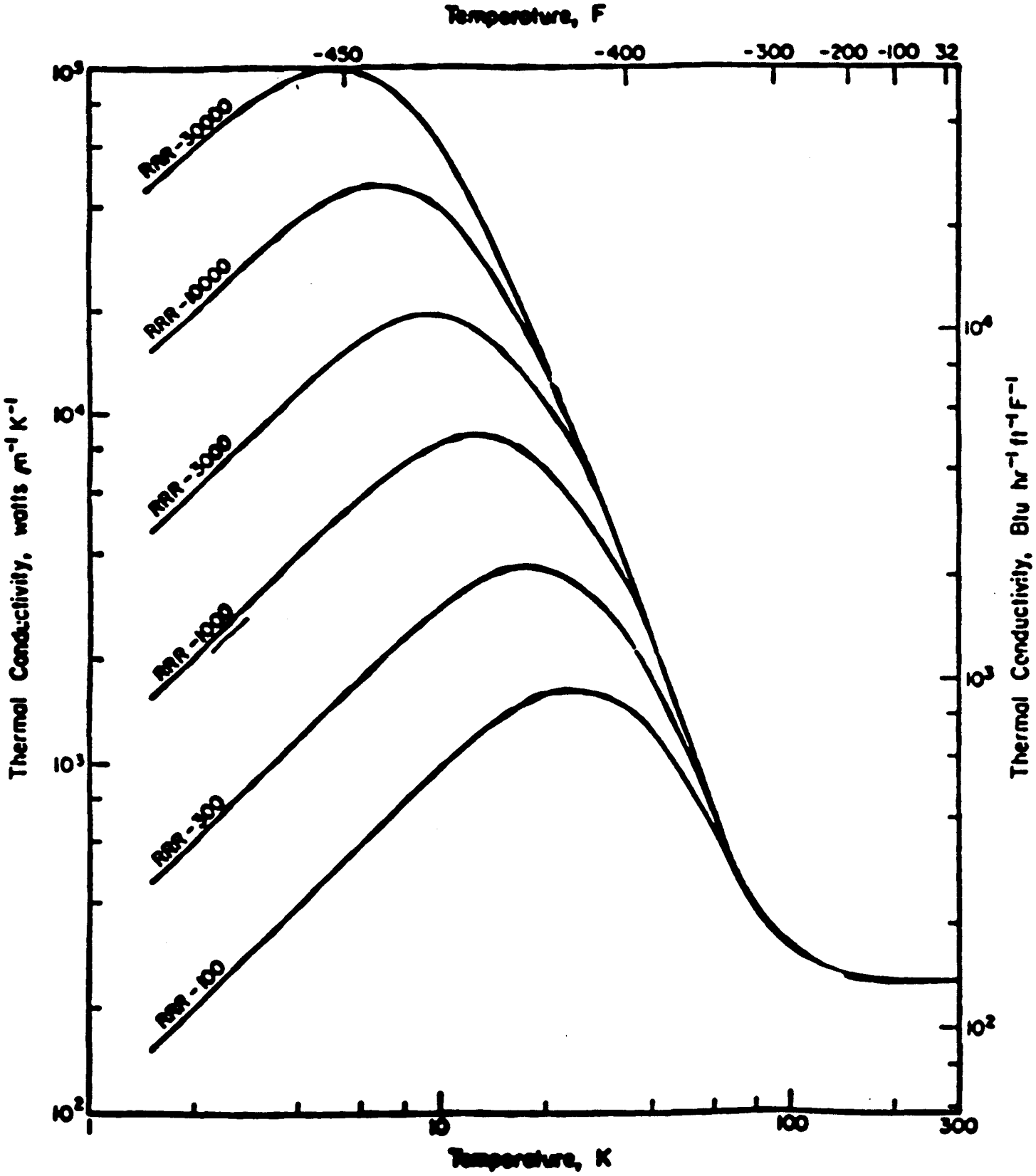

FIGURE 4.1.1-C1. THERMAL CONDUCTIVITY VERSUS TEMPERATURE [illegible] ALUMINUM

Thin coils Thickness $\lesssim 2X_0$: Tolerable ?
$\wr$
$4X_0$

Energy resolution
SF03 lead glass ($18X_0$)
K. Ogawa et al. NIM A238, 328 (1985)

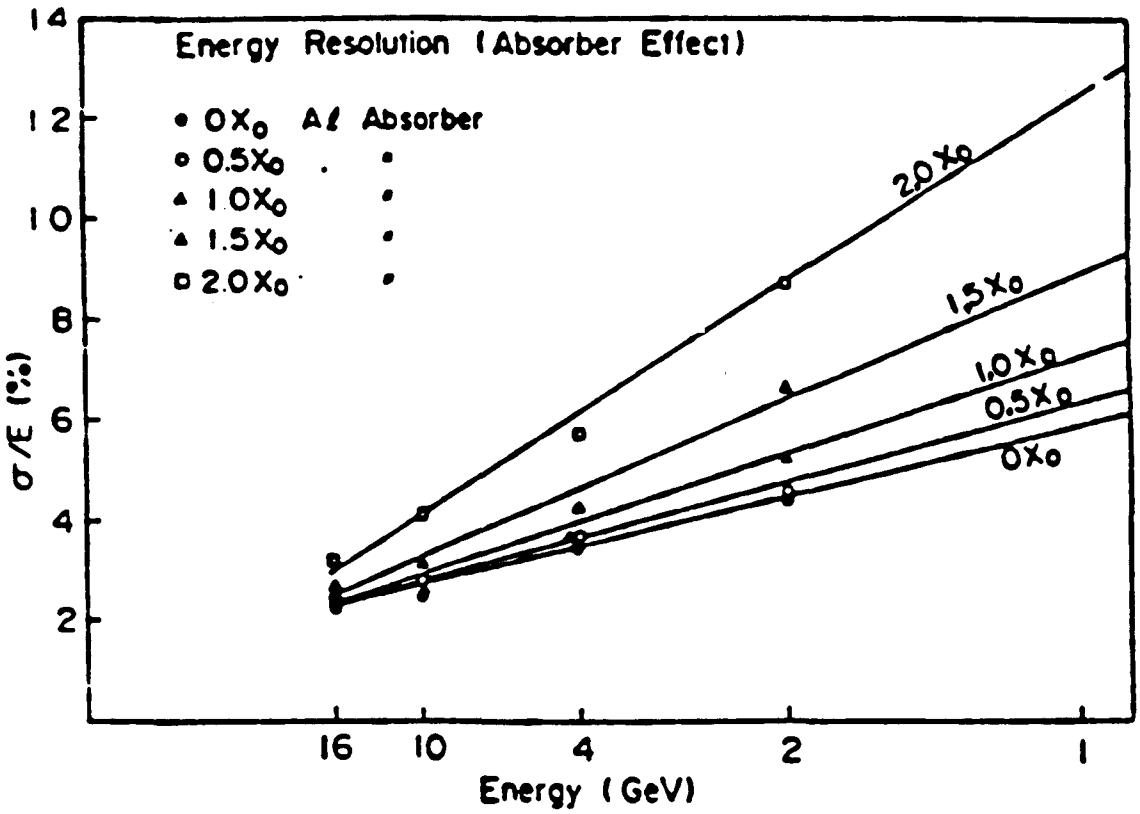

- Pion rejection : Diebold et al.

$\pi^- p \to \pi^0 n$

zero prong interaction

rate $\sim 0.8 \times 10^{-3}$ in 7.6cm of Al at 30 GeV (π^-

$\approx 0.1\%$ / 1 r.l. Al.

Calorimetry

P.R. 5, 2677 (72)

Electromagnetic shower development:

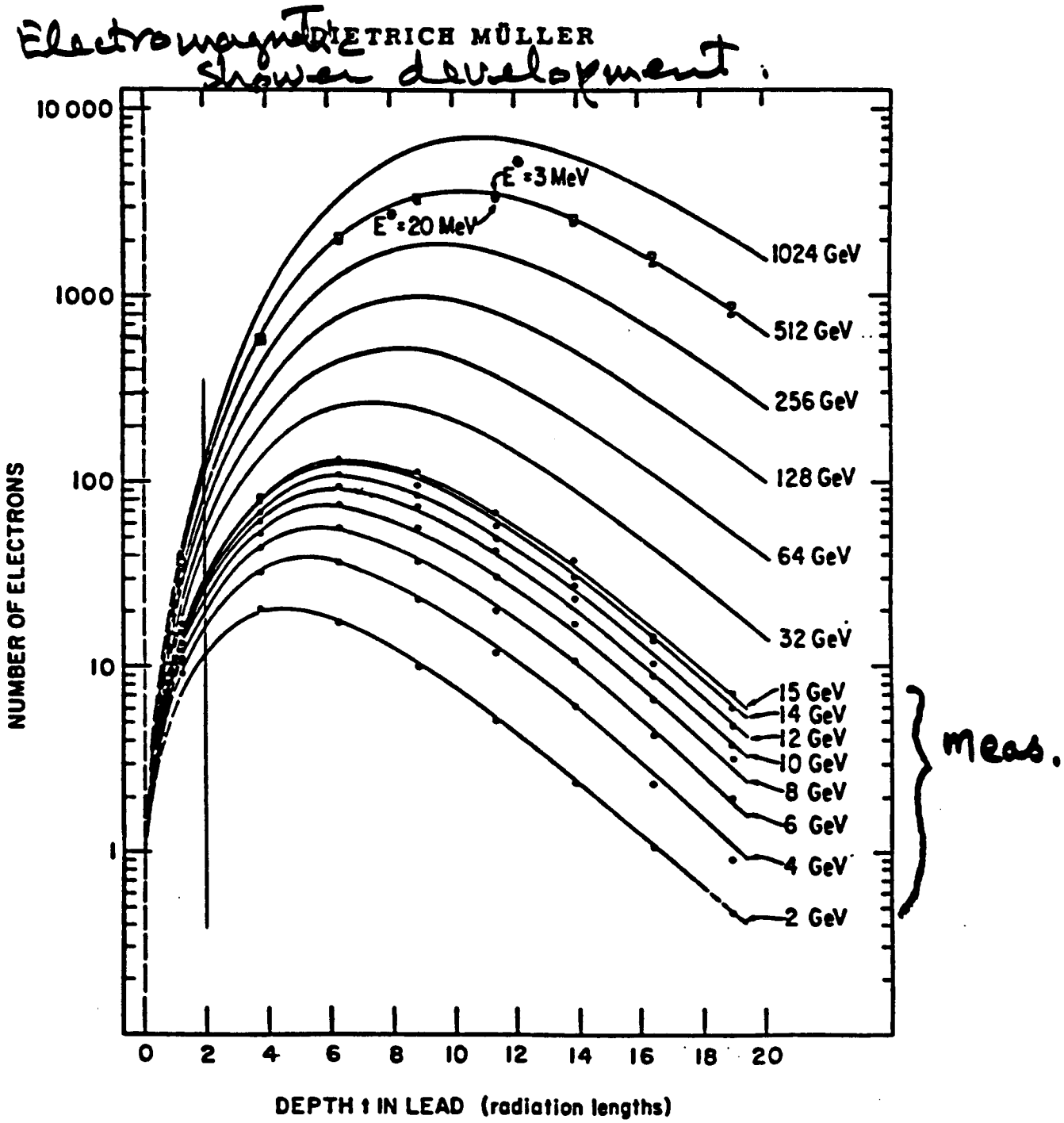

FIG. 6. Shower profiles in the energy region 2 to 1024 GeV. The data points at lower energies (2–15 GeV) are measured values, while the solid lines are calculated profiles according to the fitting procedure described in Sec. IV with $E^* = 7.4$ MeV. For 512 GeV, also calculated profiles with $\rho(s)$ corresponding to $E^* = 3$ MeV and 20 MeV are sh

Y. Hayashide et al. NIM 204, 361 (83)

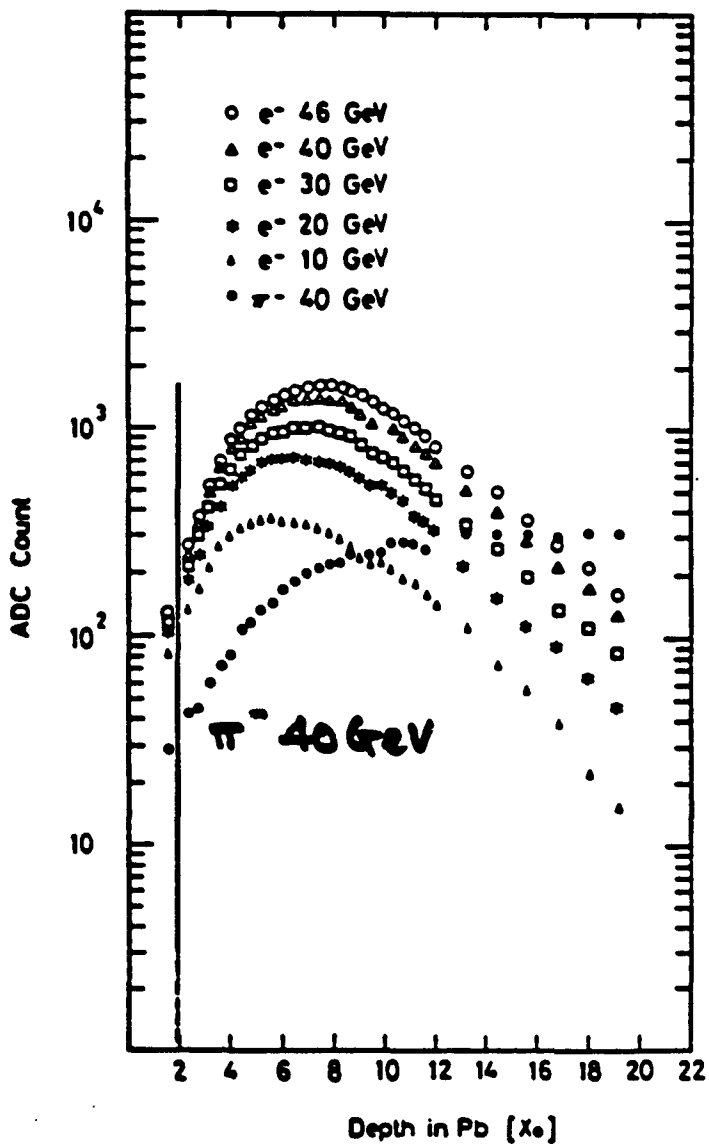

Fig. 4. Longitudinal shower development for electrons and pions in terms of radiation lengths (X_0).

M. Chishima

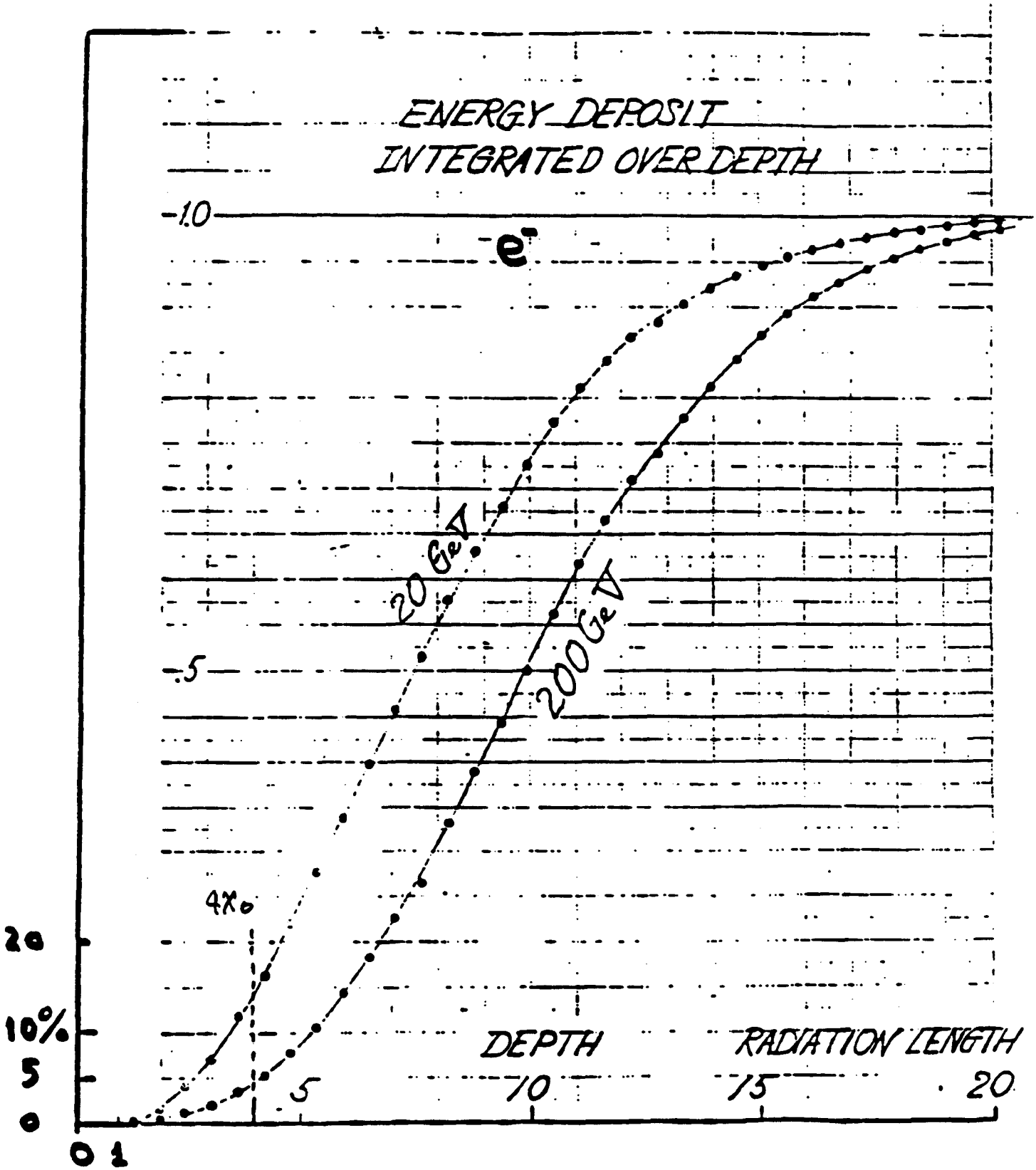
ENERGY DEPOSIT
INTEGRATED OVER DEPTH
1.0
e⁻
.5
20 GeV
200 GeV
4X₀
20
10%
5
0
0 1
5
10
15
20
DEPTH
RADIATION LENGTH

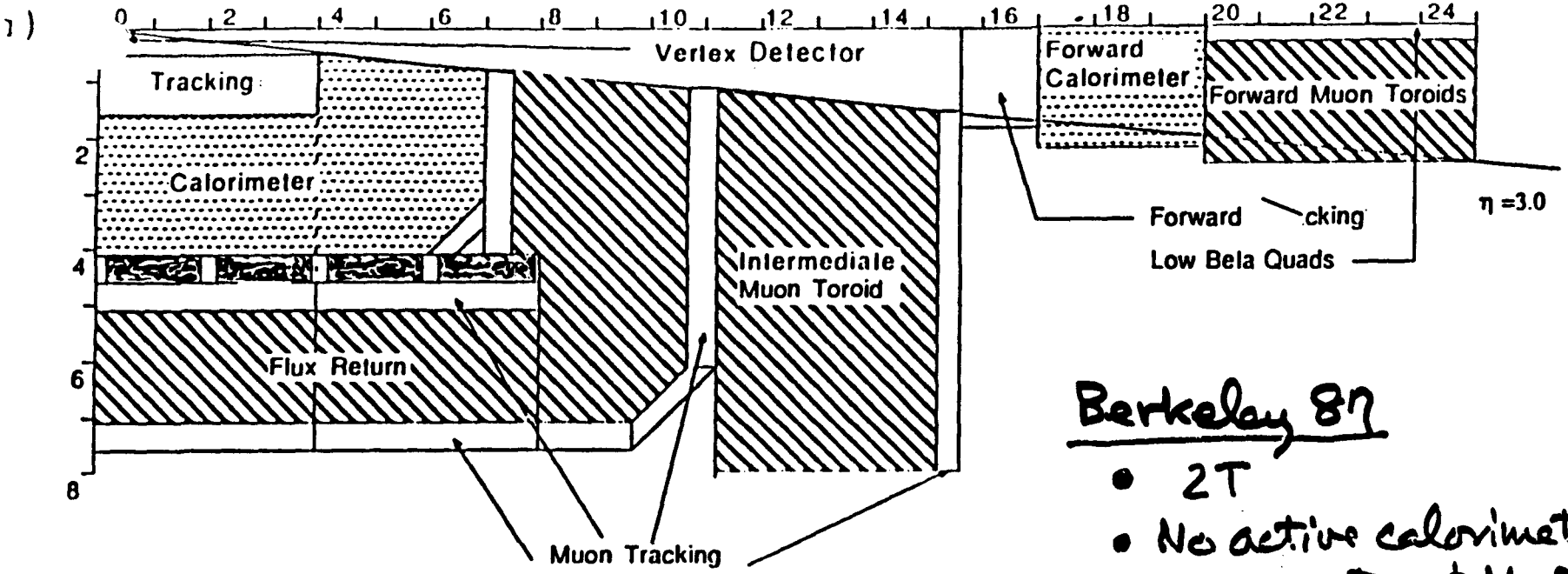

Berkeley 87

- 2T
- No active calorimeter components outside the coil
  No limitation for material thickness
- No additional muon toroids (Barrel)

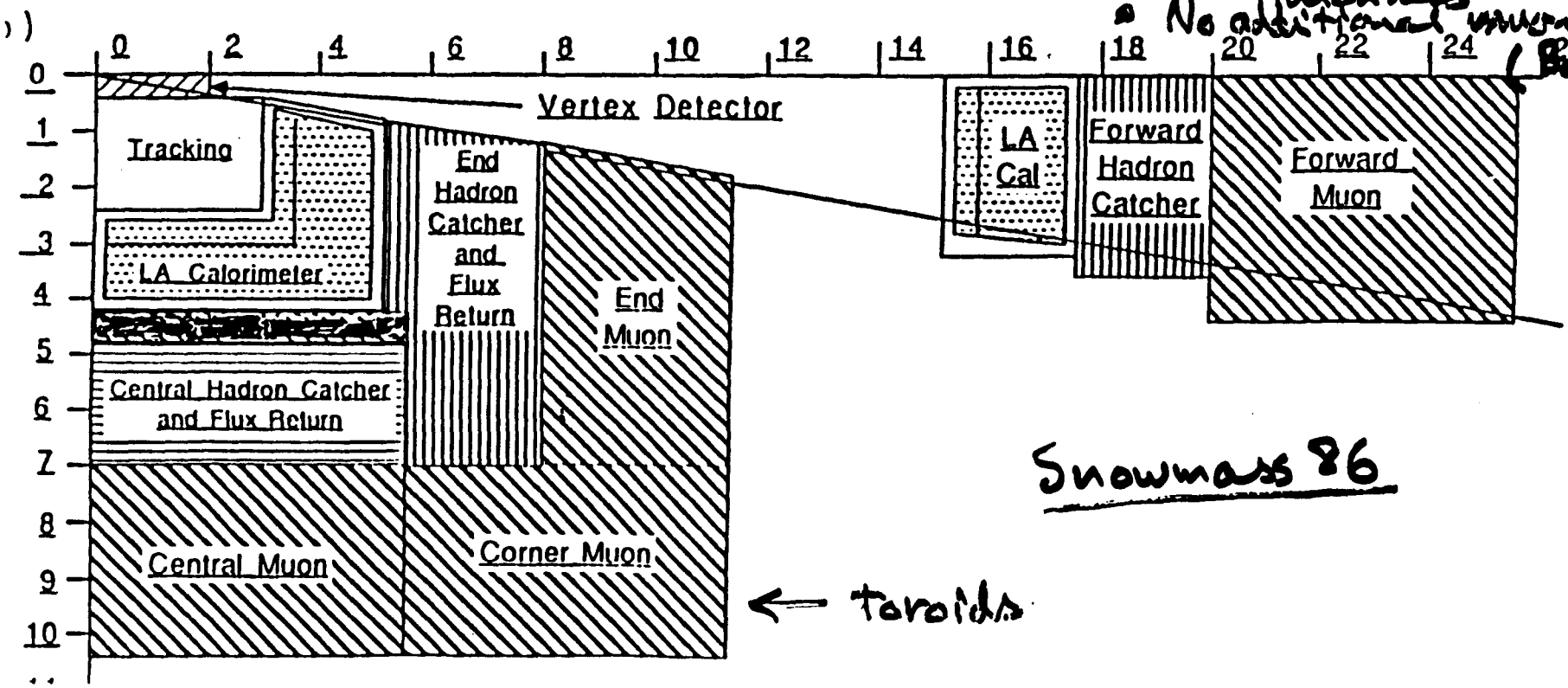

Snowmass 86

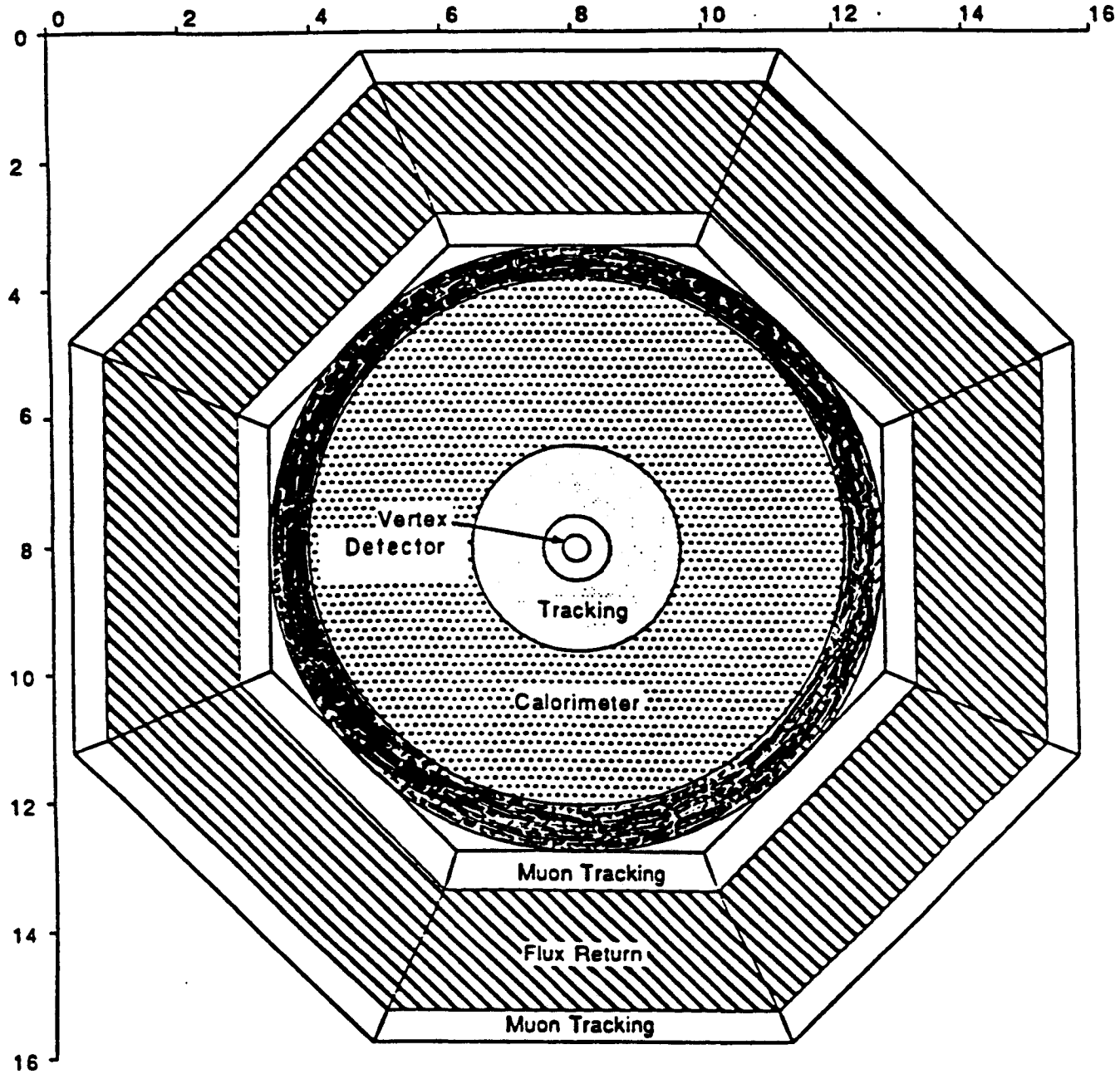
0
2
4
6
8
10
12
14
16
Vertex
Detector
Tracking
Calorimeter
Muon Tracking
Flux Return
Muon Tracking

Small.

(Hori)

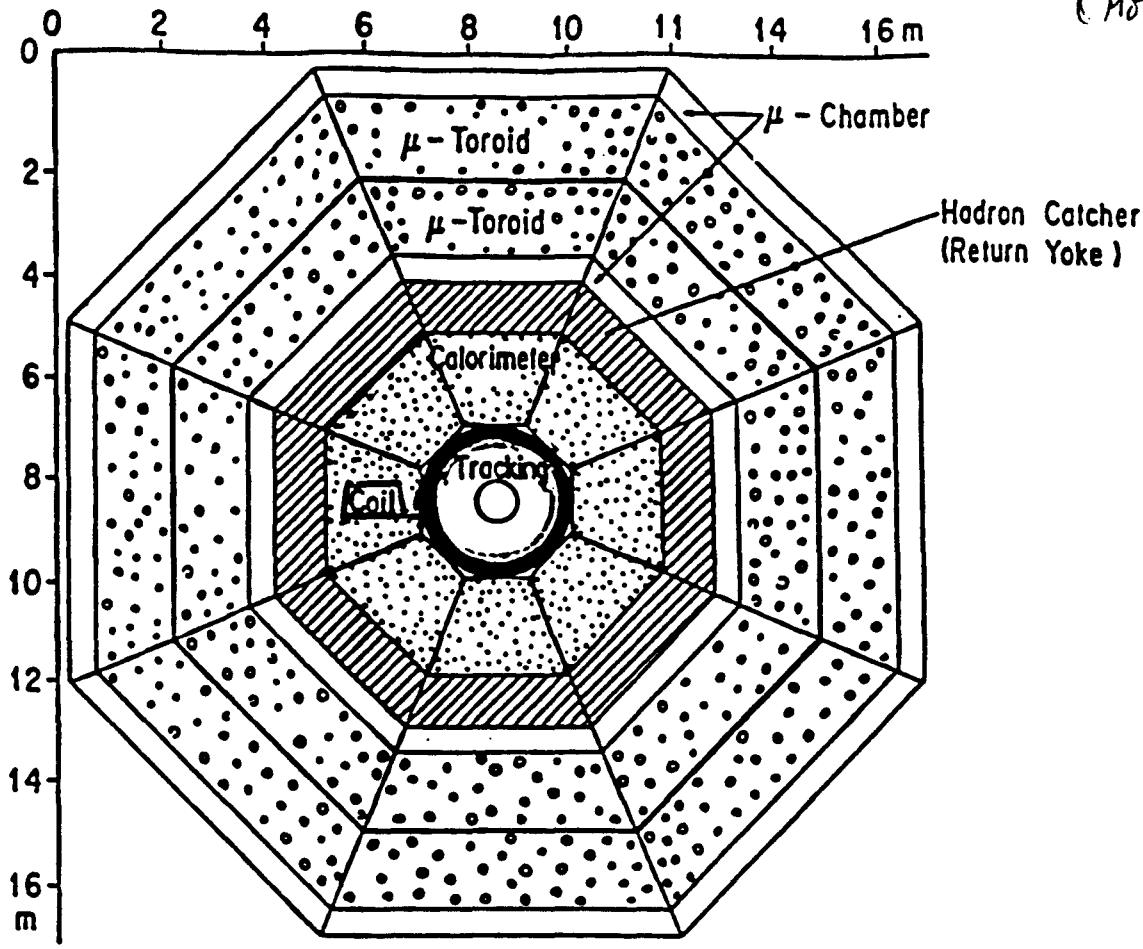
0 2 4 6 8 10 11 14 16 m
μ - Chamber
μ - Toroid
μ - Toroid
Hadron Catcher
(Return Yoke)
Calorimeter
Tracking
Coil
16 m

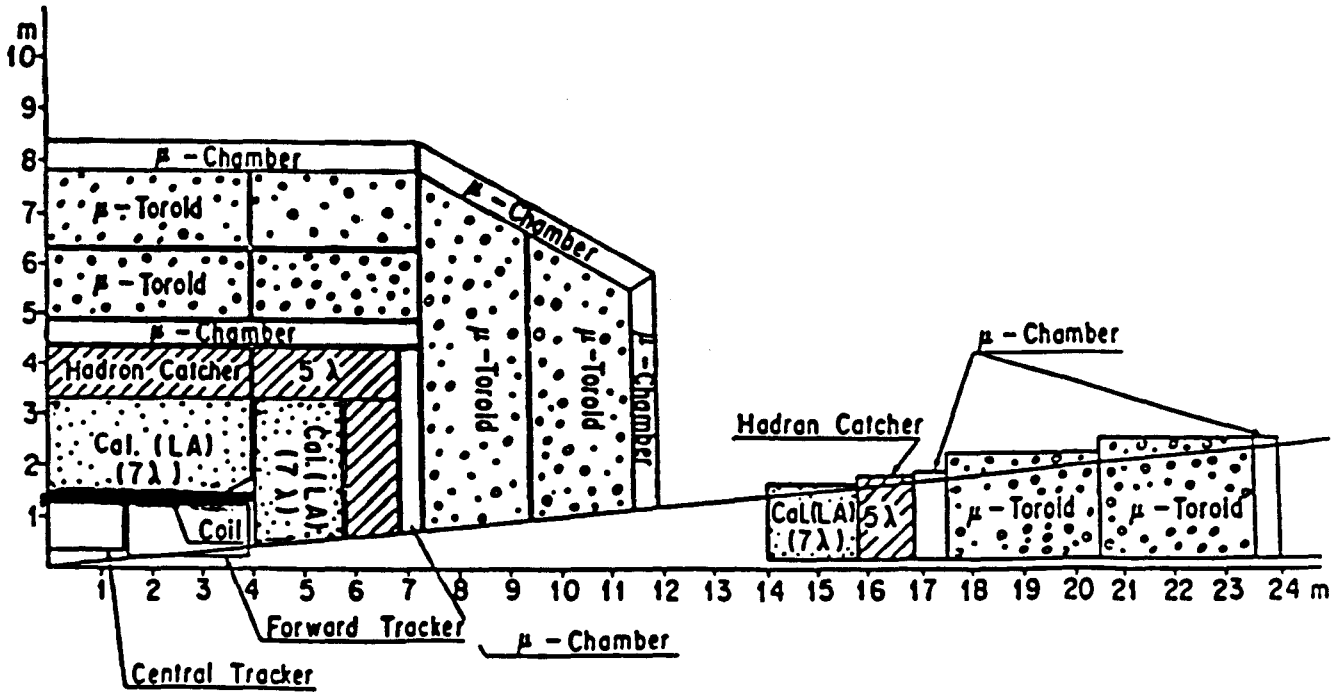
m
μ - Chamber
μ - Toroid
μ - Toroid
μ - Chamber
Hadron Catcher
5 λ
Cal. (LA) (7 λ)
Coil
μ - Toroid
μ - Toroid
μ - Chamber
μ - Chamber
Hadron Catcher
Cal(LA) (7 λ)
5 λ
μ - Toroid
μ - Toroid
1 2 3 4 5 6 7 8 9 10 11 12 13 14 15 16 17 18 19 20 21 22 23 24 m
Forward Tracker
μ - Chamber
Central Tracker

FIELD CONTOUR PLOT

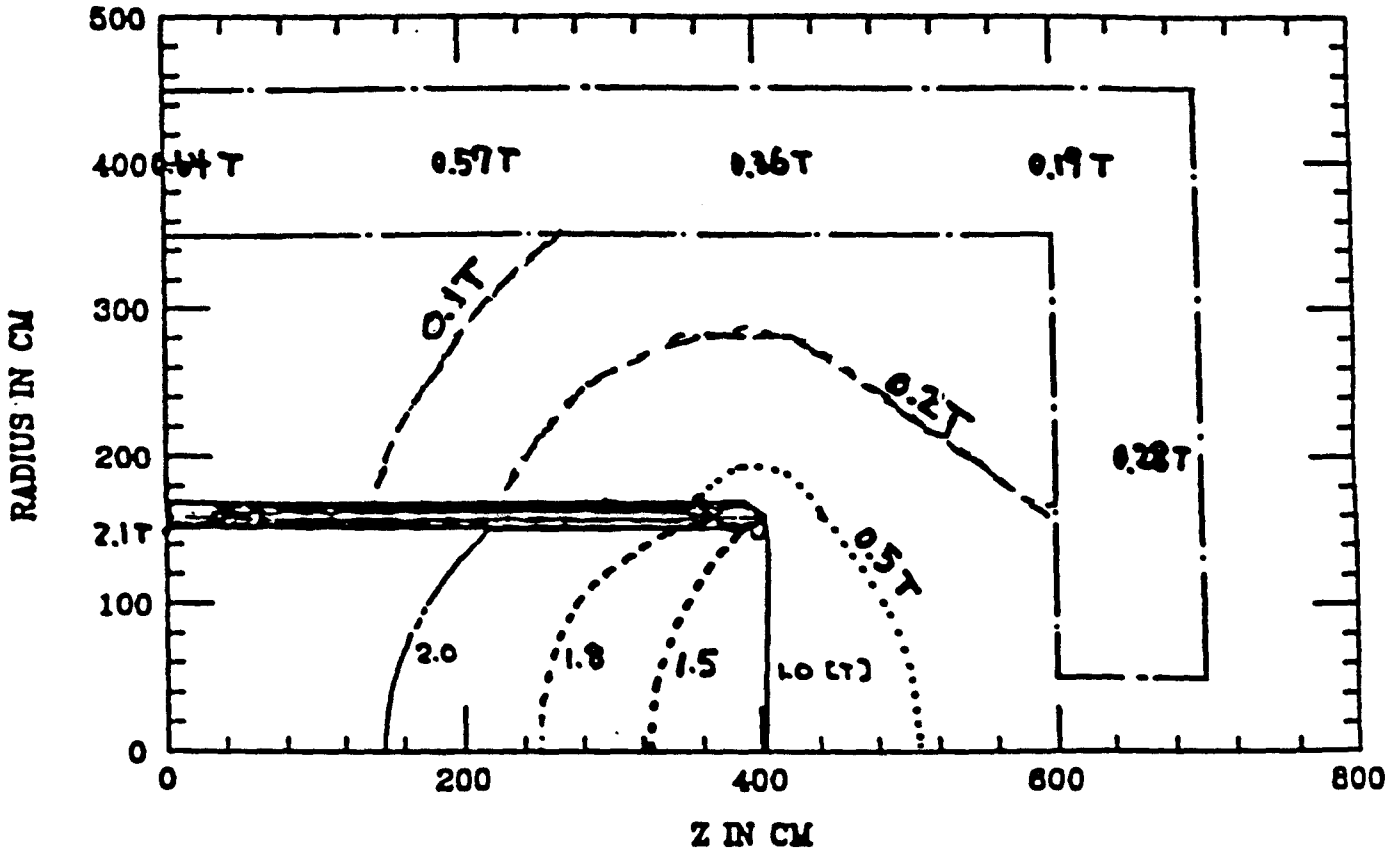

SCD – Snowmass 84
1.5T, 7mϕx11m
~360MJ.

ALEPH (DELPHI) 1.5T, 5.2mϕx7m. 137MJ.

A CONVENTIONAL MAGNETIC DETECTOR FOR THE SUPERCONDUCTING SUPER COLLIDER

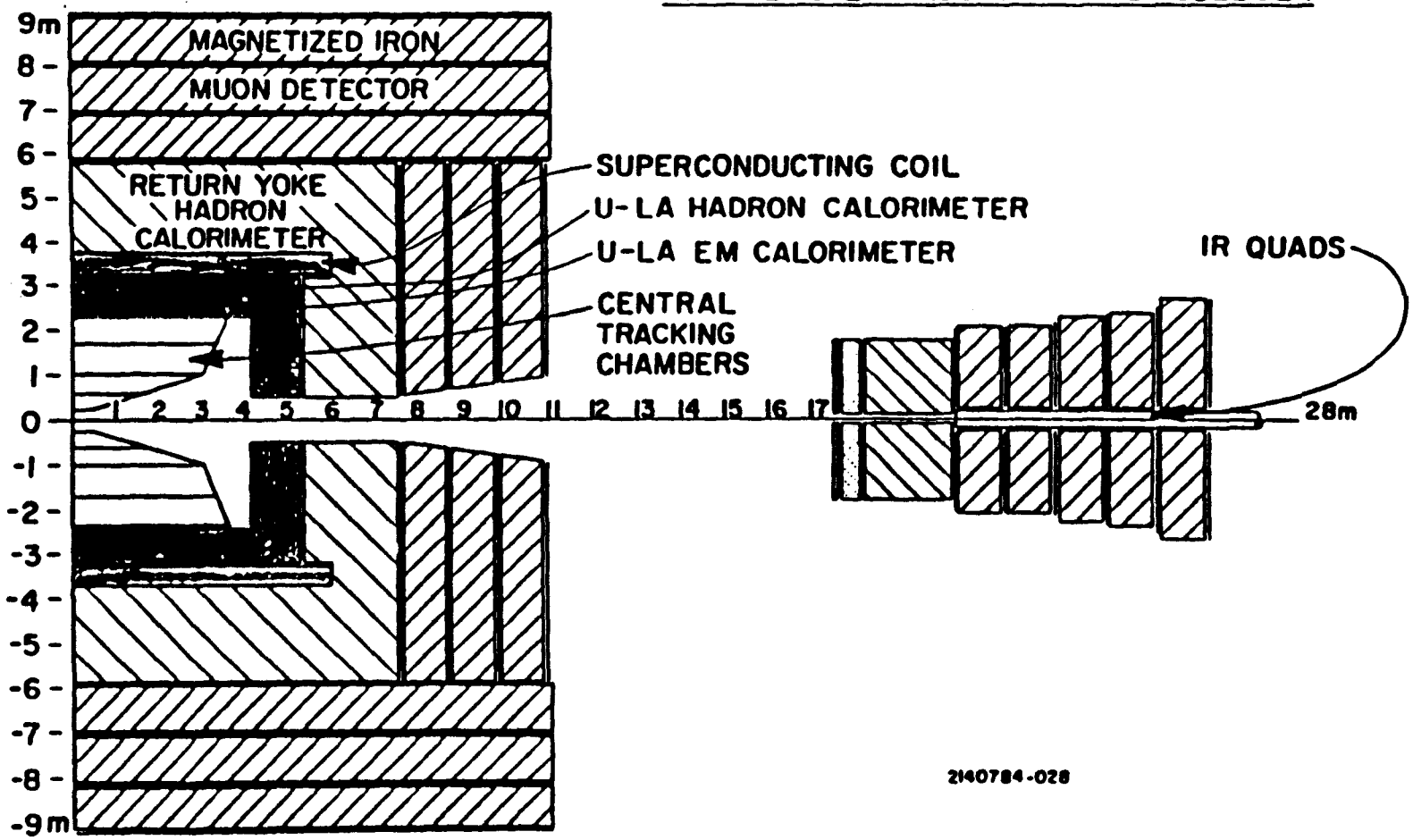

Simple (educated) extrapolation from CDF, TOPAZ, VENUS

M. Wa

$$t_{tot} \approx t_o + t_i + 2 \cdot t_{hoop}$$

$$t_o \sim \left(\frac{P_c \cdot 1.5\, L R^{1.5}}{0.807\, E} \right)^{0.4}$$

$$t_i \sim \frac{1.5\, P}{\sigma} R$$

$$P_{hoop} = 0.01 \cdot (2B)^2$$

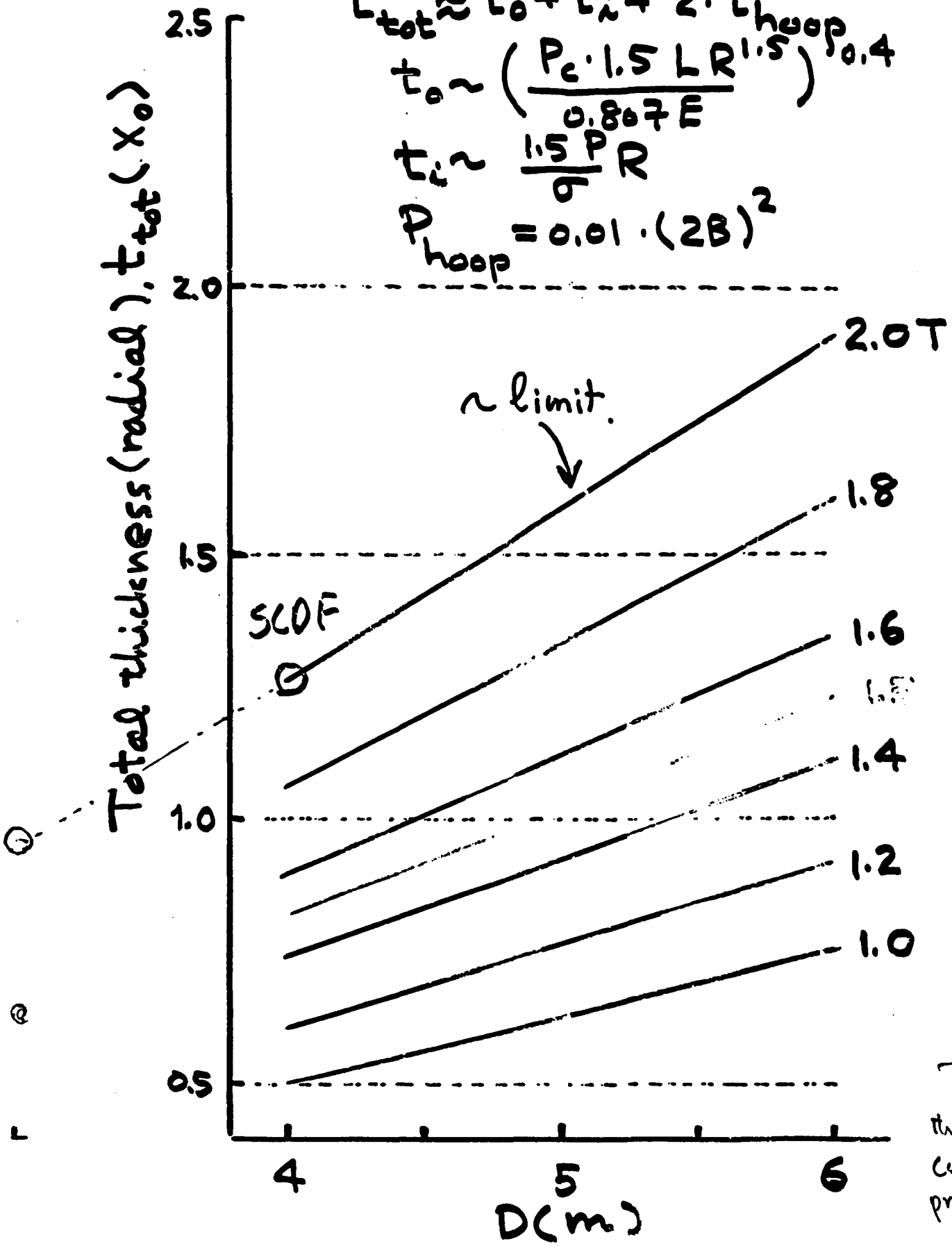

This as
that
compressive
problem

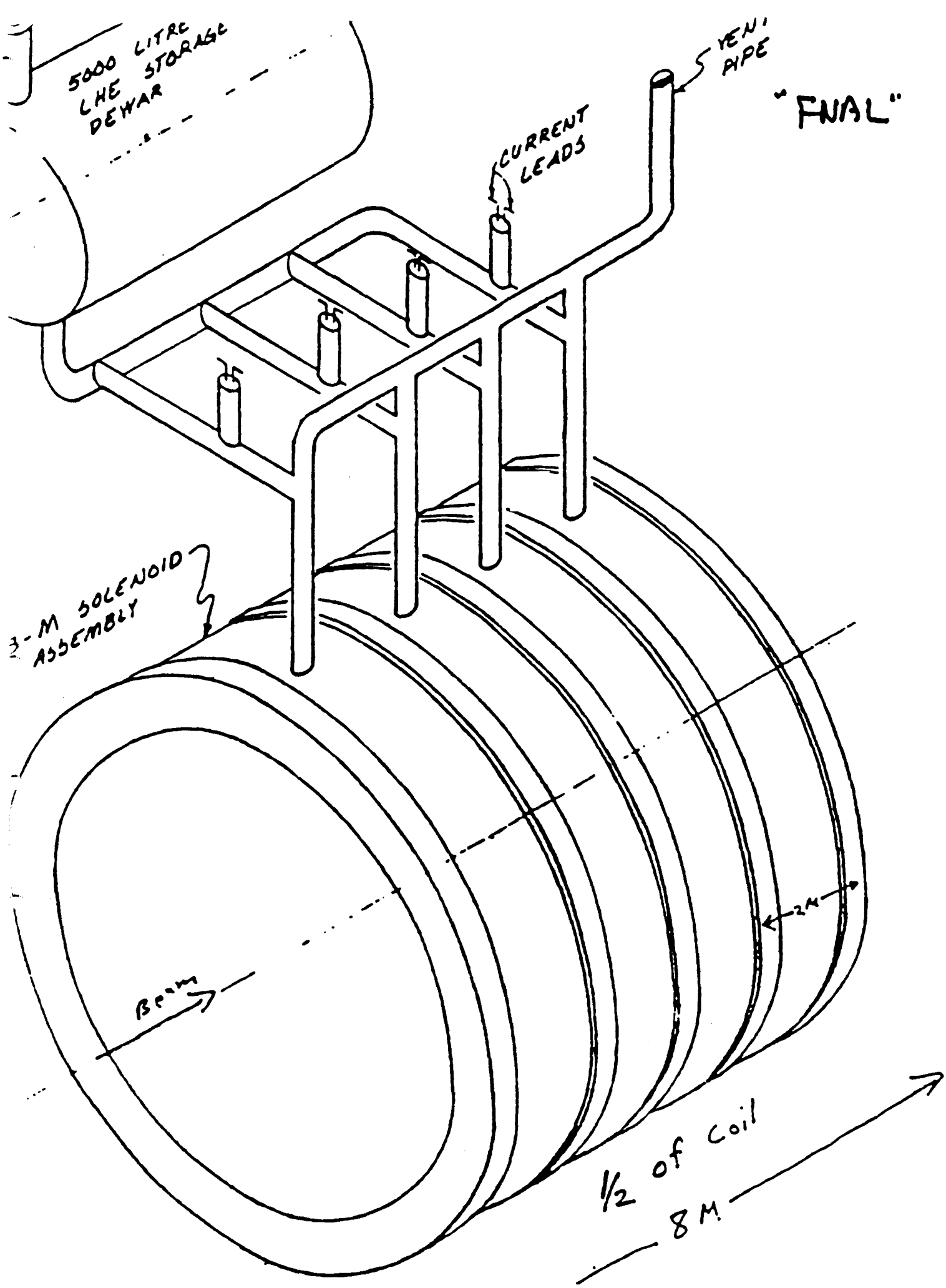
5000 LITRE
LHE STORAGE
DEWAR
VENT
PIPE
"FNAL"
CURRENT
LEADS
3-M SOLENOID
ASSEMBLY
2M
Beam
1/2 of Coil
8 M

FNAL

Coil Cross Section

① Cooling by immersion in LHe @ 4.5K

② He flow via Thermosiphon from Dewer To bottom of each module

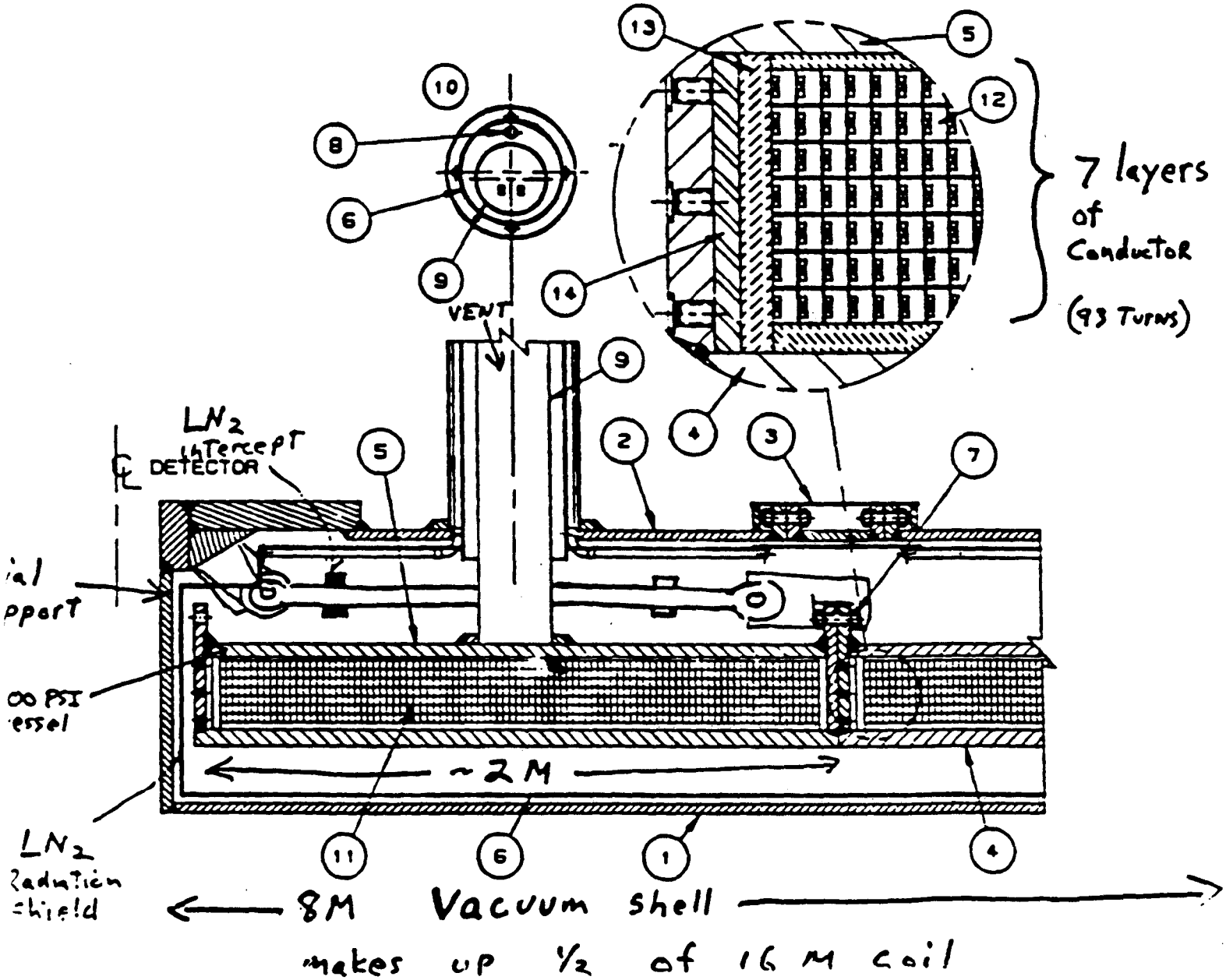

89/01/26 16.52.26 92507

1989.

表3.4.1 超伝導導体の仕様

項目		記号	仕様	備考
AMY-type 構造・寸法			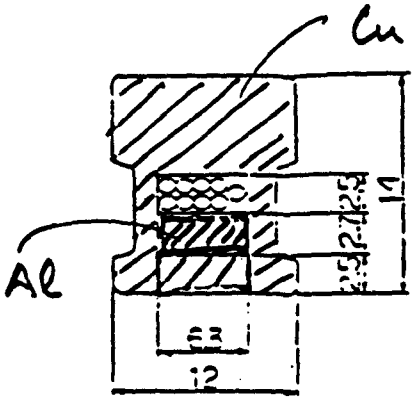	
基本外形寸法			12mm×14mm	
臨界電流		Ic	≧9000A at 4.4T 4.2K	
超伝導素線	材質		NbTi	
	フィラメント径		30μmφ	
	本数		約 1013 本	
	素線径		1.35mmφ	
	銅比	m	1.0	
	ツイストピッチ	ℓt	30 mm	
ストランド	本数	ns	9 本	
	ストランドピッチ	ℓs	50 mm	
	外形寸法		6.3mm×2.5mm	
銅被アルミ	外形寸法		6.3mm×2.7mm	
	銅部分の割合		25 %	
	アルミ電気比抵抗	ρAℓ	≦0.3×10^{-8} Ωcm at 3T	
安定化基材	材質		1/2H 無酸素銅	
	電気比抵抗	ρcu	<3×10^{-8} Ωcm at 3T	
	0.2%耐力	σ0.2	≧30 kg/mm^2	
銅断面積		Acu	116.0mm^2	
アルミ断面積		AAℓ	11.8mm^2	
等価電気比抵抗		ρeff	1.64×10^{-8} Ωcm at 3T	

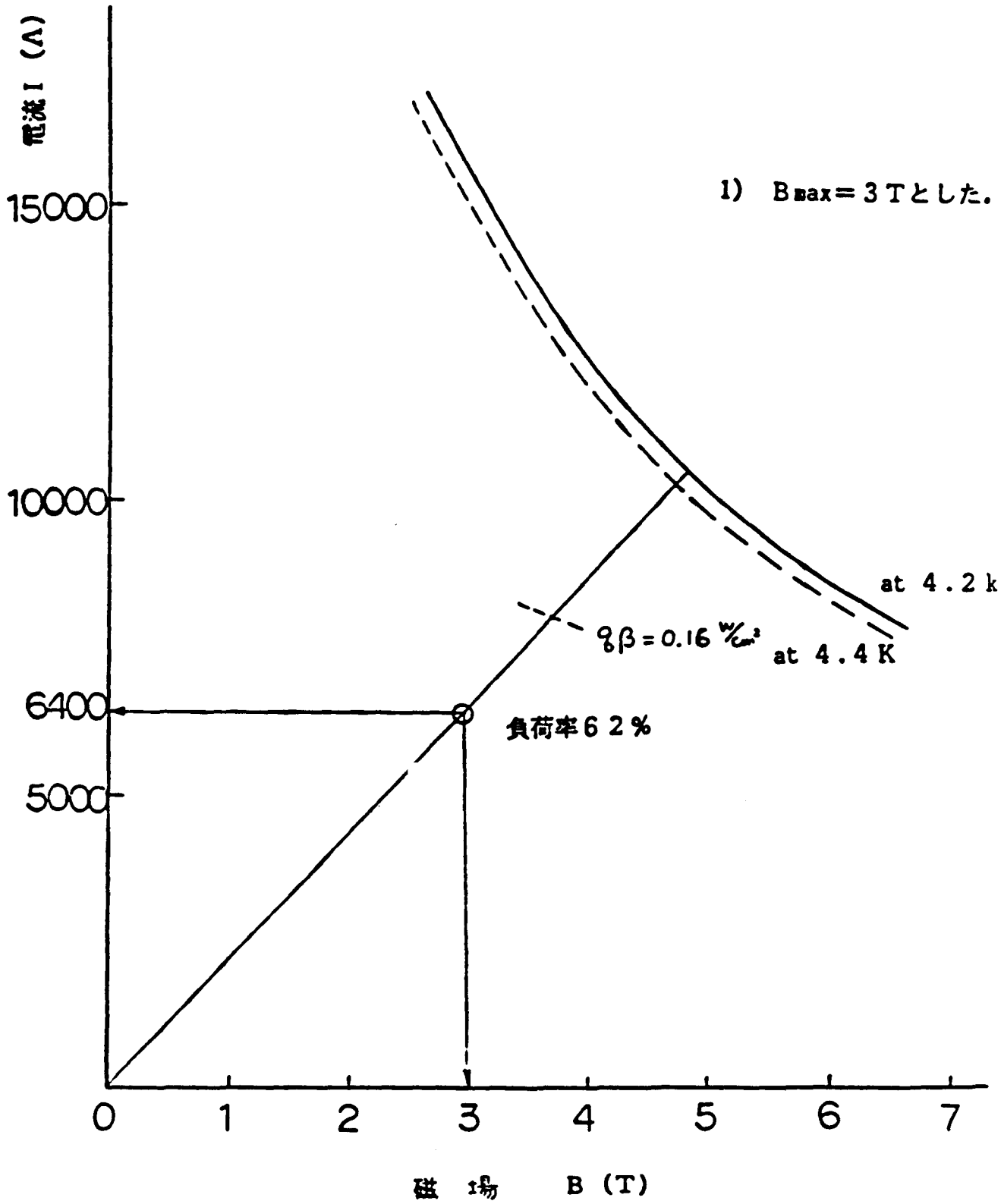
電流 I (A)
15000
10000
6400
5000
1) Bmax＝3Tとした。
at 4.2 k
at 4.4 K
qβ = 0.16 W/cm²
負荷率62%
0
1
2
3
4
5
6
7
磁 場 B (T)

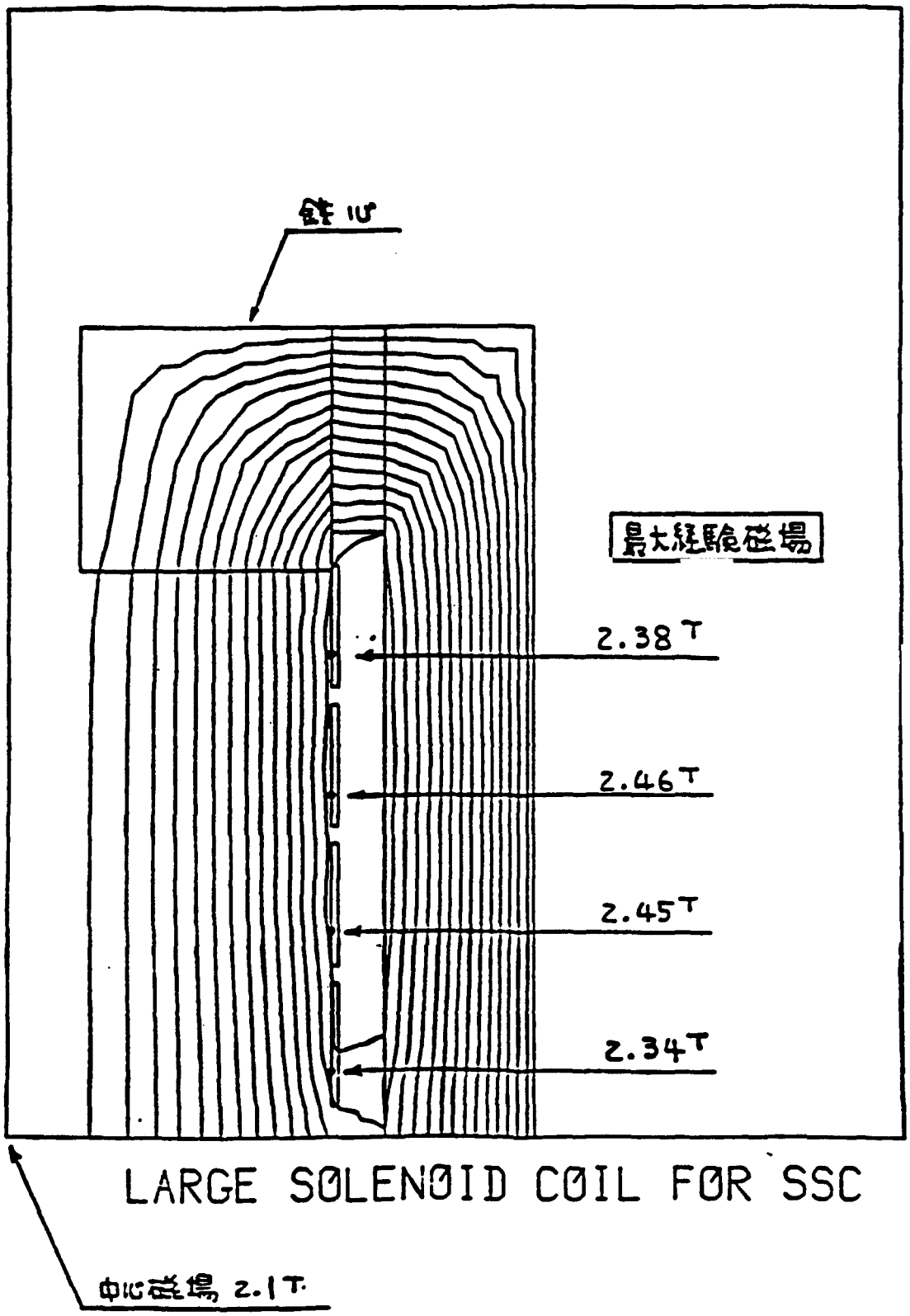
鉄心
最大経験磁場
2.38 T
2.46 T
2.45 T
2.34 T
LARGE SOLENOID COIL FOR SSC
中心磁場 2.1 T

図3.3.2

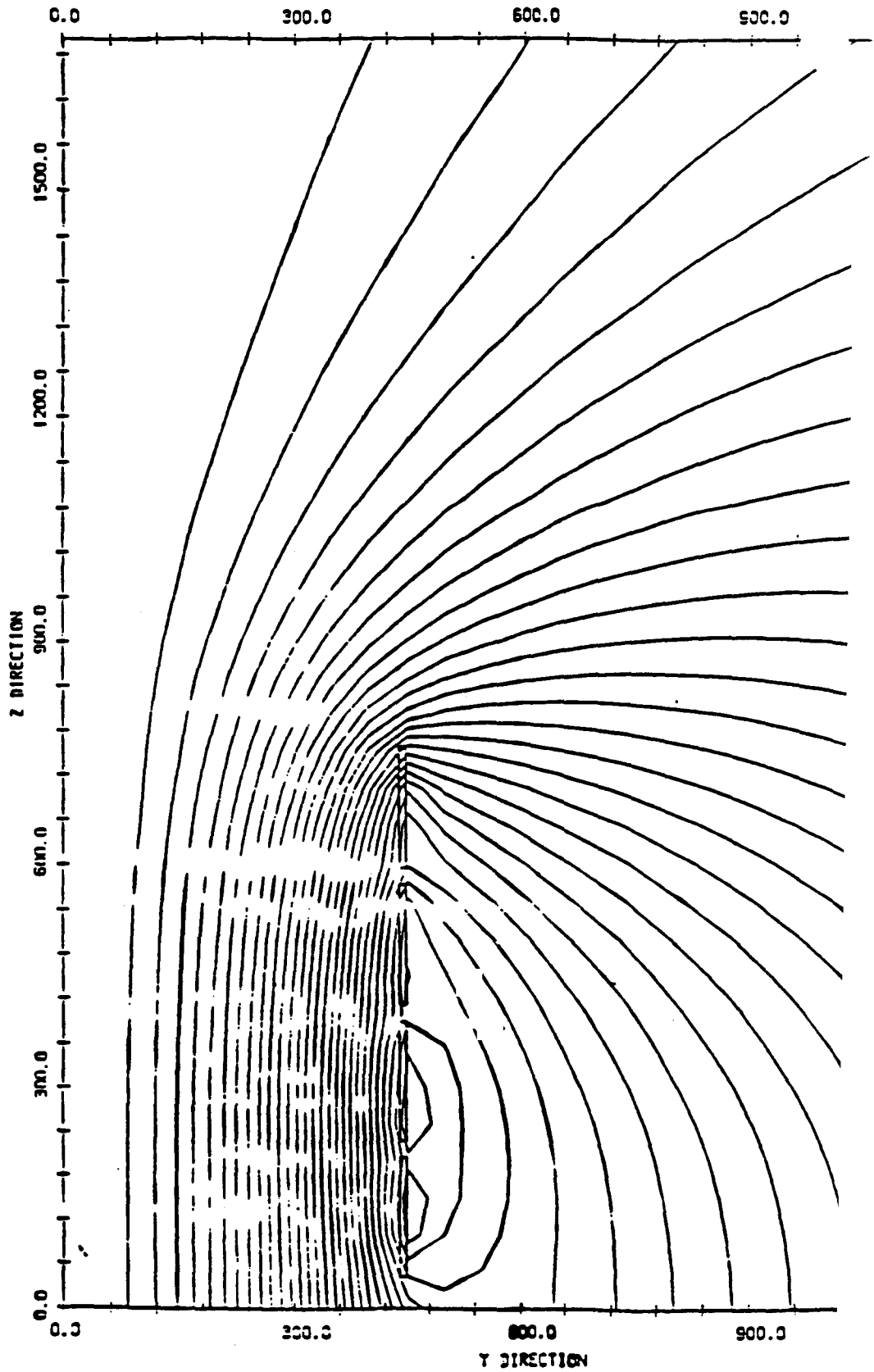

FIG. LARGE SOLENOID COIL

☑ 3.3.3

Quench simulations

表3．6．1　計算ケース

ケース	回路条件										動作条件				
	X電源　Y保護方式				導体．設計電流		保護抵抗				コイル間カップリング		1コイルクエンチ後の他コイル動作		遮断器が動作しない時
	X≡8 Y≡8	X≡4 Y≡4	X≡2 Y≡2		導体(1) I=6400A	導体(2) I=5000A	0.1Ω	0.15Ω	0.2Ω		考慮	考慮せず	遮断	遮断せず	
(1)		○			○			○			○		○		
(2)		○			○		○				○		○		
(3)		○			○				○		○		○		
(4)		○			○			○			○			○	
(5)		○			○			○			○			○	○
(6)		○				○		○			○		○		
(7)		○				○		○			○			○	
(8)		○				○		○			○			○	○

(注1)　導体(1)　：　今年度設計

(注2)　導体(2)　：　前年度設計

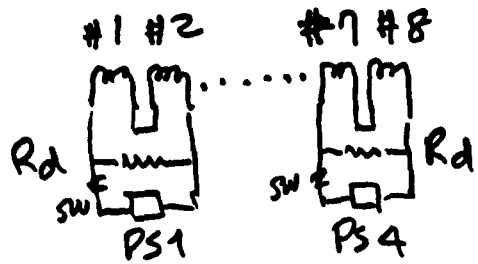

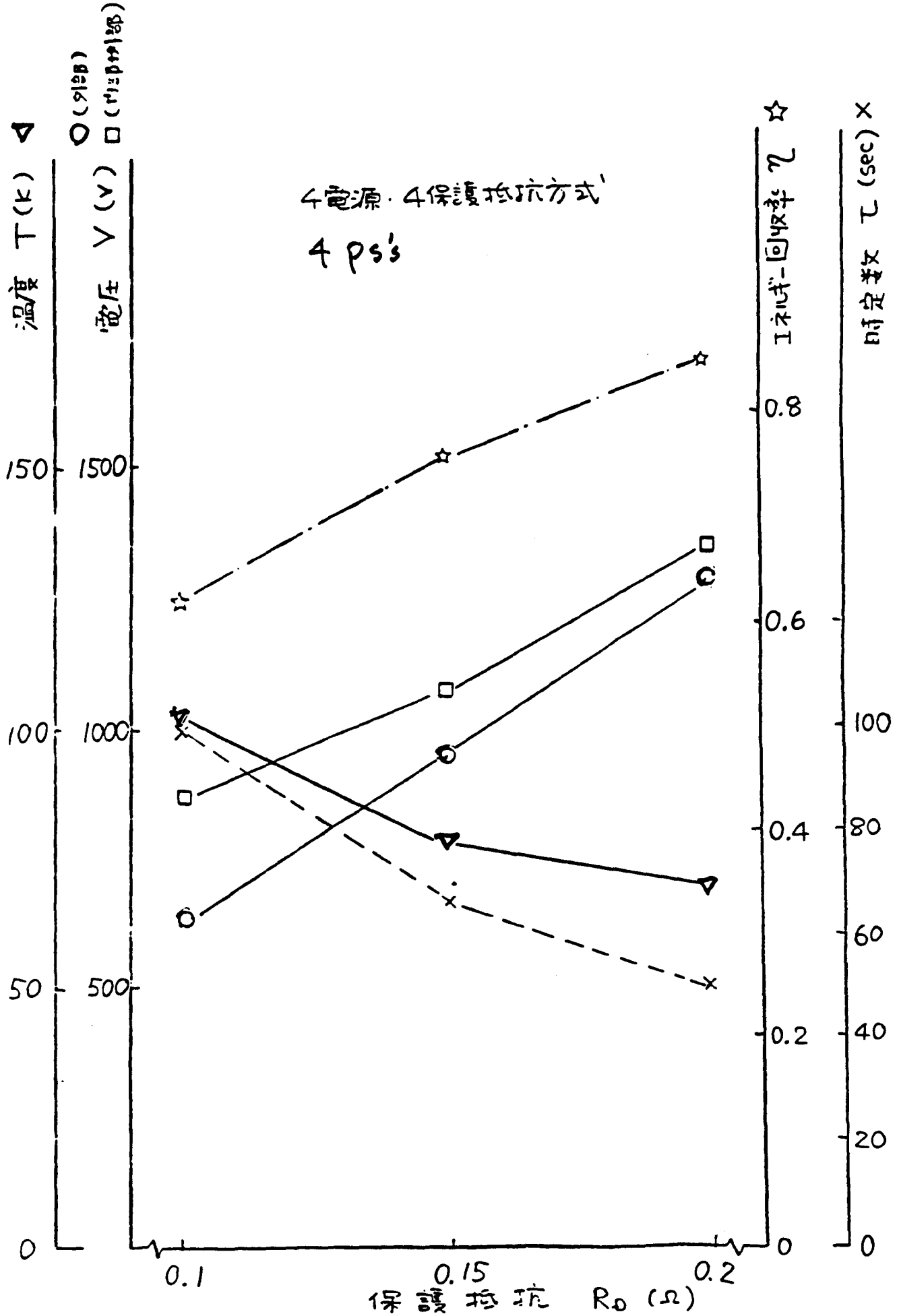

図3.6.7 クエンチ解析（保護抵抗依存性）

遮断条件を変えた場合の検討

次に、R＝0.15Ωの場合で、遮断条件を変えた場合(表3.6.1のNo④,⑤)についての計算結果を以下に示す。表3.6.1のNo5は、保護動作失敗を想定したものである。

ケースNO	t = 0 ~ 200 sec			t = 0 sec	図NO
	電流(A)	到達温度(K)	内部電圧(V)	外部(端子)電圧(V)	
3	① 650 ② 1350 ③ 1350 ④ 1100	① 80	① 115	① 960	図3.6.3
4	① 400 6750 ③ 6500 ④ 6400	① 58	① 60	① 960	図3.6.6
5	① 1600 ② 6800 ③ 6500 ④ 6400	① 220	① 960	① ~~960~~ 0	図3.6.7

(注) ○内数字はモジュールNOを示す。

コイルNo	ケース④		ケース⑤	
	$\lvert F_R \rvert$ (kg)	$\lvert F_z \rvert$ (kg)	$\lvert F_R \rvert$ (kg)	$\lvert F_z \rvert$ (kg)
#1	3.20×10^{6}	1.34×10^{5}	3.94×10^{6}	1.84×10^{5}
#2	3.08×10^{6}	2.33×10^{5}	3.85×10^{6}	2.46×10^{5}
#3	1.23×10^{7}	1.37×10^{6}	1.24×10^{7}	1.17×10^{6}
#4	1.22×10^{7}	2.67×10^{6}	1.13×10^{7}	2.64×10^{6}

net $|F_z| \sim 3\times10^{6}$ kg

Construction schedule

表11.1 製作工程・スケジュール（案）

~5 years

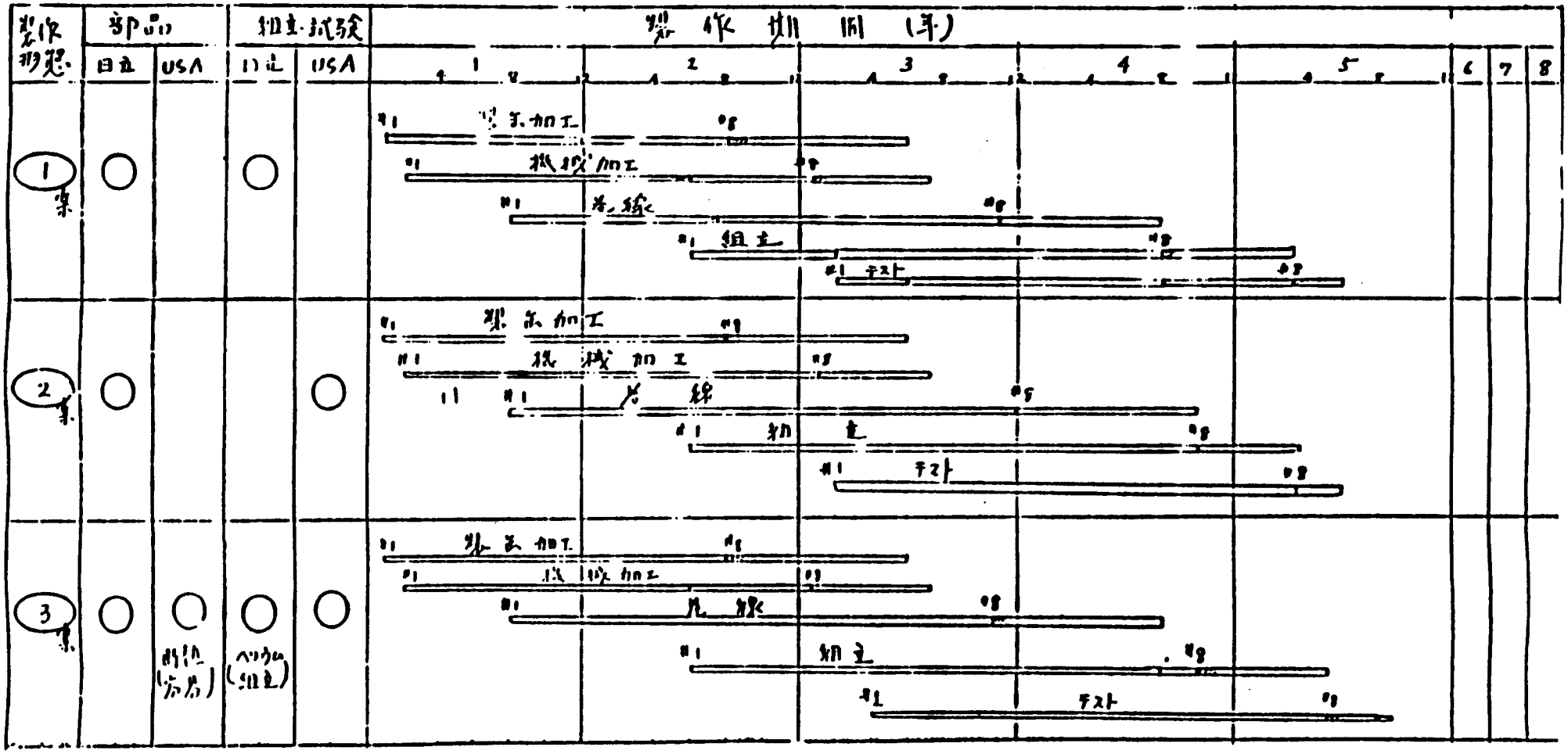

超伝導マグネット(モジュール状態)の超伝導性能試験は、その予冷から通電までかなり膨大な設備を必要とする。実機大型超伝導ソレノイドに使用されるLN_2設備、LHe関連設備・システムを先行・設置することにより、共用可能な構成に配置しておくことが、関連設備の重複設置を避け、効率的運転が可能となる。

試験完了した超伝導マグネットは速やかにビームライン近接の組立ホールへ搬出し、スペースを有効に活用する必要がある。

図12.3.1に以上の概念を組み入れた Site shopの構成例を示す。

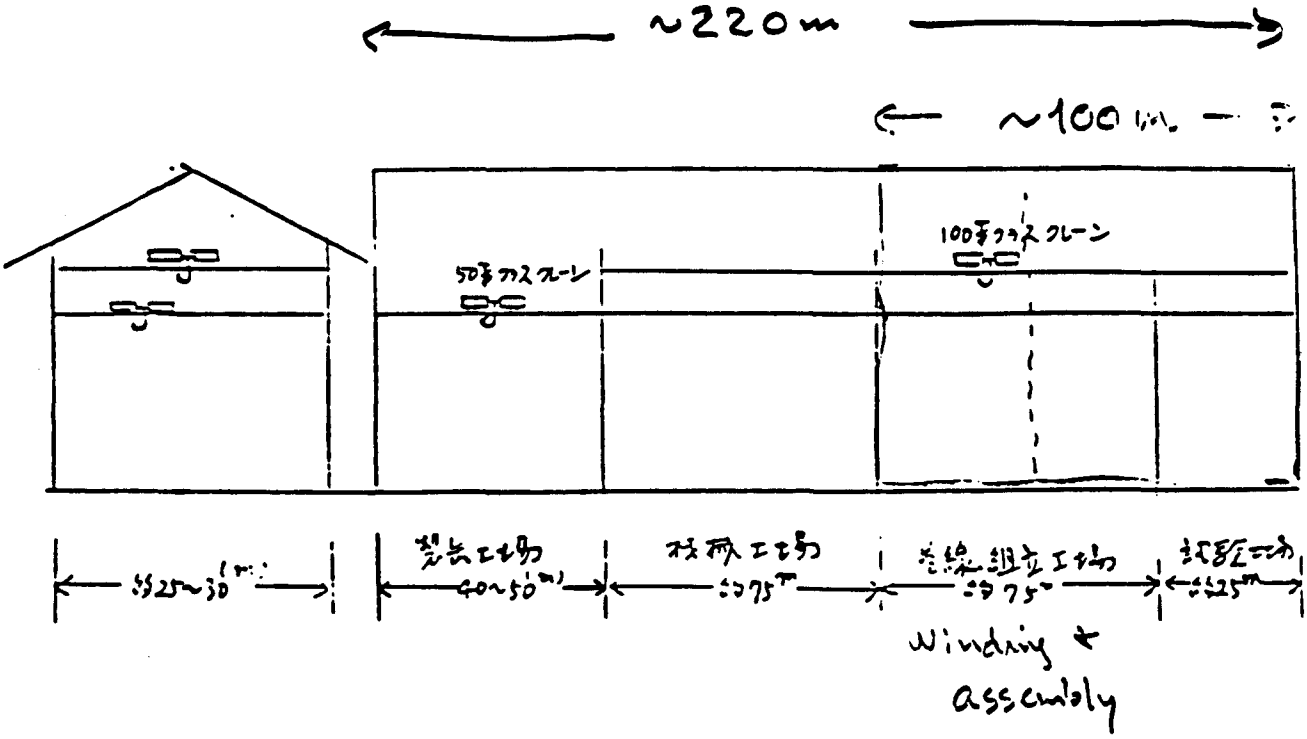

図１２．３．１ 工場構成(例)

注(1) 機械工場には、機械加工物の他に、部分的な部品に一時保管場所を確保する。

(2) 超伝導性能確保試験を完了した超伝導マグネット(モジュール)は速かにビームラインに近接の組立ホールへ搬出するものである。

Comparison of Parameters of the Large Solenoid
Tsukuba/Hitachi vs. Fermilab

Items	Tsukuba/Hitachi (1989)	Fermila
Conductor		
Dimensions	14x12 mm^2	16x18
Current	6400 A	5000
Critical current	11.6 kA at 4.4T	10 kA
Stabilizer current	4000 A/cm^2	1765
Coil		
Number of layers	6	7
Number of modules	8	8
Number of PSs	4	1
PS connection	#1-#8, #2-#7 #3-#6, #4-#5	–
Cold mass	390 t	880 t
Vacuum shell	(1)8 m x 2 or (2)16 m x 1	8 m x

T_{max}, Γ : fixed

#1 #2 #8

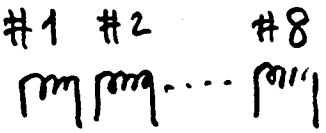

$$V_{max} \sim \frac{J_0^2}{I_0}$$

$$\left(\left(\frac{4000}{1765}\right)^2 \right.$$

Axial Supports **Tsukuba/Hitachi Design**

Items	(1)8 m x 2	(2)16 m x 1
Axial load	2.5×10^6 kg[(A)]	70×10^3 kg
Axial supports		
Materials	Inconel 718	Inconel 718
Cross section		
Inner/outer diameter (mm)	100/70	30/20
Length (mm)	1000	300
Number of supports	18 x 2	6
Stress (magnetic forces)	35.4 kg/mm^2 (tension)	29.7 kg/mm^2 (tens./compr.)
Thermal leak		
LHe system	67 W	3.6 W
LN_2 system	1376 W	74 W

(A) This load corresponds to the static electromagnetic forces. During quenches it is expected to be near or above 3×10^6 kg. Careful analyses will be carried out soon.

hoop stress:
$P \approx B^2/2\mu \sim 9\,atm.$

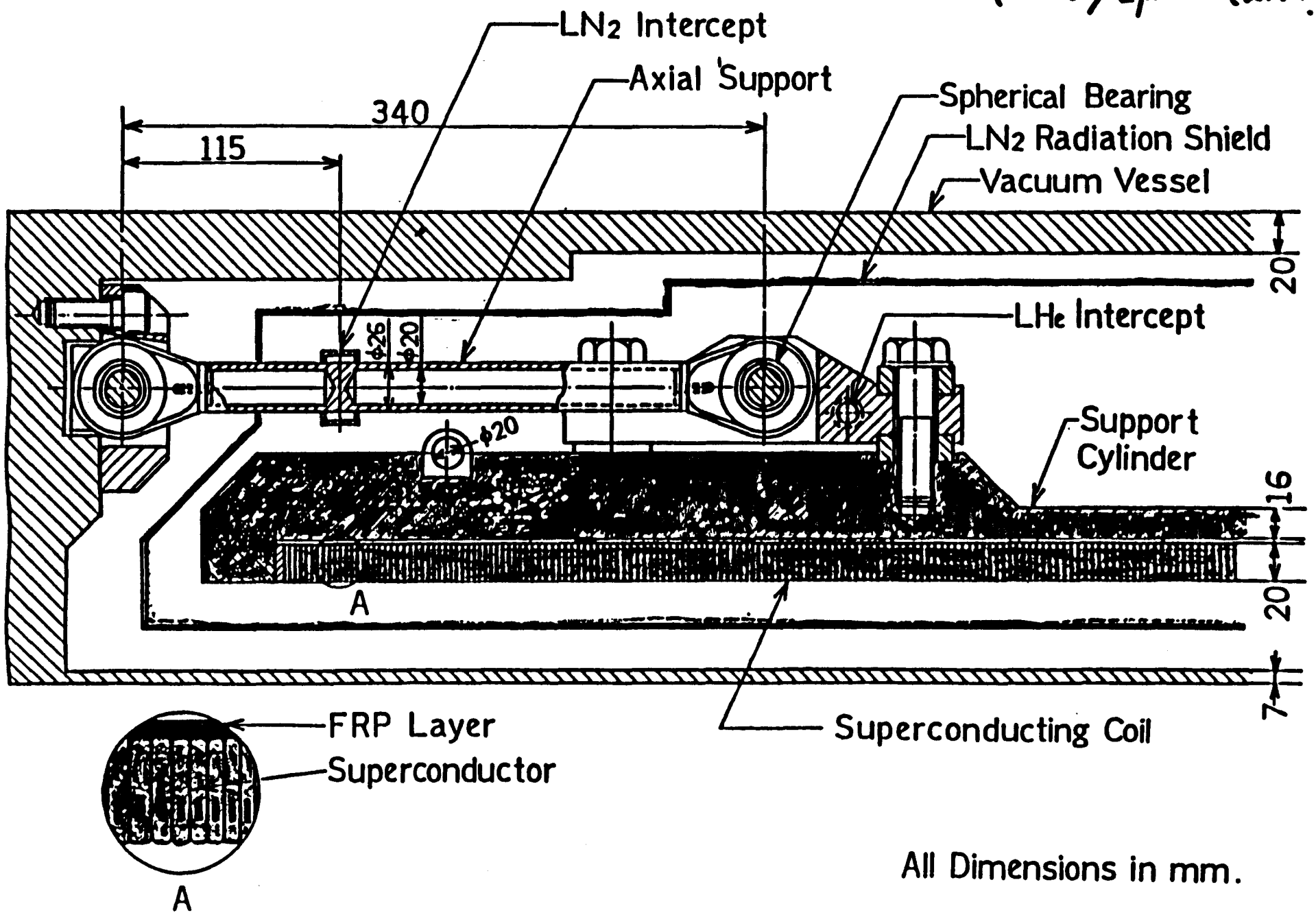

Figure 2.

R. Kephart.
4/89

COIL MANUFACTURING /TRANSPORTATION ISSUES

PROBLEM:

Even if divided into 2 M modules
- LARGE dia > 33 feet
- HEAVY weight > 125 tons
- yet Delicate

Is it feasible to build the coil in industry and move it to the site ?

MANUFACTURING:

Few companies have machine tools that accept 33 foot dia. objects. (eg vertical lathes or winding machines)

- Large = special = expensive
- Limits vendors (or develop NEW construction methods ?)

TRANSPORTATION

- Can't transport it by RAIL or AIR
  1) eg CDF coil move from Japan --CSA ? weight ok but < 14 feet AN125 ?
  2) rail limit < 15 feet
- Ship/barge OK but limits vendors to those with sea access.
- Transport by Truck
  1) practical only for short distances. (eg interstate bridge < 28')
  2) LEP coils near practical max size for Europe.

BUT (Some help from BIG sky country !)

It appears to be possible to move 2M modules by land from a deep water port at Freeport, Tex. to the Waxahachie SSC site.

1) EXPENSIVE... - not much BELDING estimate $ 350 K from Freeport.
2) Moving an 8M coil half (500 T) appears to be not practical.
3) Conclude that significant on-site assembly and testing facilities will be required.

R.K.

CONCLUSIONS

1) The proposed SSC LARGE SOLENOID MAGNET can be built assuming a reasonable extrapolation of existing superconducting magnet technology.

2) The main engineering challenges are those posed by its LARGE SIZE and STORED ENERGY.

3) Severe transportation problems may require significant on site assembly and testing facilities.

4) Additional work is still needed :

   a) Engineering Analysis (eg forces during a quench)
   b) Yoke design
   c) Coil manufacturing techniques
   d) Costs
   e) Realistic time estimates
      (long ! 4-5 years must start soon!)

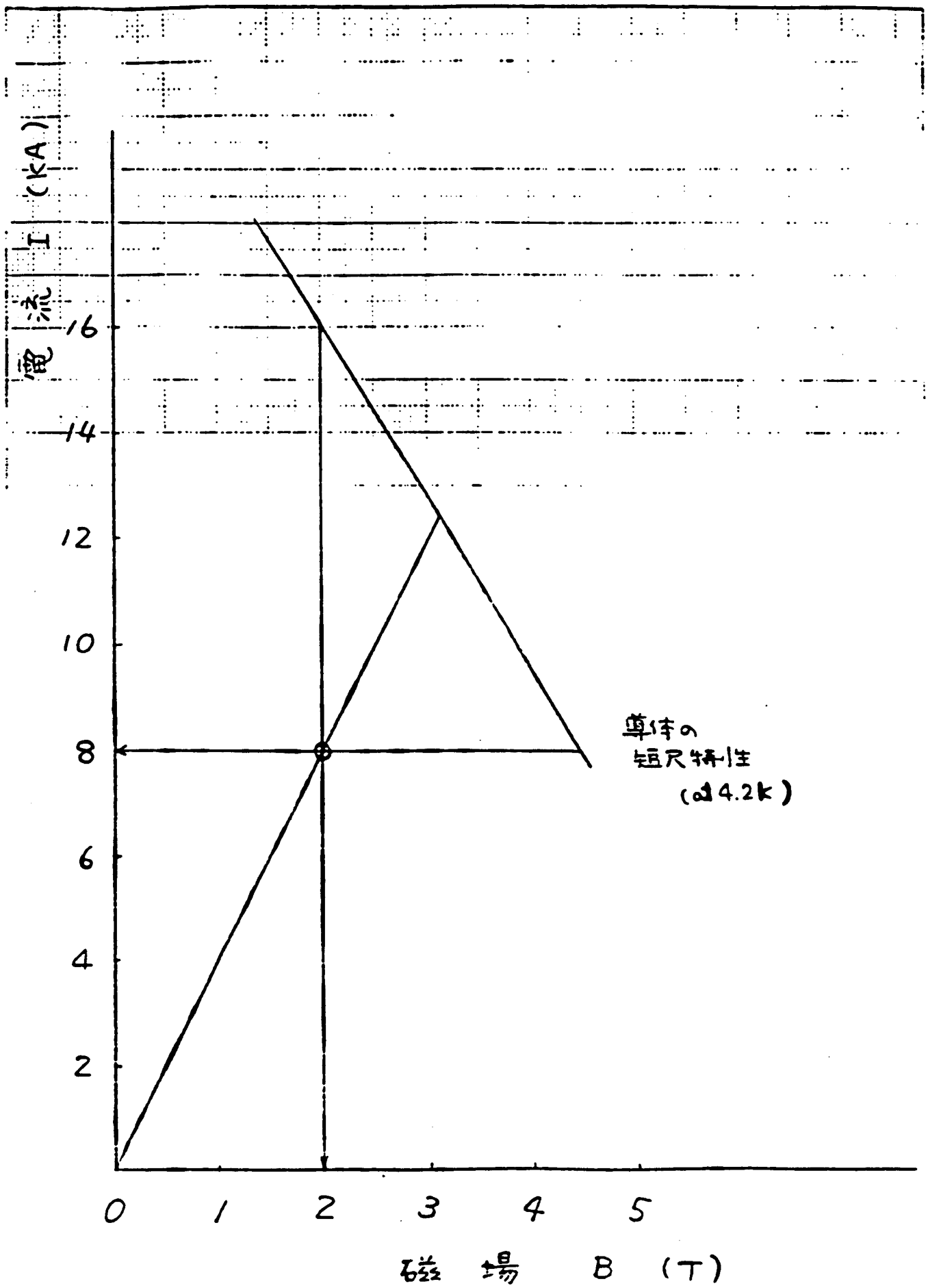
電流 I (KA)
16
14
12
10
8
6
4
2
0
1
2
3
4
5
磁場 B (T)
導体の
短尺特性
(at 4.2K)

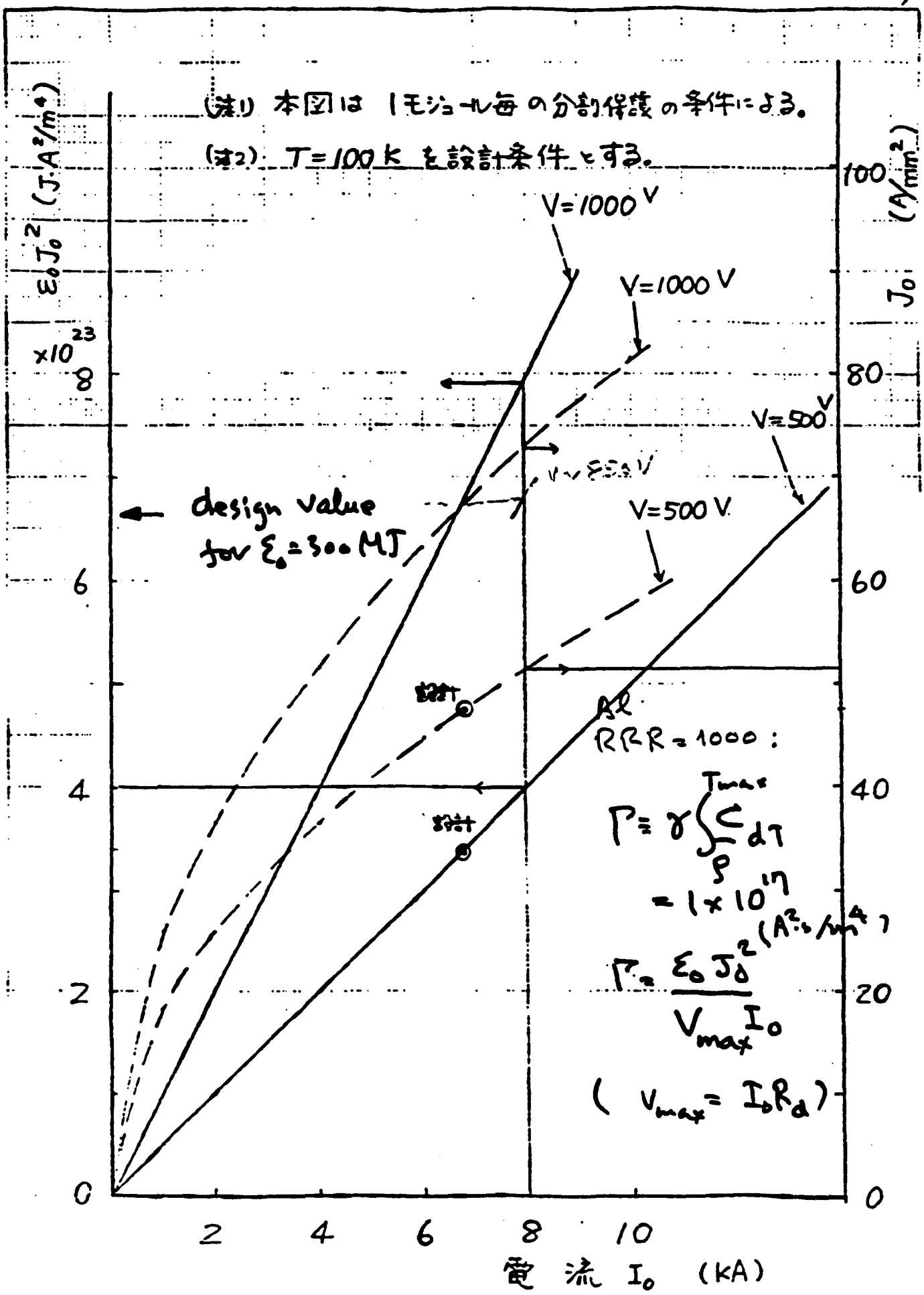
(注1) 本図は 1モジュール毎の分割保護の条件による。
(注2) T=100K を設計条件とする。
$\varepsilon_0 J_0^2$ (J·A²/m⁴)
×10²³
J_0 (A/mm²)
V=1000 V
V=1000 V
V=500 V
V=500 V
design value for ε_0=300 MJ
設計
設計
Al
RRR=1000 :
$\Gamma = \gamma \int_{\rho}^{T_{max}} \frac{C}{\rho} dT$
$= 1 \times 10^{17}$ (A²·s/m⁴)
$\Gamma = \frac{\varepsilon_0 J_0^2}{V_{max} I_0}$
($V_{max} = I_0 R_d$)
電流 I_0 (kA)

Thin Solenoids without Return Yokes

*Aluminum-stabilized NbTi/Cu

*Indirectly cooled, forced flow two-phase helium

Items	CDF (Yoke)	ZEUS	Small
Diameter (m)	3	2	3
Length (m)	5	2.8	8
Field (T)	~~0.84~~ 0.72 (1.5)	1.8	2
Energy (MJ)	9.4 (30)	16	99
Conductor			
Dimension (mm^2)	4x20	4.3/5.5 x15	5.6x35
RRR of Al	2000	700	?
Winding			
Layer	1	2	1
Axial preload (kg/mm^2) (room temperature)	1.0	2	?
Axial comp. load (4k)			
Total (t)	170 (540)	390	1460
Stress (kg/mm^2) (Conductor only)	0.9 (2.9)	2.2	4.4

CDF R.Y. Jan 81

Fig. 5 3 m ϕ, 5 m long (200") Solenoid

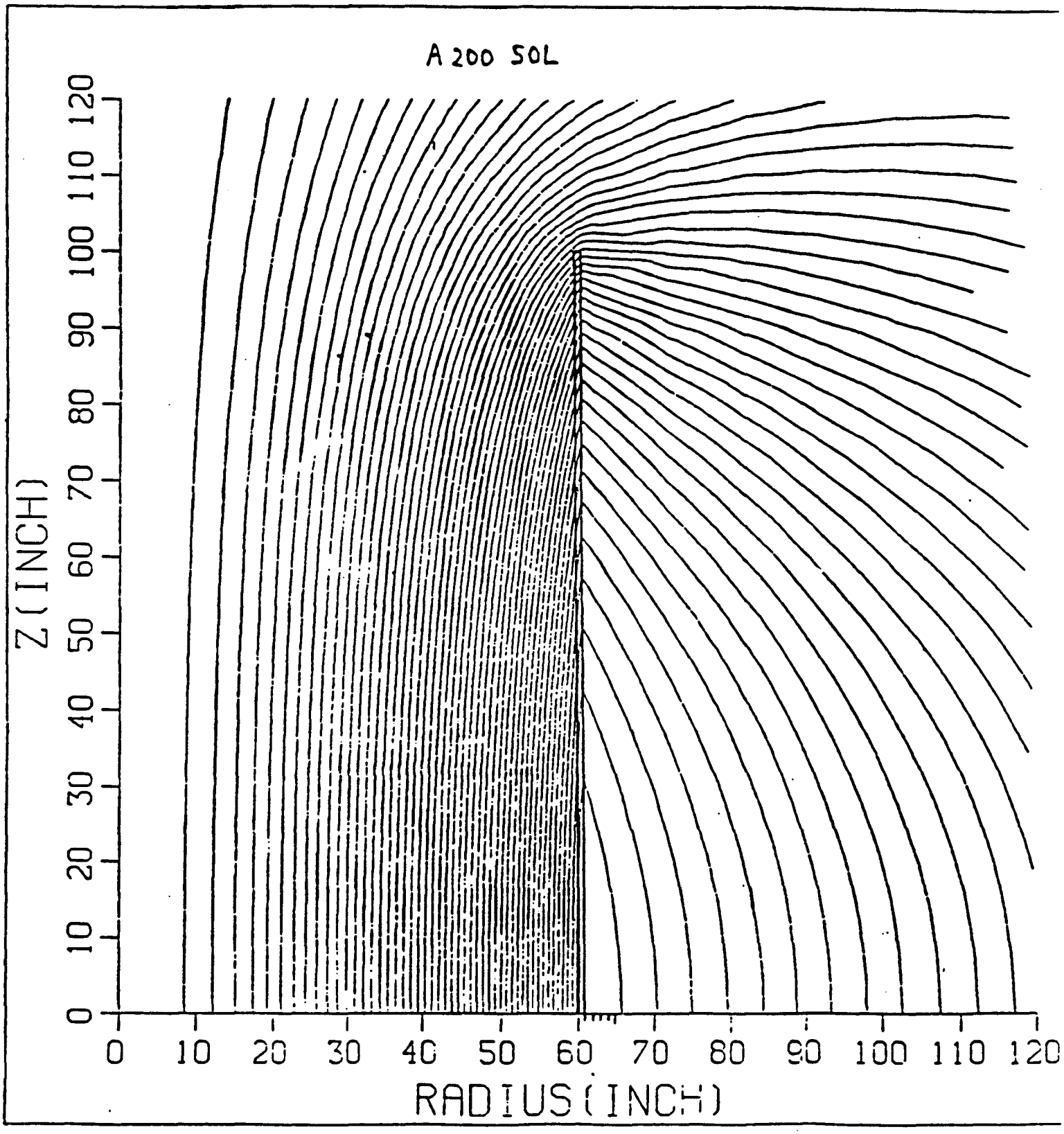

Coil $r = 60" \sim 61"$

$z = 0 \sim 100"$

"CDF"

R.Y. Jan 81

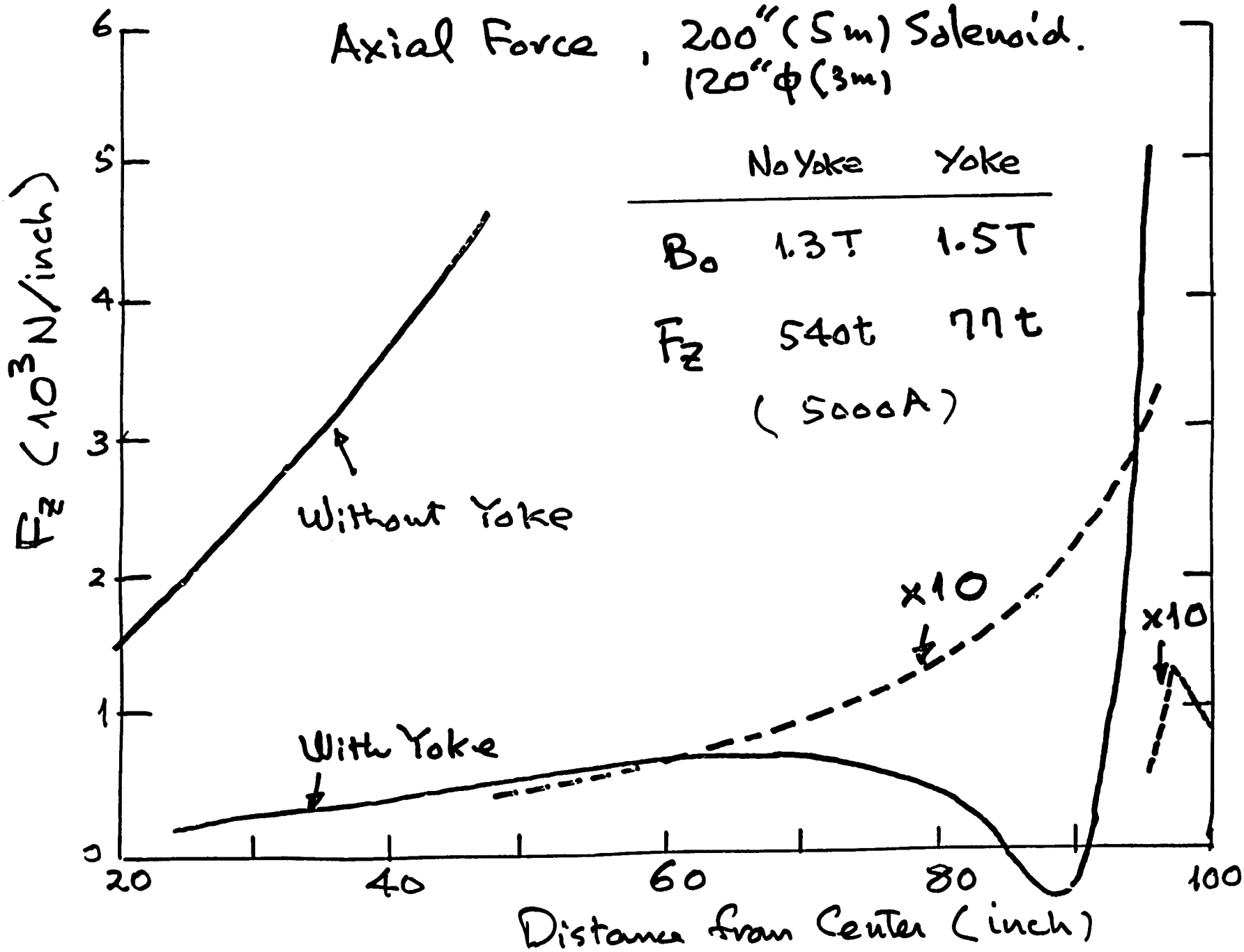
Axial Force, 200" (5m) Solenoid.
120" φ (3m)
No Yoke
Yoke
B_0 1.3T 1.5T
F_z 540t 77t
(5000A)
Without Yoke
With Yoke
x10
x10
F_z (10^3 N/inch)
0
1
2
3
4
5
6
20
40
60
80
100
Distance from Center (inch)

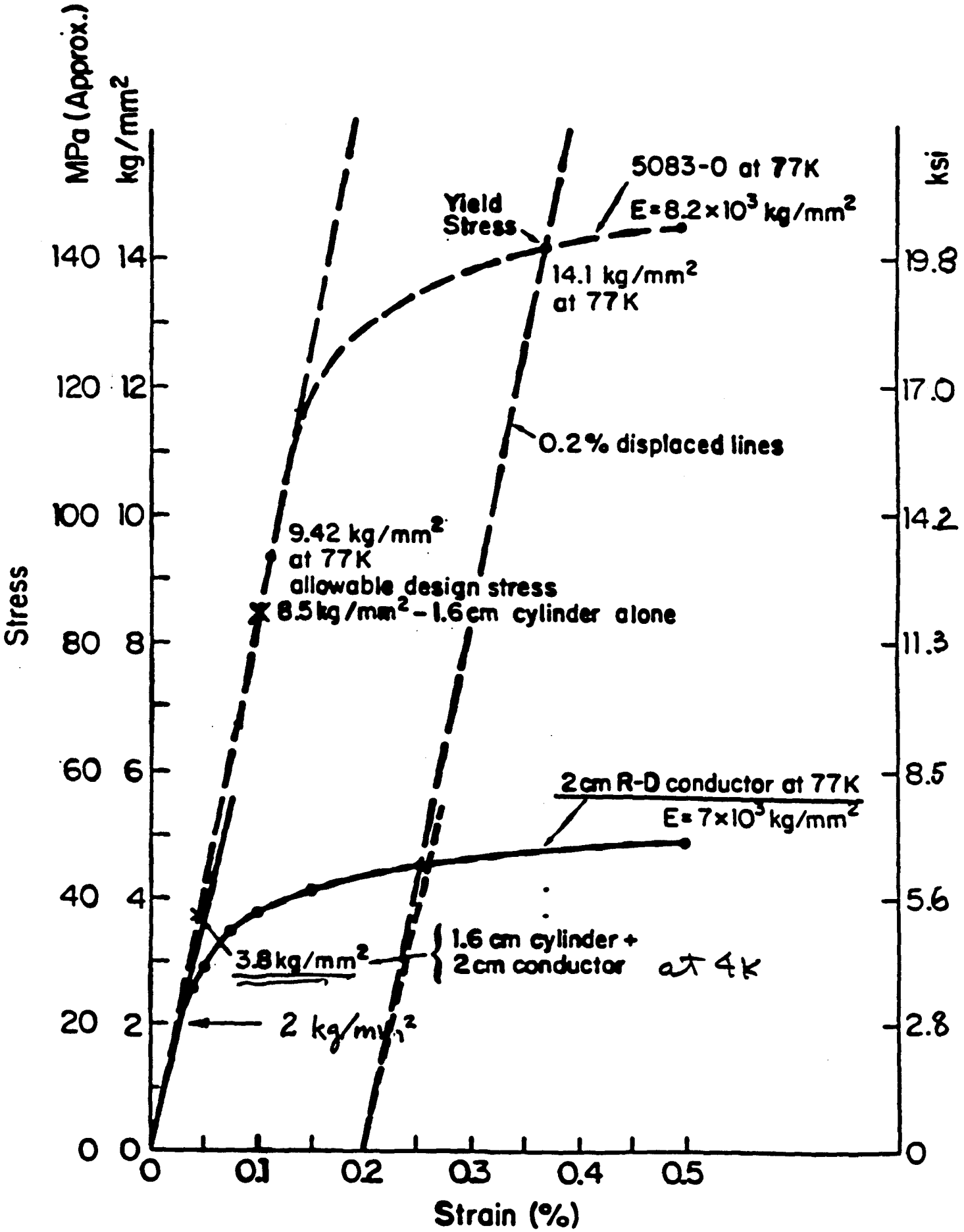

Fig. III(6). Estimated stress-strain curve

Conclusion

Large:

1. It can be constructed with reasonable extrapolation of existing technology.
2. On-site fabrication seems to be too expensive because large-sized facilities are required.
3. Transportation problems must be solved.
4. Detailed stress analyses for axial supports during quenches must be performed. Is an arrangement with a single vacuum chamber feasible?
5. Costs.

SCDF:

Modest extrapolation from the CDF and ALEPH solenoids.

SCD-Snowmass 84:

ALEPH

Small:

1. Axial compressive load seems to be prohibitively high for aluminum-stabilized NiTi/Cu superconductor.
2. If serious, more realistic optimization of parameters must be made.

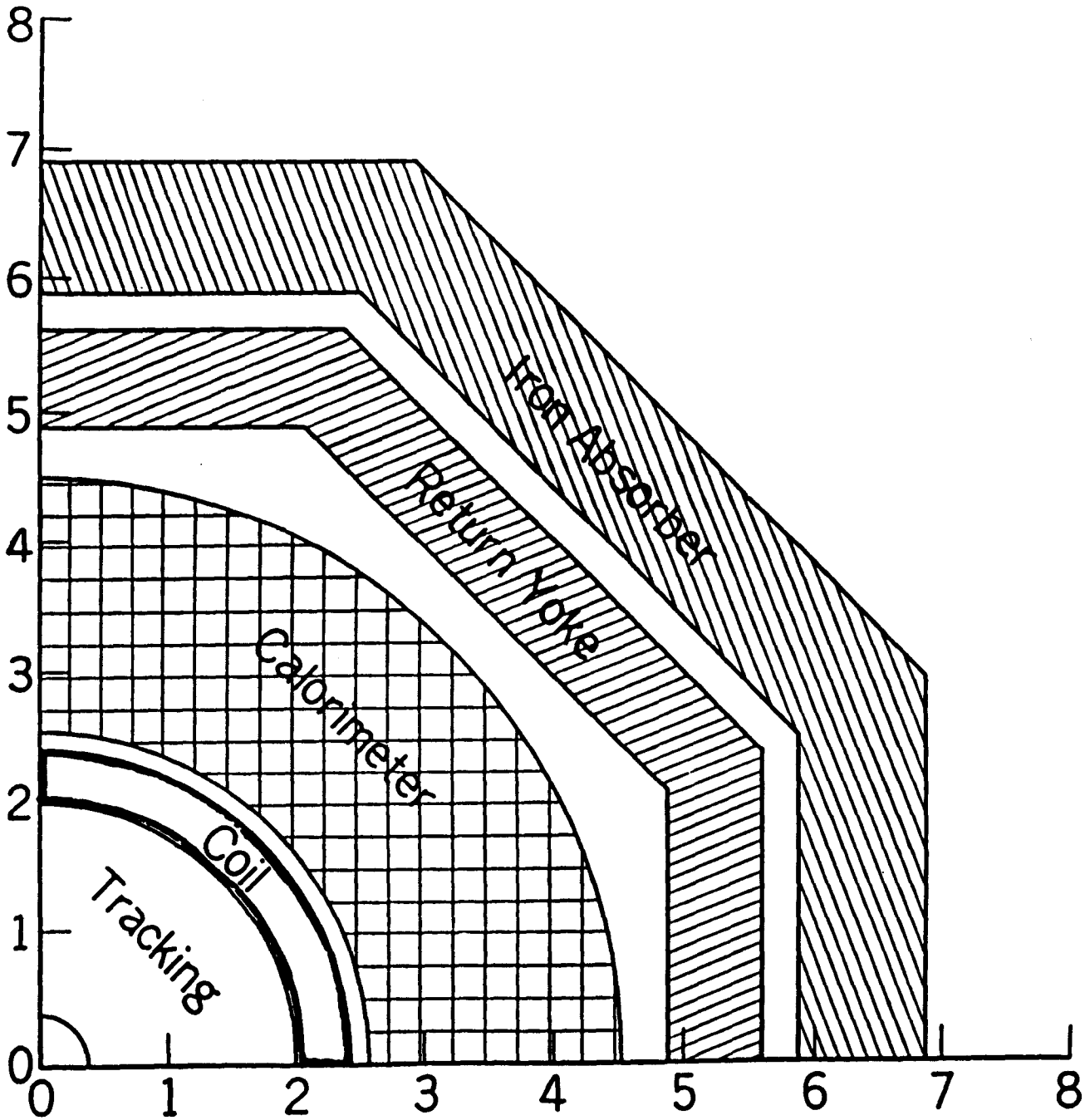
Iron Absorber
Return Yoke
Calorimeter
Coil
Tracking
0
1
2
3
4
5
6
7
8

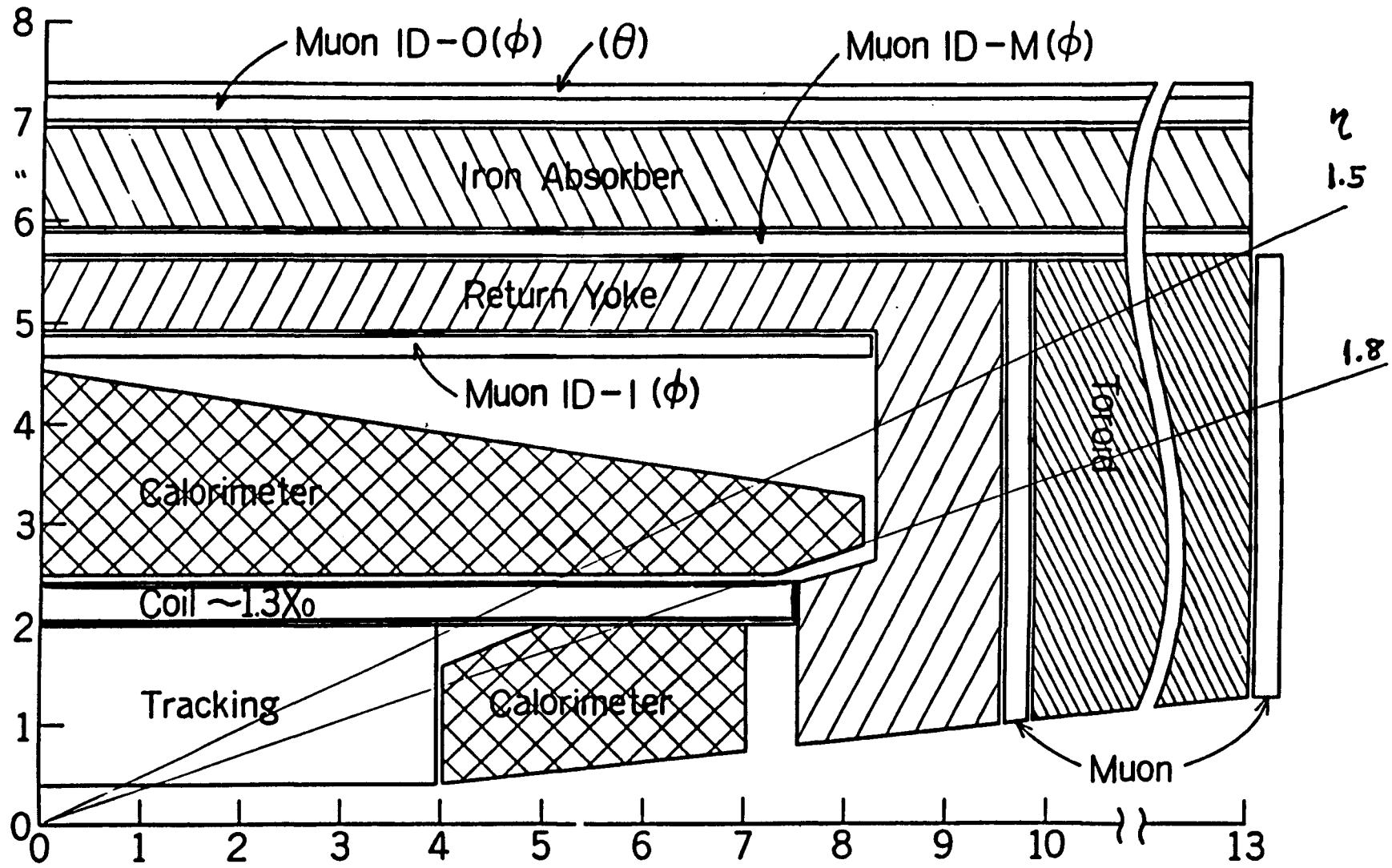

SCDF

- $\Delta p_T/p_T = 0.30$ at $p_T = 1$ TeV
  same central tracker as LSD
- d_{min} (cal.) ≈ 2.5 m

c. H. Ogren
June 26, 1989
Dallas, Tx

SSC

WIRE CHAMBER

TRACKING

REVIEW

PROGRESS REPORT

WORKSHOP TOPICS

Charged particle tracking

Lepton Id:

Lepton Sign for Momentum < 1 TeV/c
e tracking from vertex into calorimeter
μ tracking from vertex matching to muon chamber
matching leptons to correct vertex

Complex event analysis

Separation of multiple interactions in crossing

Identify secondary vertices

Determine invariant masses ,energy , momentum

Improve missing ET and verify calorimetery

Establish Credibility of New Physics, Redundancy

Tracking Chamber Parameters

What determines the size of the wire tracking system?

$$\frac{\sigma_{P_T}}{P_T} = \sqrt{720}\,\frac{\sigma_x}{0.3\,q\,B\,L^2\sqrt{N}}\,P_T$$

Suppose:

$\sigma x = 200\ \mu$
B=2 T
L=0.5 m to 1.5 m
N=100

$\sigma/P_T \sim .6\,P_T$

This gives a sign measurement up to about 500 GeV, (3σ)

with beam constraint up to 1 TeV.

(minimum acceptable level - 1/40 of total E_{CM})

If the field is .7 T :

the tracking distance must go up to 2.6 m.

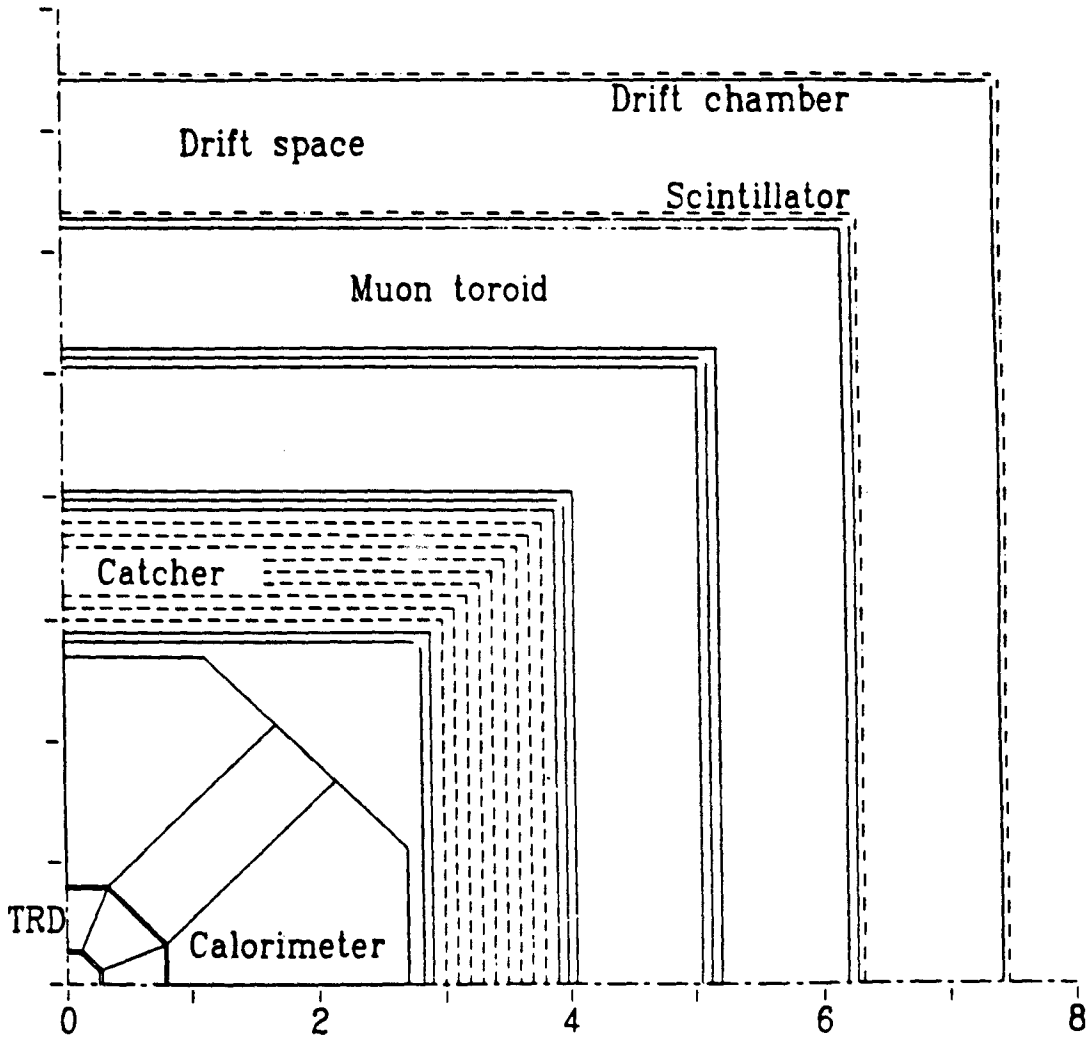

Fig. 1b. Cross Sectional View of the "Non-Magnetic Detector."

The central and intermediate tracking systems are shown in Fig. 8. The momentum resolution as a function of polar angle and rapidity is shown in Fig. 9.

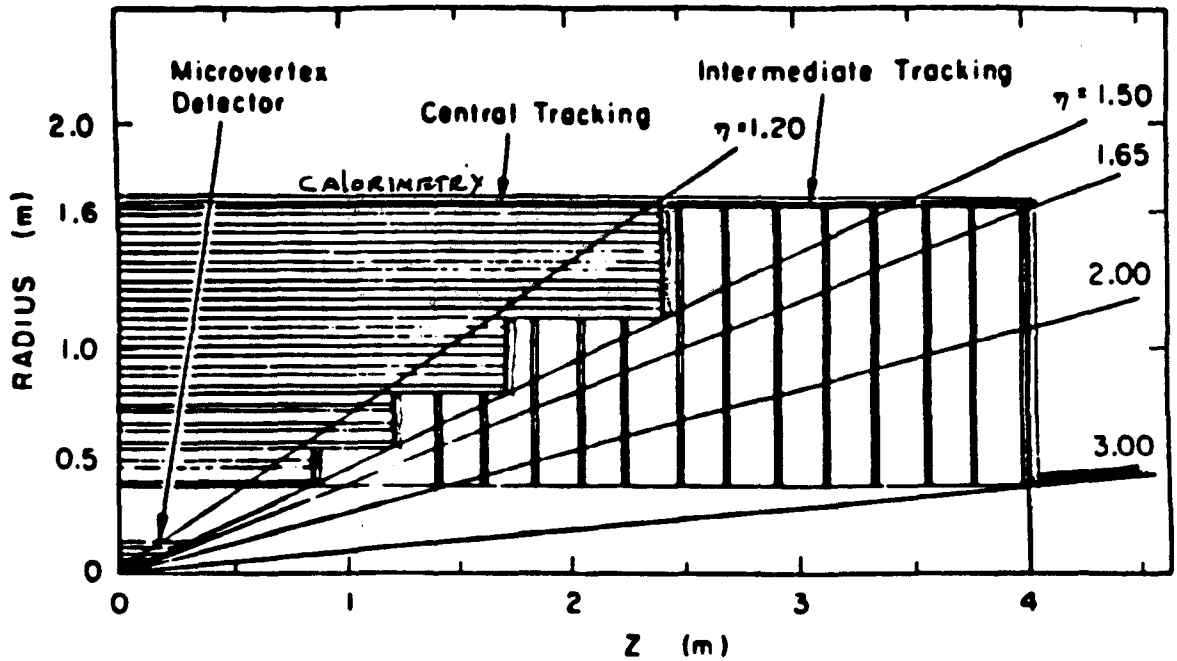

Fig. 8. Schematic view of central and intermediate tracking systems in the Large Solenoid Detector.

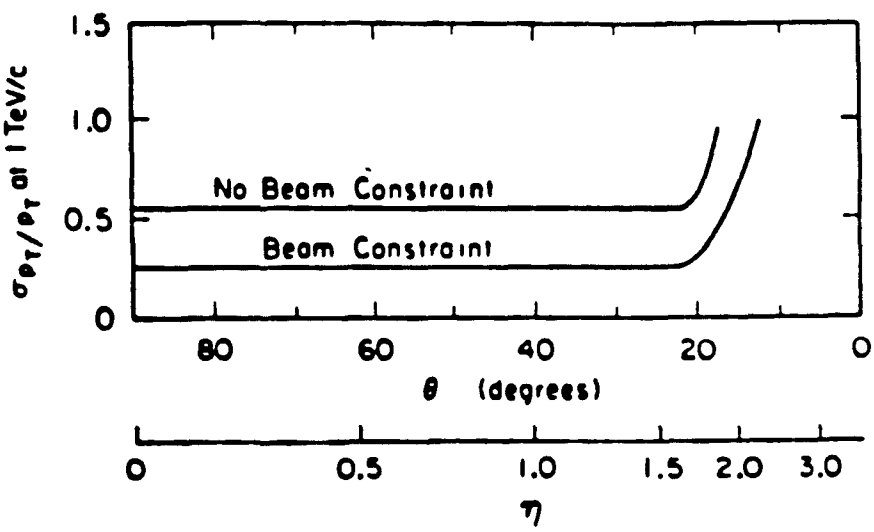

Fig. 9. Momentum resolution as a function of polar angle and rapidity in the Large Solenoid Detector for the 13 superlayers at radii > 50 cm in the central tracking system and intermediate tracking Option A.

4 mm STRAWS

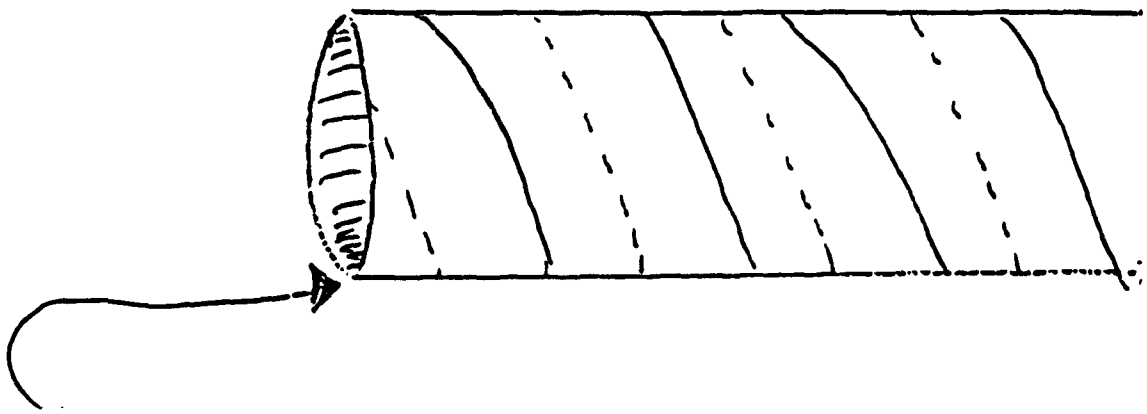

Wall thickness - 37 microns (→ 20 μ)

Lexan film, aluminized. 200 ohms (→ 50 Ω)

mylar film outside

50 straws, 2 meters long

$1000
Precision Paper Tube Co.

QUESTIONS:

Thinner walls?
RADIATION HARDNESS?
CATHODE COATING? GOLD?
ATTENUATION?
MAXIMUM LENGTH?

STRAW CHAMBERS

The result of about 4 years of workshop effort.

Conventional wire chamber technology with well understood properties, tracking 0.5m to 2 m from beam.

New ideas are always welcome.

- The sensitive volume can be made small.
  Singles rates, occupancy , and current are reasonable 50 cm from the beam.

- The drift times 20-30 ns
  Good match to the SSC. (faster gasses ?)

- Mass introduced by tube walls, total of 8% of Xo.
  Tracking seems to tolerate it.

File Edit Search Project Run Debug Windows 11:43:00

Observe

1500.000000	v0
0.000000	bf[3]
0.010800	w0 FAST GAS
18.750000	t ns

gas .p

```
screen(xs, ys);                    (get screen coor
lineto(xs, ys);
end;
{ savedrawing(doctorhoo : gpic);}
end.
```

Drawing

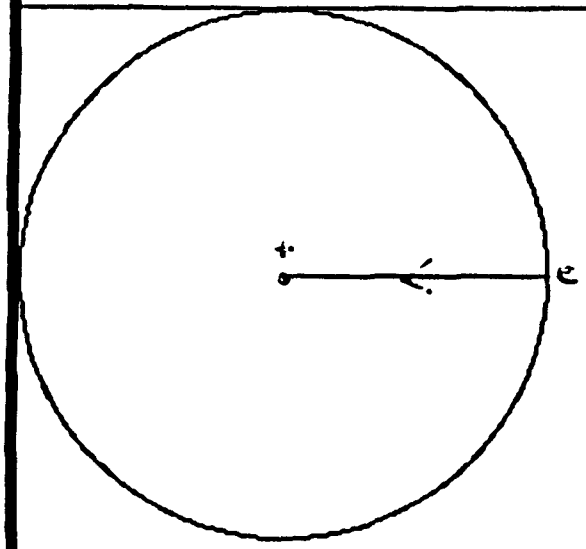

ZERO FIELD

File Edit Search Project Run Debug Windows 11:19:24

Observe

1500.000000	v0
2.000000	bf[3]
0.010800	w0 FASTGAS
31.750000	t (v.c)

gas .p

```
    screen(xs, ys);                    {get screen coor
    lineto(xs, ys);
  end;
{ savedrawing(doctorhoo : gpic);}
end.
```

Drawing

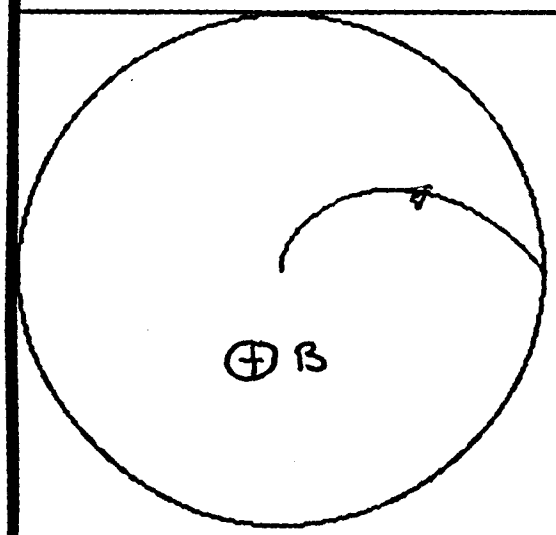

2T: 1 ie!!

1940 V → 27 ms Ar-CO_2

2600 V → 24 ms CF_4

-1.3e-4	-2.1e-3	-1.3e-1	3.0e+1
-8.3e-10	-1.1e-3	-1.4e-1	13.0e+1 ⊥ to field

Drawing

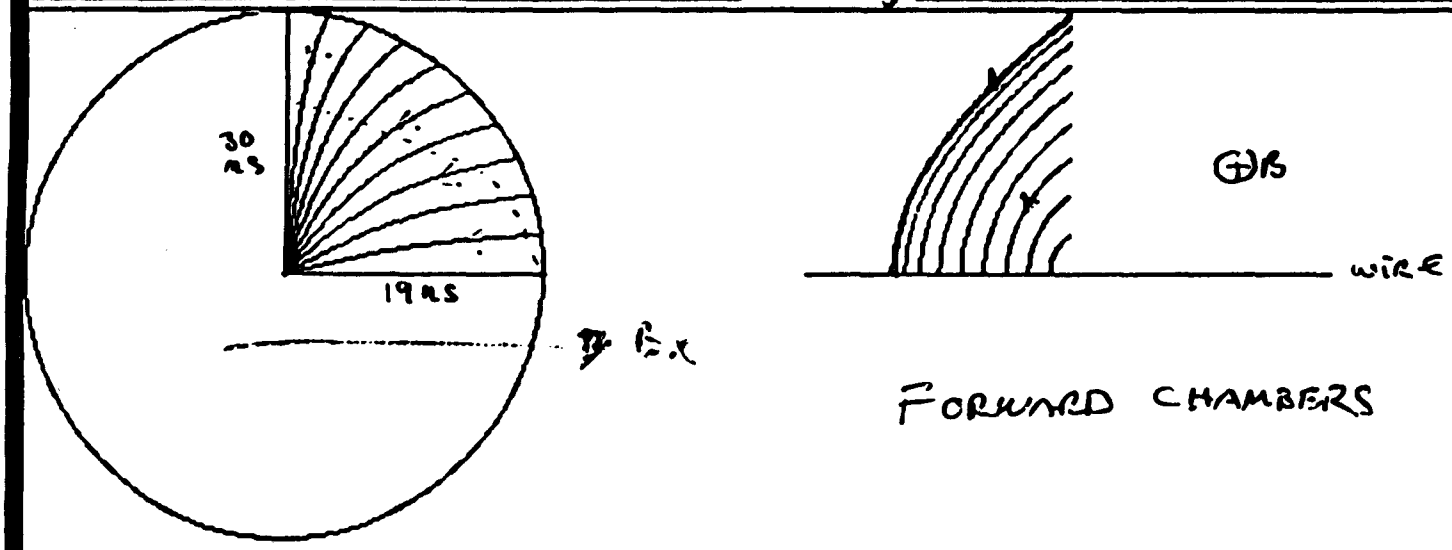

File Edit Search Project Run Debug Windows 16:38:59

Text

1.0e-1	-1.6e-1	2.6e+1
1.0e-1	-1.5e-1	2.4e+1
1.0e-1	-1.4e-1	2.3e+1
1.0e-1	-1.3e-1	2.1e+1
1.0e-1	-1.2e-1	2.0e+1
1.0e-1	-1.1e-1	1.8e+1
1.0e-1	-1.0e-1	1.7e+1
1.0e-1	-9.0e-2	1.6e+1
1.0e-1	-8.0e-2	1.5e+1
1.0e-1	-7.0e-2	1.4e+1
1.0e-1	-6.0e-2	1.3e+1
1.0e-1	-5.0e-2	1.2e+1
1.0e-1	-4.0e-2	1.2e+1
1.0e-1	-3.0e-2	1.2e+1
1.0e-1	-2.0e-2	1.1e+1
1.0e-1	-1.0e-2	1.1e+1
1.0e-1	3.0e-8	1.0e+1
1.0e-1	1.0e-2	1.0e+1
1.0e-1	2.0e-2	1.0e+1
1.0e-1	3.0e-2	1.1e+1
1.0e-1	4.0e-2	1.1e+1
1.0e-1	5.0e-2	1.2e+1
1.0e-1	6.0e-2	1.2e+1
1.0e-1	7.0e-2	1.2e+1
1.0e-1	8.0e-2	1.3e+1
1.0e-1	9.0e-2	1.4e+1
1.0e-1	1.0e-1	1.5e+1
1.0e-1	1.1e-1	1.6e+1
1.0e-1	1.2e-1	1.7e+1
1.0e-1	1.3e-1	1.8e+1
1.0e-1	1.4e-1	2.0e+1
1.0e-1	1.5e-1	2.1e+1
1.0e-1	1.6e-1	2.3e+1
1.0e-1	1.7e-1	2.4e+1
1.0e-1	1.8e-1	2.6e+1
1.0e-1	1.9e-1	2.8e+1
1.0e-1	2.0e-1	3.0e+1

accelerator text

s[1,2] * ps

* 10000.0;

gas.π

Options	File (by build order)	Size
	Runtime.lib	18256
	Interface.lib	8104
D N V R	contour.p	5164

Word Proc
Pascal 1
in disk

Runtime.lib
Interface.lib
Libraries
Utilities 1
DA Mover
rfaces
se Notes

20K Microsoft Wor
1K Microsoft Wor
5K Microsoft Wor
7K Microsoft Wor
2K Microsoft Wor
3K Microsoft Wor
8K Microsoft Wor
3K Microsoft Wor
2K Microsoft Wor
3K Microsoft Wor
4K Microsoft Word d... Wed, Mar 1, 1989

Drawing

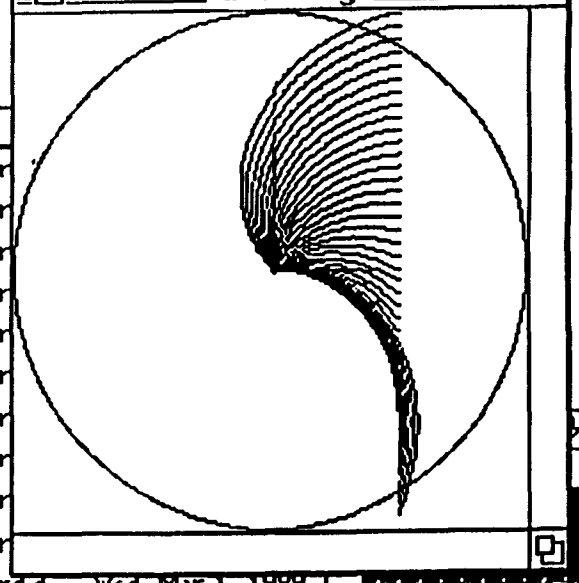

Trash

Constraints due to SSC Environment

Central Axial Chambers:

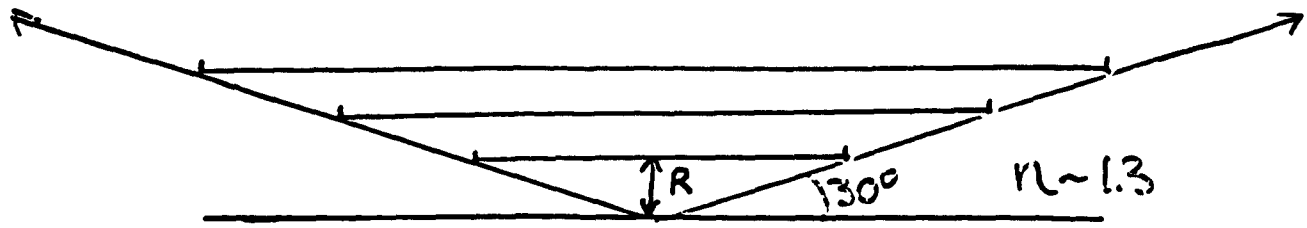

Rate: $\mathcal{L} = 10^{33}\ cm^{-2}\ sec^{-1}$ $\sigma_{inel} = 100\ mb$

$$\frac{dN_{CH}}{da} \approx \frac{120\ MHz}{r_\perp^2} \quad (cm) \qquad N_{CH} = \int da\ (straw)$$

integrate over straw diameter

Occupancy:

$$O = \frac{\text{Max drift Time}}{\text{ave Time between Hits}} \quad (20 \to 30\,ns) \quad \approx 1/N_{CH}\ \text{rate}$$

Current draw:

$$i = N_{CH}\ e\ (100 e^-/cm)\ \underline{Lev} \cdot gain$$

$$Q = \int_{5\,years} i\, d\tau \quad \simeq \underline{5 \times 10^7 s}$$

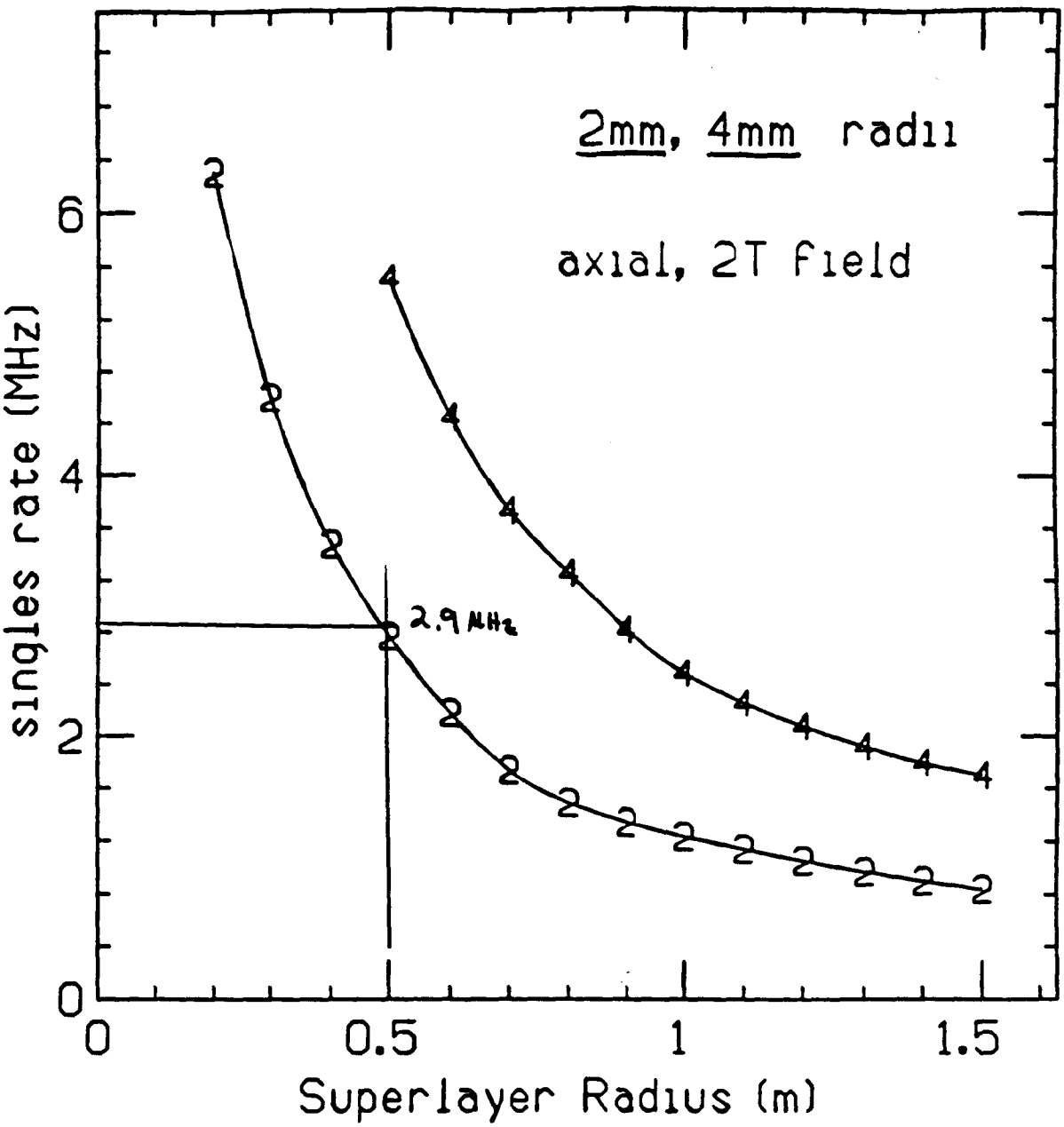
2mm, 4mm radii
axial, 2T field
2.9 MHz
singles rate (MHz)
Superlayer Radius (m)
0
2
4
6
0
0.5
1
1.5

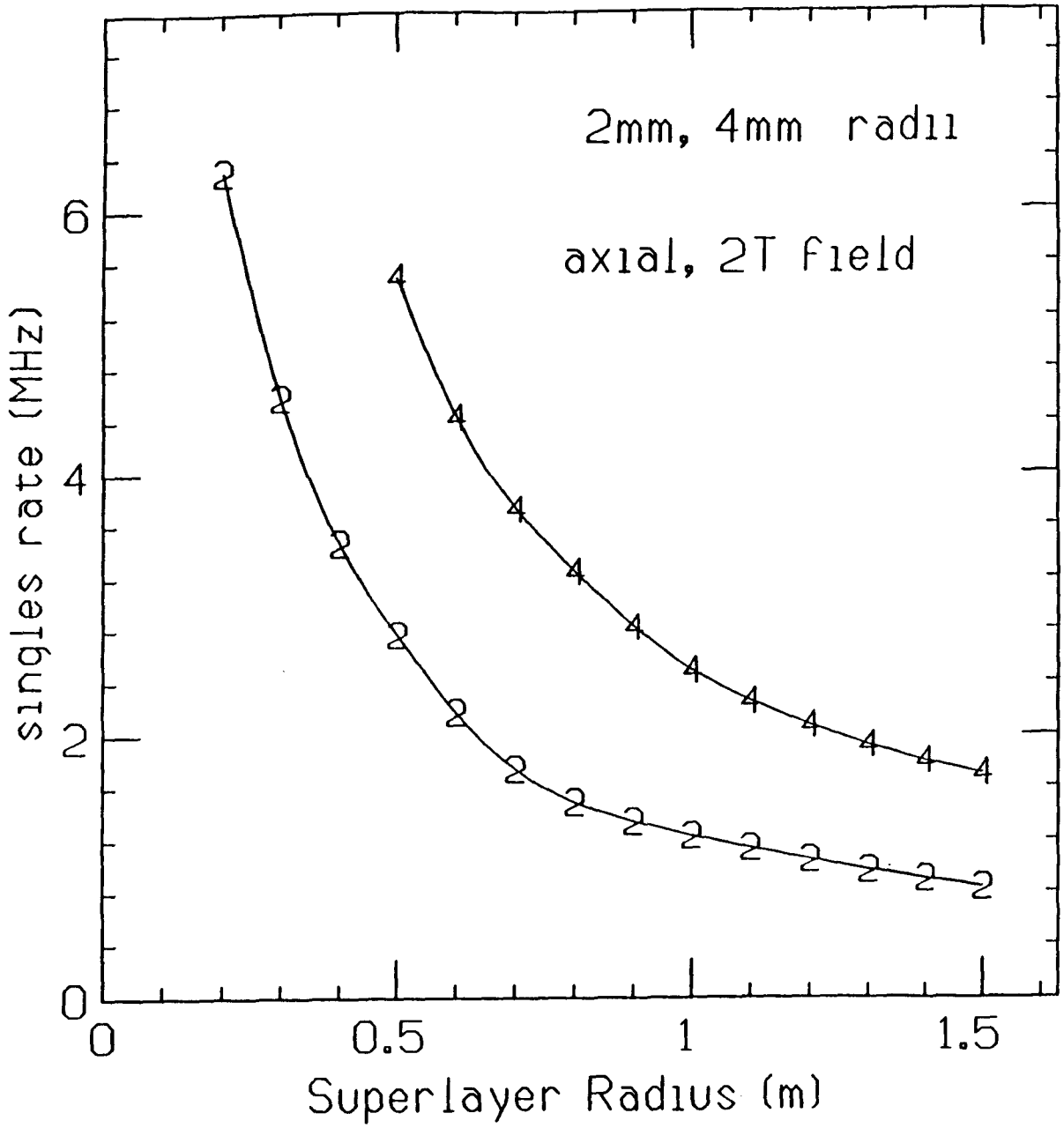
2mm, 4mm radii
axial, 2T field
singles rate (MHz)
Superlayer Radius (m)
0
2
4
6
0
0.5
1
1.5

Forward Chambers

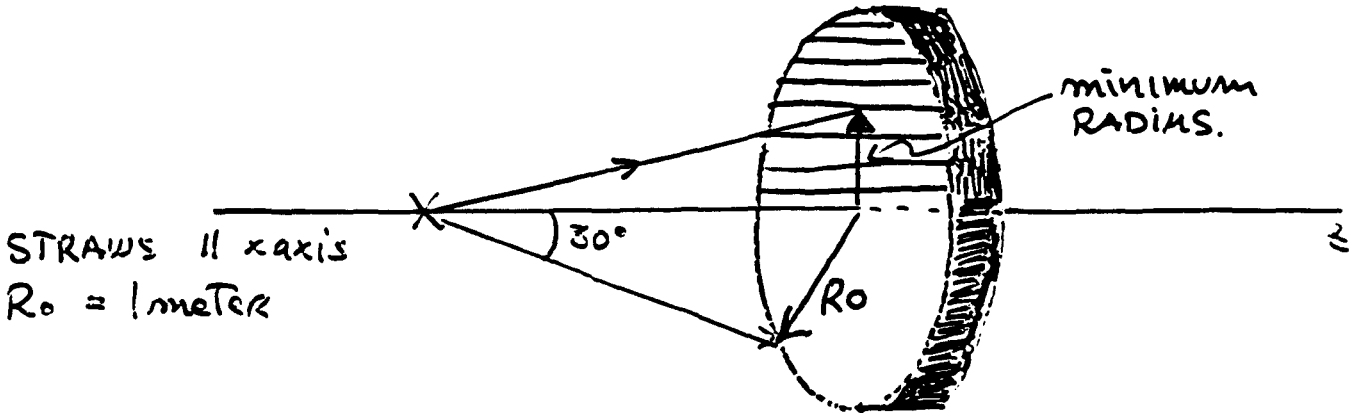

rates:

$$\frac{dN_{CH}}{dq} = \frac{120\,\text{MHz}}{v_\perp^2}\ (\text{cm}) \qquad N_{CH} = \int \underline{\text{STRAW}}\ dA$$

occupancy:

$$O = \frac{\text{max drift time}}{\text{ave time between hits}}$$

current draw:

$$i = N_{CH}\ e\ (100\ e^-/\text{cm}) \cdot \text{Len} \cdot \text{Gain}$$

$$Q = \int_{5\ \text{years}} i\,dt$$

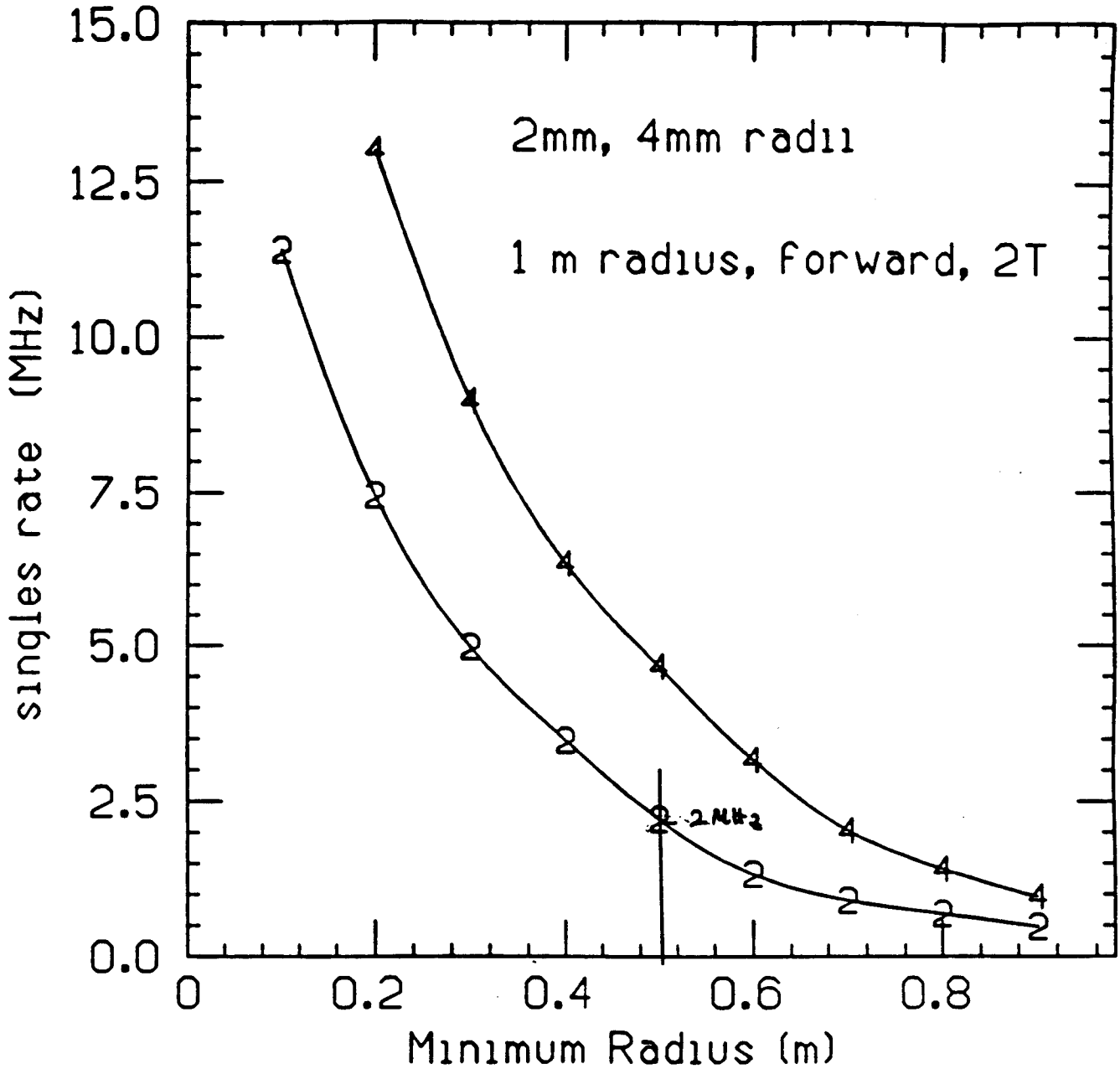
2mm, 4mm radii
1 m radius, forward, 2T
singles rate (MHz)
Minimum Radius (m)
15.0
12.5
10.0
7.5
5.0
2.5
0.0
0
0.2
0.4
0.6
0.8
2 MHz

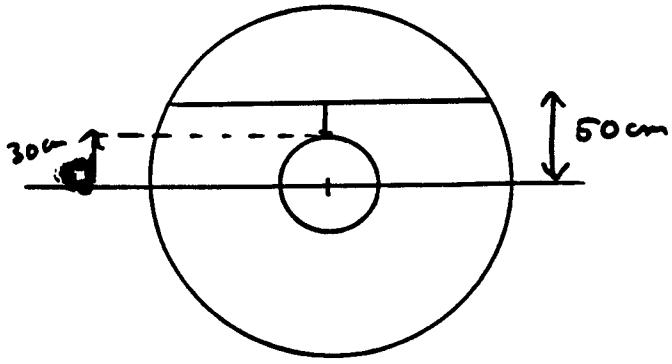
30cm
50cm

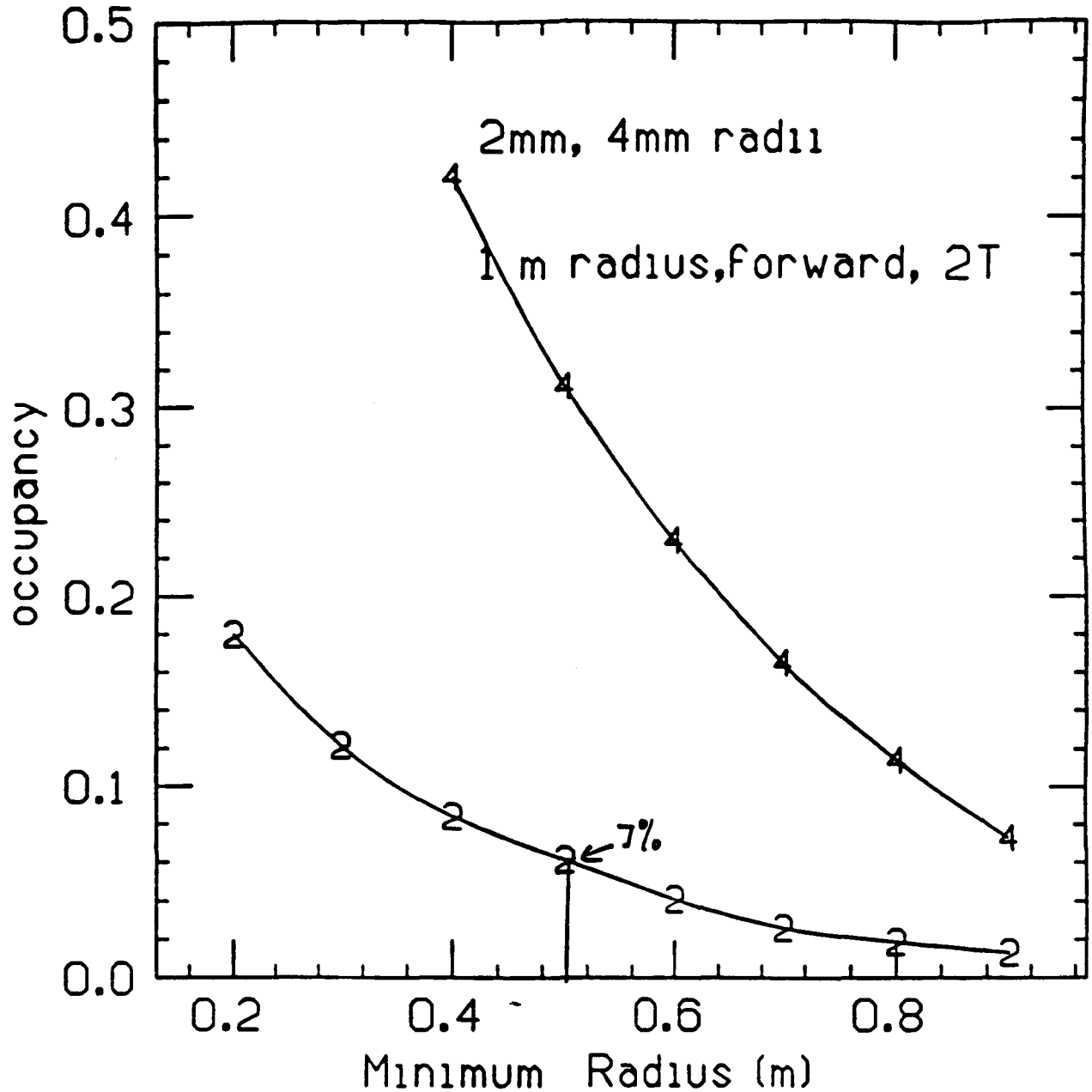
2mm, 4mm radii
1 m radius,forward, 2T
7%
occupancy
Minimum Radius (m)
0.0
0.1
0.2
0.3
0.4
0.5
0.2
0.4
0.6
0.8

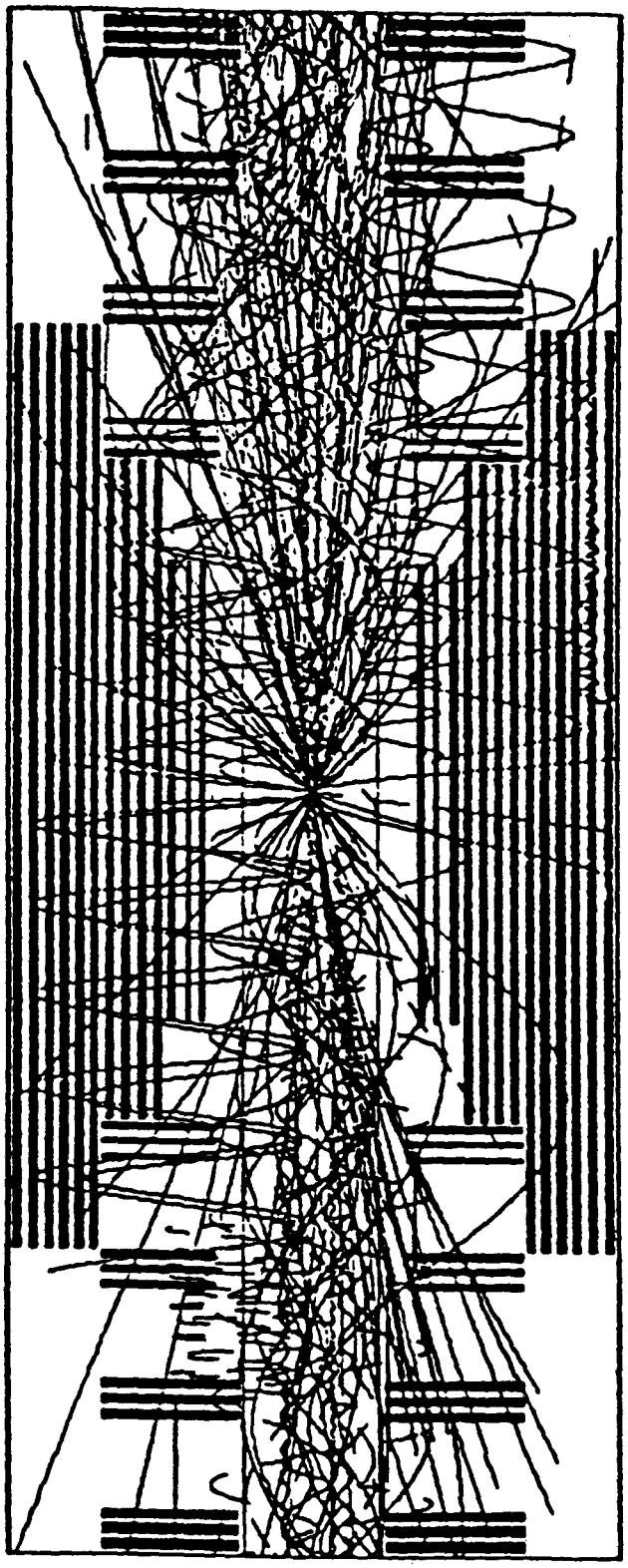

)

gs :

(ns)

Radiu

ssing

ISAJET TWOJET EVENT

$p_T = 1$ TeV

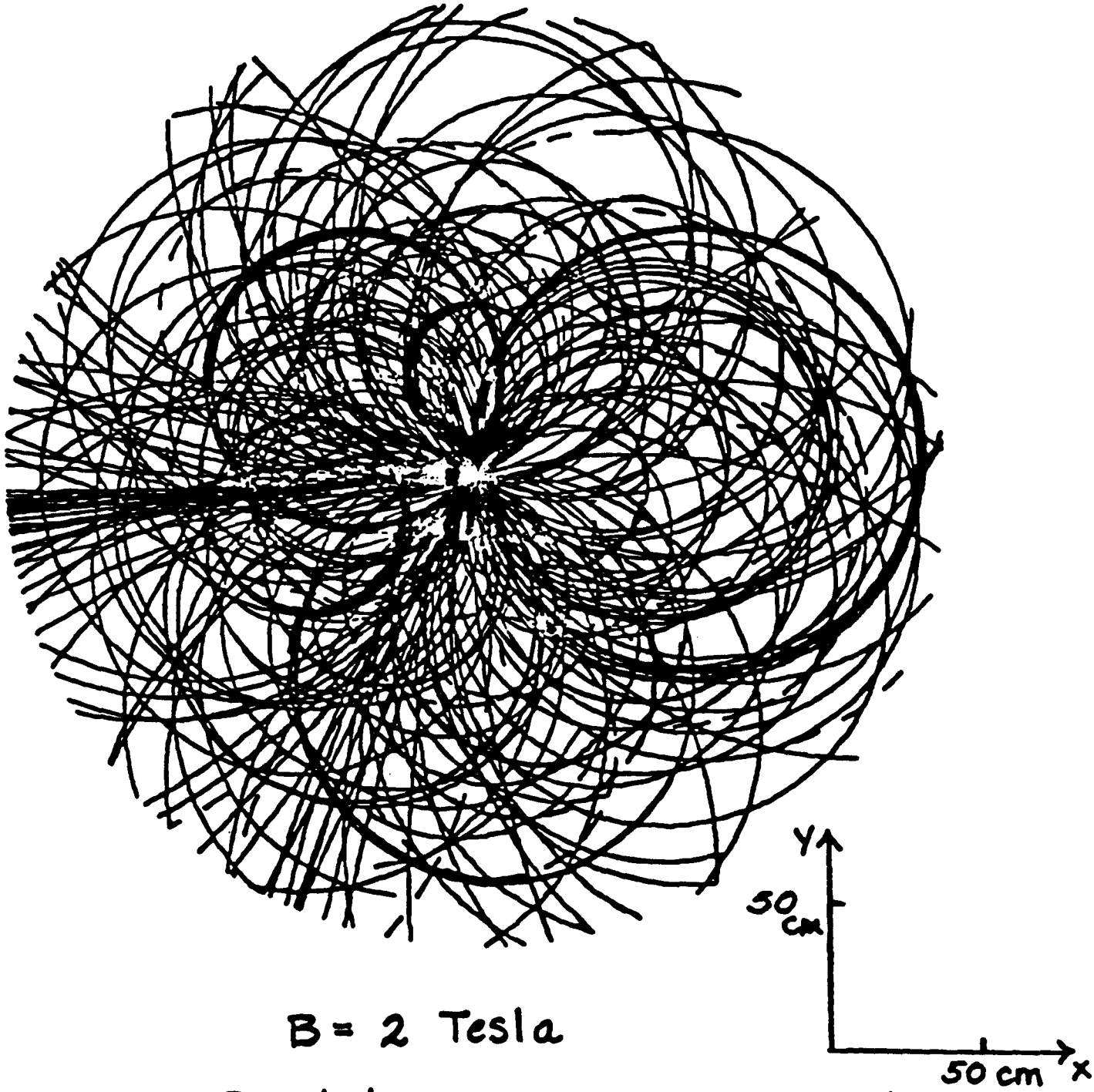

B = 2 Tesla

223 Particles $p_T > 200$ MeV, $|y| < 1.5$

($p_T < 200$ MeV $\rightarrow$ $r < 0.67$ m)

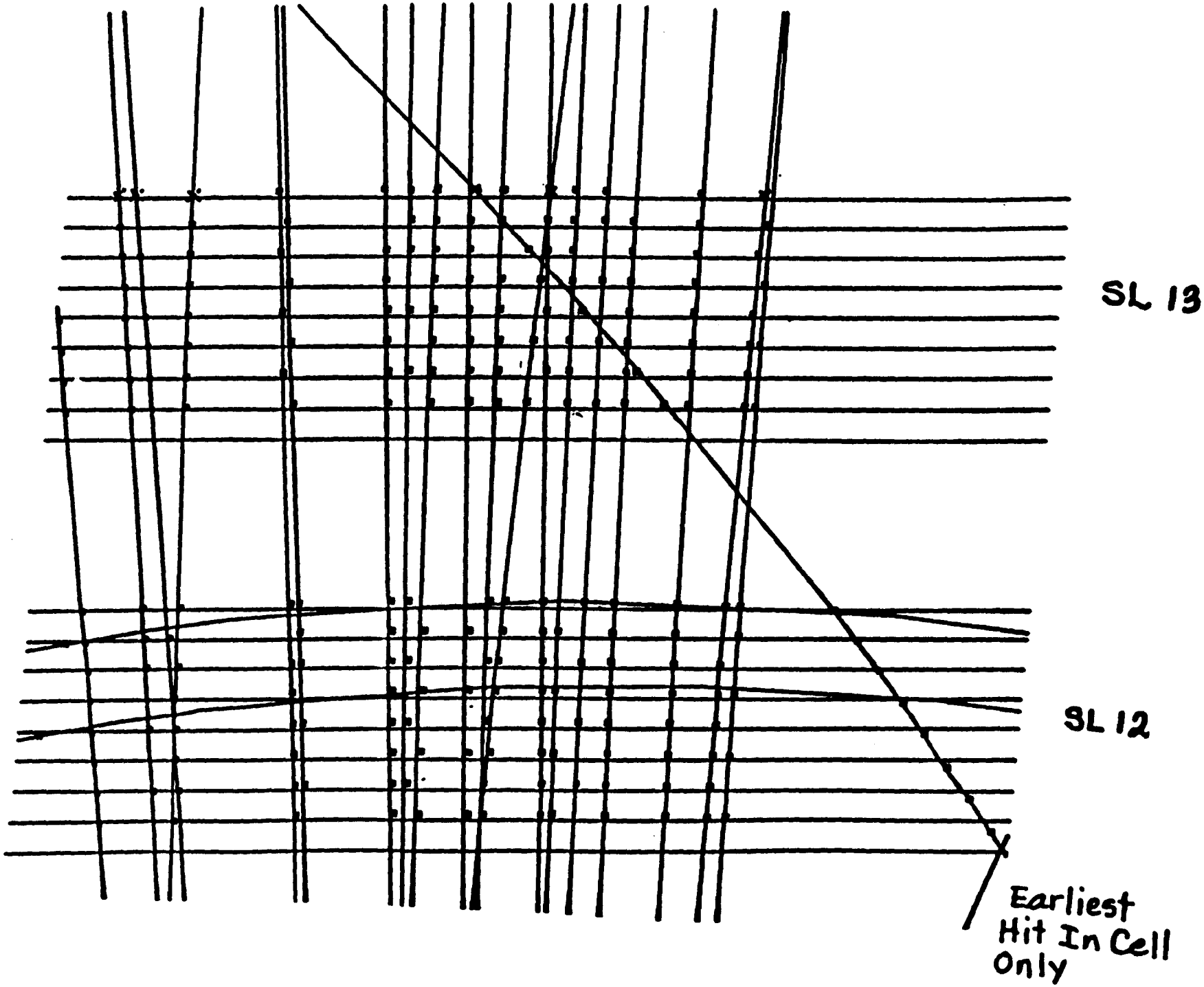
SL 13
SL 12
Earliest
Hit In Cell
Only

$H \rightarrow ZZ$

$\hookrightarrow e^+e^-$

$\hookrightarrow \mu^+\mu^-$

$m_H = 400\ \mathrm{GeV}/c^2$

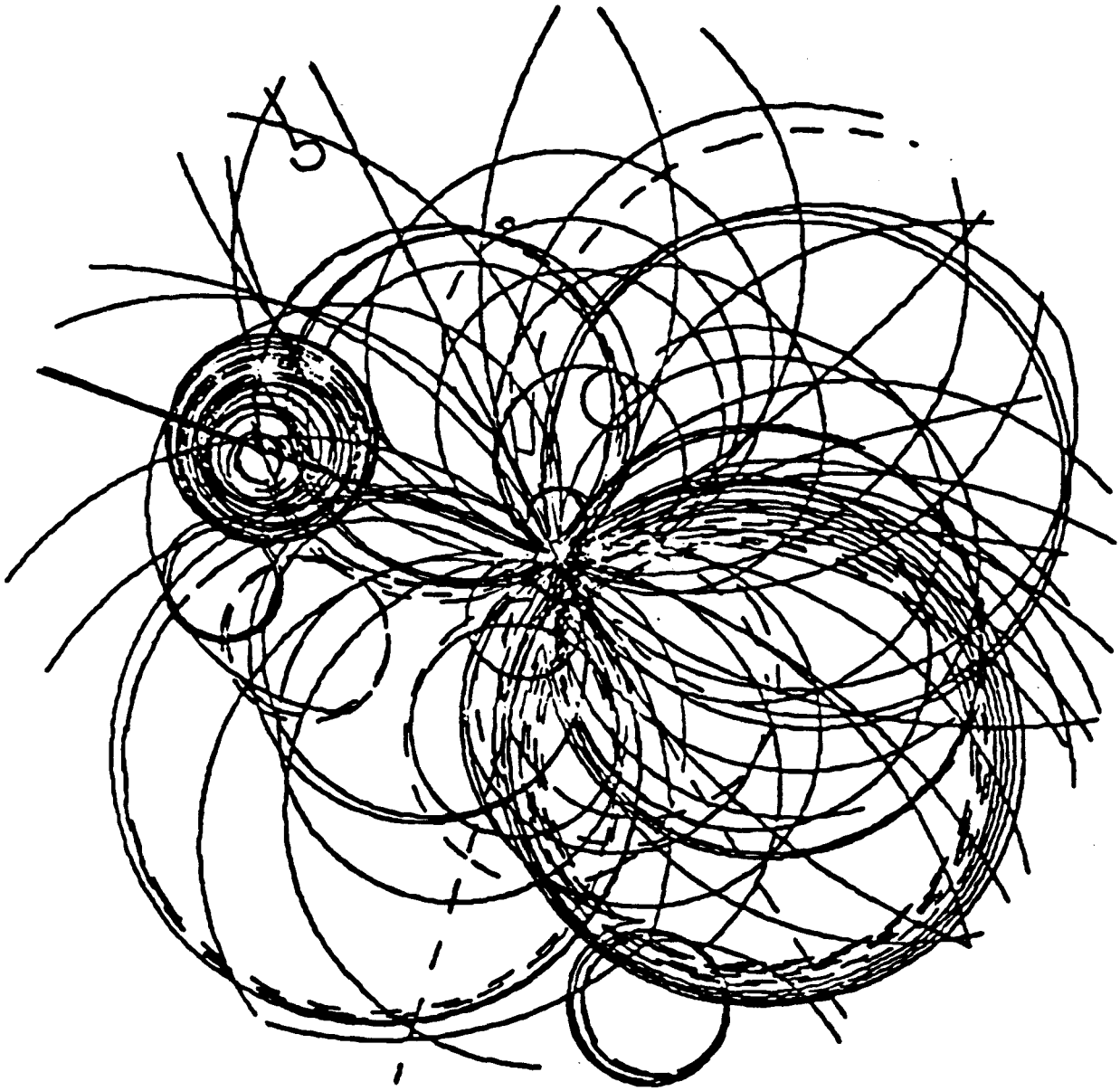

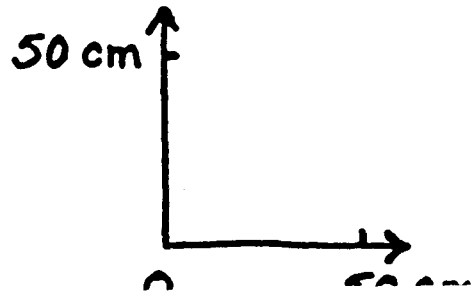

PATTERN RECOGNITION

Find Track Segments In Superlayers:

8 Layers

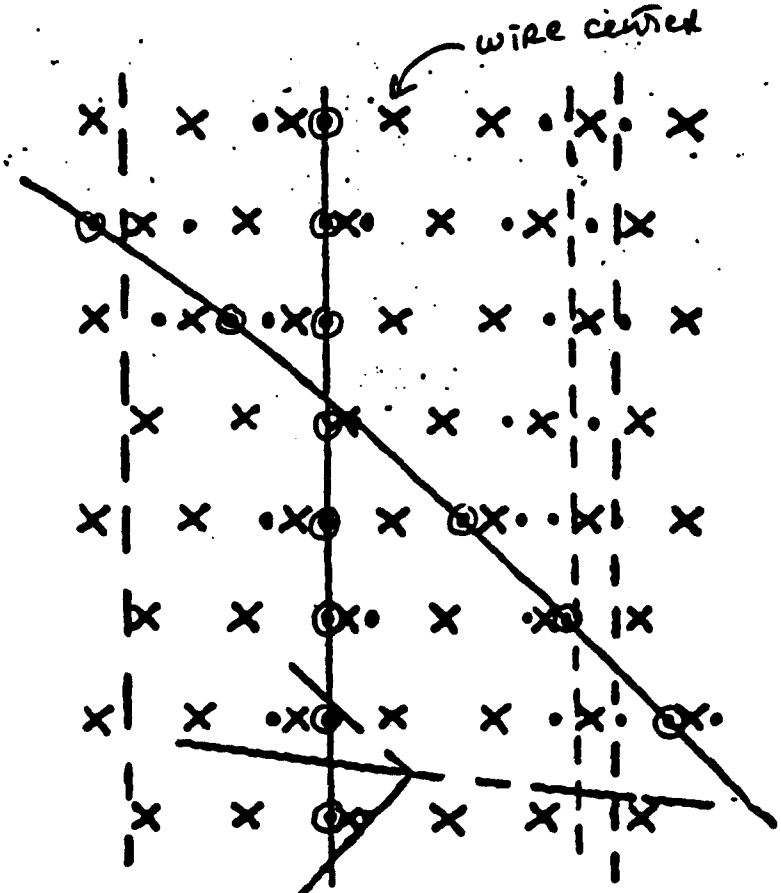

1. Find Groups of Hits (Road) On Same Wire Number ± 2 (Discriminates Against Low-p_T Tracks)
2. Require ≥ 3 Hits On Segment (≥ 1 Odd)
3. Look For Consistency With Straight Line, Resolve Left-Right Ambiguities (Discriminates Against Hits From Out-of-Time Bunch Crossings)

Wire Positions
Displayed for Hits

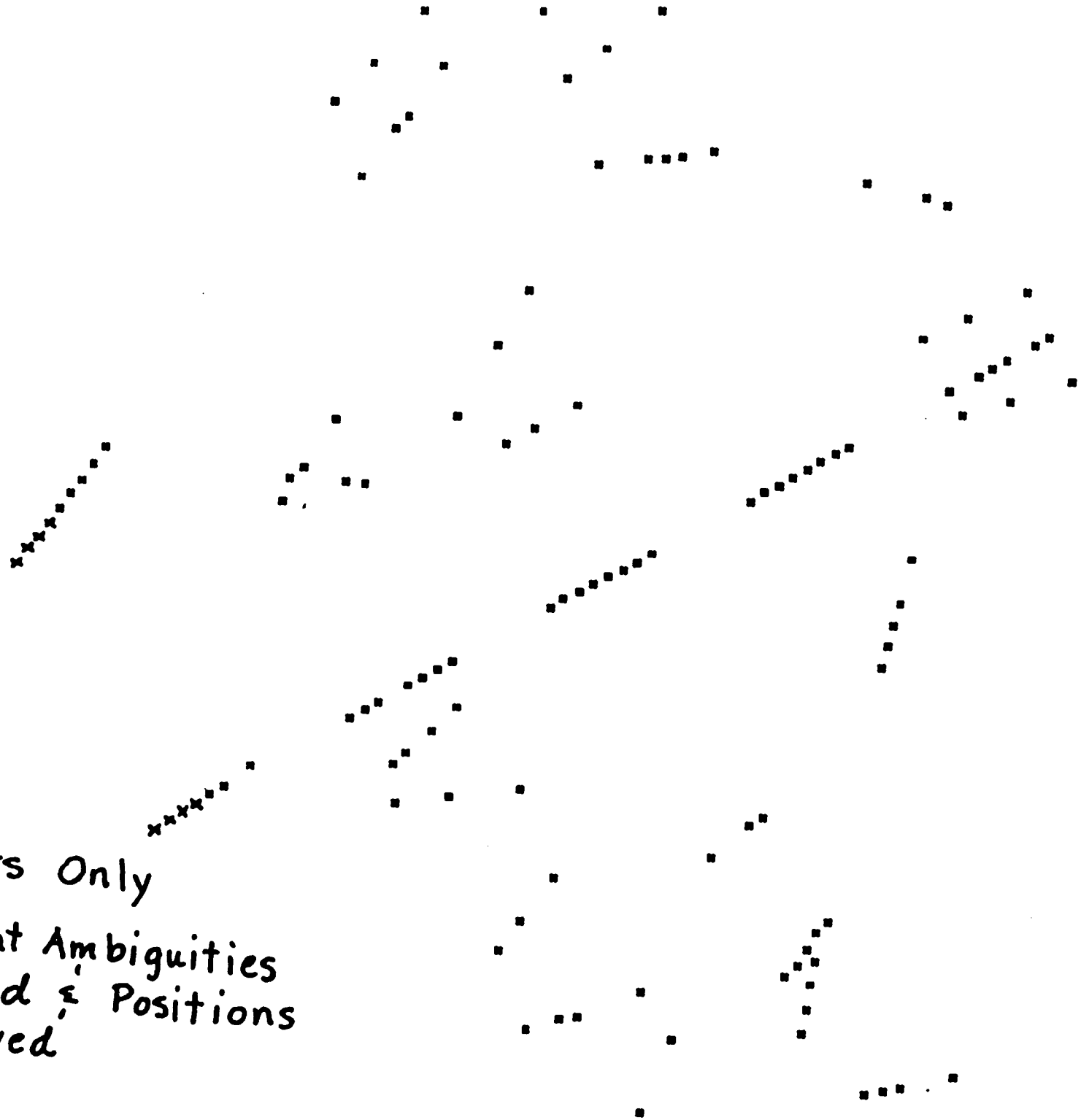

Segments Only

Left-Right Ambiguities Resolved & Positions Displayed

Construction of a LARGE system

a) 2T design

2T - LARGE SOLENOID TRACKING

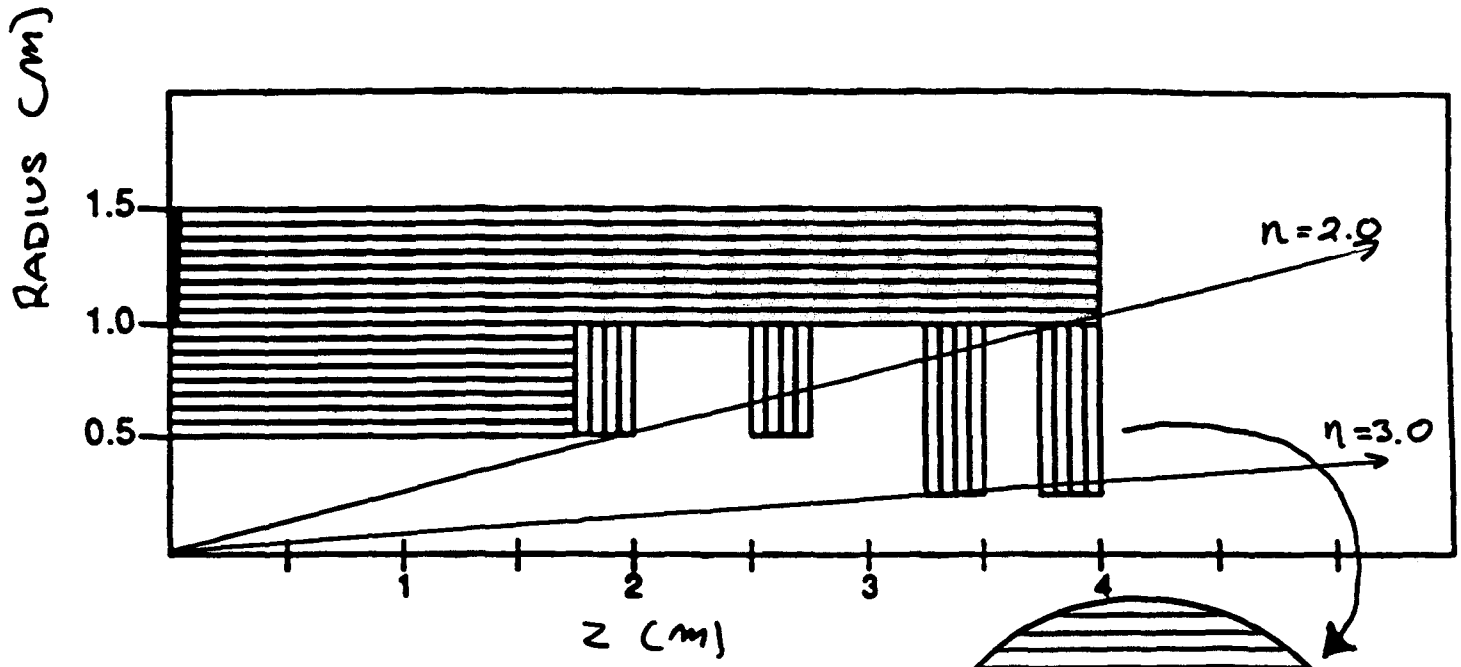

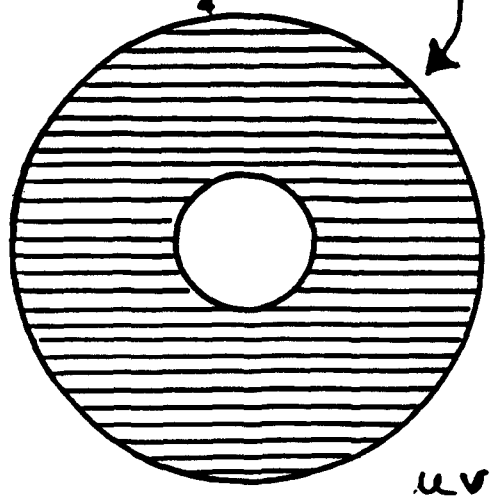

CENTRAL (15 superlayers - 8 Tubes ea)

.5 → 1.0	63,200	wires
1.0 → 1.5	152,200	wires

Forward 150,000 WIRES

UVH
TOTAL 24 planes
each DISK

365,000 TOTAL (minimum)

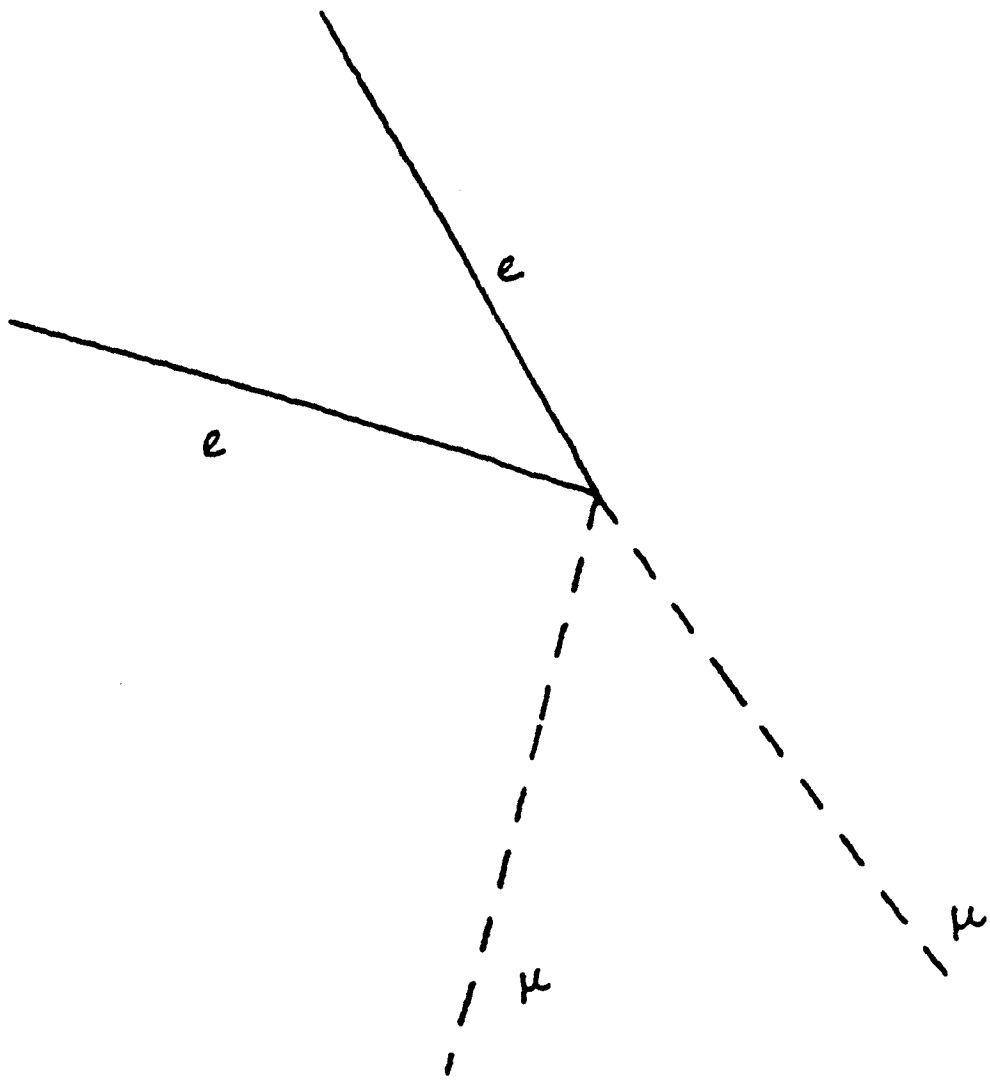
e
e
μ
μ

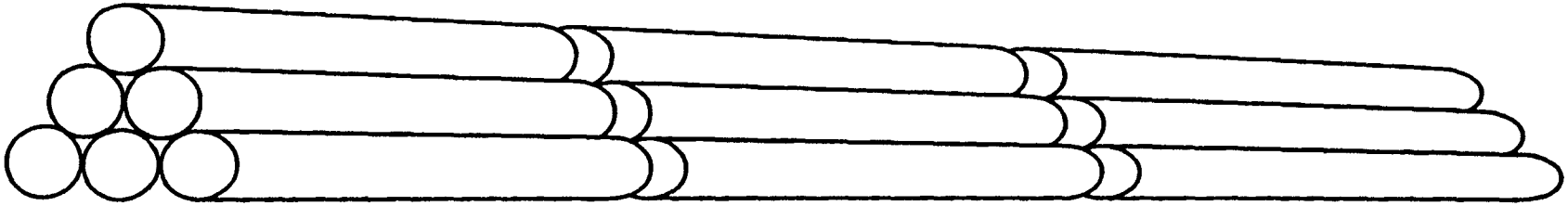

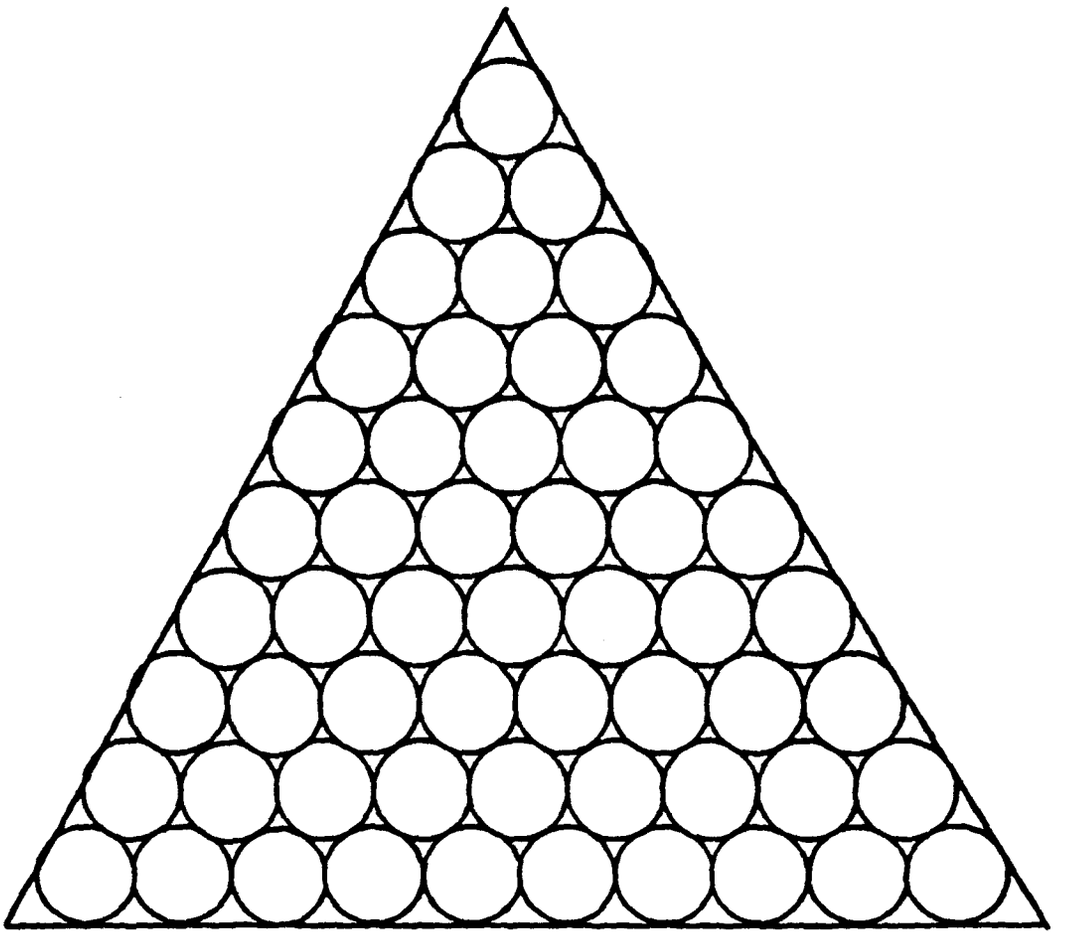

SUPER MODULES ?

~ 16 Tube ARRAY on a side required for 1 meter of free Tubes.

.7T LARGE SOLENOID TRACKING

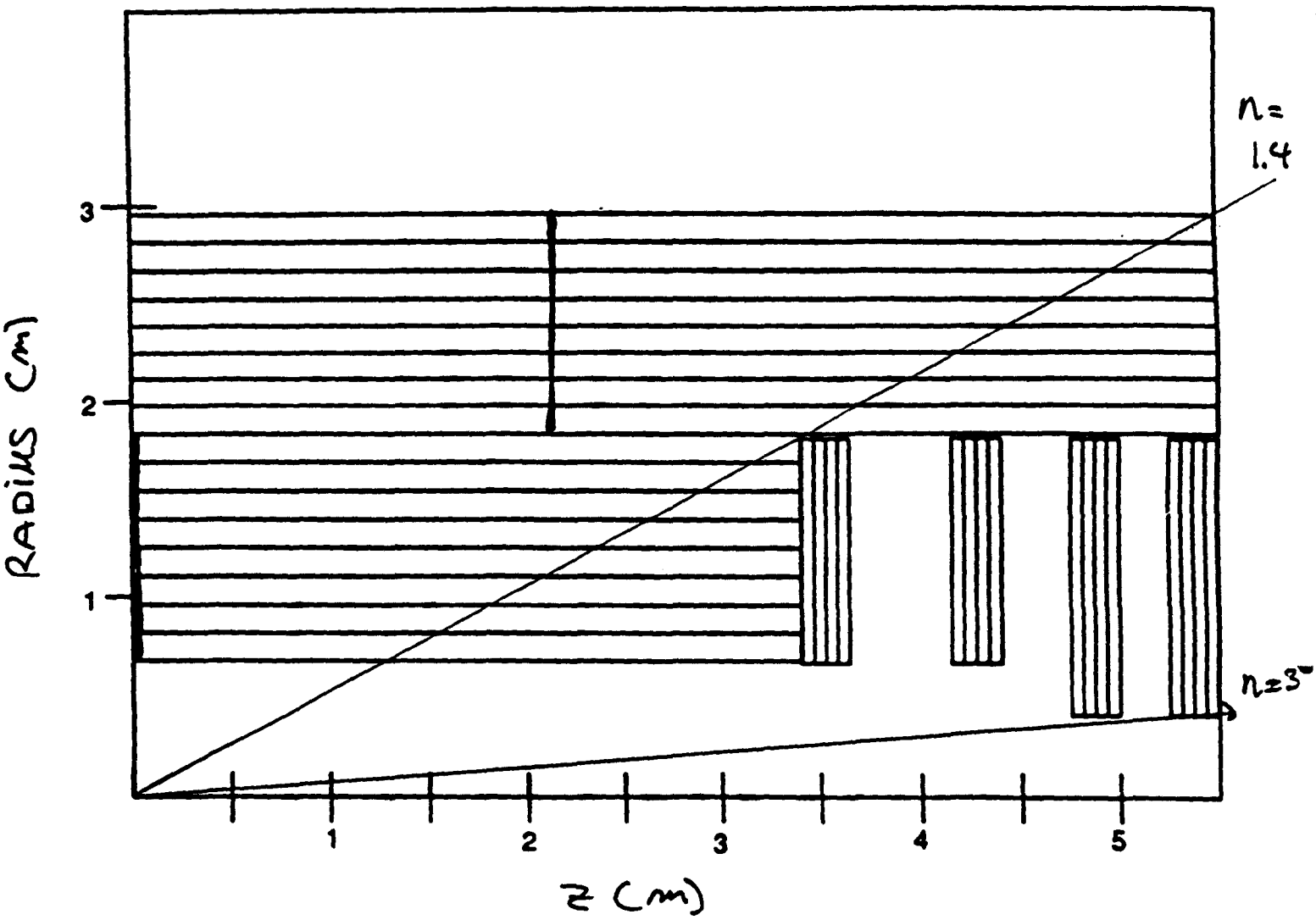

CENTRAL

.7 → 1.8m 150,000 WIRES

1.8 → 3.0m 360,000 WIRES

FORWARD 300,000 WIRES

810,000

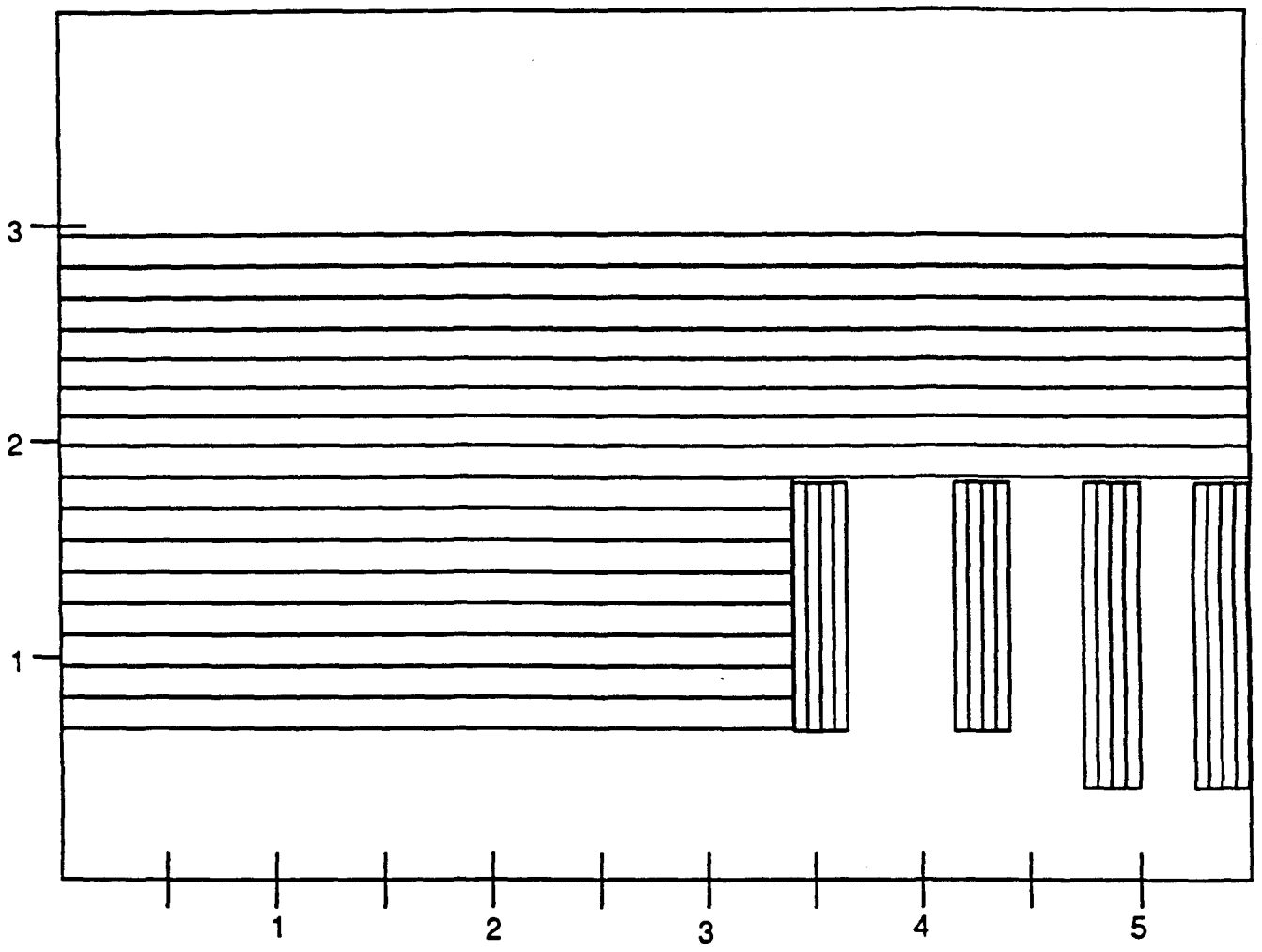
3
2
1
1
2
3
4
5

Topics to consider at workshop

1) Trade offs- tracking radius and field.
How much tracking do we need?

2) Integration of forward and central tracking.

3) Information on the Z coordinate.

4) Effects of field inhomogeneities.

5) How do we accommodate electron ID?

a) TRD
b) Preconvertors

TRACKING SIMULATION:

OPTIMUM CELL SIZE FOR SEGMENT FINDING

EFFECTS OF STEREO WIRES

EFFECTS OF INCREASED TUBE MATERIAL + MECHANICAL SUPPORTS

d. Sadrozinski

TRACKING with SILICON DETECTORS at the SSC

HARTMUT F.-W. SADROZINSKI

Santa Cruz Institute for Particle Physics

University of California Santa Cruz

Santa Cruz, CA 95064

1) Tracking Goals and Characteristics of Silicon Trackers

2) Systems Design Questions

3) future R&D

ds Sa K dro

Characteristics of SSC Events

10^8 interactions/sec

Stiff tracks

Narrow, dense jets

Many extra low energy tracks

Complicated events

Large data volume (mainly from tracking devices)

Characteristics of Si Tracking System

Fast collection device → separate different interactions

Good position resolution ($\frac{25\,\mu m}{\sqrt{12}}$)

Very small cells → low occupancy

Local stereo → unambiguous z measurement

Good 2 track resolution (100 μm)

few noise hits (signal 25000 e^-/300 μm)

Data reduction and storage possible in VLSI on detector

TRACKING GOALS

1) Lepton ID with calorimeter and μ toroid
   electrons are identified by E/P ratio

   $\rightarrow$ P should be measured with same precision as .

   measure e and μ with the same precision and systemat

2) Lepton Mass Reconstruction for $H \rightarrow ZZ \rightarrow e^+e^-$ $\mu^+\mu^-$
   efficiency and good momentum resolution

   $\rightarrow$ lepton pair mass resolution less than Z width

   $\rightarrow$ good coverage in η:

$$\frac{N_{ZZ}(\eta < 2.5)}{N_{ZZ}(\eta < 1.5)} \approx 2.5 \rightarrow 3$$

3) Measurement of Event Structure

   a) Multiplicity

   b) Energy flow with good timing to comple
      calorimeter

4) Vertex Reconstruction

   a) Disentangle multiple events in same time bu

   b) Measure impact parameter of $< 300\mu$m in
      decays
      Pixel (low occupancy, close to vertex) + st
      tum determination)

Figure 22 shows a possible arrangement for the tracking detector. It contains about 40m^2 of silicon detectors. Going out in θ this arrangement gives:

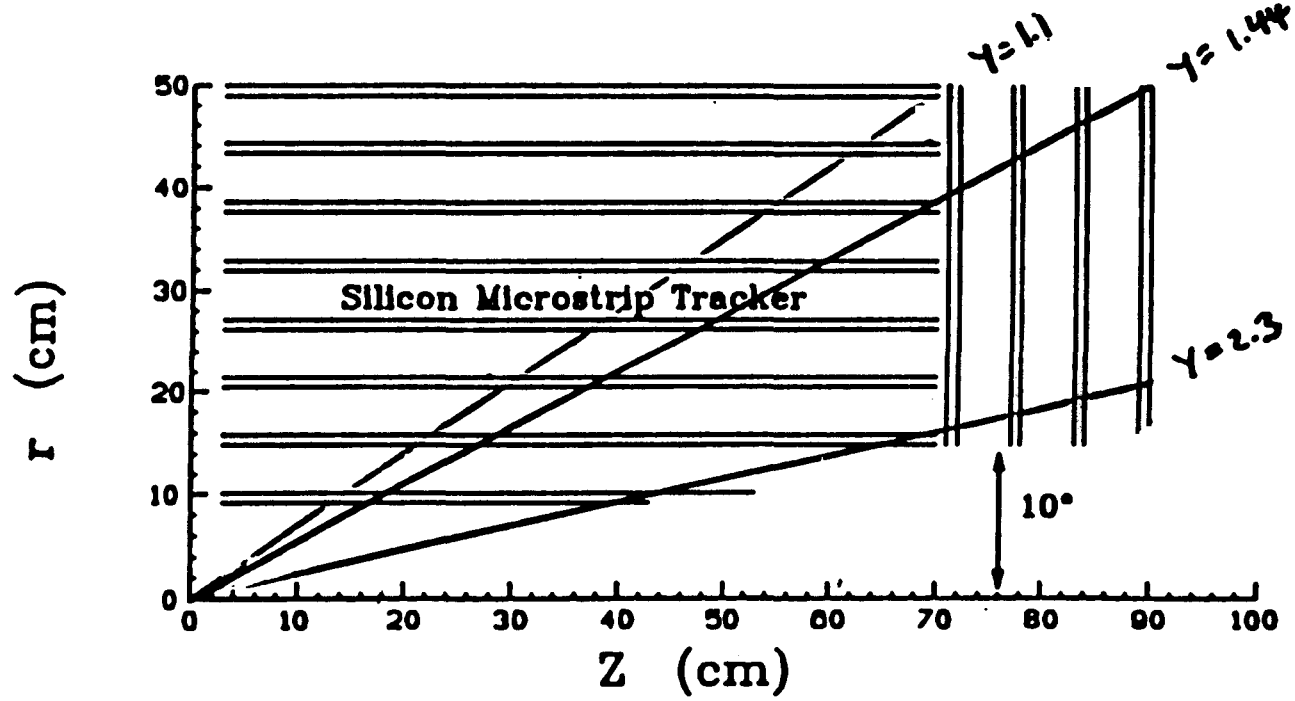

Fig. 22. Silicon Tracking System

ⓐ Tracking with ≥ 6 superlayers for $170° \geq \theta \geq 10°(|Y| \leq 2.3)$.

b Tracking with 8 superlayers for $160° \geq \theta \geq 20°(|Y| \leq 1.75)$.

ⓒ Tracking over a fixed radius of 50cm for $154° \geq \theta \geq 26°(|Y| \leq 1.44)$.

ⓓ Tracking with axial strips for $143° \geq \theta \geq 37°(|Y| \leq 1.10)$.

$$\frac{\sigma_{P_T}}{P_T^2} = \frac{2}{0.3B}\sqrt{\frac{\sum_{i=1}^{m}\frac{r_i^2}{\sigma_i^2}}{\sum_{i=1}^{m}\frac{r_i^2}{\sigma_i^2}\sum_{i=1}^{m}\frac{r_i^4}{\sigma_i^2} - \left(\sum_{i=1}^{m}\frac{r_i^3}{\sigma_i^2}\right)^2}}$$

For B=2.5 Tesla, 25 μm St

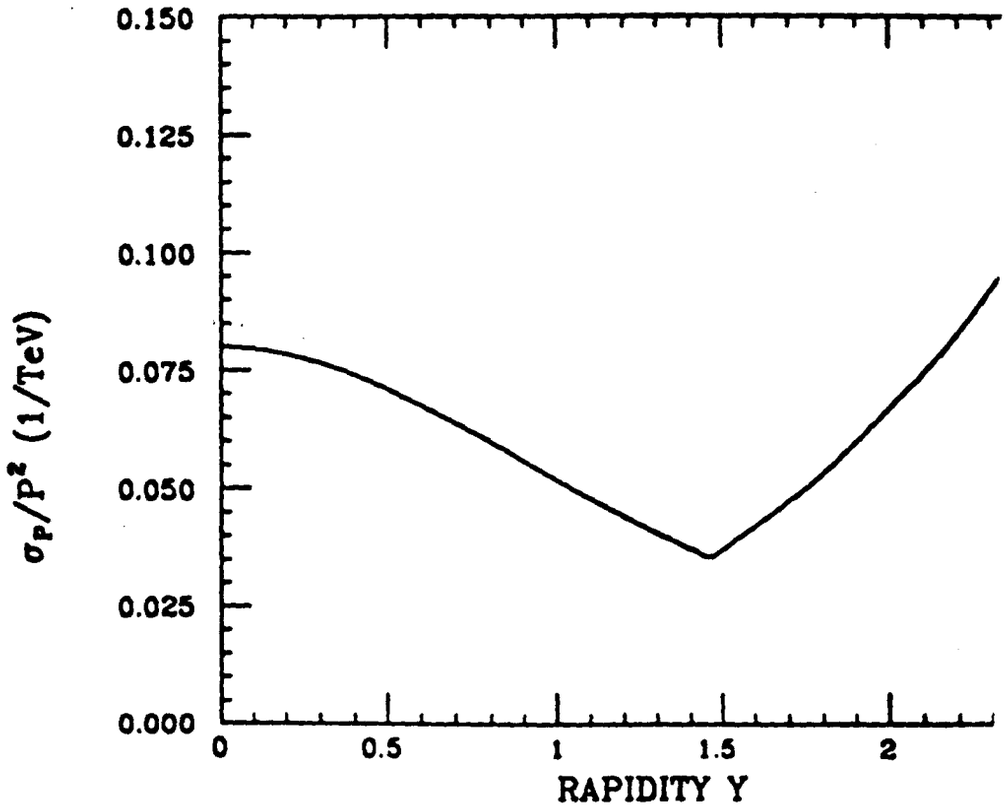

Momentum resolution vs. rapidity.

BOTH μ and e

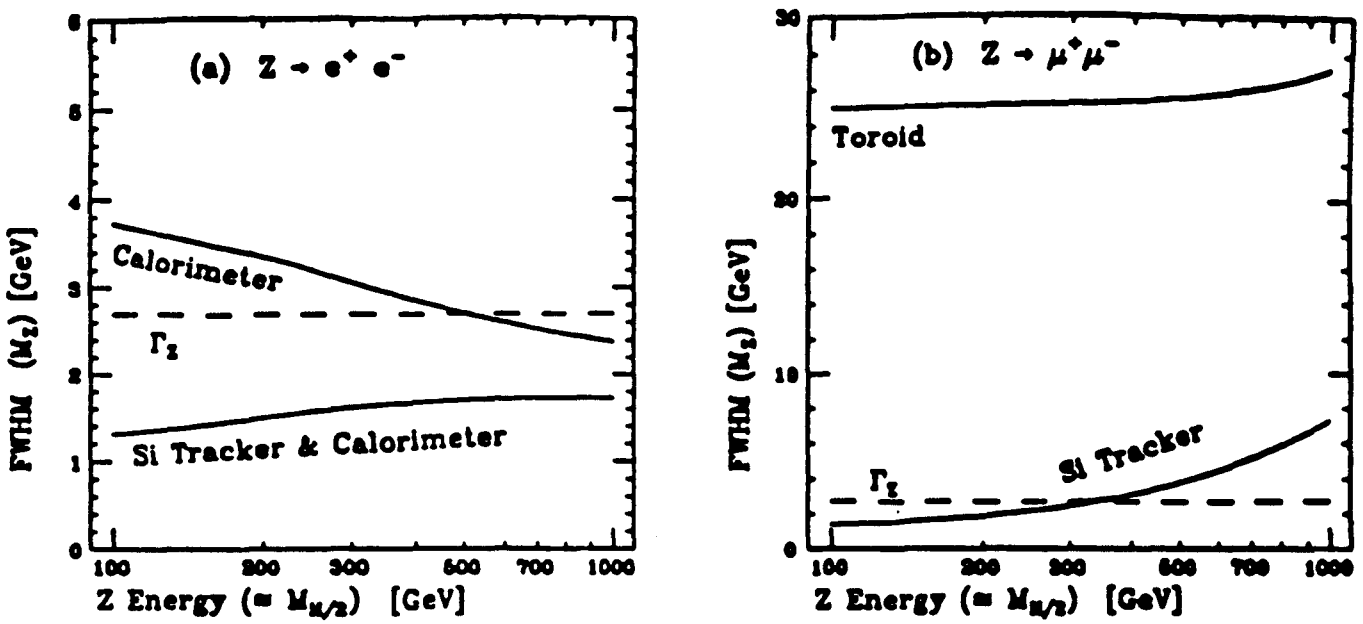

FWHM resolution of the Z^0 mass as a function of Z^0 energy for a detector with calorimetry only, and for a detector including precision Si tracking. a) $Z^0 \to e^+e^-$. b) $Z^0 \to \mu^+\mu^-$.

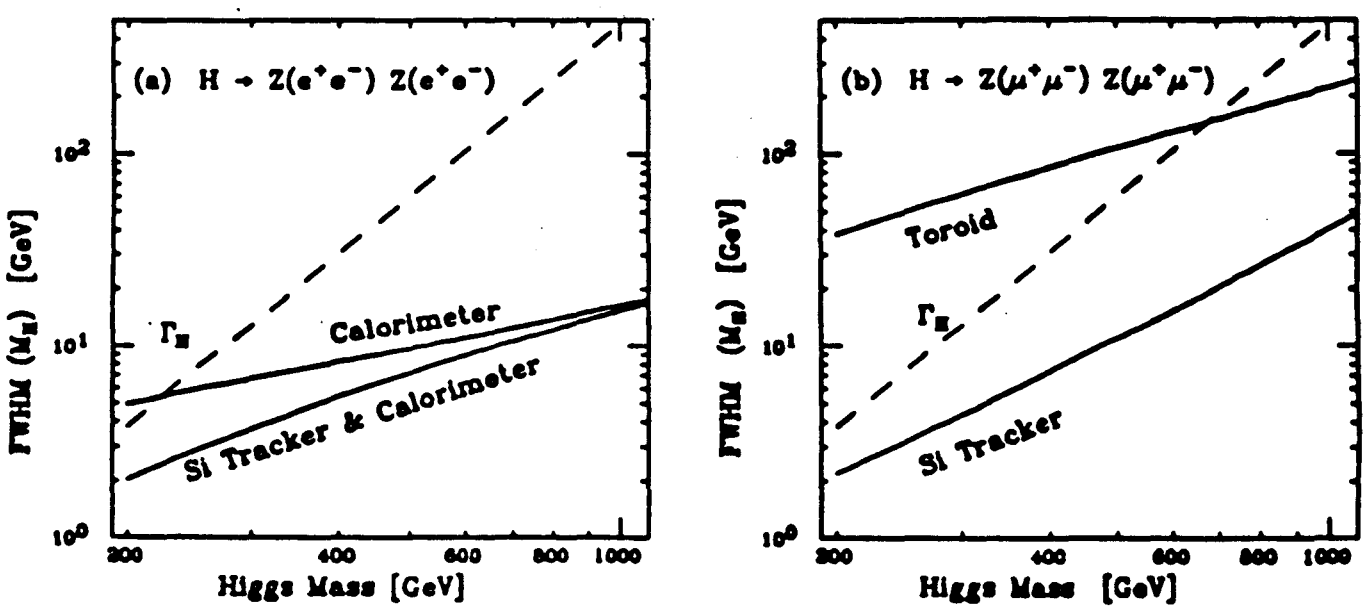

Z^0Z^0 invariant mass resolution for different detector configurations, compared with the expected Higgs width Γ_H (dashed line). a) $Z^0 \to e^+e^-$. b) $Z^0 \to \mu^+\mu^-$.

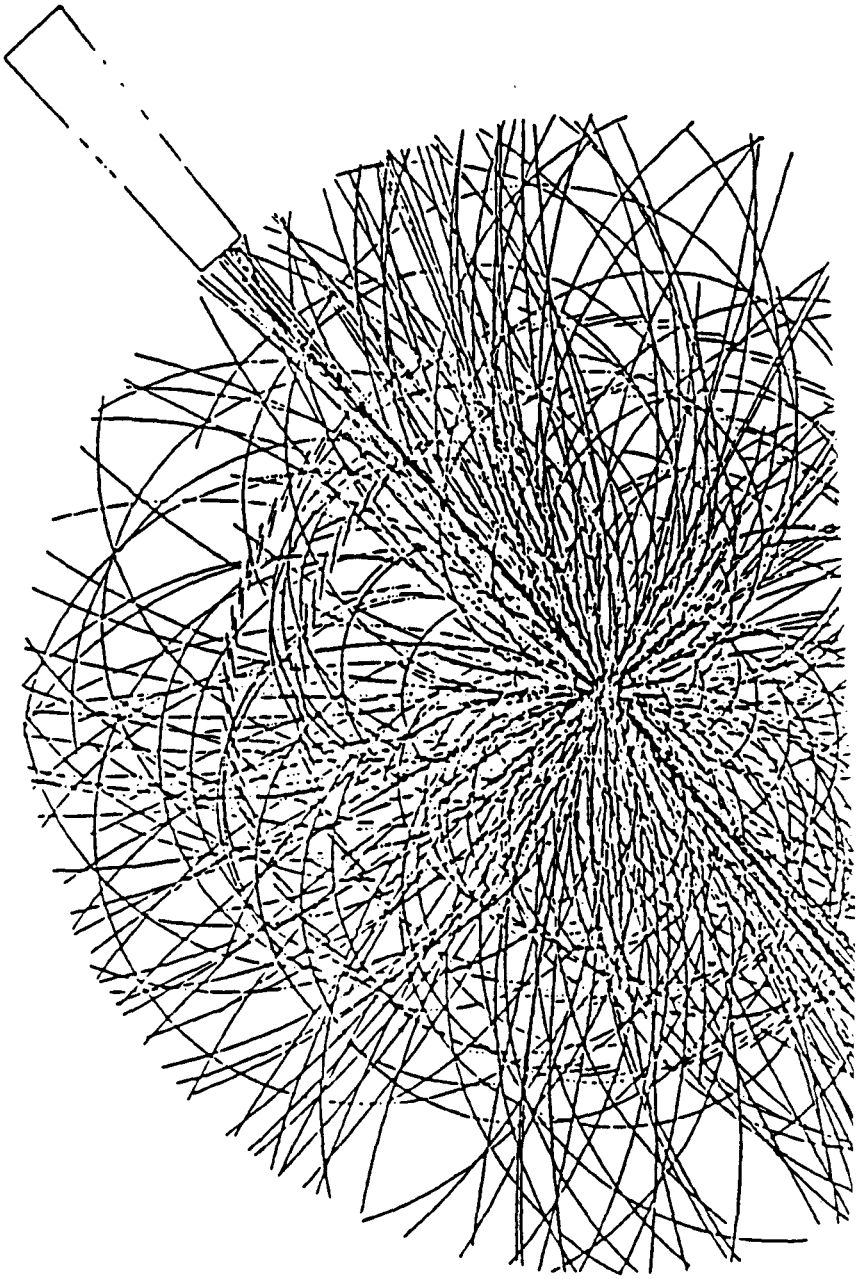

M.C. STUDY OF TRACK FINDING 1 TeV DETS

Δ = SEPARATION OF SUPERLAYERS = 6 CM

(r_{min} = 8 cm, r_{out} = 50 cm) $\langle\theta\rangle \cdot r = \varepsilon$ AT r = 20 cm

δ = SEPARATION OF DETECTORS INSIDE SUPERLAYERS

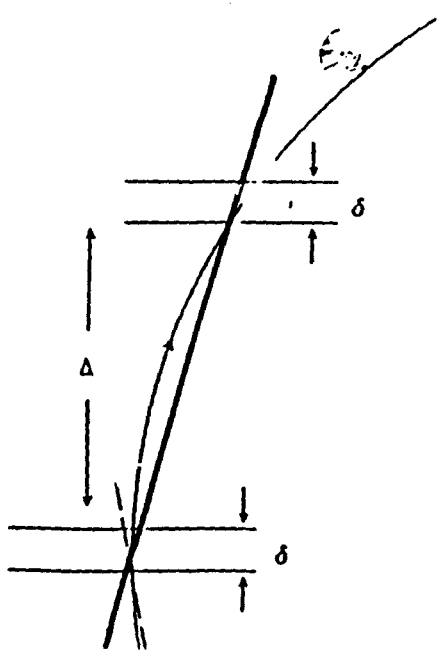

1.) VECTOR FINDING $\Rightarrow$ δ SMALL

2.) VECTOR ASSOCIATION $\Rightarrow$ ε LARGE

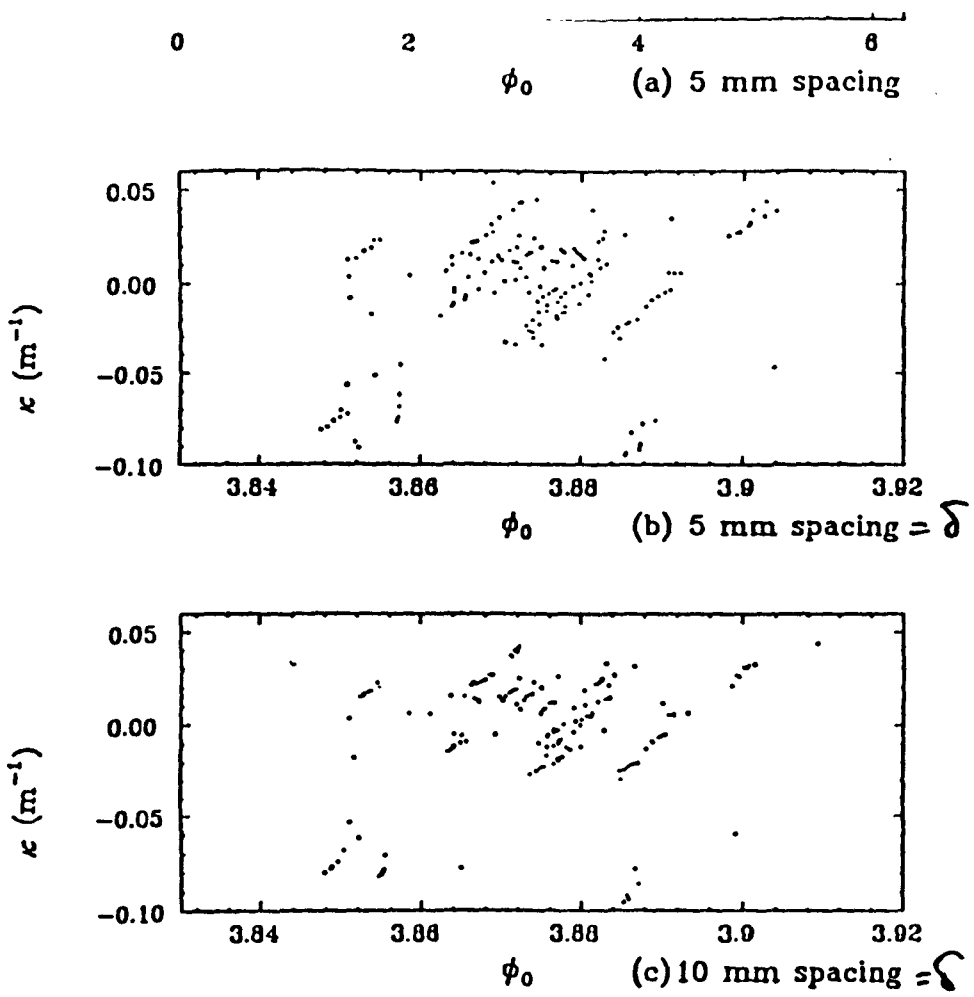

$$\kappa = \frac{}{2 \cdot \rho_{TRACK}}$$

TRACKS ARE DEFINED AS POINTS IN κ, ϕ_0 SPAC

FIG 17

M.C. EFFICIENCY

$\sigma = 1$ CM

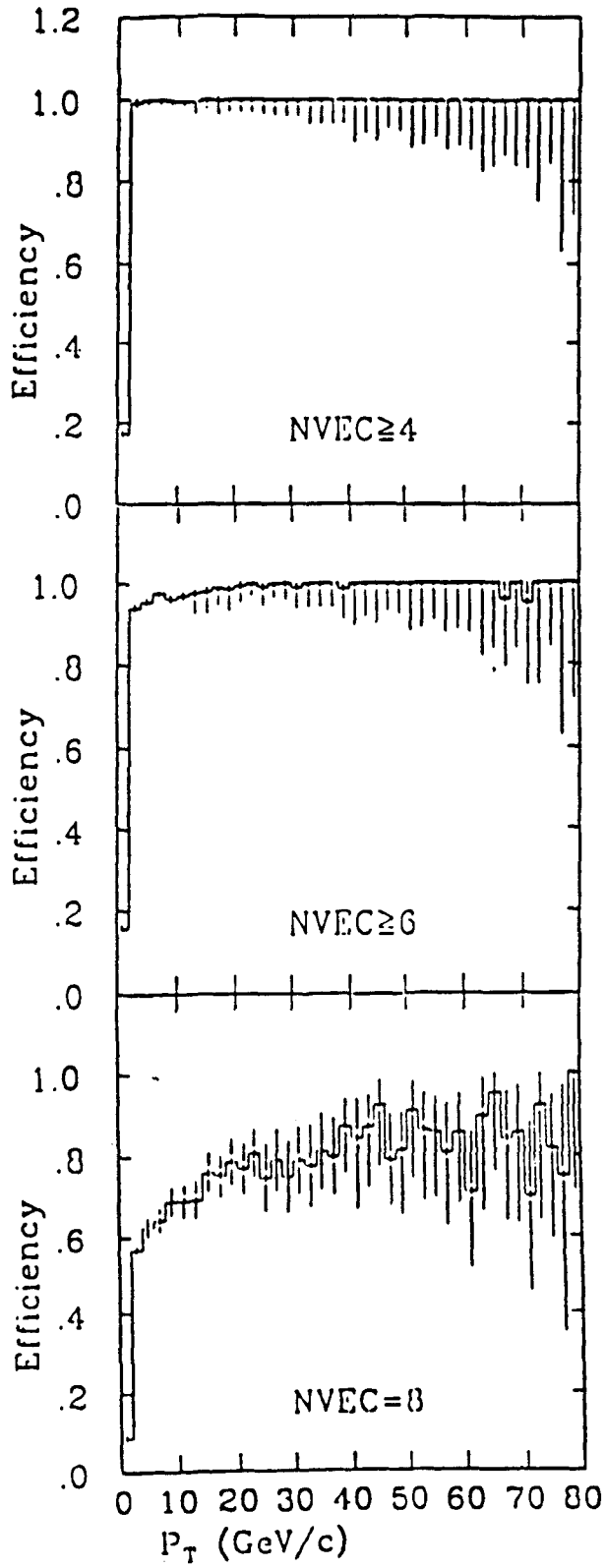

NVEC IS NUMBER OF VECTORS REQUIRED FOR TRACK

LOCAL Z- MATCH

U, V STRIPS ON SAME DETECTOR AS AXIAL

CONFUSION $\sim L \cdot \alpha$ → α SMALL (5 mrad)

σ (Z VERTEX) ≈ [illegible] (VERTEX IS ABOUT 7 CM LONG)

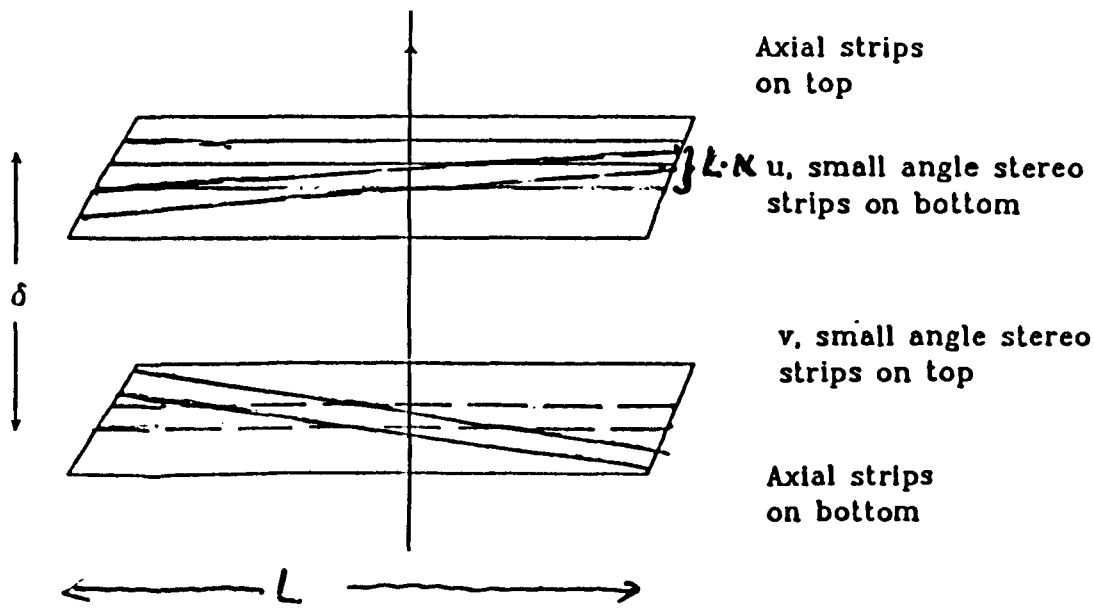

SYSTEM DESIGN

1) Strips from r=8cm to r=50cm
   Pixels from r=3cm to r=8cm

2) The exact configuration depends on the solution to t
   tions:
   - Power dissipation
   - Alignment
   - Radiation Hardness
   - Complexity (Cost)

   These issues are part of the generic SSC R &D ar
   cussed in this Workshop. Of great importance are M
   optimize the design.

   Example :

Study the effects of a system with much fewer channel

a) System with only 25μm wide strips:
   excellent momentum resolution, vey low occupancy

b) Fixed occupancy system- strip width grows with ra
   (25μm at r=8cm, 100μm at r=50cm):
   occupancy still very low because strip width $\leq$ 2 tr
   momentum resolution worse by factor 2 than for a
   some loss in pattern recognition power in outer lay
   but
   much less stringent alignment criteria and much fe

c) Combine b) with the outer driftchamber to restore
   resolution

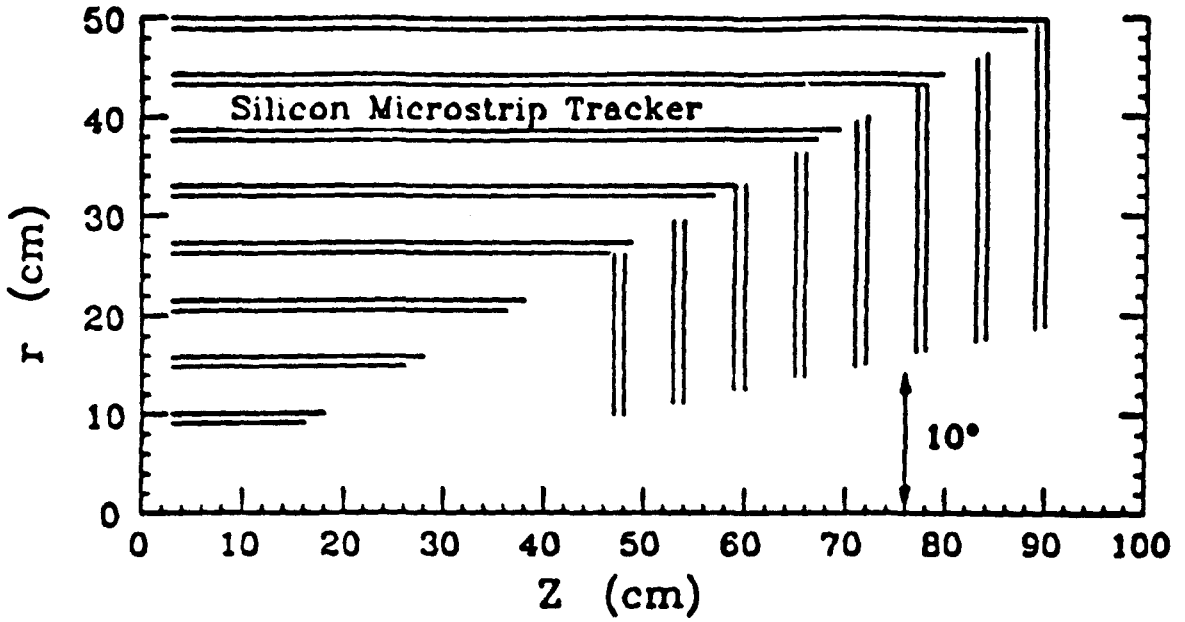

Silicon tracking system

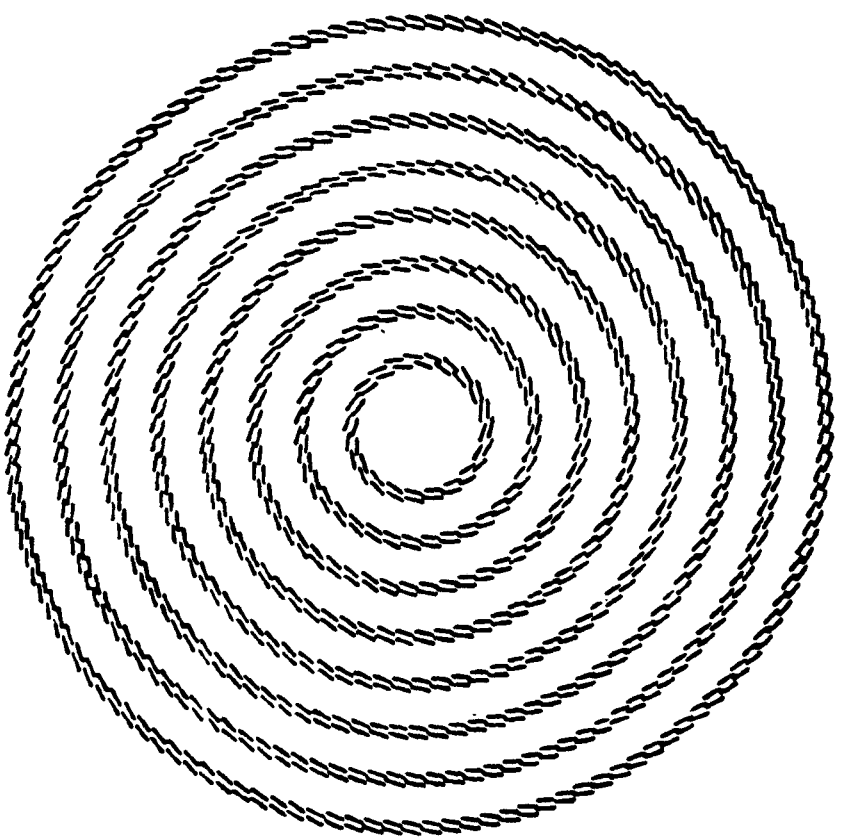

Central silicon tracker

SYSTEM MOMENTUM RESOLUTION

$$\frac{\sigma_P}{P} = \frac{C(\theta)}{B(\text{Tesla})}\, P\ (\text{TeV})$$

SYSTEM	C(90°)	σ_P/P $P = 1$ TeV, $B = 2.5$ T, $\theta = 90°$
A Silicon 8 cm–50 cm		
8 S.L. 25 μm strips	0.26	10%
B Drift 50 cm–150 cm		
100 L. $\sigma = 200$ μm	0.51	20%
A + B	0.14	5.6%
C Silicon 8 cm–50 cm		
3 S.L. 25 μm strips		
2 S.L. 50 μm strips	0.52	21%
3 S.L. 100 μm strips		
C + B	0.15	6.0%

Fixed occupancy

High Backgrounds (Only back half of detectors is usable) :

Back of B	1.06	42%
Back of C	1.30	52%
Back of C + Back of B	0.18	7.2%

OTHER PROPERTIES OF FIXED OCCUPANCY

SI TRACKER :

4 UNITS

2 CENTRAL $-1.35 \leq \eta \leq 0$, $0 \leq \eta \leq 1.35$

2 FORWARD $-2.4 \leq \eta \leq -1.35$, $1.35 \leq \eta \leq 2.4$

EACH UNIT HAS ABOUT 20 TRACKS / TIME BUCKET FROM MIN. BIAS EVENTS (+ CURLERS)

$\rightarrow$ OCCUPANCY $\leq 4 \cdot 10^{-3}$ (SETS SCALE FOR S/N)

LEAKAGE CURRENTS : (AFTER ONE YEAR)

AT $\mathcal{L} = 10^{33} (cm^2 sec)^{-1}$ neutron fluence $= 10^{12} \frac{n}{cm^2} \frac{1}{YEAR}$

		YEARLY CHARGED FL.	CURRENT/STRIP (μA) neutron	charged	total
CENTRAL REGION	INNER LAYER	$4 \cdot 10^{13} \frac{1}{cm^2}$	0.08	1.3	1.4
	OUTER LAYER	10^{12} "	0.95	0.4	1.4

This corresponds to ENC = 400 e .

LEAKAGE IN FORWARD UNITS SMALL .

R&D for the SSC SILICON TRACKER

1) Monte Carlo Simulations of designs (Radii, Length and width of strips and pixels, Number of layers)

2) Detector Research (Double sided,Collection,Radiation hardness, Bonding,Integration with electronics)

3) Electronics (Radiation hardness,Speed,Low Power,Read-out, Interaction with trigger)

4) Mechanical integration (Supports, Alignment, Temperature stability)

5) Cooling

THERE IS CONSIDERABLE EXPERIENCE WITH SI STRIPS:

a) FIXED TARGET

b.) COLLIDING BEAMS (MK II, CDF)

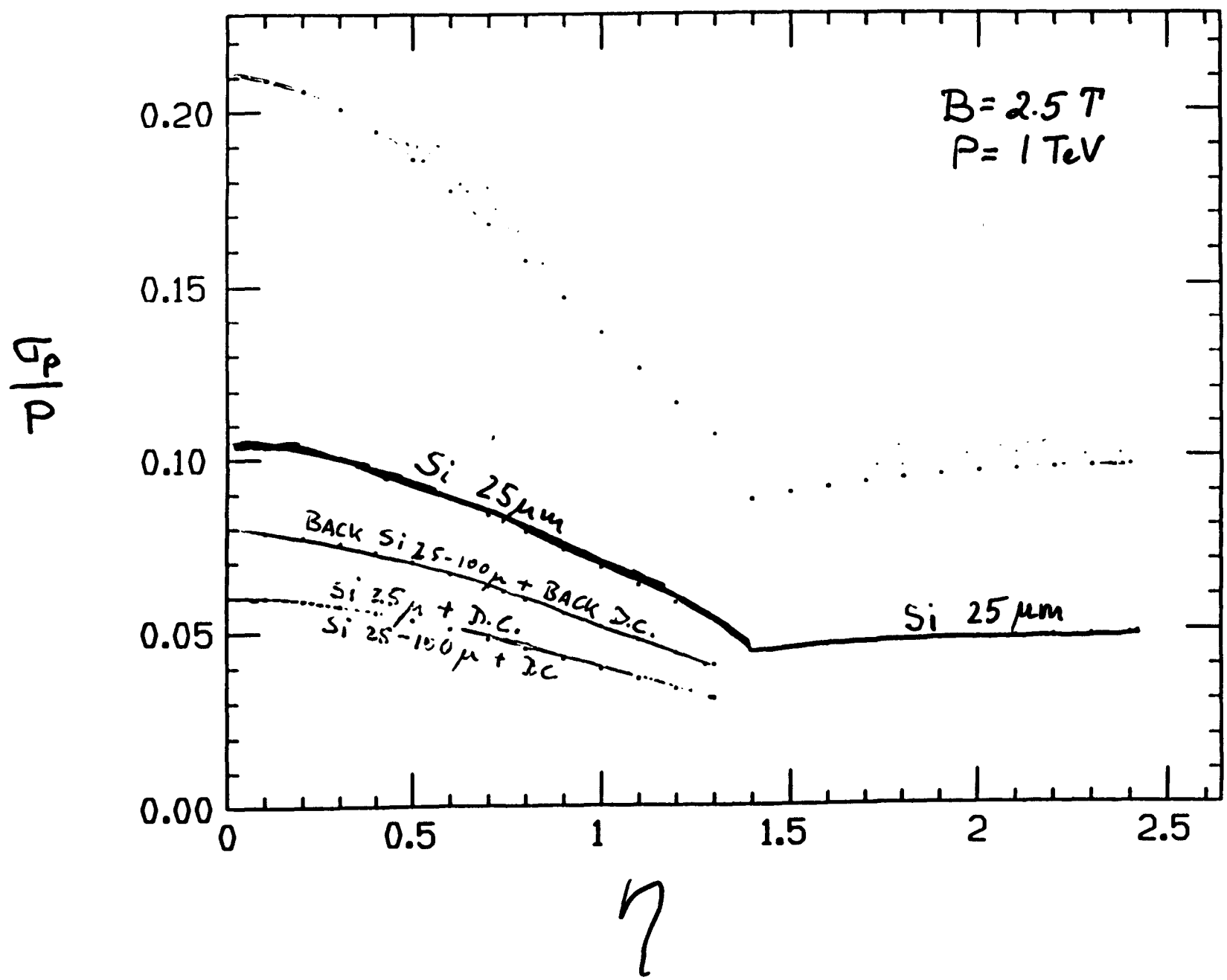

SIRES TOPDRAW 81 created on 24 Jun 1988 at 22:32.

Readout – VLSI chips.

H. Gordon
6/26/89 - DALLA.

PROGRESS in the DESIGN of a LIQUID ARGON CALORIMETER FOR the SSC

Lots of Progress at the Alabama workshop

- Engineering
- Hermeticity
- Nitty Gritty Details
- Electronics

We are preparing a "Major Subsystem R+D Proposal for Oct. 1, 1989

e. H. Gordon

CALORIMETRY REQUIREMENTS

H. Gordon.

Further Study

- **Radiation Resistance:**

  $\approx 10^6$ rads/year; $\approx 10^{12}$ neutrons/cm^2 year

- **Energy Resolution:**
  - EM , $\approx 0.15/E^{1/2}$, constant term $\approx 1\%$ (low PT electrons)
  - Hadronic , $< 1.0/E^{1/2}$ sufficient, $\leq \underline{0.5/E^{1/2}}$ very good

- **Systematics, Calibration, Uniformity, Stability:** 1% if easy, 2% if hard ✓

- **Electron/hadron Response:** $\leq \underline{1.1}$ direct response, or by weighting (quark compositeness signal!) ✓

- **Dynamic Range:**

  EM, 5 TeV lepton ($\approx$ 2.5 TeV in one channel)
  Lepton isolation test $\approx$ 100 MeV/channel } $\underline{2.5 \times 10^4}$ -10^5
  Hadronic, QCD jets $\approx$ 5-6 TeV in one jet cone

- **Noise (electronic-, uranium-):**
  - Lepton isolation $E_T < 4$GeV in $\Delta R \approx 0.4$
  - Missing PT $\sigma_{el} < 20$ GeV

- **Speed and Pileup:**
  - Timing (associate events and bunch crossings), $\sigma_t \approx \underline{1\text{-}2 \text{ nsec}}$
  - Integration time (hadron response) $t_m \approx \underline{100\text{-}150}$ nsec ✓
  - Pileup time, impact of overlap of n (e.g., 10) bunch crossings ✓

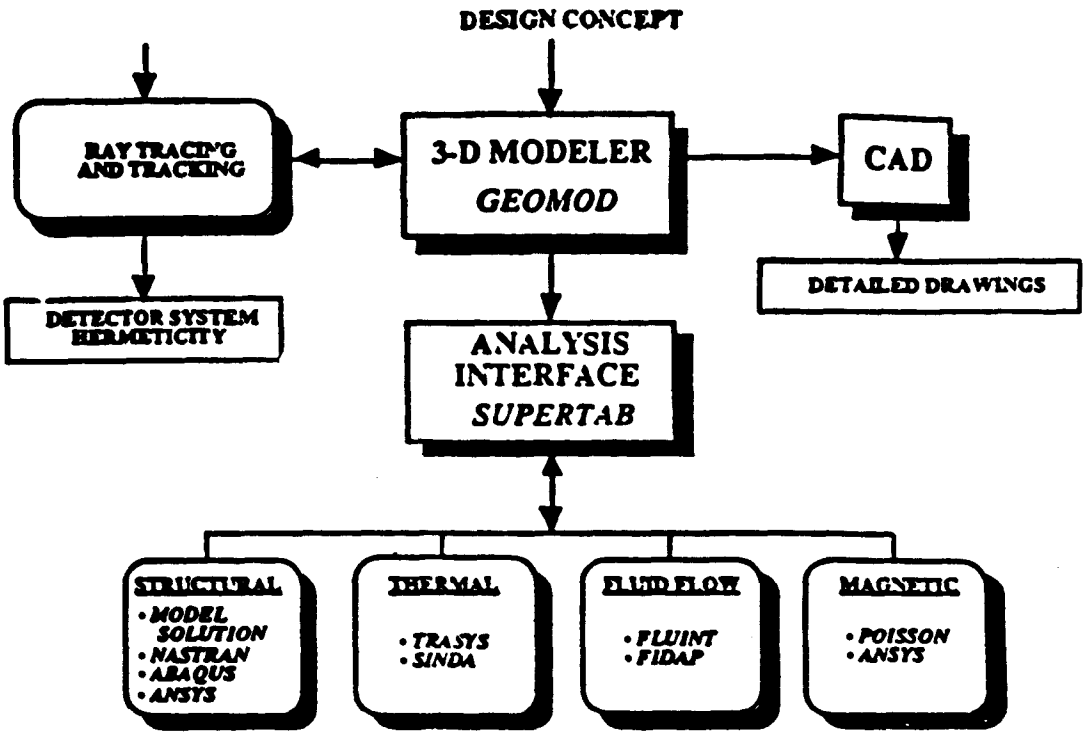

Figure 1: The integrated design, modeling and analysis system.

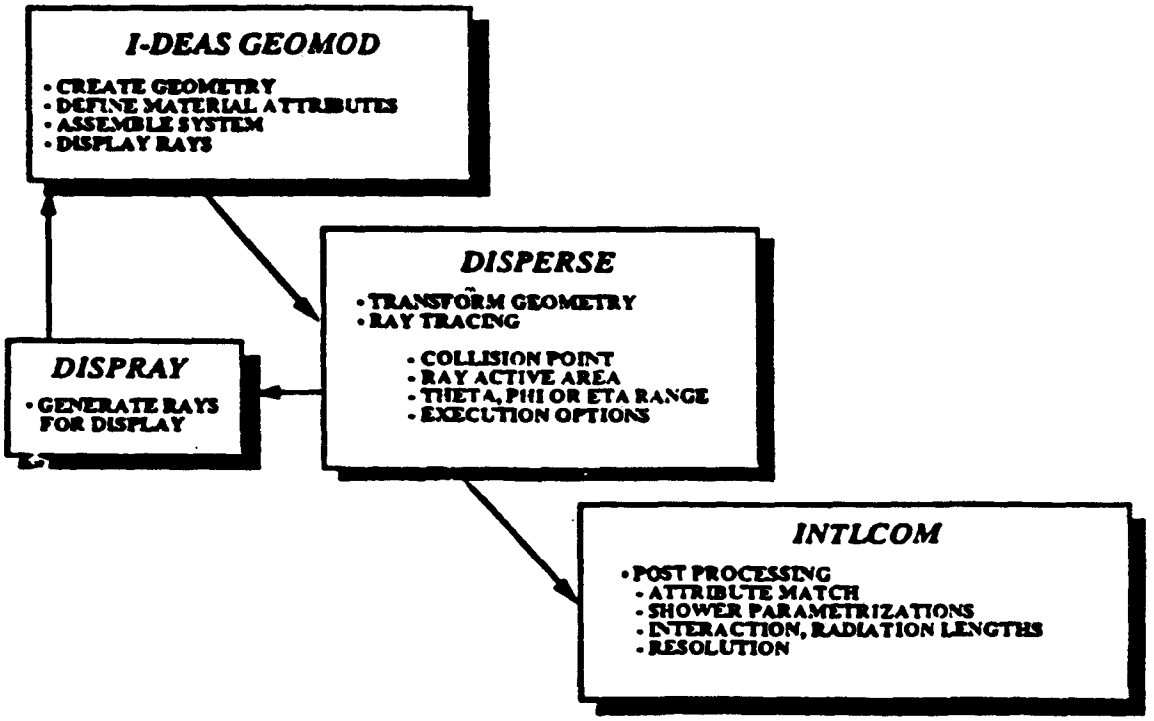

Figure 2: The ray tracing and tracking section of the design, modeling and analysis system.

I. Engineering

"Martin Marietta" Design for LSD

Report is a snapshot of work in progress

Future plans

Minimize wall thickness in end cap

Finish Details of support

Assembly scenarios, design of handling eg.

$r = 1\,m$

$\rho = 10\ g/cm^3$

solenoid inside calorimeter — hermeticity?

split @ 90°

Schedule and cost $68–93M scaled from DØ/SLD

STATUS REPORT OF AN ENGINEERING DESIGN STUDY OF HERMET LIQUID ARGON CALORIMETRY FOR THE SSC

T. Adams[2], M. Davis[2], N. J. DiGiacomo[2]*, B. Easom[2], H. Gordon[1], J. Hupp
K. Killian[2], P. Kroon[1], M. Lajczok[2], M. Marx[3,4], L. Mason[2], J. Pohlen[2],
R. Watt[4], and T. Wright[2]

(1) Brookhaven National Laboratory, Upton, NY 11973
(2) Martin Marietta Astronautics, Denver, CO 80201
(3) State University of New York at Stony Brook, Stony Brook, NY 11794
(4) SSC/CDG, Lawrence Berkeley Laboratory, Berkeley, CA 94720

FERMILAB-Conf-89/109
D0 Note 839

Hermeticity of Three Cryogenic Calorimeter Geometries *

M. Strovink
University of California, Berkeley / Fermilab

W.J. Womersley
University of Florida

G.E. Forden
State University of New York, Stony Brook

FERMILAB-Conf-89/109
D0 Note 839

Hermeticity of Three Cryogenic Calorimeter Geometries *

M. Strovink
University of California, Berkeley / Fermilab

W.J. Womersley
University of Florida

G.E. Forden
State University of New York, Stony Brook

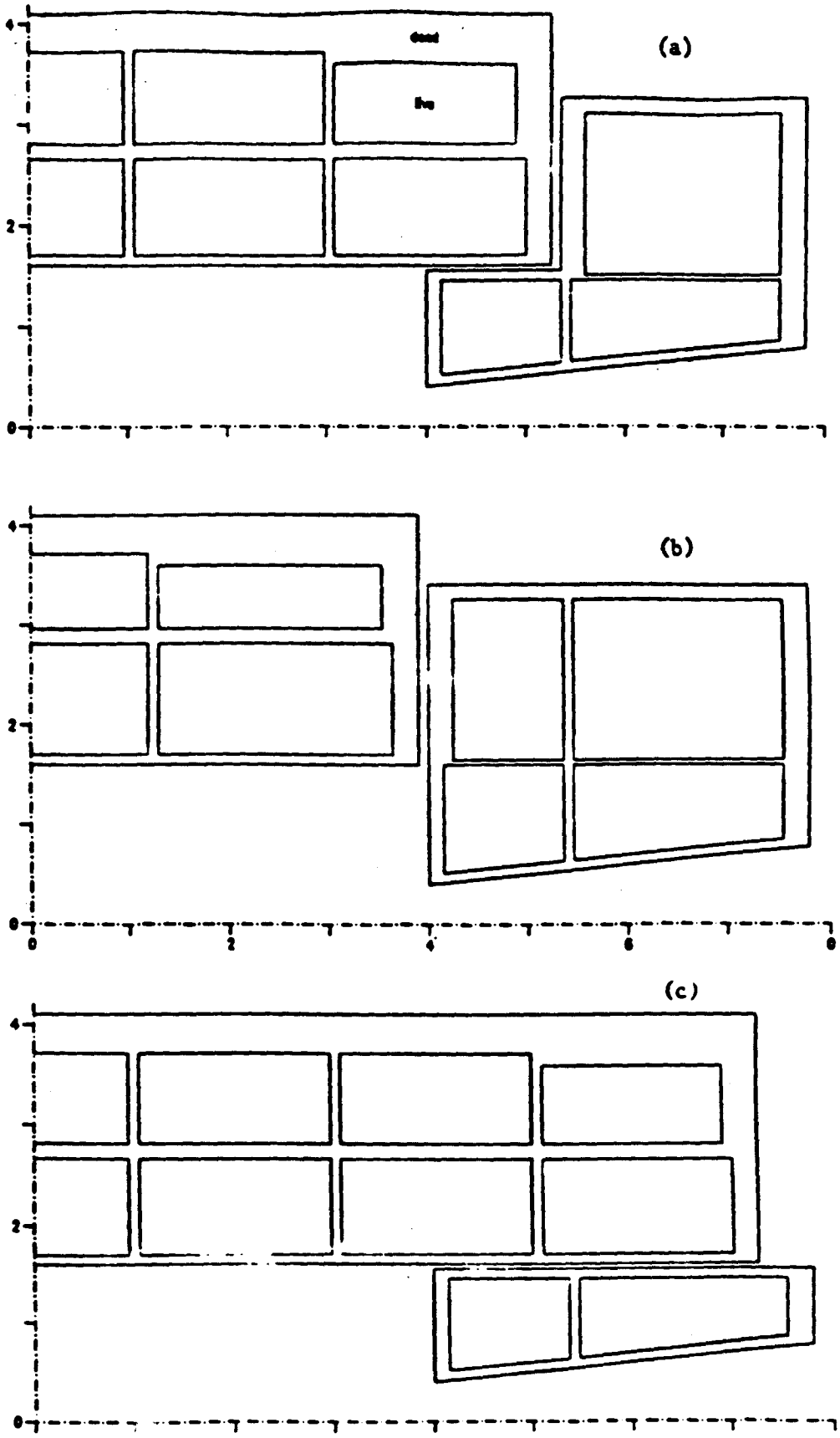

Fig. 1

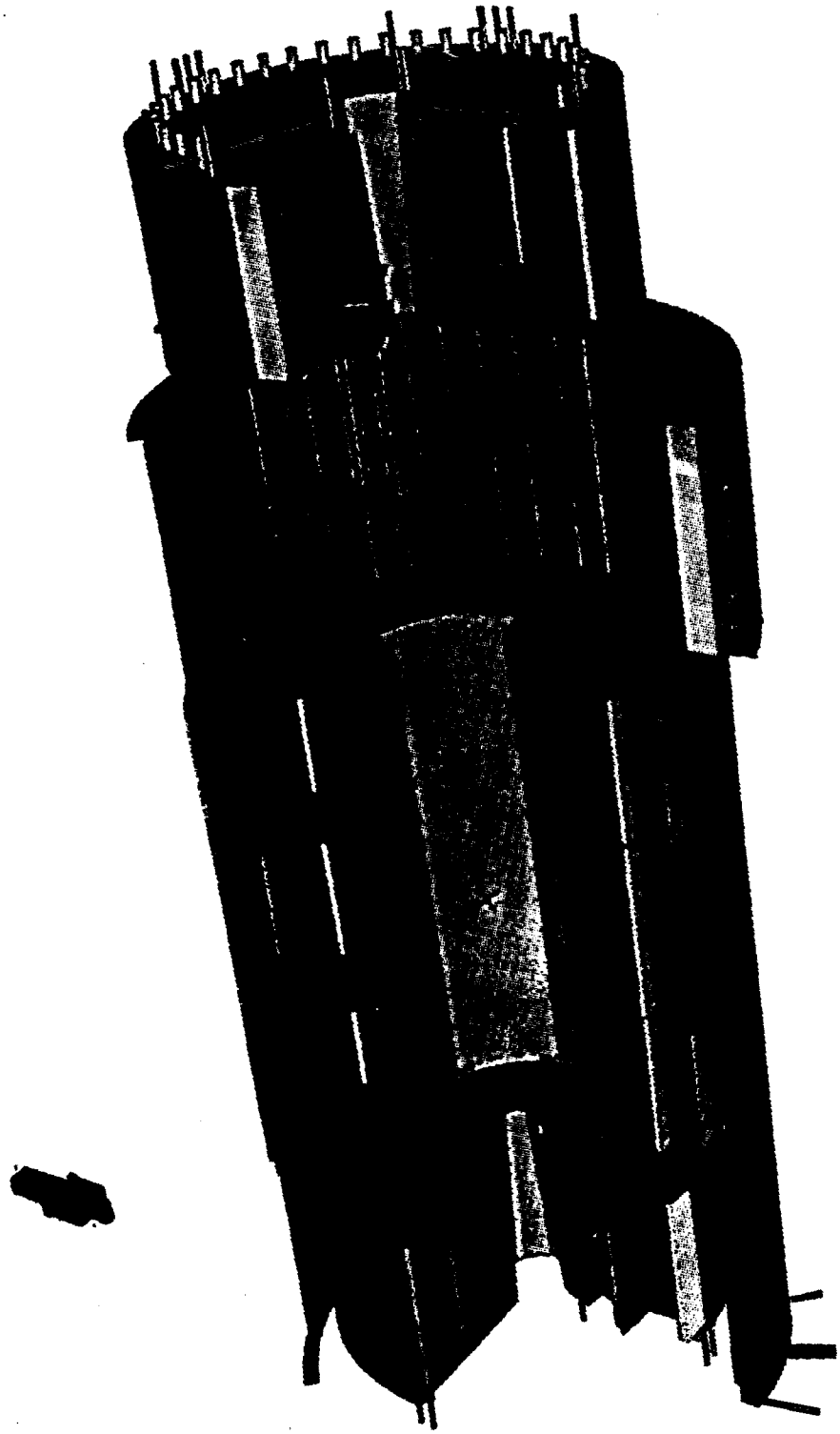

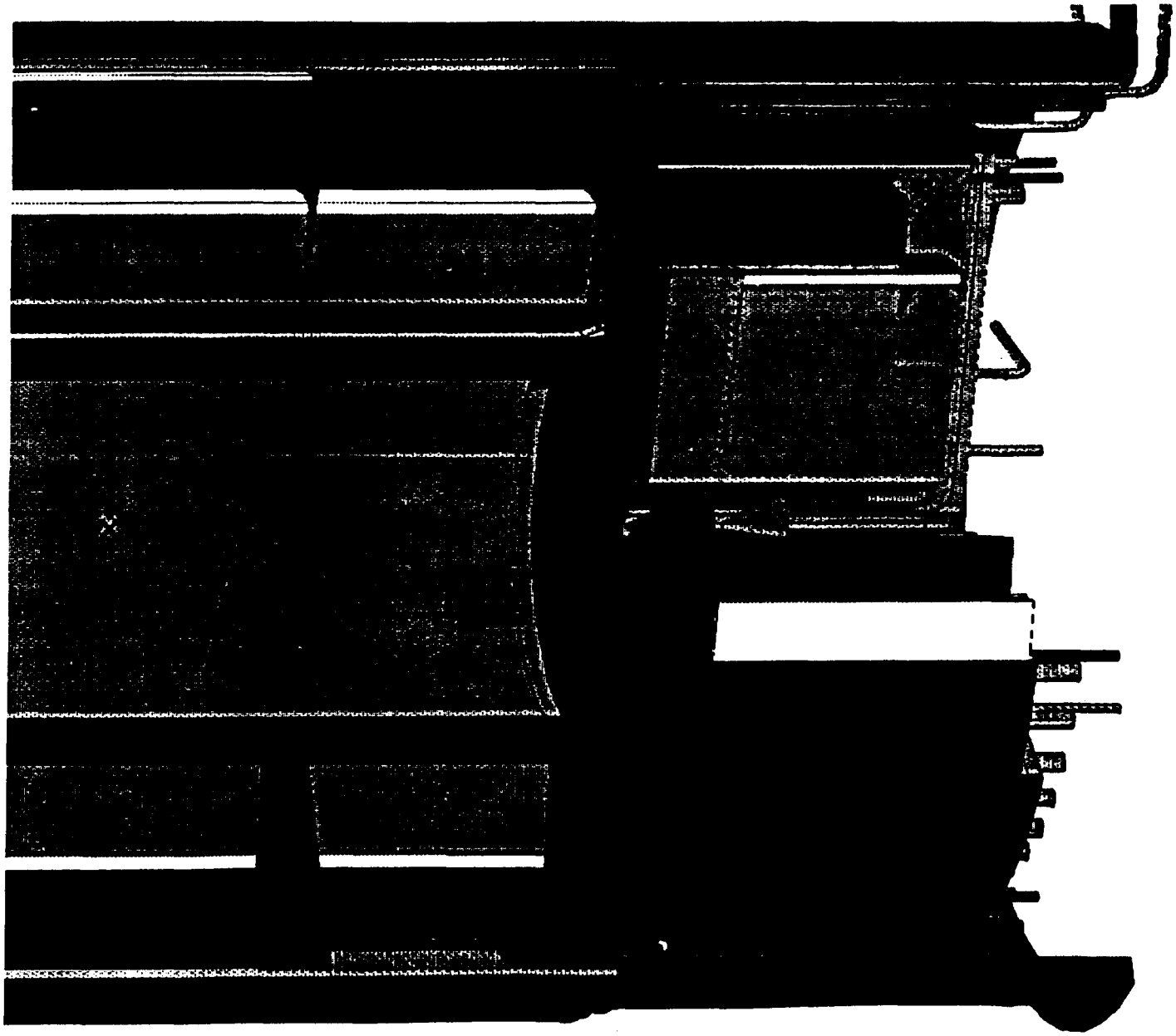

1A1B 6

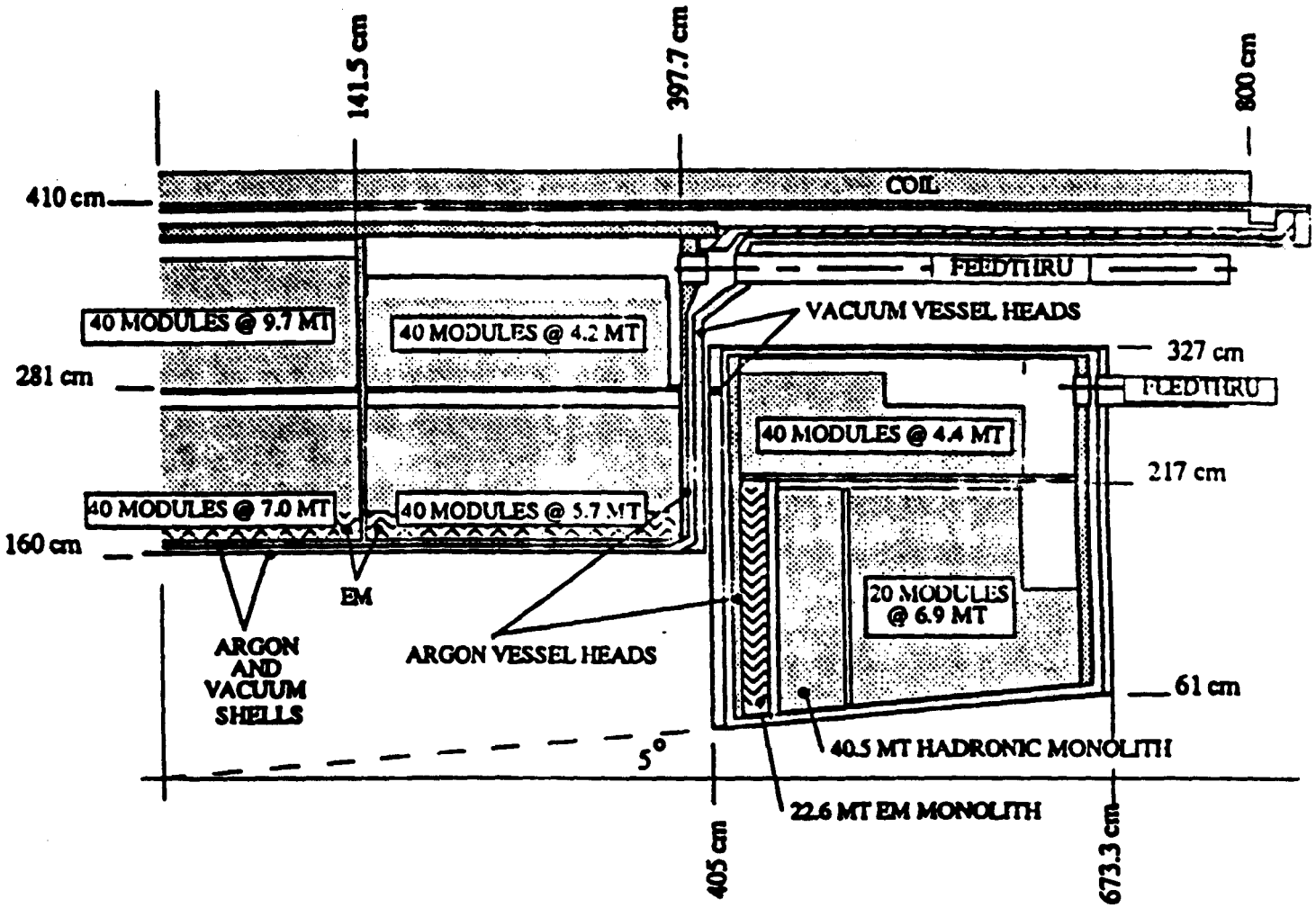

Figure 5: Schematic view of LAC, showing overall dim... each region ...

	ARGON VESSELS BARREL	ARGON VESSELS END CAPS		VACUUM VESSELS BARREL	VACUUM VESSELS END CAPS
Inner Shell	3.8 cm	2.5 cm	Inner Shell	1.9 cm	7.6 cm
Corner	3.8	10.9 to 2.5			
Outer Shell	7.1	4.8	Outer Shell	5.1	4.5
Heads	6.1	8.9	Heads	5.3	[illegible]
Washers	5.6	[illegible]			

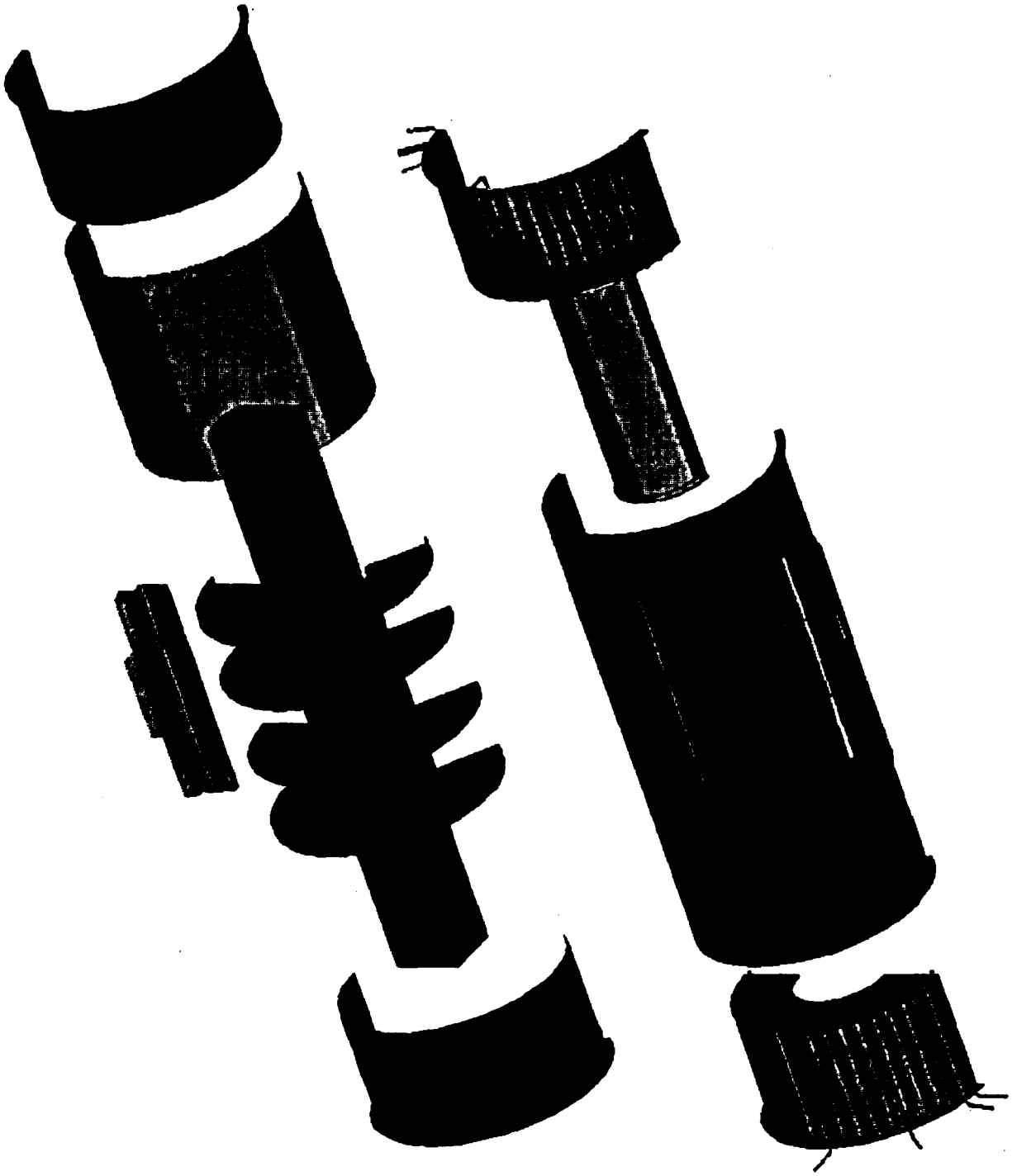

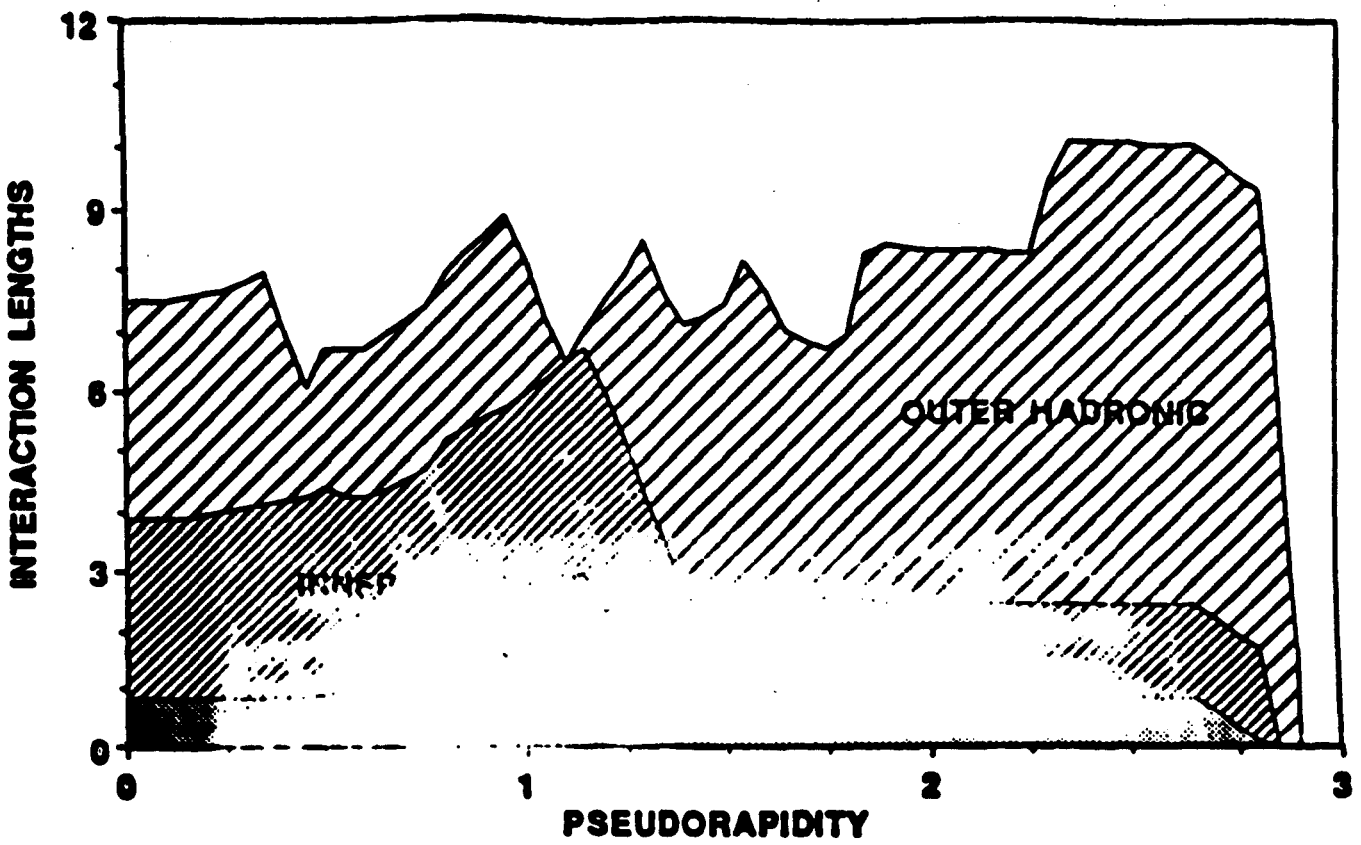

gure 9: Active interaction lengths of calorimeter (i.e. not including vessels, structural [illegible] in the LAC [illegible] assuming ρ = 7.5 g/cm^3, λ = 25 cm and X_o = 0.80 cm.

	Al	Steel	Ti
SHELLS			
t/t_{Al} (Stress: $S^{1.0}$)	1	.53	.18
(t/t_{Al}) (l_{Al}/l)	1	1.25	.26
(t/t_{Al}) (X_{oAl}/X_o)	1	2.69	.46
t/t_{Al} (Stability: $E^{1/3}$)	1	.71	.86
(t/t_{Al}) (λ_{Al}/λ)	1	1.66	1.24
(t/t_{Al}) (X_{oAl}/X_o)	1	3.58	2.16
HEADS/WASHERS			
t/t_{Al} (Bending: $S^{1/2}$)	1	.73	.43
(t/t_{Al}) (λ_{Al}/λ)	1	1.71	.61
(t/t_{Al}) (X_{oAl}/X_o)	1	3.69	1.07
t/t_{Al} (Stability: $E^{1/2}$)	1	.60	.80
(t/t_{Al}) (λ_{Al}/λ)	1	1.40	1.15
(t/t_{Al}) (X_{oAl}/X_o)	1	3.02	2.01
ρ (g/cm^3)	2.70	7.87	4.54
λ (cm)	39.40	16.80	27.50
X_o (cm)	8.90	1.76	3.56
S (10^3 psi)	10.0	18.75	55.
E (10^6 psi)	10.0	28.	15.5
Relative Cost (fabricated)	1.0	2.5	3.0

Table 4: Cryostat material performance, referenced to aluminum.

DESIGN EVOLUTION

MODULE SCHEDULE

MINIMUM TIME (FAST) SCHEDULE

	YEARS
SELECT GAP + ABSORBER STRUCTURE	1/2
DESIGN MODULES	1
VERIFY DESIGN (LAR, COSMIC + BEAM TESTS)	1
FIRST ARTICLES FROM INDUSTRY	3/4
ASSEMBLE + TEST FIRST ARTICLES	1/4
PRODUCTION + SIMULTANEOUS TESTING	2
COMPLETE TESTING	1/2
INSTALLATION INTO VESSELS + TESTING	1
VESSEL CLOSURE + EXTERNAL CONNECTIONS	1/2
	7 1/2

CONSERVATIVE (SLOW) SCHEDULE

R+D ON PB COMPENSATION, U PLATING/ CLADDING, SUB-UNIT TYPE GAPS	2
MODULE DESIGN	1
VERIFY DESIGN	1
TECHNOLOGY TRANSFER TO INDUSTRY	1 1/2
FIRST ARTICLES	1/2
TEST FIRST ARTICLES	1/2
REDESIGN	1/2
PRODUCTION + SIMULTANEOUS TESTING	2
COMPLETE TESTING	1/2
INSTALLATION INTO VESSELS + TESTING	1 1/2
VESSEL CLOSURE + EXTERNAL CONNECTIONS	1 1/2
	12 1/2

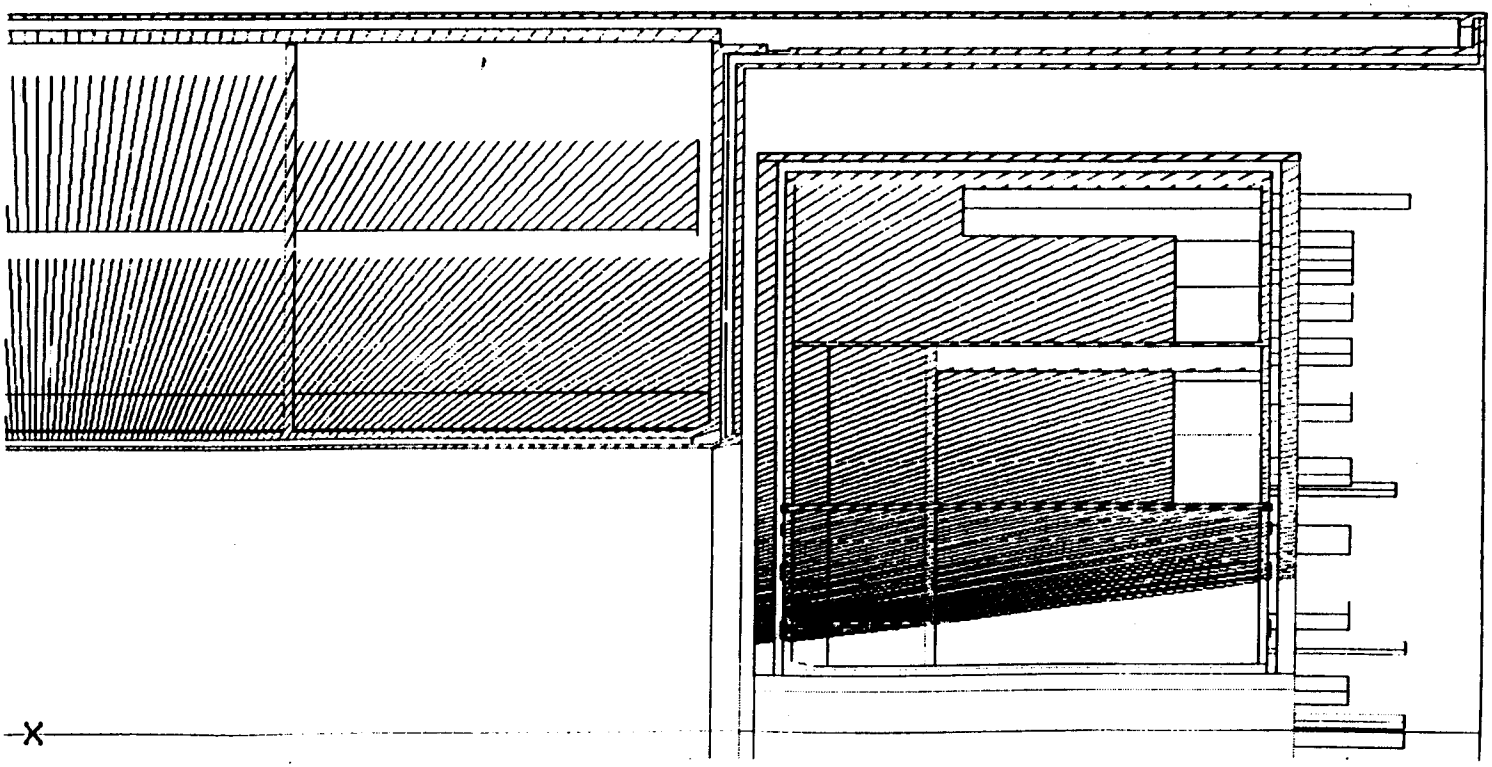

A1A1

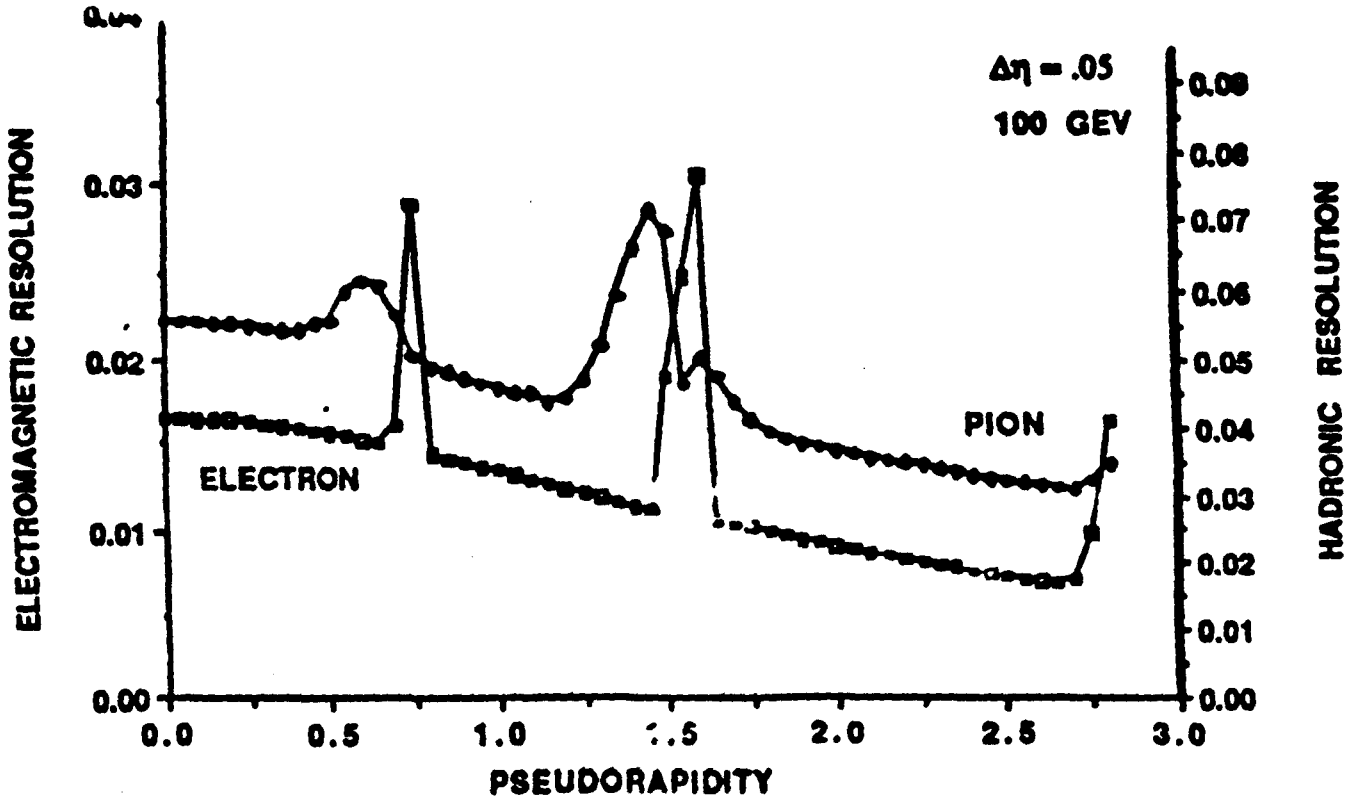

Figure 13: Resolution versus pseudorapidity for 100 GeV transverse energy electrons

II HERMETICITY

- DEAD MATERIAL
- DEPTH

LSD (Pb ⇒ ~7λ ; U ⇒ ~10λ)

Jürgen Krüger (Zeus)

in 6.6λ 90% of 135GeV Jets >95% energy

in ~9λ 99%

Need specification from $\not{p}_T$ physics

III. Nitty-gritty details

Absorber choice e/π

SLD tests Pb/LA ~1.2±0.1

HELIOS (NA34)] U/LA

DØ (1988)]

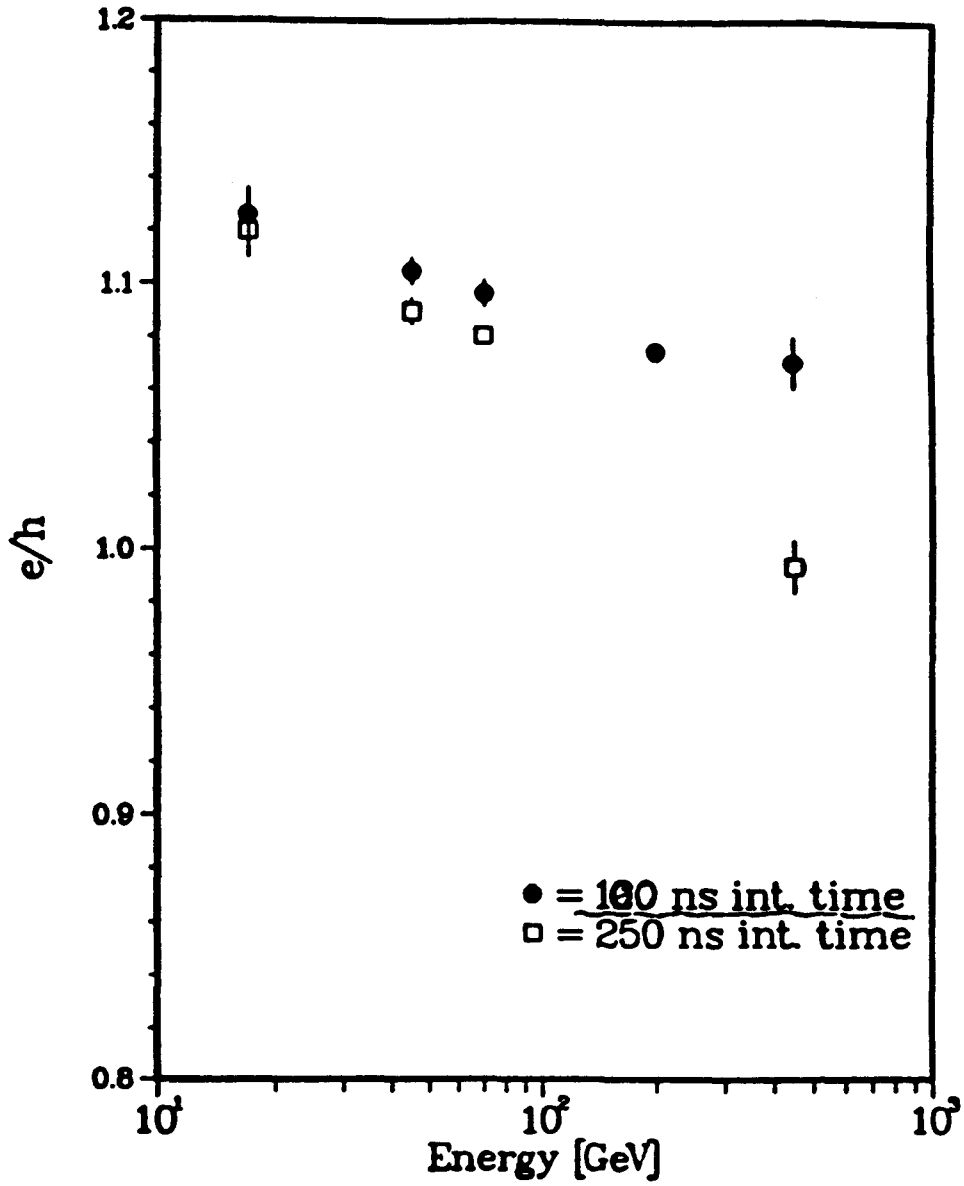

Uranium - Liquid Argon Calorimeter for HELIOS exp.

e/h ratio vs E

NA34

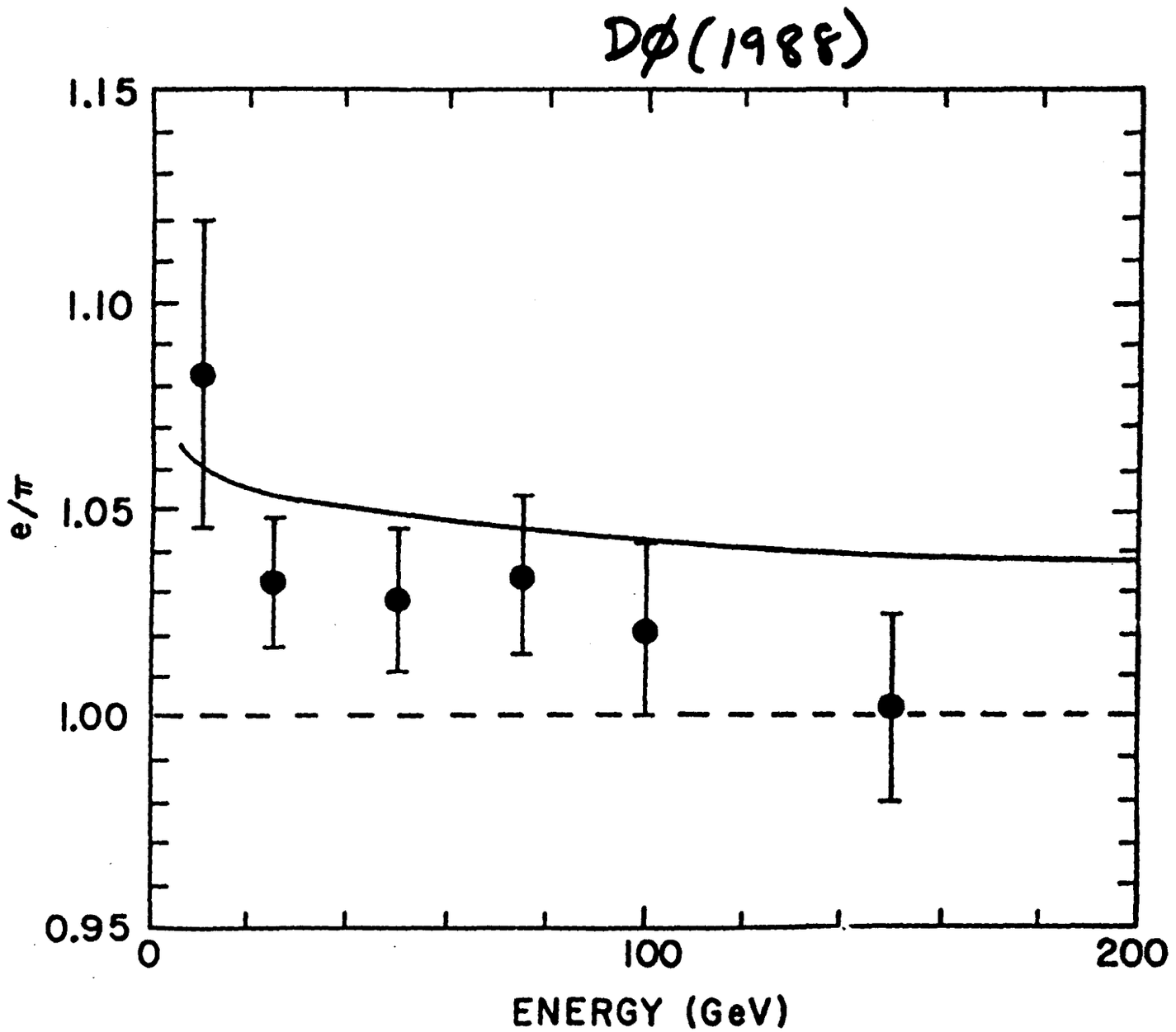
DØ (1988)
1.15
1.10
1.05
1.00
0.95
e/π
0
100
200
ENERGY (GeV)

DØ

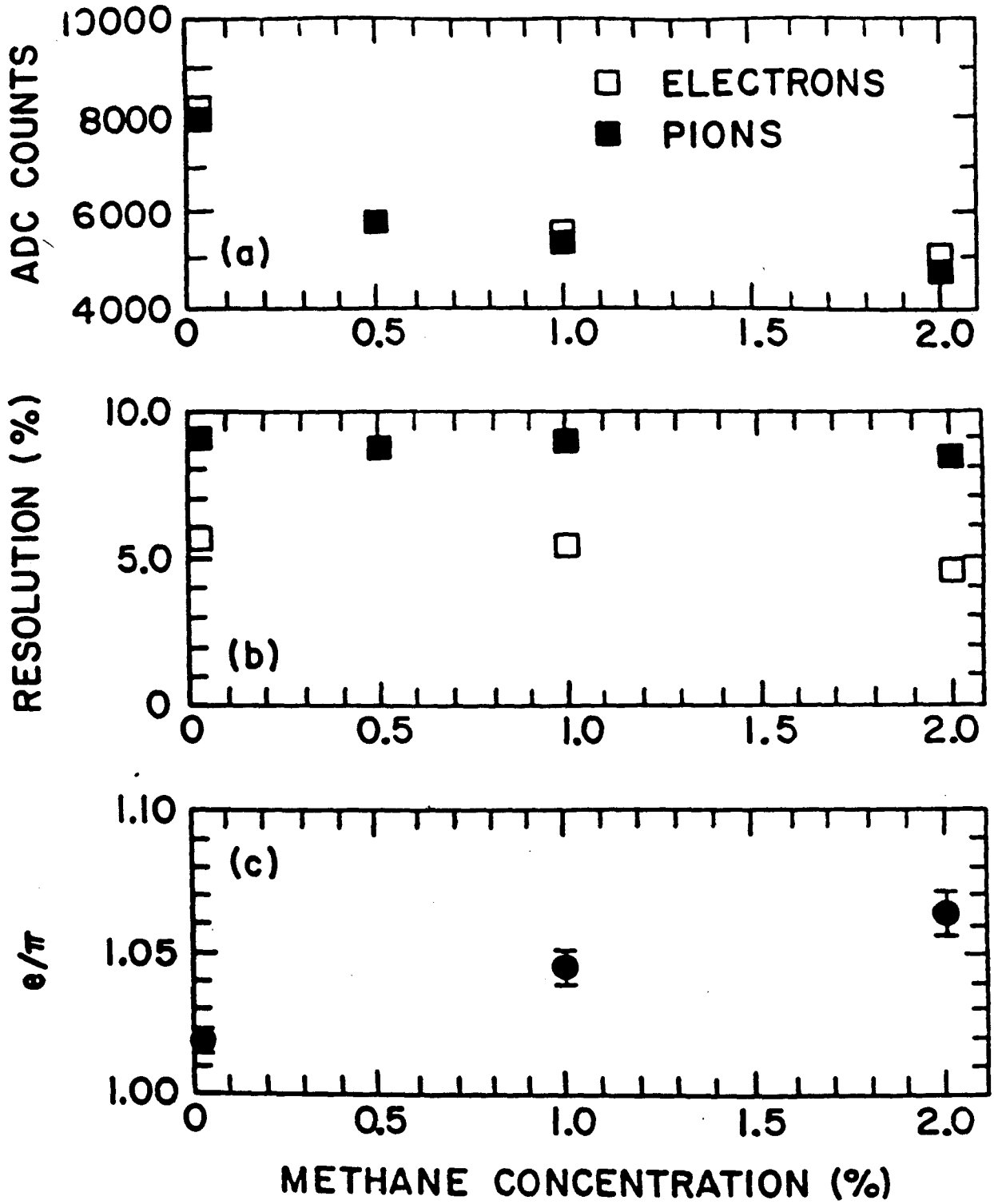
ADC COUNTS
10000
8000
6000
4000
ELECTRONS
PIONS
(a)
0
0.5
1.0
1.5
2.0
RESOLUTION (%)
10.0
5.0
0
(b)
e/π
1.10
1.05
1.00
(c)
METHANE CONCENTRATION (%)

IV. Electronics

Speed? Problem is getting charge to preamps

∴ preamps in liquid — cooling problem (some other opinions)

Towers - need to be short for timing

$\delta \geq 6\%$ S/N

Ferrite transformers $\lesssim \sim 0.5$ T

a) reduce power 2-3

b) protect preamp from sparks

c) reduce noise

Alternatives are being discussed

- "Electrostatic transformers" parallel → series
- long low impedance lines ?

Block diagram exists

Charge transfer vs time – long connections

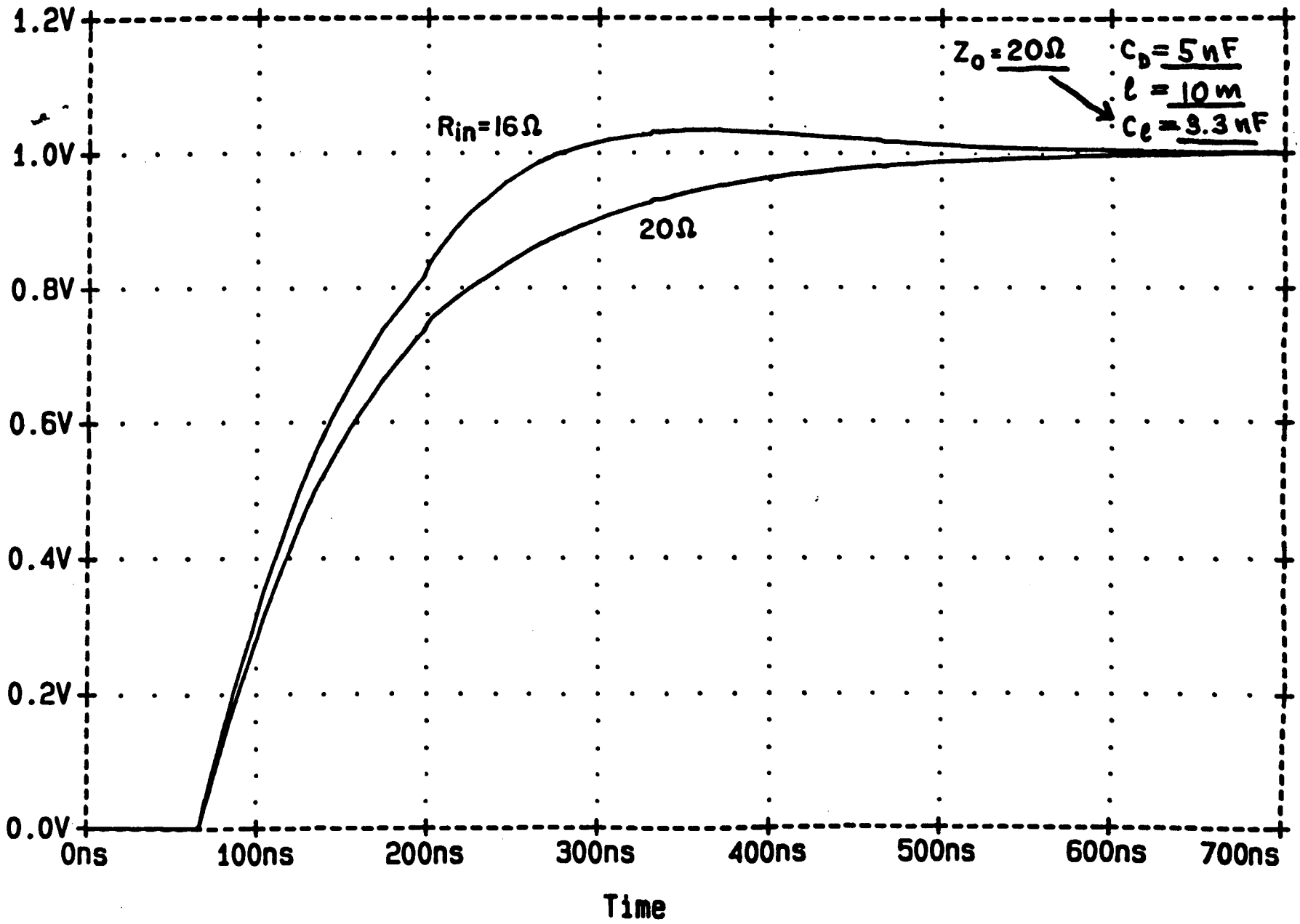

Ch ge transfer vs time — short connections

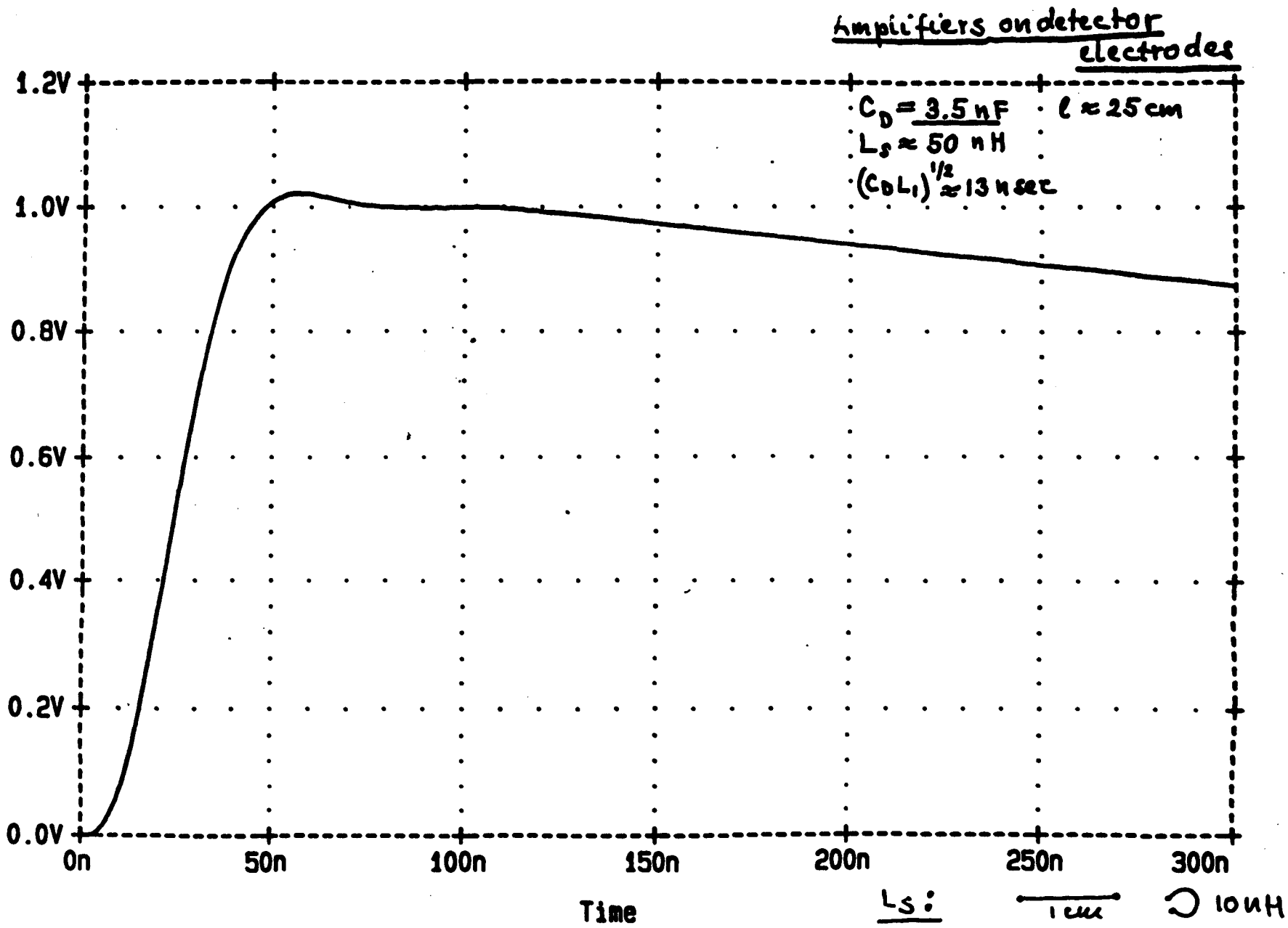

$t_r \approx 3.5 (L_s C_D)^{1/2}$

$[nF \cdot nH]^{1/2} = [nsec]$

Z_0	100 Ω	1.5 cm
($\varepsilon' \approx 4$)	50 Ω	3 cm
	20 Ω	7.5 cm

5C7 KODAK 5C7 KODAK 5C7 KODAK

Uranium - Liquid Argon Calorimeter
for HELIOS (NA 34) exp.

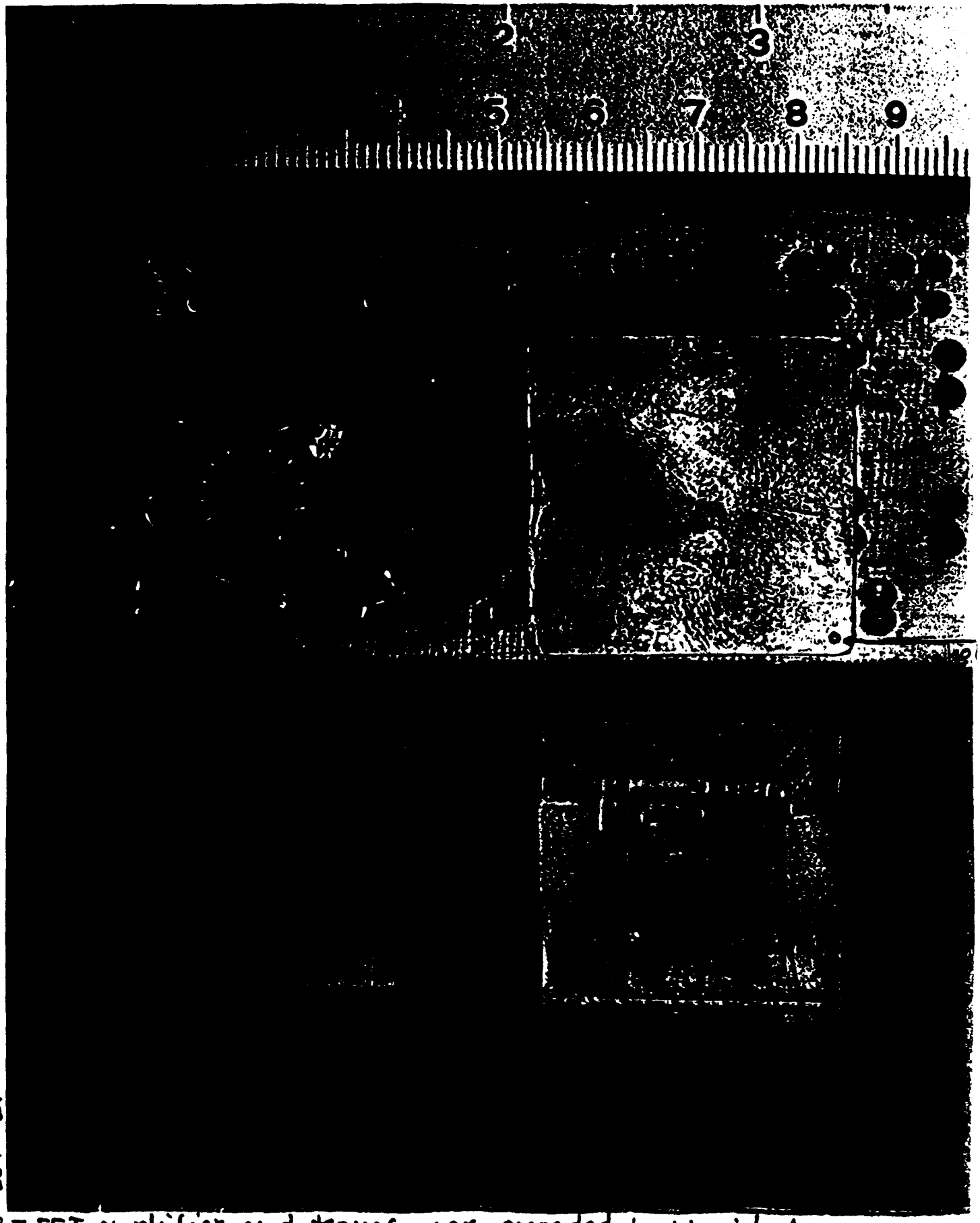

CMZ-437-86

J FET amplifier and transformer operated in Liquid Argon

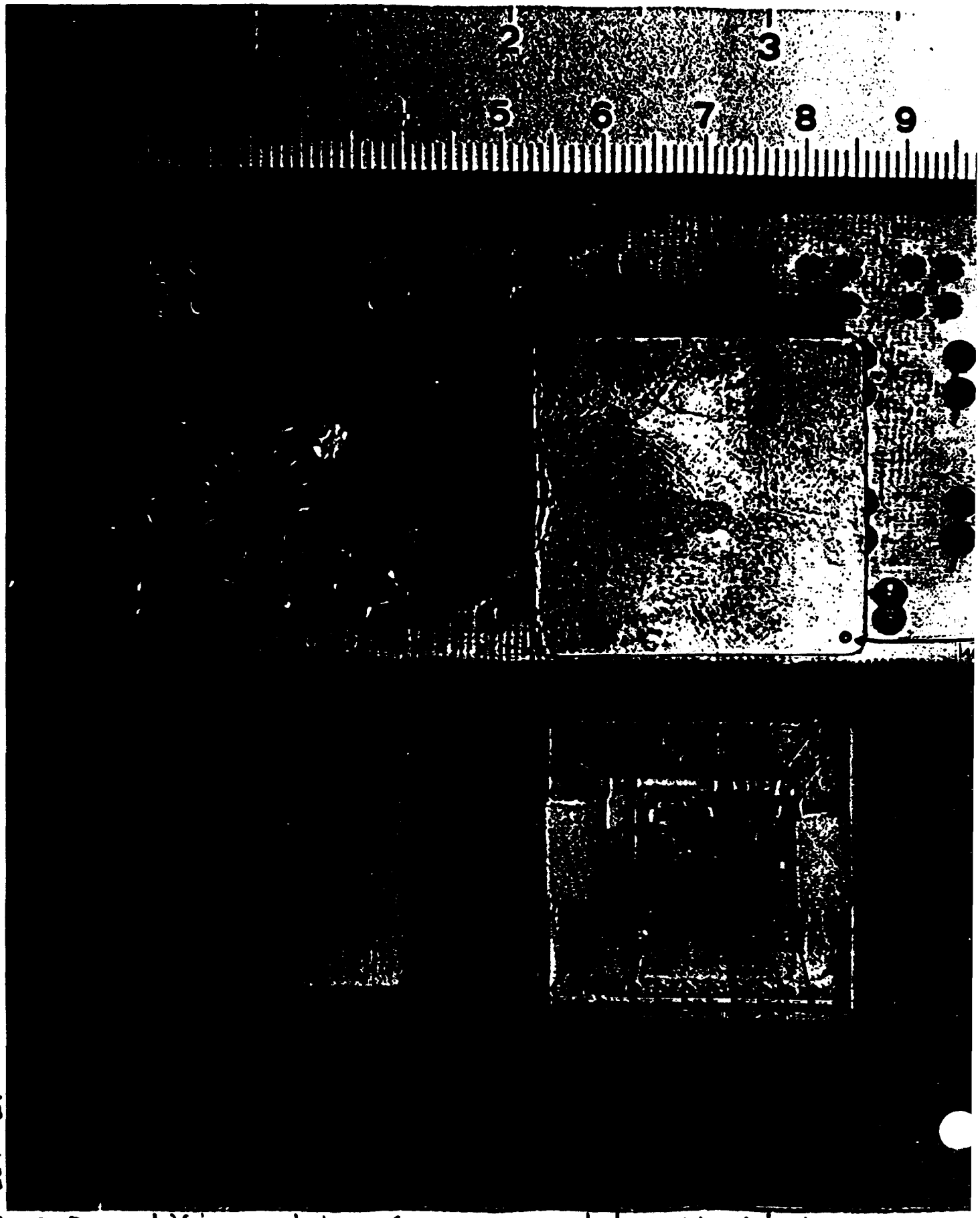

FET amplifier and transformer operated in Liquid Argon

CN2-437-86

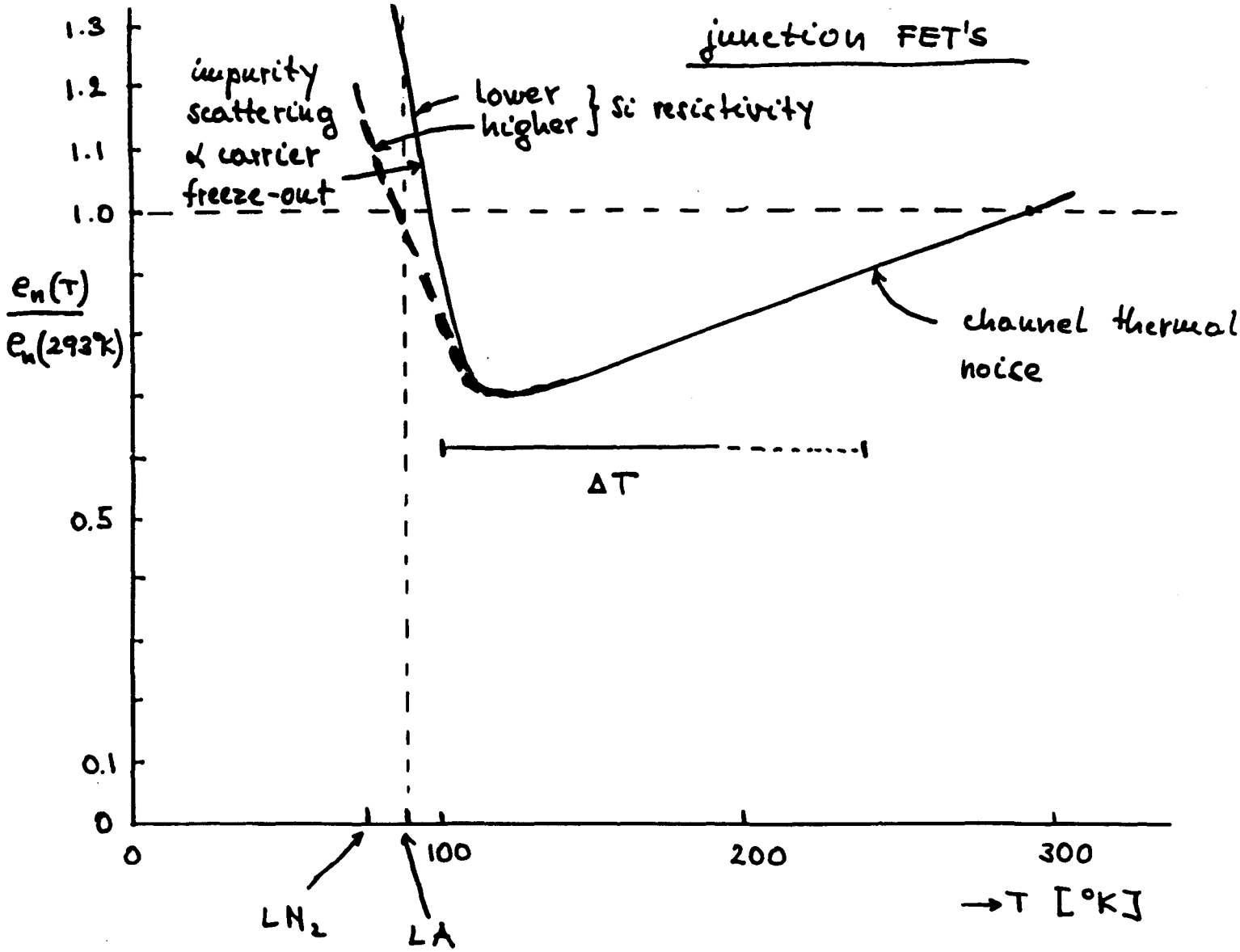

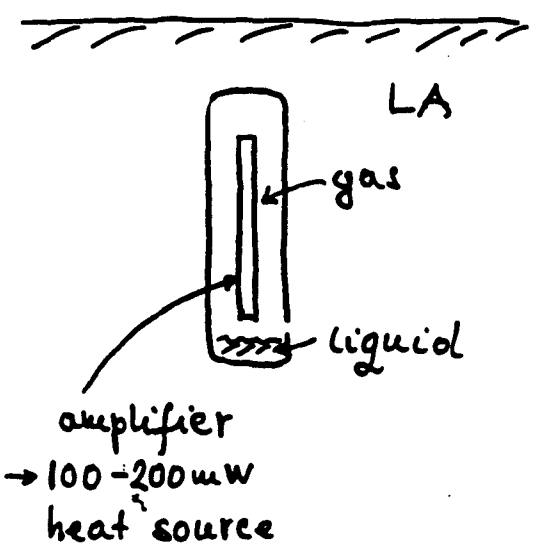

Necessary temperature difference achieved by amplifier power dissipation

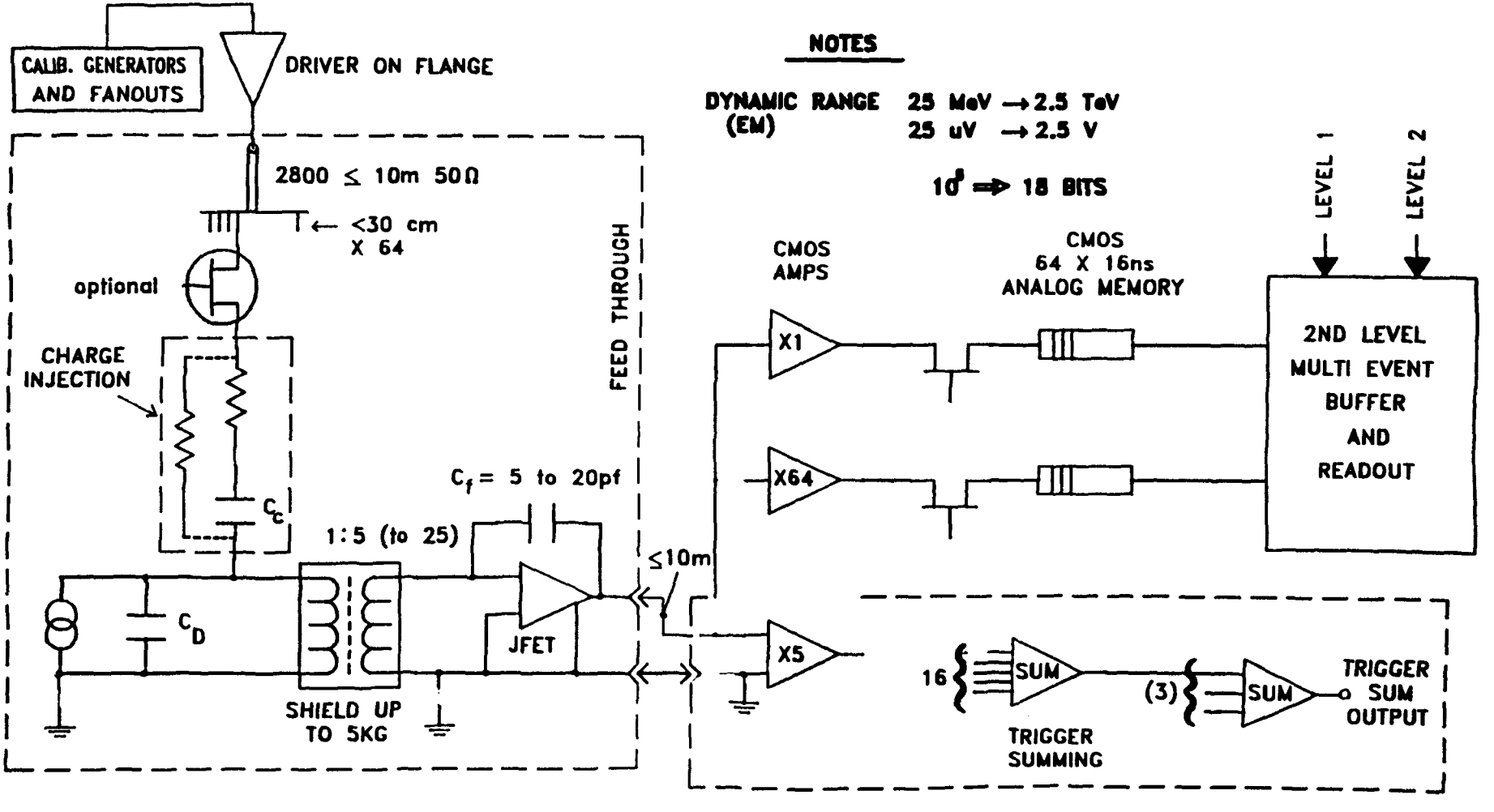

BNL-OMEGA JMH
SSC LA CAL SSCTA01

$\tau_m = 50$ ns

	$\Delta\eta \times \Delta\phi$	PAD SIZE (cm)	$C_D + C_c$	S	NOISE PREAMPS IN L. Ar	+ TRANS FORMER
EM 1	0.04 x 0.04	7	400pf	11.4%	75 MeV	
EM 2	0.02 x 0.02	3.4	300pf		94 MeV	
EM 3	0.04 x 0.04	7	660pf		142 MeV	
H1+H2	0.04 x 0.04	8.4 9.9	3.8nf	5.7%	0.8 GeV	0.21 GeV
H3+H4	0.04 x 0.04	12.1 13.9	5.5nf		1.15 GeV	0.24 GeV

	$\Delta\eta$ $\Delta\phi$			
Trigger Tower	(0.32x0.32)	EM	1.8 GeV	
		EM+H	10 GeV	3.2GeV
Electron Tower	(0.08x0.08)		0.45 GeV	

TIMING (0.32x0.32)

1 ns	100GeV
4 ns	25GeV

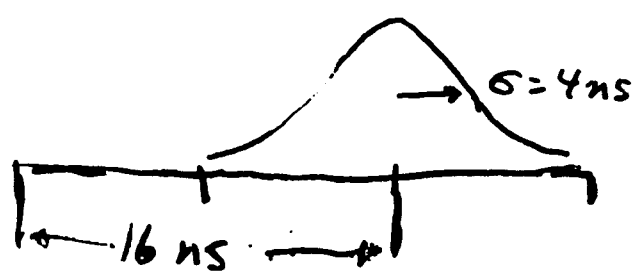

All components need to be ±2ns

PULSE SHAPING, NOISE and PILEUP

Final shaping for triggers will be done after the sums are formed.

Final shaping for individual channels will be done by a combination of weighted samples taken every 16 ns.

Thus, the effective integration time t_m can be chosen to optimize the electronic noise against pileup for different physics requirements at a given luminosity:

t_m	50 ns		100 ns
		Timing	
	1 ns	100 GeV Jet	0.67 ns
	4 ns	25 GeV Jet	2.7 ns
	2.8 GeV	σ	0.9 GeV

$\sigma_{pileup} \sim \sqrt{t_m}$

<u>Other improvements</u>

- Methane S/N ↑2 problems with purification radiation damage?
- S → 12% S/N ↑
- Electrostatic transformer (See warm liquid talk)???

Subsystem Proposal

BNL, LBL, FSU, U of Rochester, MSU, FNAL, ...
Stony Brook, KEK, U of Washington

Absorber? Beam test of Pb Pb/Fe

Module design
- connections
- segmentation

Cooling of preamps

Shielding of transformers

Development of Brite Pads

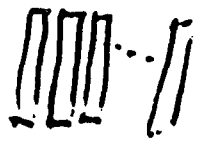

Signal + HV feedthroughs

Optimization of S/N

Calibration

⋮

Paul Mockett

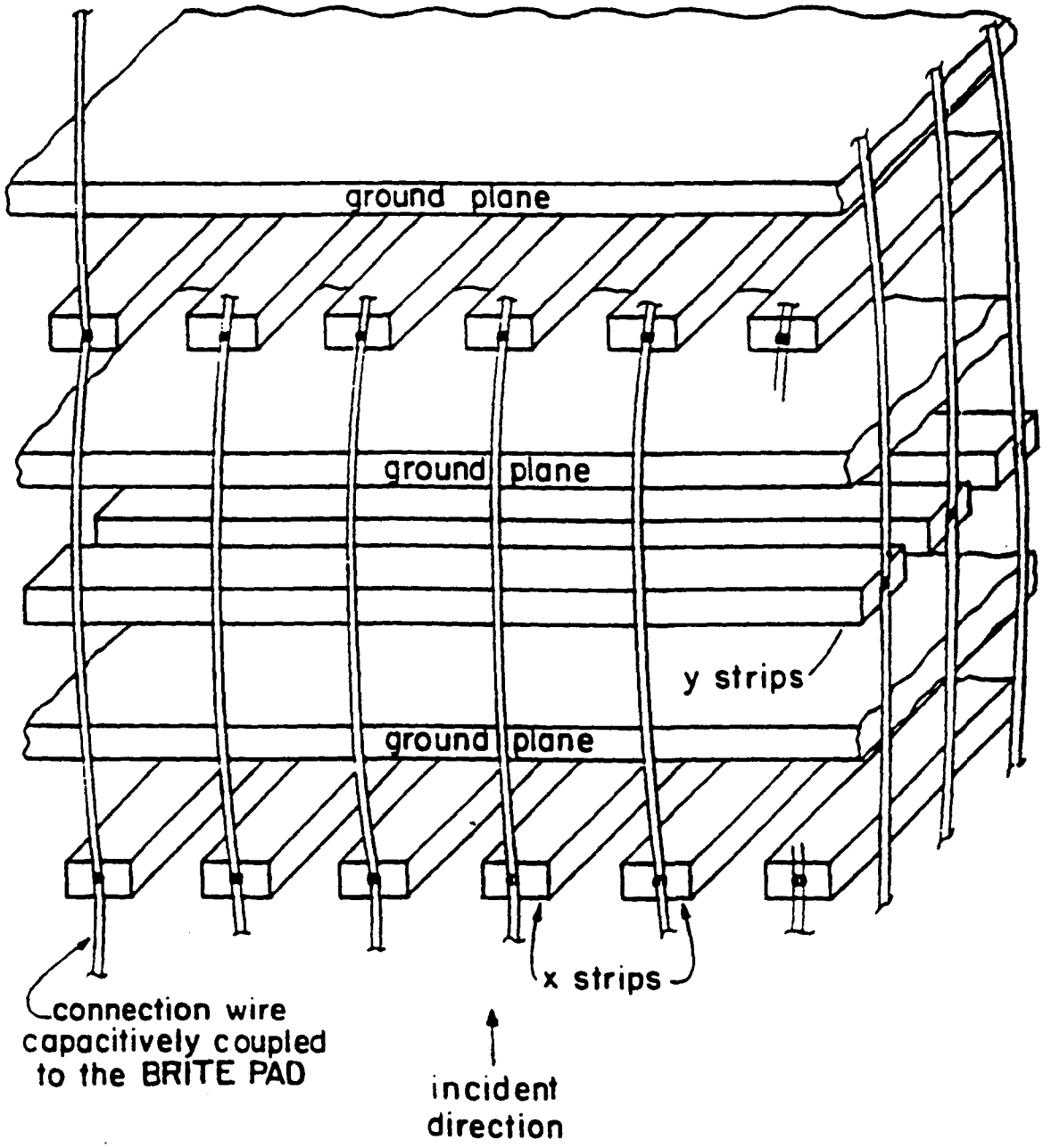

Fig. 1

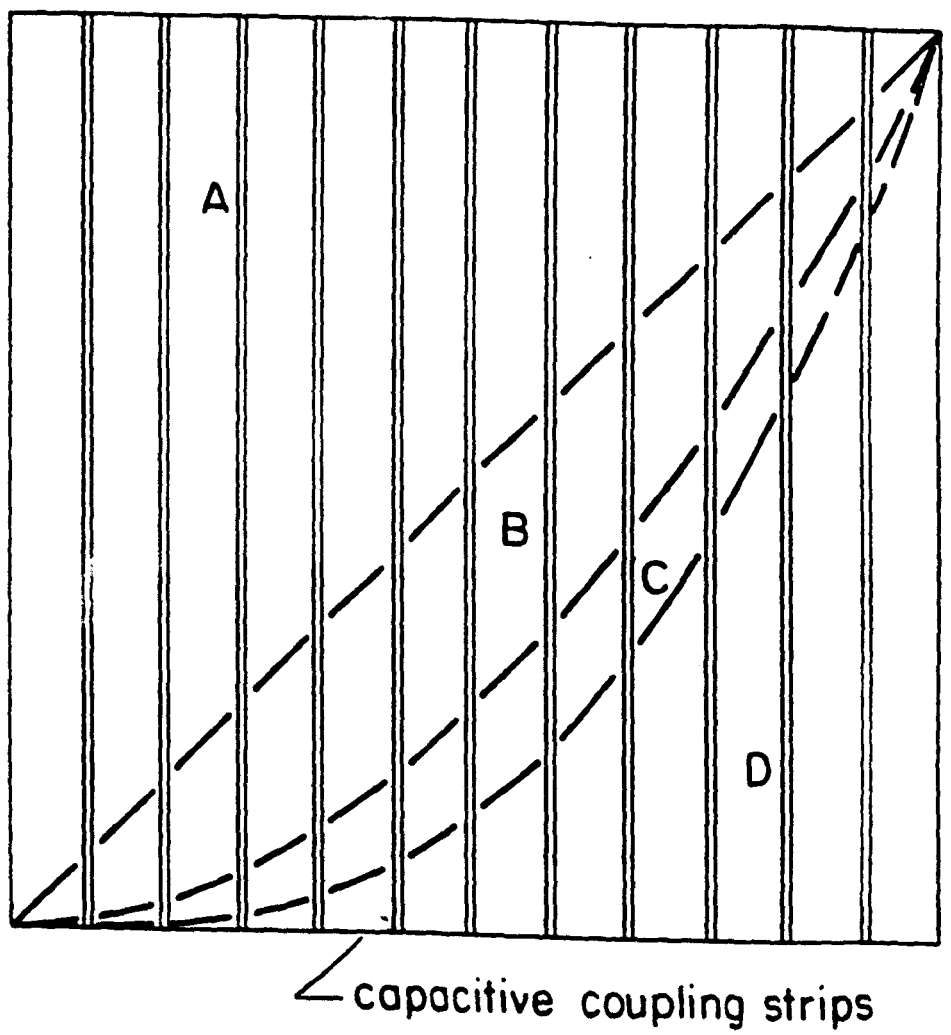

Fig. 3

Improves: position resolution ~ 1 mm

e/π separation

2 showers

redundancy (dead channels or shorts)

channel count ≲ 1/2

Tentative Schedule for
SSC Liquid Argon Major Subsystem R& D Proposal

June 27 Suite 210 SSC Laboratory

12:00 ~~9:00~~ AM	Organization Details
9:10 AM	V. Radeka/S. Rescia – Progress on electrode configurations, shower and signal propagation in a tower, measurements of transformer shielding and status of high resistivity preamps
9:50 AM	P. Mockett – Discussion of Methane, Interleaving and survival with buried electronics – Brite Pates
10:30 AM	LBL – Progress on Tiles/Readout boards, connection details, HV and cold feedthroughs
11:10 AM	H. Gordon – Estimate of funds and manpower for a beam test
11:40 AM	N. DiGiacomo– Martin Marietta's resources to help this proposal
12:00	Lunch
12:30 PM	Discussion of Proposal – writing assignments
2:15 PM	Senator Phil Gramm
3:15 PM	Continued Discussion
	T. Kondo – Calibration of VENUS Liquid Argon System

E. pected Attendees:

M. Levi, H. Gordon, N. DiGiacomo, G. Abrams, J. Siegrist,
A. Lankford, M. Marx, V. Radeka, V. Polychronakos,
V. Hagopian, S. Rescia, T. Kondo, P. Mockett, F. Lobkowicz

CONCLUSIONS

Lots more work is needed! (5° region!!

Liquid Argon look very promising

Living at 2T will be hard (for all?)

Physics Benchmarks need definition

- Can $W_L W_L$ scattering be studied by using $W \to$ jet + jet ?
- Do we need to search for $80 < m_{h^0} < 180$ GeV $h^0 \to \gamma\gamma$
- Missing p_T – how well do we need to measure it – how does noise and pileup contribute

⋮

H. Sadrozinski

TRACKING with SILICON DETECTORS at the SSC

HARTMUT F.-W. SADROZINSKI

Santa Cruz Institute for Particle Physics

University of California Santa Cruz

Santa Cruz, CA 95064

1) Tracking Goals and Characteristics of Silicon Trackers

2) Systems Design Questions

3) Ongoing and future R&D

Dallas, TX, June 26, 1989

Characteristics of SSC Events	Characteristics of Si Tracking System
10^8 interactions/sec	Fast collection device $\rightarrow$ separate different interactions
Stiff tracks	Good position resolution ($\frac{25\mu m}{\sqrt{12}}$)
Narrow, dense jets	Very small cells $\rightarrow$ low occupancy
Many extra low energy tracks	Local stereo $\rightarrow$ unambiguous z measurement
Complicated events	Good 2 track resolution (100 μm)
Large data volume (mainly from tracking devices)	few noise hits (signal 25000 e,h/300 μm)
	Data reduction and storage possible in VLSI on detector

TRACKING GOALS

1) Lepton ID with calorimeter and μ toroid
   electrons are identified by E/P ratio

   $\rightarrow$ P should be measured with same precision as .

   measure e and μ with the same precision and systemat

2) Lepton Mass Reconstruction for $H \rightarrow ZZ \rightarrow e^+e^-$ $\mu^+\mu^-$
   efficiency and good momentum resolution

   $\rightarrow$ lepton pair mass resolution less than Z width

   $\rightarrow$ good coverage in η:

$$\frac{N_{ZZ}(\eta < 2.5)}{N_{ZZ}(\eta < 1.5)} \approx 2.5 \rightarrow 3$$

3) Measurement of Event Structure

   a) Multiplicity

   b) Energy flow with good timing to comple
      calorimeter

4) Vertex Reconstruction

   a) Disentangle multiple events in same time bu

   b) Measure impact parameter of $< 300\mu$m in
      decays
      Pixel (low occupancy, close to vertex) + st
      tum determination)

Figure 22 shows a possible arrangement for the tracking detector. It contains about 40m^2 of silicon detectors. Going out in θ this arrangement gives:

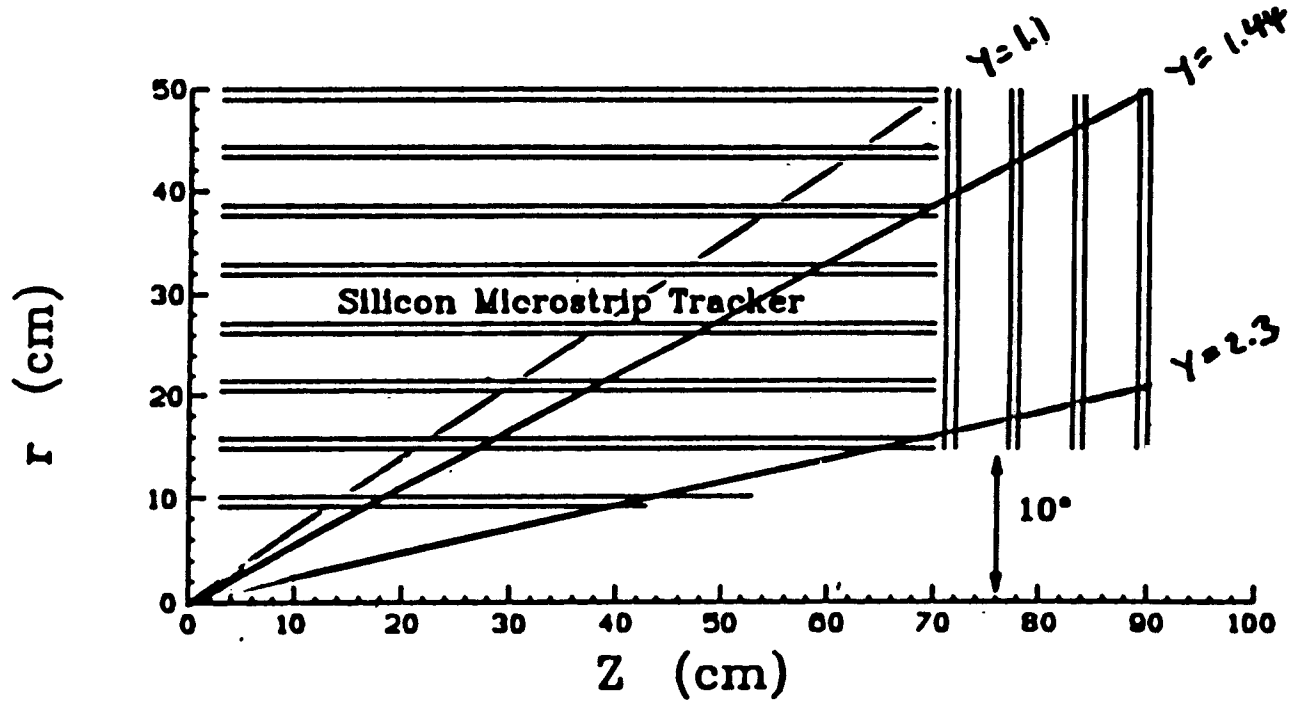

Fig. 22. Silicon Tracking System

ⓐ Tracking with ≥ 6 superlayers for $170° \geq \theta \geq 10°(|Y| \leq 2.3)$.

b Tracking with 8 superlayers for $160° \geq \theta \geq 20°(|Y| \leq 1.75)$.

ⓒ Tracking over a fixed radius of 50cm for $154° \geq \theta \geq 26°(|Y| \leq 1.44)$.

ⓓ Tracking with axial strips for $143° \geq \theta \geq 37°(|Y| \leq 1.10)$.

$$\frac{\sigma_{P_T}}{P_T^2} = \frac{2}{0.3B}\sqrt{\frac{\sum_{i=1}^{m}\frac{r_i^2}{\sigma_i^2}}{\sum_{i=1}^{m}\frac{r_i^2}{\sigma_i^2}\sum_{i=1}^{m}\frac{r_i^4}{\sigma_i^2} - \left(\sum_{i=1}^{m}\frac{r_i^3}{\sigma_i^2}\right)^2}}$$

For B=2.5 Tesla, 25 μm St

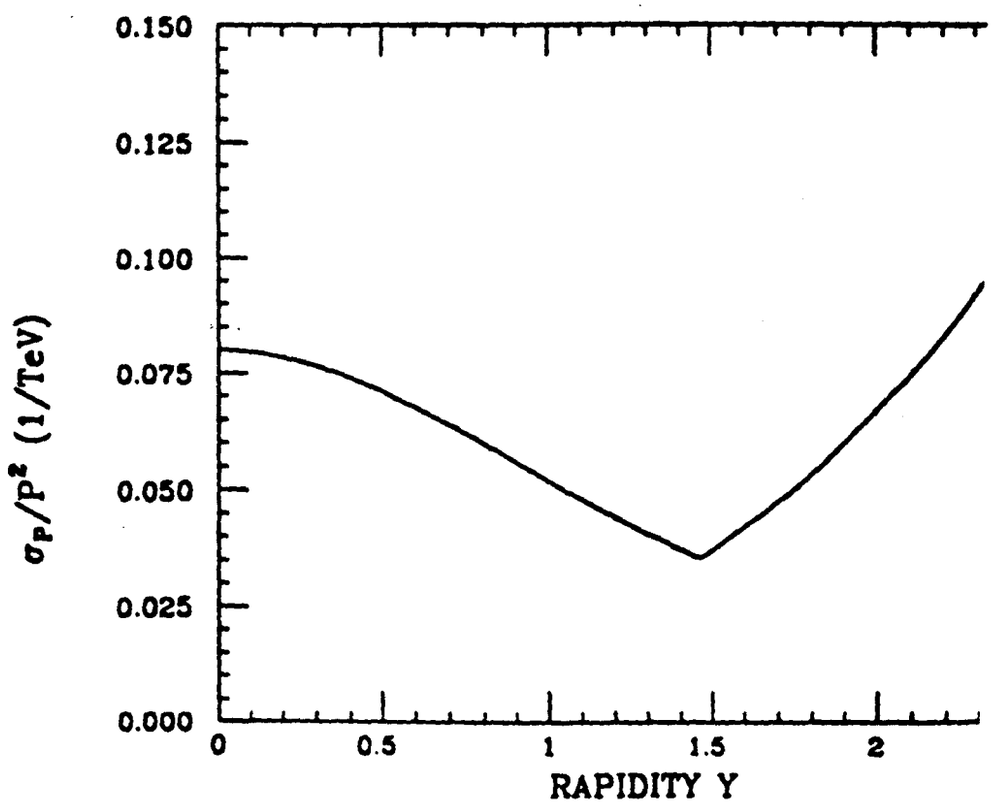

Momentum resolution vs. rapidity.

BOTH μ and e

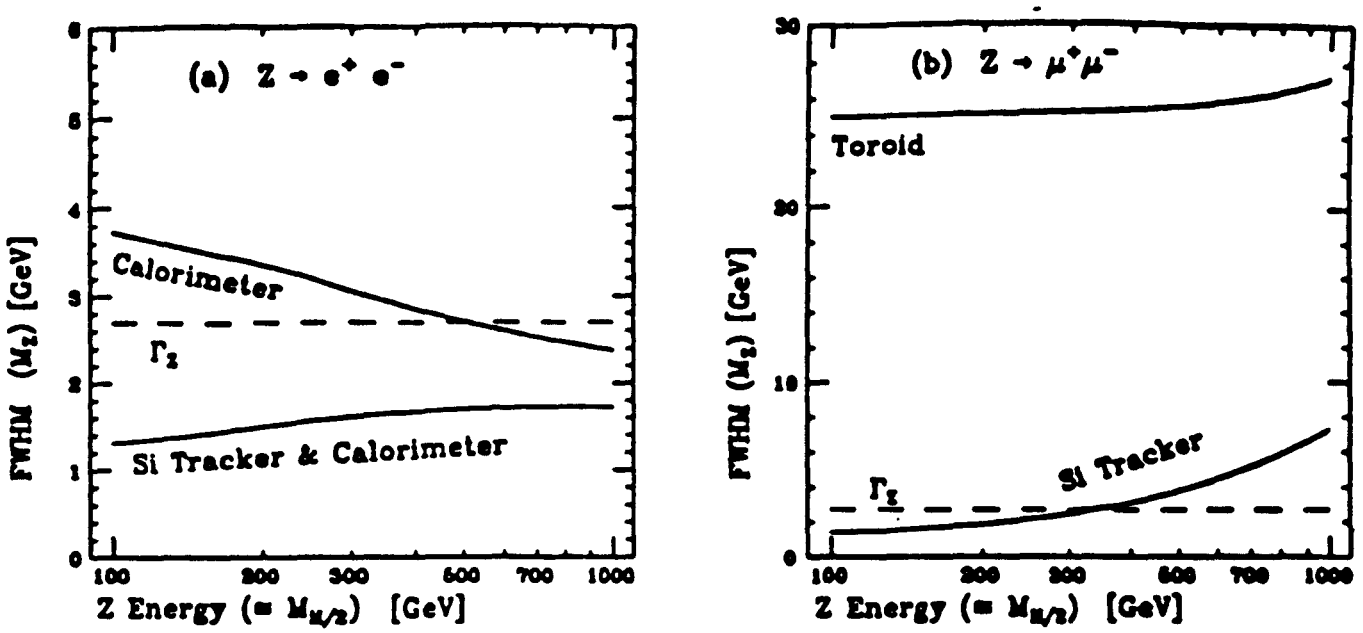

FWHM resolution of the Z^0 mass as a function of Z^0 energy for a detector with calorimetry only, and for a detector including precision Si tracking. a) $Z^0 \to e^+e^-$. b) $Z^0 \to \mu^+\mu^-$.

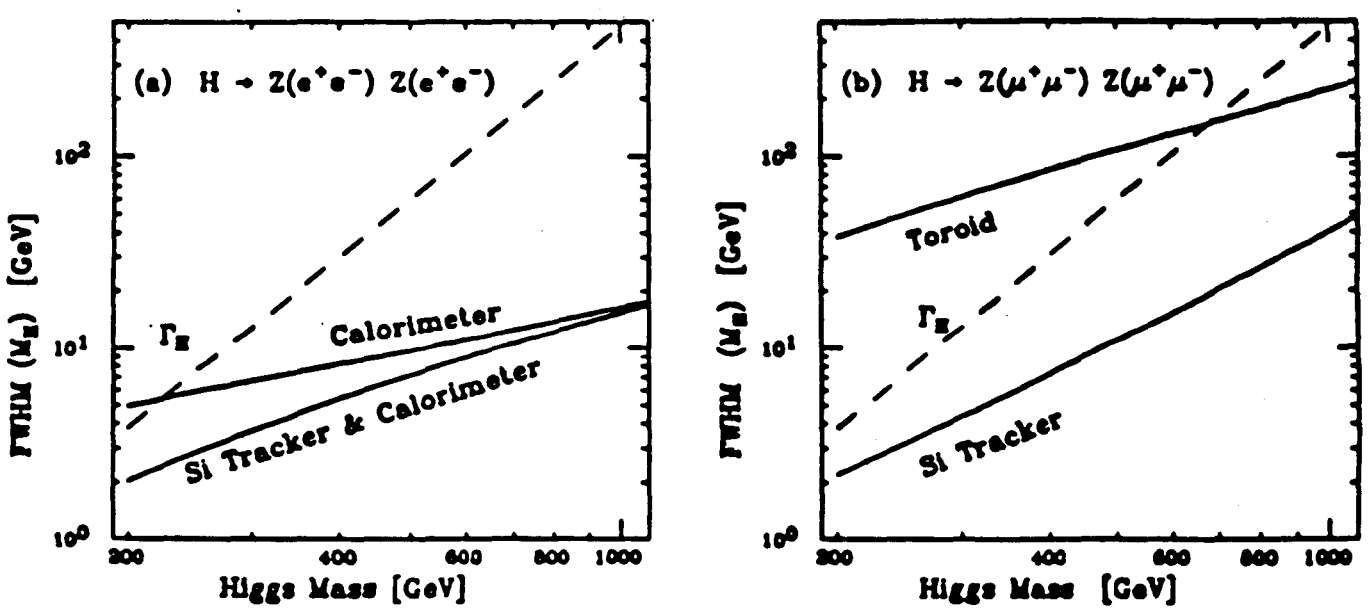

Z^0Z^0 invariant mass resolution for different detector configurations, compared with the expected Higgs width Γ_H (dashed line). a) $Z^0 \to e^+e^-$. b) $Z^0 \to \mu^+\mu^-$.

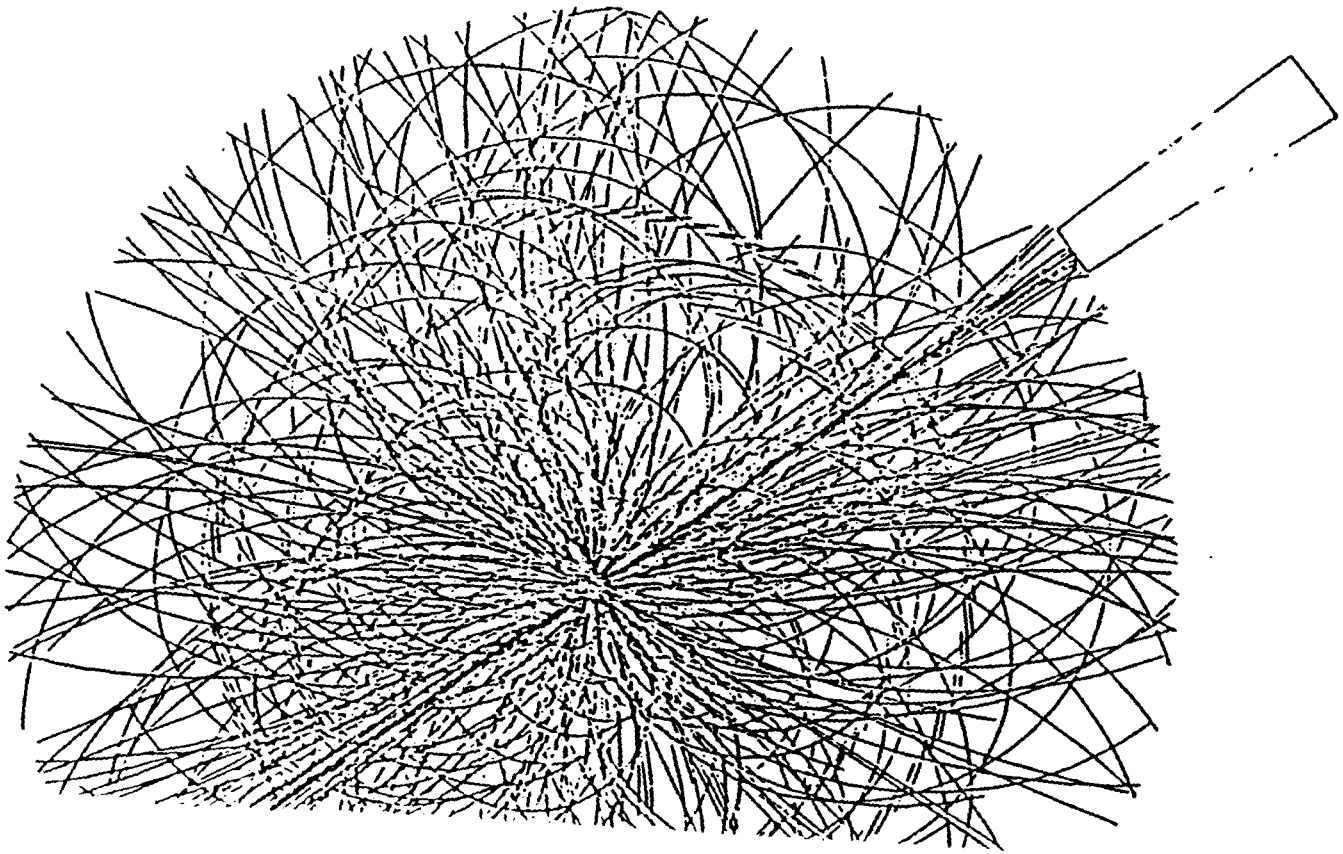

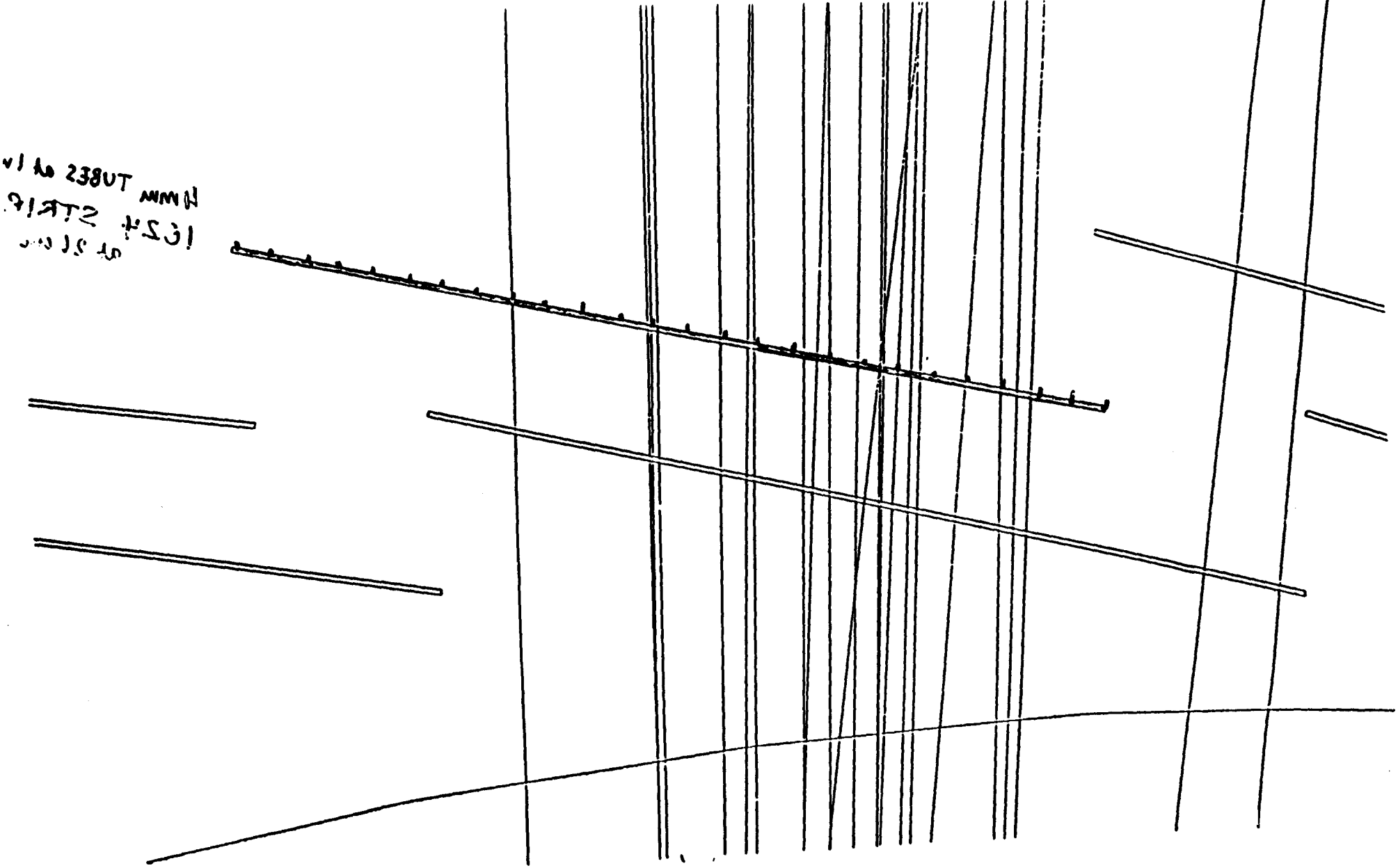

M.C. STUDY OF TRACK FINDING 1 TeV DETS

Δ = SEPARATION OF SUPERLAYERS = 6 CM

(r_{min} = 8 cm , r_{out} = 50 cm) $\langle\theta\rangle \cdot r = \varepsilon$ AT r = 20 cm

δ = SEPARATION OF DETECTORS INSIDE SUPERLAYERS

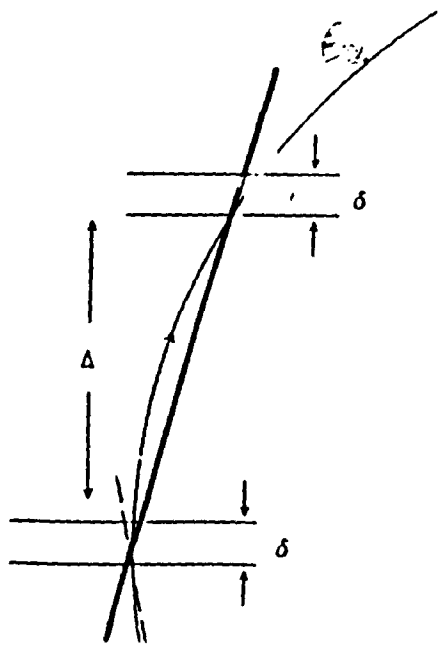

1.) VECTOR FINDING $\Rightarrow$ δ SMALL

2.) VECTOR ASSOCIATION $\Rightarrow$ δ LARGE

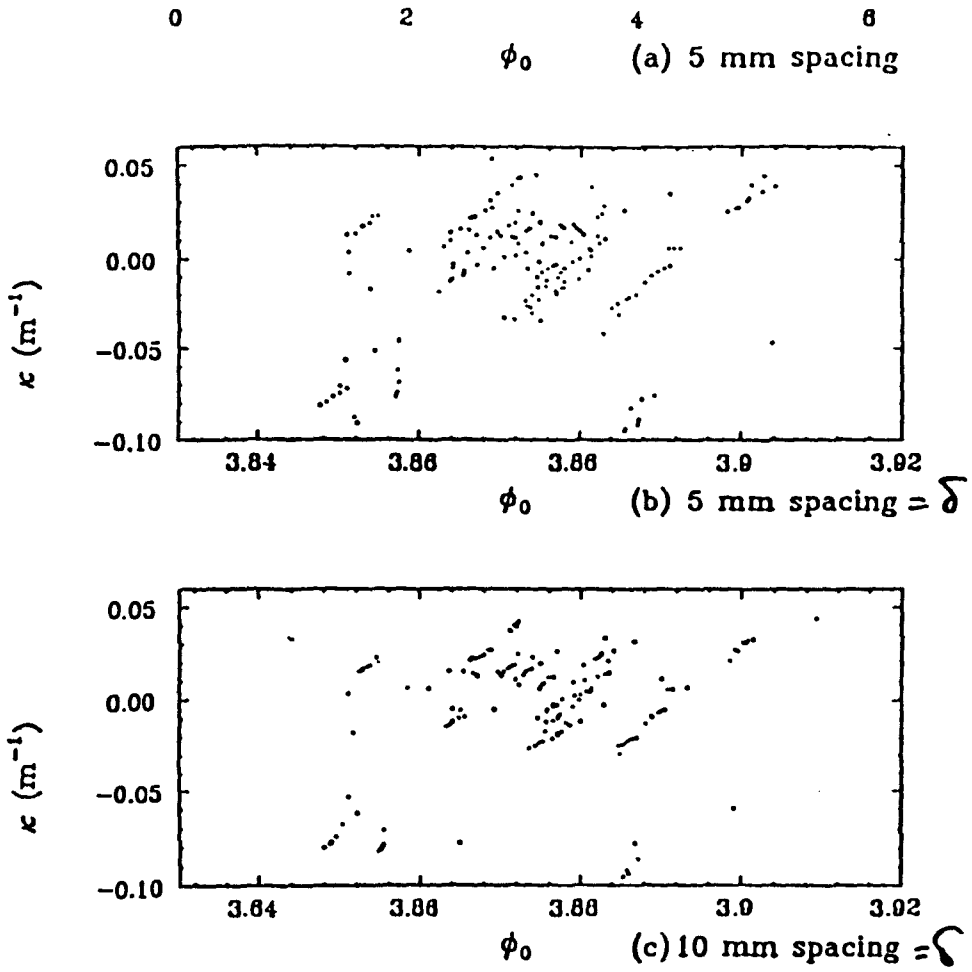

$$\kappa = \frac{}{2 \cdot \rho_{TRACK}}$$

TRACKS ARE DEFINED AS POINTS IN κ, ϕ_0 SPAC

FIG 17

M.C. EFFICIENCY

$\sigma = 1$ CM

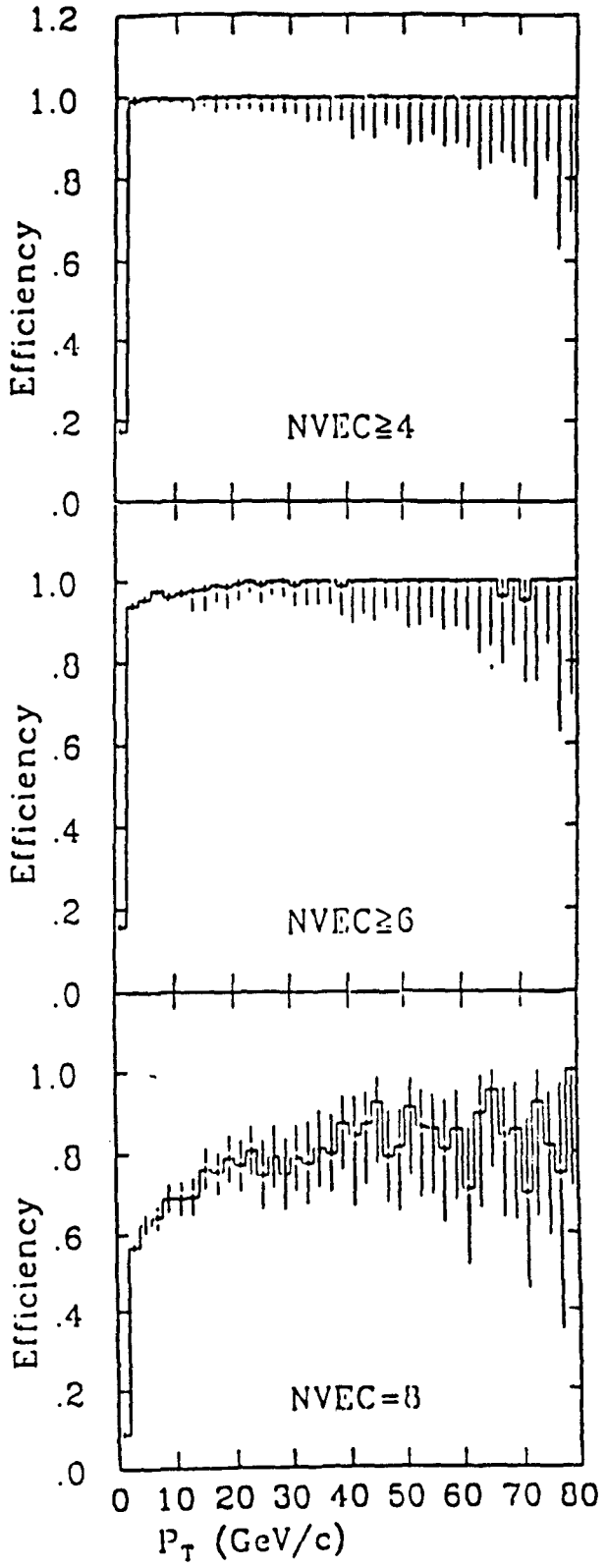

NVEC IS NUMBER OF VECTORS REQUIRED FOR TRACK

LOCAL Z- MATCH

U, V STRIPS ON SAME DETECTOR AS AXIAL

CONFUSION $\sim L \cdot \alpha$ $\rightarrow$ α SMALL (5 mrad)

σ (A VERTEX) $\approx$ [illegible] (VERTEX IS ABOUT 7 CM LONG)

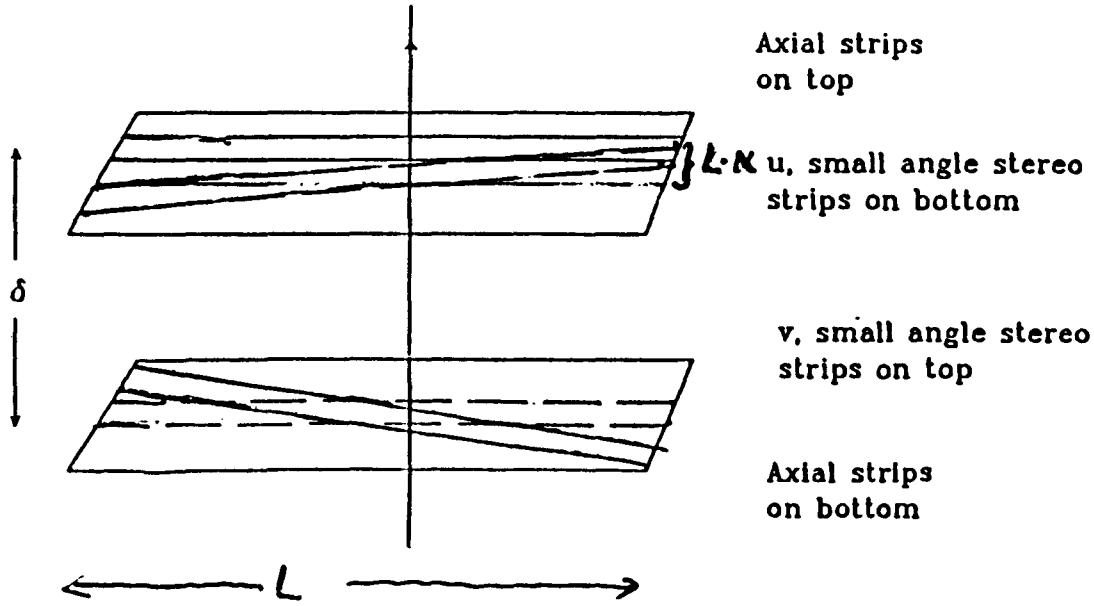

SYSTEM DESIGN

1) Strips from r=8cm to r=50cm
   Pixels from r=3cm to r=8cm

2) The exact configuration depends on the solution to te
   tions:
   - Power dissipation
   - Alignment
   - Radiation Hardness
   - Complexity (Cost)

   These issues are part of the generic SSC R &D ar
   cussed in this Workshop. Of great importance are M
   optimize the design.

   Example :

Study the effects of a system with much fewer channel

a) System with only 25μm wide strips:
   excellent momentum resolution, vey low occupancy

b) Fixed occupancy system- strip width grows with ra
   (25μm at r=8cm, 100μm at r=50cm):
   occupancy still very low because strip width $\leq$ 2 tr
   momentum resolution worse by factor 2 than for a
   some loss in pattern recognition power in outer lay
   but
   much less stringent alignment criteria and much fe

c) Combine b) with the outer driftchamber to restore
   resolution

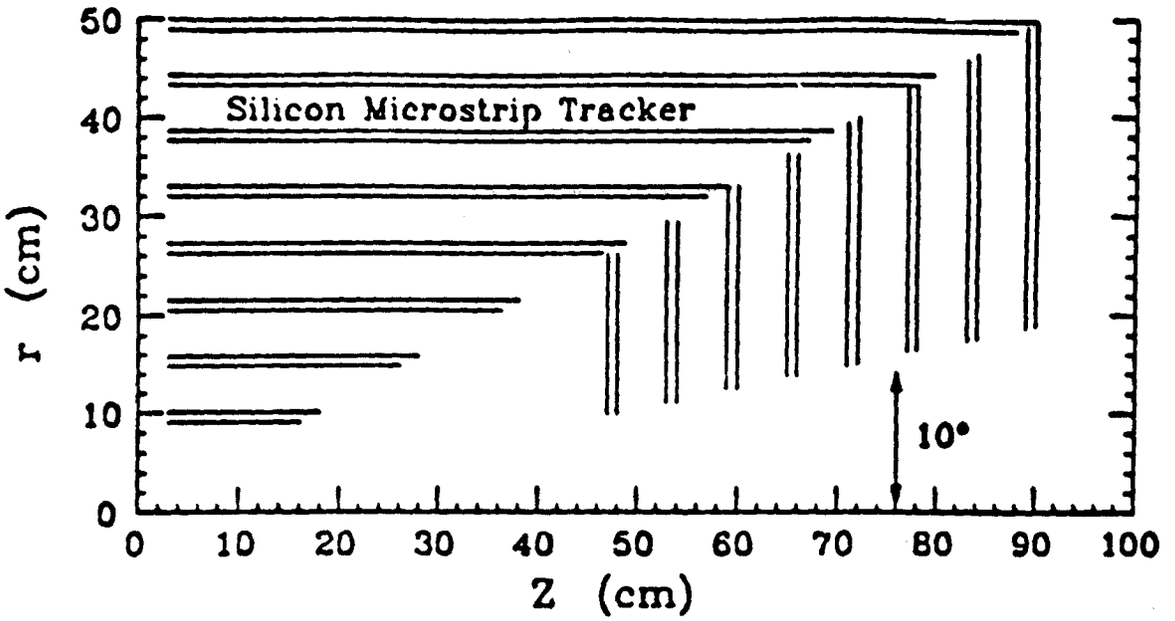

Silicon tracking system

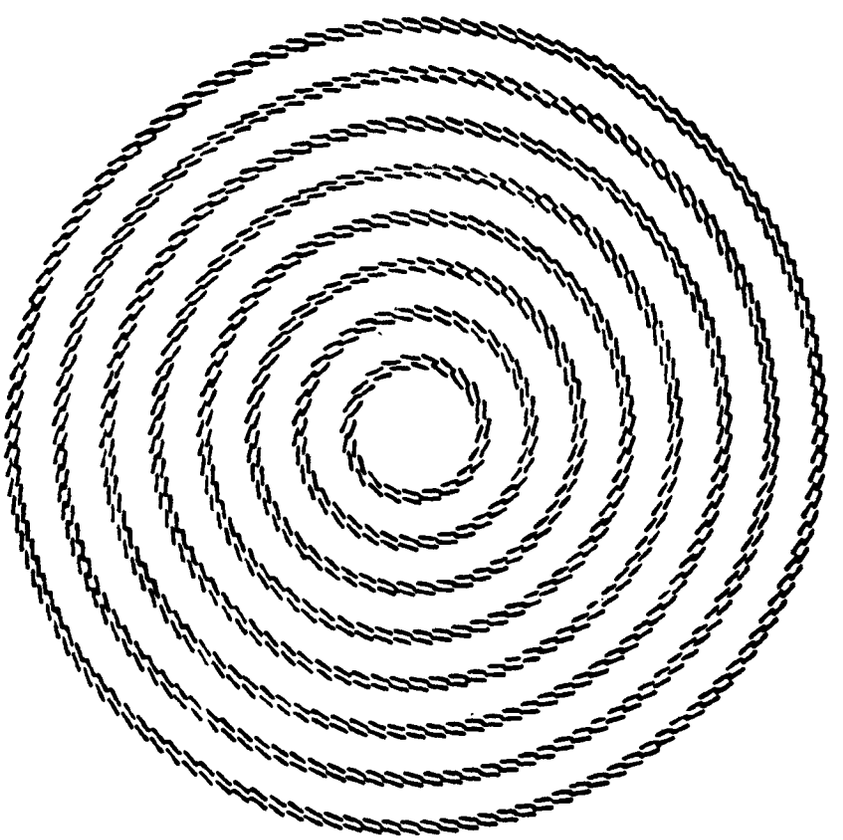

Central silicon tracker

SYSTEM MOMENTUM RESOLUTION

$$\frac{\sigma_P}{P} = \frac{C(\theta)}{B(\text{Tesla})}\, P\ (\text{TeV})$$

SYSTEM			C(90°)	σ_P/P $P = 1$ TeV, $B = 2.5$ T, $\theta = 90°$
A	Silicon	8 cm–50 cm		
	8 S.L.	25 μm strips	0.26	10%
B	Drift	50 cm–150 cm		
	100 L.	$\sigma = 200$ μm	0.51	20%
A + B			0.14	5.6%
C	Silicon	8 cm–50 cm		
	3 S.L.	25 μm strips		
	2 S.L.	50 μm strips	0.52	21%
	3 S.L.	100 μm strips		
C + B			0.15	6.0%

Fixed occupancy

High Backgrounds (Only back half of detectors is usable) :

Back of B	1.06	42%
Back of C	1.30	52%
Back of C + Back of B	0.18	7.2%

OTHER PROPERTIES OF FIXED OCCUPANCY

SI TRACKER :

4 UNITS

2 CENTRAL $-1.35 \leq \eta \leq 0$, $0 \leq \eta \leq 1.35$

2 FORWARD $-2.4 \leq \eta \leq -1.35$, $1.35 \leq \eta \leq 2.4$

EACH UNIT HAS ABOUT 20 TRACKS / TIME BUCKET FROM MIN. BIAS EVENTS (+ CURLERS)

$\rightarrow$ OCCUPANCY $\leq 4 \cdot 10^{-3}$ (SETS SCALE FOR S/N)

LEAKAGE CURRENTS : (AFTER ONE YEAR)

AT $\mathcal{L} = 10^{33} (cm^2 sec)^{-1}$ neutron fluence $= 10^{12} \frac{n}{cm^2} \frac{1}{YEAR}$

		YEARLY CHARGED FL.	CURRENT/STRIP (μA) neutron	charged	total
CENTRAL REGION	INNER LAYER	$4 \cdot 10^{13} \frac{1}{cm^2}$	0.08	1.3	1.4
	OUTER LAYER	10^{12} "	0.95	0.4	1.4

This corresponds to ENC = 400 e .

LEAKAGE IN FORWARD UNITS SMALL .

R&D for the SSC SILICON TRACKER

1) Monte Carlo Simulations of designs (Radii, Length and width of strips and pixels, Number of layers)

2) Detector Research (Double sided,Collection,Radiation hardness, Bonding,Integration with electronics)

3) Electronics (Radiation hardness,Speed,Low Power,Read-out, Interaction with trigger)

4) Mechanical integration (Supports, Alignment, Temperature stability)

5) Cooling

THERE IS CONSIDERABLE EXPERIENCE WITH SI STRIPS:

a) FIXED TARGET

b.) COLLIDING BEAMS (MKII, CDF)

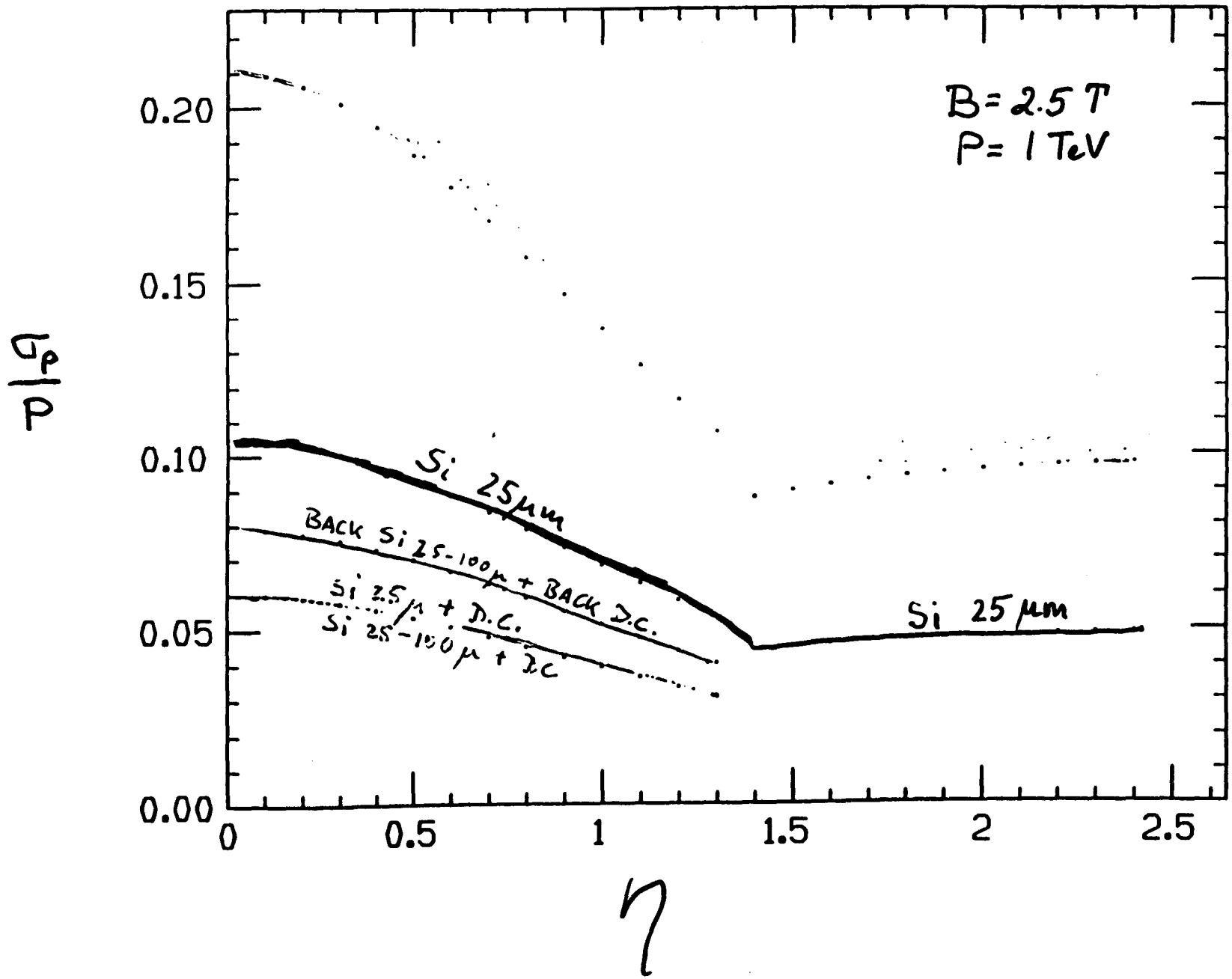

SIRES TOPDRAW BI created on 24 Jun 1988 at 22:32.

Readout – VLSI chips.

H. Gordon
6/26/89 - DALLA:

PROGRESS in the DESIGN of a LIQUID ARGON CALORIMETER FOR the SSC

Lots of Progress at the Alabama Workshop

- Engineering
- Hermeticity
- Nitty Gritty Details
- Electronics

We are preparing a "Major Subsystem R+D Proposal for Oct. 1, 1989

e. H. Gordon

CALORIMETRY REQUIREMENTS

H. Gordon.

Further Study

- **Radiation Resistance:**

  $\approx 10^6$ rads/year; $\approx 10^{12}$ neutrons/cm^2 year

- **Energy Resolution:**
  - EM , $\approx 0.15/E^{1/2}$, constant term $\approx$ 1% (low PT electrons)
  - Hadronic , $< 1.0/E^{1/2}$ sufficient, $\leq \underline{0.5/E^{1/2}}$ very good

- **Systematics, Calibration, Uniformity, Stability:** 1% if easy, 2% if hard ✓

- **Electron/hadron Response:** $\leq \underline{1.1}$ direct response, or by weighting ✓
  (quark compositeness signal!)

- **Dynamic Range:**

  EM, 5 TeV lepton ($\approx$ 2.5 TeV in one channel)
  Lepton isolation test $\approx$ 100 MeV/channel } $\underline{2.5 \times 10^4}$ -10^3
  Hadronic, QCD jets $\approx$ 5-6 TeV in one jet cone

- **Noise (electronic-, uranium-):**
  - Lepton isolation $E_T < 4$GeV in $\Delta R \approx 0.4$
  - Missing PT $\sigma_{el} < 20$ GeV

- **Speed and Pileup:**
  - Timing (associate events and bunch crossings), $\sigma_t \approx \underline{1\text{-}2 \text{ nsec}}$
  - Integration time (hadron response) $t_m \approx \underline{100\text{-}150}$ nsec ✓
  - Pileup time, impact of overlap of n (e.g., 10) bunch crossings ✓

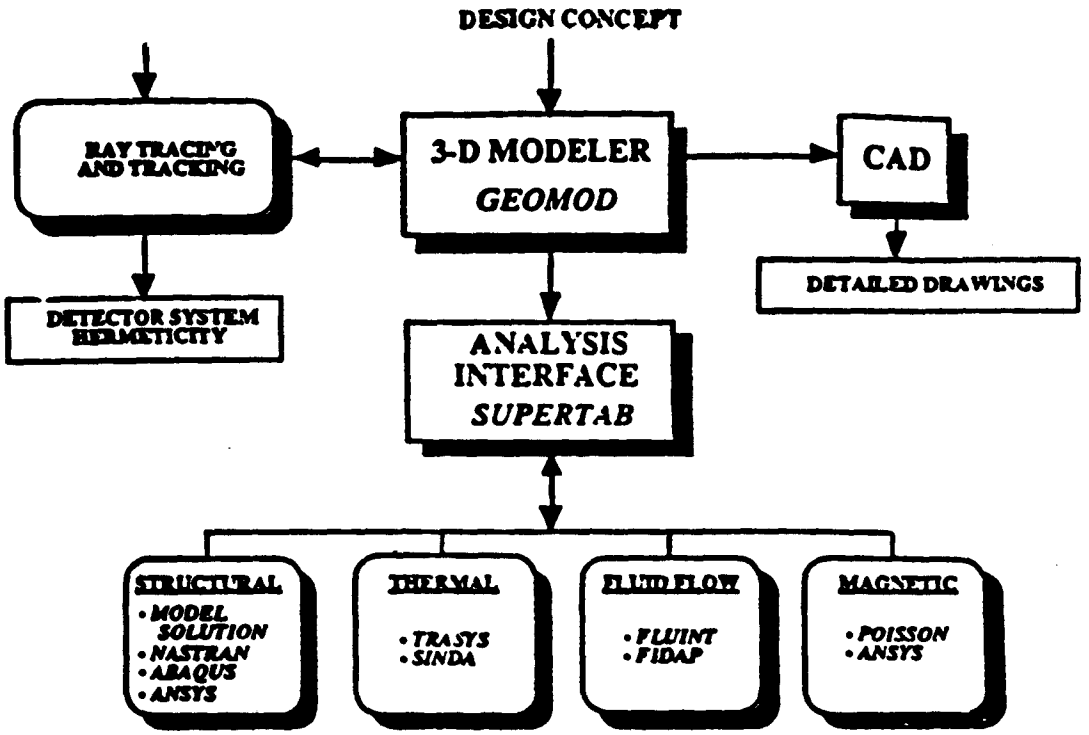

Figure 1: The integrated design, modeling and analysis system.

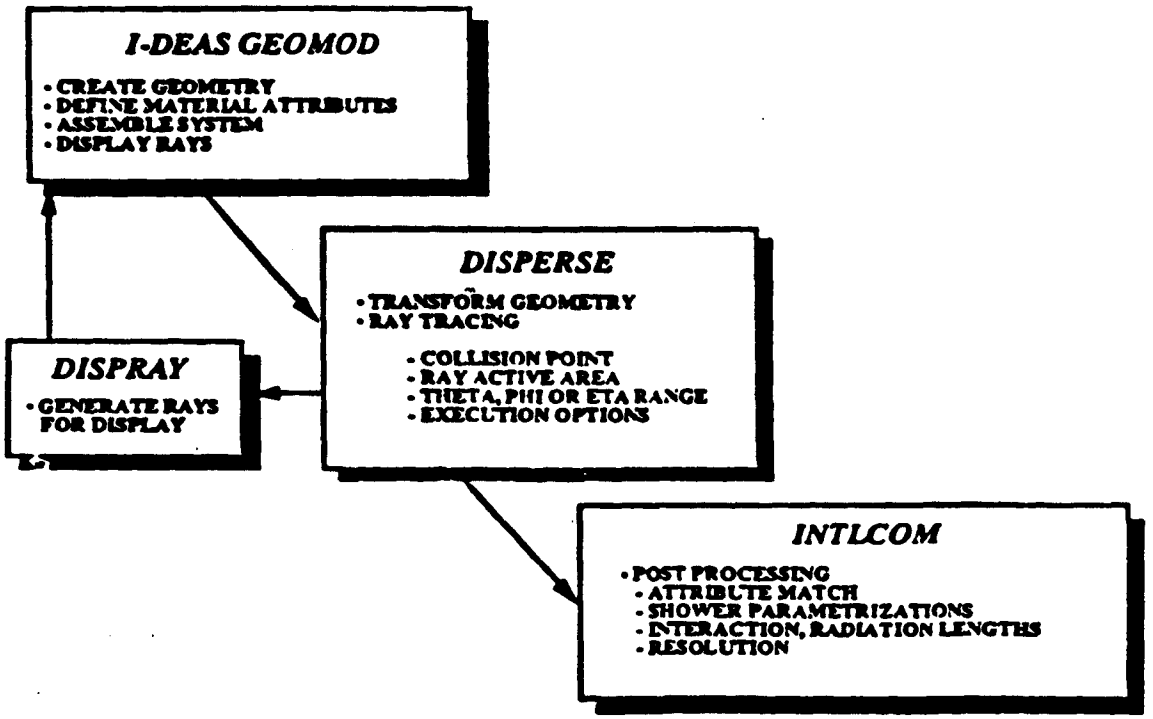

Figure 2: The ray tracing and tracking section of the design, modeling and analysis system.

I. Engineering

"Martin Marietta" Design for LSD

Report is a snapshot of work in progress

Future plans

Minimize wall thickness in end cap 5

Finish Details of support

Assembly scenarios, design of handling eq.

$r = 1\ m$

$\rho = 10\ g/cm^3$

solenoid inside calorimeter – hermeticity?

split @ 90°

Schedule and cost $68–93M scaled from DØ/SLD

STATUS REPORT OF AN ENGINEERING DESIGN STUDY OF HERMET LIQUID ARGON CALORIMETRY FOR THE SSC

T. Adams(2), M. Davis(2), N. J. DiGiacomo(2)*, B. Easom(2), H. Gordon(1), J. Hupp
K. Killian(2), P. Kroon(1), M. Lajczok(2), M. Marx(3,4), L. Mason(2), J. Pohlen(2),
R. Watt(4), and T. Wright(2)

(1) Brookhaven National Laboratory, Upton, NY 11973
(2) Martin Marietta Astronautics, Denver, CO 80201
(3) State University of New York at Stony Brook, Stony Brook, NY 11794
(4) SSC/CDG, Lawrence Berkeley Laboratory, Berkeley, CA 94720

FERMILAB-Conf-89/109
D0 Note 839

Hermeticity of Three Cryogenic Calorimeter Geometries *

M. Strovink
University of California, Berkeley / Fermilab

W.J. Womersley
University of Florida

G.E. Forden
State University of New York, Stony Brook

FERMILAB-Conf-89/109
D0 Note 839

Hermeticity of Three Cryogenic Calorimeter Geometries *

M. Strovink
University of California, Berkeley / Fermilab

W.J. Womersley
University of Florida

G.E. Forden
State University of New York, Stony Brook

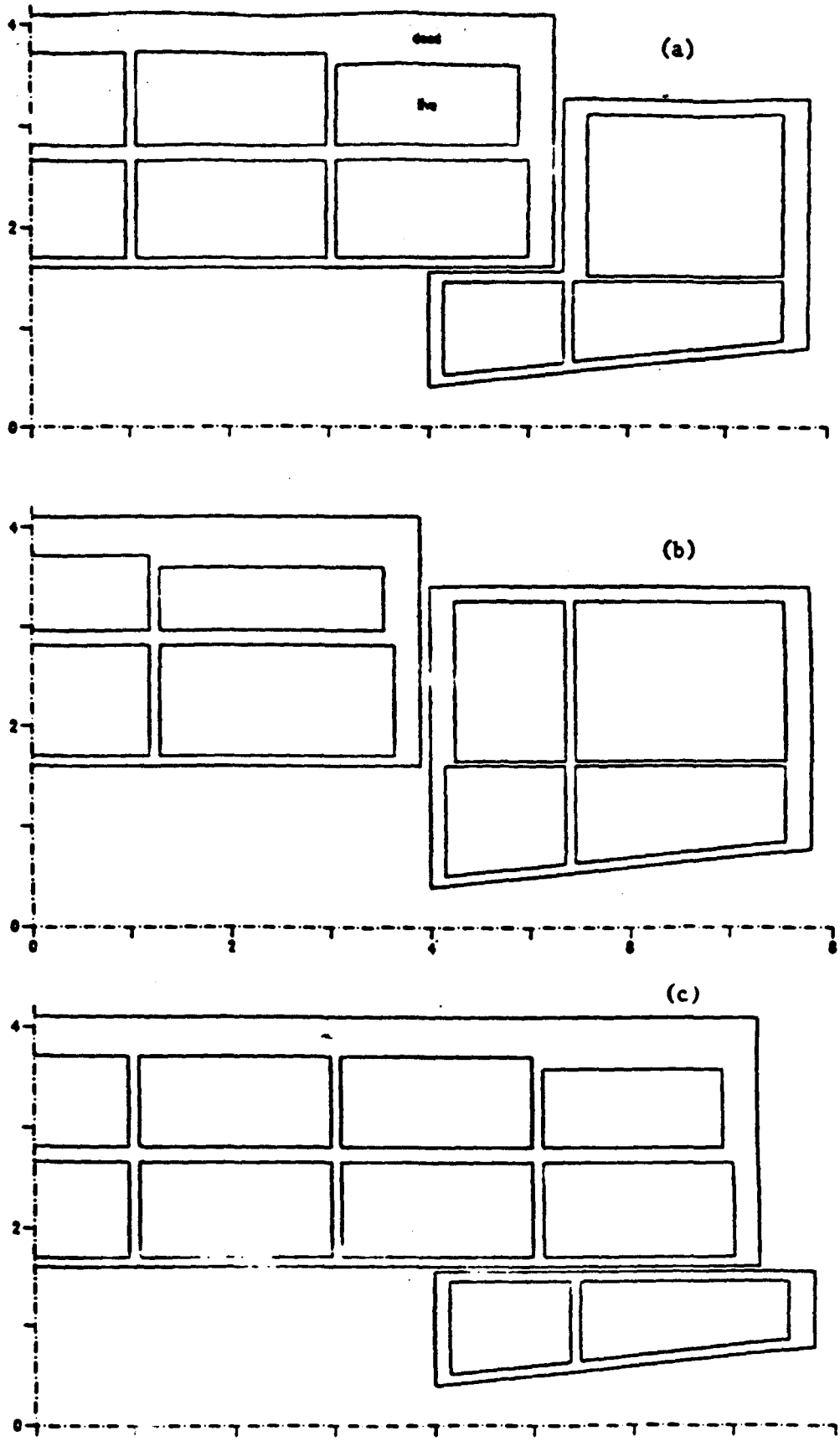

Fig. 1

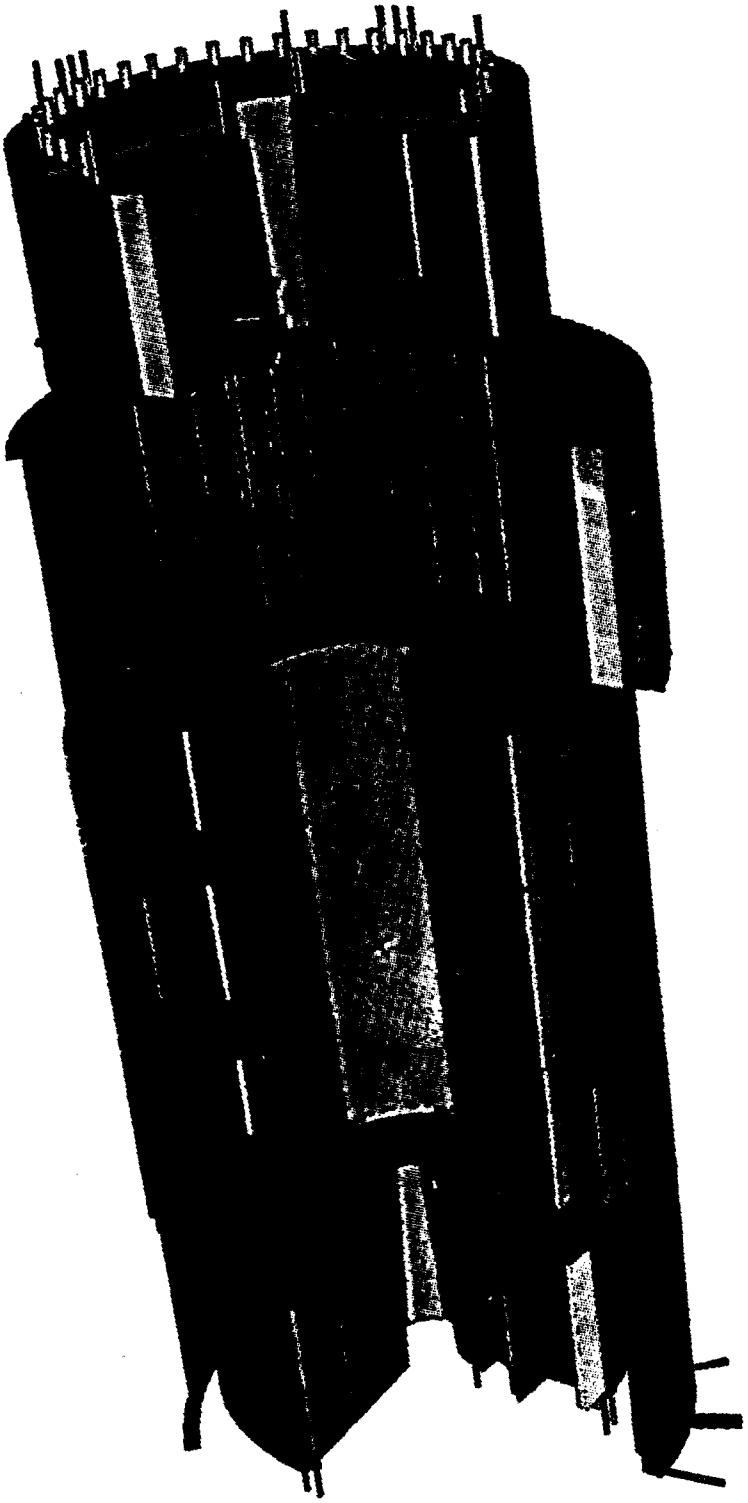

1A1B 6

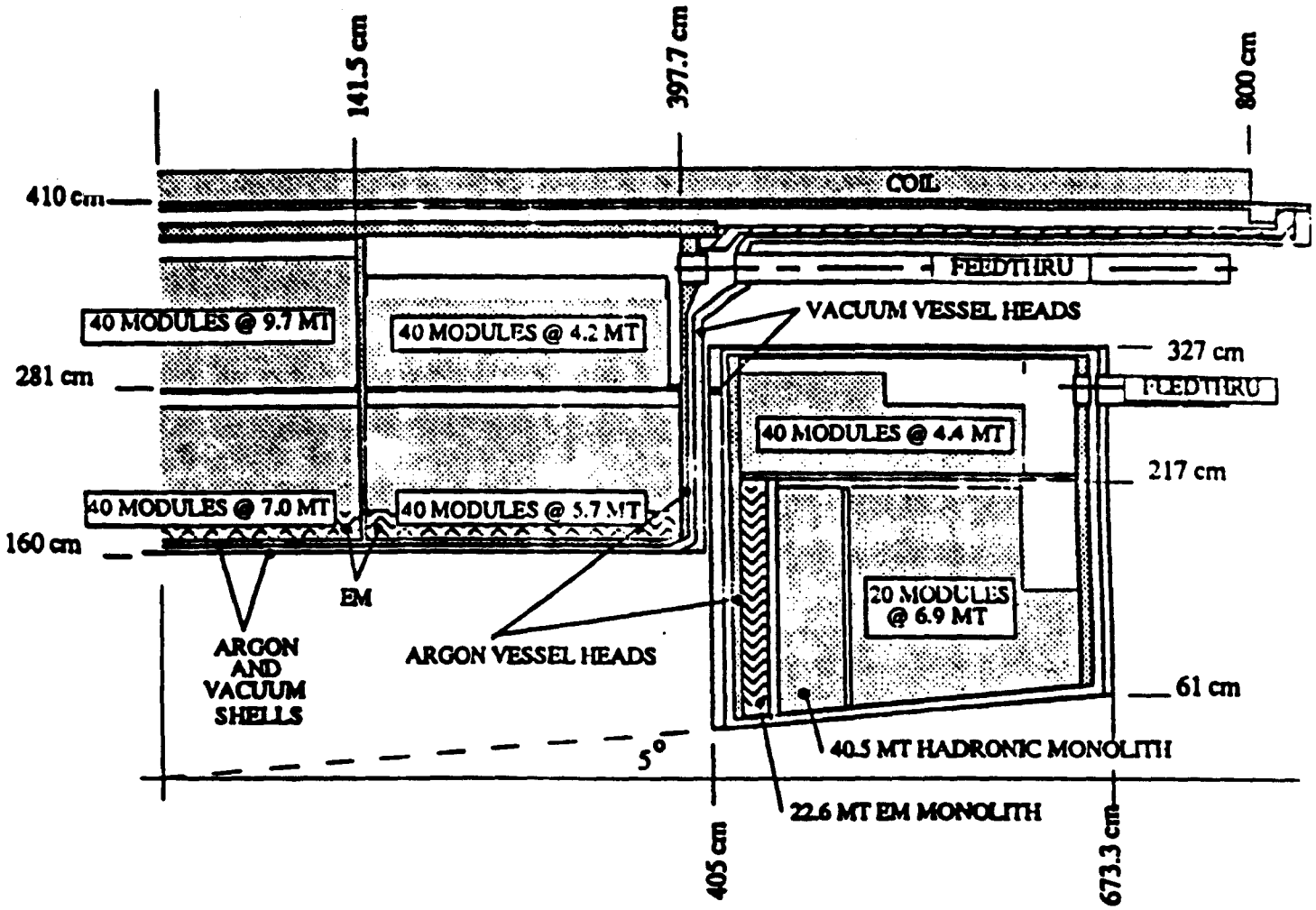

Figure 5: Schematic view of LAC, showing overall dim...
each major ...

	ARGON VESSELS BARREL	ARGON VESSELS END CAPS		VACUUM VESSELS BARREL	VACUUM VESSELS END CAPS
Inner Shell	3.8 cm	2.5 cm	Inner Shell	1.9 cm	7.6 cm
Corner	3.8	10.9 to 2.5			
Outer Shell	7.1	4.8	Outer Shell	5.1	4.5
Heads	6.1	8.9	Heads	5.3	10.2
Washers	5.6	5.6			

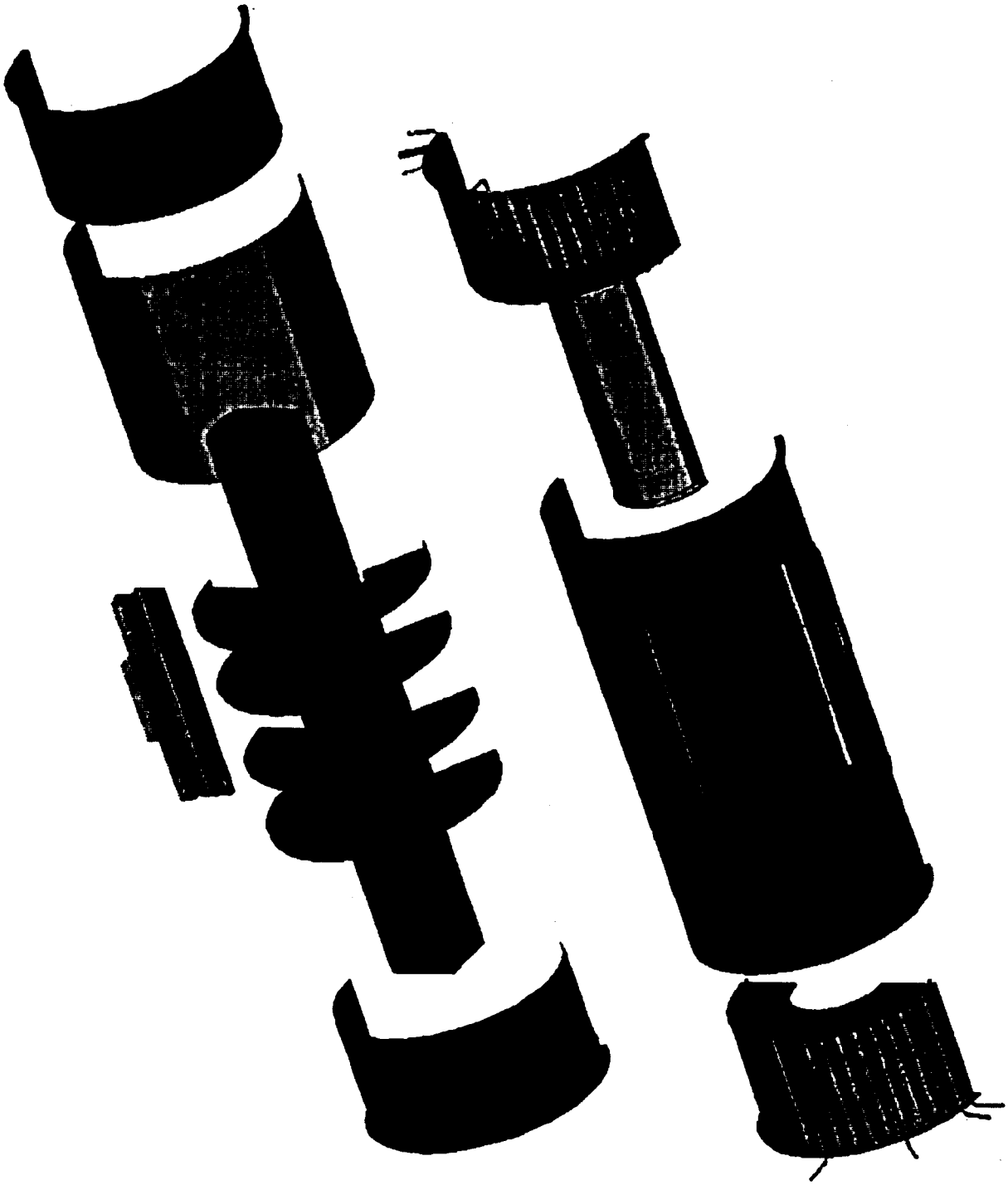

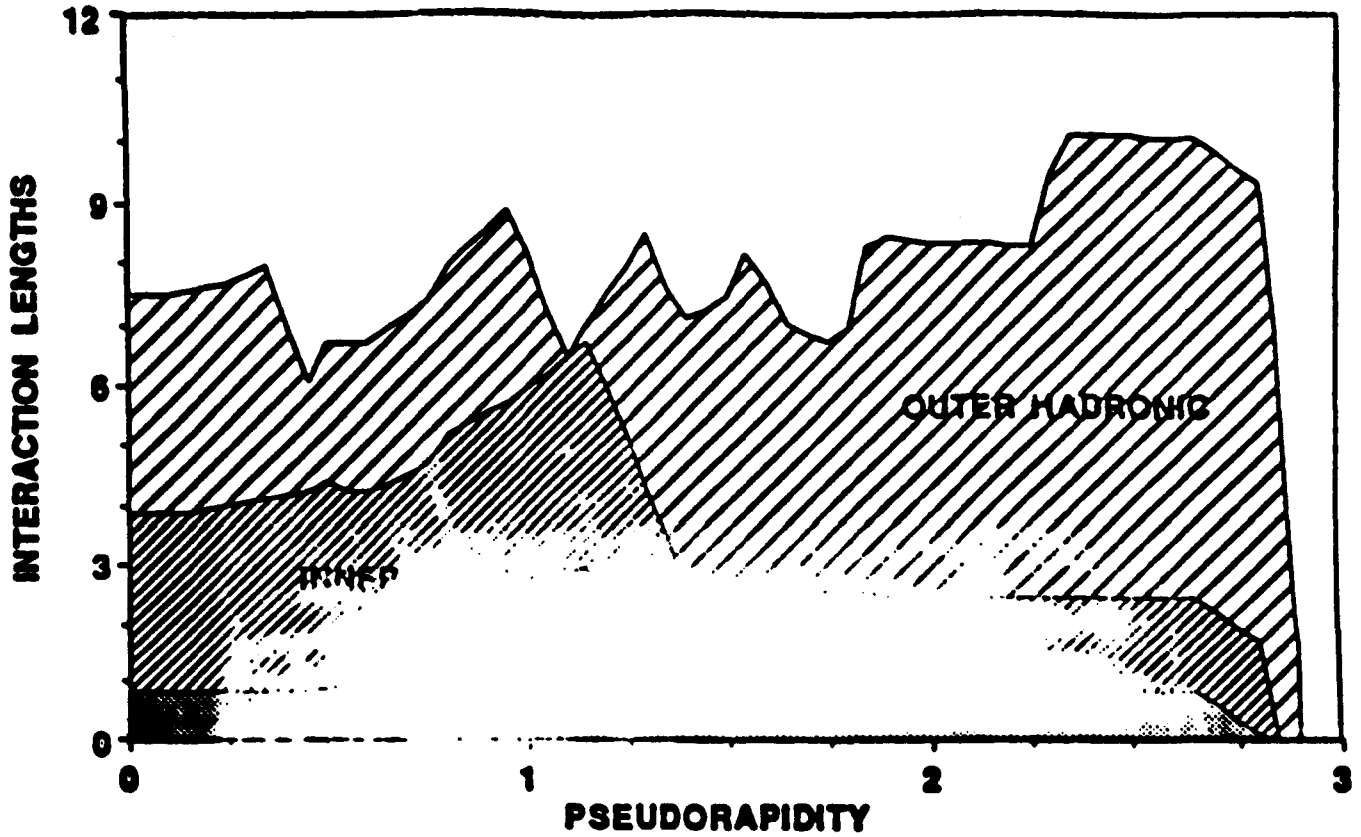

Figure 9: Active interaction lengths of calorimeter (i.e. not including vessels, structural members, etc.) in the LAC assuming $\rho = 7.5$ g/cm^3, $\lambda = 25$ cm and $X_0 = 0.80$ cm.

	Al	Steel	Ti
SHELLS			
t/t_{Al} (Stress: $S^{1.0}$)	1	.53	.18
(t/t_{Al}) (l_{Al}/l)	1	1.25	.26
(t/t_{Al}) (X_{oAl}/X_o)	1	2.69	.46
t/t_{Al} (Stability: $E^{1/3}$)	1	.71	.86
(t/t_{Al}) (λ_{Al}/λ)	1	1.66	1.24
(t/t_{Al}) (X_{oAl}/X_o)	1	3.58	2.16
HEADS/WASHERS			
t/t_{Al} (Bending: $S^{1/2}$)	1	.73	.43
(t/t_{Al}) (λ_{Al}/λ)	1	1.71	.61
(t/t_{Al}) (X_{oAl}/X_o)	1	3.69	1.07
t/t_{Al} (Stability: $E^{1/2}$)	1	.60	.80
(t/t_{Al}) (λ_{Al}/λ)	1	1.40	1.15
(t/t_{Al}) (X_{oAl}/X_o)	1	3.02	2.01
ρ (g/cm^3)	2.70	7.87	4.54
λ (cm)	39.40	16.80	27.50
X_o (cm)	8.90	1.76	3.56
S (10^3 psi)	10.0	18.75	55.
E (10^6 psi)	10.0	28.	15.5
Relative Cost (fabricated)	1.0	2.5	3.0

Table 4: Cryostat material performance, referenced to aluminum.

DESIGN EVOLUTION

MODULE SCHEDULE

MINIMUM TIME (FAST) SCHEDULE

	YEARS
SELECT GAP + ABSORBER STRUCTURE	1/2
DESIGN MODULES	1
VERIFY DESIGN (LAR, COSMIC + BEAM TESTS)	1
FIRST ARTICLES FROM INDUSTRY	3/4
ASSEMBLE + TEST FIRST ARTICLES	1/4
PRODUCTION + SIMULTANEOUS TESTING	2
COMPLETE TESTING	1/2
INSTALLATION INTO VESSELS + TESTING	1
VESSEL CLOSURE + EXTERNAL CONNECTIONS	1/2
	7 1/2

CONSERVATIVE (SLOW) SCHEDULE

R+D ON PB COMPENSATION, U PLATING/ CLADDING, SUB-UNIT TYPE GAPS	2
MODULE DESIGN	1
VERIFY DESIGN	1
TECHNOLOGY TRANSFER TO INDUSTRY	1 1/2
FIRST ARTICLES	1/2
TEST FIRST ARTICLES	1/2
REDESIGN	1/2
PRODUCTION + SIMULTANEOUS TESTING	2
COMPLETE TESTING	1/2
INSTALLATION INTO VESSELS + TESTING	1 1/2
VESSEL CLOSURE + EXTERNAL CONNECTIONS	1 1/2
	12 1/2

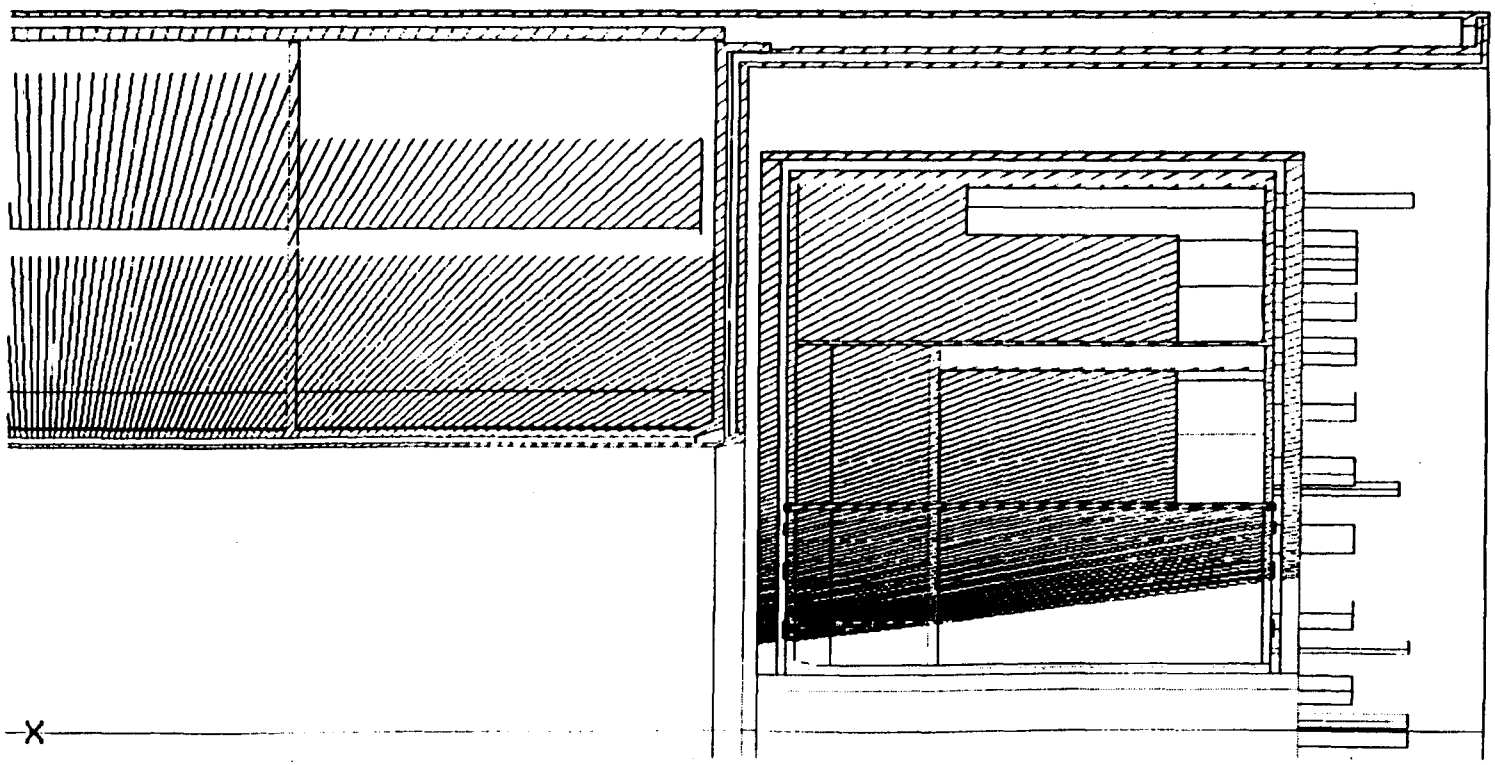

A1A1

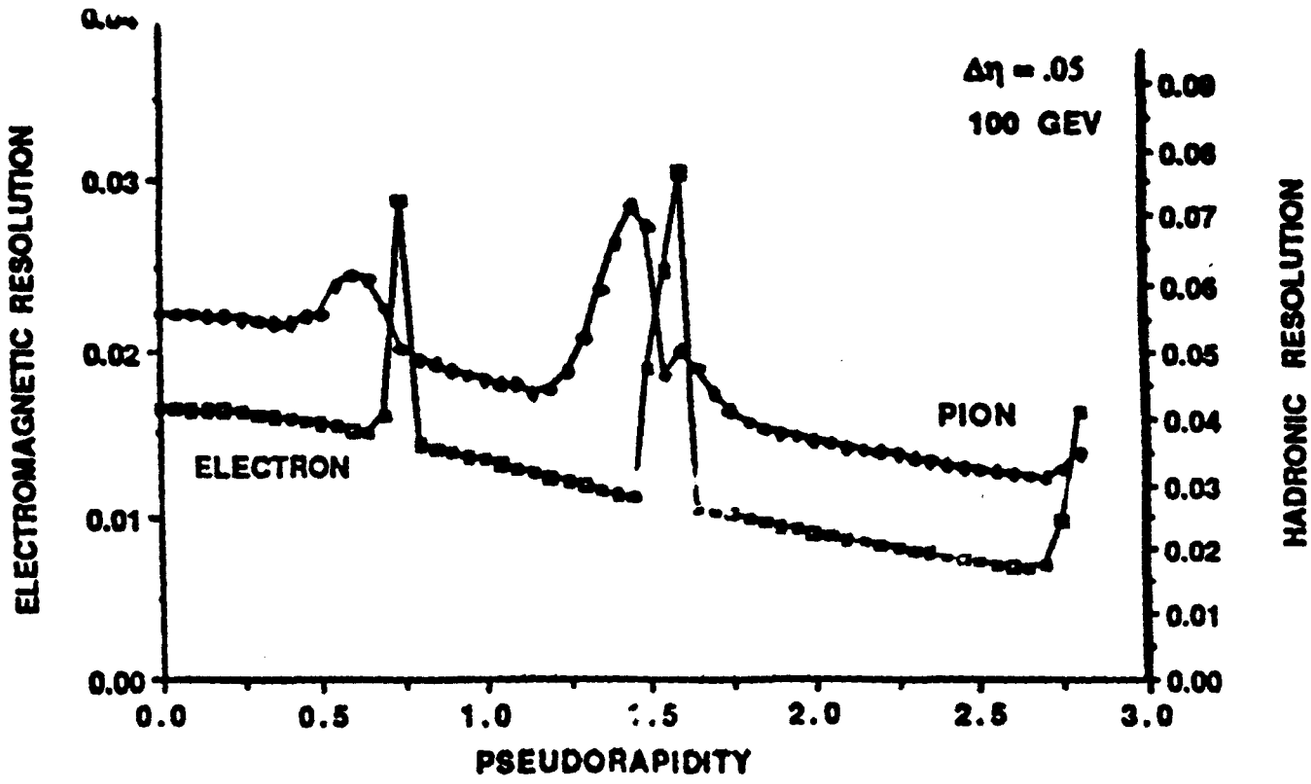

Figure 13: Resolution versus pseudorapidity for 100 GeV transverse energy electrons

II HERMETICITY

- DEAD MATERIAL
- DEPTH

LSD (Pb ⇒ ~7λ ; u ⇒ ~10λ)

Jürgen Krüger (Zeus)

in 6.6λ 90% of 135GeV Jets >95% energy

in ~9λ 99%

Need specification from $\not{p}_T$ physics

III. Nitty-gritty details

Absorber choice e/π

SLD tests Pb/LA ~1.2±0.1

HELIOS (NA34)] U/LA

DØ (1988)]

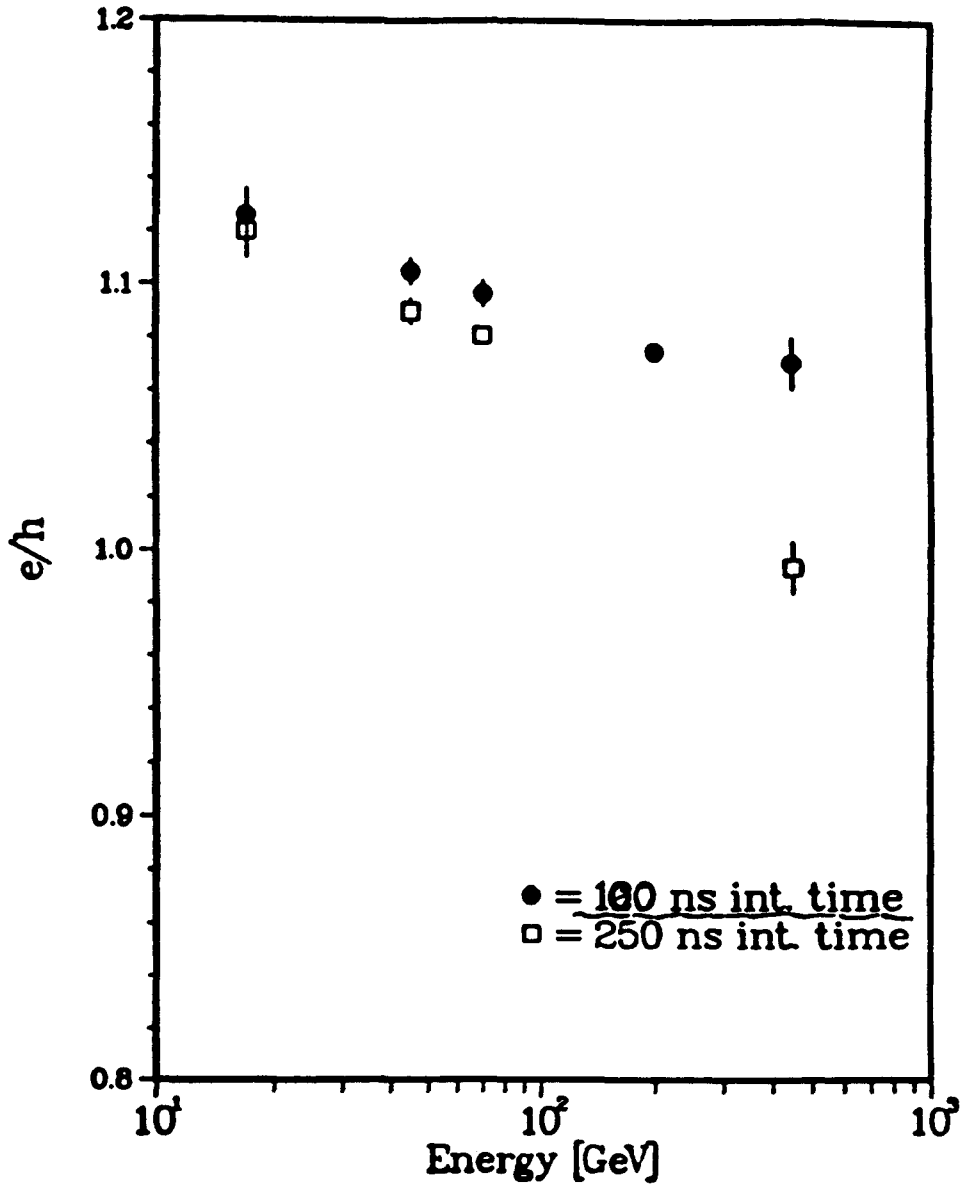

Uranium - Liquid Argon Calorimeter for HELIOS exp.

e/h ratio vs E

NA34

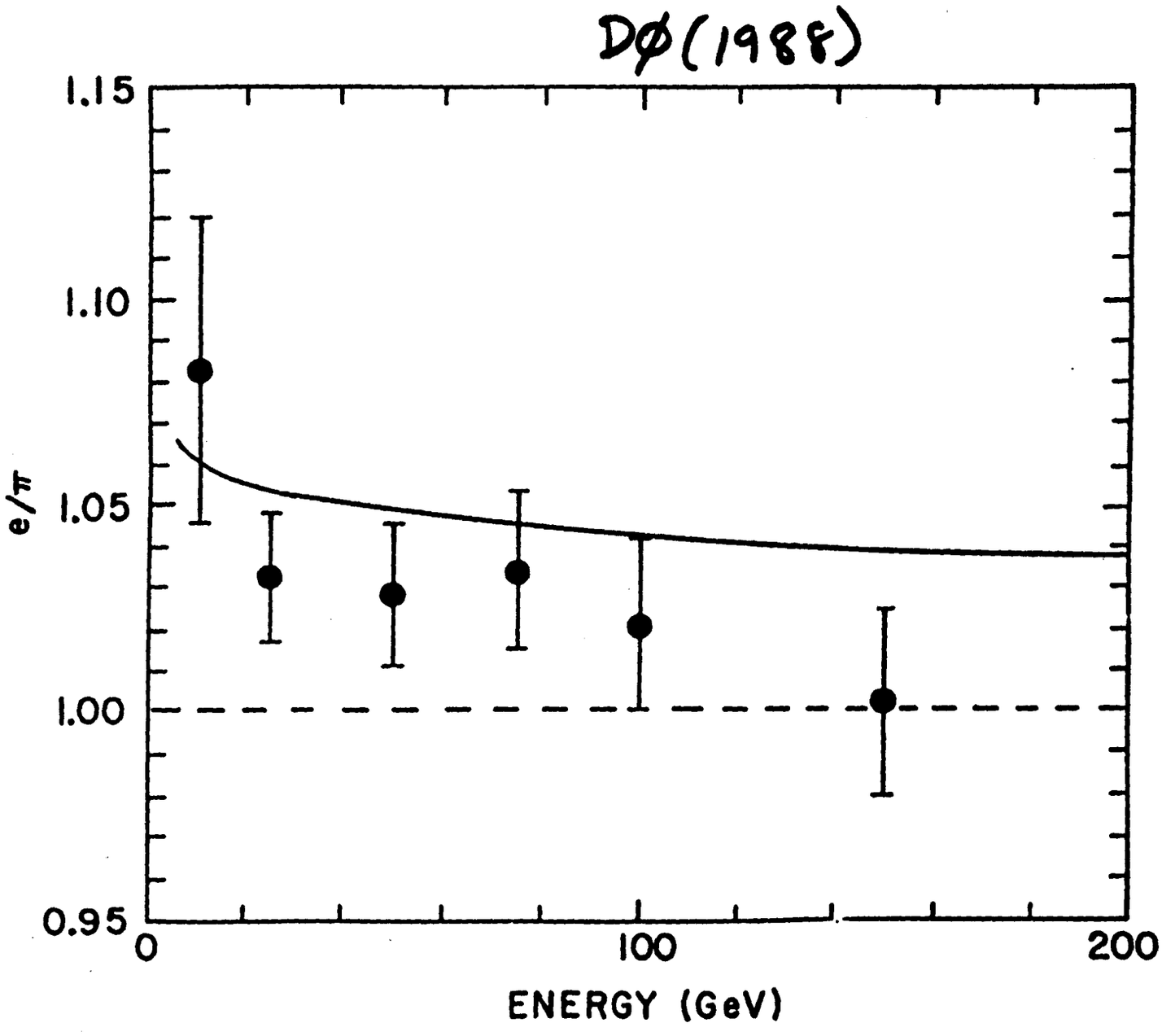
DØ (1988)
1.15
1.10
1.05
1.00
0.95
e/π
0
100
200
ENERGY (GeV)

DØ

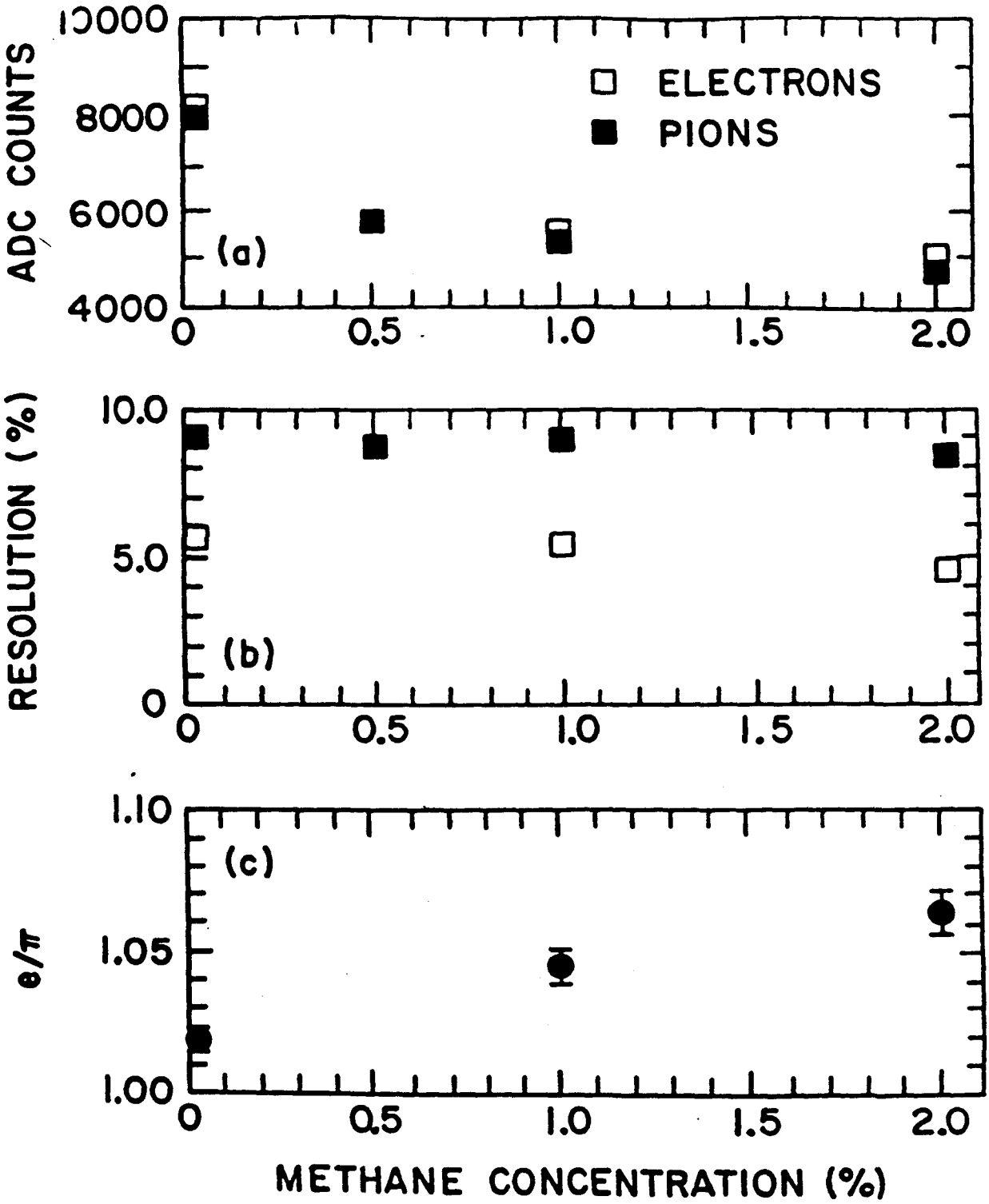
ADC COUNTS
10000
8000
6000
4000
ELECTRONS
PIONS
(a)
0
0.5
1.0
1.5
2.0
RESOLUTION (%)
10.0
5.0
0
(b)
e/π
1.10
1.05
1.00
(c)
METHANE CONCENTRATION (%)

IV. Electronics

Speed? Problem is getting charge to preamps

∴ preamps in liquid — cooling problem (some other opinions)

Towers - need to be short for timing

$S \geq 6\%$ S/N

Ferrite transformers $\leq \sim 0.5$ T

a) reduce power 2-3

b) protect preamp from sparks

c) reduce noise

Alternatives are being discussed

- "Electrostatic transformers" parallel → series
- long low impedance lines ?

Block diagram exists

Charge transfer vs time – long connections

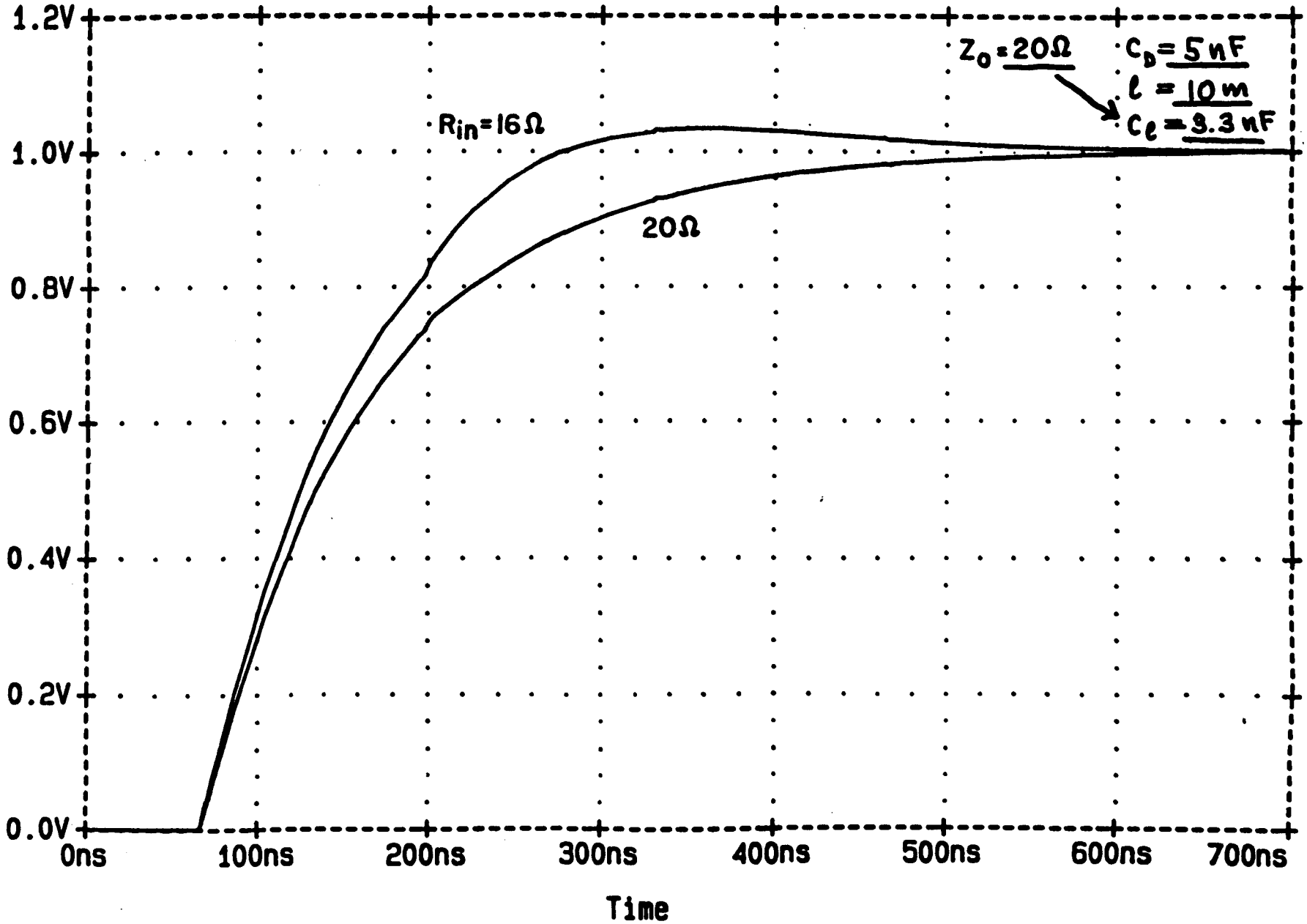

Ch ge transfer vs time — short connections

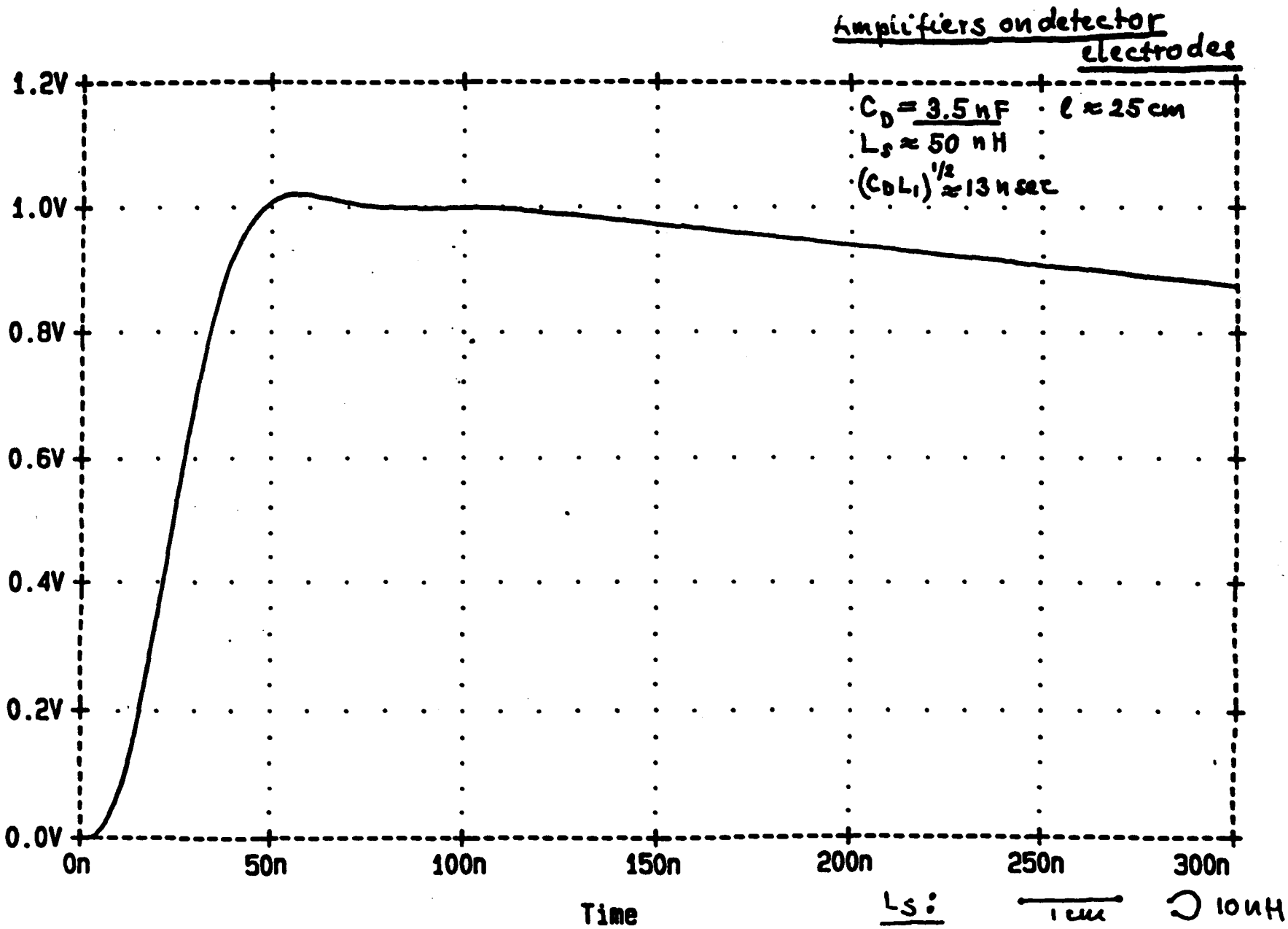

$t_r \approx 3.5 (L_s C_D)^{1/2}$

$[nF \cdot nH]^{1/2} = [nsec]$

L_s:		1 cm	10 nH
Z_0	100 Ω		1.5 cm
($\varepsilon' \approx 4$)	50 Ω		3 cm
	20 Ω		7.5 cm

5C7 KODAK 5C7 KODAK 5C7 KODAK

Uranium - Liquid Argon Calorimeter
for HELIOS (NA 34) exp.

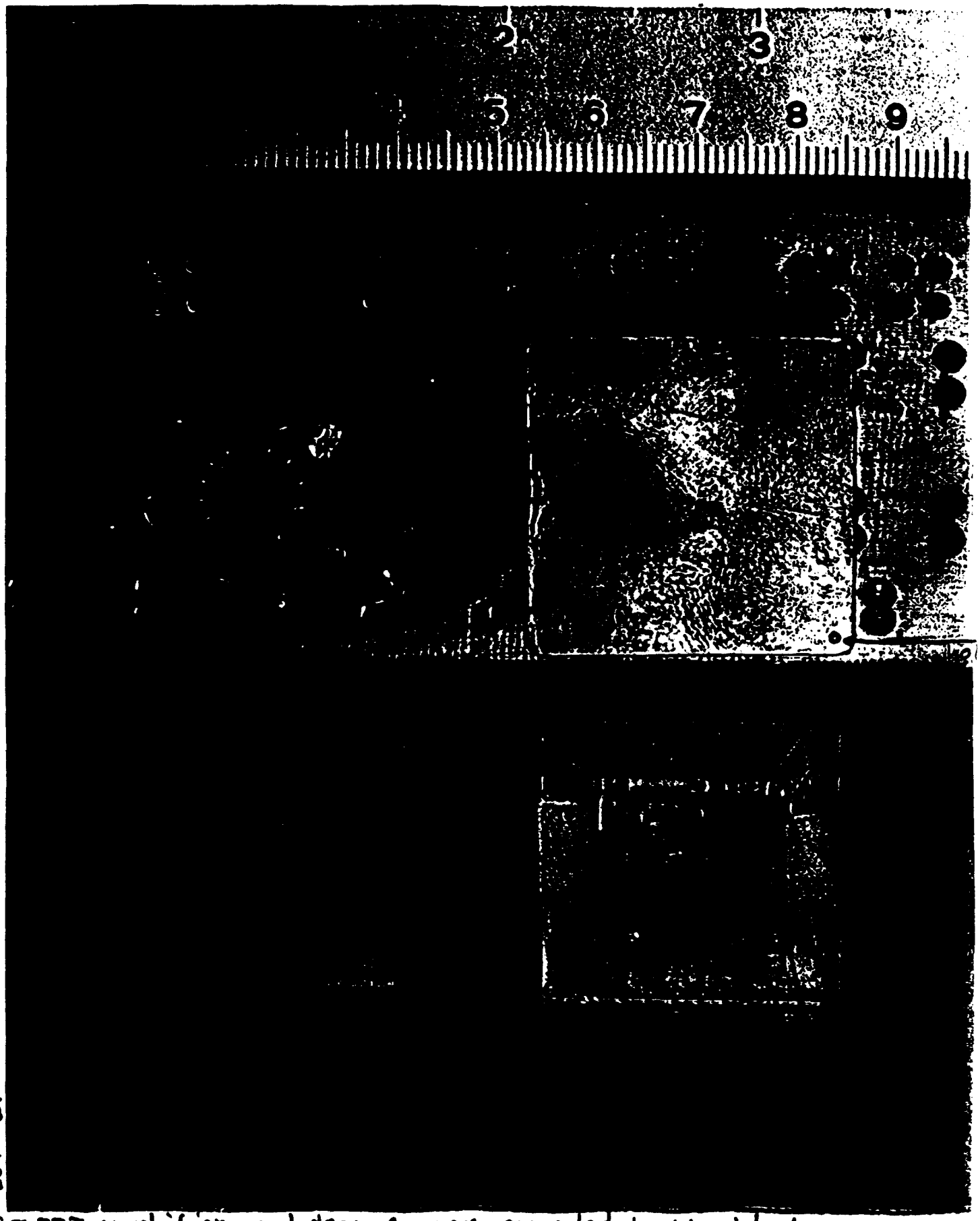

CN2-437-86

J FET amplifier and transformer operated in Liquid Argon

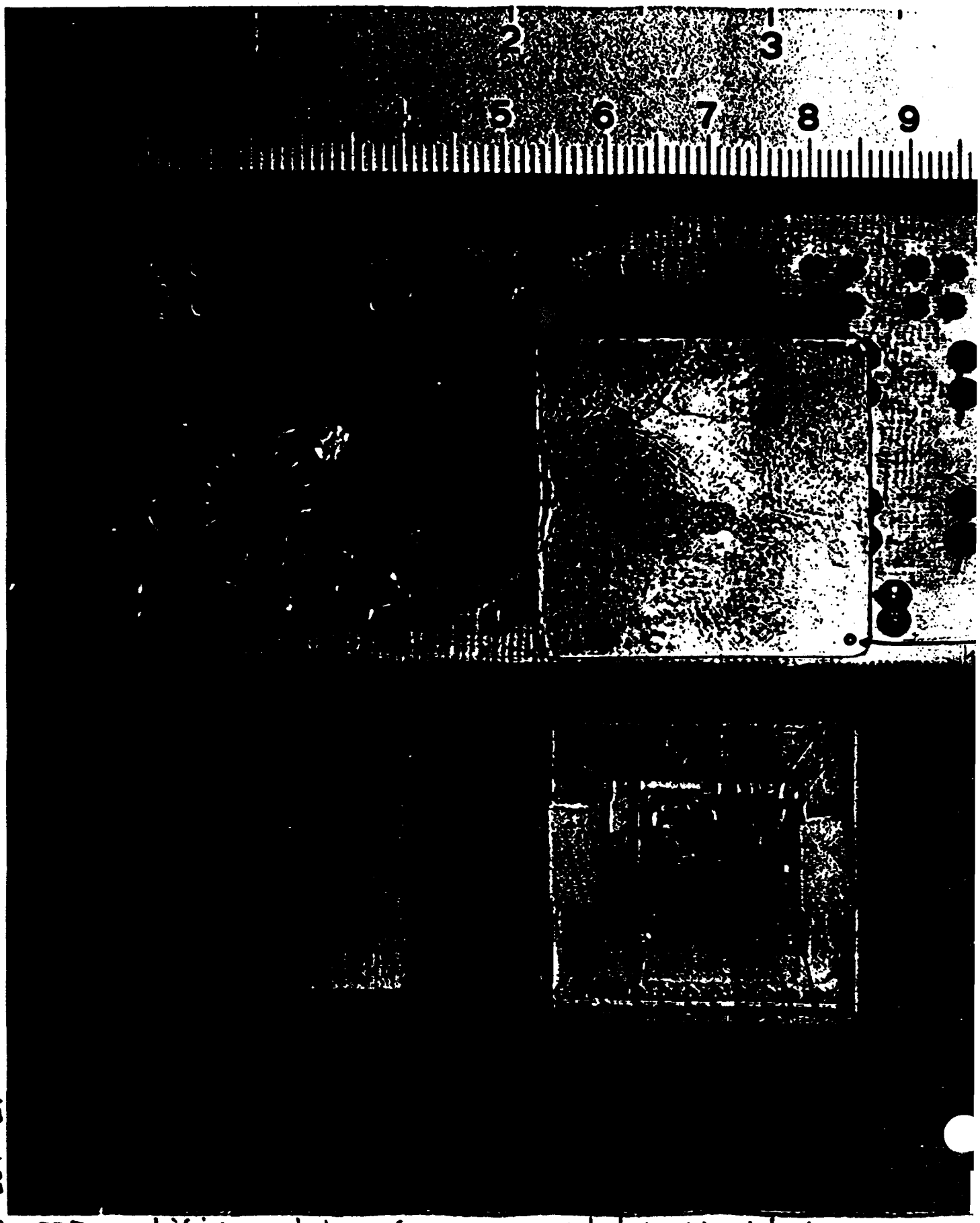

CMZ-437-86

J FET amplifier and transformer operated in Liquid Argon

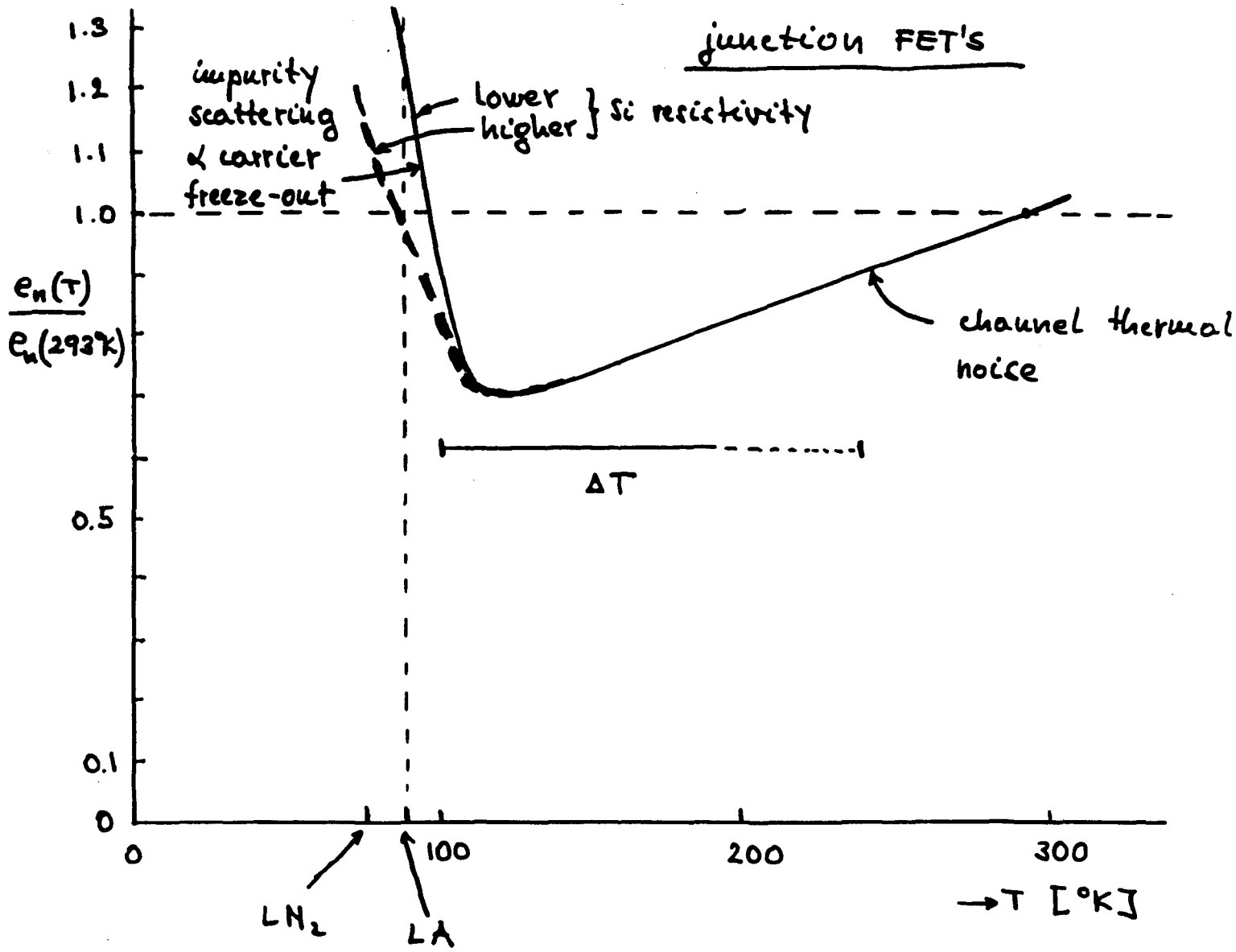

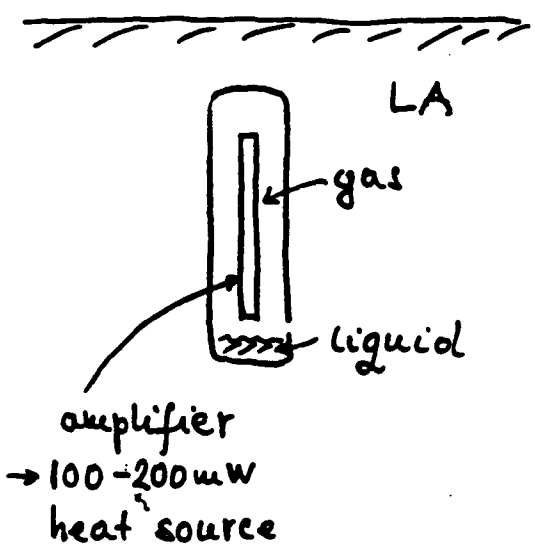

Necessary temperature difference achieved by amplifier power dissipation

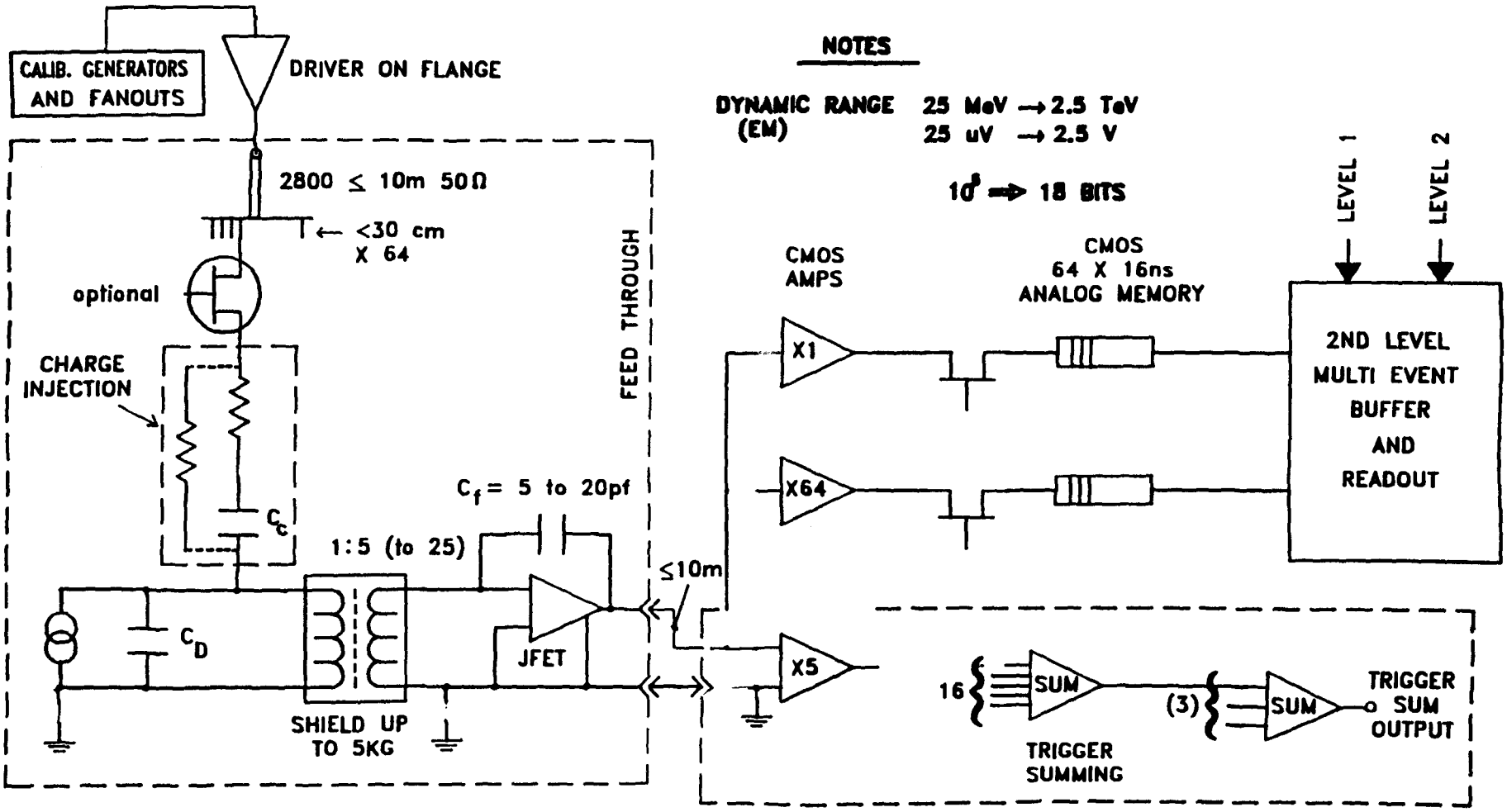

BNL-OMEGA JMH
SSC LA CAL SSCP001

	$\Delta\eta \times \Delta\phi$	PAD SIZE (cm)	$C_D + C_c$	S	NOISE PREAMPS IN L. Ar	+ TRANS FORMER
EM 1	0.04 x 0.04	7	400pf	11.4%	75 MeV	
EM 2	0.02 x 0.02	3.4	300pf		94 MeV	
EM 3	0.04 x 0.04	7	660pf		142 MeV	
H1+H2	0.04 x 0.04	8.4 9.9	3.8nf	5.7%	0.8 GeV	0.21 GeV
H3+H4	0.04 x 0.04	12.1 13.9	5.5nf		1.15 GeV	0.24 GeV

	$\Delta\eta$ $\Delta\phi$			
Trigger Tower	(0.32x0.32)	EM	1.8 GeV	
		EM+H	10 GeV	3.2GeV
Electron Tower	(0.08x0.08)		0.45 GeV	

TIMING (0.32x0.32)

1 ns	100 GeV
4 ns	25 GeV

All components need to be ±2ns

PULSE SHAPING, NOISE and PILEUP

Final shaping for triggers will be done after the sums are formed.

Final shaping for individual channels will be done by a combination of weighted samples taken every 16 ns.

Thus, the effective integration time t_m can be chosen to optimize the electronic noise against pileup for different physics requirements at a given luminosity:

t_m	50 ns		100 ns
		Timing	
	1 ns	100 GeV Jet	0.67 ns
	4 ns	25 GeV Jet	2.7 ns
	2.8 GeV	σ	0.9 GeV

$\sigma_{pileup} \sim \sqrt{t_m}$

<u>Other improvements</u>

- Methane S/N ↑2 problems with purification radiation damage ?
- S → 12% S/N ↑
- Electrostatic transformer (See warm liquid talk) ???

Subsystem Proposal

BNL, LBL, FSU, U of Rochester, MSU, FNAL, ...
Stony Brook, KEK, U of Washington

Absorber? Beam test of Pb Pb/Fe

Module design
- connections
- segmentation

Cooling of preamps

Shielding of transformers

Development of Brite Pads

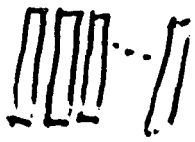

Signal + HV feedthroughs

Optimization of S/N

Calibration

⋮

Paul Mockett

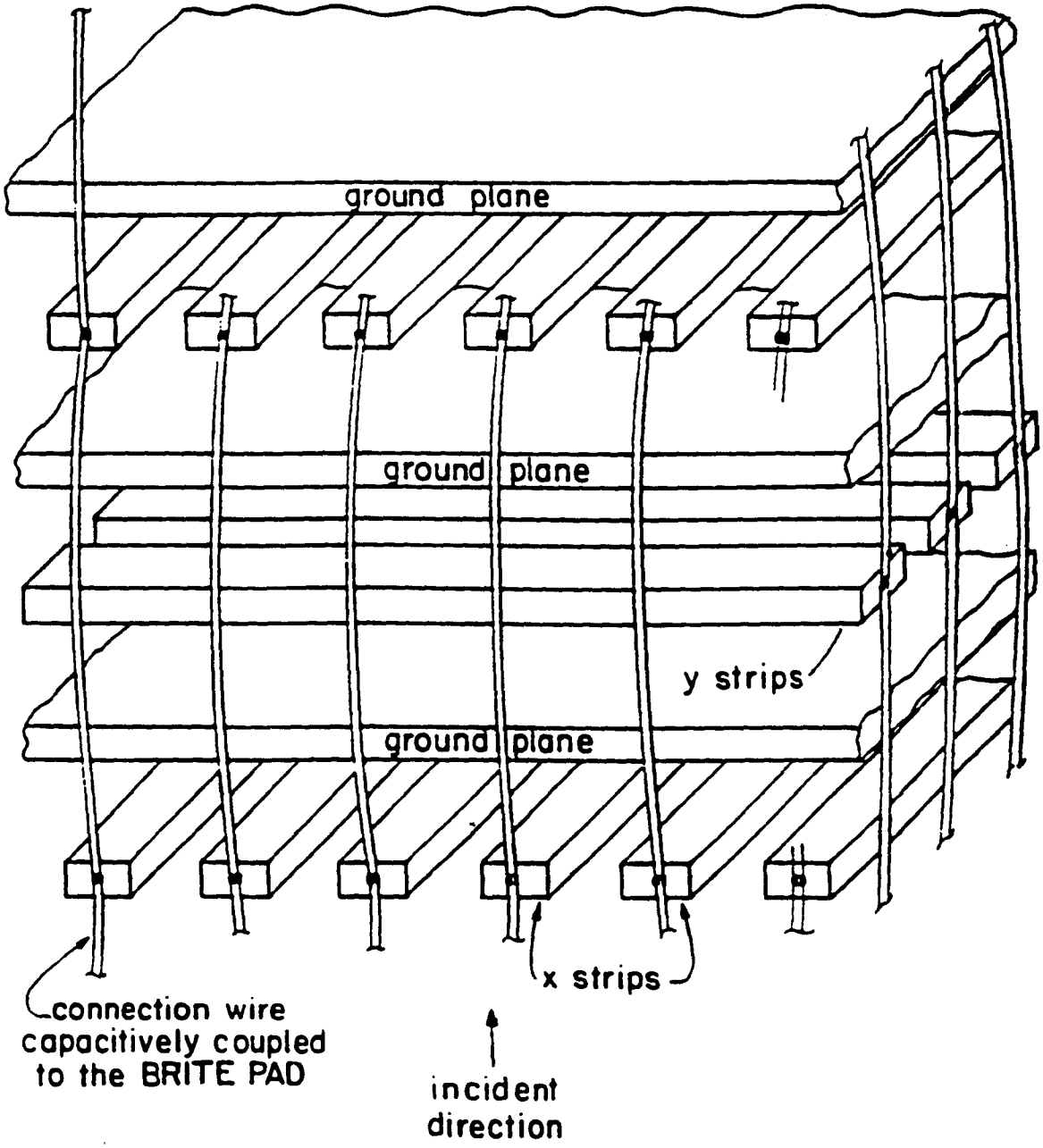

Fig. 1

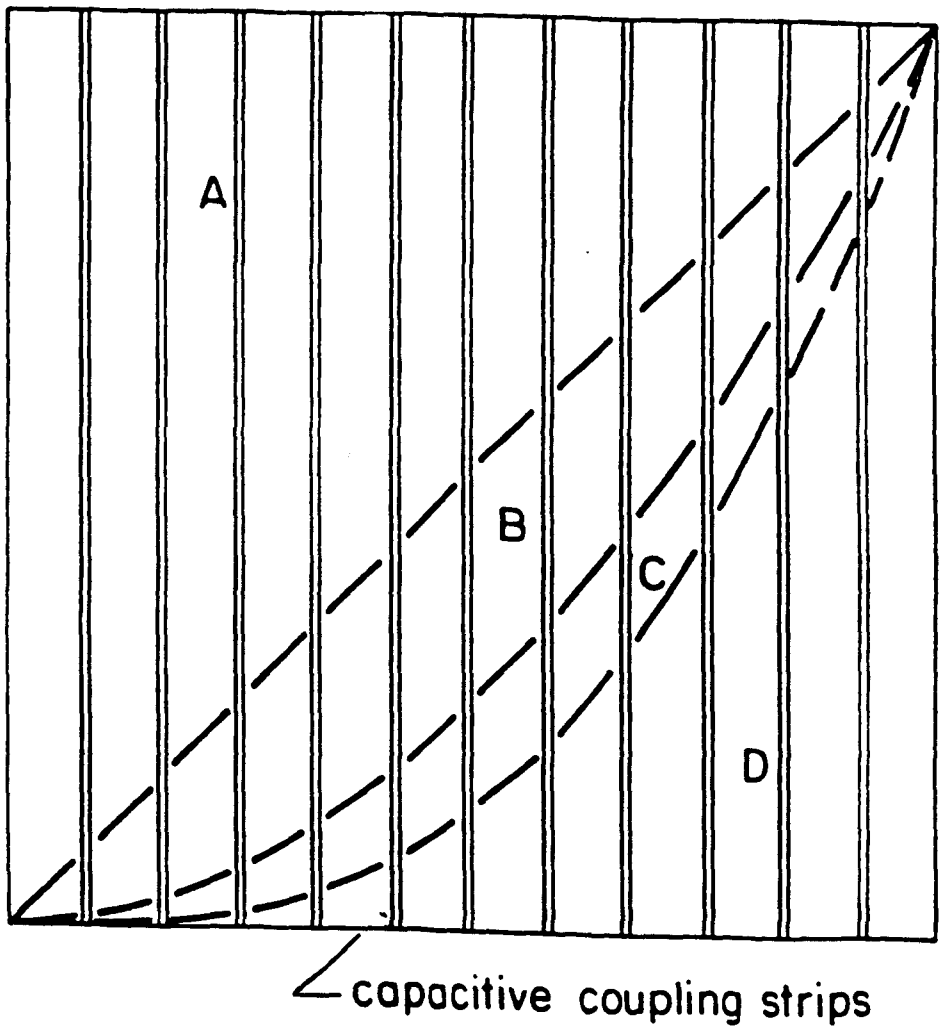

Improves: position resolution ~ 1 mm

e/π separation

2 showers

redundancy (dead channels or shorts)

Fig. 3

channel count ≲ 1/2

Tentative Schedule for
SSC Liquid Argon Major Subsystem R& D Proposal

June 27 Suite 210 SSC Laboratory

12:00 ~~9:00~~ AM	Organization Details
9:10 AM	V. Radeka/S. Rescia – Progress on electrode configurations, shower and signal propagation in a tower, measurements of transformer shielding and status of high resistivity preamps
9:50 AM	P. Mockett – Discussion of Methane, Interleaving and survival with buried electronics – Brite Pates
10:30 AM	LBL – Progress on Tiles/Readout boards, connection details, HV and cold feedthroughs
11:10 AM	H. Gordon – Estimate of funds and manpower for a beam test
11:40 AM	N. DiGiacomo– Martin Marietta's resources to help this proposal
12:00	Lunch
12:30 PM	Discussion of Proposal – writing assignments
2:15 PM	Senator Phil Gramm
3:15 PM	Continued Discussion
	T. Kondo – Calibration of VENUS Liquid Argon System

Expected Attendees:

M. Levi, H. Gordon, N. DiGiacomo, G. Abrams, J. Siegrist,
A. Lankford, M. Marx, V. Radeka, V. Polychronakos,
V. Hagopian, S. Rescia, T. Kondo, P. Mockett, F. Lobkowicz

CONCLUSIONS

Lots more work is needed! (5° region!!

Liquid Argon look very promising

Living at 2T will be hard (for all?)

Physics Benchmarks need definition

- Can $W_L W_L$ scattering be studied by using $W \to$ jet + jet ?
- Do we need to search for $80 < m_{h^0} < 180$ GeV $h^0 \to \gamma\gamma$
- Missing p_T – how well do we need to measure it – how does noise and pileup contribute

⋮

M. Prest
6/26/89
DALLA

ROOM-TEMPERATURE OR WARM-LIQUID* CALORIMETRY

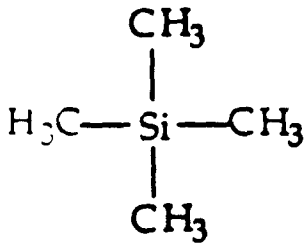

TMS ($(CH_3)_4Si$)

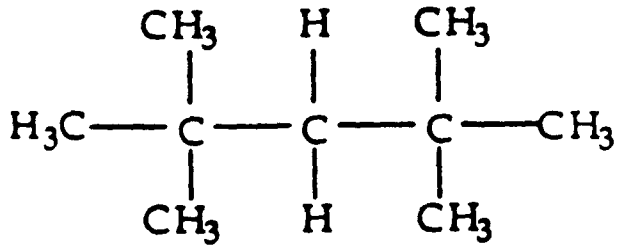

TMP (C_9H_{20})

(*- Liquids which at room temperature can sustain the existence of free ionization electrons and their drifting in an external electric field)

OUTLINE

- AN ASSESSMENT OF THE TECHNOLOGY
- DESIGN OF A FAST, HERMETIC, COMPENSATING CALORIMETER

WHY CONSIDER WARM LIQUIDS

- ***Advantages of liquid ionization chambers***
  - Direct collection of charge is most absolute and stable way of recording ionization signal
  - Thousands of ion pairs -- statistical fluctuations are negligible compared with sampling fluctuations
  - Spatially uniform
  - Easy to segment in depth as well as in surface area
  - Insensitive to magnetic fields
  - Requires little space for readout cables
  - Radiation resistant
- ***Some advantages of warm liquids relative to LAr***
  - No cryogenic insulation
  - Modules can be smaller, with thinner single-wall boundaries
  - More hermetic
  - Hydrogenous medium -- possible compensation without uranium
  - Preamp location ~~inner near~~ OUTSIDE liquid AND NEAR ELECTRODES -- matching transformers may not be needed -- with high voltage, signal pulses are short
- ***Limitations*** ("CHALLENGES")

CRITICAL ISSUES

- *VIABILITY OF TECHNOLOGY*

  - **Detector Scale (Large Solenoidal Detector - LSD)**
  - **Extreme Requirements of Liquids and Containers**
  - **Purity:** Long-Term High Purity (ppb) in situ for Large Volumes (>100,000 Liters)
  - **Safety:** May determine choice of liquid (TMP, TMS, TMGe, TMPb, etc.)
  - **Materials Compatibility:** Profound Impact on Design. Thus far, UA-1 long-term experience for stainless steel and ceramic. If no other, then ⇒ discrete boxes, spaghetti calor?
  - **Cleaning Procedures:** UA-1 very stringent, e.g. bakeout at 900° C.
  - **Radiation Damage.** Mostly OK (Groom & Holroyd)
  - **Recirculating Liquid to Ameliorate Radiation Damage and Impurities Build-up?**
  - **Cost, Filling Strategies, etc.**
  - [redacted] **Large-Scale Detector ⇒ UA-1.** (RETROFIT)

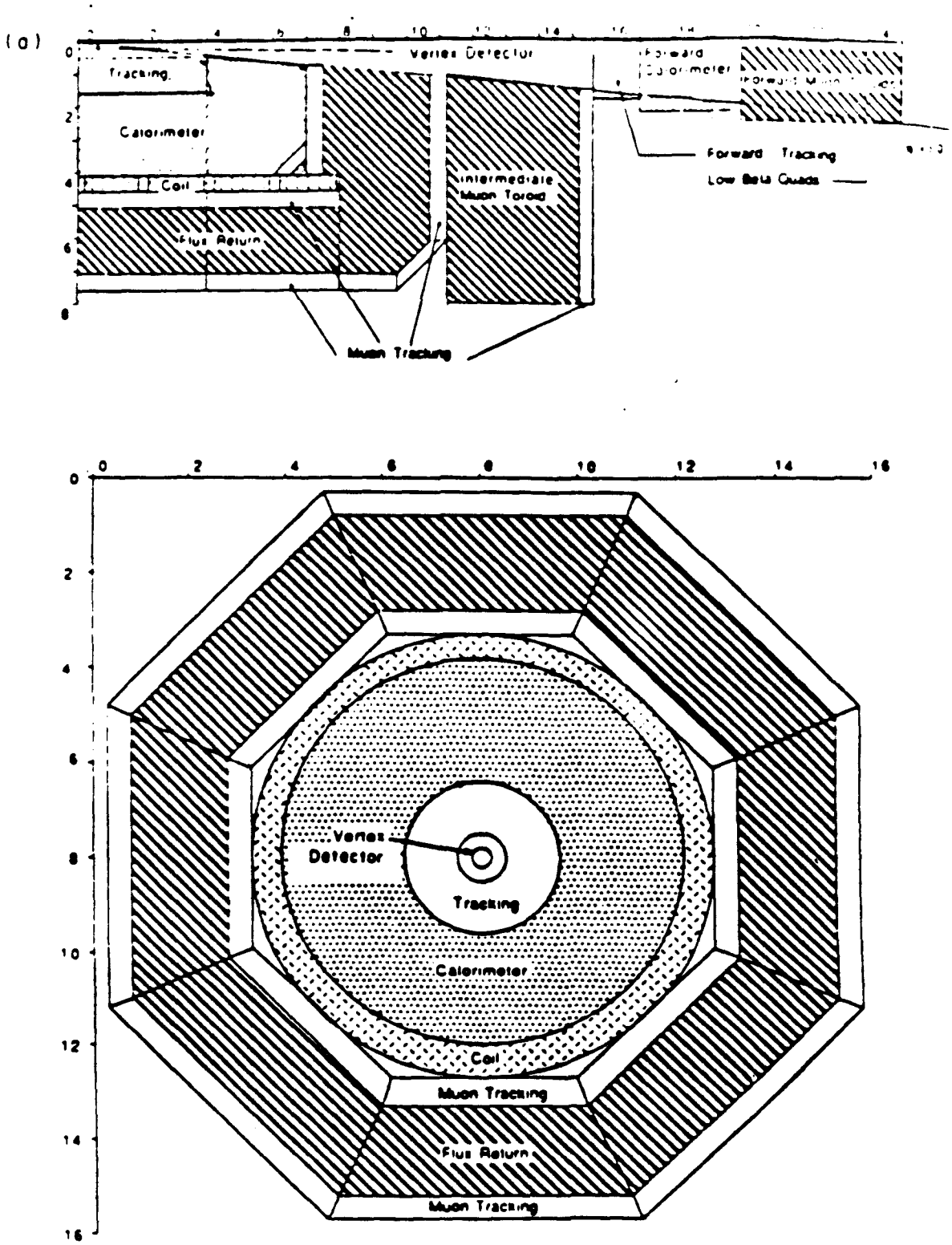

Fig. 2. End view of the Large Solenoid Detector.

ELECTRON LIFETIMES (τ_e) IN TMS AS A FUNCTION OF IMPURITY CONCENTRATIONS FOR VARIOUS IMPURITIES

- WANT $\tau_e > 10 \times$ DRIFT-TIME, i.e $\tau_e \gtrsim 1\mu s$

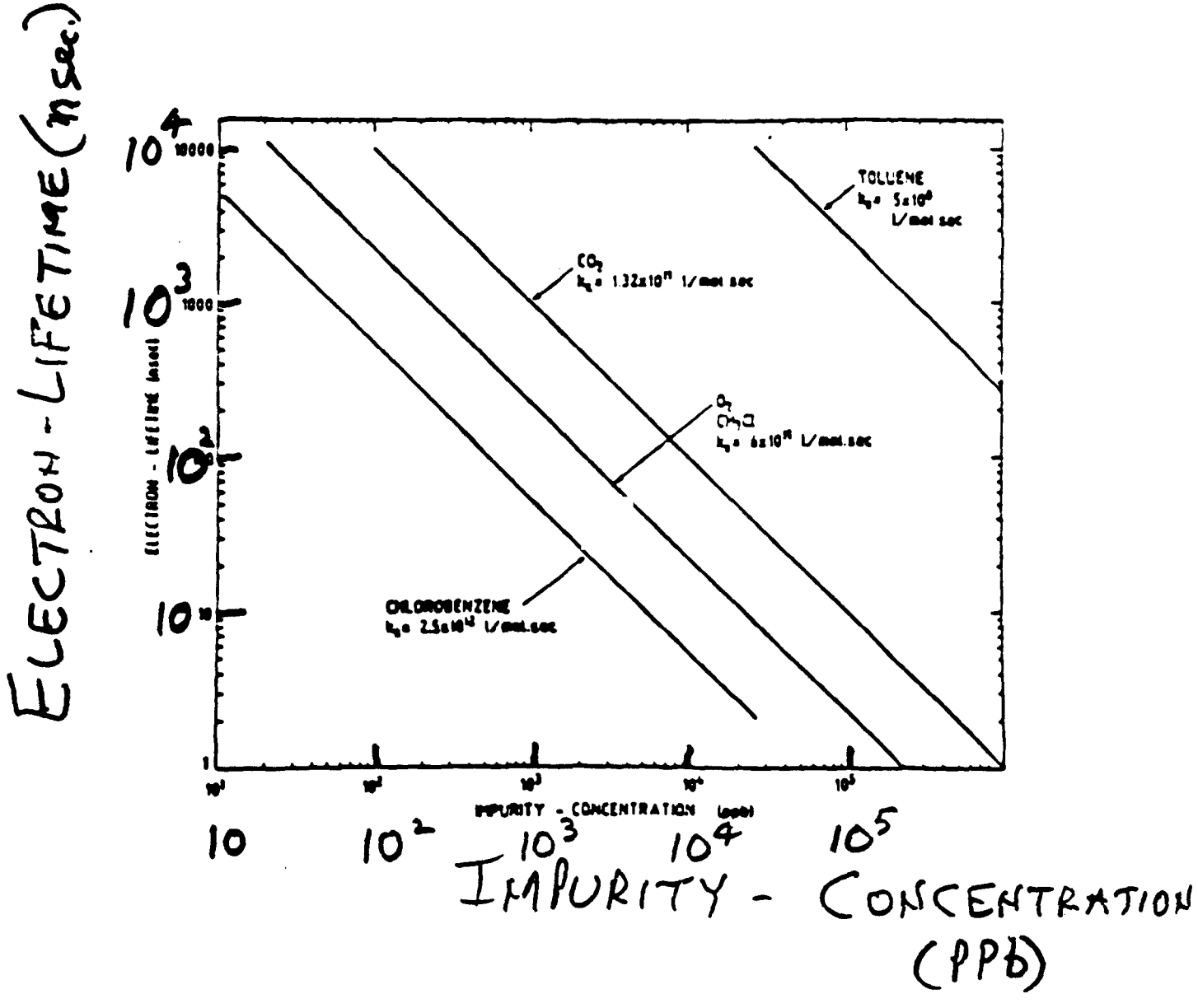

Fig. 6

UA-1

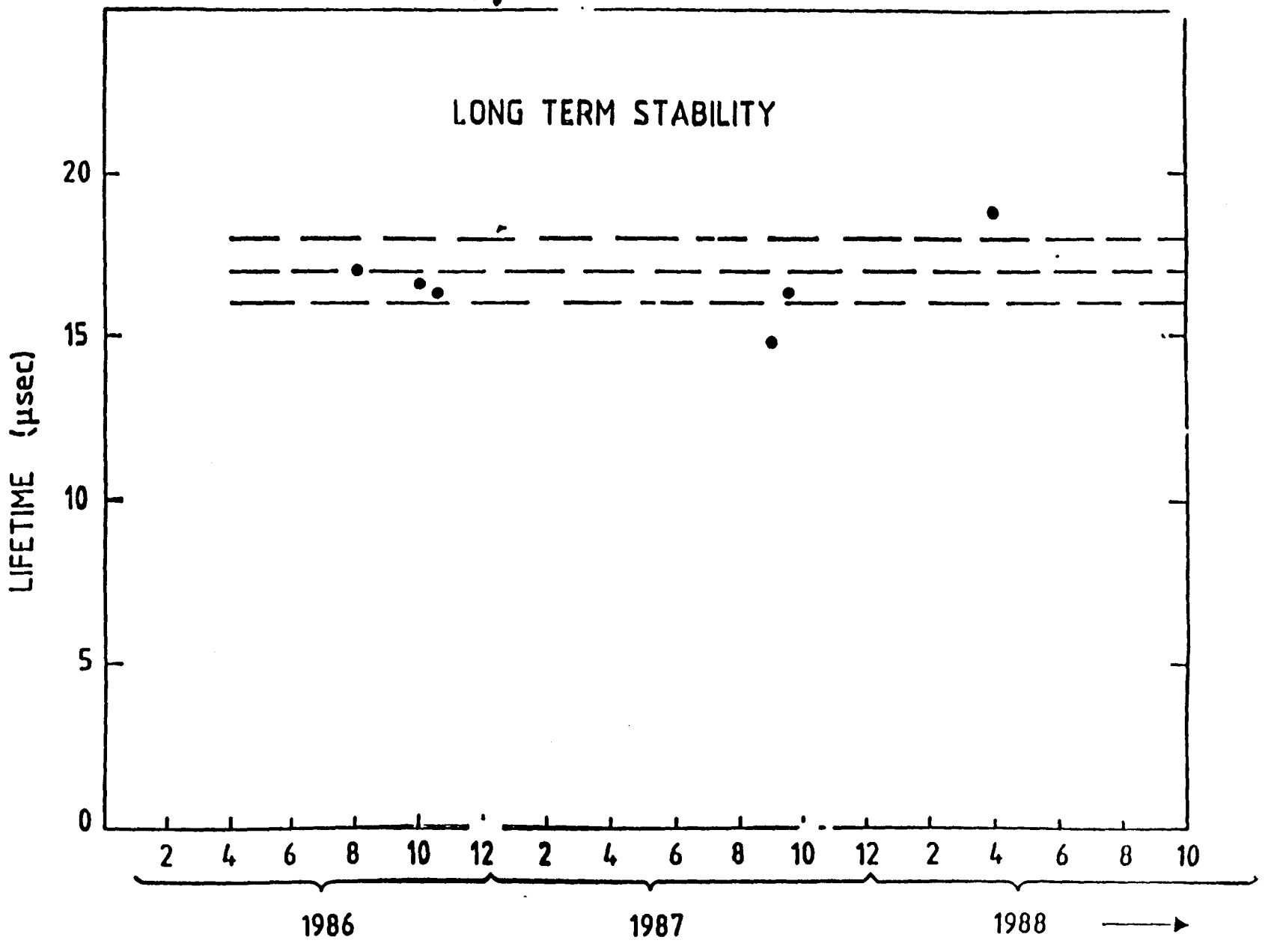

LIFETIME OF RECENT SAMPLES = 280μ.

ISOLATED COMPARTMENTS

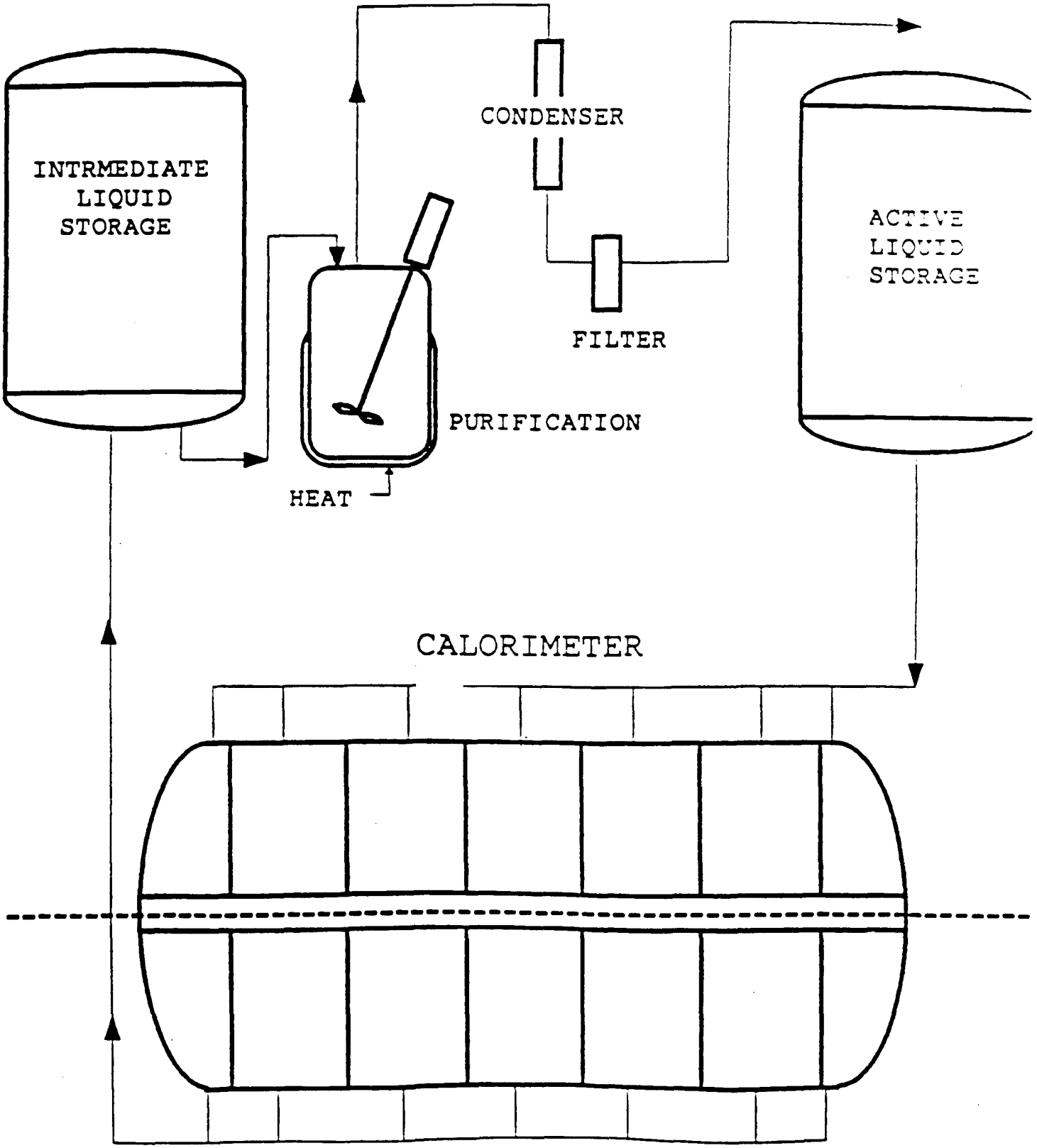

WILEY ORGANICS,INC

3/3/89

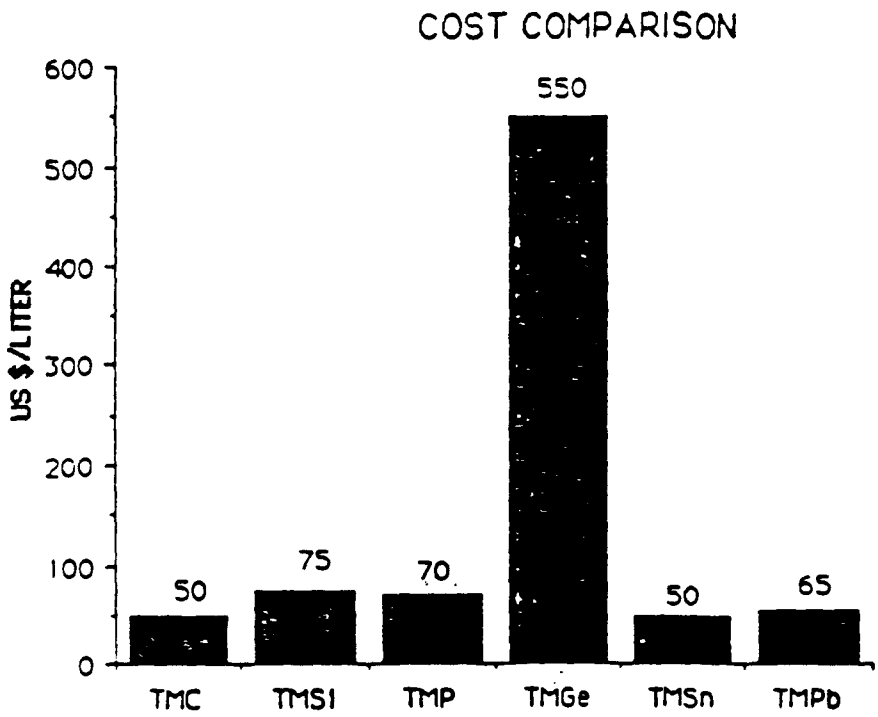

IF CAN GET TMS AS BYPRODUCT OF SILANE PRODUCTION, THEN PRICE ~$35/LITER

COST ESTIMATE
(PRIOR TO ENGINEERING)

1. 'Warm Liquid'	7,250,000
2. Piping, valves, etc.	700,000
3. Transport tanks (6 required)	600,000
4. Instrumentation & vacuum	350,000
5. Repurification system	500,000
6. Cleaning & startup	550,000
7. Contingencies	1,000,000
TOTAL	10,950,000

Notes:

1. 'Warm Liquid' cost was the average between TMP & TMSi
2. All piping 316 stainless, high vacuum rated & cleaned
3. Assume 20,000l transport tanks @ $100,000 each.
4. Pressure, temperature indicators, controllers, etc.
5. Skid mounted, no building is included.
6. Purification and de-gas loop only.

Typical peak yearly doses in Gy for operation of the SSC at the design luminosity of 10^{33}

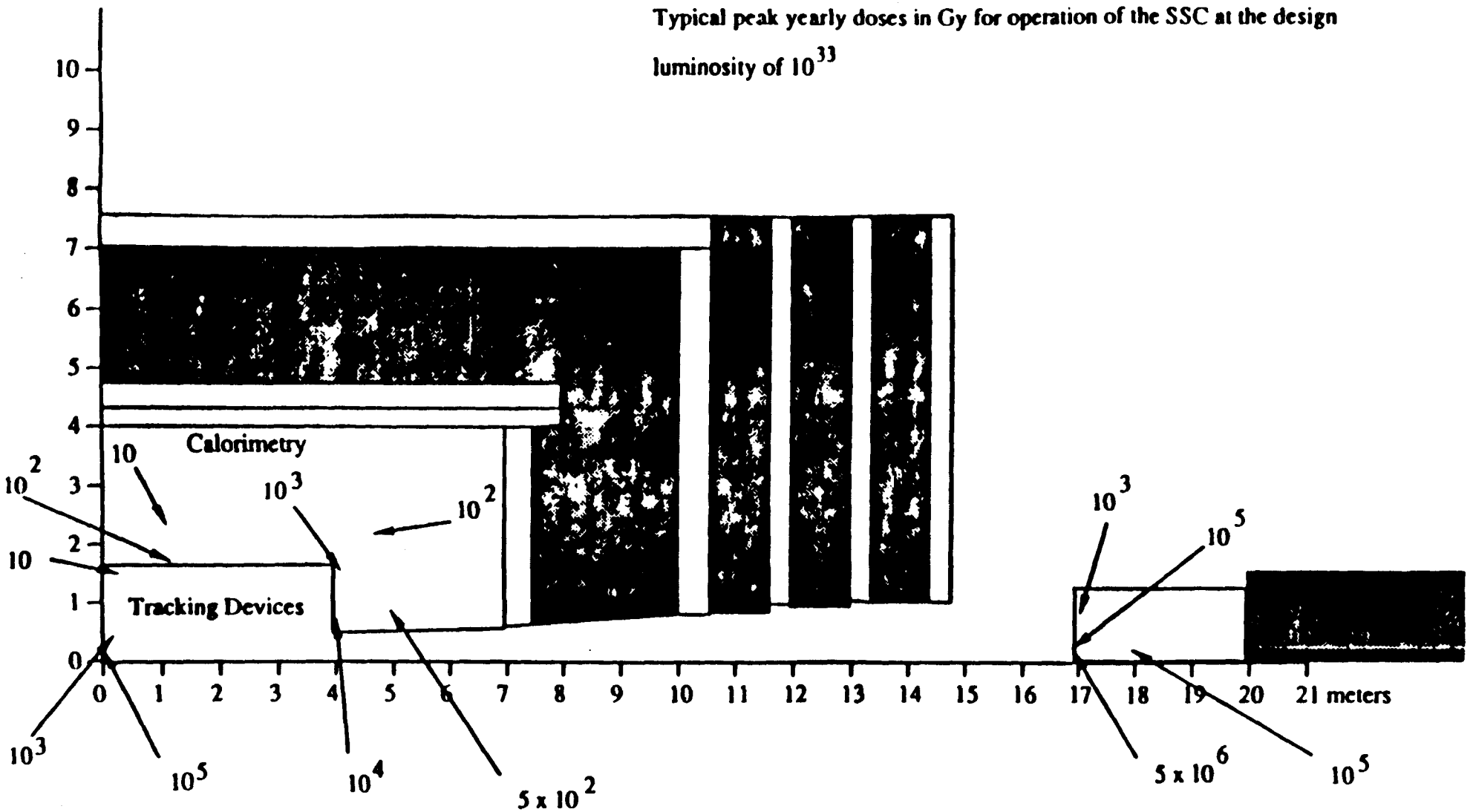

- LIFETIME, DRIFT VELOCITY (NEGLIGIBLE)
- PRESSURE, FOR 10^5 GY IN TMS, P = 4.4 ATM (H_2) + 1.7 ATM (

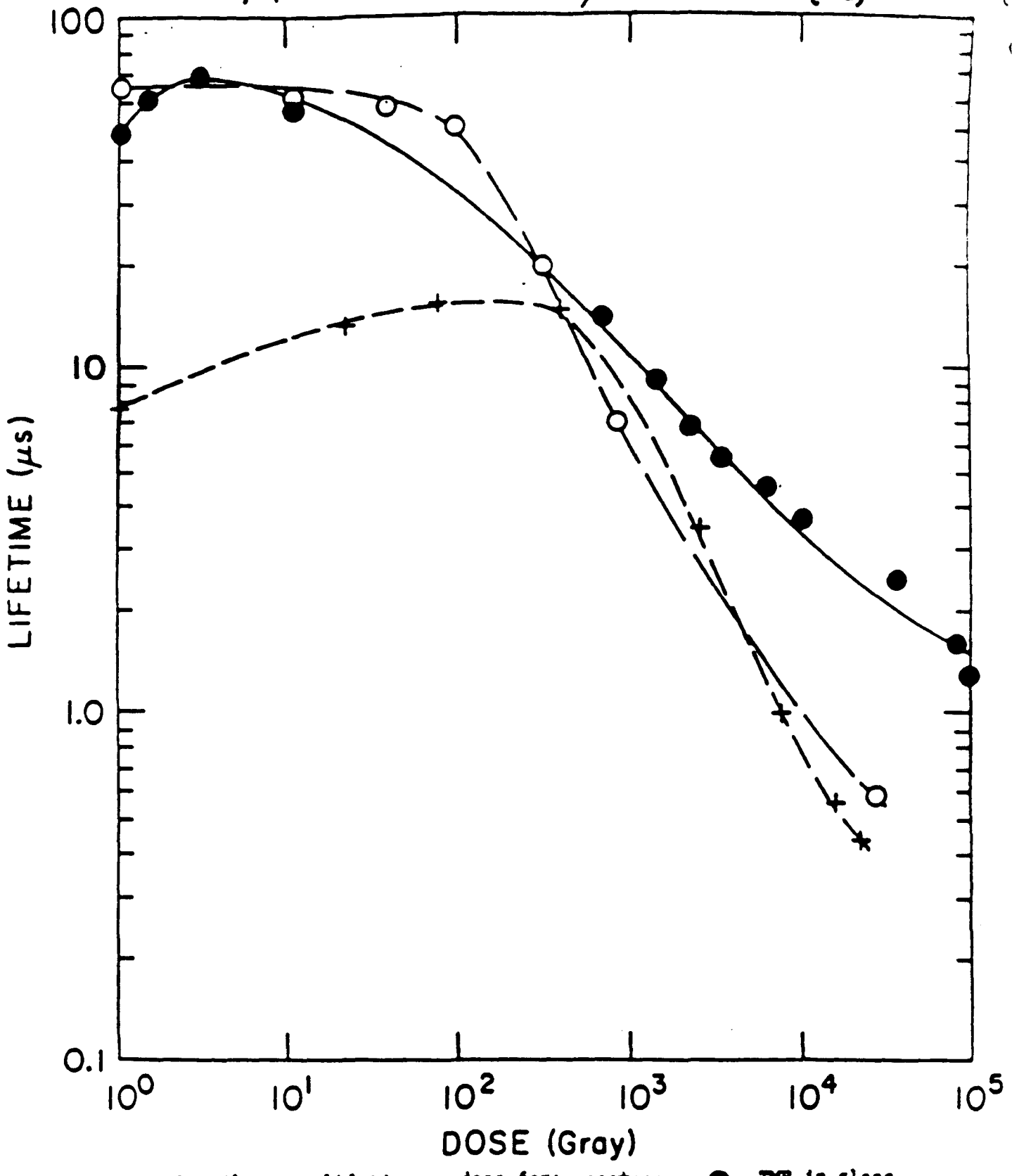

Figure 2. Electron lifetime vs dose for: ···+···, —●— TMP in glass cell with Pt electrodes; and for —○— 2,2,4-trimethylpentane in stainless steel cell.

CRITICAL ISSUES (continued)-

- *QUALITY OF PERFORMANCE*

  - Signal Response Speed, Signal/Noise, Pileup

    (SSC Constraints: Beam Crossing Every 16ns and an Average of 1.5 Interactions/Beam Crossing for 10^{33} Luminosity)

    Depends on Charge Collection Time (Drift Time) and Charge Transfer Time from Electrodes to Preamps

    (Drift Time depends on <u>GAP</u> and <u>ELECTRIC FIELD.</u>
    e.g. for UA-1: 1.25mm gap, E ~ 10 *kV/cm* ⇒
    t_d ~ 400ns for TMP
    ~ 120ns for TMS

    For WALIC: 1mm gap, E ~ 60 *kV* / cm
    t_d ~ 60ns for TMP
    ~30ns for TMS)

    Charge Transfer Time Depends on Cable Lengths and Impedances.
    Need small C_D. (⇒ EST)

  - Fast, Low-Noise Electronics (LARGE DYNAMIC & LOW POWER DISSIP. IN

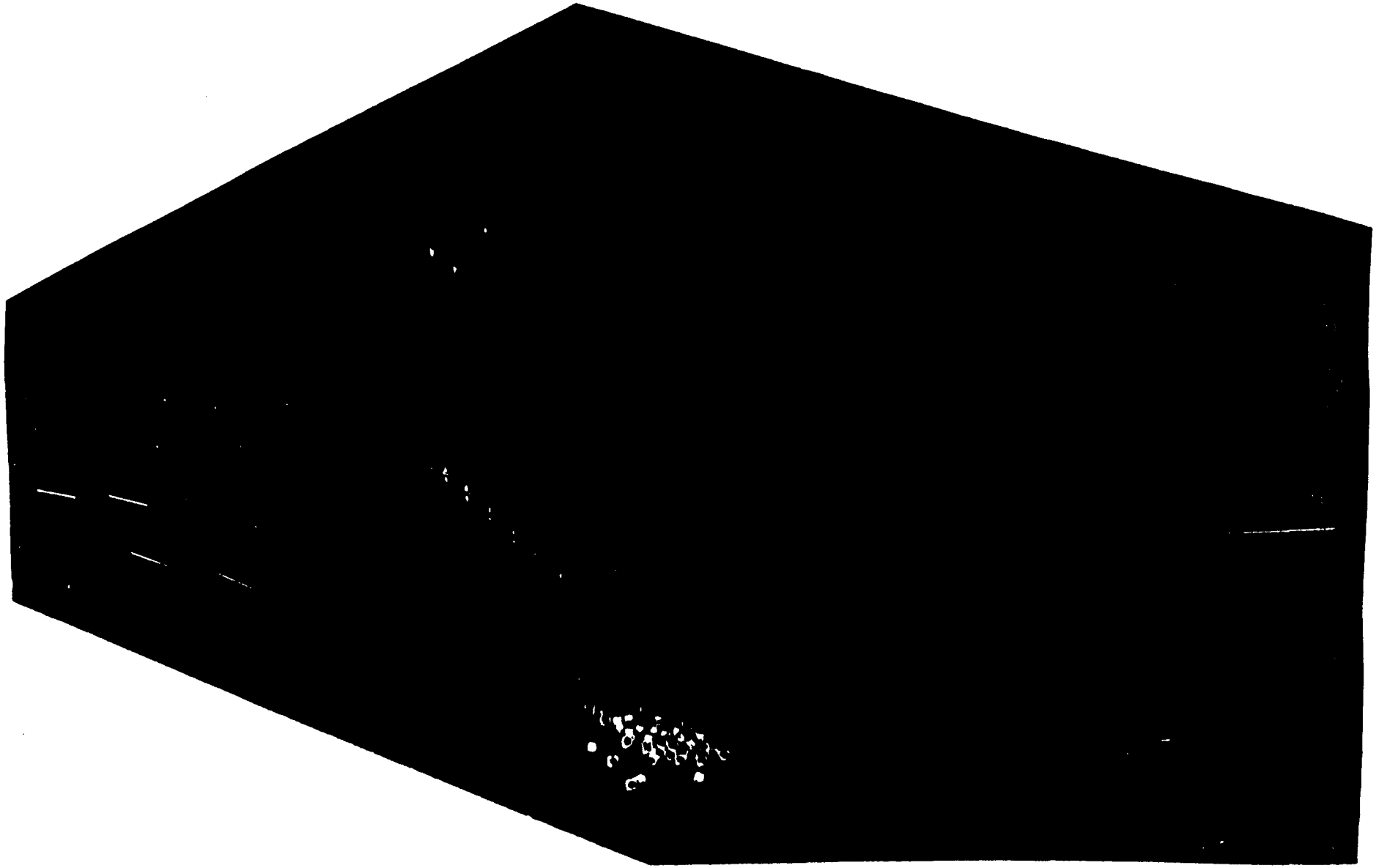

BBC 8506-4828

QUALITY OF PERFORMANCE (Continued)

Compensation (e/h = 1) without Uranium

- Hydrogenous
- Effect of Saturation on e/h (see Wigmans) $\frac{dI}{dx} \propto \frac{dE/dx}{1 + k_B \cdot dE/dx}$
- Saturation Measurements
  (WALIC, Ochsenbein/Holroyd, Engler)
- More Measurements needed, especially for ~ 1-2MeV protons:
  - From n-p scattering
  - From hadron showers with warm liquid calorimeter in hadron test beam (e.g., WALIC SETUP)
  - Other measurements, at CERN SC

Hermeticity

TWO EXTREMES:

(1) Small discrete boxes a la UA-1 (i.e. with liquid not in contact with absorber). More conservative construction but more dead spaces, H.V. feedthroughs, fill-tubes.

(2) [redacted] "swimming pool" type container, i.e. with absorbers immersed in liquids (e.g. Engler et. al.). Similar to liquid argon, but must exploit room temperature liquid properties to minimize dead space and signal cable length, yet keep electronics outside of liquid vol. Sensitive to materials compatibility, [redacted]

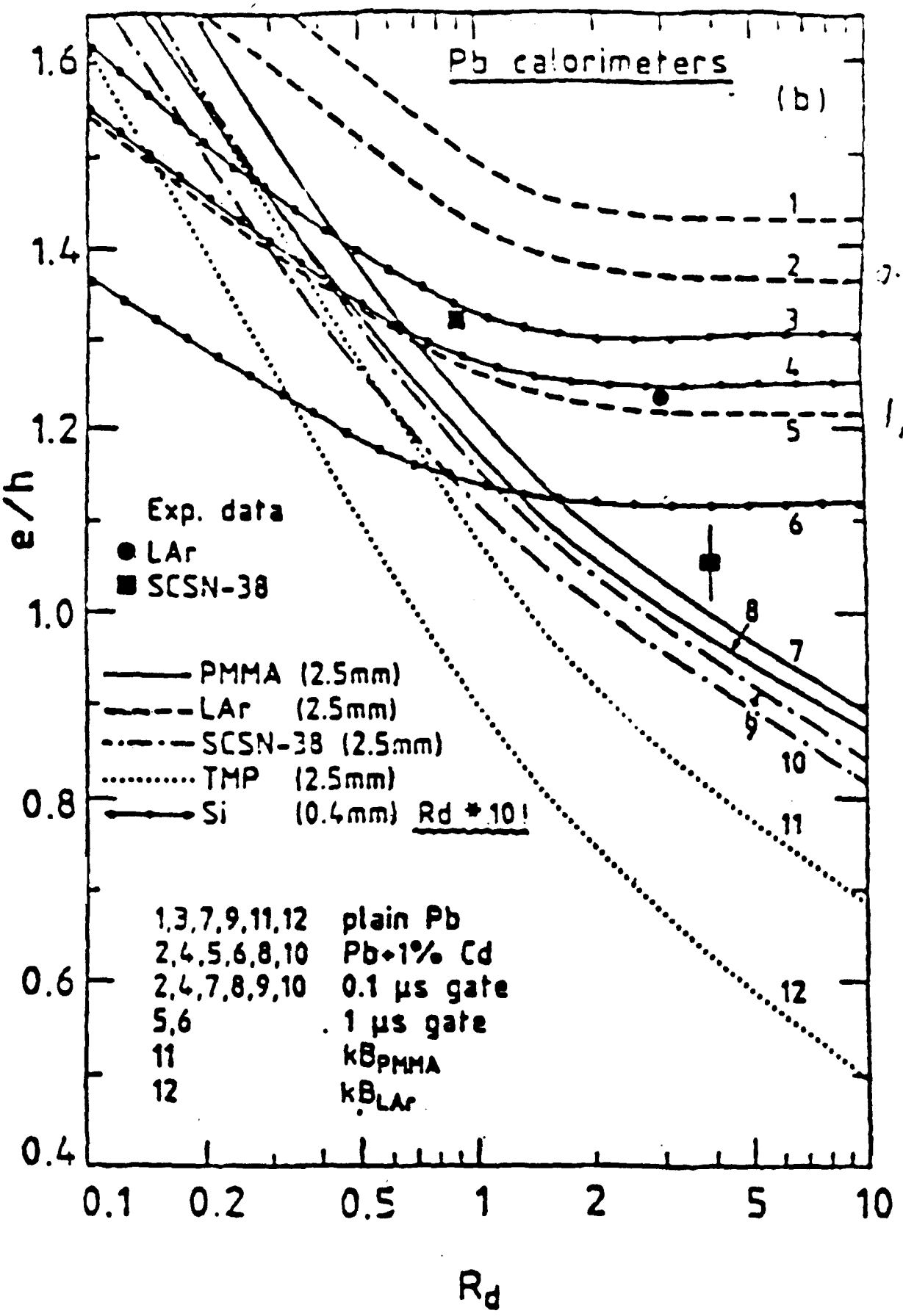
Pb calorimeters
(b)
e/h
Rd
Exp. data
LAr
SCSN-38
PMMA (2.5mm)
LAr (2.5mm)
SCSN-38 (2.5mm)
TMP (2.5mm)
Si (0.4mm) Rd * 10!
1,3,7,9,11,12 plain Pb
2,4,5,6,8,10 Pb+1% Cd
2,4,7,8,9,10 0.1 μs gate
5,6 1 μs gate
11 kBPMMA
12 kBLAr
1
2
3
4
5
6
7
8
9
10
11
12
1 μs

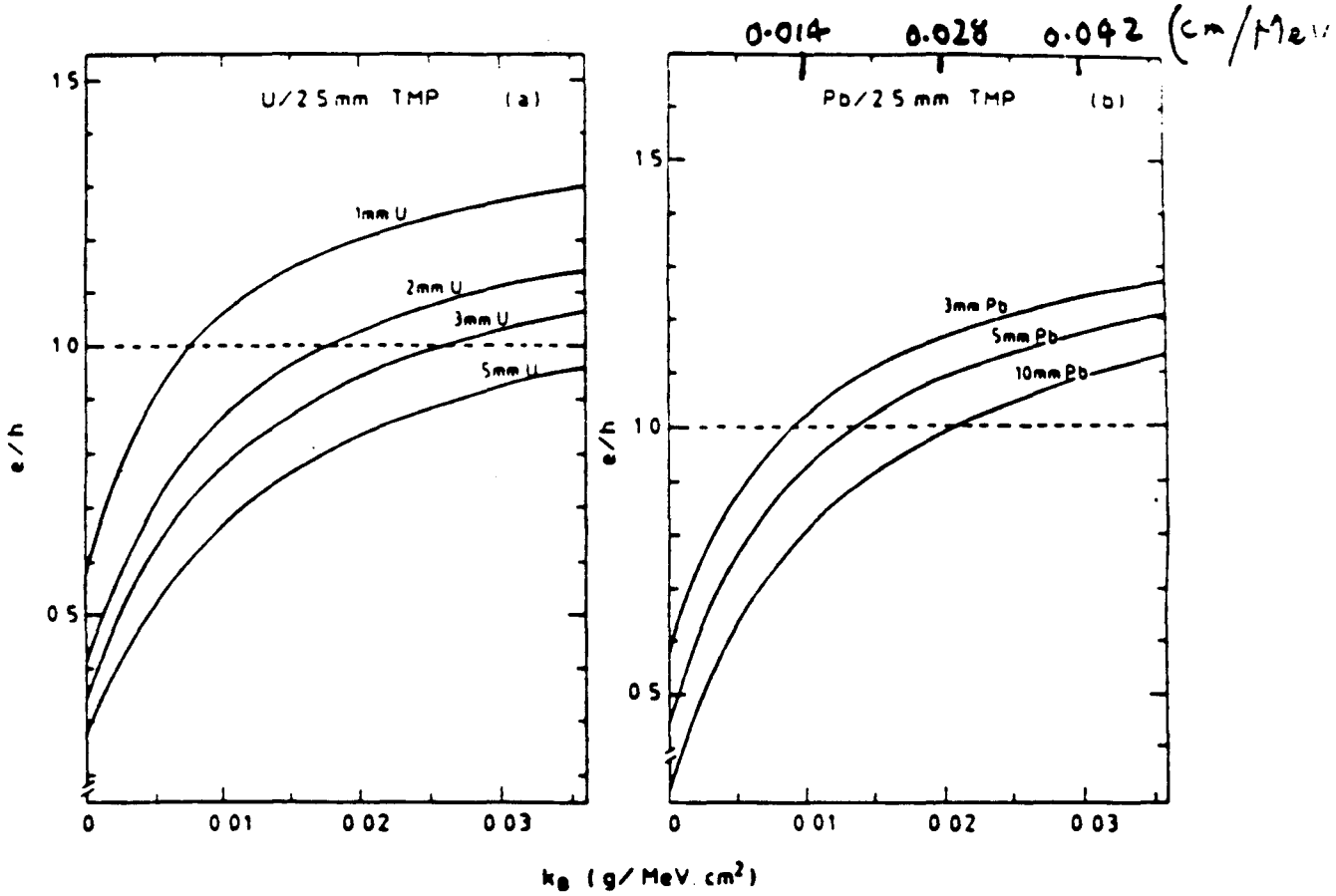

Figure 8

8. The e/h signal ratio as a function of Birk's constant k_B, for TMP calorimeters with uranium (a) or lead absorber (b). The liquid gaps are 2.5 mm wide.

WALIC COLLABORATION

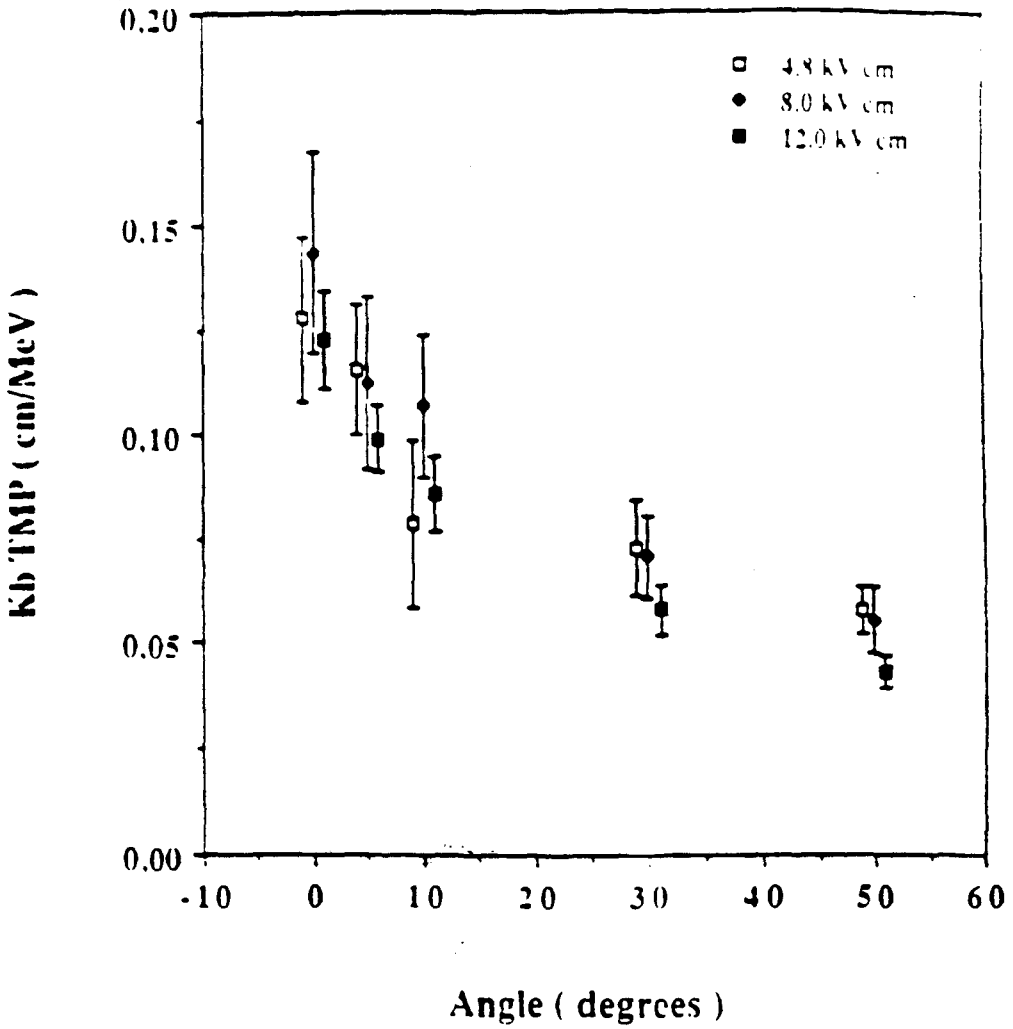

Figure 7: Kb in the TMP box as a function of the incident angle for 4.8, 8.0 and 12.0 kV/cm
The 4.8 (12.0) kV/cm data are shifted by -1 (+1) degree for better readability (errors are sta
).

WALIC

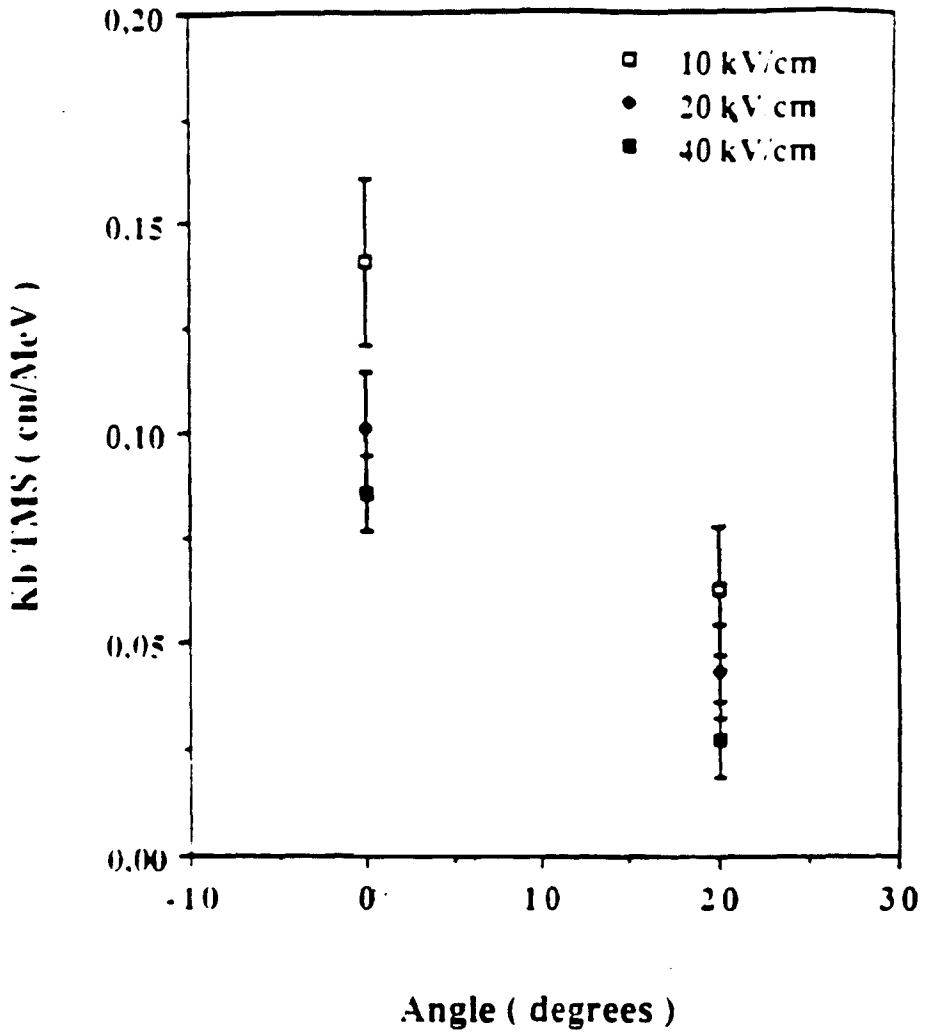

Figure 9 Kb in the TMS cell for 0 and 20° incident angle and 10, 20 and 40 kV/cm. The errors are only statistical (dominant compared to syst.. see text).

Saturation effects in TMS

(Ochsenbein)

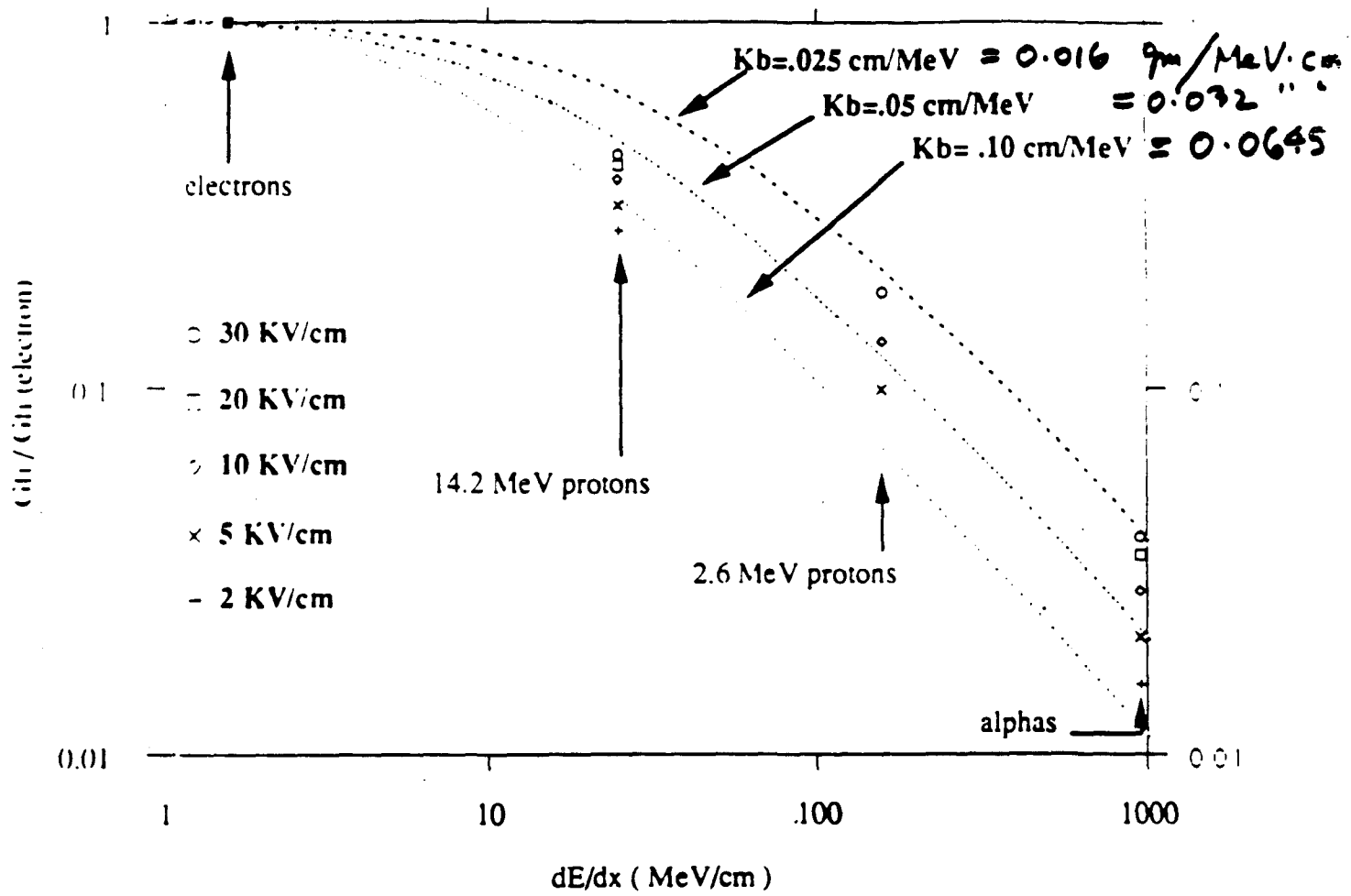

DUHM et al, NIM A277 (1989) 565

USING PROTONS 8 - 23 MeV + INTEGRATING OVER θ

FOR TMS, k_b = 0.0191 gm/MeV·cm²

CALORIMETER STACK-WALIC

to measure e/h vs sampling ratio for Pb-TMP and Fe-TMP

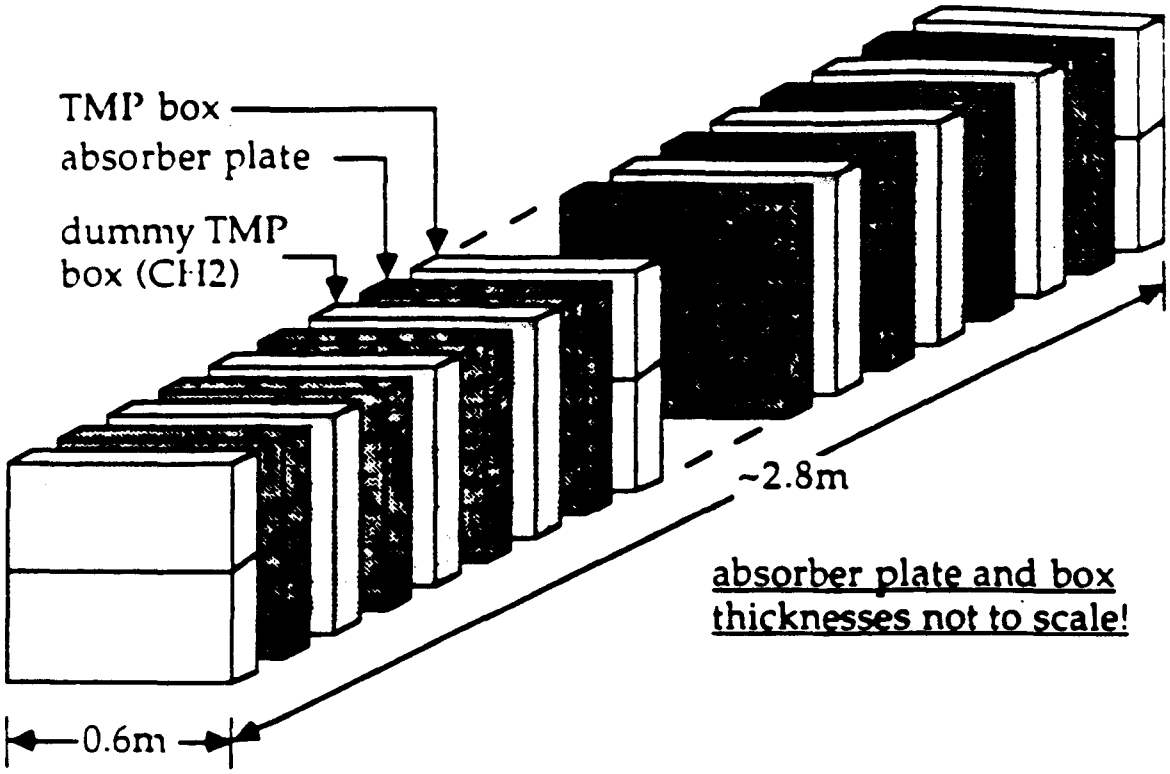

Example Stacks with Differing Hydrogen Concentrations

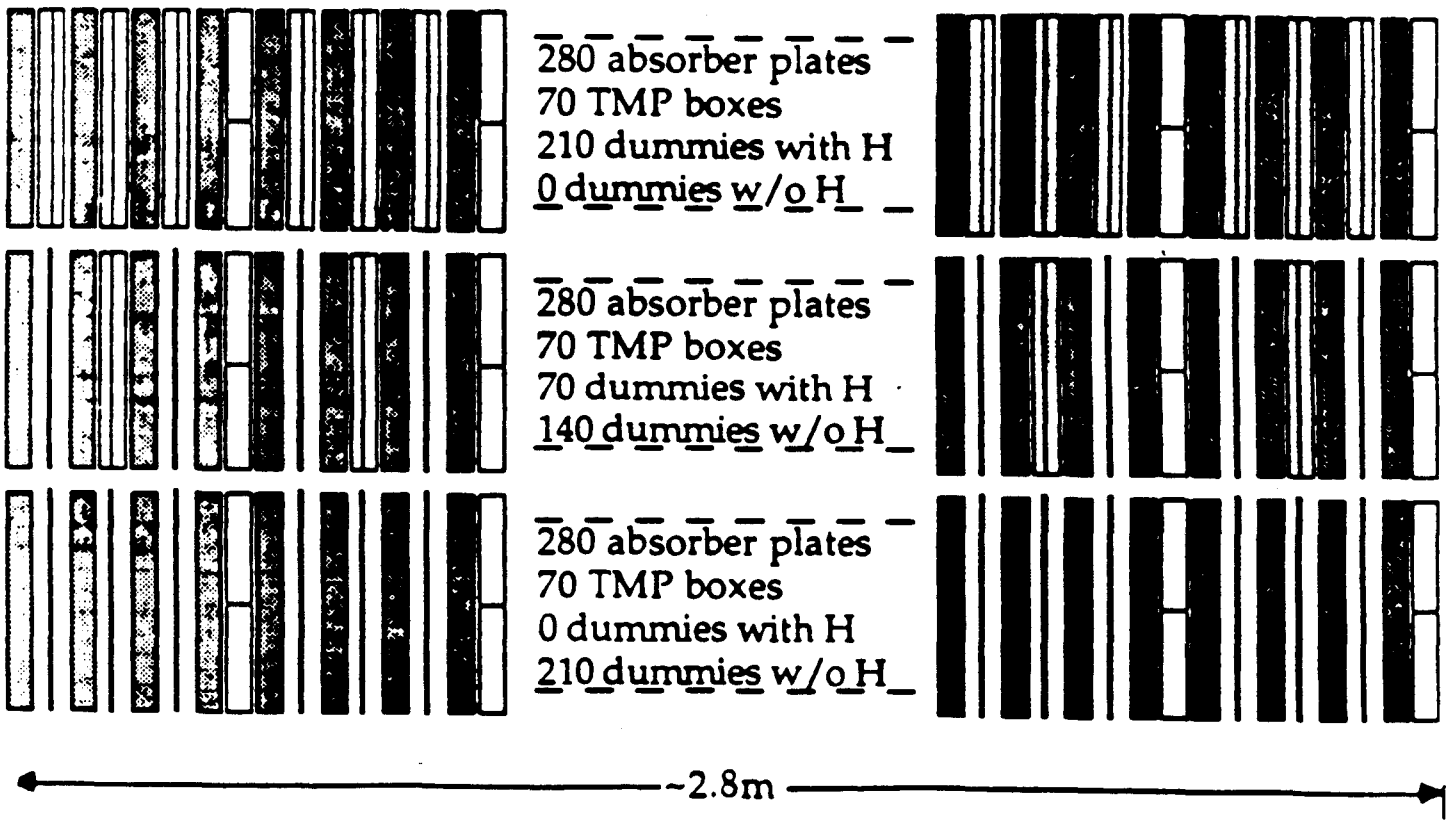

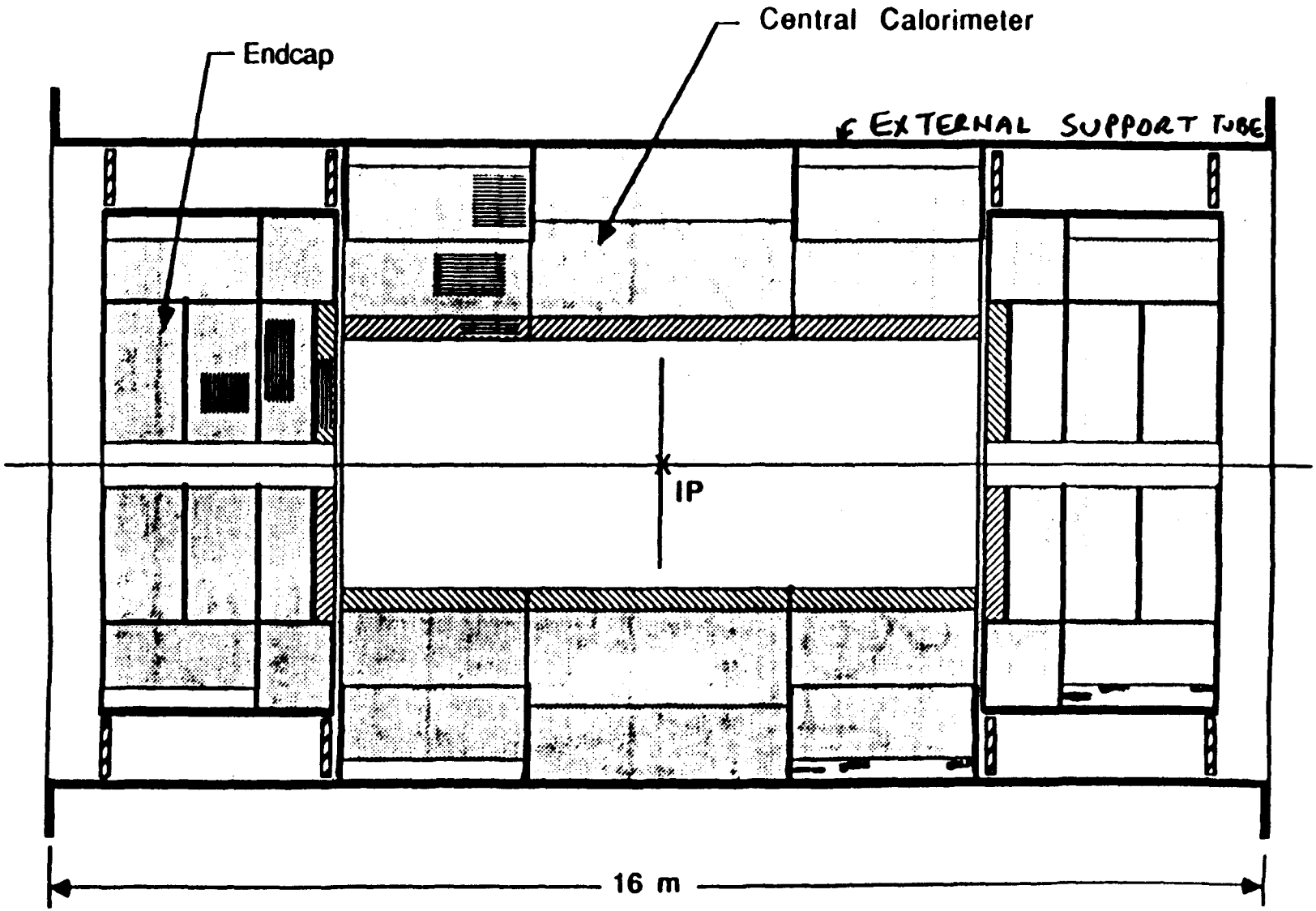

Warm Liquid Calorimeter R-Z Plane Cross Section

Plate Orientation

W R Edwards
6/22/89

WASHER

Barrel X-Sectior

WRE/WW/MS.DT
3/16/89

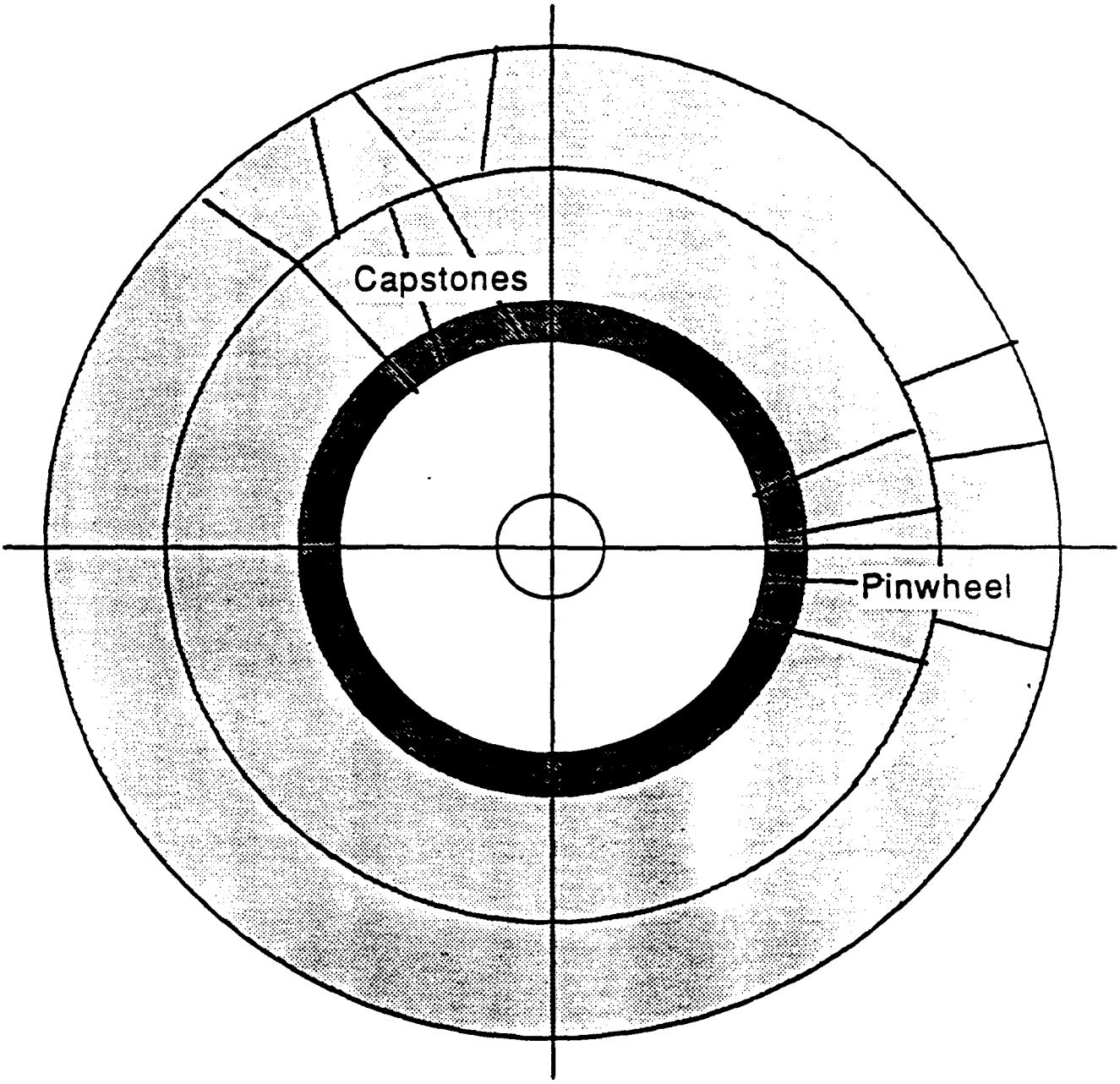

MODULE WEIGHT ~ 20 T

W R Edwards
6/22/89

Endcap Cross Sections:

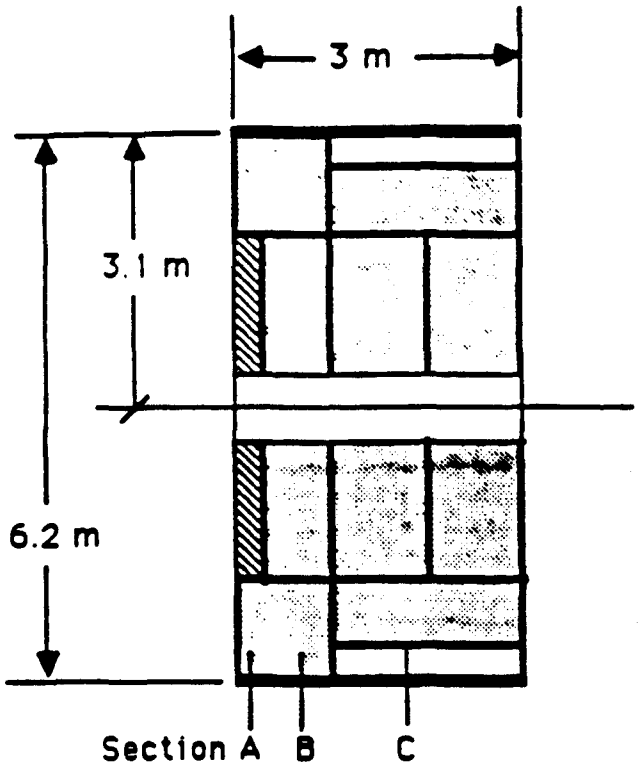

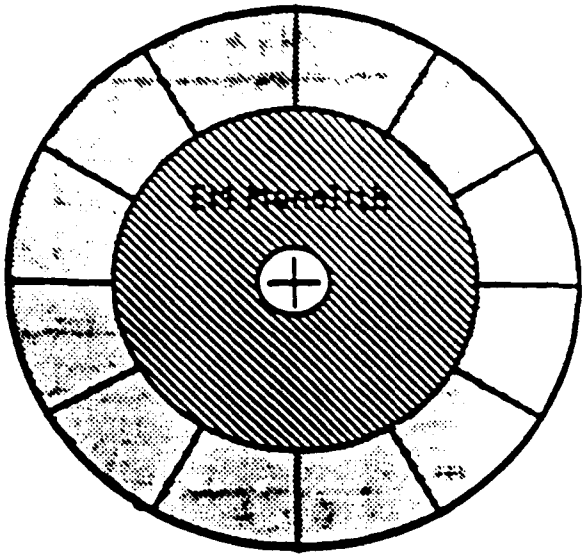

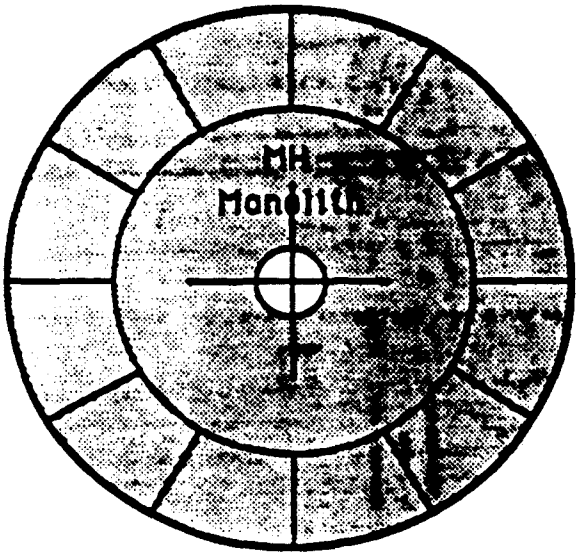

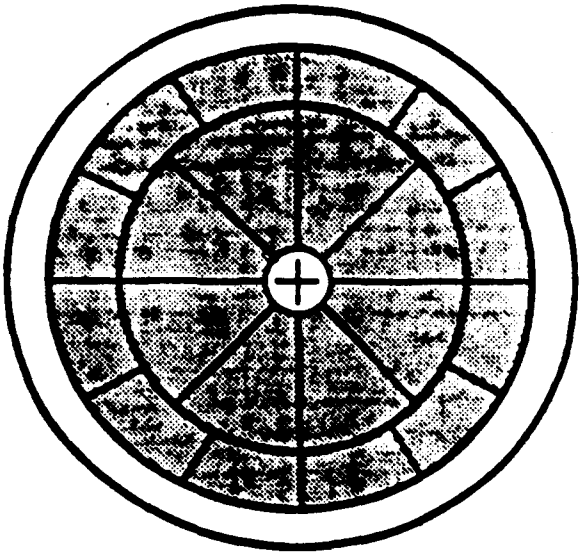

Section B

Section C

Electro-Magnetic Calorimeter

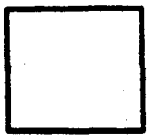

Hadronic Calorimeter

Empty Volume

Room Temp. Liquid Wedge

12 mm Lead - 2x1.5 mm TMP Gap

NOT TO SCA

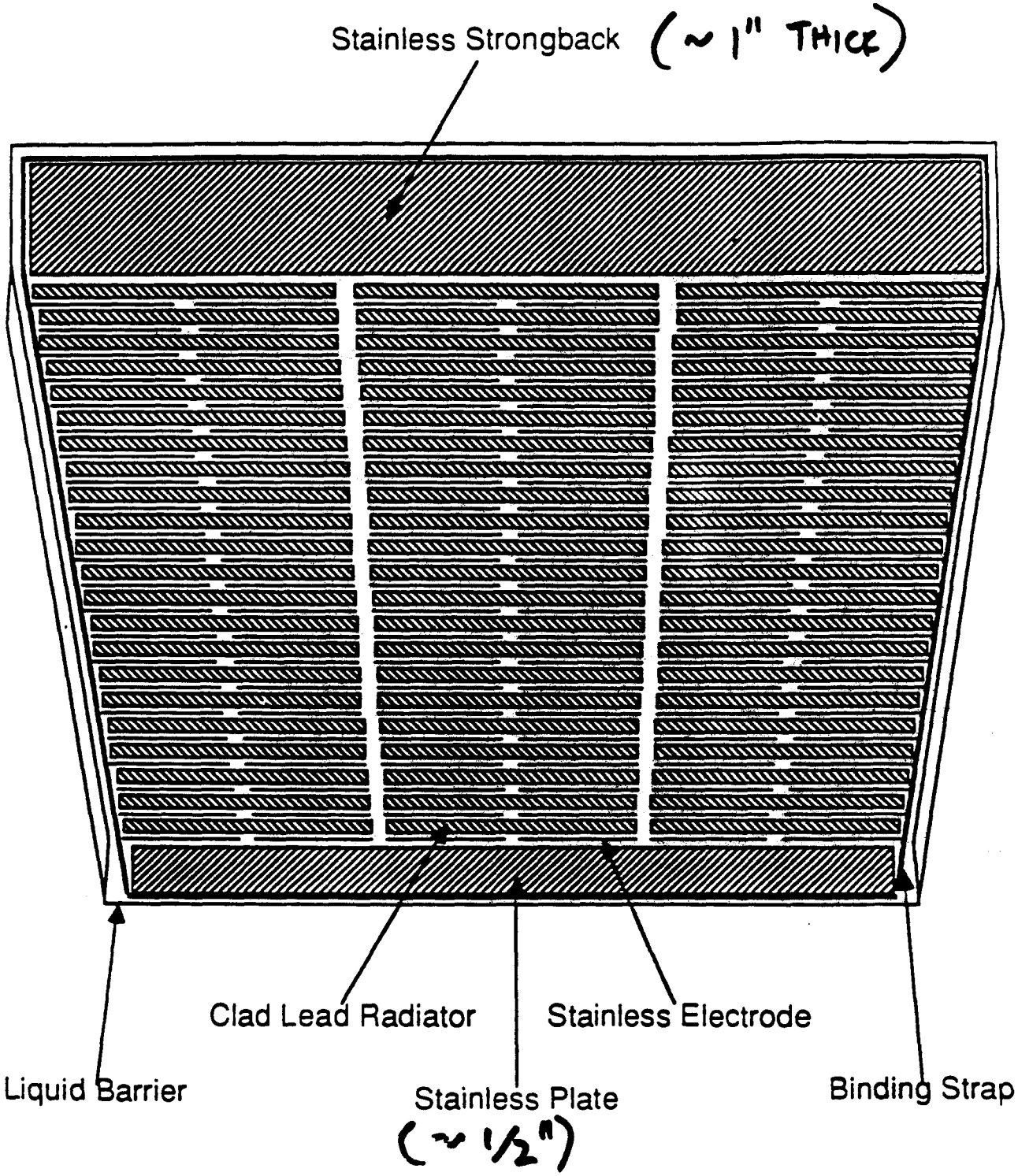

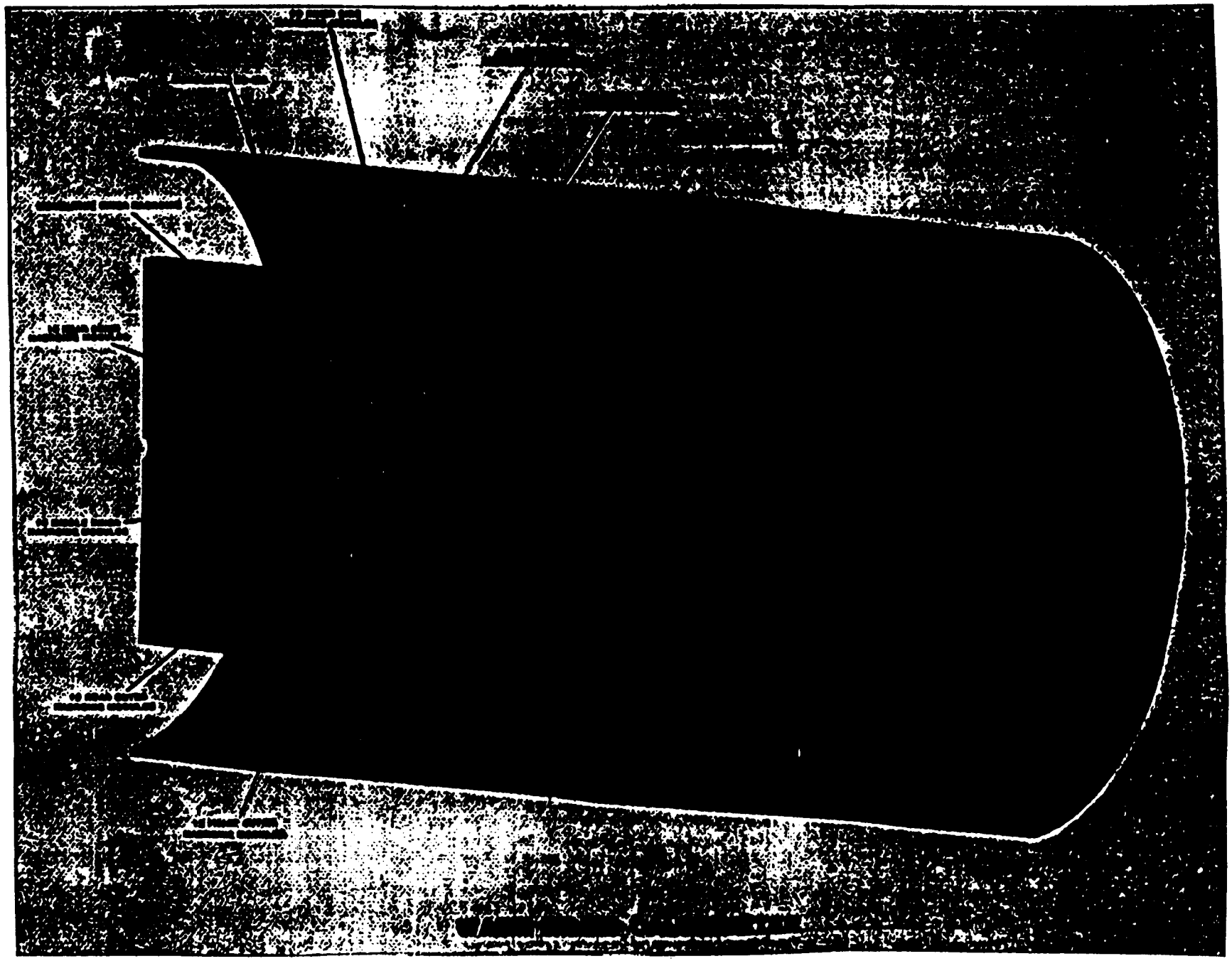

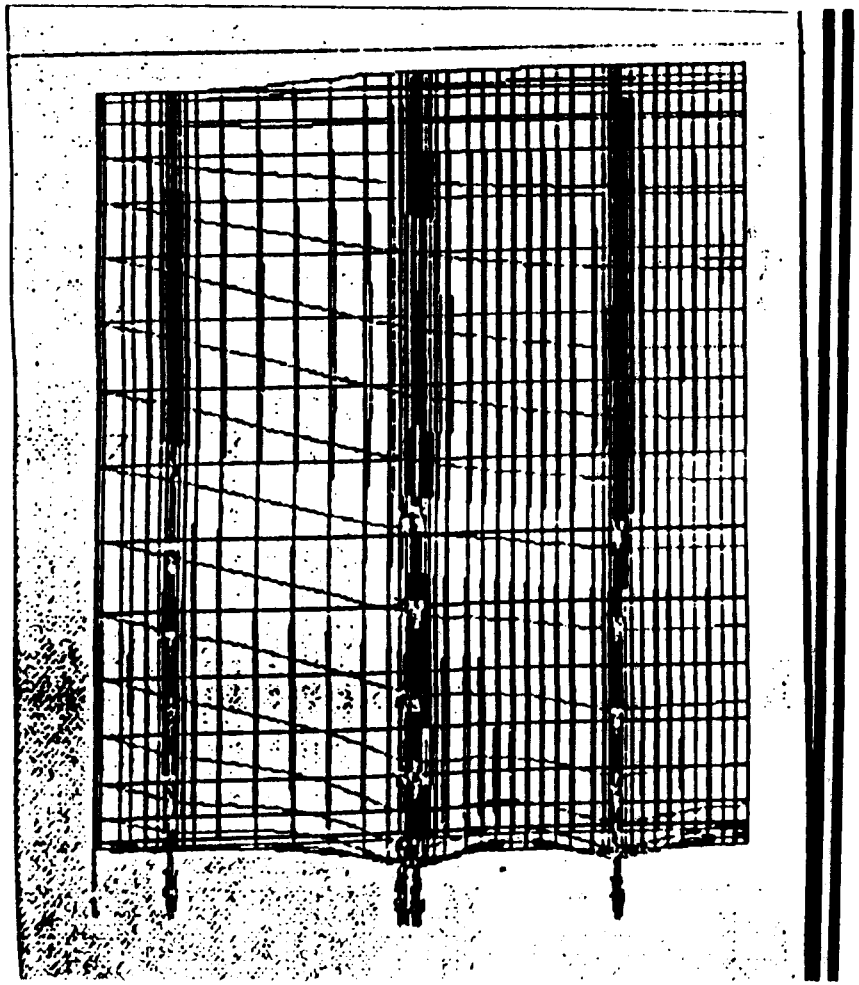

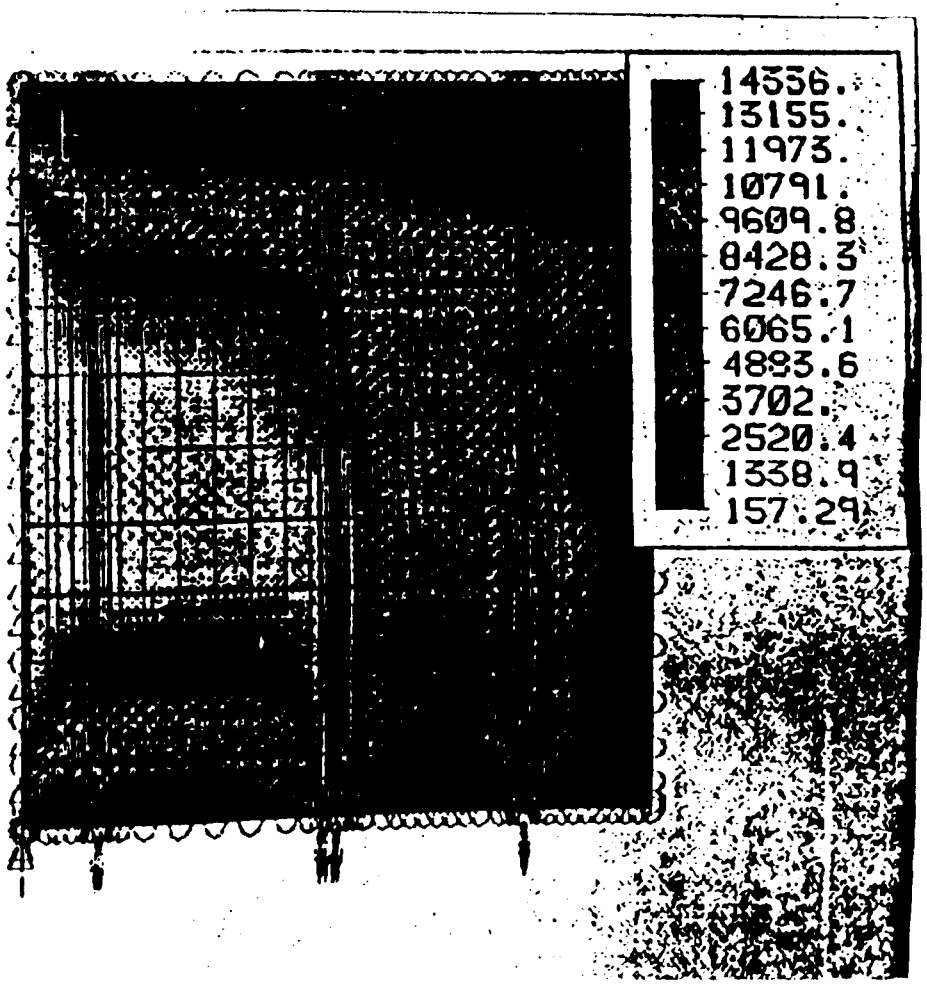
14536.
13155.
11973.
10791.
9609.8
8428.3
7246.7
6065.1
4883.6
3702.
2520.4
1338.9
157.29

SUMMARY

1. PRESENT DESIGN OF A FAST, HERMETIC, COMPENSATING CALORIMETER IS BASED ON CONSERVATIVE CHOICES

2. PROMISING PROSPECTS FOR EVEN BETTER PERFORMANCE CHARACTERISTICS IN THE NEAR FUTUR

3. WORKSHOP PROVIDED FERTILE GROUND FOR NEW IDEAS

AS A RELATIVELY NEW TECHNOLOGY, MORE R+D NEEDED VERY SOON:

- HIGH VOLTAGE
- MATERIALS COMPATIBILITY
- PROPERTIES OF VARIOUS ROOM TEMP. LIQUID
- FASTER READOUT
- ENGINEERING STUDIES
- TEST BEAM STUDIES OF LARGE PROTOTYP

D Bin

Scintillation Calorimetry

Options : Fiber, Plate, ---

Advantages:
- Fast
- Low Noise
- Compensating
- Good Resolution
- Constructable (Fiber?)

Issues:
- ☆ Radiation Survivability
- Calibration and Monitoring
- Uniformity of Response
- Coil Placement
- Schedule and Cost

TIMING - IMPORTANT

TIME STRUCTURE
CALORIMETER SIGNALS

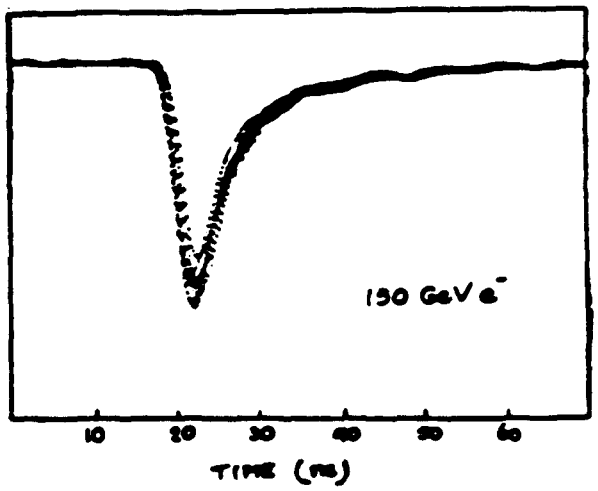

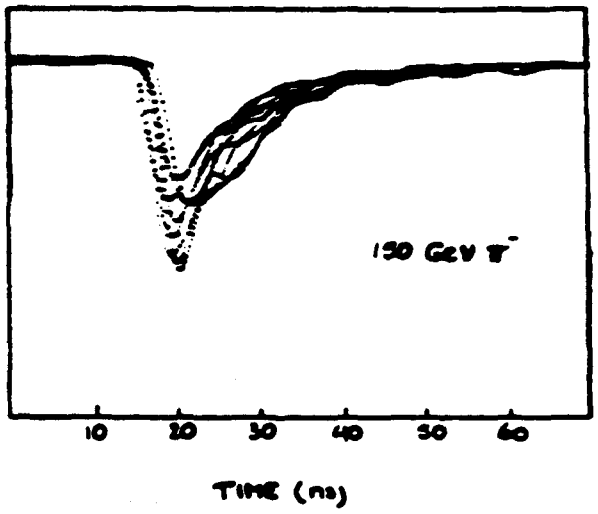

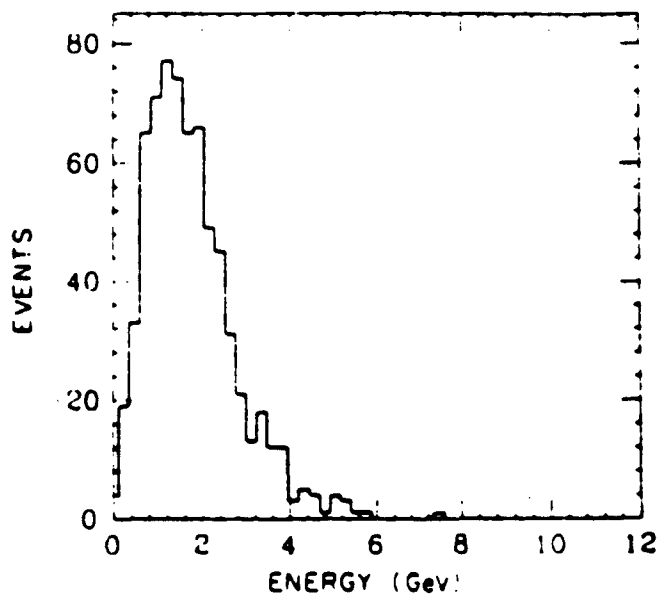

Fig. 11. Muon spectrum for an endwall tower. The peak corresponds to about 2 GeV energy deposition for a hadronic cascade.

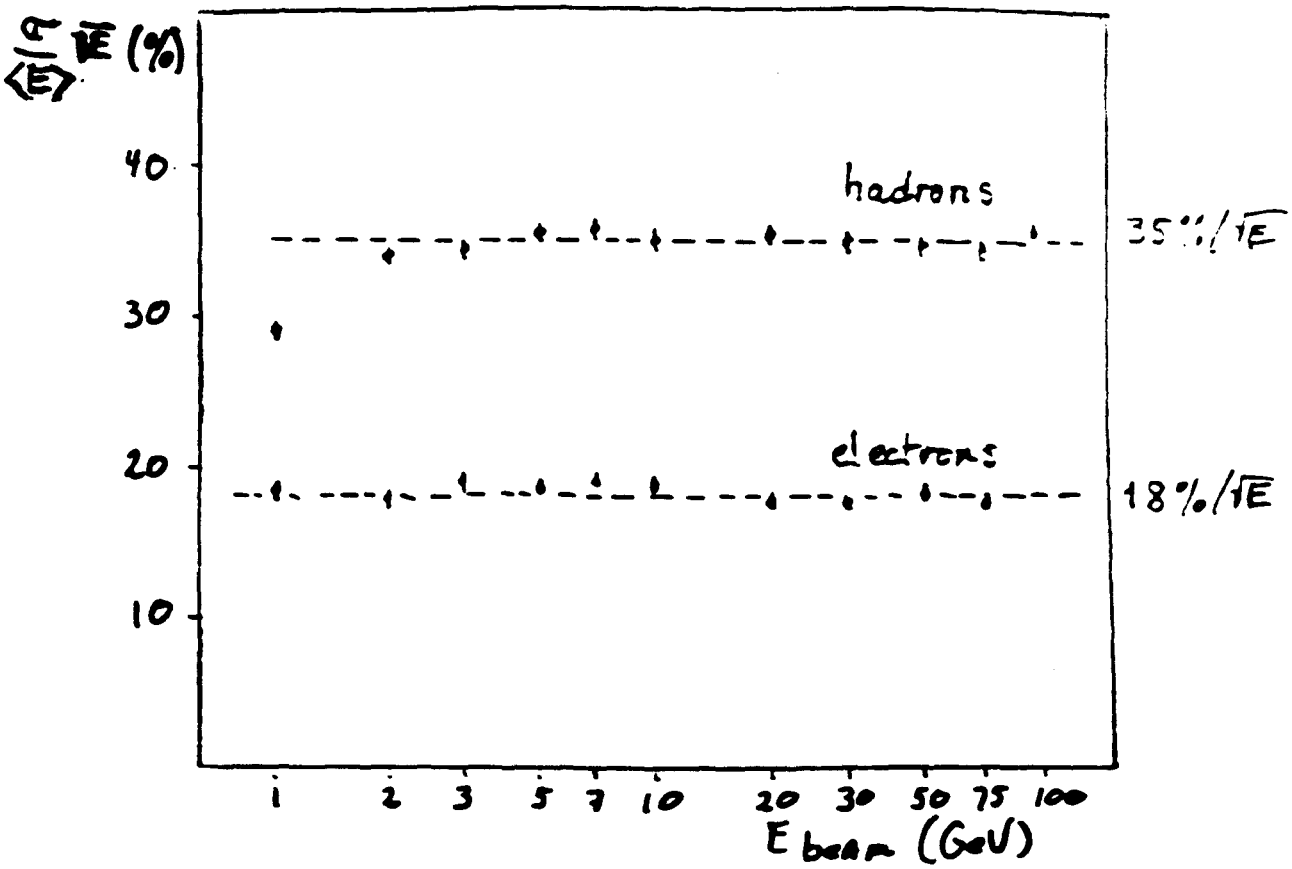
$\frac{\sigma}{\langle E \rangle}$ (%)
40
30
20
10
hadrons
35%/√E
electrons
18%/√E
1
2
3
5
7
10
20
30
50
75
100
E beam (GeV)

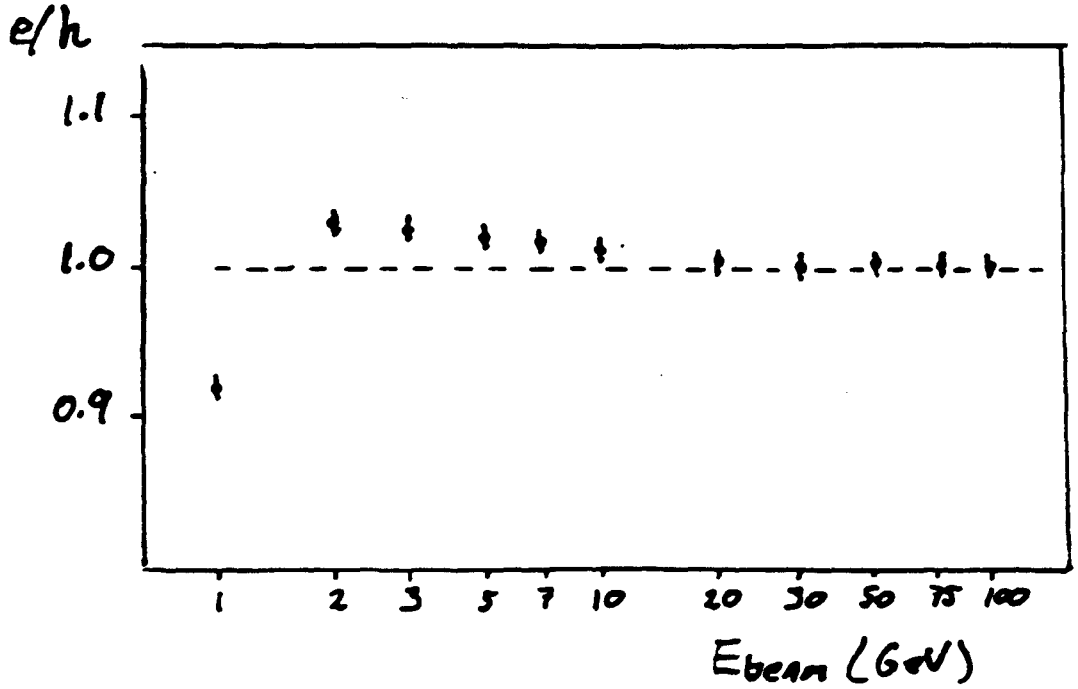
e/h
1.1
1.0
0.9
1
2
3
5
7
10
20
30
50
75
100
Ebeam (GeV)

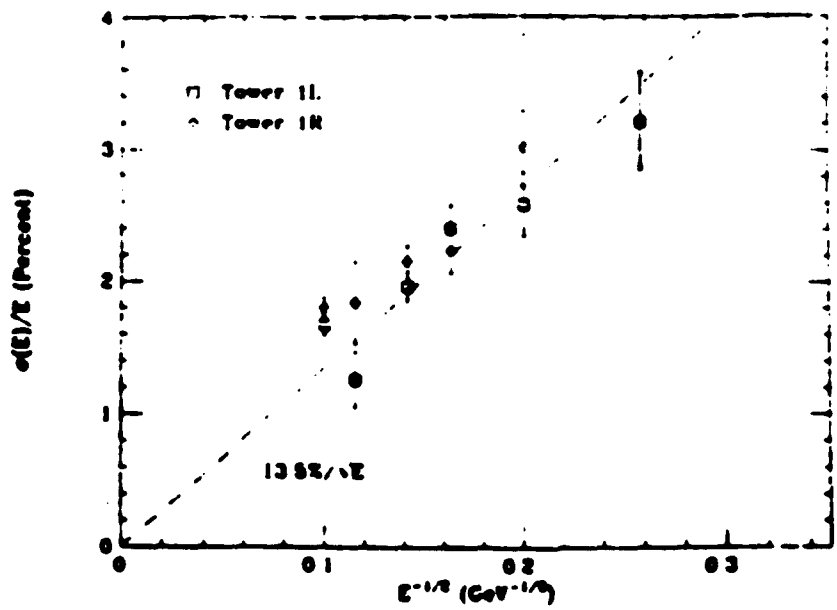

Fig. 4. Central electromagnetic calorimeter energy resolution as a function of the energy for both phototubes of tower 1 of a typical calorimeter module. The large errors at higher values of $E^{-1/2}$ are due to lower beamline delivery of low energy electrons.

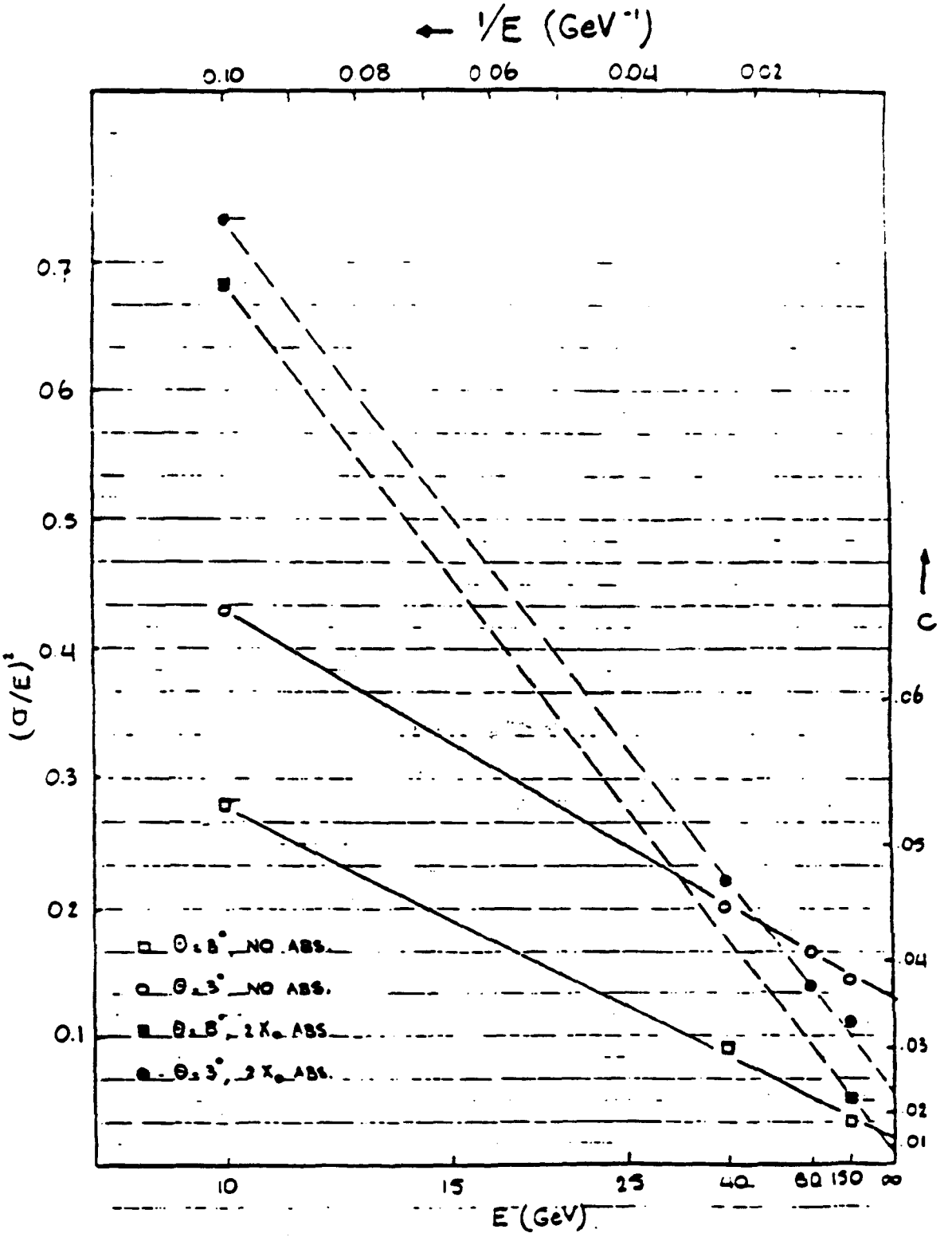
← 1/E (GeV⁻¹)
0.10
0.08
0.06
0.04
0.02
0.7
0.6
0.5
0.4
0.3
0.2
0.1
(σ/E)²
C
.06
.05
.04
.03
.02
.01
10
15
25
40
60
150
∞
E (GeV)
θ = 8°, NO ABS.
θ = 3°, NO ABS.
θ = 8°, 2 X₀ ABS.
θ = 3°, 2 X₀ ABS.

Figure 12

(c) Dose at electromagnetic and hadronic cascad maximum

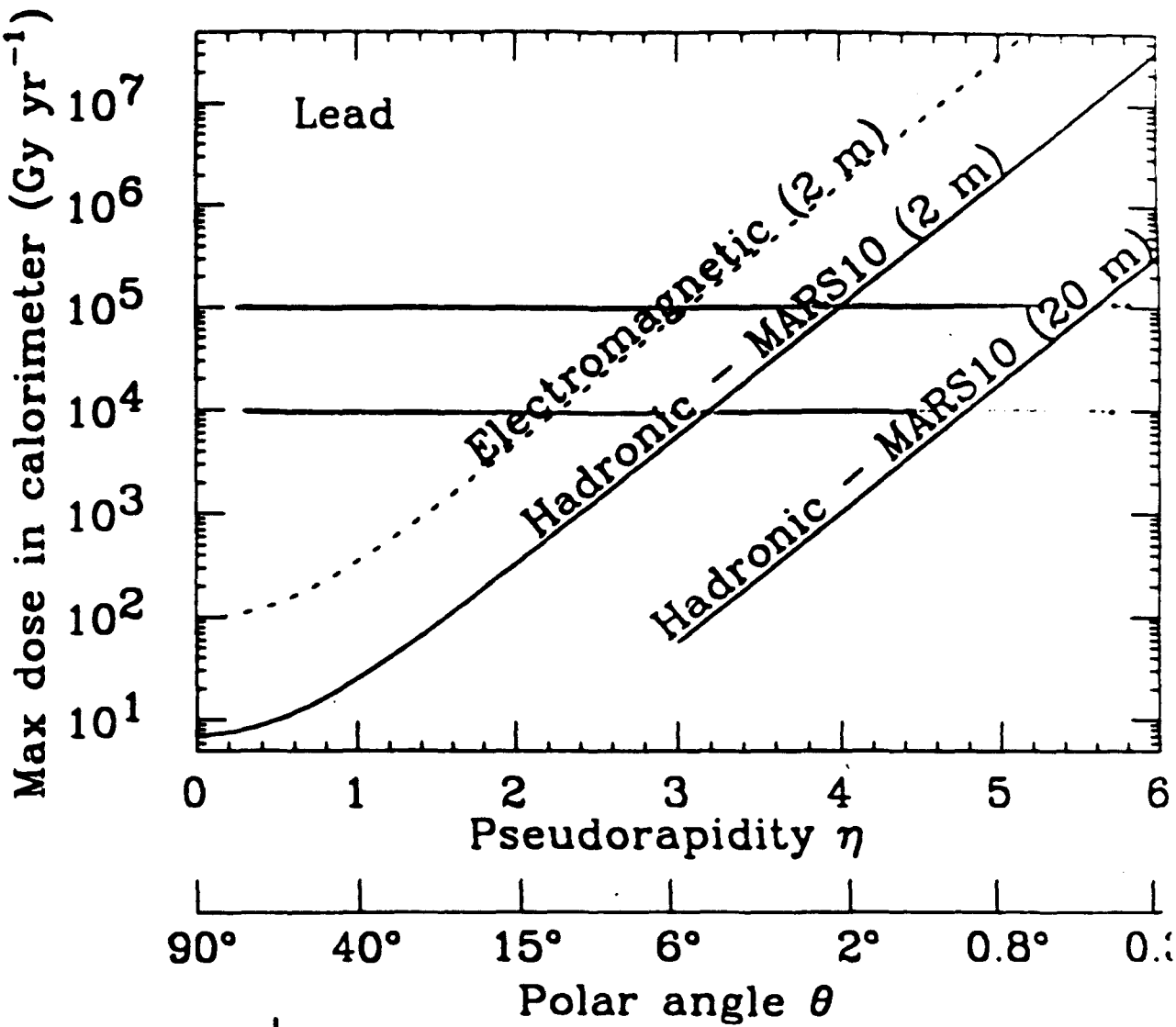

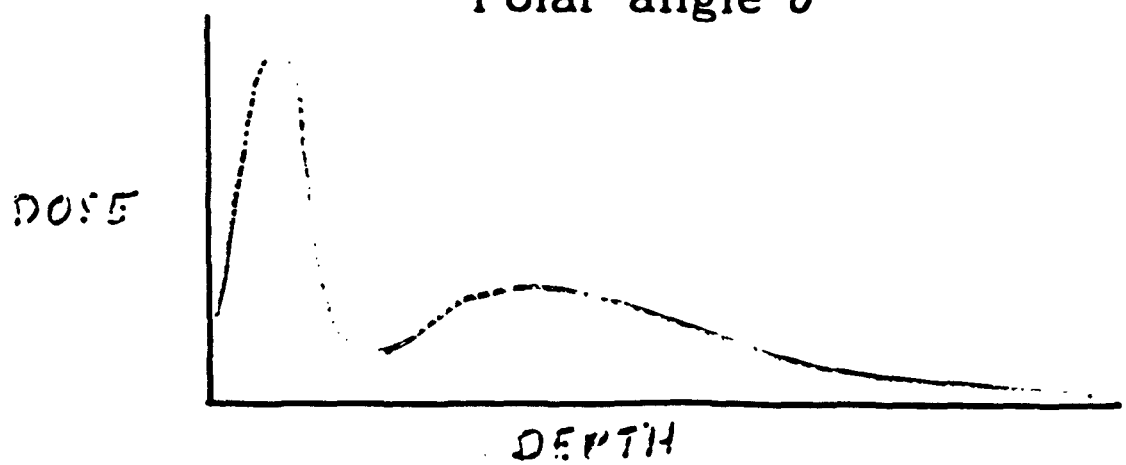

RPM 11 May 1959
D. E. Groom G/π 3

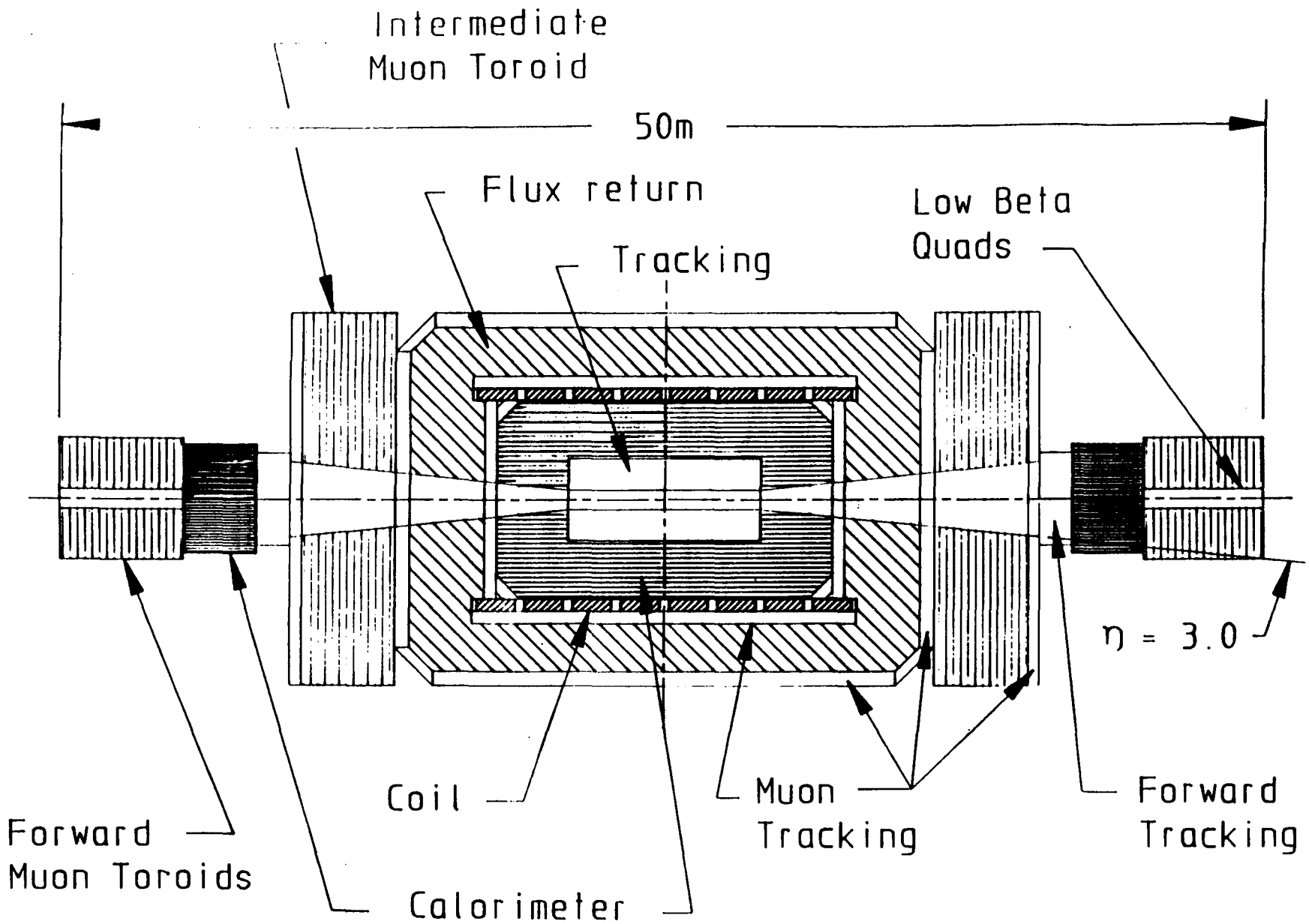

Large Soleno d Detector

GROOM lg ec etr1
GROOM/FONG ay89

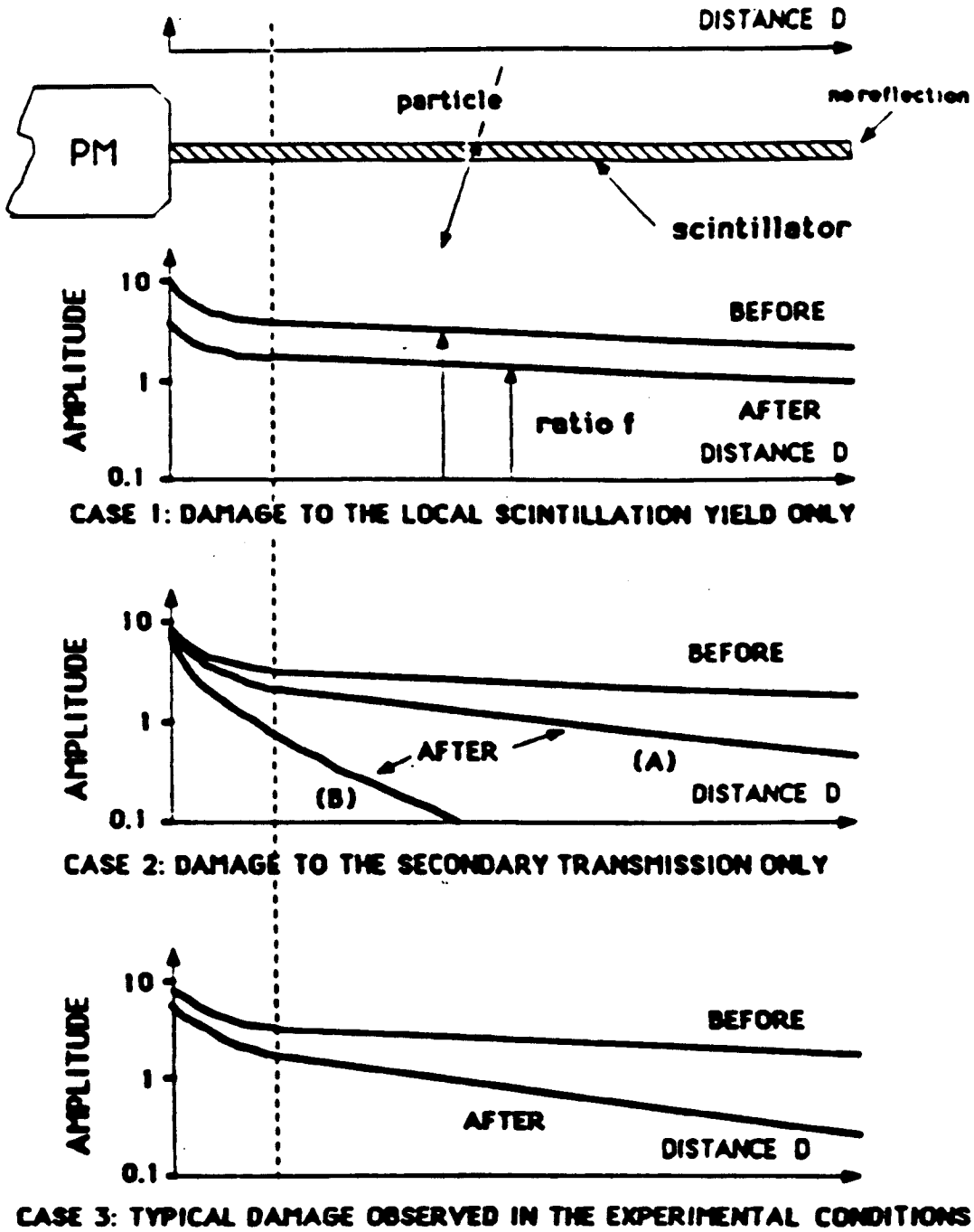

Fig. 2. Radiation damage effects on a scintillation output from a long scintillator, under the assumption of damage to the local scintillation yield only (case 1), damage only to the secondary transmission for two different levels of damage (A) and (B) (case 2), and finally due to a mixture of the two effects (case 3).

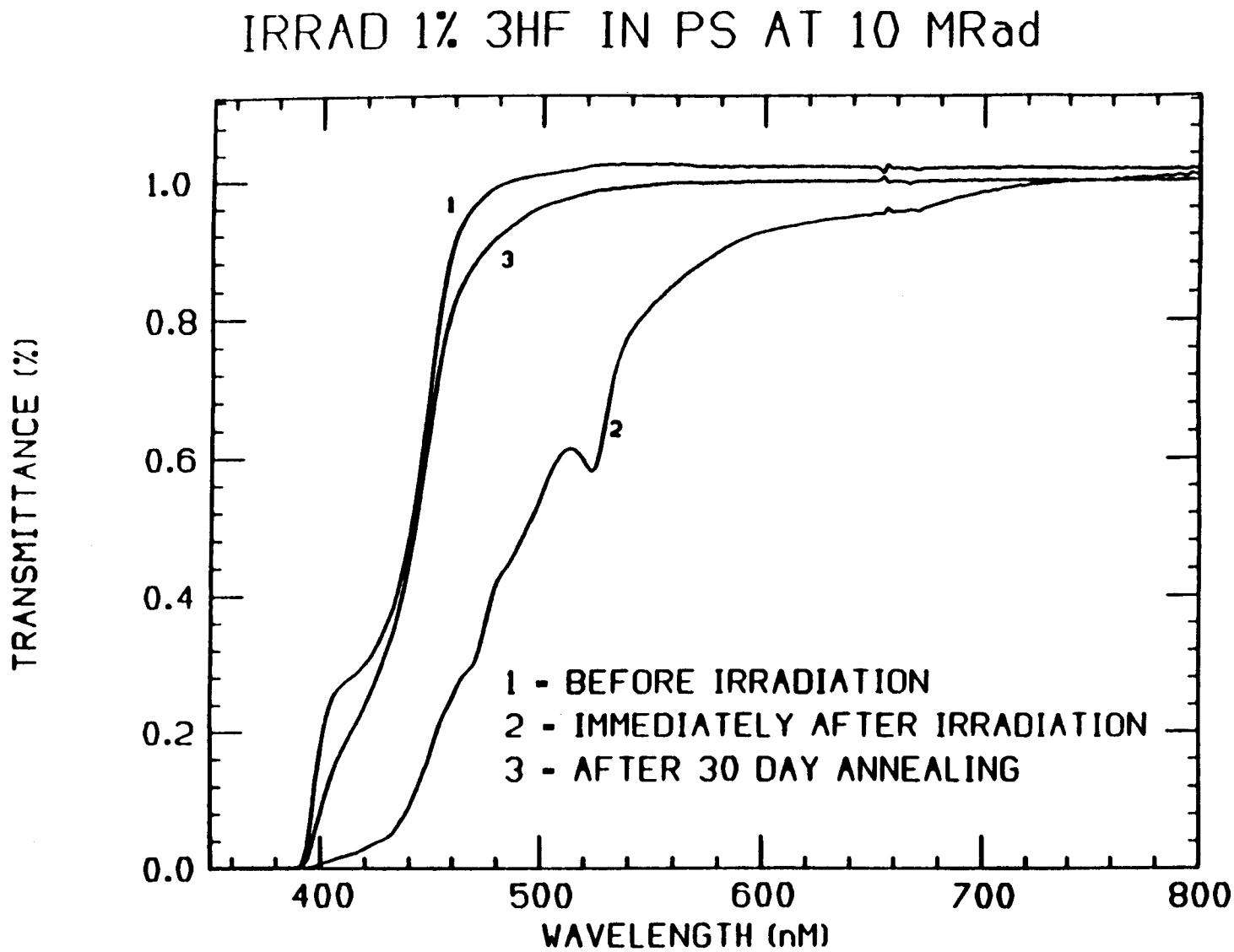
IRRAD 1% 3HF IN PS AT 10 MRad
TRANSMITTANCE (%)
1.0
0.8
0.6
0.4
0.2
0.0
400
500
600
700
800
WAVELENGTH (nM)
1
2
3
1 - BEFORE IRRADIATION
2 - IMMEDIATELY AFTER IRRADIATION
3 - AFTER 30 DAY ANNEALING

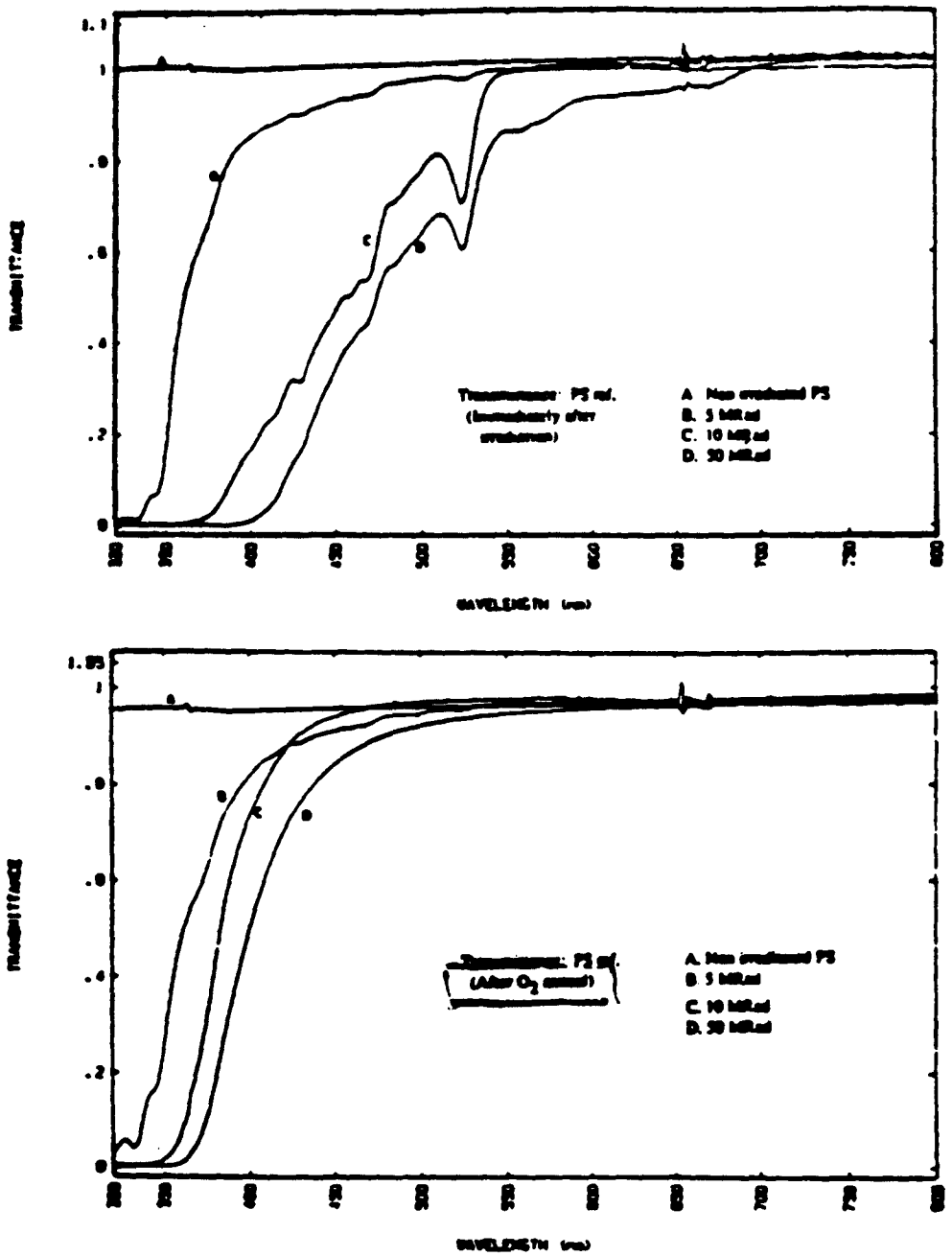

Fig. 6. Transmittance of 1 cm thick polystyrene samples after gamma doses of 5-50 MRad as measured immediately after irradiation (upper figure) and after annealing in oxygen (lower figure). Also, transmittance of a non-irradiated sample (curve A) is shown for comparison (from [19]).

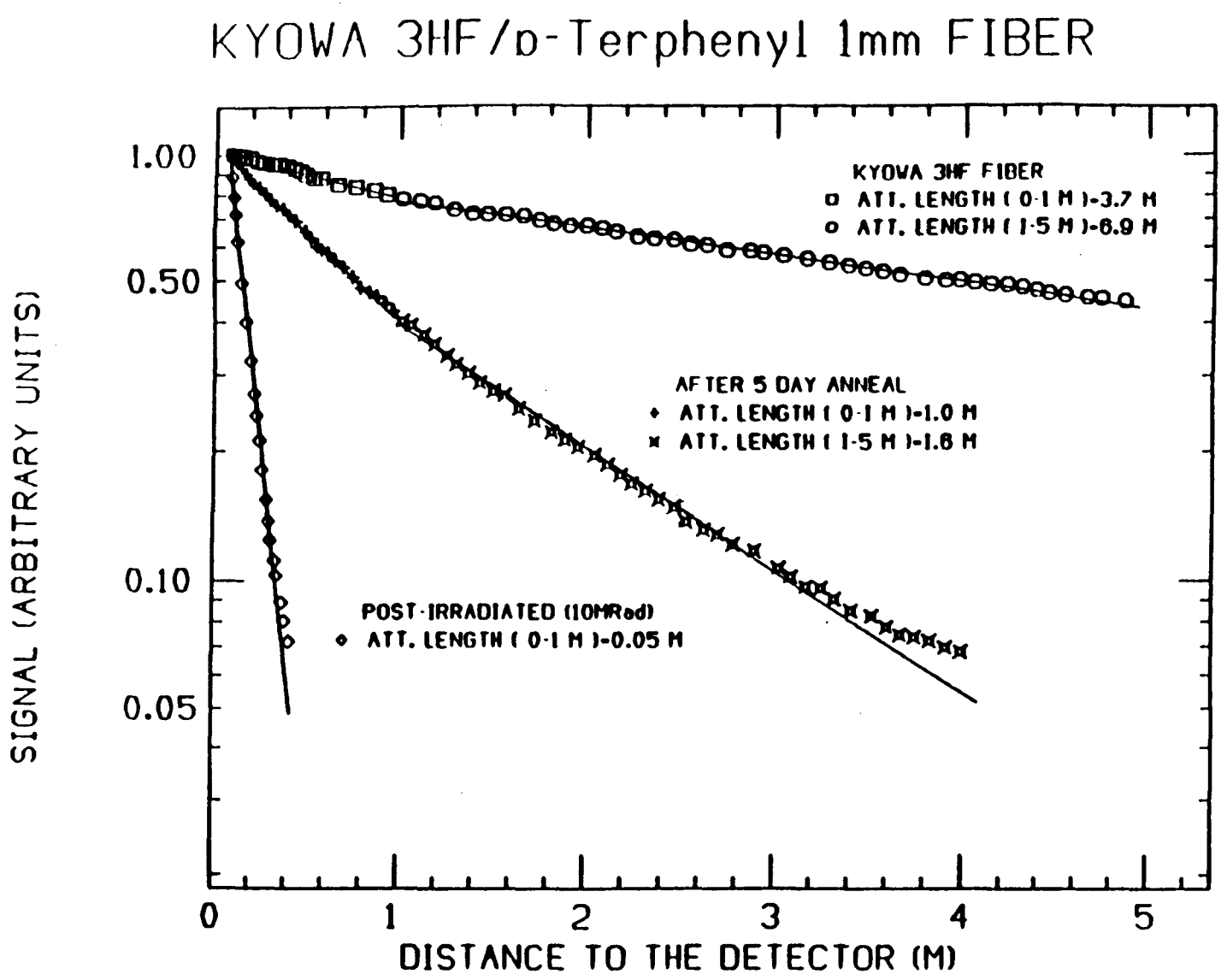
KYOWA 3HF/p-Terphenyl 1mm FIBER
KYOWA 3HF FIBER
ATT. LENGTH (0-1 M)-3.7 M
ATT. LENGTH (1-5 M)-6.9 M
AFTER 5 DAY ANNEAL
ATT. LENGTH (0-1 M)-1.0 M
ATT. LENGTH (1-5 M)-1.6 M
POST-IRRADIATED (10MRad)
ATT. LENGTH (0-1 M)-0.05 M
SIGNAL (ARBITRARY UNITS)
1.00
0.50
0.10
0.05
0
1
2
3
4
5
DISTANCE TO THE DETECTOR (M)

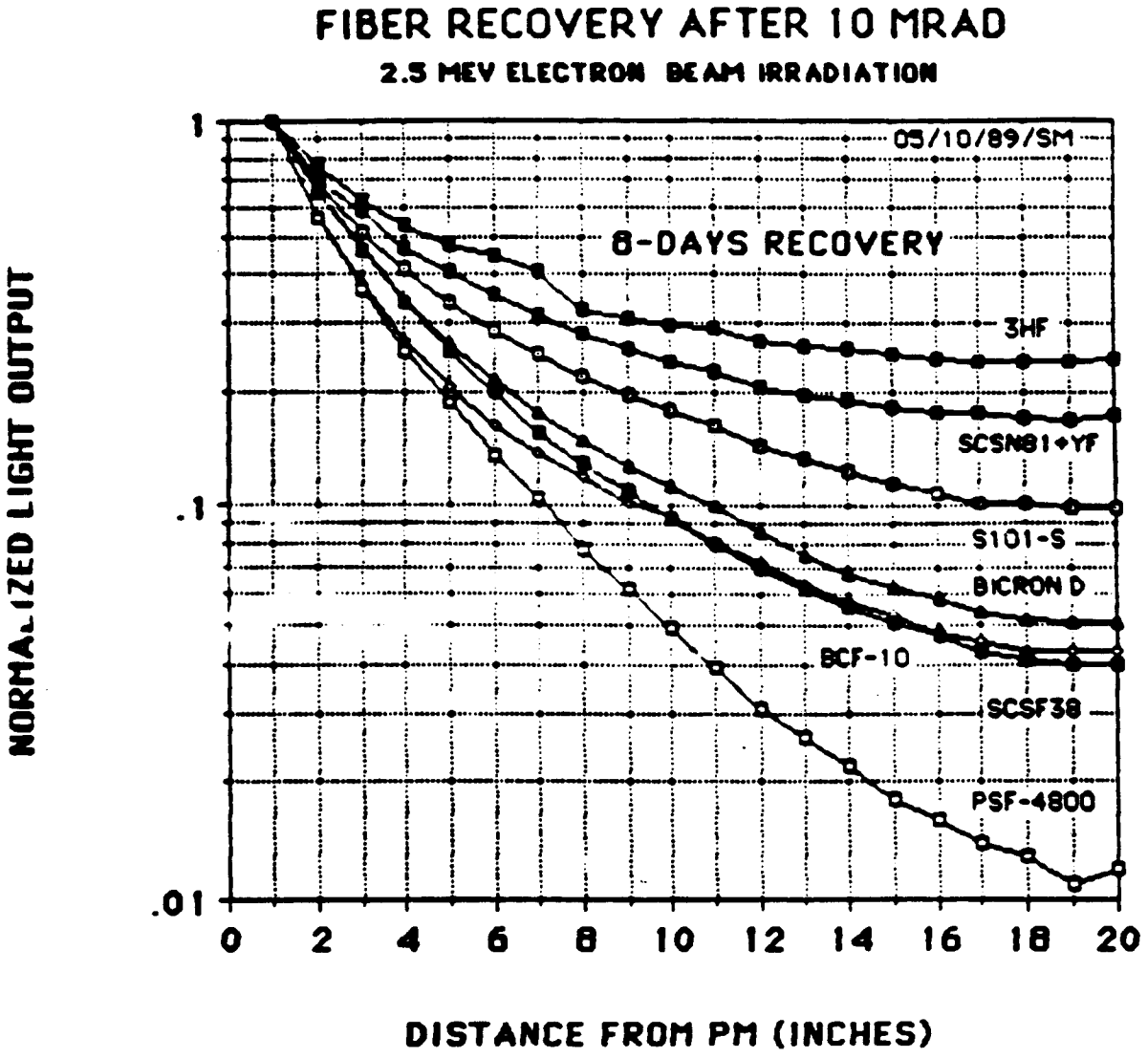
FIBER RECOVERY AFTER 10 MRAD
2.5 MEV ELECTRON BEAM IRRADIATION
05/10/89/SM
8-DAYS RECOVERY
3HF
SCSN81+YF
S101-S
BICRON D
BCF-10
SCSF38
PSF-4800
NORMALIZED LIGHT OUTPUT
1
.1
.01
0
2
4
6
8
10
12
14
16
18
20
DISTANCE FROM PM (INCHES)

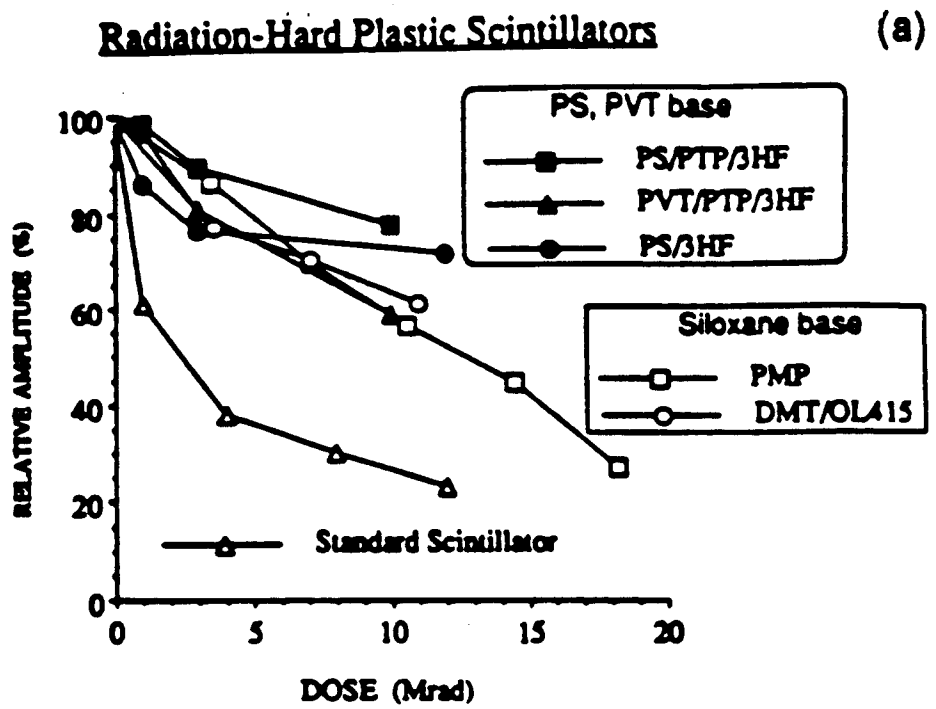

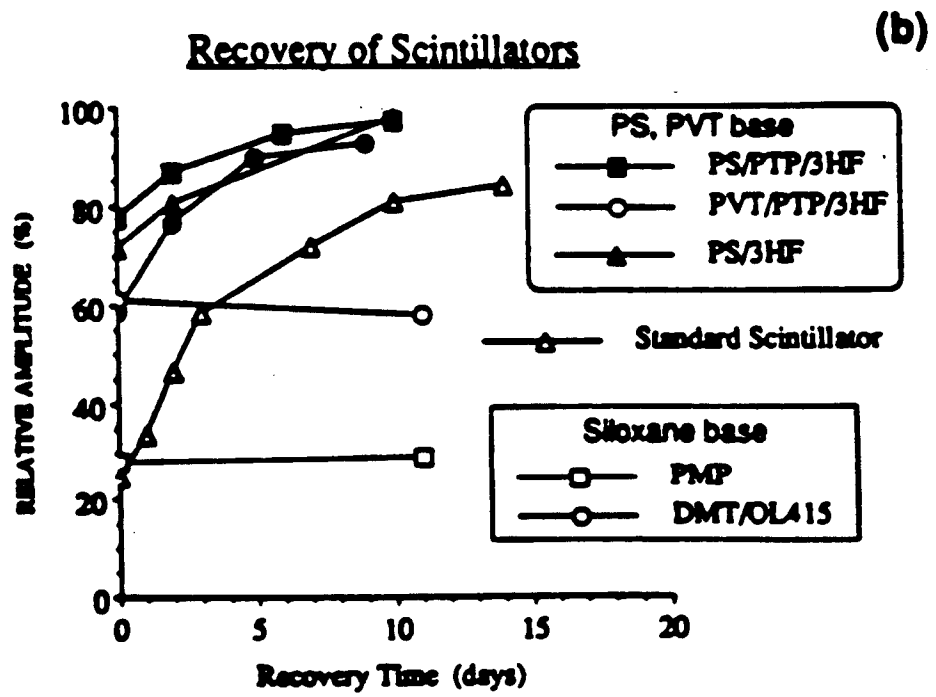

Fig. 22. Irradiation results for polysiloxane-based scintillators and for standard base (PVT, PS) plastic scintillators doped with 3HF. BC408 (standard scintillator) was used as a reference. Scintillation output as measured during irradiation (a), and recovery (b) [46].

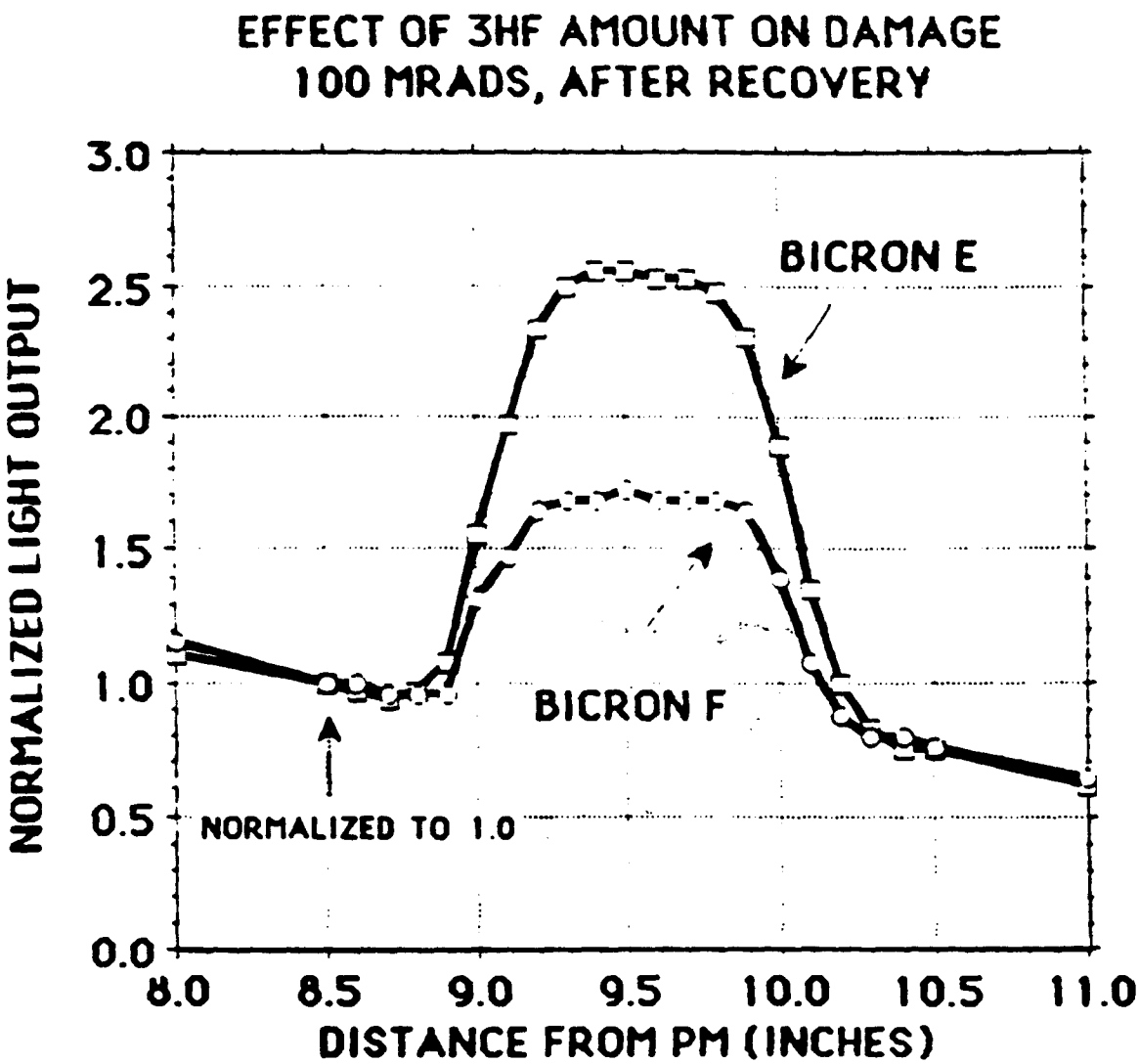
EFFECT OF 3HF AMOUNT ON DAMAGE
100 MRADS, AFTER RECOVERY
NORMALIZED LIGHT OUTPUT
3.0
2.5
2.0
1.5
1.0
0.5
0.0
BICRON E
BICRON F
NORMALIZED TO 1.0
8.0
8.5
9.0
9.5
10.0
10.5
11.0
DISTANCE FROM PM (INCHES)

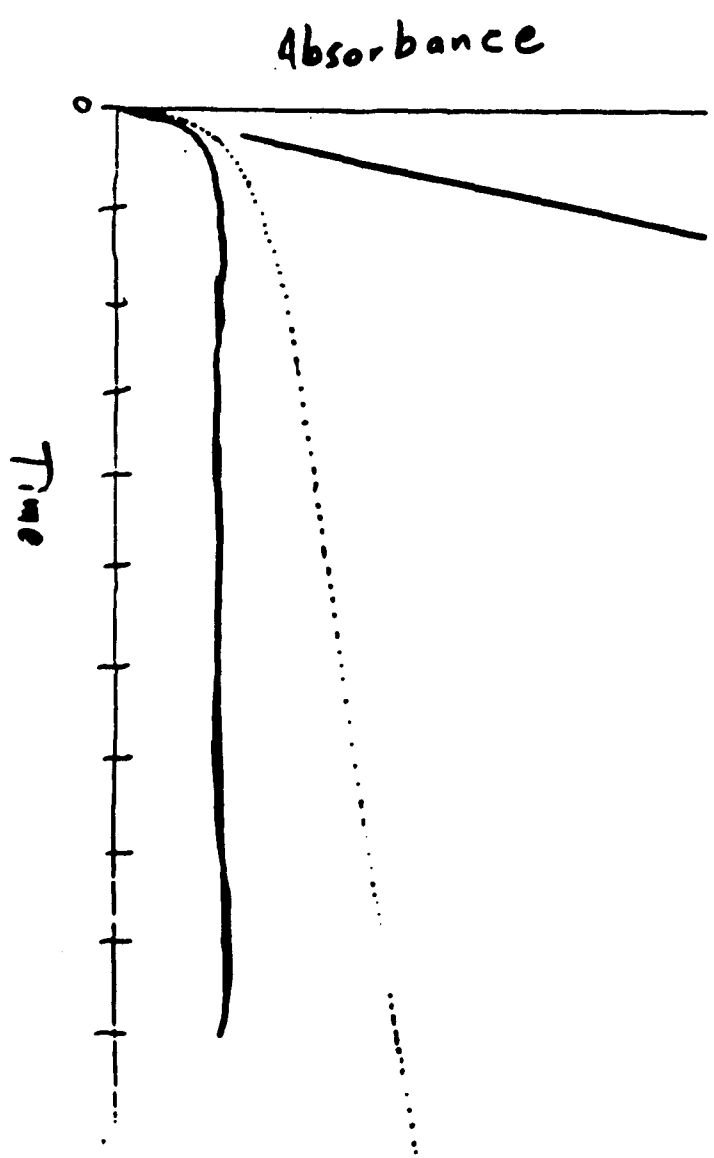
Absorbance
0
Time

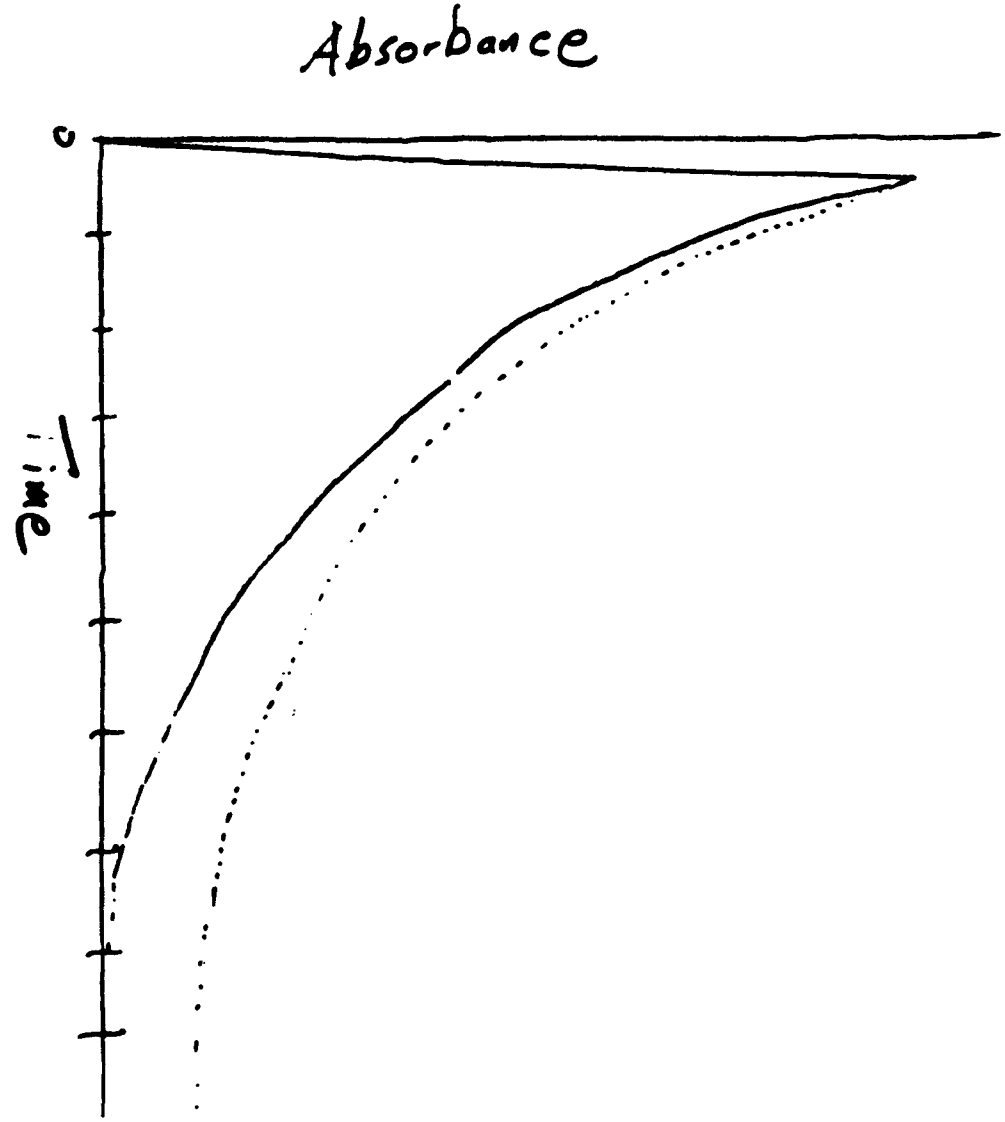
Absorbance
0
Time

4. SUMMARY OF THE RADIATION DAMAGE RESULTS

(1) The main conclusion from all the presented data is that the major contribution to radiation damage in plastic scintillators comes from the radiation-induced absorption/discoloration in the plastic matrix. In some cases, additional transmissional effects due to fluors were observed.

(2) Recovery of transmission after the accelerated irradiation tests is a very important and well-documented experimental fact that demonstrates the existance of a process of continuous dynamic repair which shall take place in the real experimental conditions. However, at present the exact predictions of the speed and extent of this cure are impossible, especially for air conditions.

JPTb

10MRad

(3) Damage to the intrinsic scintillation yield of many fluors seems to be relatively unimportant, with some fluor molecules exhibiting in plastic matrices an exceptional radiation resistance approaching our set goal of 100 MRad (example: TPB in polystyrene).

(4) From the above, it stems that the best remedy for the damage problem is to bypass the (permanently) damaged region in the transmission spectrum by long waveshifting of the scintillation light, preferably in a small number of steps by utilizing large Stoke's shift fluors, such as molecules undergoing intra-molecular proton transfer, the examples of which are 3-HF, BPD and HBT.

?

(5) Oxygen plays an important role in the damage and recovery processes, and from the still preliminary data it seems that the negative effects outweigh the stimulating effect it has on accelerating recovery of transmission in plastics.

?

(6) Contrary to the original "common wisdom", polystyrene- and PVT-based scintillators seem to recover (in transmission) in argon and nitrogen, though much more slowly than in air or oxygen.

(7) The additional effect of radiation damage to the local primary scintillation yield is probably due to direct transfer of excitation energy in plastic matrices into heat. The experimental data indicate that this is the second non-recovering part of the radiation damage, in addition to residual transmission damage.

Objectives

- Identify Crucial Factors in the Loss of Scintillation Efficiency:
  - Influence of Polymer Molecular Structure
  - Influence of Dye Molecular Structure
  - Role of Oxygen
  - Role and Nature of Impurities
  - Identify Color Centers
- Evaluate Potential Stabilizer Additives
- Develop Predictive (Accelerated) Aging Methods
- Make Lifetime Predictions for Candidate Materials Under Application Environments
- Iterative Development of Improved Radiation-Resistant Materials

(CERN)

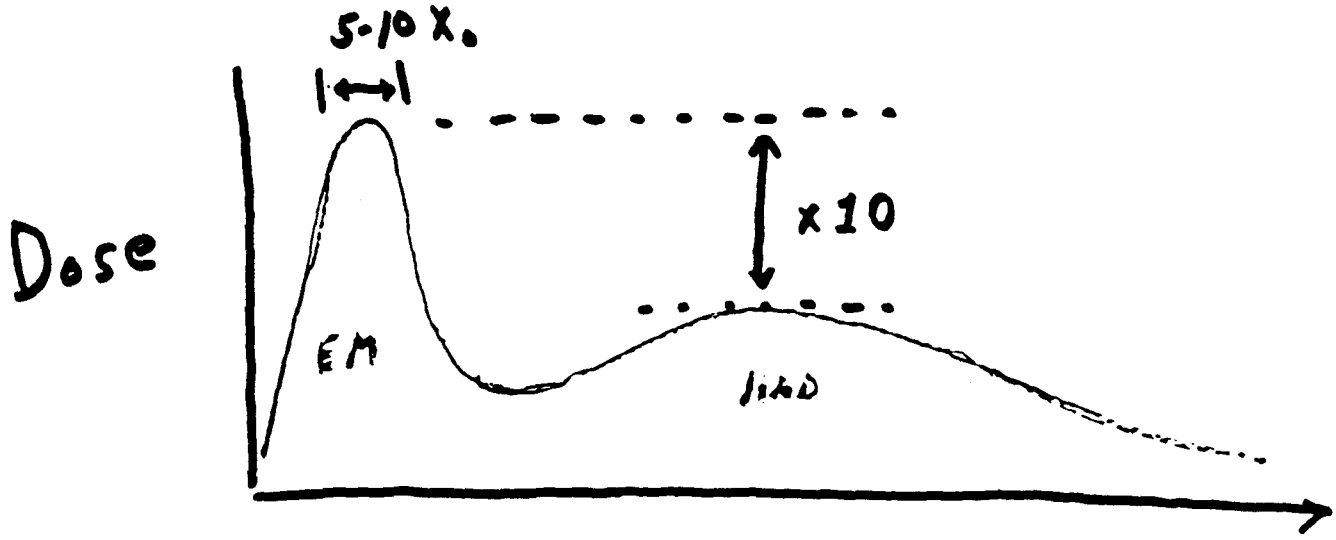

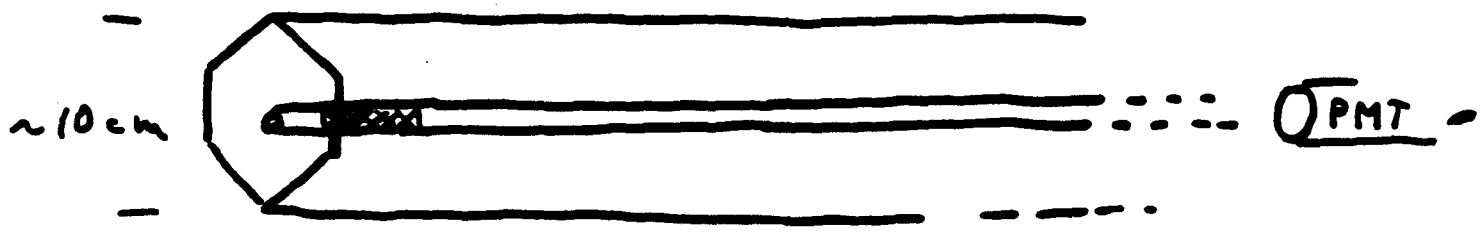

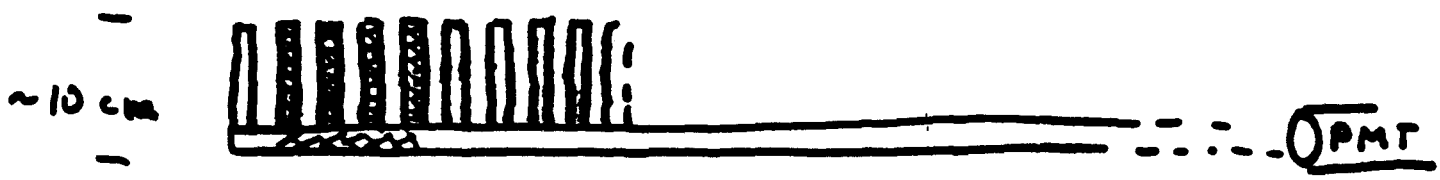

Need Real Calorimeter Test

EXTREME EXAMPLE

10 GeV SHOWER ~AVE AT $\eta \simeq 4$

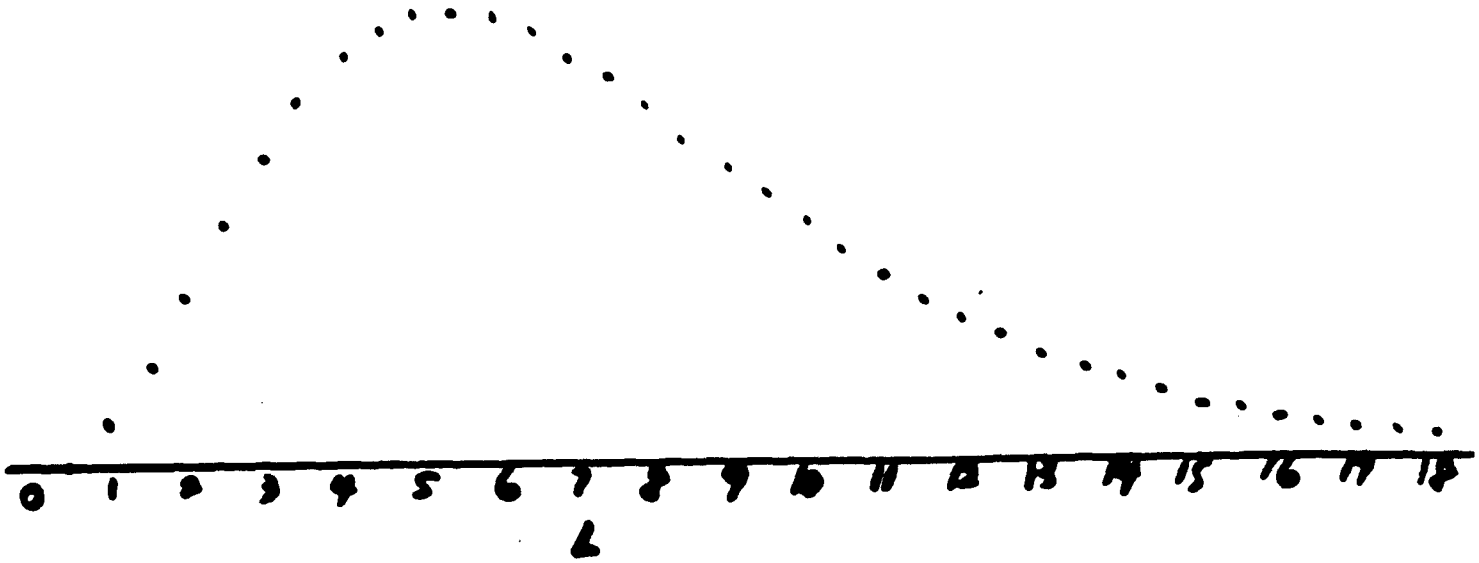

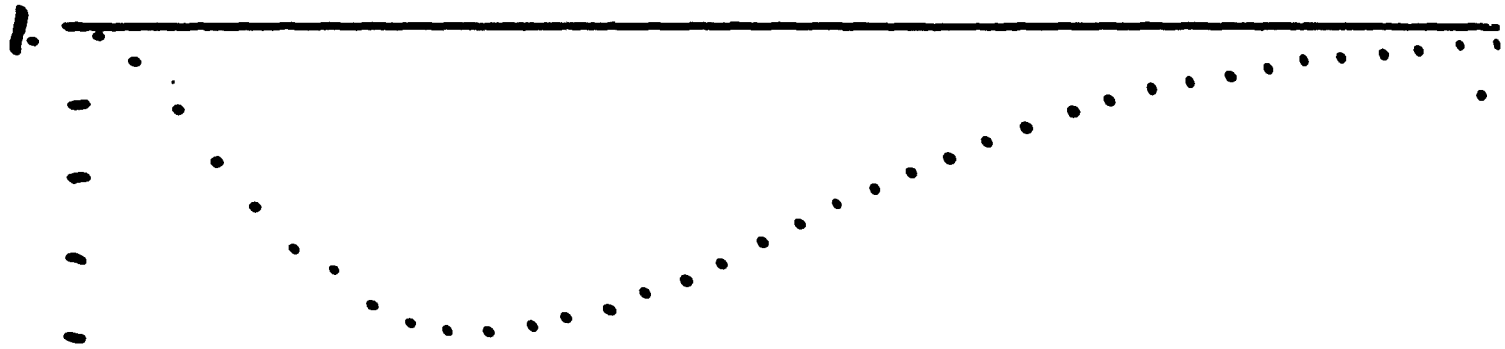

MULTIPLIER DUE TO RADIATION DAMAGE.

GIVES $\int \frac{dE}{dx}$ ~.7 × ORIGINAL ENERGY

1 MR AT $\eta = 4$ IF NO RECOVERY SCSN38).

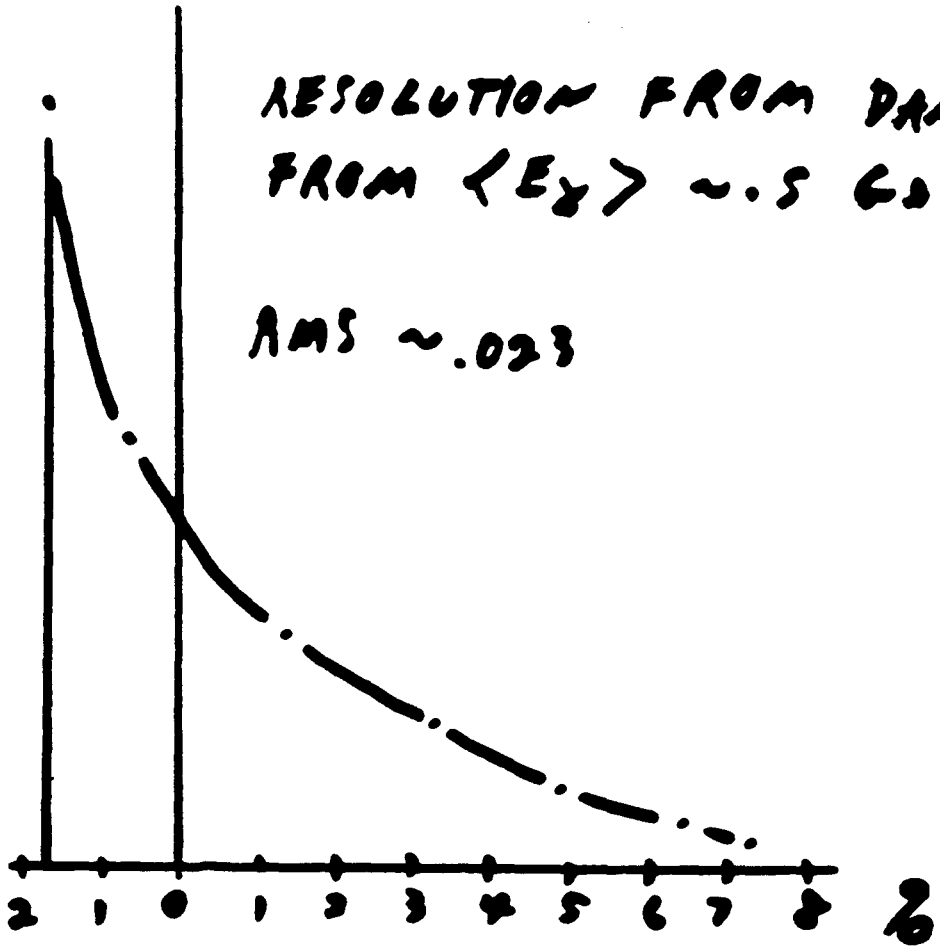
RESOLUTION FROM DAMAGE
FROM ⟨Eγ⟩ ~.5 GeV
RMS ~.023
2 1 0 1 2 3 4 5 6 7 8
%

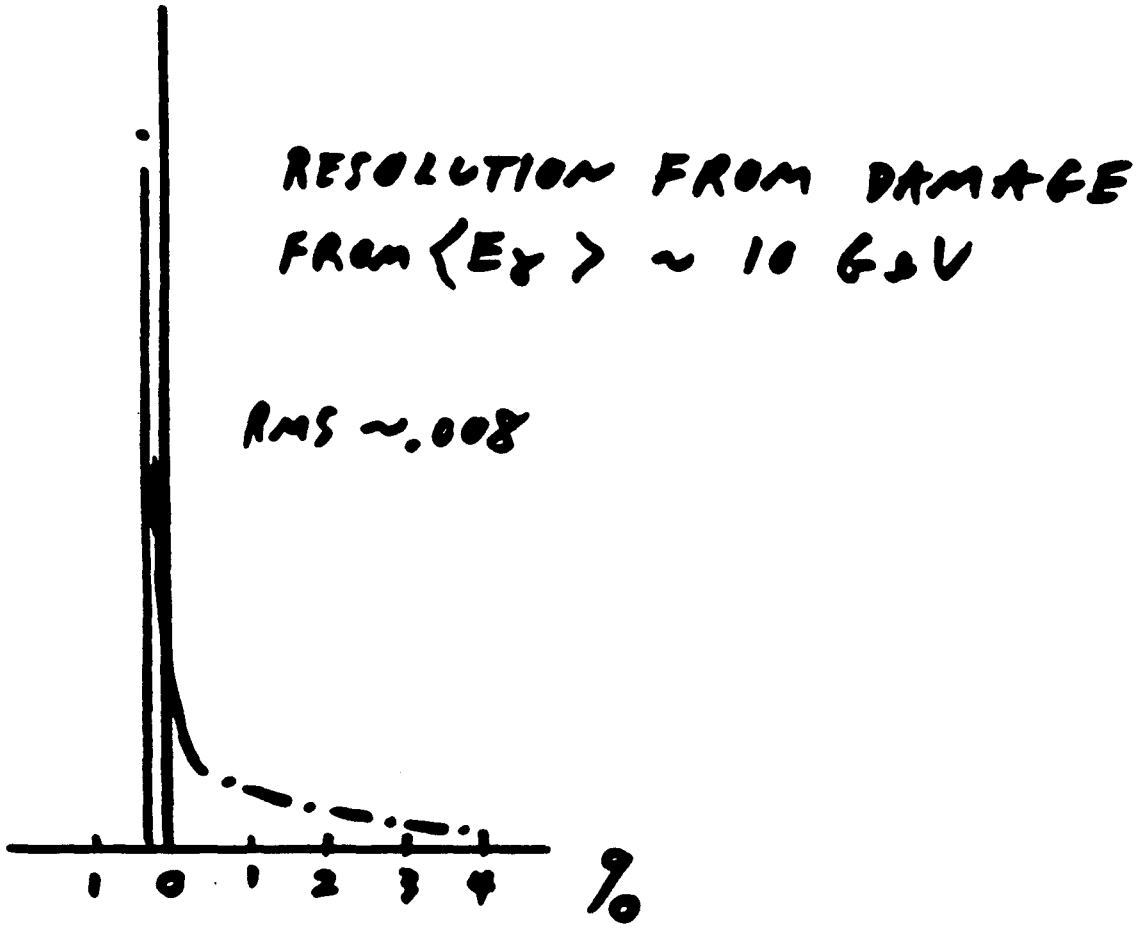
RESOLUTION FROM DAMAGE
FROM ⟨Eγ⟩ ~ 10 GeV
RMS ~.008
1 0 1 2 3 4
%

ZEUS Calorimeter Calibration

Tools: DU current
Monitors overall gain of calorimeter + PMT + electronics

Radioactive point source
Monitors longitudinal uniformity of calorimeter

Laser Monitors PMT + electronic

Particles
μ - monitors transverse uniformity + overall gain

e - measures local response (front of EMC section)

h - measures global response of calorimeter

Co^{60} scan

Iov 'suppressed

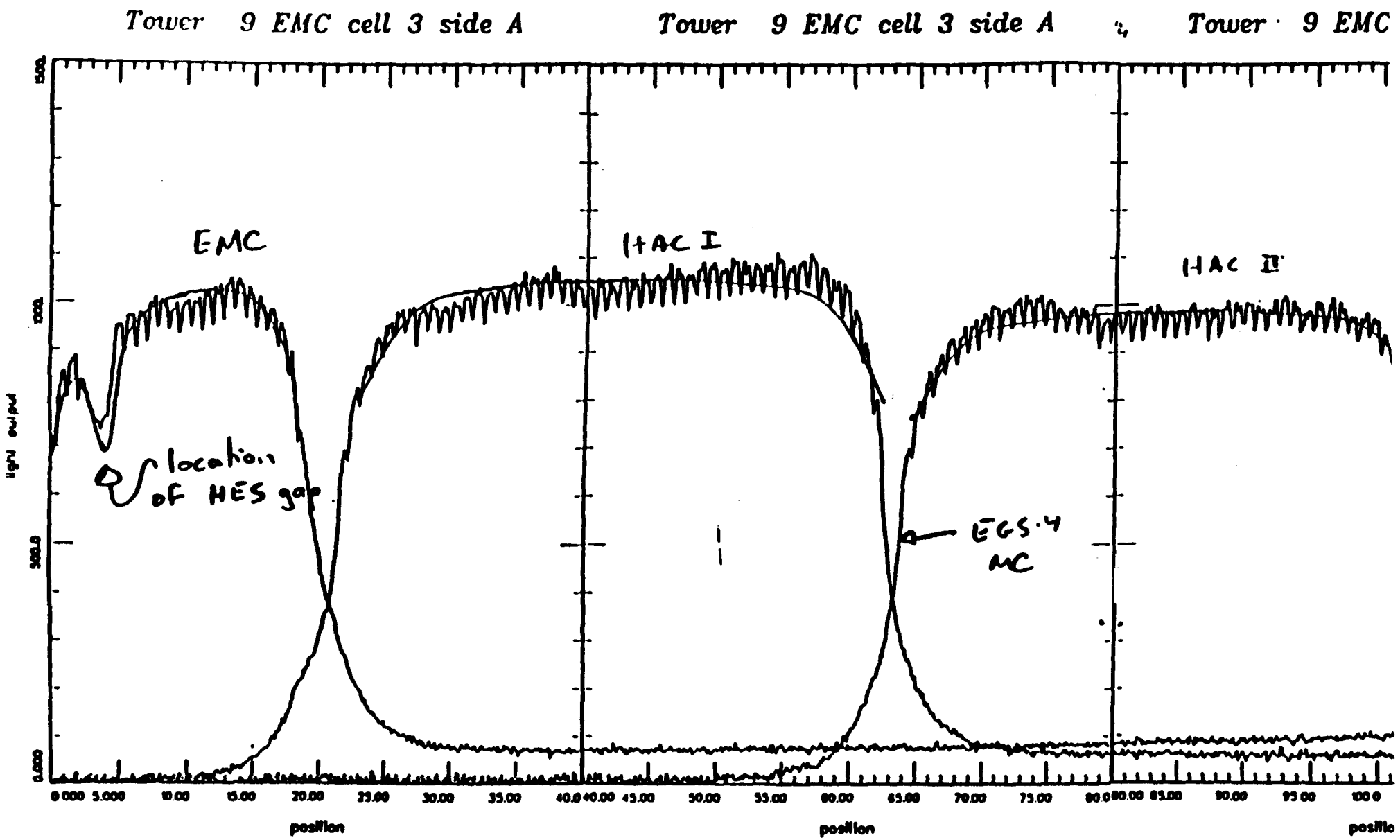

SUMMARY

ZEUS U-scinti. calorimeter

$$\frac{\sigma}{E} = \begin{array}{ll} 18\ \% / \sqrt{E} & \text{for electron} \\ 35\ \% / \sqrt{E} & \text{for hadron} \end{array}$$

$e/h = 1$ (1 - 100 GeV)

calibration and stability

electronics < 0.5 ADC channels after 24 hours

UNO < 1 % after 8 hours

UNO calibration

EMC 3.5 % (e)

HAC 1.2 % (μ), 1.6 % (h)

Conclusions about Radiation Damage in a Calorimeter

Zone of Concern: η 2.5 → 3
depth 5 to 10 cm at front

Attenuation Length Decrease (to ~1m, 10 MRad, Reco
Light at PMT decrease ~ 10 %
Resolution increase ~ 1 %
Readout balance (plate-WLS) ?

Scintillation Light Decrease (~20%, 10 MRad, Reco
Light at PMT decrease ~20% EM
e/h decreases ?
Resolution increase ~ 1 %

Damage to other components ?

Need Real Calorimeter Test

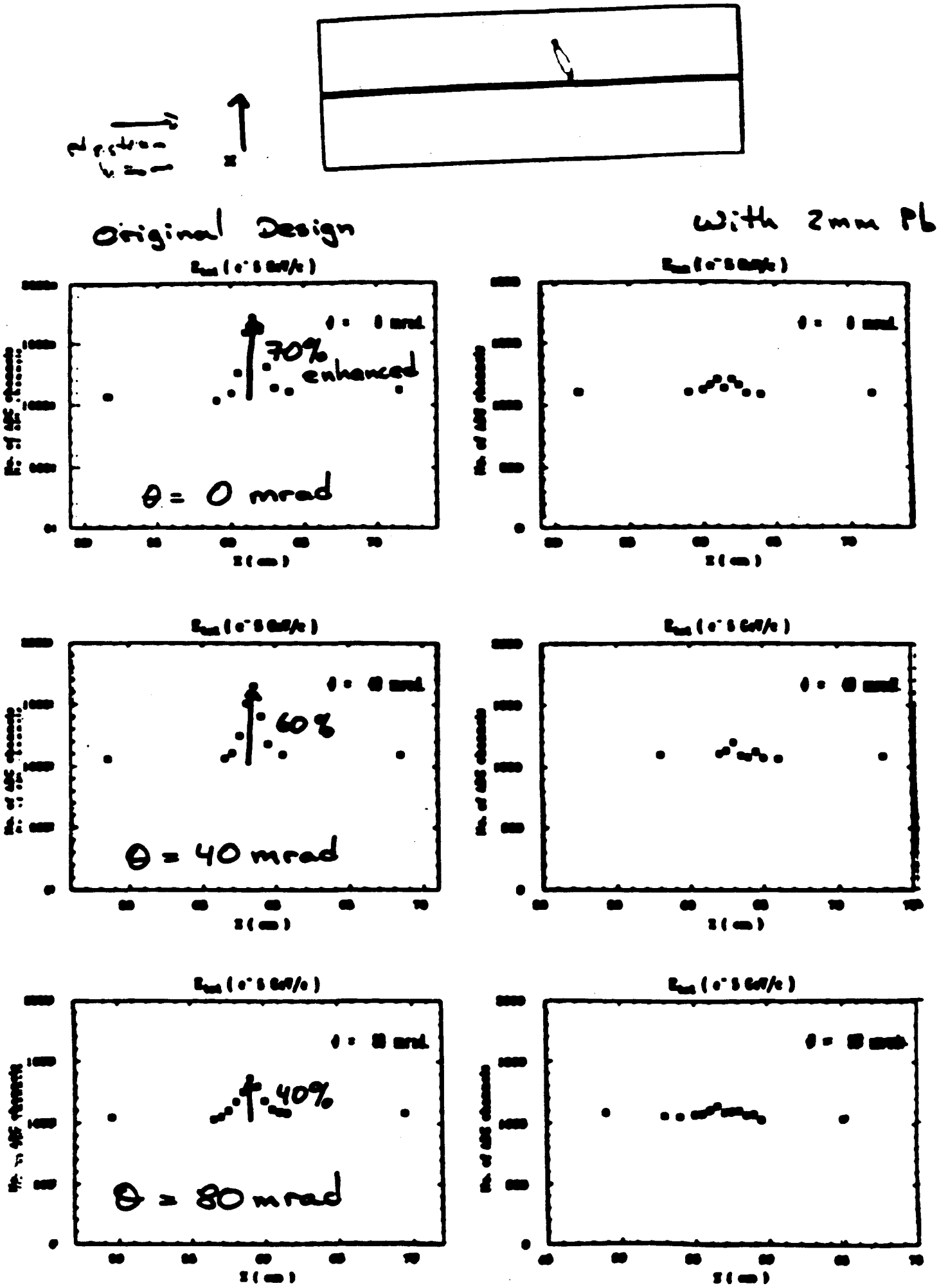
Original Design
With 2mm Pb
70% enhanced
θ = 0 mrad
60%
θ = 40 mrad
40%
θ = 80 mrad

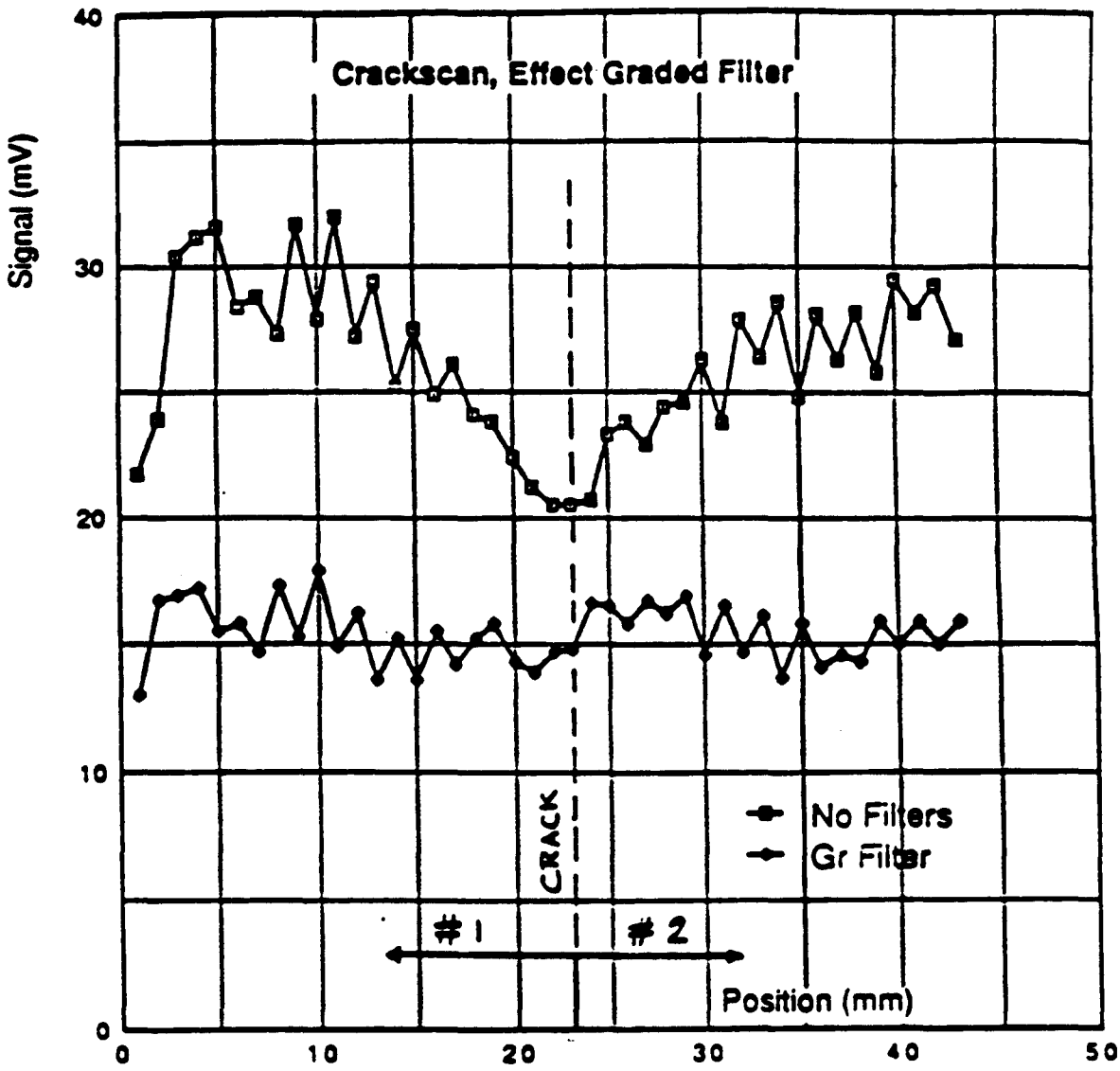
Crackscan, Effect Graded Filter
Signal (mV)
40
30
20
10
0
0
10
20
30
40
50
CRACK
No Filters
Gr Filter
1
2
Position (mm)

Figure 5

Coil Placement

Inside: 1.0 - 1.5 X_0 at 90°
η 0 → 1.6

Resolution: no problem E > 10 GeV

Hermeticity: Requirements ?
Magnet Supports + Supply
Biggest Problem at $\eta = 3$

Field Quality: Requirements ?

e/hadron Separation: Effects of Coil
1. Fiber
2. Plate

Effect of Field on Calorimetry, PMTs

Outside:

PMTs in High Field

Effect of Field on Calorimetry

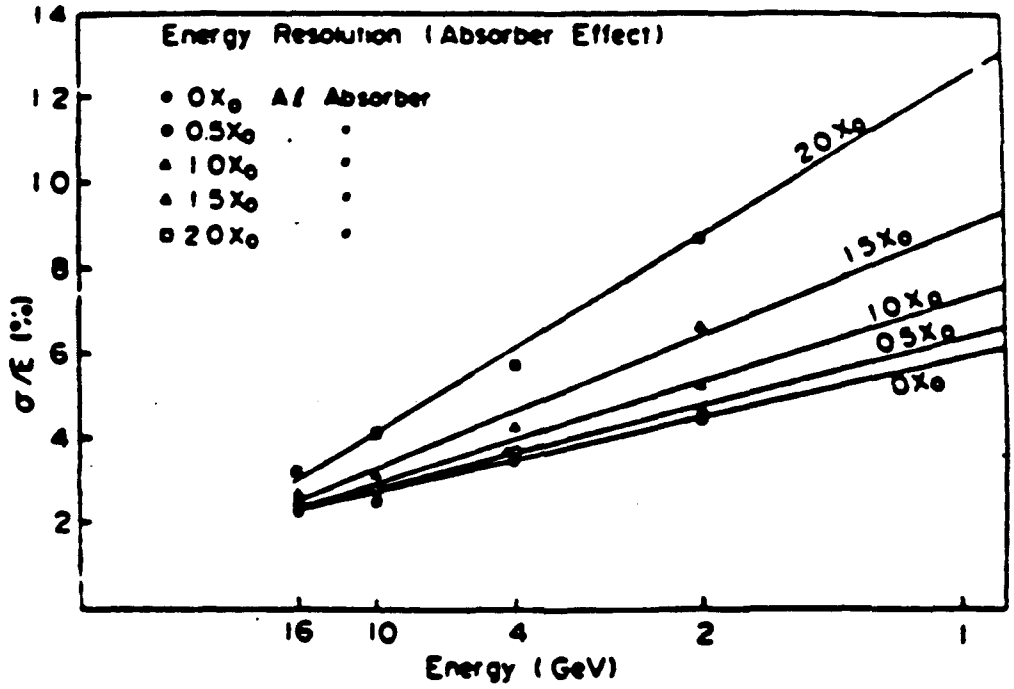

Fig. 5.3.3 Energy resolution of and SF03 lead glass counter ($18X_0$) with aluminium absorbers of different thickness in front (ref. 14).

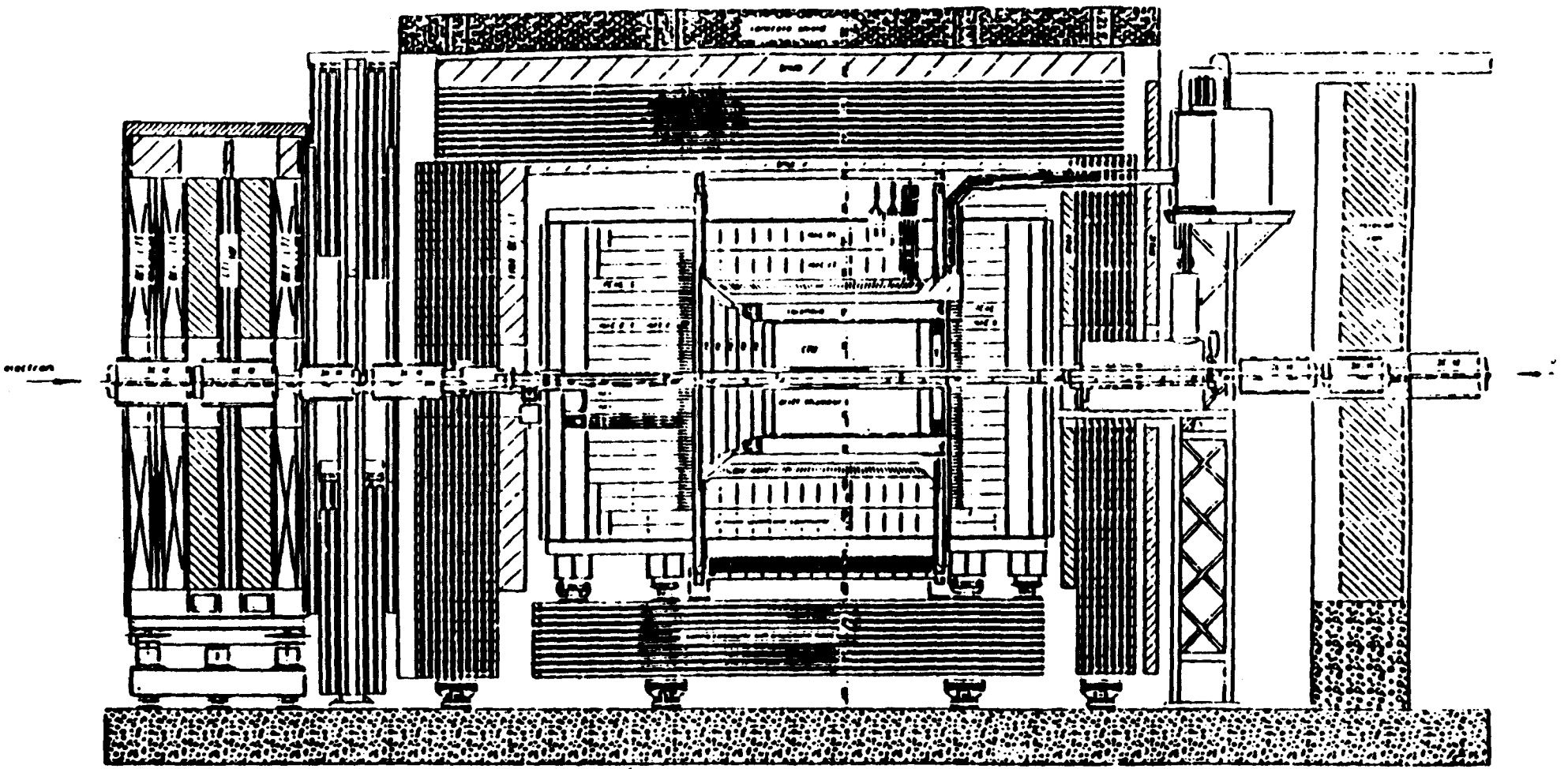

Fig. 2.1 Section of the ZEUS detector along the beam

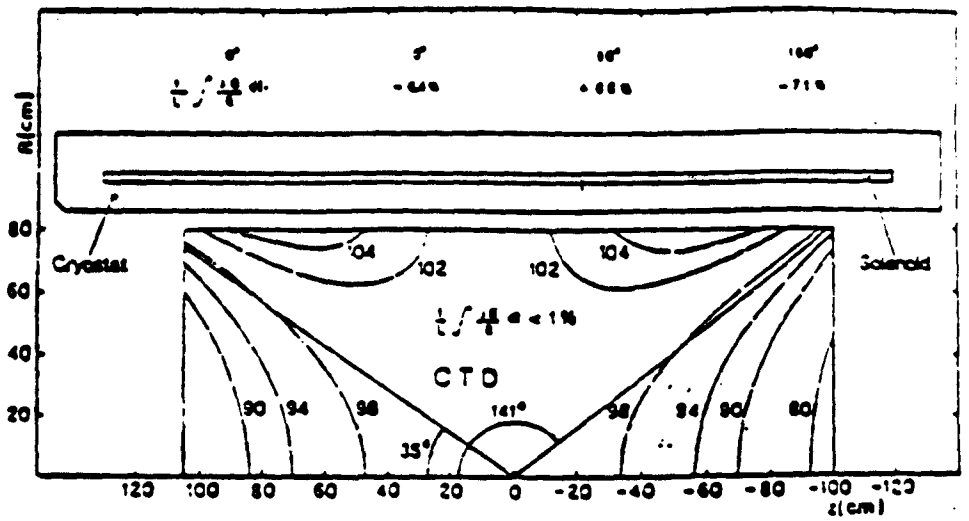

Fig. 3.3.5.a Isocontour lines of the magnetic field in percent of the axial field in the region of the CTD.

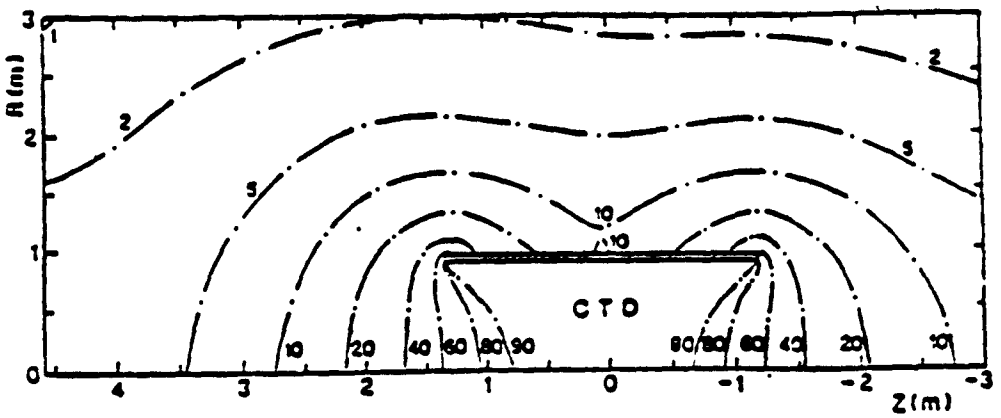

Fig. 3.3.5.b Isocontour lines of the magnetic field in percent of the axial field in the region of the calorimeter.

The hadron calorimeter consists of 34 2.54cm-thick iron plates with 1.6cm gaps containing 1cm thick scintillator. Most of the measurements were made with 7.6cm of aluminum in front of the module in order to simulate the effects of a coil-cryostat. Figure 5.3.1 shows typical pion and electron pulse height distributions in the EM shower counter and hadron calorimeter at 30 GeV. For a momentum resolution of $\delta p/p = 0.002p$ (GeV/c), a pion rejection of approximately 10^{-3} was obtained for an electron efficiency of 70%. Table 5.3.2 gives typical cut efficiencies for 30 GeV e and π. The energy dependence of the pion rejection factor from 15 GeV to 46 GeV was found to be small, although some improvement was observed at higher energies. They also studied the dependence of the pion rejection on the amount of material in front of the calorimeter. The ratios for pion rejection for 14 cm/7.6 cm/2.5 cm aluminum were observed to be (1.9±0.3)/1/(1.0±0.3).

Table 5.3.2

Electron Selection Criteria

Cut	Electron Survival	Pion Survival	Remaining Pion Survival After All Other Cuts
EM scintillator	0.87	0.0076	0.29
Hadron calorimeter	0.94	0.013	0.54
W1 pulse height ($25X_0$)	0.94	0.24	0.54
W2 pulse height ($6X_0$)	0.97	0.041	0.90
W1 width	0.99	0.24	0.89
W2 width	0.97	0.23	0.69
Total	0.72	7×10^{-4}	

Y. Hayashide et al.[7] used another test shower counter of 31 layers of lead/scintillator for the CDF. A proportional chamber is placed at $5.6X_0$ depth, near the shower maximum of electrons. A likelihood method incorporating Fourier analyses of lateral profiles of electron and pion showers was employed

appears at a depth of $5X_0$ to $10X_0$ for the energy range of the SSC. Longitudinal segmentation and measurements of lateral shower distributions at various depths can improve electron-hadron separation.

Table 5.3.1 lists some recent reports on π/e separation using EM shower calorimeters. Common techniques used to identify an electron are:

- comparison of the shower energy with the momentum if the particle momentum is analyzed by a magnetic spectrometer;
- ratio of shower energies in EM and hadron calorimeters;
- ratio of the front end energy to the total shower energy in an EM shower detector;
- measurement of the lateral shower profile near the shower maximum of an electron.

A pion rejection factor of approximately 10^{-3} has been obtained at high energies with a reasonable electron acceptance. At very high energies (> few hundred GeV to a TeV), where the momentum resolution of a magnetic spectrometer becomes poor, the total energy of a particle must be measured by a calorimeter system. Therefore, finer lateral segmentation of both EM and hadron calorimeters are required. Among the measurements listed in Table 5.3.1 we describe test results of prototype calorimeters designed for the CDF detector and also measurements made to study effects due to material in front of EM shower detectors.

R. Diebold et al.[6] studied the performance of the full-scale prototype model of the central calorimeter for the CDF.[15] The EM shower counter consists of 33 layers of lead/scintillator, each having 0.32 cm of lead and 0.64cm of plastic scintillator, $0.6X_0$ per layer, for a total of $20X_0$. Two layers of wire chambers are placed at $2.6X_0$ and $6.2X_0$ depths.

Micke, Trines, and Wallraff[11] studied the pion misidentification probability after inserting 10cm of aluminum in front of their lead liquid argon calorimeter, which corresponds to a total amount of $1.3X_0$ material in front of the active part of the detector. They observed a small increase in the misidentification probability at 2, 5, and 10 GeV. They pointed out that an improvement of π/e discrimination could be achieved by cutting on the pulse height in the first strip system. Combining all cuts they obtained a pion rejection rate of $(4\pm2)\times10^{-3}$ at 10 GeV for an electron efficiency of 97%.

It can be concluded that additional material in front of an EM shower detector can in principle degrade the energy resolution for electrons and the pion rejection factor, but in practice effects due to an aluminum absorber of 1 to $1.5X_0$ are small at electron energies greater than about 10 GeV.

Electron identification can be provided by calorimetry over the full electron energy range expected at the SSC. Pion rejection factors of $\sim10^{-3}$ can be expected by using combinations of E/p and shower development criteria. At energies above ~1 TeV, only shower development is likely to be viable as magnetic tracking resolution becomes very poor, at least in a typical 4π detector. The limitations to measuring shower development in large calorimeter systems will arise primarily from mechanical complexity and cost considerations, not the fundamentals of electromagnetic showers. Finally, for those experiments at the SSC which are investigating high mass/high energy phenomena, the effects of inert absorbing material preceding electromagnetic calorimetry will be small, possibly simplifying the mechanical design of detectors.

5.3.2 Electron Identification: Transition Radiation

A number of reviews[18,19] of the principles of transition radiation detectors (TRD) exist in the literature and we will not discuss them here. Transition radiation is a well established method of electron identification and

Tubes for High Magnetic Environments

Type No.	Tube Diameter (Inches)	Outline No.	Spectral Response: Curve Code	Spectral Response: Range (nm)	Spectral Response: Peak Wavelength (nm)	No. of stage	Cathode Luminous Sensitivity Typ. (μA/lm)	Anode to Cathode Supply Voltage (Vdc)	Anode-Luminous Sensitivity Typ. (A/lm)	Current Amplification: at 0 gauss Typ.	Current Amplification: at 5 kilo-gauss Typ.	Current Amplification: at 10 kilo-gauss Typ.	Current Amplification: Anode Dark Current Typ.
Triode Tubes													
R2148 ▼	1	❶	400K	300 – 650	420	1	65	750	7.8×10^{-4}	12	7.8	7.2	3.7
R2184 ▼	2	❷											
R2046 ▼	3	❸											
Tetrode Tubes													
R2149 ▼		❶	400K	300 – 650	420	2	65	750	3.3×10^{-3}	50	25	17.5	1.0
R2185 ▼	2	❷											
R2186 ▼	3	❸											
High Gain Types													
R2181 ▼	1.5	❹	400K	300 – 650	420	8	70	1500 ⑦	0.07	1×10^3	500	70	5
R2182 ▼	2	❻											
R2021 ▼	1.5	❺				12	70	2000 ⑦	3.5	5×10^4	1.5×10^4	600	30
R2063 ▼	2	❻											

▼: Newly listed in this catalog.
Typical spectral response characteristics are shown on pages 65 and 66.
The supply voltage for Triode and Tetrode tubes is equally distributed to each electrode.
For High gain types, see page 50 for the voltage distribution ratios.

For further information, technical data sheet is available.

Unit: mm

❶ R2148, R2149

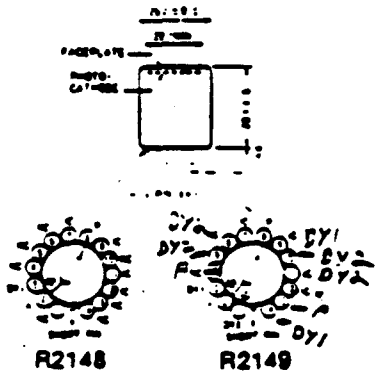

❷ R2184, R2185

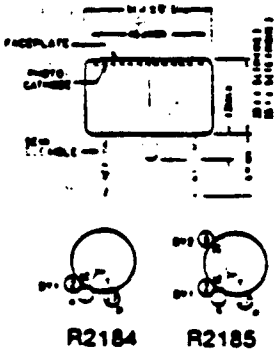

❸ R2046, R2186

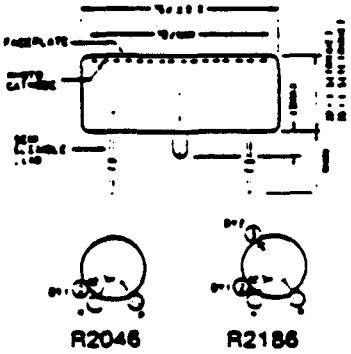

❹ R2181

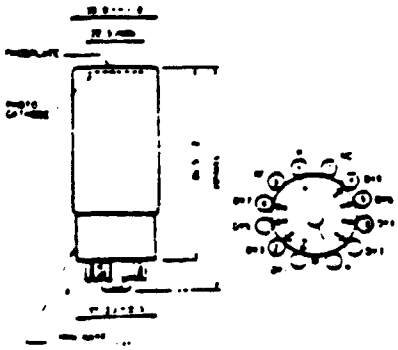

❺ R2021

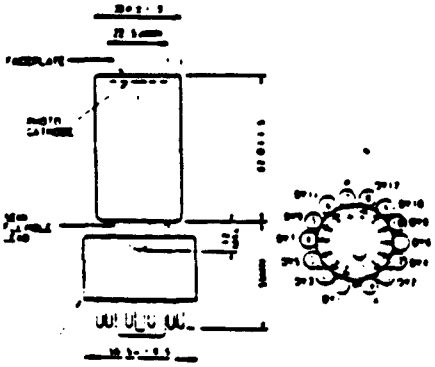

❻ R2182, R2063

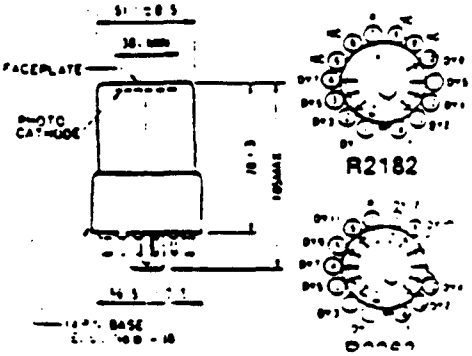

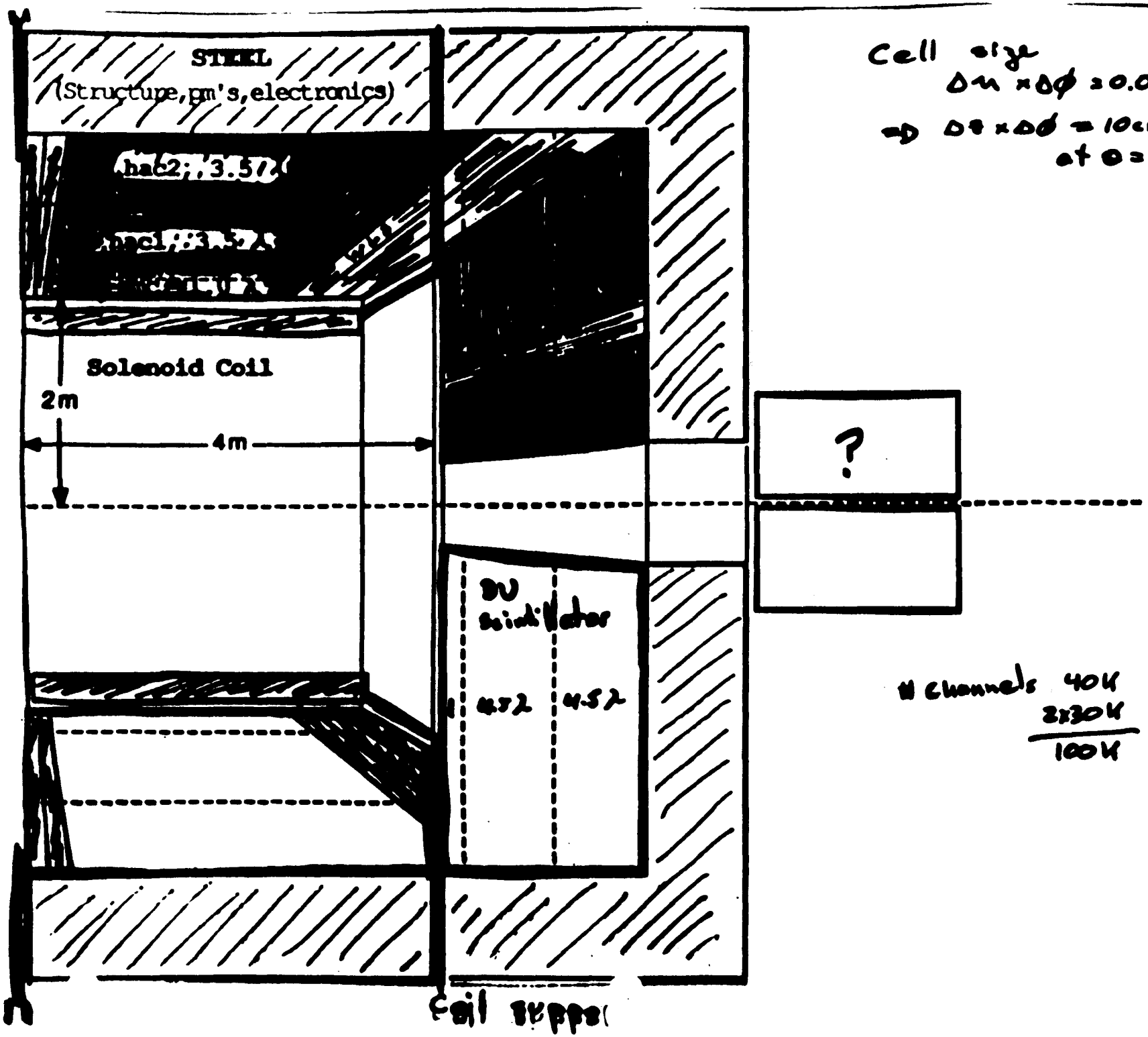

Cell size
$\Delta\eta \times \Delta\phi = 0.05 \times 0.05$
$\Rightarrow \Delta z \times \Delta\phi = 10cm \times 10cm$
at $\theta = 90°$

channels 40K Barrel
2x30K Ends
100K

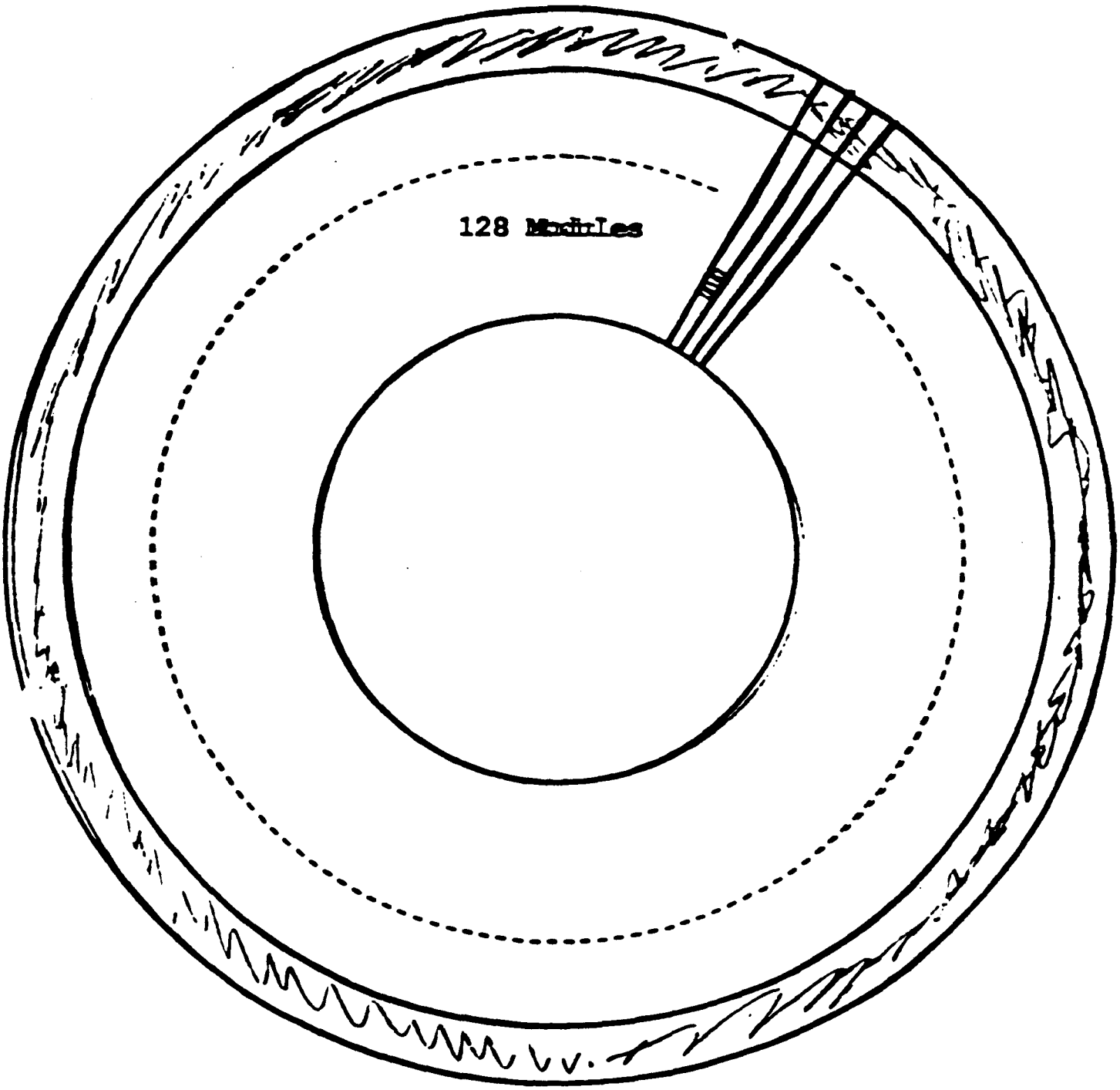

-128 wedge shaped modules 12 Tons/module

- 10 cm base width at R=2 m
- outer radius 3.6 m => 8 lambda
- 5 mm inter module gap for WLS readout
- 1 m steel support (houses PMT's, electronics, return path fo

Cost Estimate

For Barrel

$R_{in} \sim 2\,m$
$R_{out} \sim 3.6\,m$
$L_{1/2} \sim 4\,m$
$\langle \rho \rangle \sim 9\ g/cm^3$

} ≈ 2500 Ton
40K channe

End cap

$R_{in} \sim 0.4\,m$
$R_{out} \sim 3.6\,m$
depth $\sim 2\,m$

} ~800 Tons
30K channels

DU rolled, machined, clad ~ 10$/lb

Mechanical structure ~ 5 M$

Optical Readout (scint + WLS)	200$/chan
PM's + Bases	200$/chan
Analog Electronics	100$/chan
Digital Electronics	100$/chan
Triggering (I, II level)	100$/chan

Total	4000 Tons DU	80 M$
	100K Channels	70 M$
	Mechanical support	5 M$
		155 M$

Note: DU will be available

E. Fowler
DOE

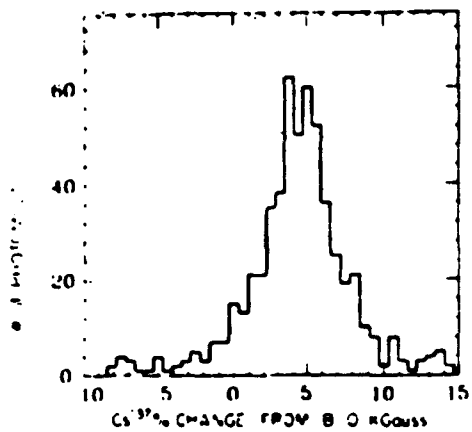

Fig. 29. Distribution of percentage differences of I_{Cs} currents in endwall tubes, when measured in the presence of no magnetic field and with the superconducting solenoid at 15 kG, representing combined scintillator, WLS and PM response changes.

ratio of the I_{Cs} currents. Fig. 27 shows the distribution of the percentage difference between corresponding pion peaks of the recalibrated modules, scaled by the I_{Cs} ratios: the standard deviation of the distribution is about 1%. When all the modules were assembled in the experiment, the role of the now impractical ^{90}Sr source was taken over the laser system.

Once all the 50 central modules were tested, their degree of similarity was checked by correlating, again through I_{Sr} and I_{Cs}, the observed pion pulse heights to the average currents I_c. Fig. 28 shows that the modules can be calibrated at a level of 3–4% with the source systems only.

Endwall modules have been calibrated relying on this result. At the test beam the phototube high voltages on two endwalls modules were adjusted to provide 100 pC for 50 GeV hadronic energy deposition. At the same voltages the current induced by a ^{137}Cs line source, longitudinally irradiating the whole tower (see section 4.2), was measured for each phototube. On both modules the currents of corresponding towers proved to be equal at a 2% level for different running conditions. These calibration currents (different for each tower of a module) were set in all the other calorimeter modules by adjusting the high voltage on the phototubes. This procedure of manually using the line ^{137}Cs source required 15 min per module. Immediately after the hv setting of each module, the current induced by the movable point source (see section 4.3) and the laser pulse heights were recorded to provide a reference for each photomultiplier.

7. Magnetic field effects

Since the endwall calorimeter serves as part of the magnetic field return yoke, its scintillators and its phototubes are influenced by the magnetic fringe field. Independent current measurements with the movable point radioactive source and with the laser system allow one to separate magnetic field effects on phototubes from those on scintillators. The percentage displacements of these currents from the initial status of no field have been measured for endwall phototubes with the superconducting solenoid powered to provide 15 kG. As shown in figs. 29 and 30 the movable source currents increase on average by ~ 5%, while the mean of the laser induced pulse heights is affected by a smaller amount (about 1%). Fig. 31 shows the dif-

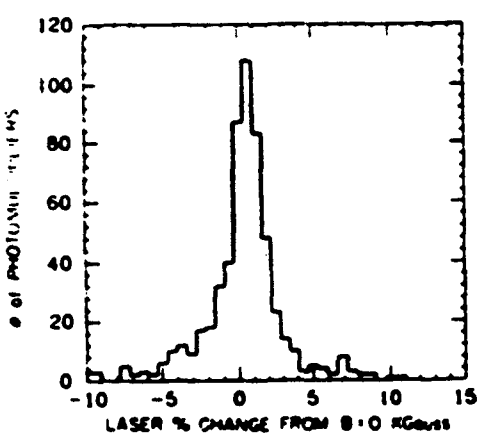

Fig. 30. Percentage differences of the charges produced by endwall PMs, exposed to light from the laser system, when measured with the magnetic field "on" (15 kG) and "off".

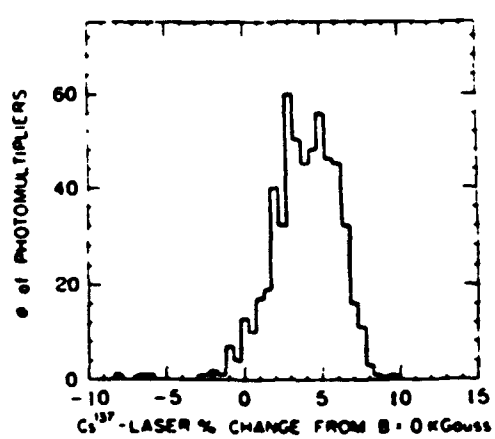

Fig. 31. Difference, tube by tube, of the quantities plotted in figs. 29 and 30, representing response change of scintillator plus WLS only.

Conclusions —

1. Radiation Damage: A Problem not A Full Stop

2. Coil Placement: Speed, Low Noise, Compensating vs Hermeticit, e/π ID, Field Quali

3. Schedule: Beam Calibration

PROGRESS REPORT ON STUDIES OF SSC TASK FORCE ON ELECTRONICS, TRIGGERING, AND DATA ACQUISITION

A. Lankford

DALLAS

JUNE 26, 1989

Scope of Task Force on Electronics, Triggering, and Data Acquisition at the SSC

Front-End VLSI and Systems

from the detector elements to the long data link

Trigger Algorithms and Architectures

prompt and higher-level triggers

Architecture, Data Flow, Event Building, Online Processing, and Data Storage

from the long data link to mass storage

Project Management

including coordination and planning, design tools,

and interaction with industry

Task Force on Electronics, Triggering, and Data Acquisition at the SSC

Steering Committee

Ed Barsotti	FNAL
Bob Downing	Illinois
Fred Kirsten	LBL
Andy Lankford, Chm.	SLAC
Jon Thaler	Illinois
Yoshiyuki Watase	KEK

TRIGGER REQUIREMENTS FOR SAMPLE PHYSICS PROCESSES

FROM GILCHRIESE AT TORONTO WORKSHOP '89

PHYSICS EXAMPLE	TRIGGER INGREDIENTS
$Q^* \to g Z \to \text{jet} + Z$	$E_T \gtrsim$ TeV ("Z")
$Q^* \to g g$ (via change in $\not{E}_T$)	$E_T \gtrsim$ [illegible] TeV
$W' \to \ell^\pm \nu$, $Z' \to \ell^+ \ell^-$ $\}\ \ell = e, \mu$	$\ell^\pm$ w/ $p_T \gtrsim 100$ GeV
$H \to Z Z \to \ell^+ \ell^-$	$\ell^+ \ell^-$ or "Z"
$H \to W W$, $W \to \ell \nu$, $W \to$ jets	$\ell^\pm$ w/ $p_T \gtrsim 50$ GeV $\not{E}_T \gtrsim 50$ GeV (jets)
$pp \to H V$, $H \to \ell \nu$, $V \to$ jets	$\not{E}_T$ [illegible] GeV $\ell^\pm$ w/ $p_T \gtrsim$ [illegible] GeV multijets w/ $p_T \gtrsim$ [illegible] GeV $\ell^\pm$ w/ relative p_T [illegible] GeV
$pp \to D \bar{D}$, $D \to W^+ \bar{t}$, $D \to W^- t$, $W^- \to b e^+ \nu$, $W^- \to e \nu$	$2\ \ell^\pm$ $p_T \gtrsim 40$ GeV $\not{E}_T \gtrsim 100$ GeV total jet $E_T \gtrsim 75$ GeV (multijets w/ $p_T \gtrsim 20$ Ge[illegible]

$\Rightarrow$ MEASURE: E_T, $\not{E}_T$

IDENTIFY, MEASURE, COUNT: jets, $e^\pm$, $\mu^\pm$, γ

Channels :

assume heavy top → BR

(Au): $ZZ \to e^+e^-/\mu^+\mu^- + e^+e^-/\mu^+\mu^-$ $4.7 \cdot 10^{-3}$

(Ag): $ZZ \to e^+e^-/\mu^+\mu^- + \bar{\nu}\nu$ .028

(Cu): $W^+W^- \to e\nu/\mu\nu + ud/cs$ .30

&

(Au): $W^\pm Z \to e\nu/\mu\nu + e^+e^-/\mu^+\mu^-$ .015

(Au_{BK}): $W^+W^+ \to e^+\nu/\mu^+\nu + e^+\nu/\mu^+\nu$ .049

$\Longrightarrow$ high p_T lepton & $\not{E}_T$ triggers

Trigger Procedure a la Snowmass '86

for leptonically decaying W from Higgs w. $m_H > 200$

1) $E_t^{cell} > 25$ GeV (80 % EM)

2) $p_T^{miss} > 40$ GeV

3) surrounding 5 cells contain < 20% of energy of central cell = isolation

4) 1 jet with $E_T > 80$ GeV

or ($\Delta R_{jet} \simeq 1.5$)

2 jets each with $E_T > 40$ GeV

$\Rightarrow$ 1 Hz — the first trigger 1) alone

$\Rightarrow$ 30 Hz still

Mixed Decays

Problem: $\sigma(W + \text{jets}) \simeq 100\ \sigma(\phi^0 \to W\ W_{\hookrightarrow \text{jets}})$
$[m_{\text{jets}} \simeq m_W]$

To overcome, need one or more pieces of additional info from final state.

a) W jet characteristics

b) multiplicity of (charged) hadrons

c) spectator jets

For triggering, primary question is whether lepton trigger on leptonically decaying W (Z) is sufficient to write to tape (30 Hz?) — if so then simply write enough info to analyze a) b) + c) above. Additional fast triggers might also be useful to review physics

Note: for basic lepton trigger, <u>isolation</u> of lepton provides additional discrimination against 'backgrounds' such as heavy quark jets

Note: need hermetic detector ($|\eta|$ to 5 or so) to reconstruct leptonically decaying W

Low Mass b) $W + \phi^0$ Looking better as $m_t \uparrow$

$\hookrightarrow b\bar{b}$

Down to $m_{\phi^0} \gtrsim 50$ GeV?

Triggering (require vertex detector)

demand i) $p_T^W \geq 50$ GeV means p^ℓ from W down to ~20 GeV + good p_T^{miss} measurement

how many Hz here? > 30 Hz?

ii) two energetic jets in $|y| < 2.5$

iii) one jet have lepton ℓ with p_T^ℓ (rel to j) $\gtrsim 1$ GeV.

iv) both jets have $\Delta R < .2$

v) ℓ: 50 micron distance in transverse plane from primary vertex

vi) another 50 micron vertex

vii) $\vec{p}_W$ (reconstructed) + $\vec{p}_T^{\,\phi^0}$ back-to-back within 23°

m_{ϕ^0}	60	80	100	120
S	760	410	377	260
B	2100	2100	2100	2100

$m_{\phi^0} \gtrsim m_Z$?

Background Rate Calculation

- Generator : ISAJET (V6.21)

  QCD TWOJET

  P_T : 5 ~ 200 GeV (6 STEP) 1500 ev

  y : −5 ~ 5 ↑ limited stat.

  $\sigma = 61$ mb

- CALORIMETER : Simple Simulation 'CASIM'

  { Energy sharing between Seg.
  EM tower info

  (No hadron shower in EM.)

SEGMENTATION : $\Delta y \times \Delta\phi = 0.15 \times \frac{2\pi}{32}$

(our standard) (Cf : CDF $0.2 \times \frac{2\pi}{24}$)

CENTRAL : $|y| < 1.5$

ENDCAP : $1.5 < |y| < 3.0$

FORWARD : $3.0 < |y| < 5.0$

(const. Δy ··· not realistic for FORWARD)

RESOLUTION : { EM $\frac{\Delta E}{E} = \frac{15}{\sqrt{E}}$ %

HAD $\frac{\Delta E}{E} = \frac{50}{\sqrt{E}}$ %

- Considered Calorimeter Info. (simple...)

  ET_TOT : total sum of E_T

  ET_MISS : total missing E_T

  E_T_e/γ : E_T of tower with HAD < 0.2× EM

  ET_CLS : E_T of tower (no overlap)

  (E_T_JET : Jet clustering GETJET
  E_{OT} = 5 GeV ΔR = 0.5)

EFFECT of Resolution

(EM, HAD) = (15, 50%) → (30, 100%)

No significant effect.

EFFECT of Segmentation

$\Delta y \times \Delta \phi = 0.15 \times \frac{2\pi}{32} \longrightarrow 0.3 \times \frac{2\pi}{16}$

No significant effect

except ET_CLS

- EFFECT of PILE UP (Event overlap)

  Superimpose QCD TWOJET events according to POISSON dist.

  1) Av = 1.5 interactions

     Detector : 1 bunch resolution for Trig.

     $L = 10^{33}$ cm^2/sec

  2) Av = 10 interactions

     ~ 6 bunches pileup in Trig.

     (actual pile up is not simulated. simply overlapped onto 1 event.)

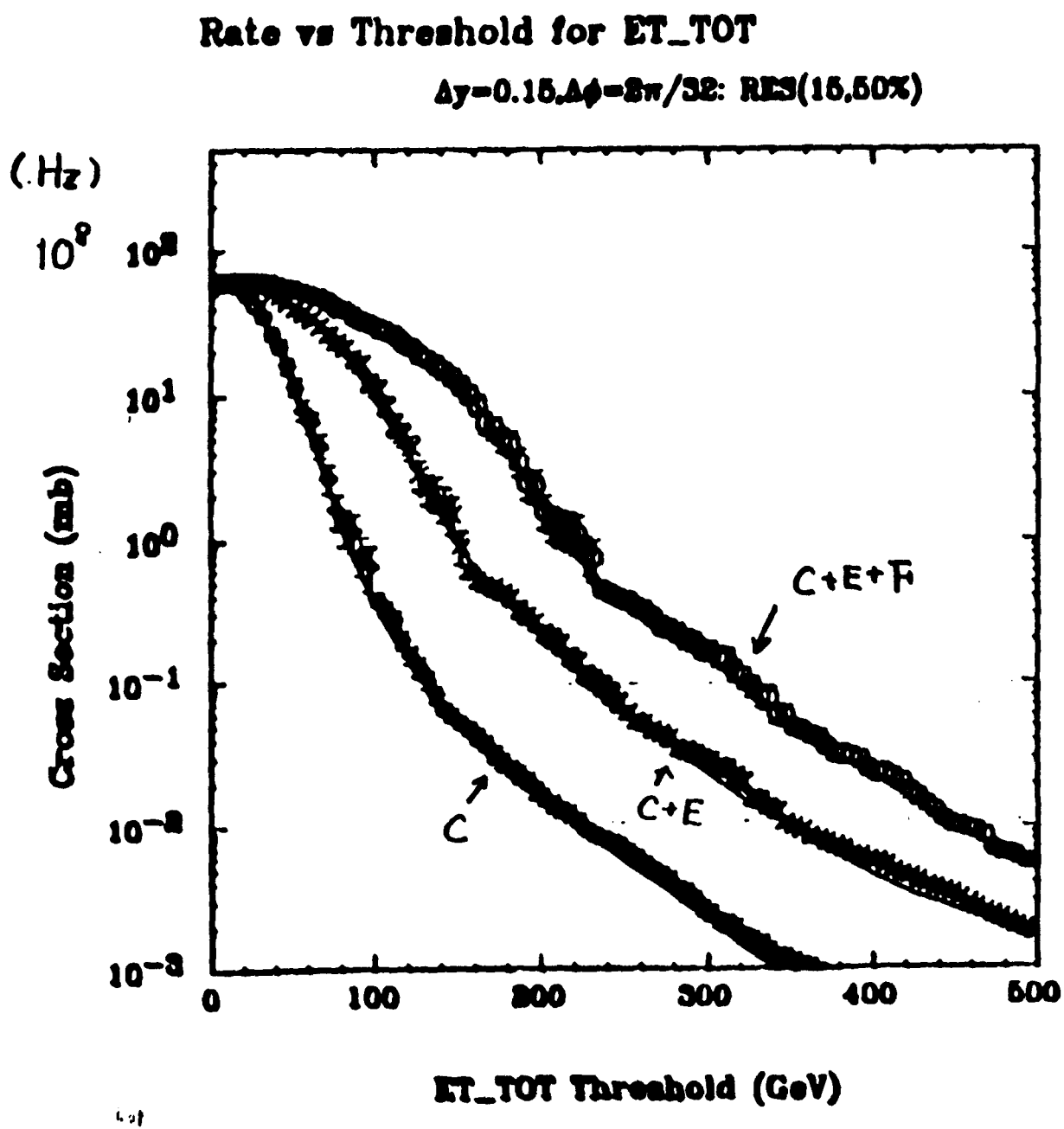

C = CENTRAL

E = END CAP

F = FORWARD

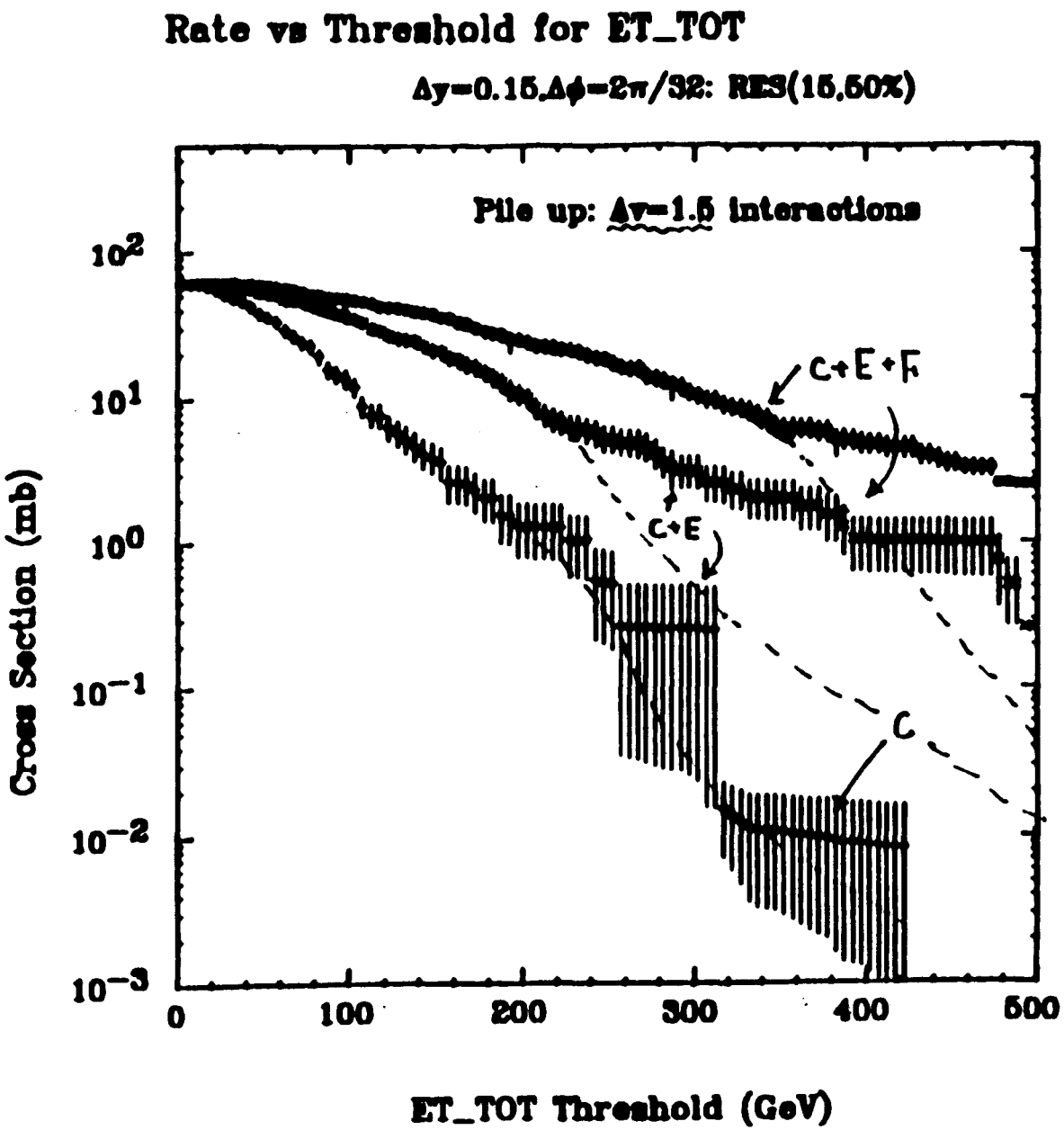
Rate vs Threshold for ET_TOT
Δy=0.15,Δφ=2π/32: RES(15,50%)
Pile up: Δν=1.5 interactions
C+E+F
C+E
C
Cross Section (mb)
10^2
10^1
10^0
10^-1
10^-2
10^-3
0
100
200
300
400
500
ET_TOT Threshold (GeV)

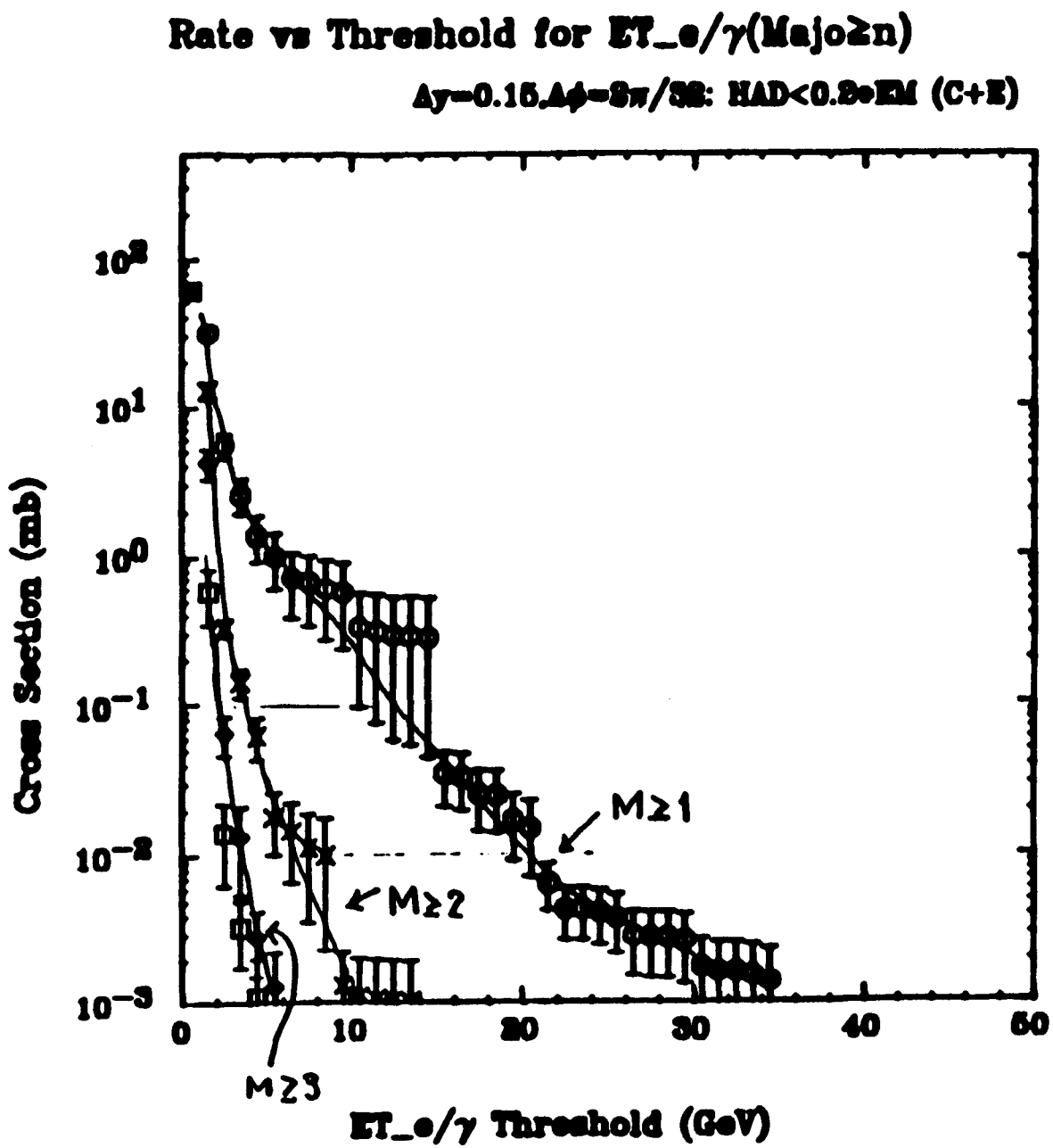
Rate vs Threshold for ET_e/γ(Majo≥n)
Δy=0.15,Δφ=8π/32: HAD<0.2*EM (C+E)
Cross Section (mb)
ET_e/γ Threshold (GeV)
M≥1
M≥2
M≥3

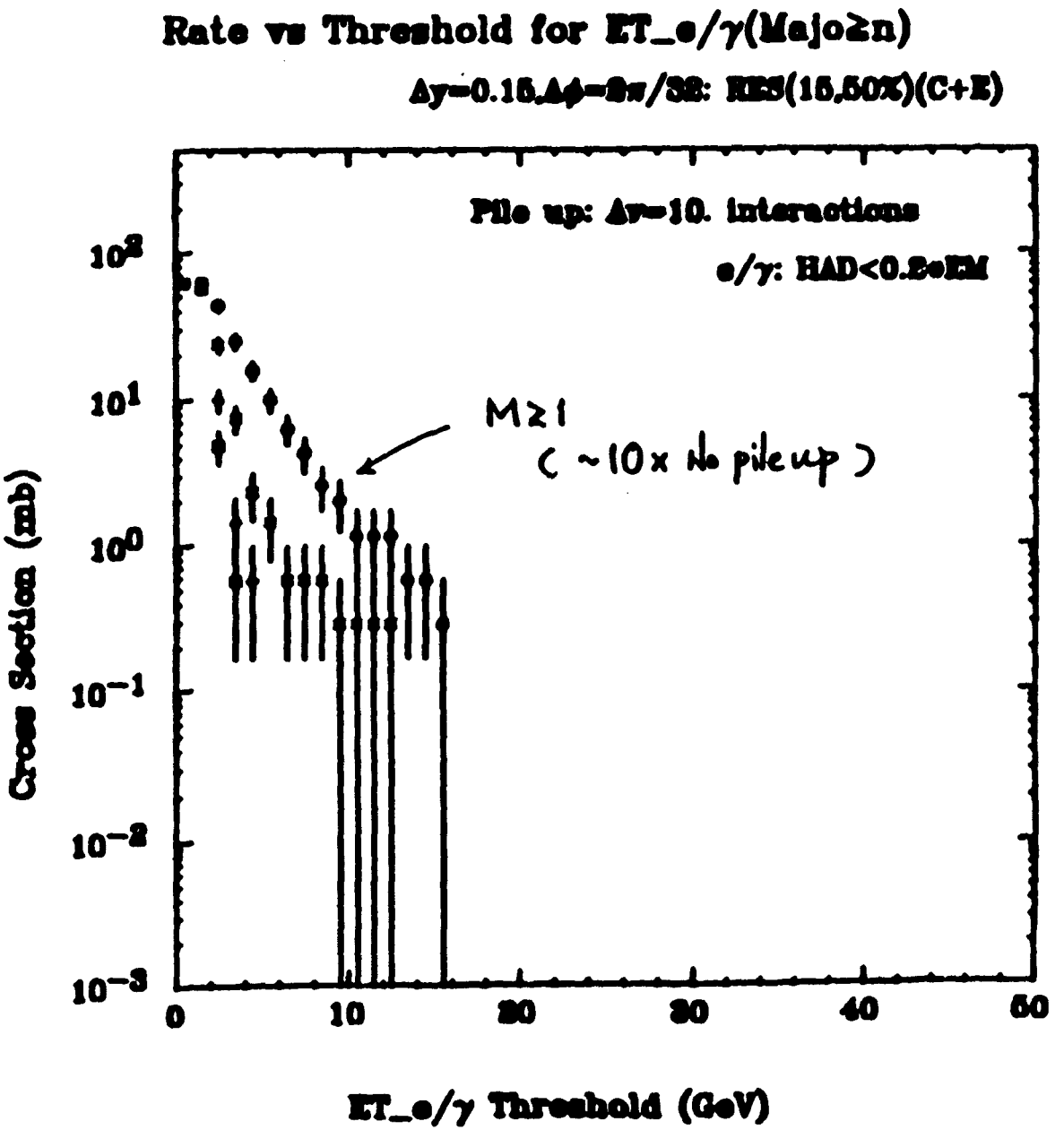
Rate vs Threshold for ET_e/γ(Majo≥n)
Δy=0.15,Δφ=2π/32: RES(15,50%)(C+E)
Pile up: Δν=10. interactions
e/γ: HAD<0.2*EM
M≥1
(~10x No pile up)
Cross Section (mb)
10^2
10^1
10^0
10^-1
10^-2
10^-3
0
10
20
30
40
50
ET_e/γ Threshold (GeV)

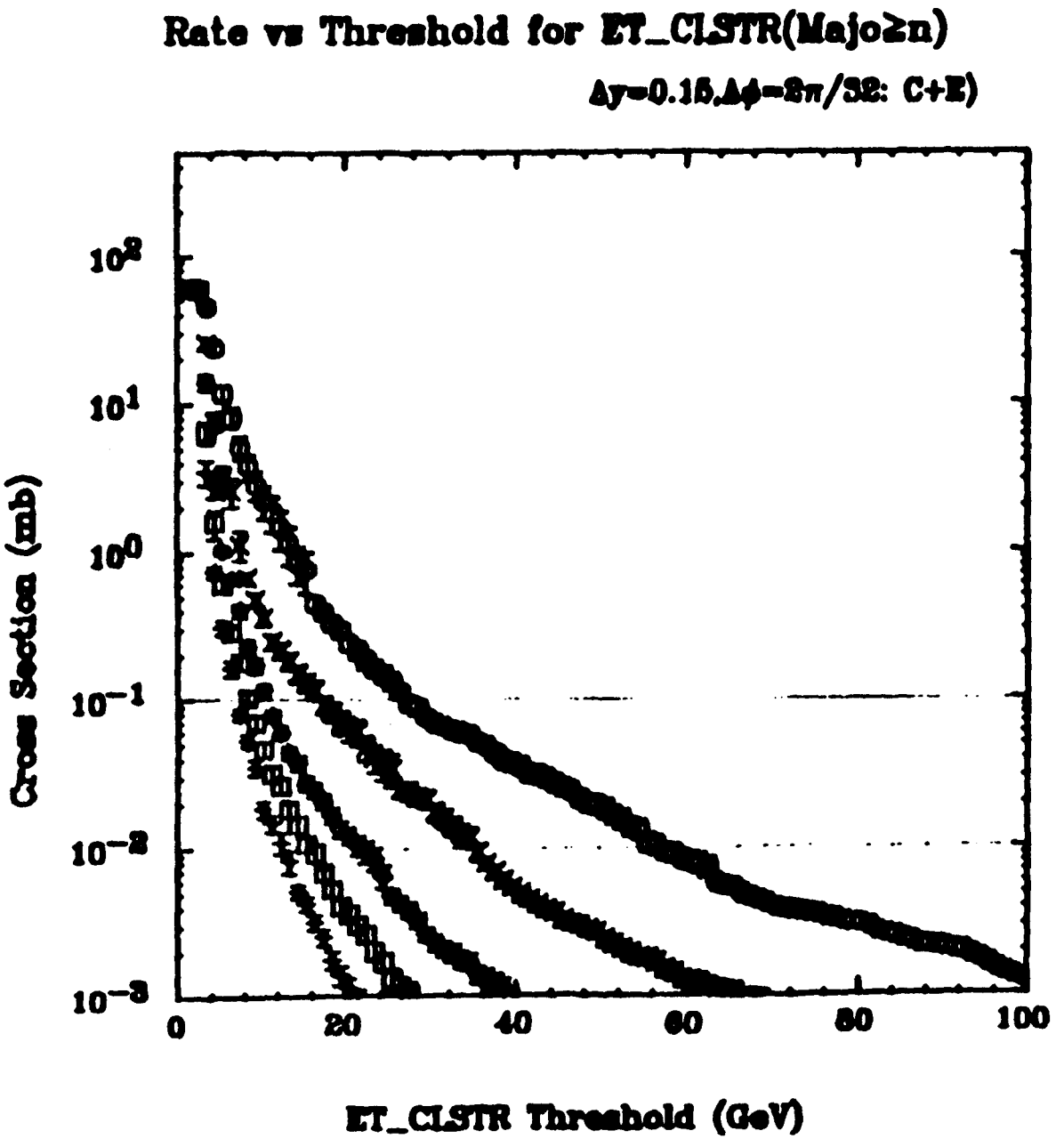
Rate vs Threshold for ET_CLSTR(Majo≥n)
Δy=0.15,Δφ=2π/32: C+E)
Cross Section (mb)
10^2
10^1
10^0
10^-1
10^-2
10^-3
0
20
40
60
80
100
ET_CLSTR Threshold (GeV)

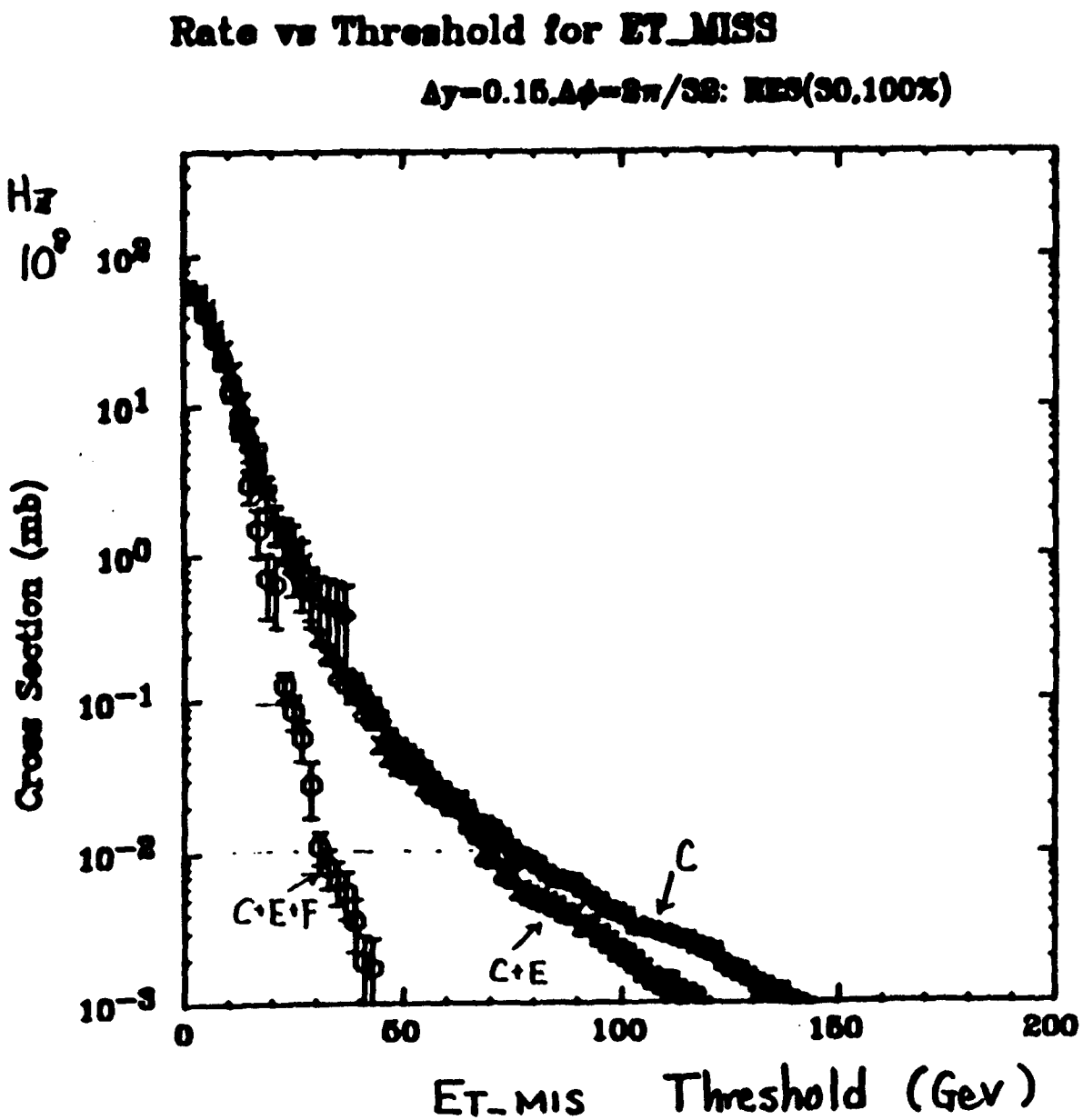
Rate vs Threshold for ET_MISS
Δy=0.15,Δφ=2π/32: RES(30,100%)
Hz
10^6
10^2
10^1
10^0
10^-1
10^-2
10^-3
Cross Section (mb)
C
C+E+F
C+E
0
50
100
150
200
ET_MIS Threshold (Gev)

- Physics Signal

As an example

$p + p \rightarrow H + x$

$\hookrightarrow WW \rightarrow e\nu$ + jets

Generated by ISAJET

$m_H = 400$ GeV

$P_T(W)$: 5 ~ 20,000 GeV

500 events. $B \cdot \sigma = .475$ pb

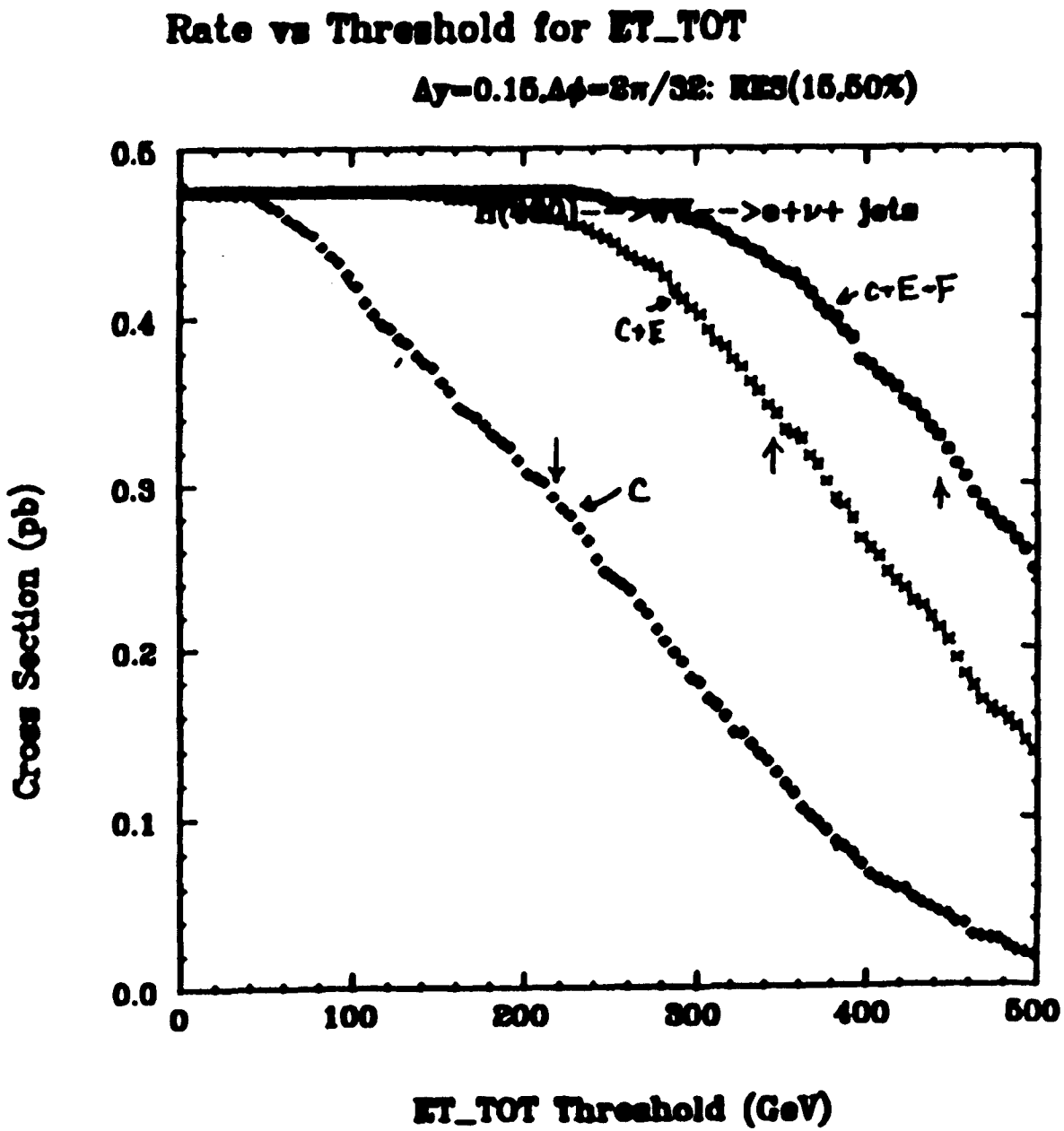
Rate vs Threshold for ET_TOT
Δy=0.15,Δφ=8π/32: RES(15,50%)
H(500)-->WW-->e+ν+ jets
C+E-F
C+E
C
Cross Section (pb)
ET_TOT Threshold (GeV)
0.0
0.1
0.2
0.3
0.4
0.5
0
100
200
300
400
500

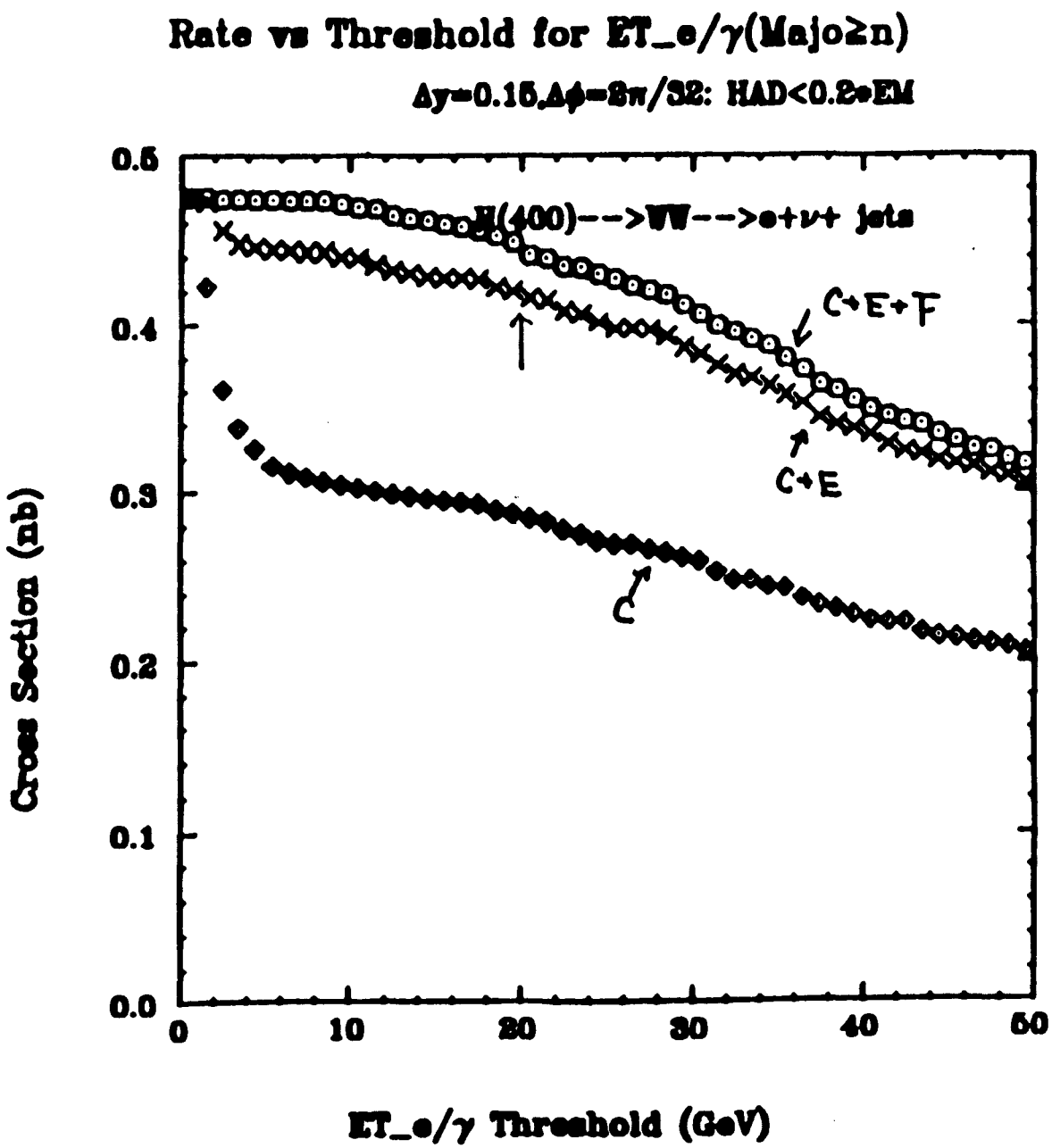
Rate vs Threshold for ET_e/γ(Majo≥n)
Δy=0.15,Δφ=2π/32: HAD<0.2*EM
H(400)-->WW-->e+ν+ jets
C+E+F
C+E
C
Cross Section (nb)
ET_e/γ Threshold (GeV)
0.0
0.1
0.2
0.3
0.4
0.5
0
10
20
30
40
50

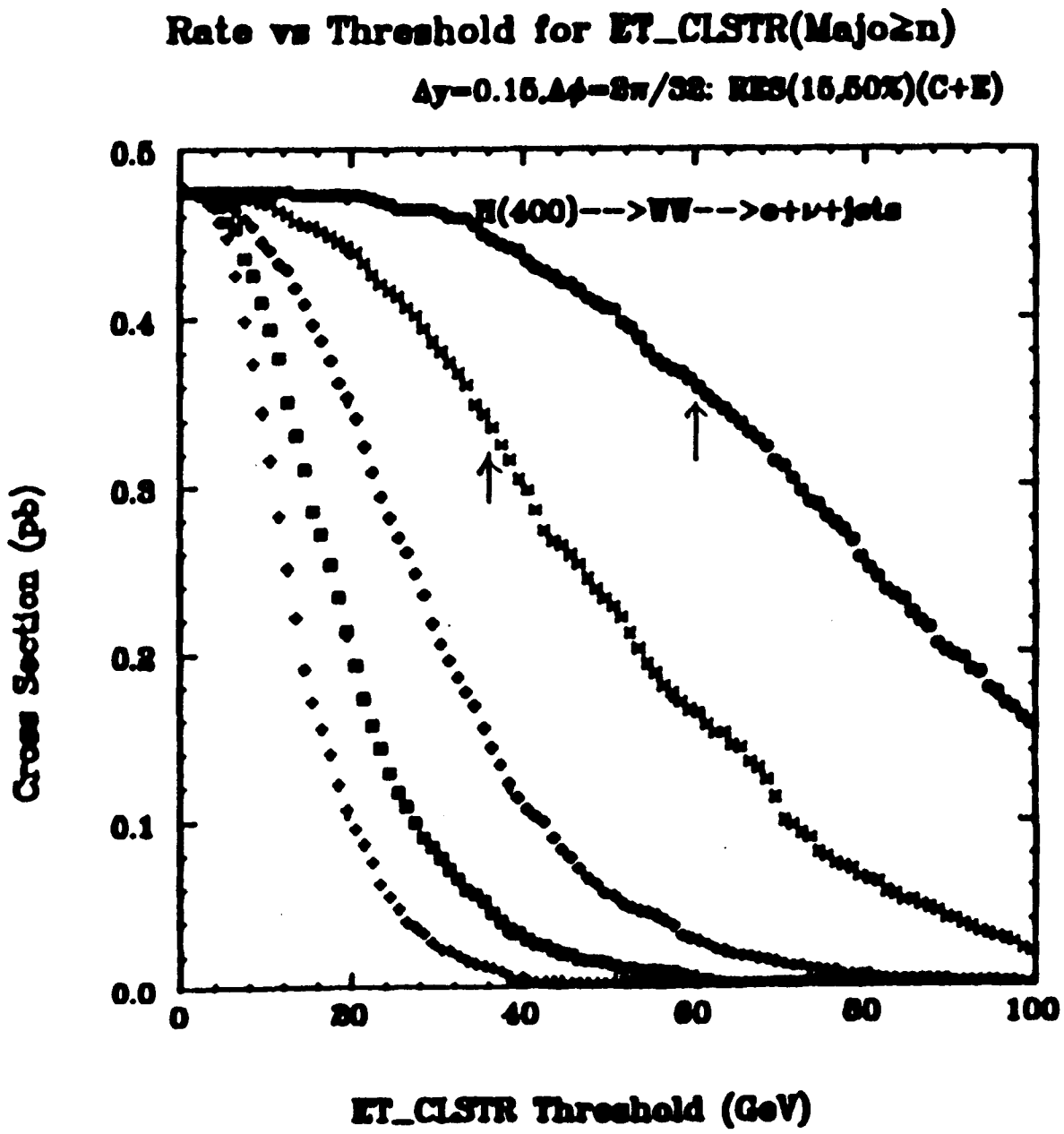
Rate vs Threshold for ET_CLSTR(Majo≥n)
Δy=0.15,Δφ=2π/32: RES(15,50%)(C+E)
H(400)--->WW-->e+ν+jets
Cross Section (pb)
0.0
0.1
0.2
0.3
0.4
0.5
0
20
40
60
80
100
ET_CLSTR Threshold (GeV)

SUMMARY OF 1ST LEVEL CAL TRIGGER STUDY

(Preliminary)

TRIG.		THRES FOR Rate ~10^4 Hz		ε (H→WW→e jets) 400Gev	
		No Pileup	Pileup 1.5 ev		
ET_TOT	CE	~350 GeV	(>500)	~72%	(<55%)
ET_MIS	CEF	~40	No effect	~86	⇐
	CE	~70	〃	~65	⇐
ET_e/γ	M≥1 CE	~20	Small effect ~20	~88	← ~Same
ET_CLS	M≥1 CE	~60	≤70	~74	≥66
(ET_JET	M≥1 CE	~100	(>100)	~72	?

- Pile up effect .... Large { ET_TOT, ET_CLS (if seg. is big)
  - → need to make pileup small.
  - → ~10 pileup is not acceptable (?)
- FORWARD is important for ET_MISS (need more study. crack ?)

(• Seems possible to get 1st level 'General' cal trigger)

FRACTIONAL ENERGY CAPTURE

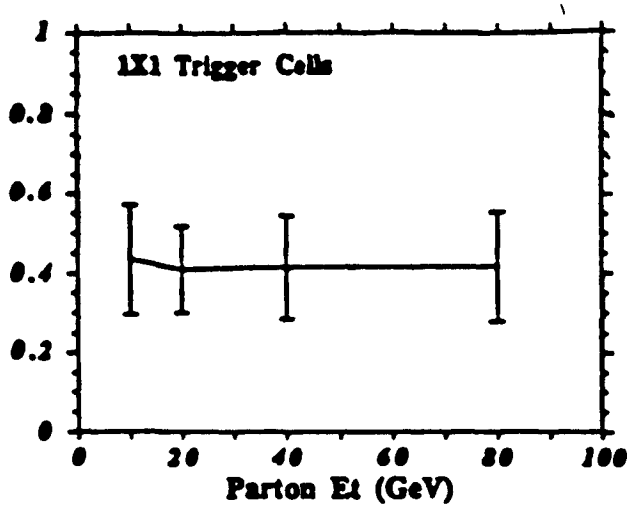

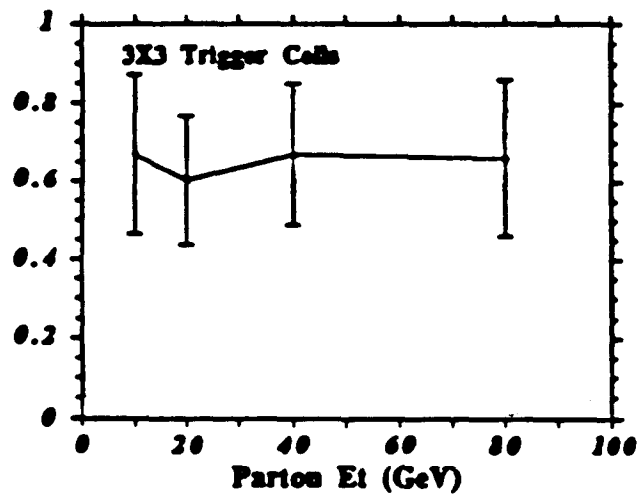

Specific Capture Fraction Dispersion

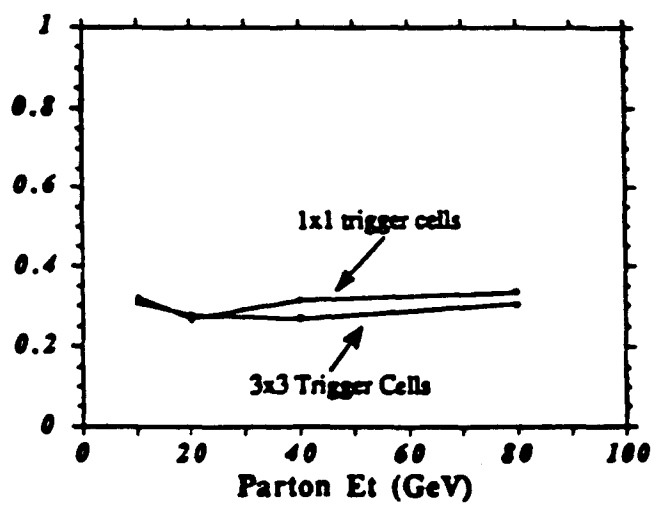

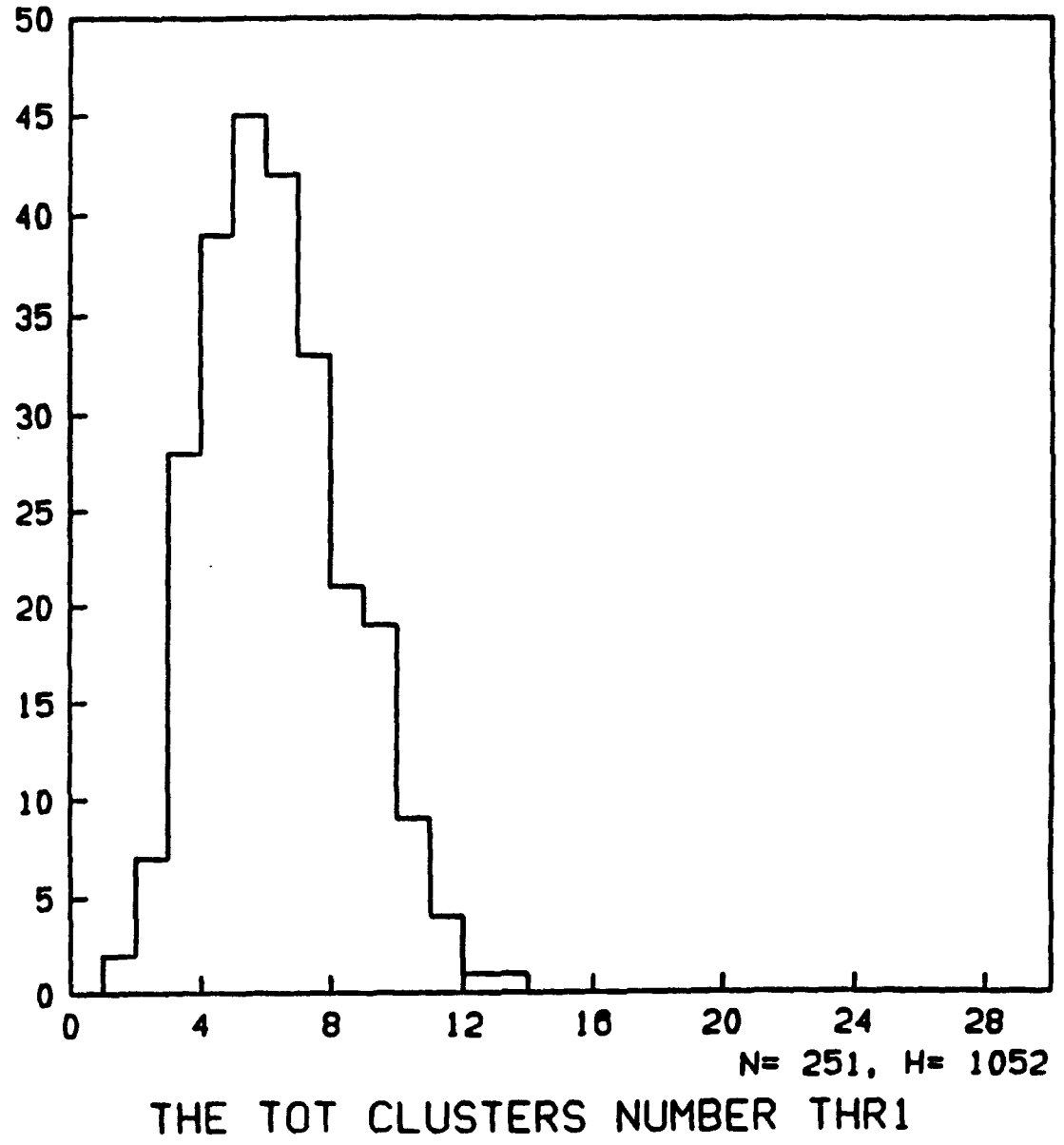

PT20 EVENTS WITH 2GEV THRLD

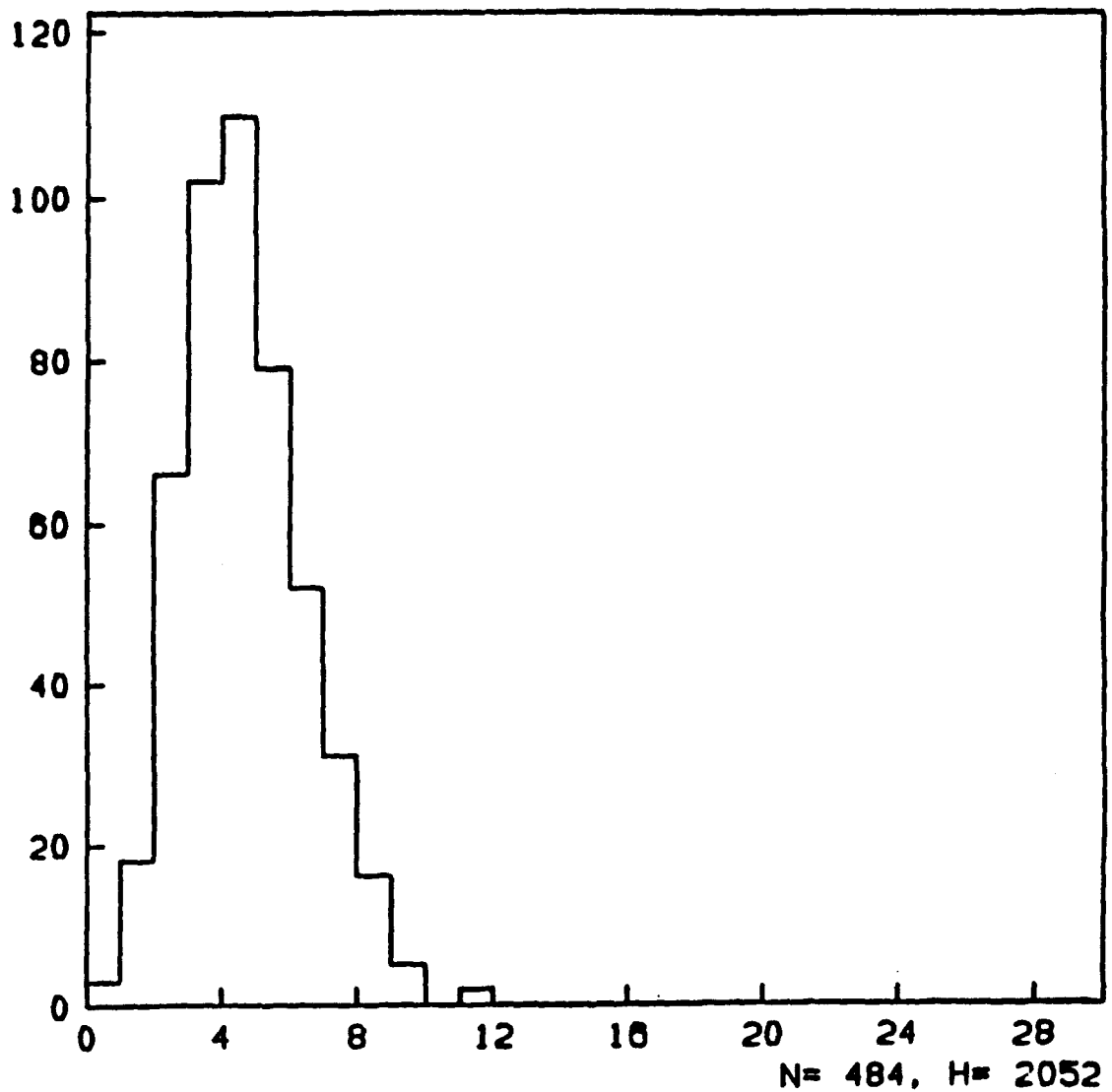

THE TOT CLUSTERS NUMBER THR1

PT40 EVENTS WITH 5GEV THRLD

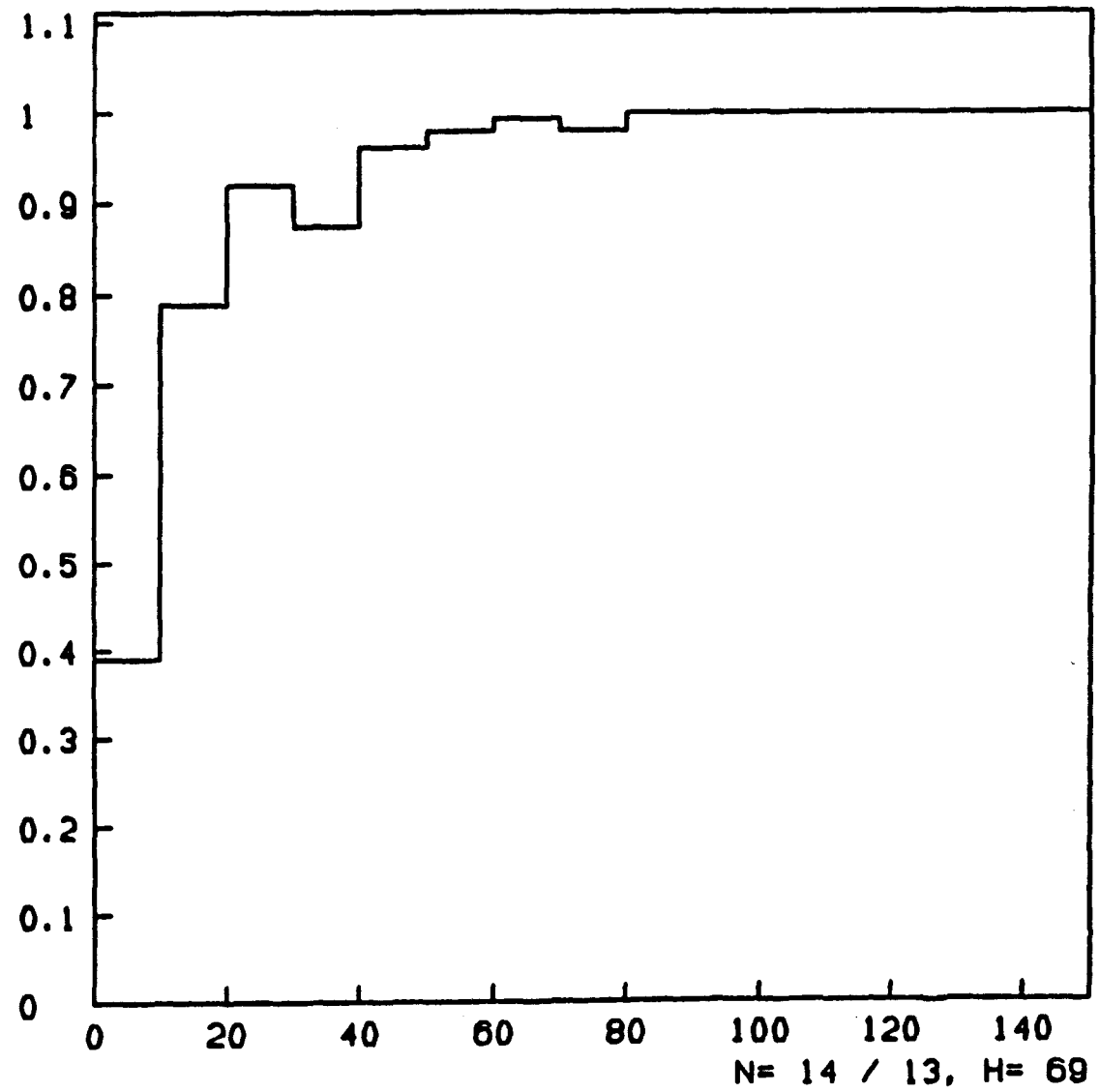

EFF OF SINGLE CORRELATED JETS

Applications of Tracking to SSC Triggers

Electron Triggers

IS SHOWER CHARGED OR NEUTRAL?

TRD LINKED TO SHOWER

$p_t > \xi \cdot E_{cal}$

SEGMENT FINDING MAY BE SUFFICIENT

Recall $p_T > 10$ GeV cut in $H \to WW \to e\nu q\bar{q}$ trigger.

THIS COULD BE PERFORMED BY FINDING A RADIAL SEGMENT IN OUTER SUPER LAYER OF CENTRAL TRACKER IN MAGNETIC DETECTOR.

(DOESN'T REQUIRE FULL TRACKING OR FULL RESOLUTION)

Muon Triggers

FIRST LEVEL TRIGGER NEEDED

$> 15°$ TRIGGER ON TRACK EXITTING MUON SYSTEM WITH MUON SYSTEM SEGMENT POINTING TO VERTEX.
(CUT ON SEGMENT ANGLE ~ p_t CUT)

$< 15°$ RATE REQUIRES p_t CUT $p_t > 10\text{-}15$ GeV

SMALL SAGITTA REQUIRES DRIFT TIME

BUILD TRACK PROCESSOR (SNOWMASS 86)

CAN SEGMENT PROCESSOR INTO TOWERS to minimize ambiguities

CAN IGNORE HIGH MULTIPLICITY PLANES

$\epsilon = 97\%$ FOR AT LEAST 3/5 LOW MULT. PLANES

CHAMBER GEOMETRY CHOSEN FOR CONVENIENCE OF TRACK FITTER

REDUCES Level 1 rate to less than 10^4 Hz

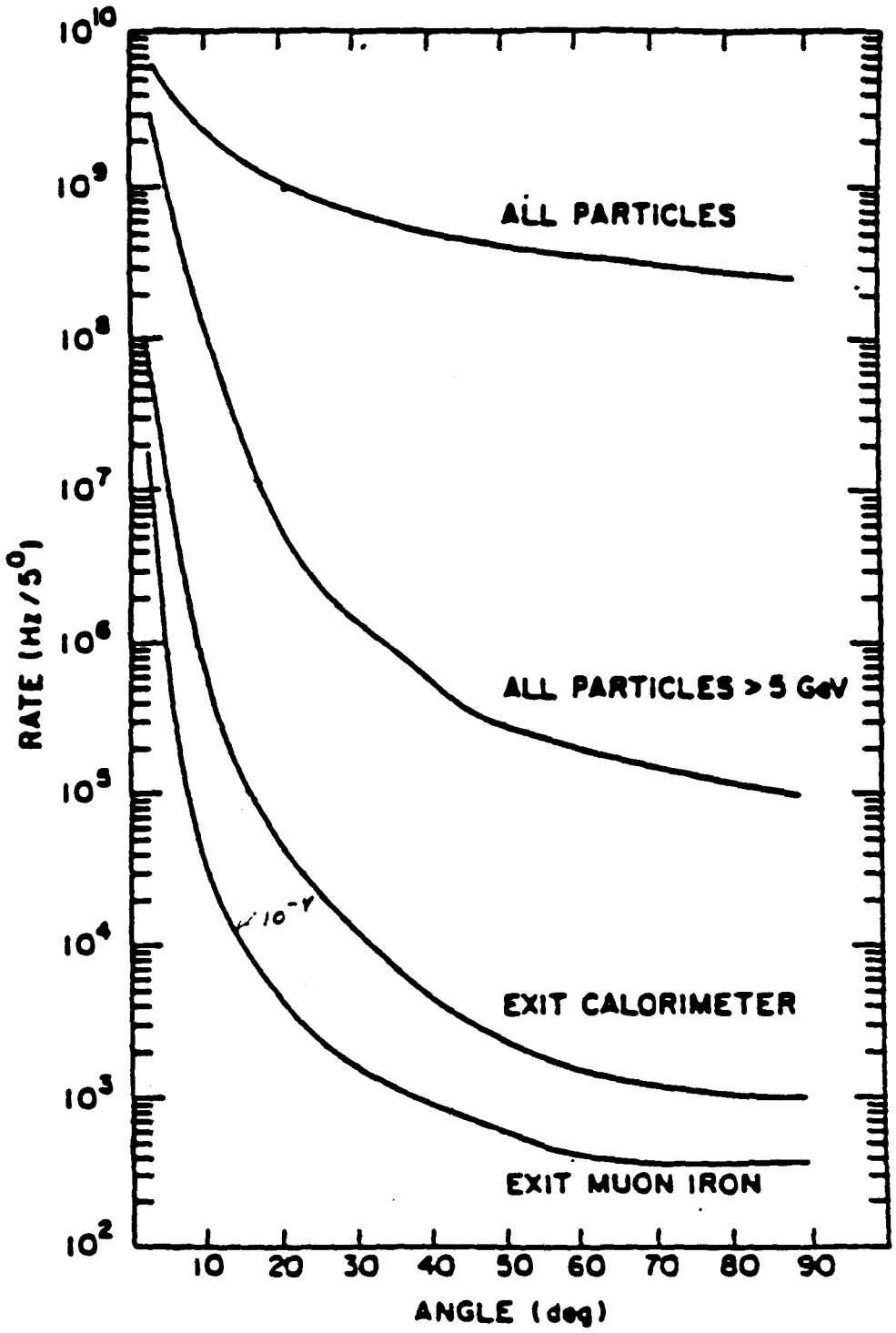

Figure 13
Estimated rates for all particles, particles with $P_t > 5$ GeV, particles exiting the calorimeter, and particles exiting the muon iron.

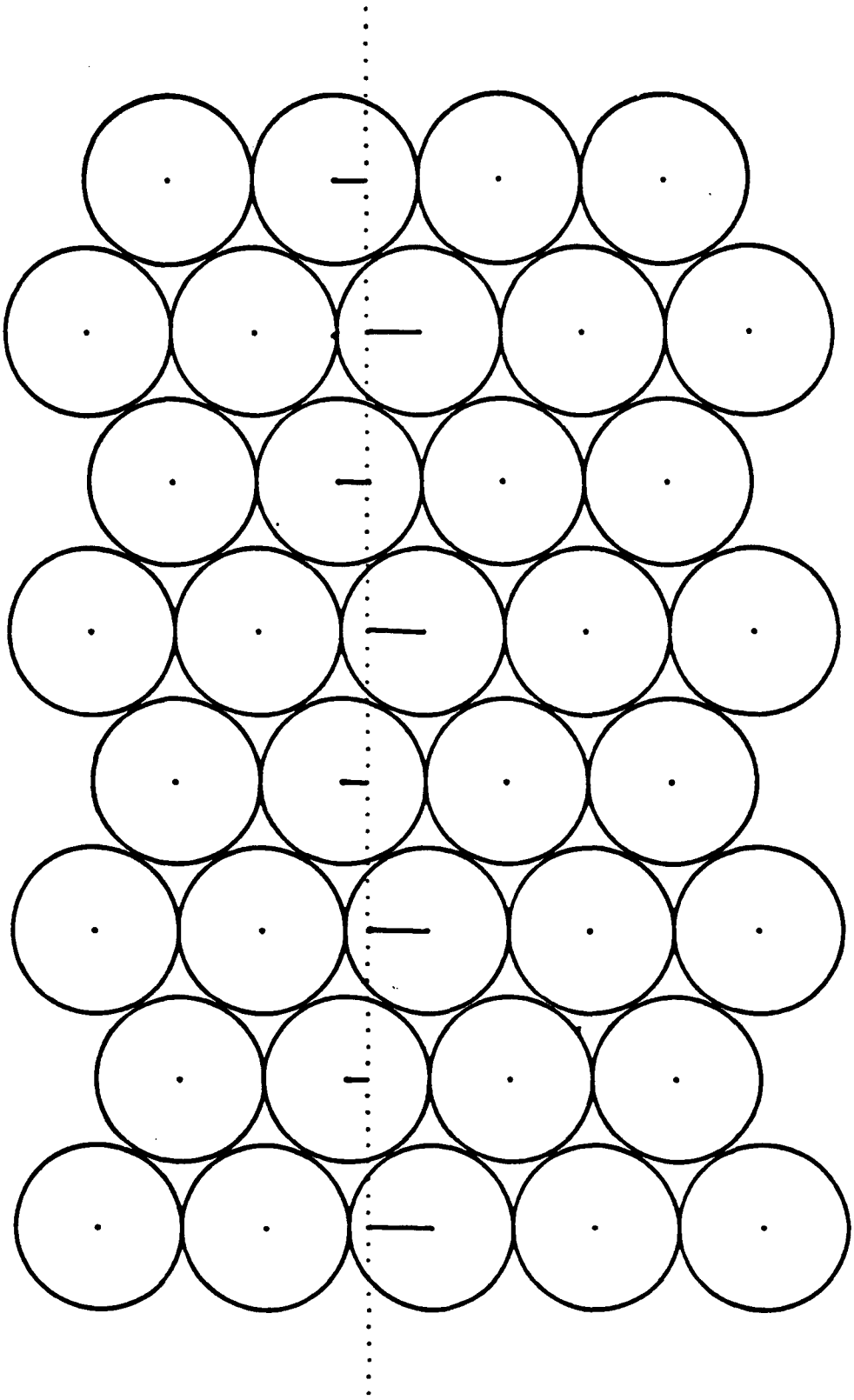

Straw Tubes

Assumes normal incidence
Use 3 of 4 coincidence - $p > 10GeV/c$

$$t_l + t_r = T$$

which for $t_r < t_l$ can be written

$$t_l - t_r + 2t_r = T$$

with the difference being positive.

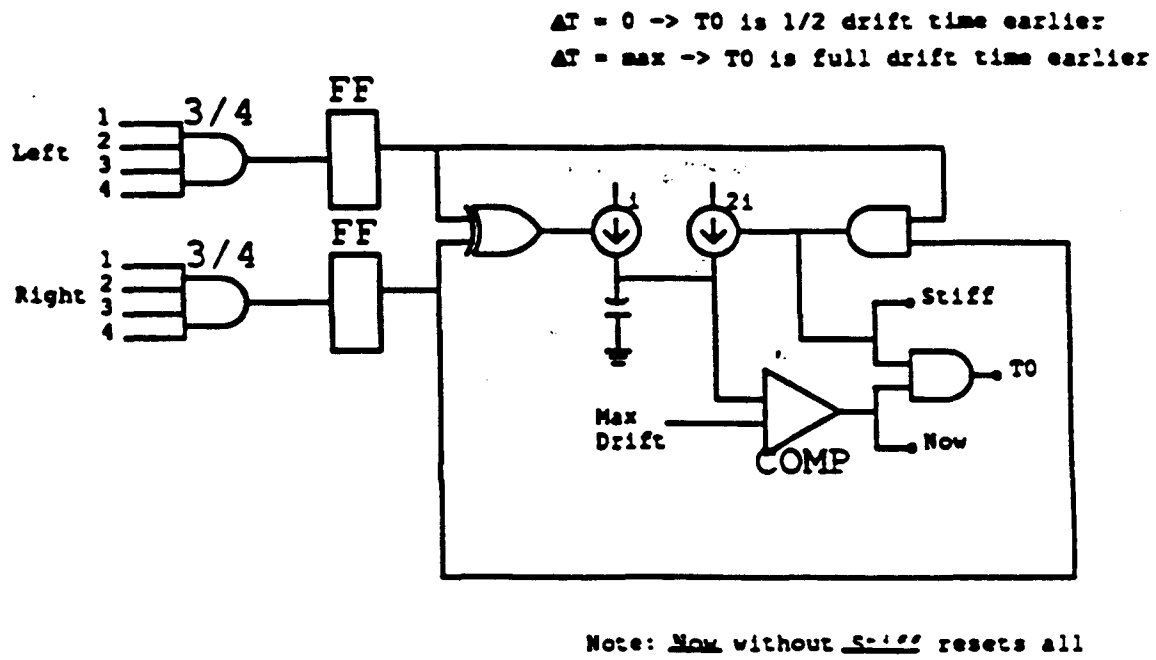

Simplified Stiff Track Finder

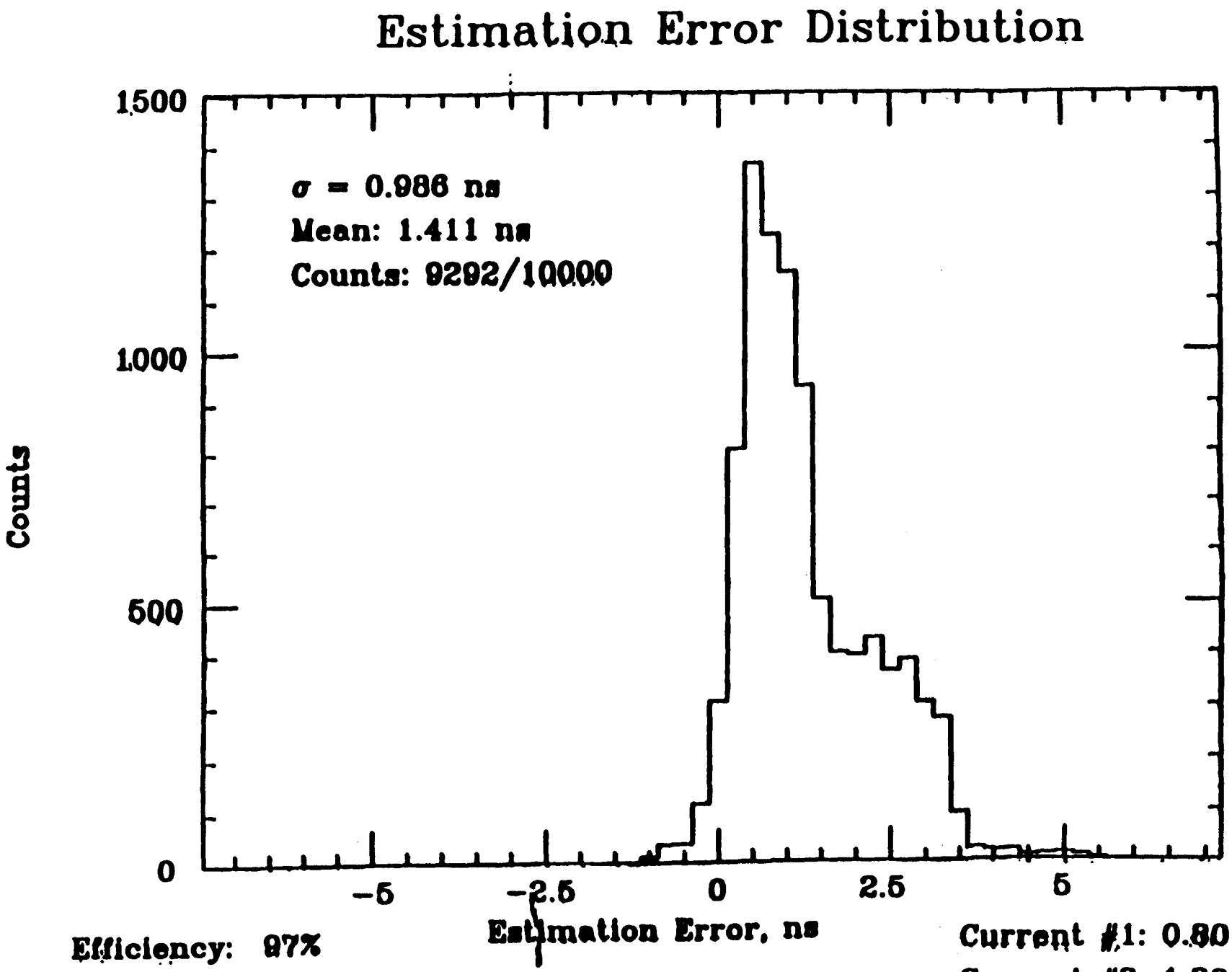

Efficiency: 97%
Noise Rate: 5%
Quadratic: 20%

Figure 3d

Current #1: 0.80
Current #2: 1.80

Tube Triads

$$t_2 + \frac{t_1 + t_3}{2} = T$$

which for $t_1 < t_3 < t_2$ can be written

$$\frac{t_3 - t_1}{2} + t_2 - t_3 + 2(\frac{t_1 + t_3}{2}) = T$$

with the differences being positive.

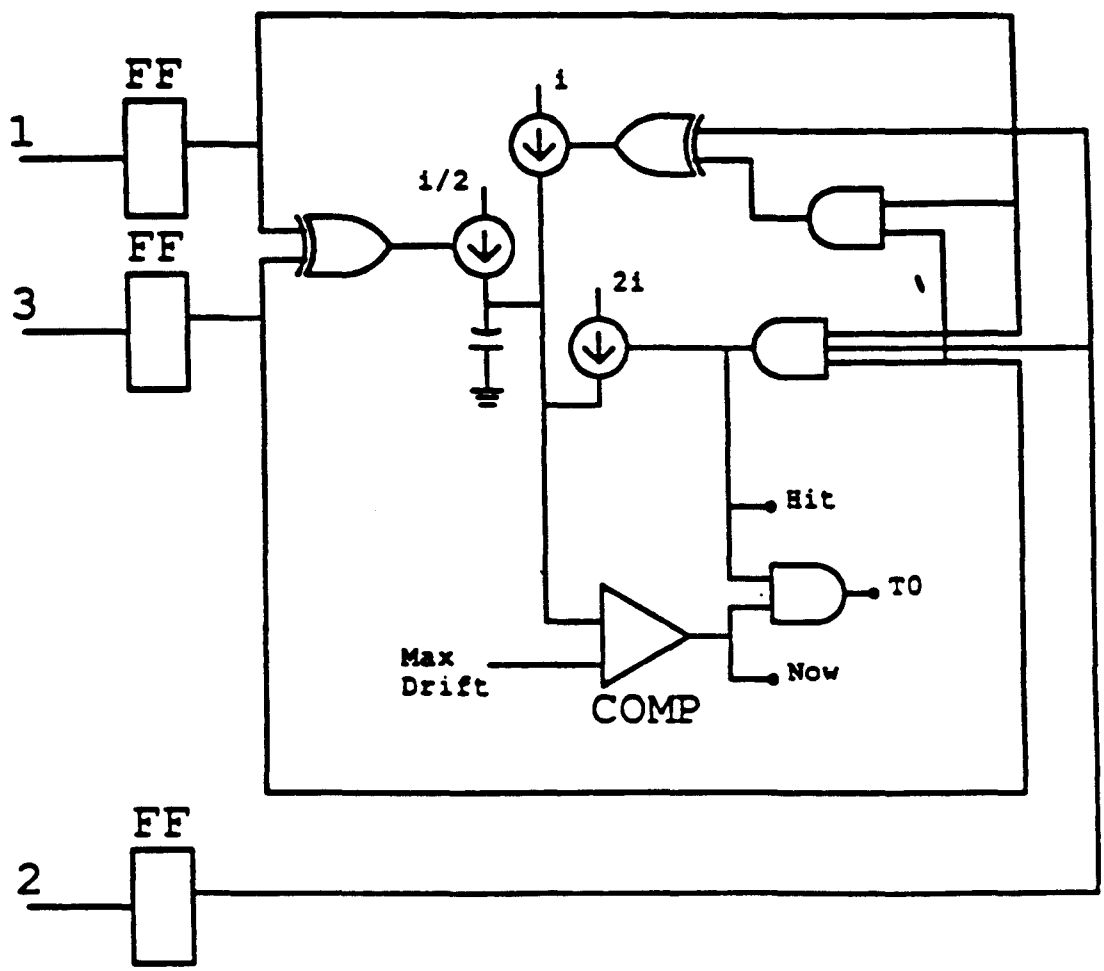

Triad T0 Generator

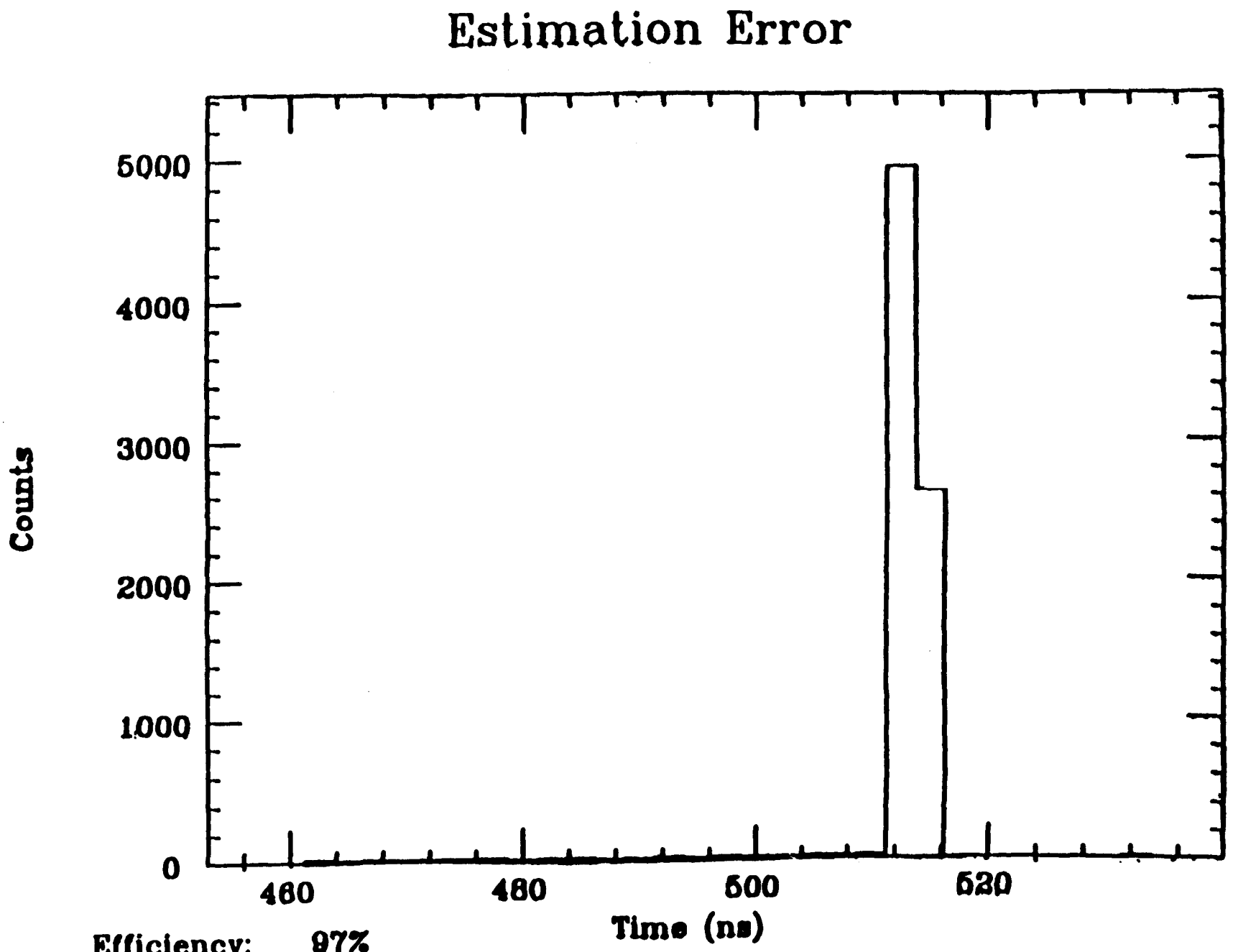

Efficiency: 97%
Nonlinearity: 20%
Random Hits: 5%

Figure 9

RECALL STEPS IN TRACKING

SEGMENT FINDING

TRACK RECOGNITION

TRACK FITTING

VERTEXING

FOR A MINI-JET CHAMBER, OR STRAW CHAMBER WITH SUPERLAYERS, OR SIMILAR SILICON TRACKER.

NOTE THAT LINKING SEGMENTS INTO TRACKS CONSISTS OF CLUSTERING SEGMENTS IN ϕ, curvature SPACE.

HIGHLIGHTS OF SOME TOOLS FOR TRACKING TRIGGER:

MEMORY LOOK-UP

ASSOCIATIVE MEMORY

- 8 address bits × 8 layers ⇒ MLU WITH 2^{64} ENTRIES
  ⇒ GREAT REDUCTION IN MEMORY OVER MLU
- OTHER CONFIGURATIONS POSSIBLE
- GOOD APPLICATION OF CUSTOM VLSI

CDF TRACK FINDER IS AN EXAMPLE OF A PATTERN MATCHING SEGMENT FINDER

FOR $P_t > 3$ GeV ~250 patterns

4-bit address 8 layers

DATA-DRIVEN PIPELINE

- FLEXIBLE STRUCTURE, PROGRAMMABLE TO A LARGE EXTENT.
- THROUGHPUT RESULTS FROM THOROUGH UNDERSTANDING OF TRACKING PROBLEM.
- ALREADY 10^5 VAX EQUIVALENTS
- SUITABLE FOR SILICON COMPILER, EXAMPLE SLD DCU CHIP

FAST, HIGHER-LEVEL LANGUAGE PROCESSORS

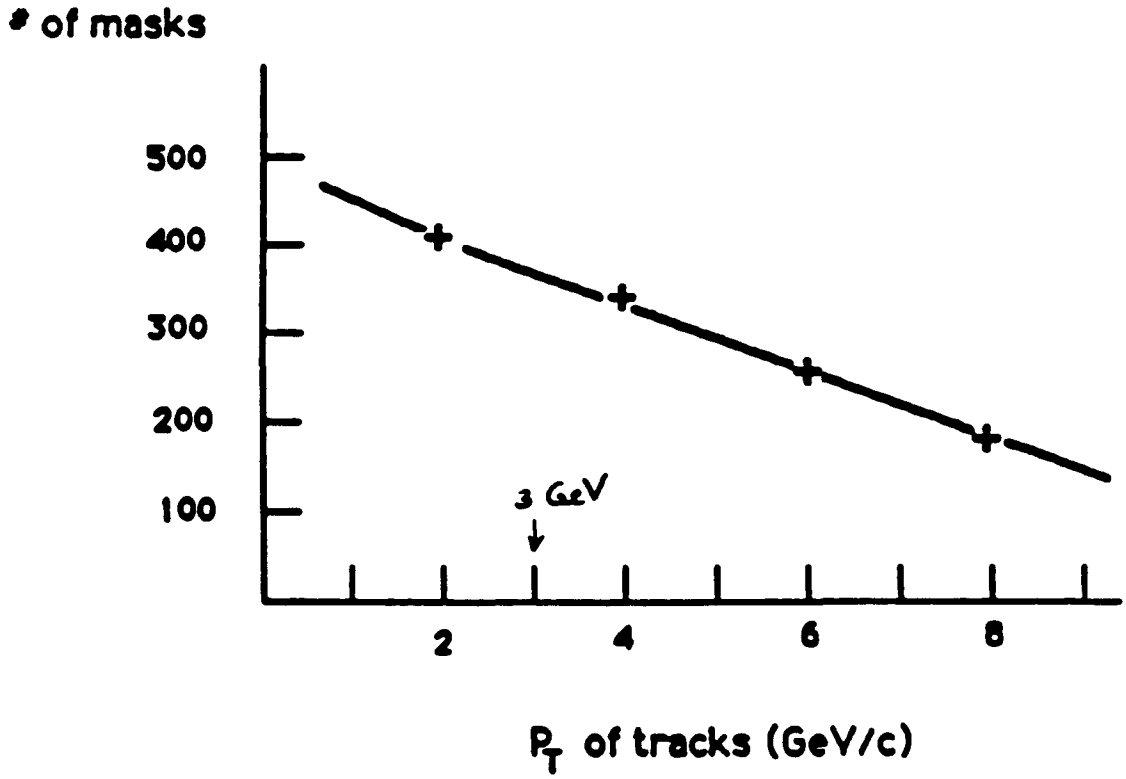

CDF SEGMENT FINDER

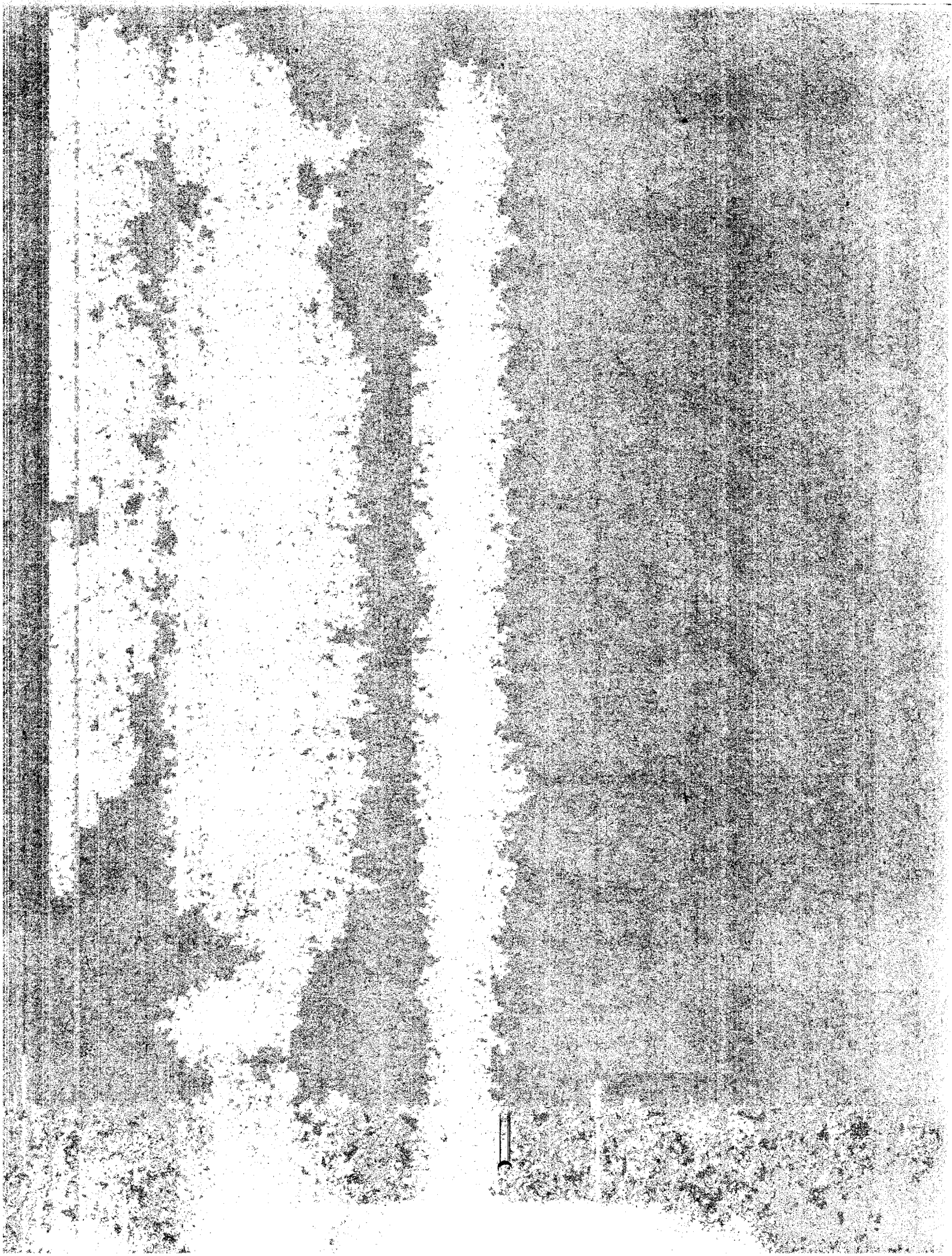

MUON SYSTEM(S)

FOR THE

LARGE SOLENOID DETECTOR

AT THE

SSC

STEVE ERREDE
TONY LISS
JIM WISS

UNIV. ILLINOIS

1.) PHYSICS w/ LEPTONS (e, μ, τ, ν...) IMPORTANT @ SSC??

ANS: YES !! e.g. Heavy Higgs $\to W^+W^-$, WZ, ZZ^0, $t\bar{t} \to \ell^+\ell^-$

$W, Z^0 \to \ell^+\ell^-$, $\to \ell\bar{\nu}_\ell$; $W^+W^- \to e^-\bar{\nu}_e$, $\to \mu^+\nu_\mu$; $ZZ^0 \to \mu^+\mu^-$, $\to e^+e^-$

2.) Nature treats Leptons symmetrically $\Rightarrow$ SSC detector should also

3.) If going to spend $\gtrsim$ 10 yrs and $\$$?? M on building an SSC detector, should do as good a job as possible, to trigger on and measure 4-momentum vectors assoc. w/ e, μ, τ...

$P_4^\ell = (\vec{P}_\ell, m_\ell)$ $\vec{P}_\ell$ = 3-momentum m_ℓ = Lepton ID

4.) MOMENTUM RESOLUTION ISSUES

A. CENTRAL REGION: $\delta P_\perp / P_\perp \lesssim 10\%$ @ 1 TeV/c

CENTRAL TRACKING vs. MAGNETIZED STEEL vs. AIR TOROIDS

— MOMENTUM RESOLUTION DEGRADED BY MUONS' PASSAGE THROUGH EM + HADRON CALORIMETER, + STEEL:

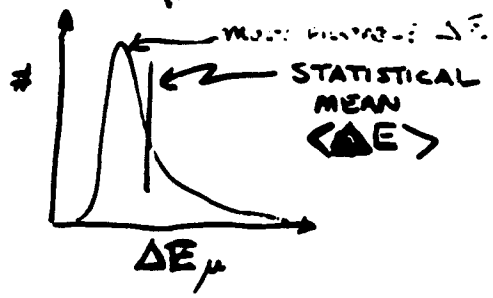

USE $\Upsilon, Z^0, Z^{0\prime} \to \mu^+\mu^-$ CALIBRATION OF MOMENTUM SCALE TO $\lesssim 0.1\%$ @ SSC:

— MEASURE $\vec{P}_\mu$ WITH HIGH RESOLUTION IN SOLENOIDAL FIELD CENTRAL TRACK CHAMBER BEFORE MULTIPLE SCATTERING IN CALORIMETER

— MEASURE $\vec{P}_\mu$ IN RETURN YOKE FOR REDUNDANCY

— IMPROVE REJECTION AGAINST PUNCHTHROUGH

CDF PRELIMINARY

LOW MASS DIMUONS

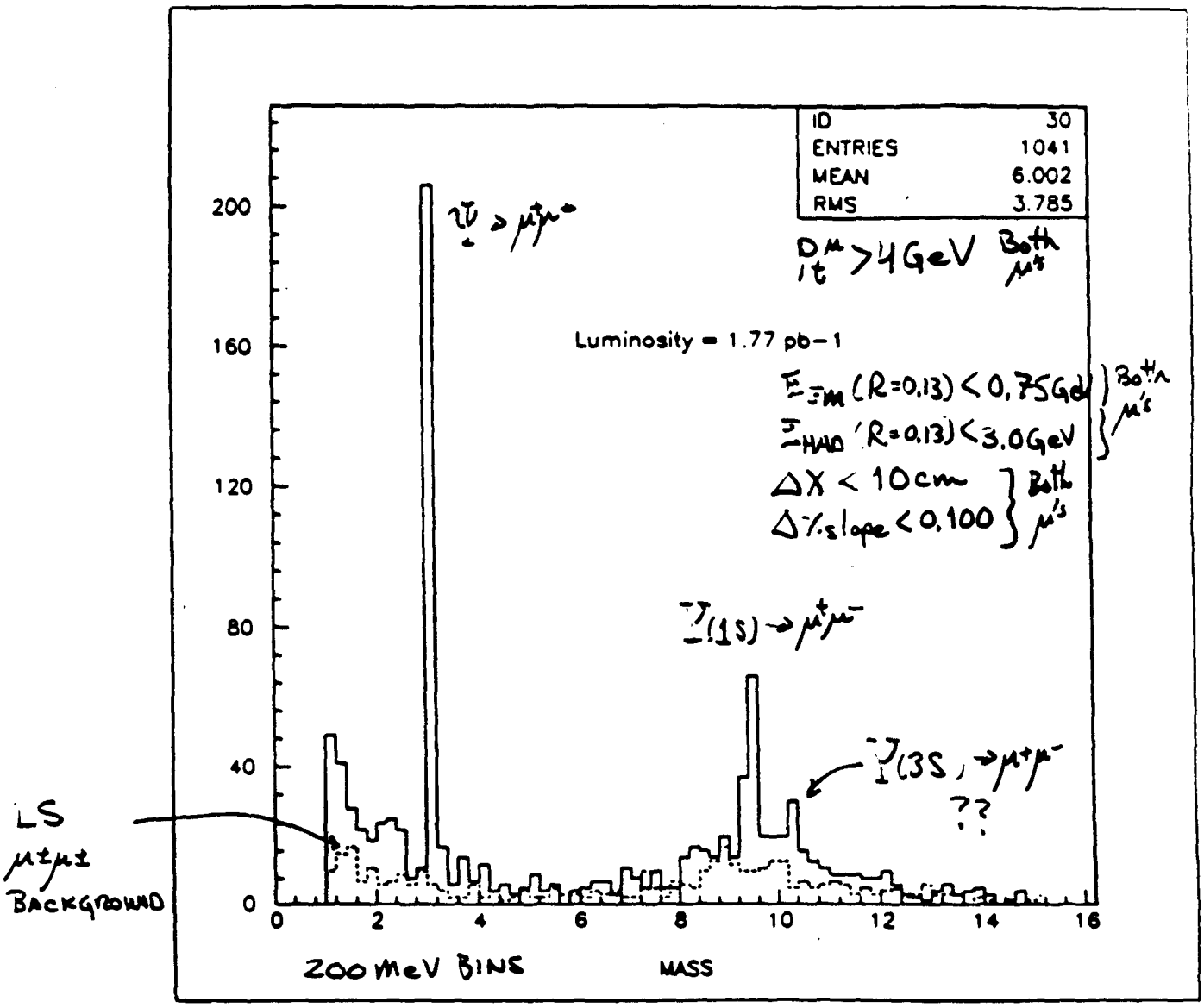

CDF PRELIMINARY

PSI INVARIANT MASS

$\Psi \to \mu^+\mu^-$

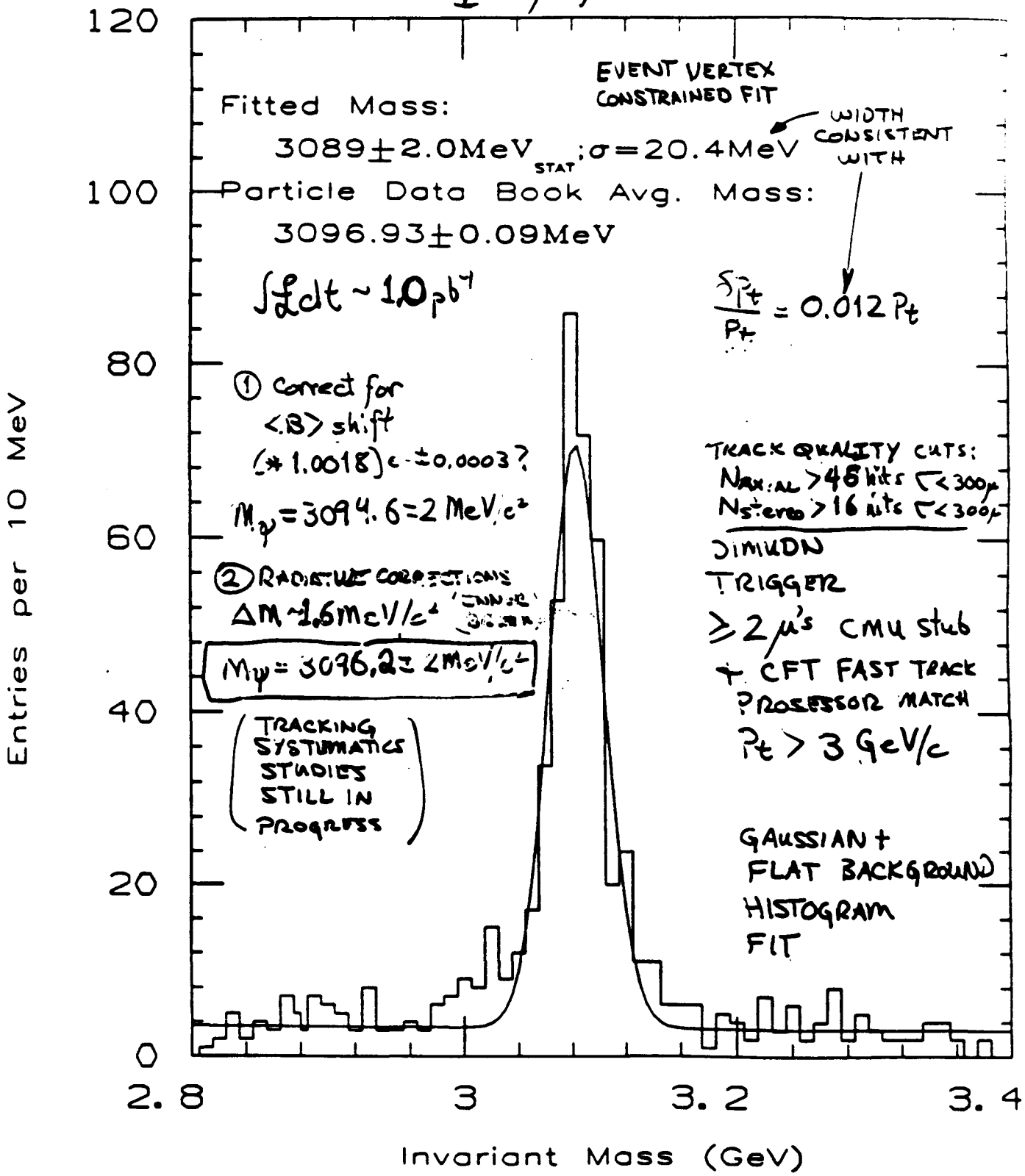

Run 17988 Event28732 C$HDHT:PSI.RET 4DEC88 5:43:34 29JAN

Pt	PHI	COT
5.7	231	0.8
-5.3	262	0.3
-1.8	62	0.6
1.6	89	0.9
-1.1	335	-0.1
-0.8	160	-0.1
0.4	310	-0.1
-0.4	114	-1.0
0.4	336	-1.0
0.4	314	0.2
-0.3	277	-1.9
0.2	279	

Ems = 3.1 GeV

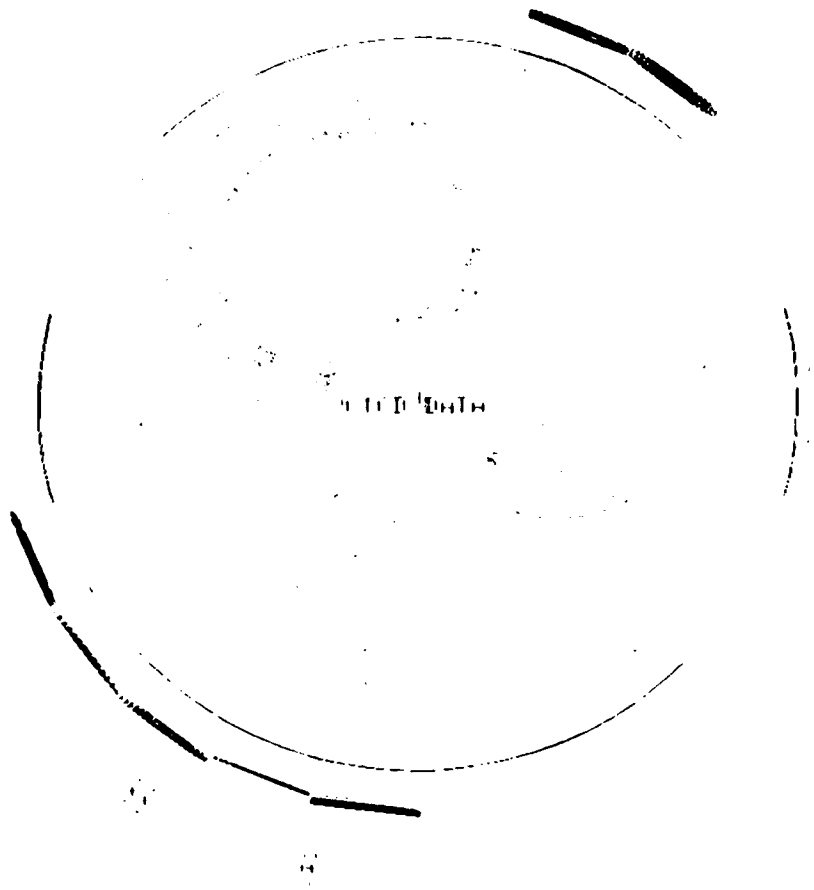

Calorimeter Energy Scale

- Use 1.4 T magnetic field and tracking chamber as reference (J/Ψ, Upsilon, and cosmic rays calibrate B).

- Energy ≠ momentum due to radiation.

$W \to e \bar{\nu}_e$

E over P distribution

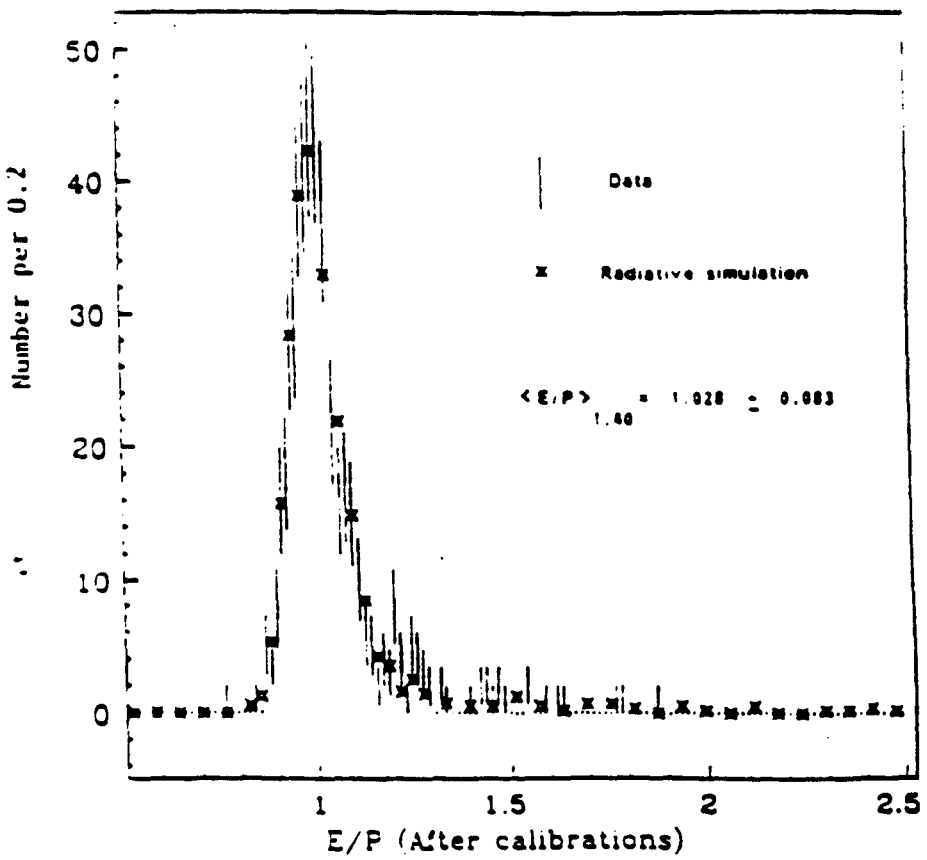

$$E_{true} = (\ 0.98 \pm 0.02\ )\ E_{measured}$$

CENTRAL TRACKING MOMENTUM RESOLUTION

$$\left(\frac{\Delta P_\perp}{P_\perp}\right)^2 = \left(\frac{\epsilon P_\perp}{0.3 \underline{BL^2}}\sqrt{\frac{720}{N+5}}\right)^2 + \left(\frac{0.056}{\underline{BL}\beta}\sqrt{\frac{L}{L_R}}\right)^2$$

BEND TERM:

$$\frac{\Delta P_\perp}{P_\perp} \sim \frac{1}{L^2} \qquad \frac{\Delta P_\perp}{P_\perp} \sim \frac{1}{B}$$

double B, double $\frac{\Delta P_\perp}{P_\perp}$

If <u>double</u> (projected) path length, quadruple $\frac{\Delta P_\perp}{P_\perp}$

MCS TERM:

$$\frac{\Delta P_\perp}{P_\perp} \sim \frac{1}{B} \qquad \frac{\Delta P_\perp}{P_\perp} \sim \frac{1}{\sqrt{L}}$$

SO: MAKE CENTRAL SOLENOID RADIUS LARGER, ~3m

MAKE $\vec{B}_{SOL}$ LARGER (IF POSSIBLE)

MAKE SOLENOID LONGER, FOR LARGER ETA ACCEPTA

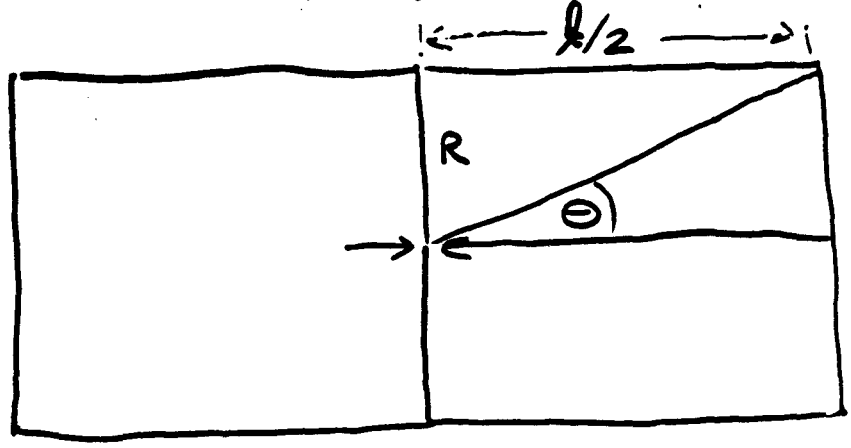

$\tan\theta = \frac{2R}{\ell}$

$\eta = \ln \tan$

$= 1.3$

$R = 3$

$\ell = 10$

B.) <u>FORWARD REGION</u> — USE AIR CORE TOROIDS (AFTER CALOR WHERE TRACKS NO LONGER HAVE FULL RADIAL PATH LENG IN CENTRAL TRACKING. (USEFUL TO HAVE REGION OF OVERLAP)

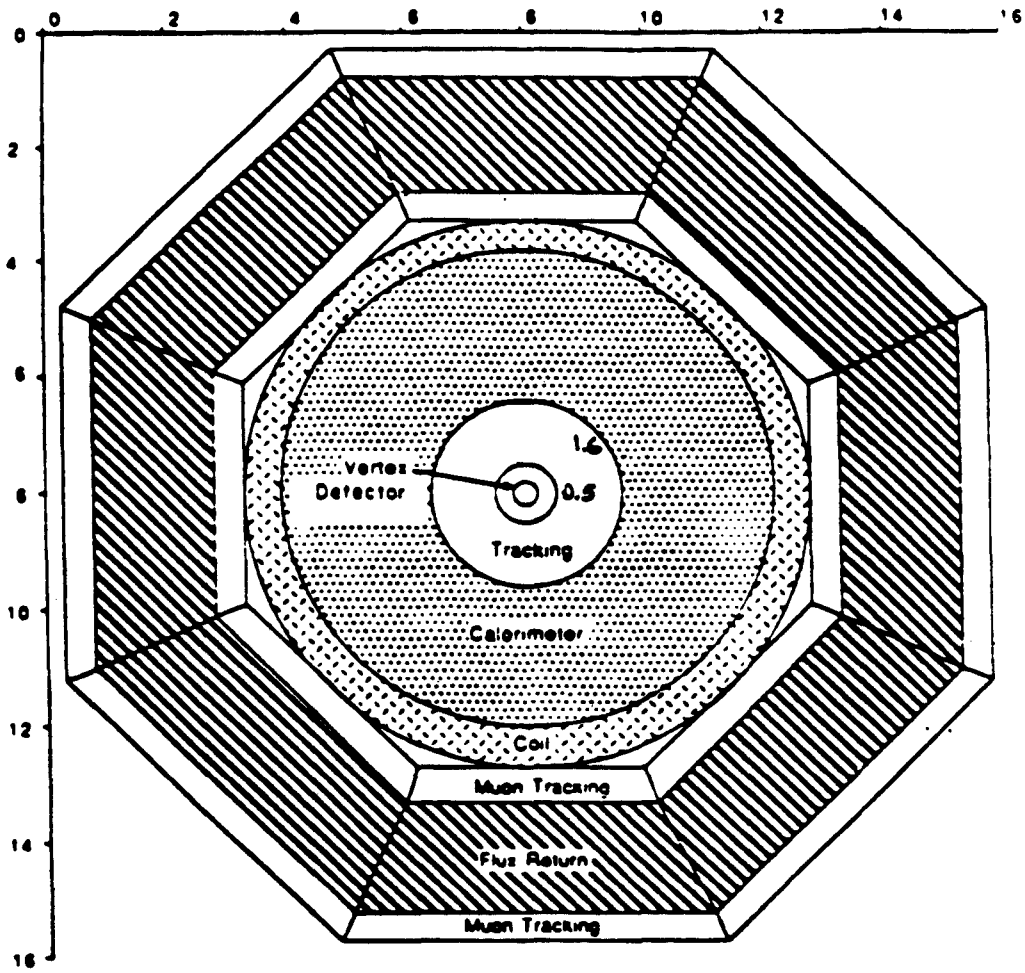

Fig. 2. End view of the Large Solenoid Detector.

Fig. 1. (a) Schematic view of the Large Solenoid Detector.

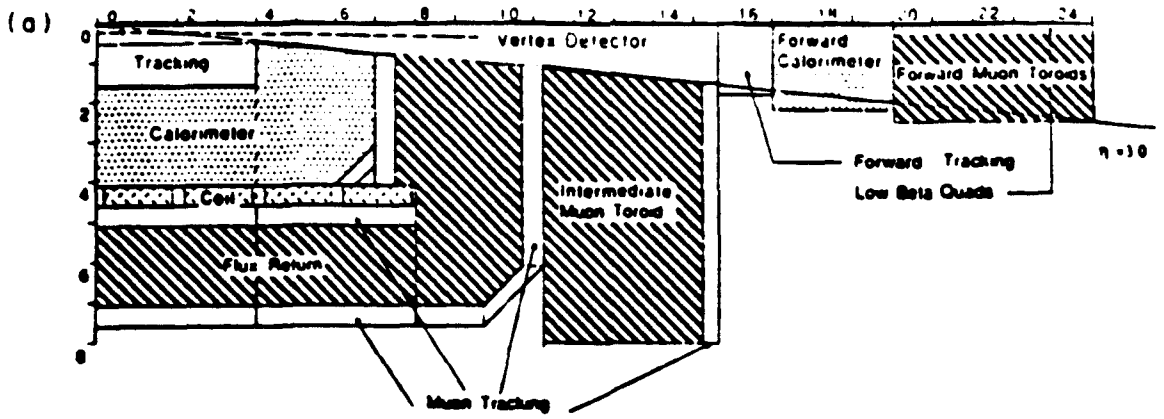

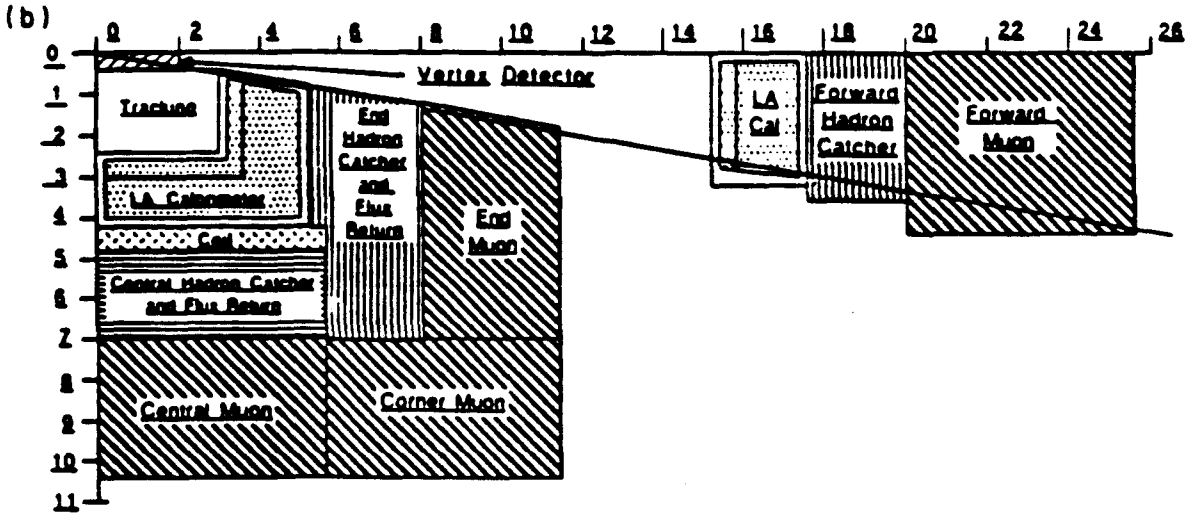

(b) Model A

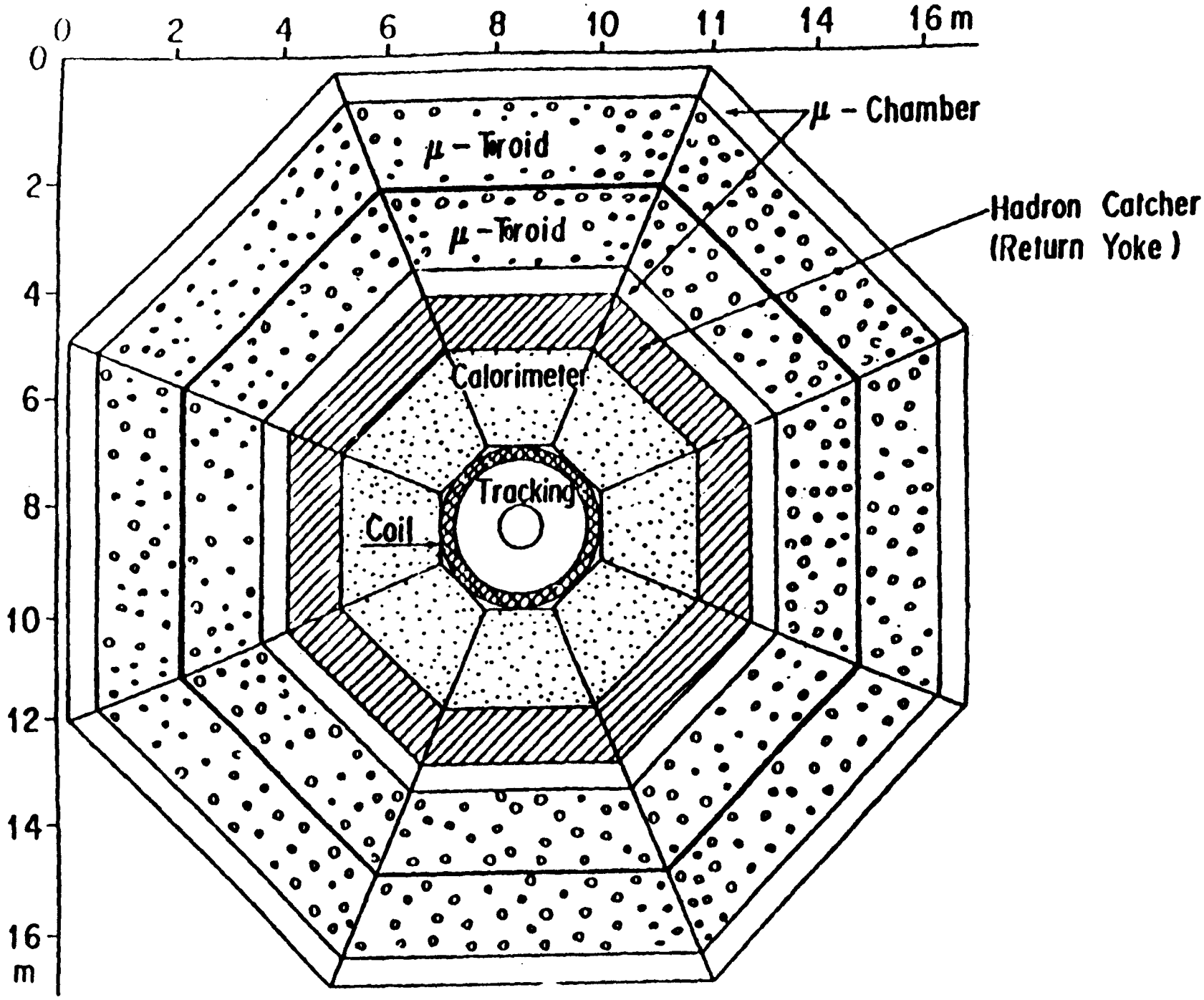
0
2
4
6
8
10
11
14
16 m
μ - Chamber
μ - Toroid
μ - Toroid
Hadron Catcher
(Return Yoke)
Calorimeter
Tracking
Coil

B = 2 Tesla

Calorimeter	Barrel	1600 tons
	Endcap	890 "
	Forward	215 "
Hadron Catcher	Barrel	2535 tons
	Endcap	530 "
	Forward	140 "
μ-Toroids	Barrel	13520 tons
	Endcap	8940 "
	Forward	1700 "
		30,070 tons

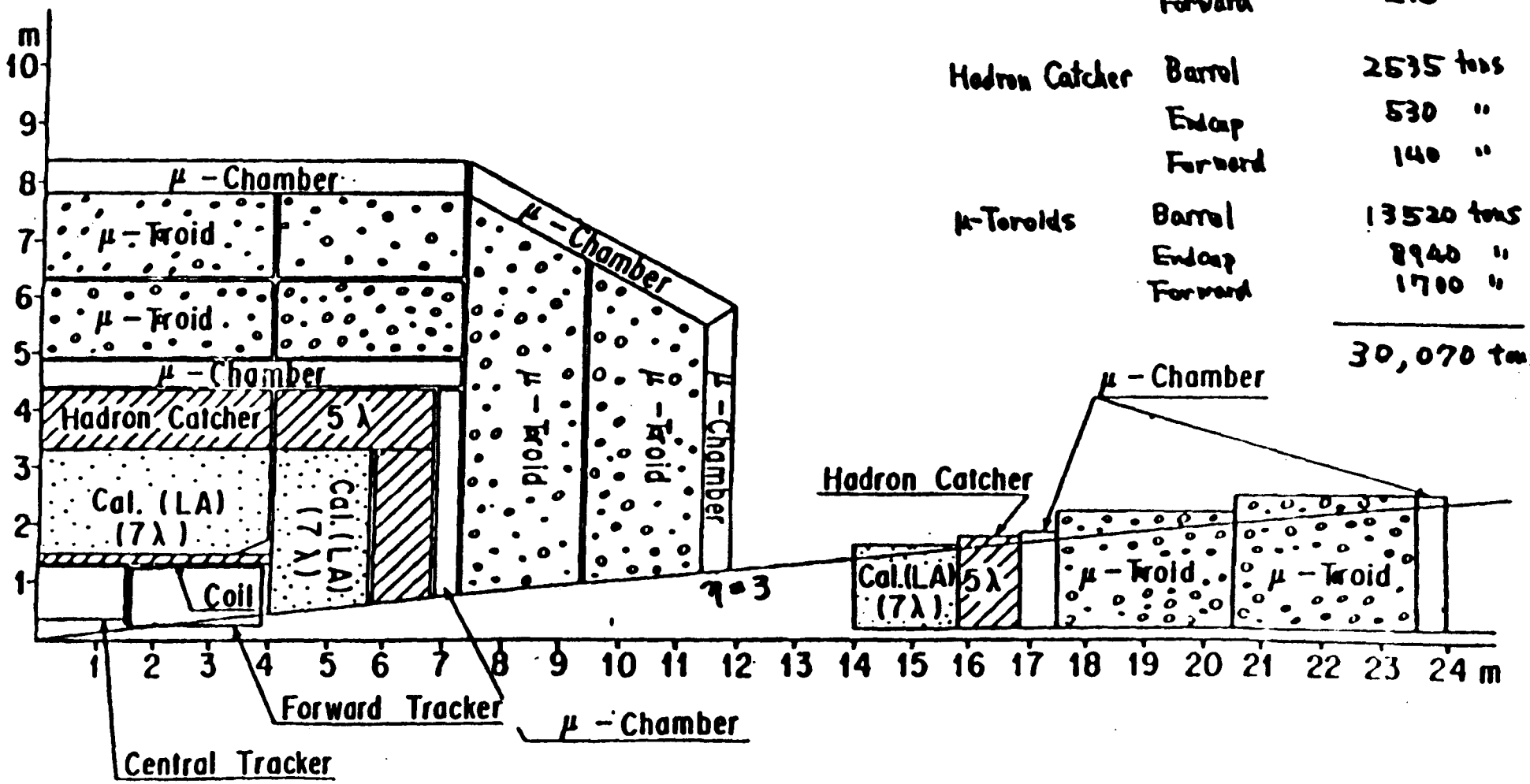

Beam Constrained Fits

	P_T	$\frac{\sigma_{P_T}}{P_T}$ MCS weighted	$\frac{\sigma_{P_T}}{P_T}$ Not wtg
"Standard" LSD	100 GeV	.043	.230
	250	.097	.230
	500	.149	.230
	1000	.185	.232
Variant 1	100 GeV	.043	.241
μ chambers	250	.096	.24[illegible]
in calorim.	500	.148	.24[illegible]
	1000	.183	.24[illegible]
Variant 2	100 GeV	.043	.221
3 additional μ	250	.097	.221
layers in return	500	.148	.222
flux	1000	.183	.223
Variant 3	100 GeV	[illegible]	[illegible]
2.0 m radius	250	[illegible]	[illegible]
tracker	500	[illegible]	[illegible]
	1000	[illegible]	[illegible]
Major Revision	100 GeV	.0097	.305
	250	.024	.305
	500	.048	.305
	$\boxed{1000}$	→ .092	.306
	1500	.131	.308

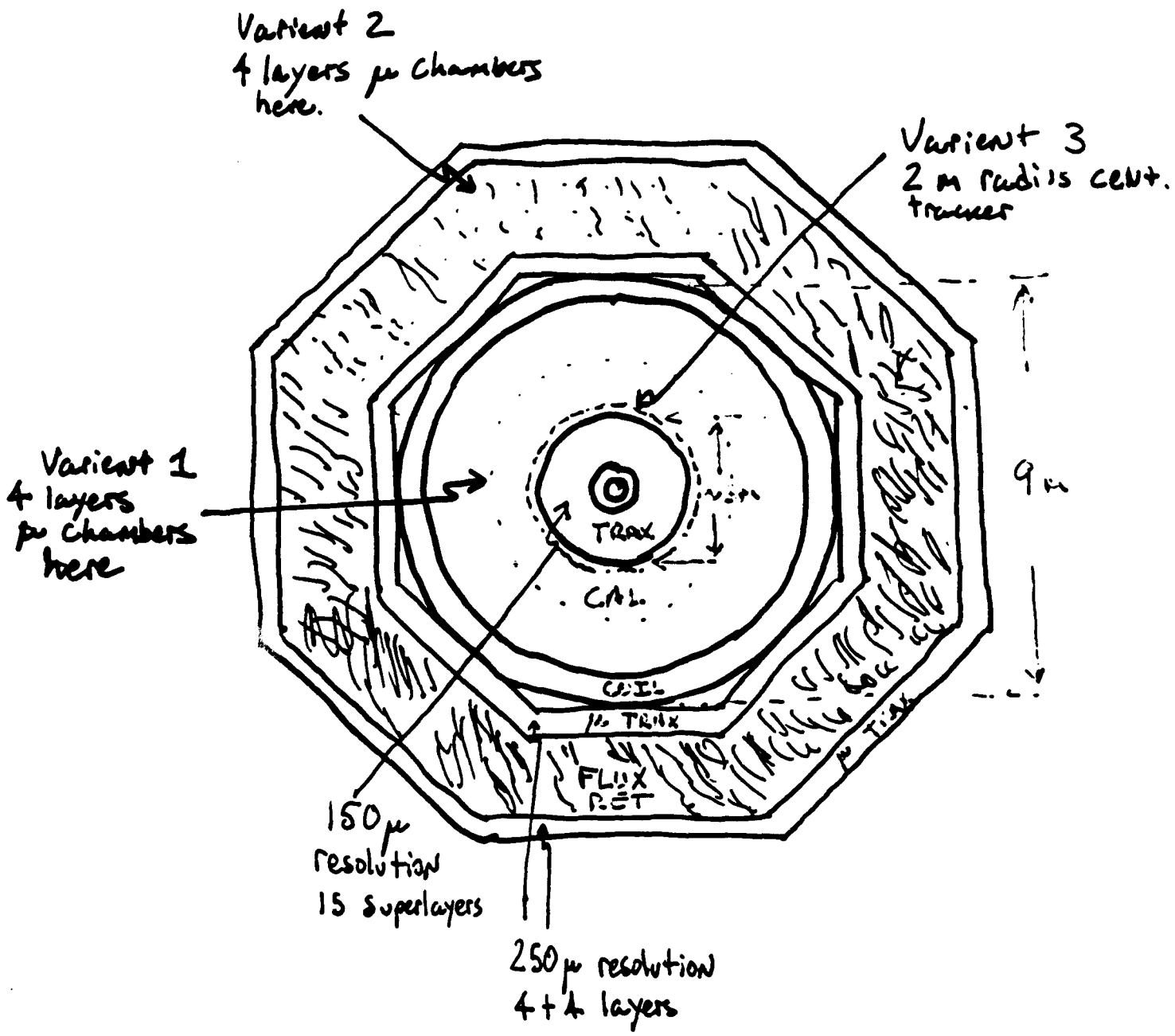
Varient 2
4 layers μ chambers here.
Varient 3
2 m radius cent. tracker
Varient 1
4 layers μ chambers here
9 m
TRAX
CAL
CAL
μ TRAX
FLUX RET
μ TRAX
150 μ resolution
15 superlayers
250 μ resolution
4 + 4 layers

"MAJOR" REVISION

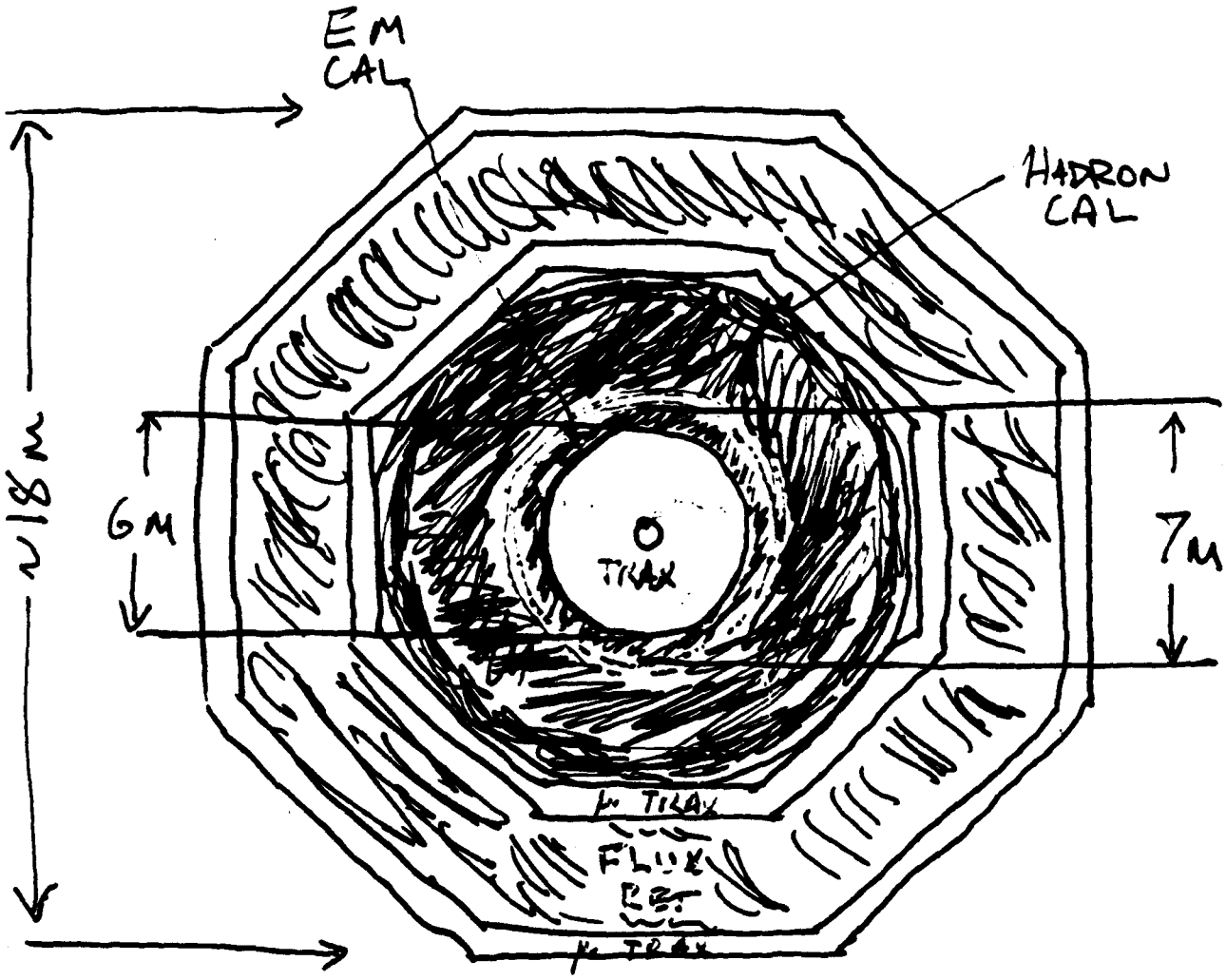

Note overall scale change from previous picture

LONG SOLENOID DETECTOR

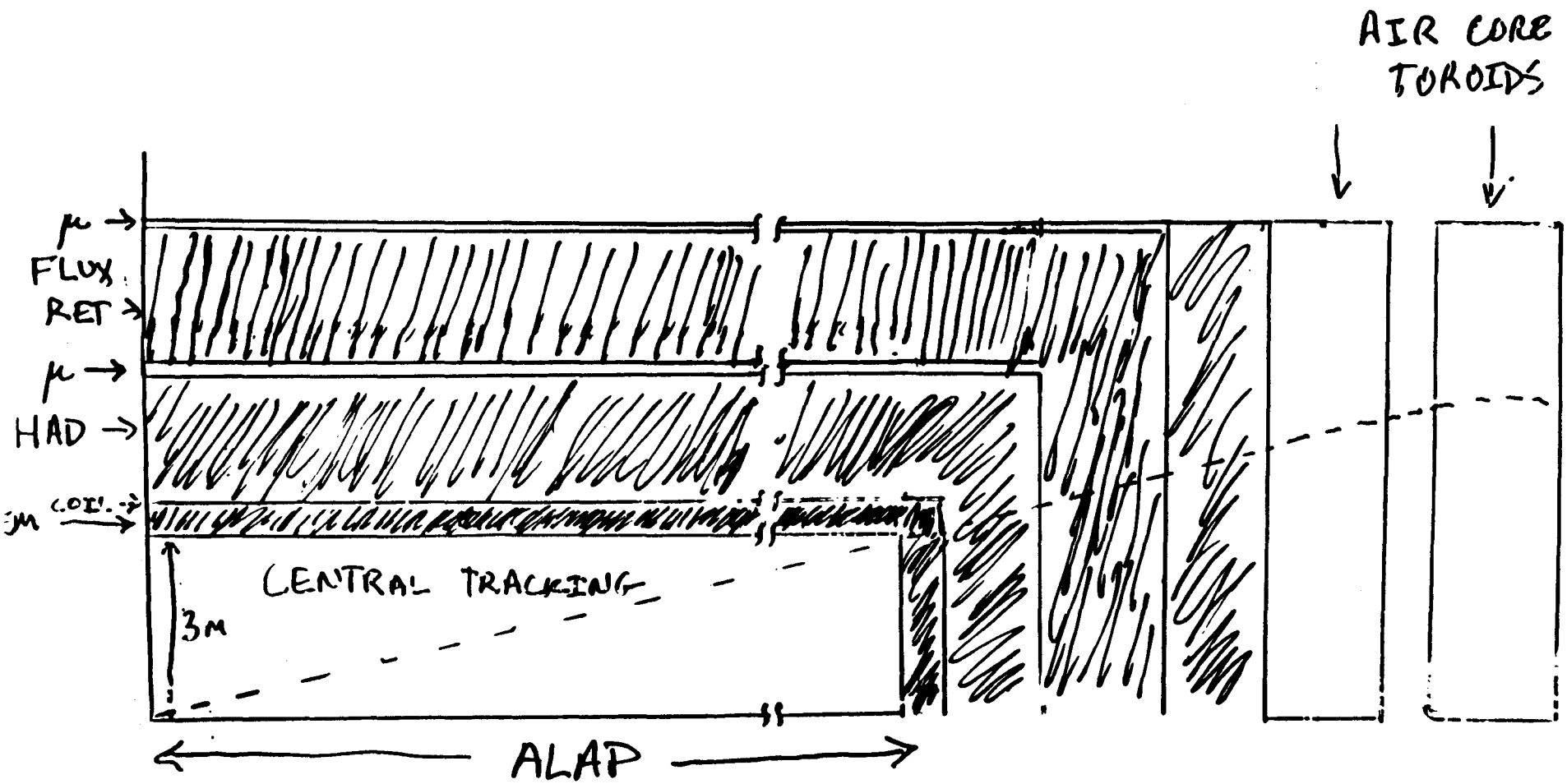

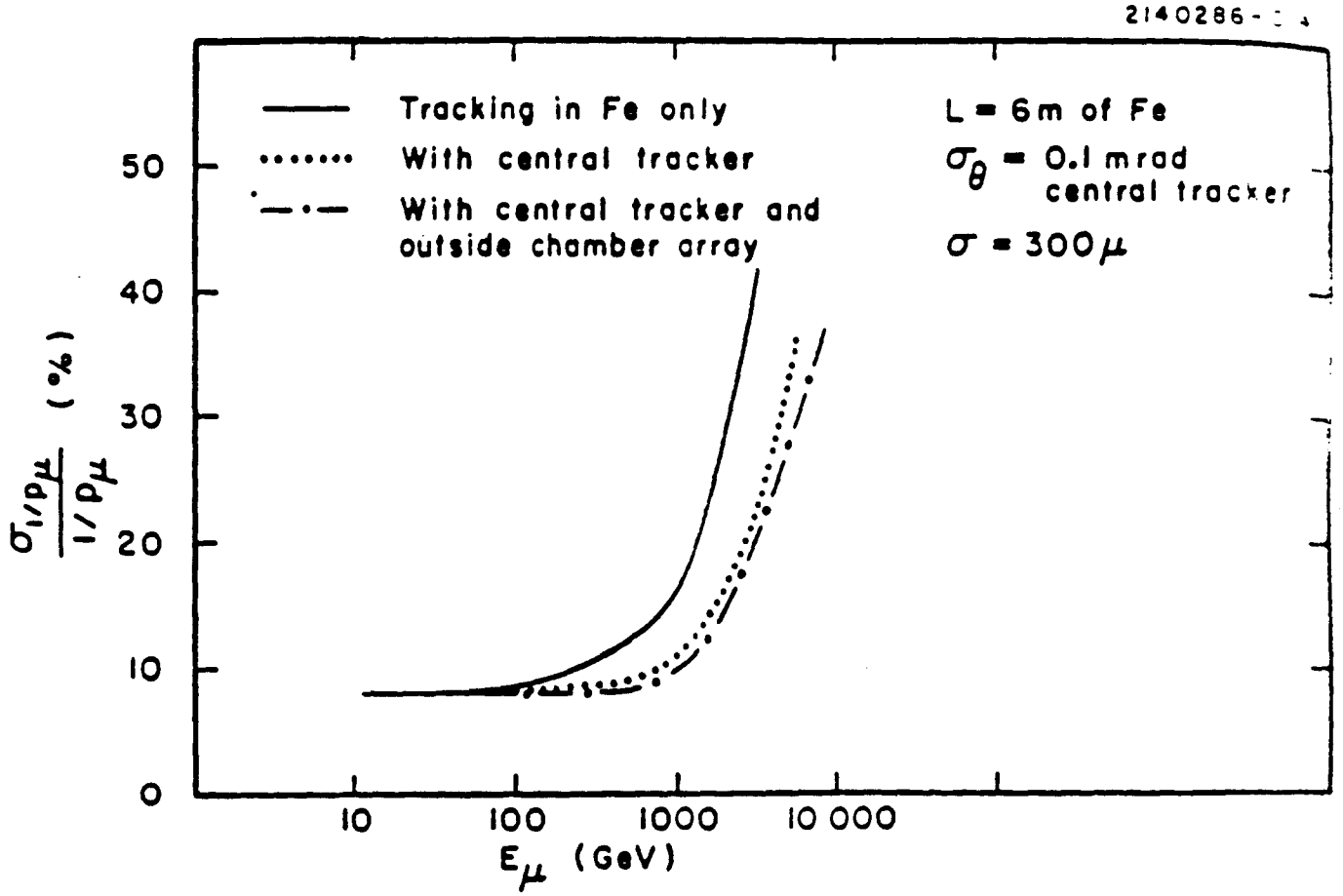

Fig. 5.2.4 Momentum resolution in an iron muon spectrometer.

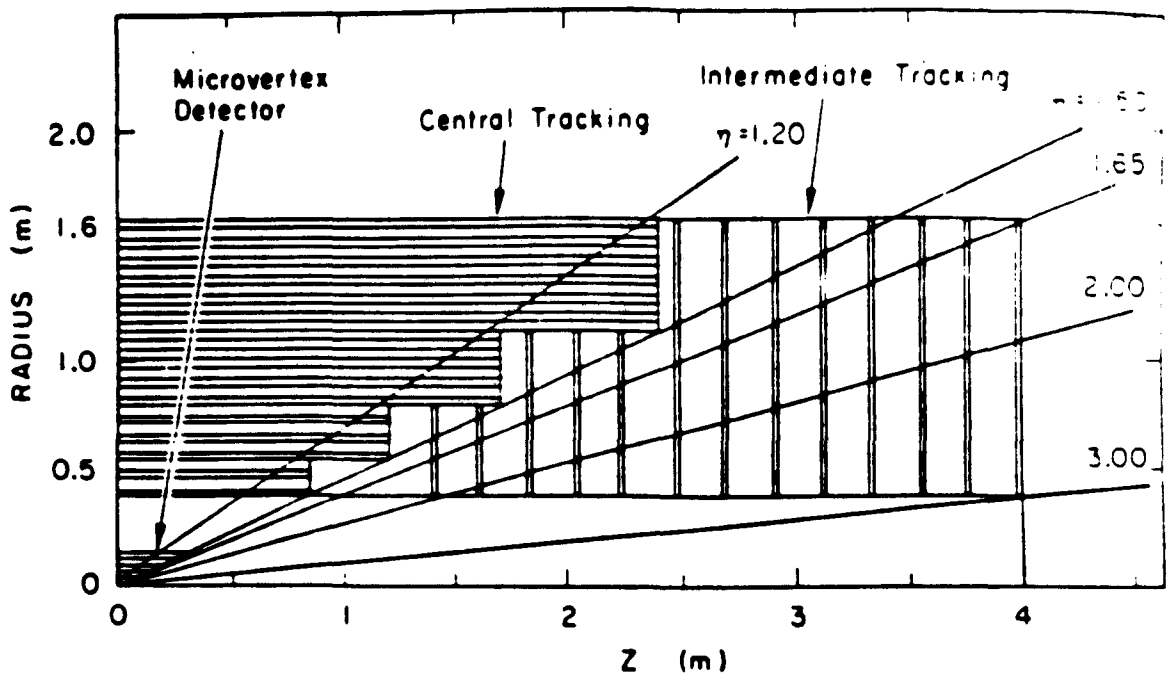

Fig. 8. Schematic view of central and intermediate tracking systems in the Large Solenoid Detector.

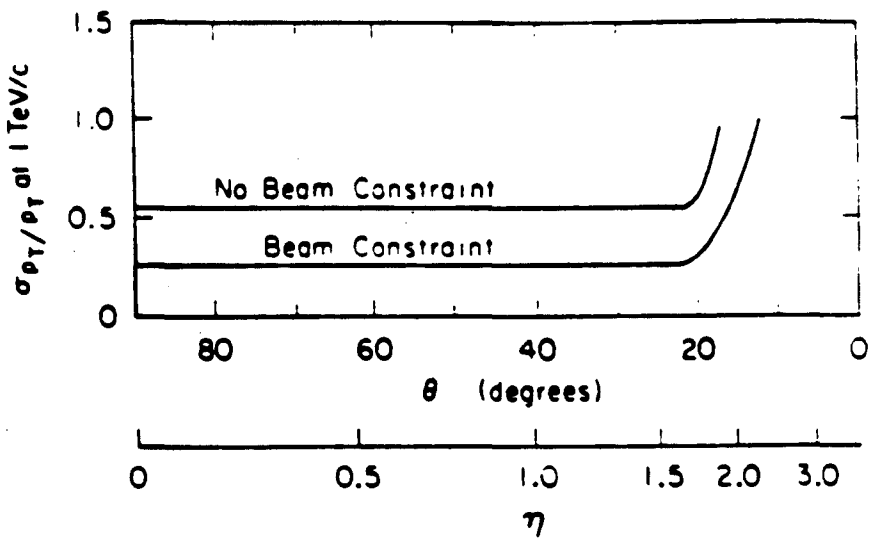

Fig. 9. Momentum resolution as a function of polar angle and rapidity in the Large Solenoid Detector for the 13 superlayers at radii > 50 cm in the central tracking system and intermediate tracking Option A.

FLUX RETURN-YOKE. MOMENTUM RESOL'N

Carlsmith, et al
Snowmass '85

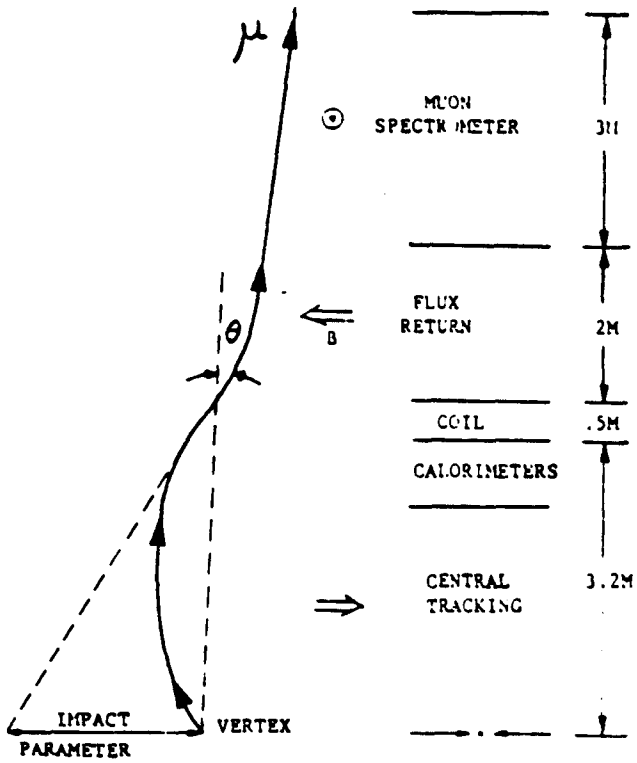

Figure 11: Measurement of muon momentum in magnetized iron by the impact parameter method.

The results are exhibited in Table 3. In performing the calculations we have assumed again that 100μ resolution in one location can be achieved and that flux return can be instrumented in such a way as to give the optimized entrance angle, i.e. θ, measurement.

Table 3
Relative Measurement Precision form Flux Return Spectrometer
1. Iron only 2. Iron plus 1 angle 3. Impact Parameter

Momentum	(i.e. sagitta meas.) 1	2	3
200 GeV	34%	34%	28%
400 GeV	39%	35%	29%
700 GeV	50%	38%	32%
1 TeV	63%	41%	35%
2 TeV	113%	50%	49%

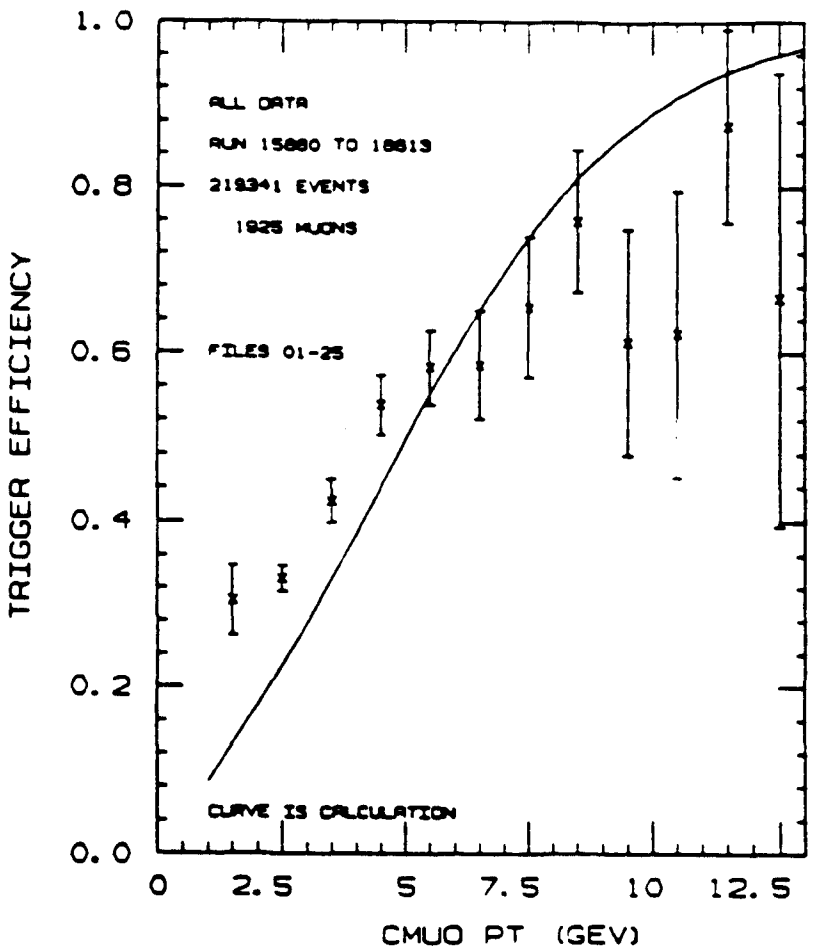

Figure 12: CMU level 1 efficiency for the 5 GeVthreshold. "Tight" cuts applied to the CMUO banks.

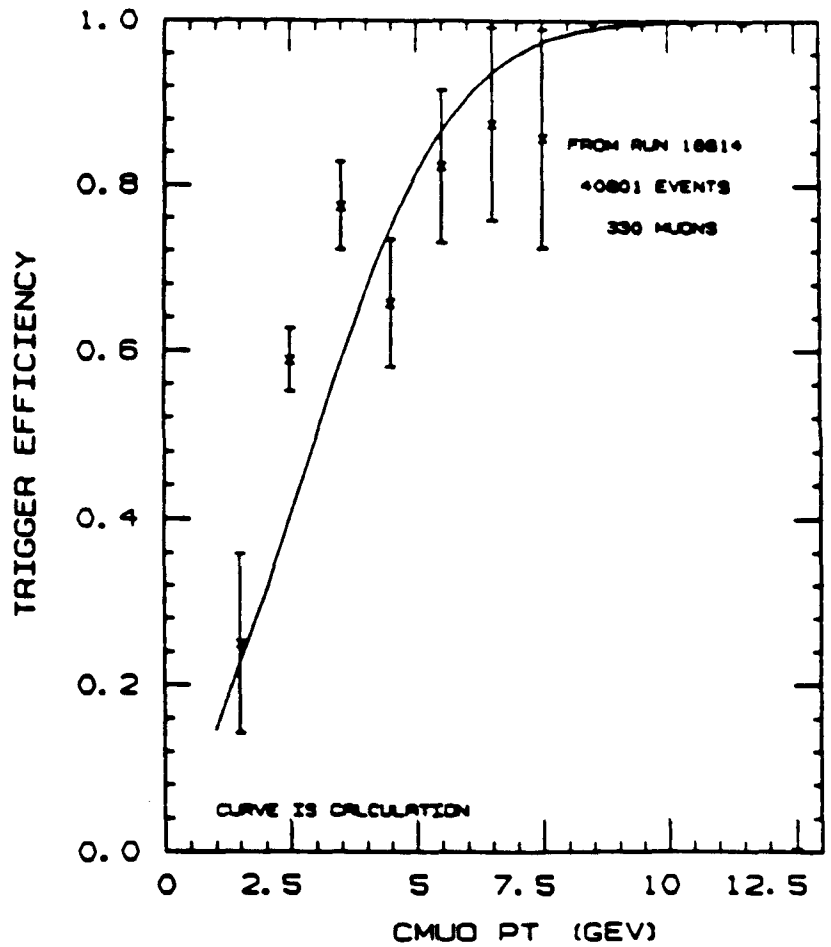

Figure 14: CMU level 1 efficiency for the 3 *GeV* threshold. "Tight" cuts applied to the CMUO banks.

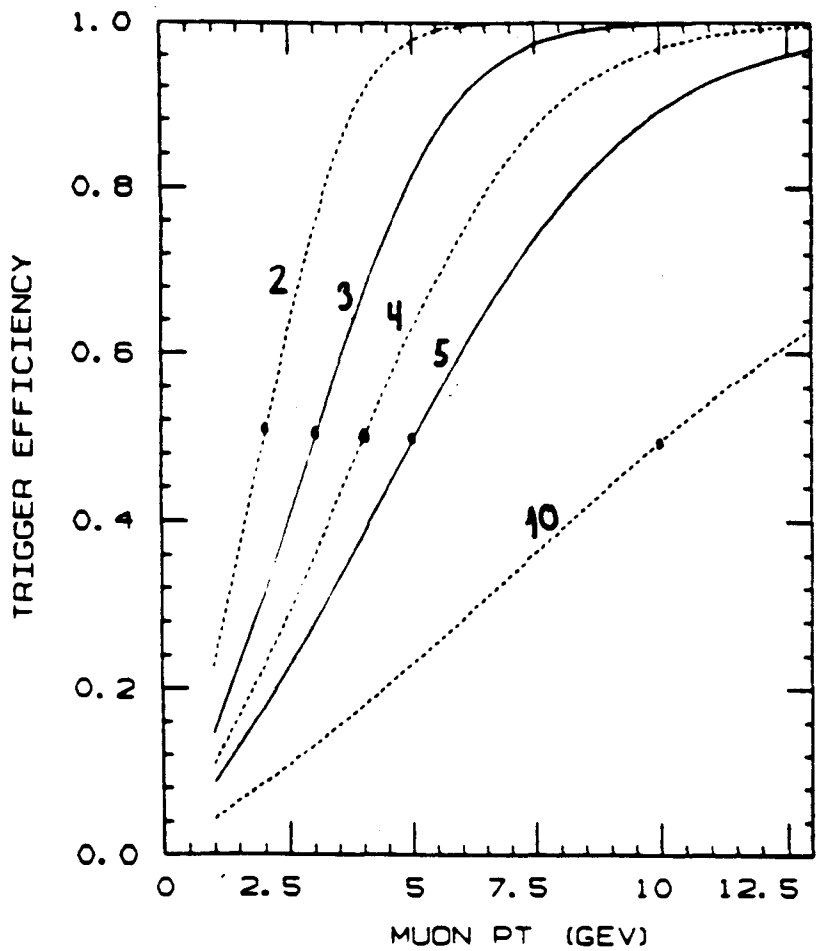

Figure 2: Trigger Efficiencies calculated by including the contribution of multiple scattering. From left to right, the curves are for a 2 GeV, 3 GeV, 4 GeV, 5 GeV, and 10 GeV threshold, respectively. At threshold, the efficiency is nominally 50%. The full lines show the two thresholds actually used in the 1988–1989 run.

CDF CENTRAL MUON CHAMBER
LEVEL-1 TRIGGERING

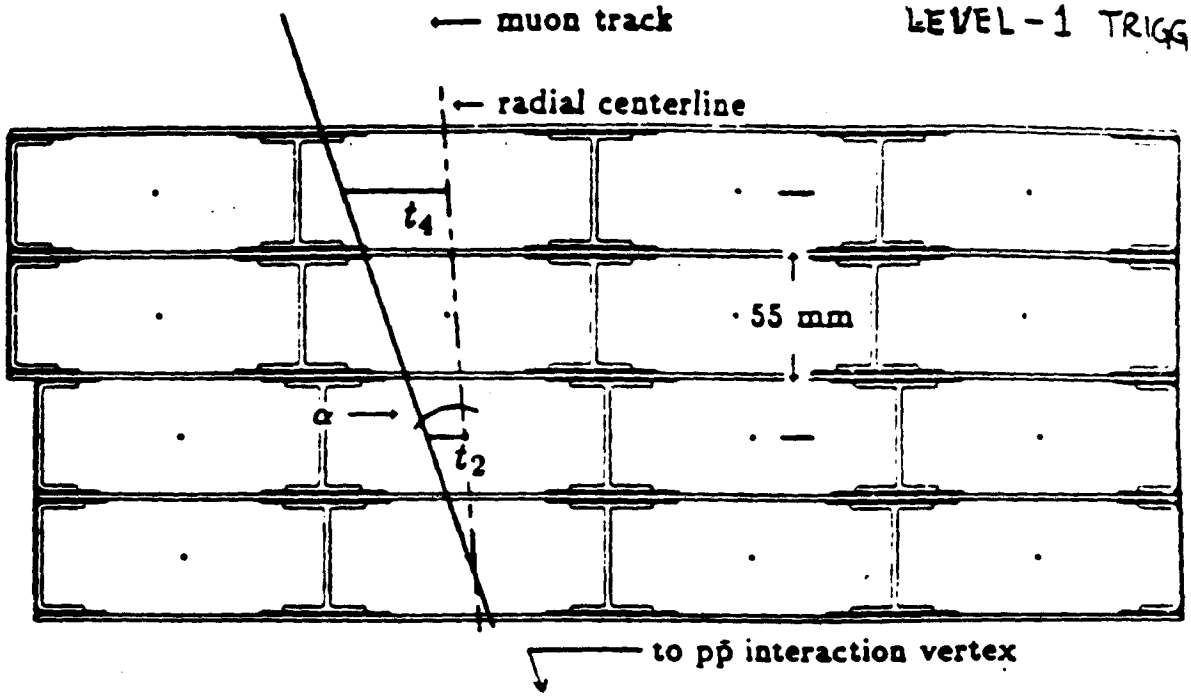

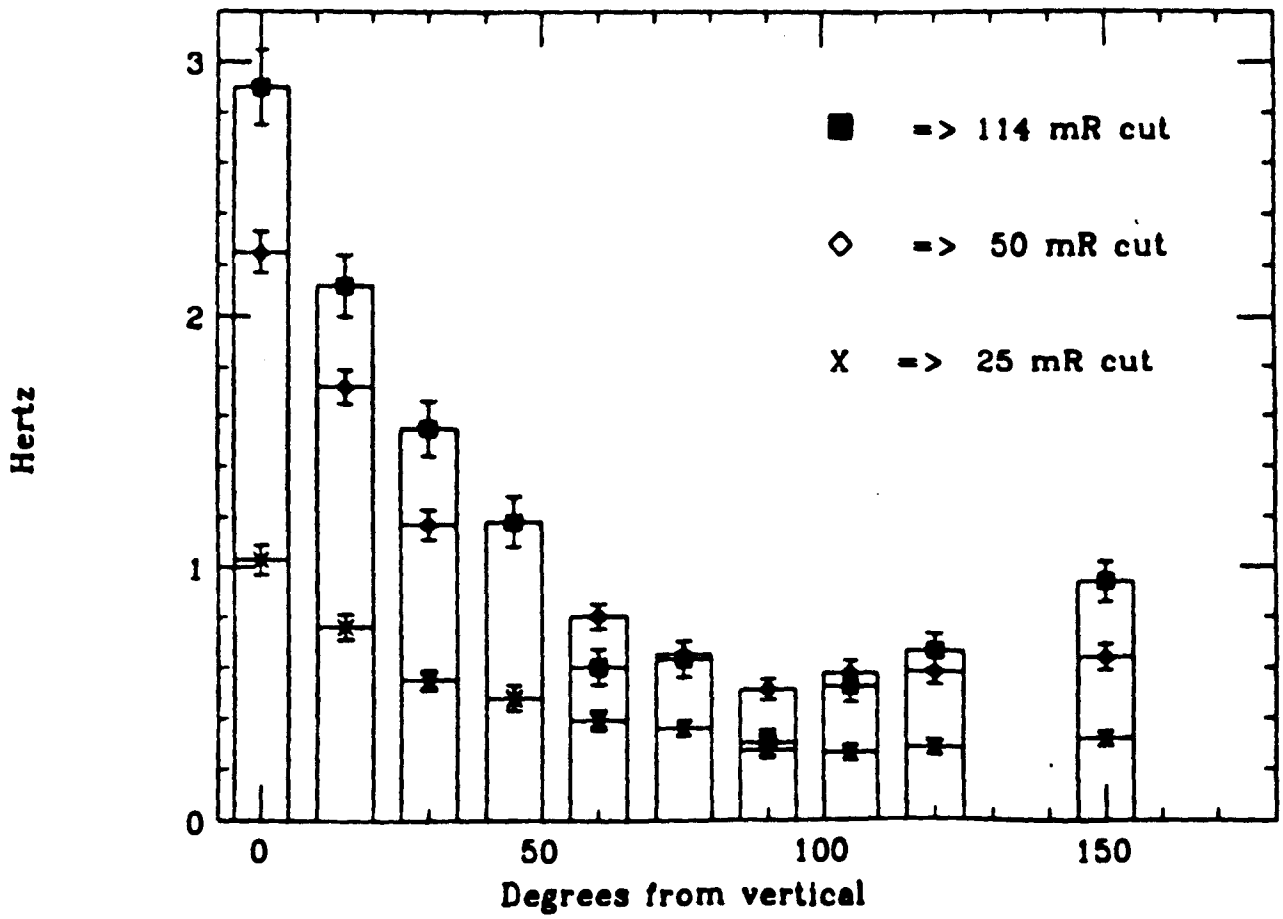

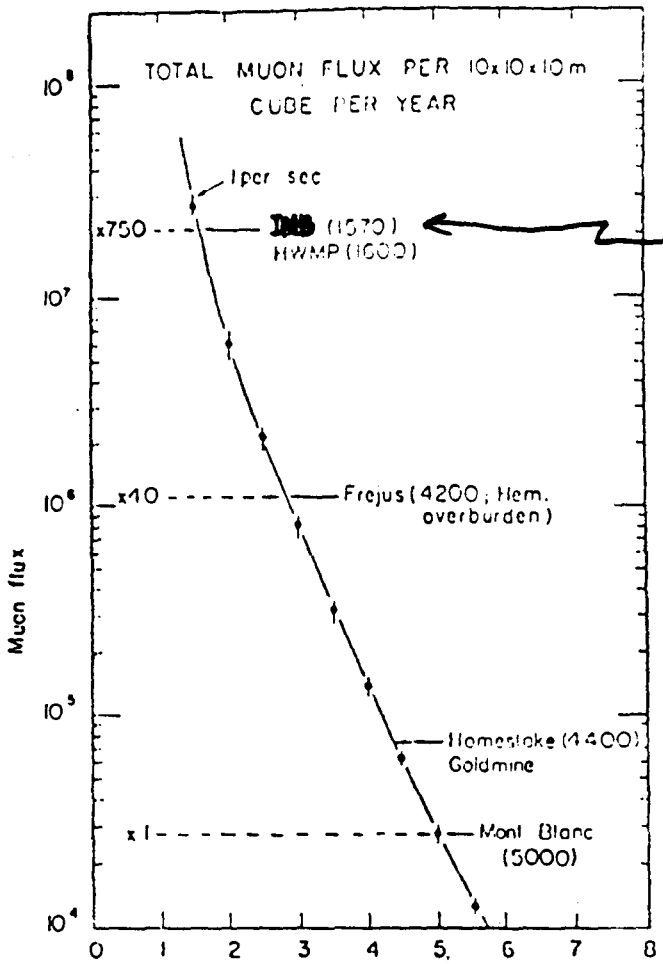

IMB DETECTOR
~ 20 m³
COSMIC RAY
3 Hz TRIGGER RATE
@ 1570 mwe

⇒ ~ 100 KHz
COSMIC RAY
RATE @ S.L.

NOT A PROBLEM
UNLESS DON'T
REQUIRE MUONS
TO POINT BACK
TO INTERACTION
REGION.

b)

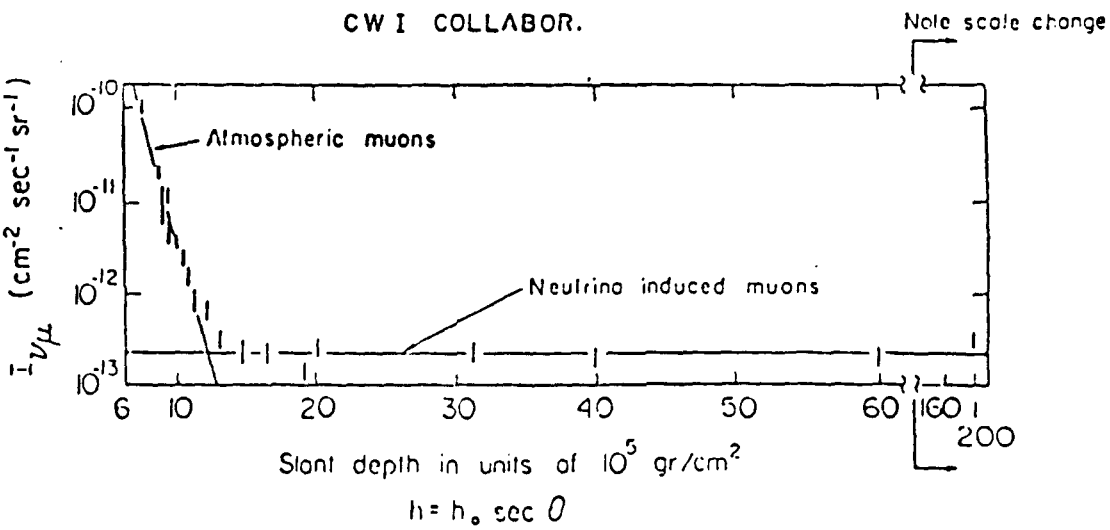

Fig. 8

COSMIC RAY BACKGROUND
A PROBLEM FOR TRIGGERING?

COMPARE WITH RAW RATES FROM PP COLLISIONS

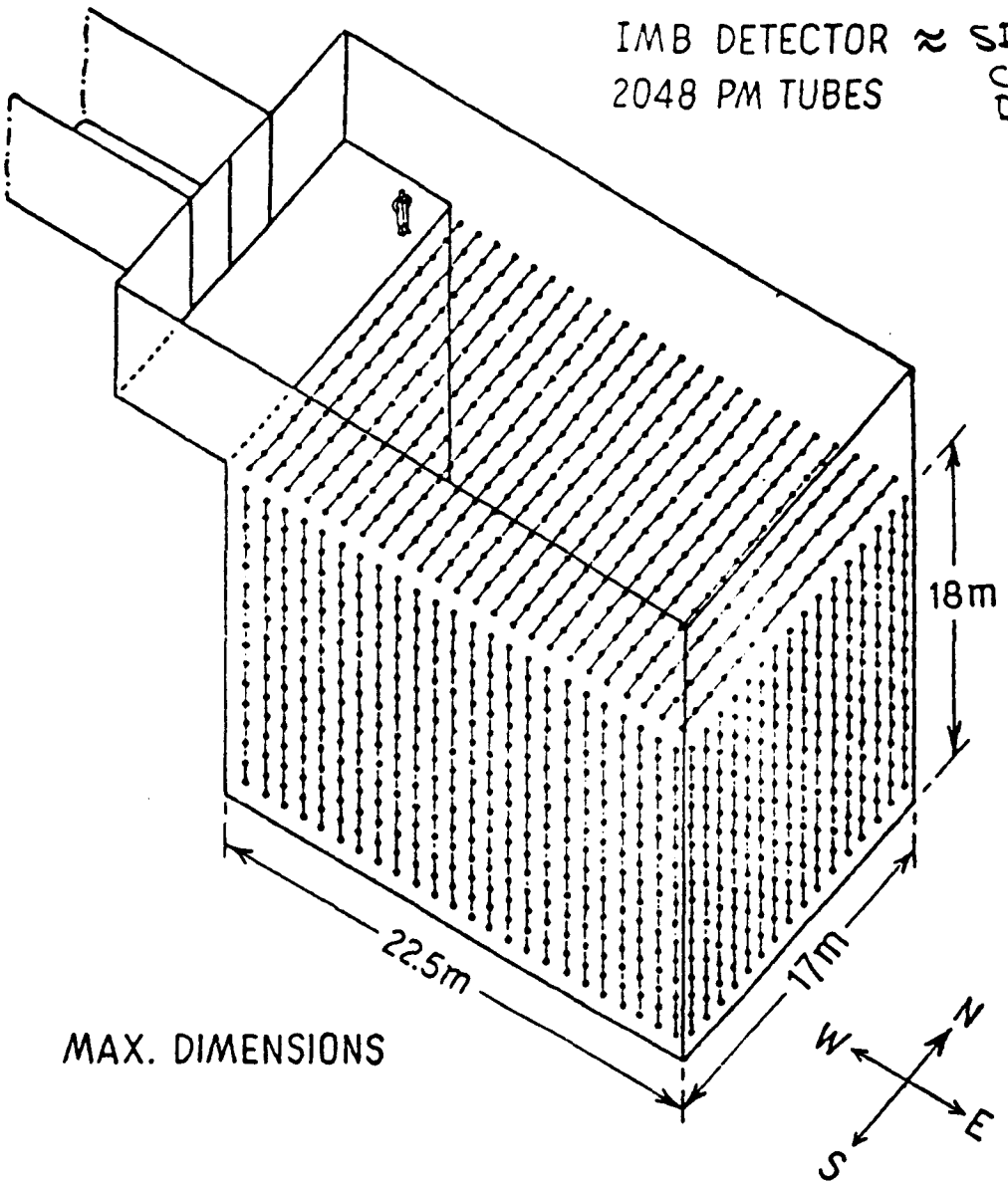

TRIGGER RATE
@ 1570 mwe
~ 3 Hz.
@ SEA LEVEL
~ 100 KHz

Figure 1. A schematic view of the IMB detector.

MUON TRIGGERING

~ RAW RATES

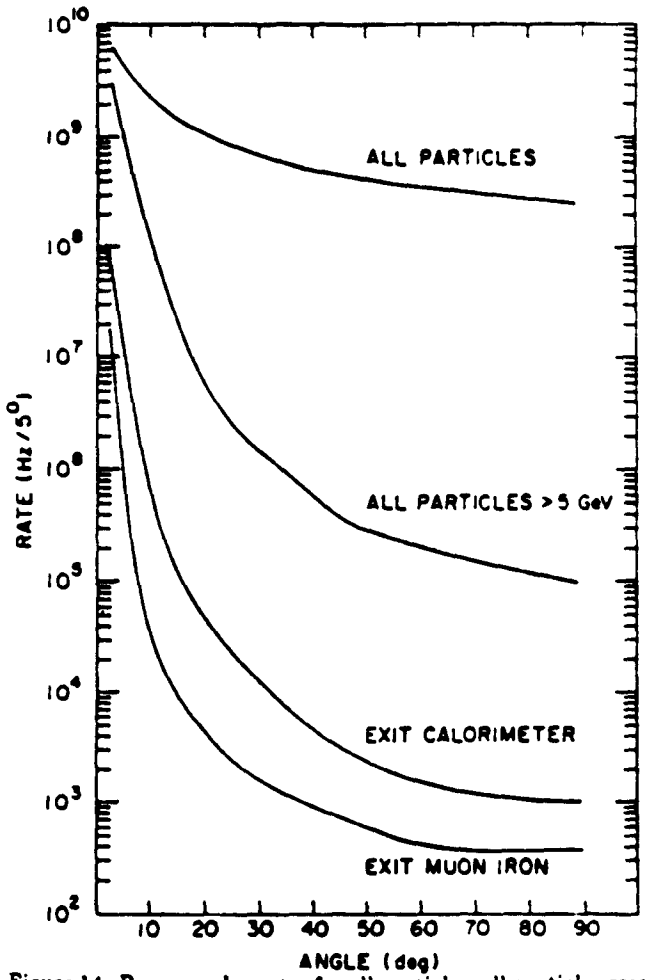

Figure 14: Raw angular rates for all particles, all particles greater than 5 GeV, all particles exiting the coarse calorimeter, and all particles exiting the muon iron.

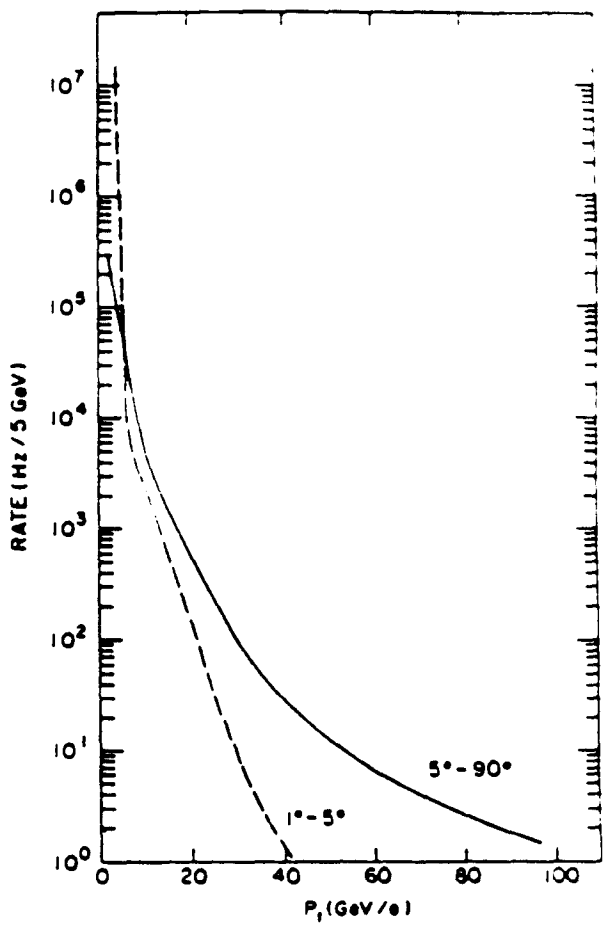

Figure 15: Rates versus p_t for particles exiting the muon iron in the end (1° – 5°) and central (5° – 90°) regions.

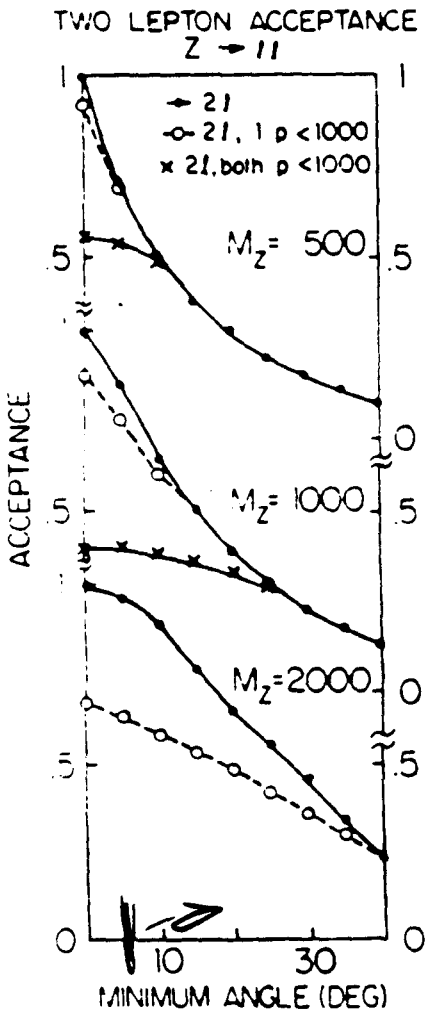

Figure 13: Two-lepton angular acceptance for $Z_x \to ll$ for Z masses of 500, 1000 and 2000 GeV.

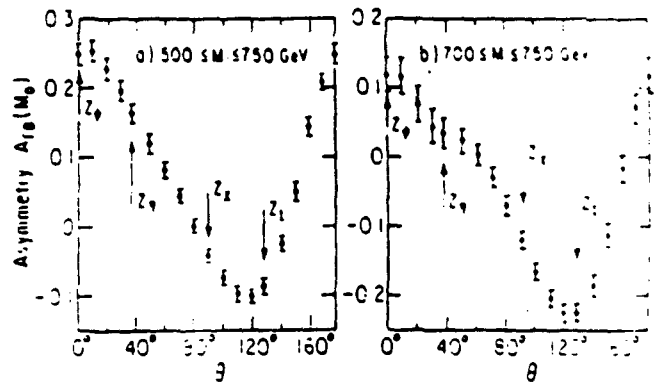

Figure 12: Forward-backward asymmetries of leptons in $pp \to l^+l^- +$ [illegible] integrated over the mass ranges a) $500 \le M(l^+l^-) \le 750 GeV$, b) $700 \le M(l^+l^-) \le 750 GeV$, as functions of mixing angle θ describing a new "$Z(\theta)$" of mass 750 GeV. Here $\sqrt{s} =$ 40 GeV. The asymmetry vanishes for y=0 and thus has been calculated using $\int_0^{y_{max}} dy(d\sigma/dy) \pm \int_{y_{min}}^0 dy(d\sigma/dy)$ in the manner [illegible] Ref. 24.

Do we need MUON COVERAGE for $|\eta| > 3.0$ $(\theta < 5°)$

MOST OF INTERESTING NEW PHYSICS @ SSC HAS EXPECTATIONS FOR SMALL % TOTAL μ's w/ $|\eta_\mu| > 3.0$

BUT, IF DOING, e.g. W, Z physics
Z^0's BACKGROUND TO W's IF MISS ONE LEG OF

⇒ IF DON'T WANT TO SWEAT BLOOD FOR μ's @ $|\eta| > 3.0$
SHOULD AT LEAST INSTRUMENT TO SEE MIN. IONIZING TRACKS THRU' STEEL + FWD CALORIMETER

Hi-P_t μ's from $Z^0 \to \mu^+\mu^-$ IF NOT DETECTED CAN ALSO DEGRADE MET RESOLN

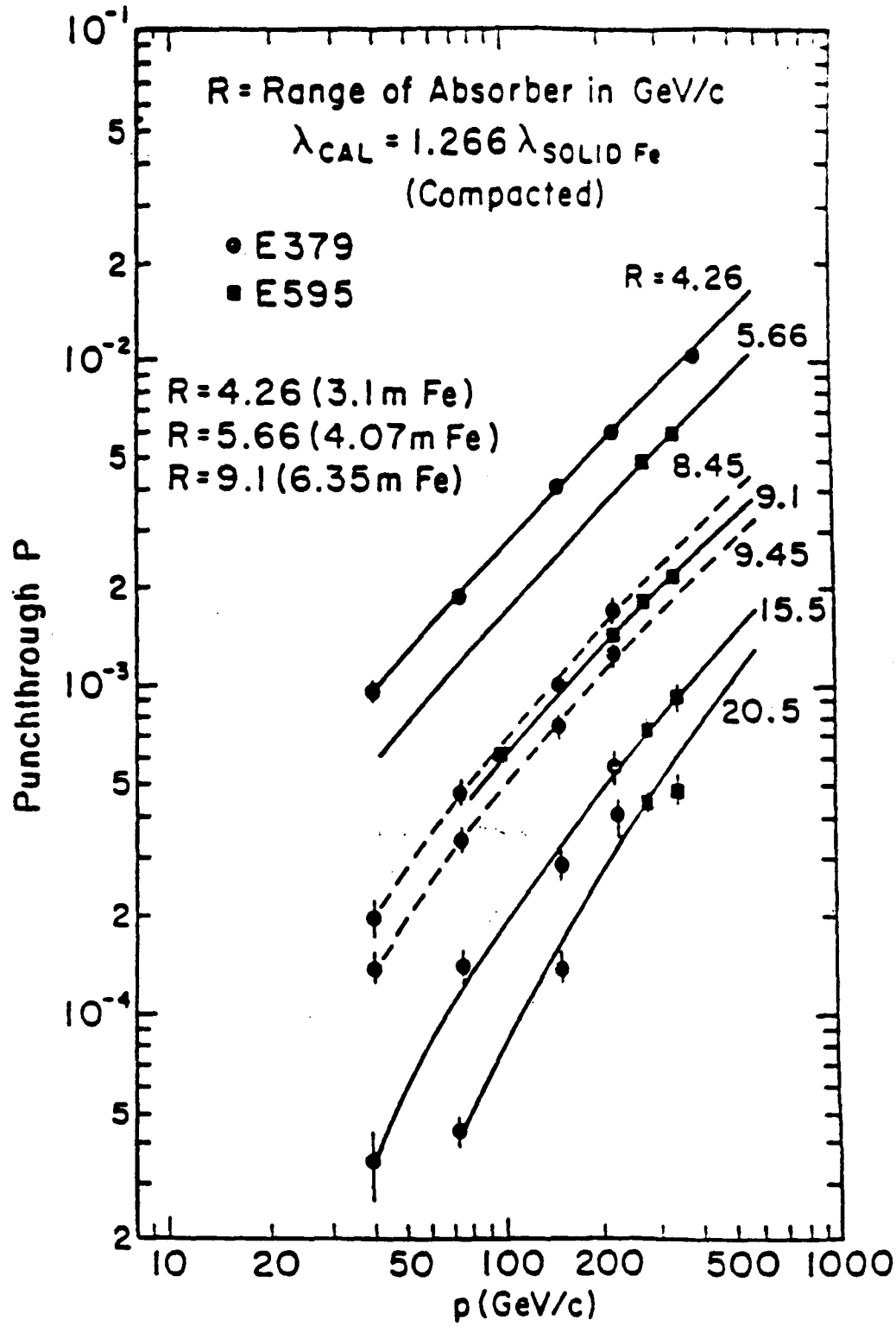

Fig. 5.2.6 Punchthrough probability vs. hadron momentum for different absorber thickness (ref. 7).

HADRON PUNCHTHROUGH

$$P = \left(\frac{p}{350\,\mathrm{GeV}}\right) 0.0095\, e^{-1.42(\sqrt{R}-2)} \left(0.22 + 0.59 f\right)$$

R = RANGE IN GEV $\qquad f = \lambda / \lambda_{Fe}$

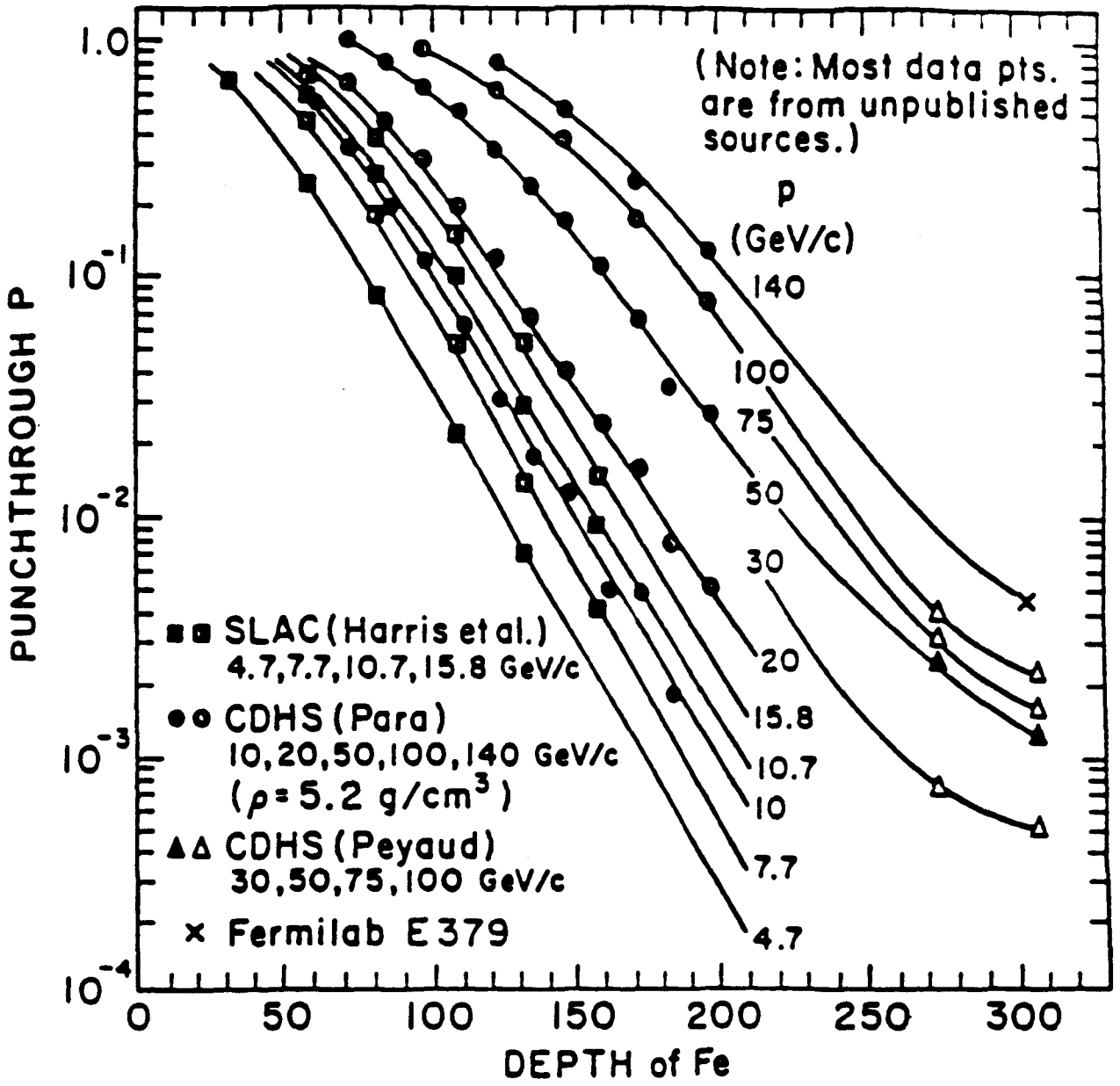

Fig. 5.2.5 Punchthrough probability vs. depth of Fe for various momenta as indicated.

Figure 3: Energy loss per muon from each of several processes for [illegible] muons in the detector of Figure 2. Shown are the contributions from *a*) bremsstrahlung; *b*) direct e^+e^- pair production; and *c*) deep inelastic scattering on nucleons. Note the substantial tails.

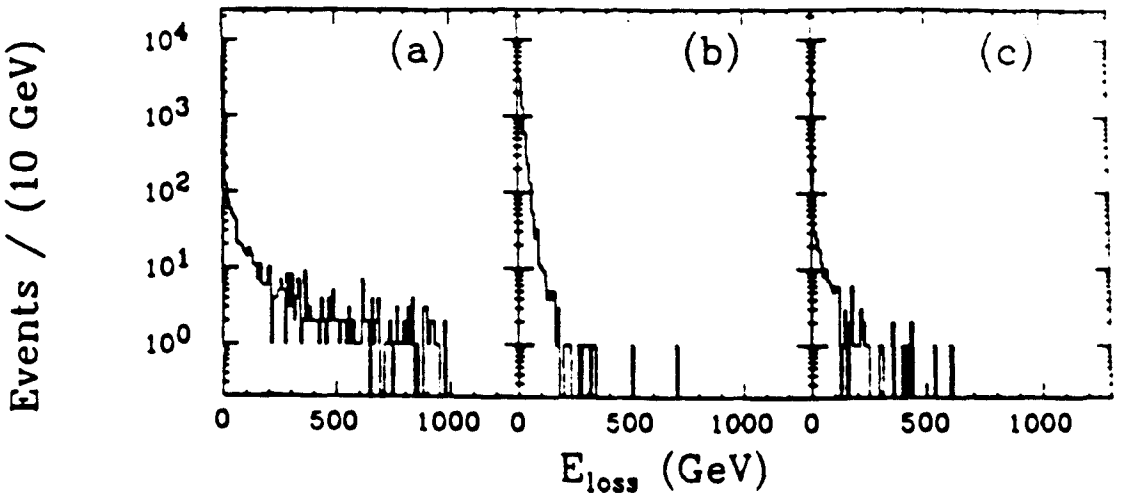

Figure 4: *a*) The hit multiplicity for 1 TeV muons in the active planes of the detector of Figure 2 and *b*) in an active plane after 90 cm of uranium.

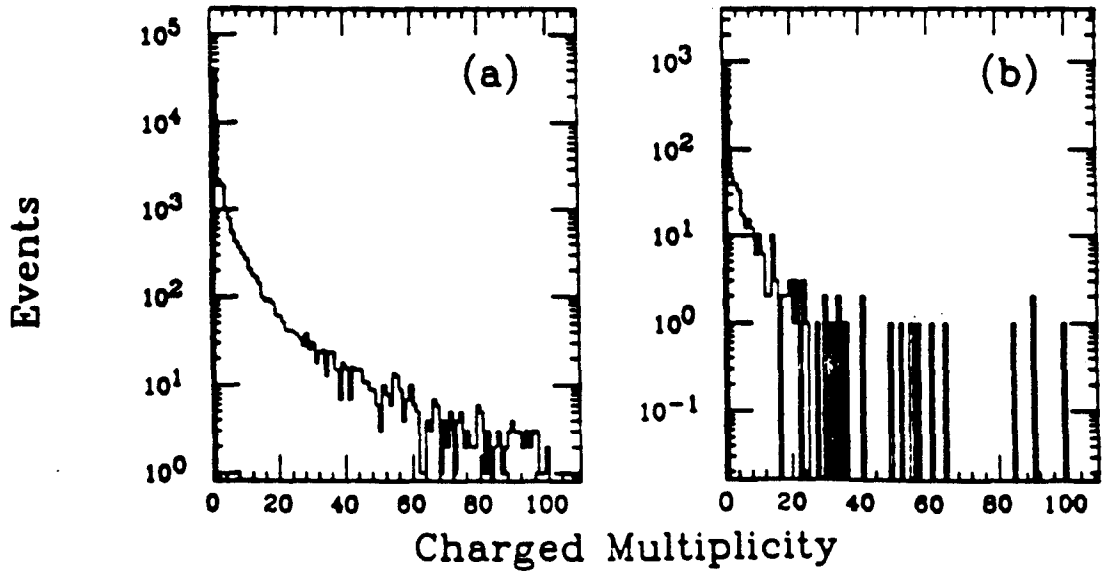

Figure 5: The probability of a clean muon hit (i.e., a muon track [illegible] by any other charged particle) in an active layer in the detector of Figure [illegible] function of E_μ (diamonds). Also included are two points for an active layer placed behind 90 cm of uranium (crosses).

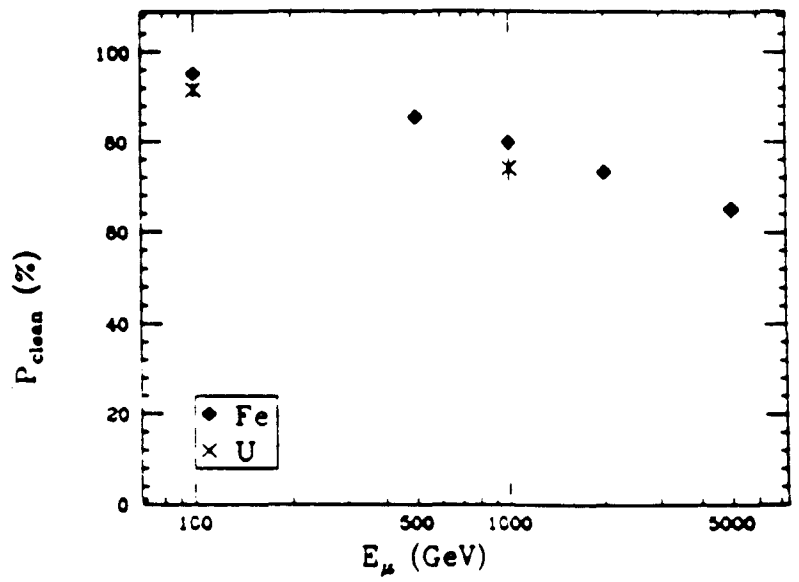

Figure 6: The probability of identifying a multiply hit chamber as a function of the chamber's two-track resolution for active planes in the detector of Figure 2 and for an active layer placed behind 90 cm of uranium. Assumptions are given in the text.

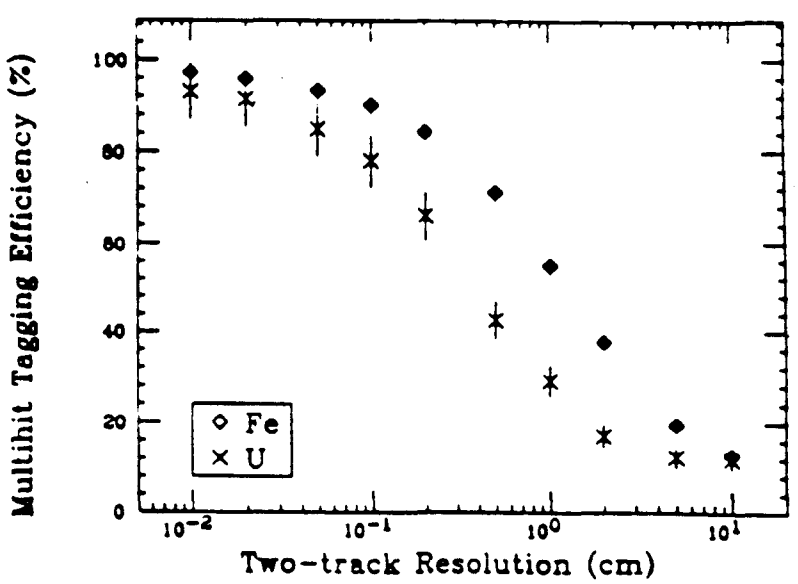

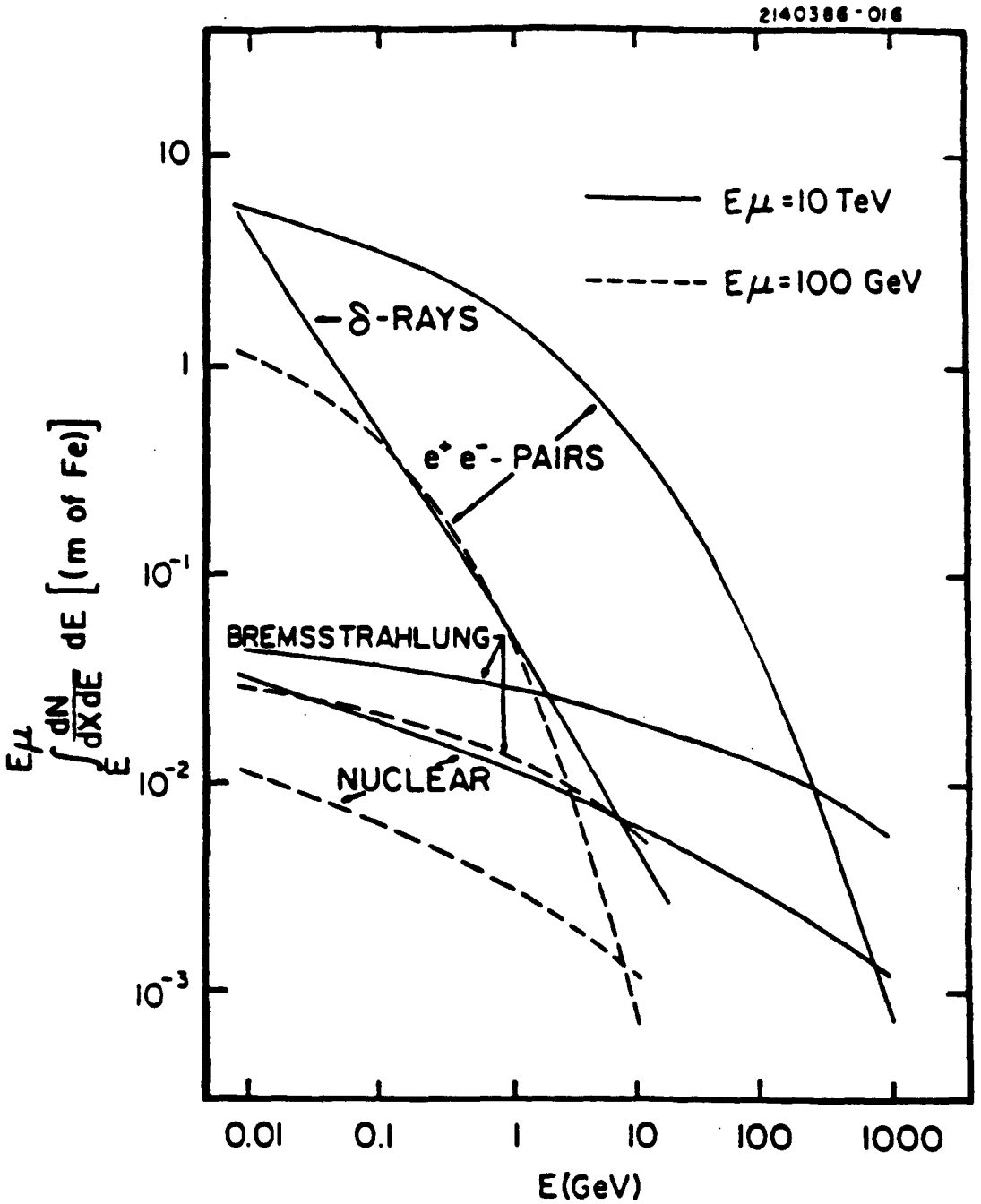

Fig. 5.2.3 The number of single events per meter of iron with muon energy loss > E, as a function of the energy loss E. Two muon energies are shown, 100 GeV and 10 TeV.

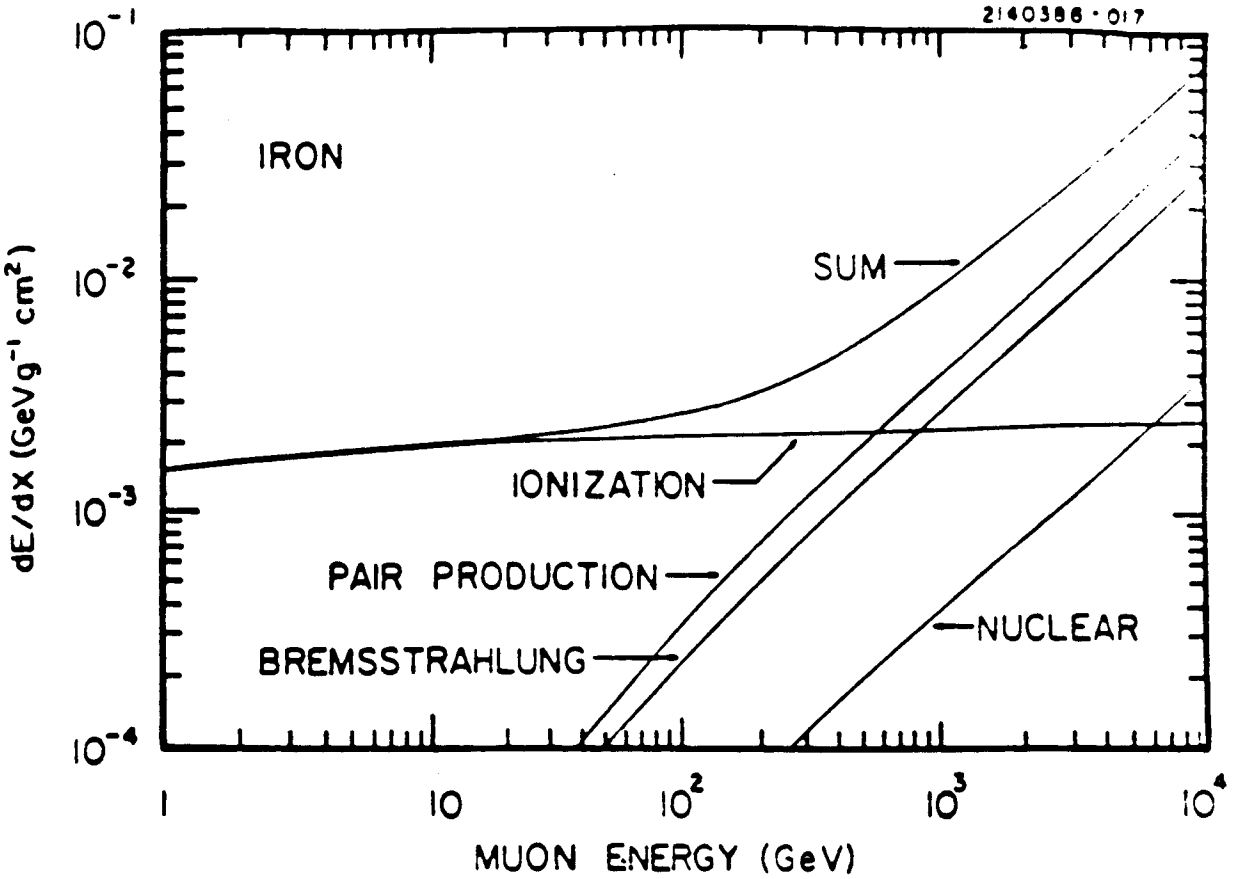

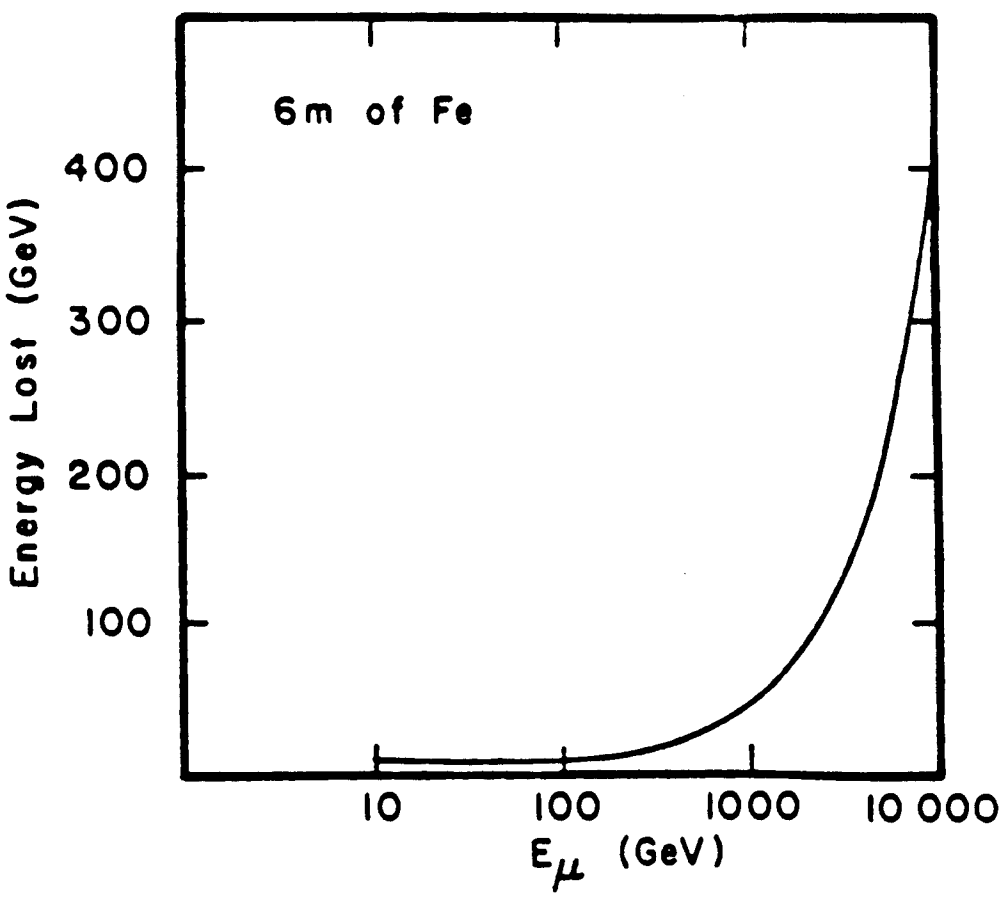

Fig. 5.2.2 Muon energy loss in 6m of iron vs. muon energy.

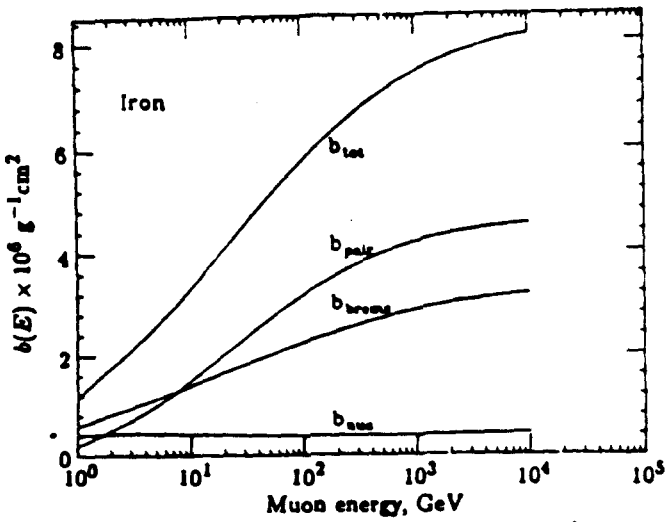

Figure 3: Contributions to the fractional energy loss by muons due to radiative processes in iron, as obtained from Lohmann *et al.*[10].

Table 1
Radiative probabilities for a muon of 1000 GeV

Type	Integrated Probability	Average length	Average energy	Weighted Probability $\int L(\epsilon) \cdot P(\epsilon, E_o)d\epsilon$
Direct Pair	0.1054E+00	18.5(cm)	4.8(GeV)	0.5708E-02
Brem.	0.7022E-02	33.7	106.9	0.2085E-03
Delta rays	0.9852E-02	17.9	6.2	0.5519E-03

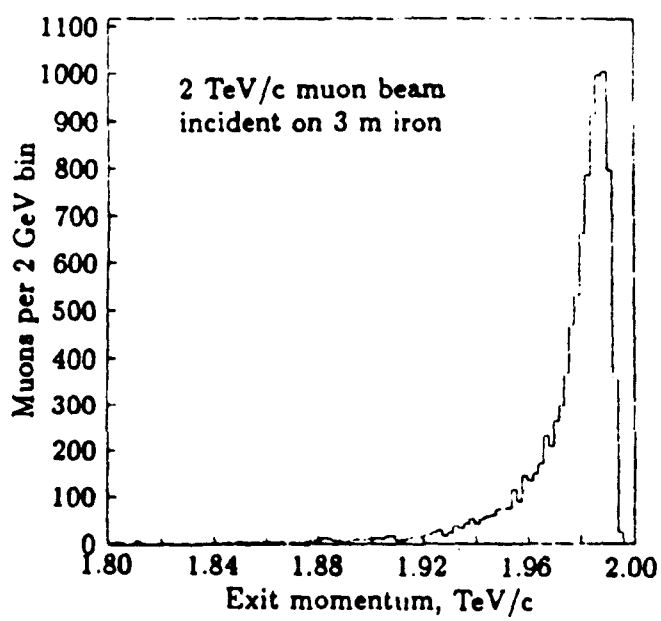

Figure 4: The momentum distribution of 2 TeV/c muons after traversing 3 m of iron, as obtained with Van Ginneken's TRAMU muon transport code. The most probable loss is 13 GeV, and the full width at half maximum 14 GeV (0.7%). Ten ·ent lost more than 2.5% of their energy, and 1.5% lost more . 10% of their incident energy.

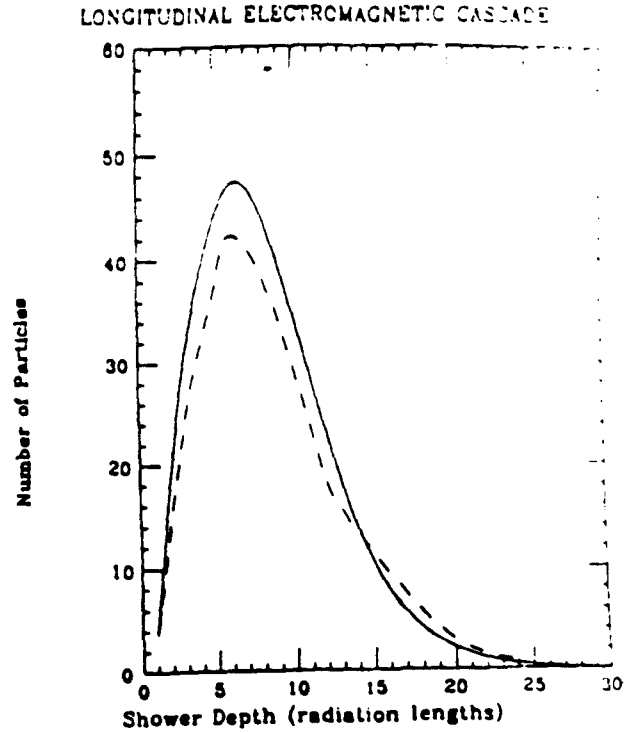

Figure 5: The longitudinal development of the electromagnetic cascade, as parameterized by the EGS program and as calculated by Messel and Crawford.

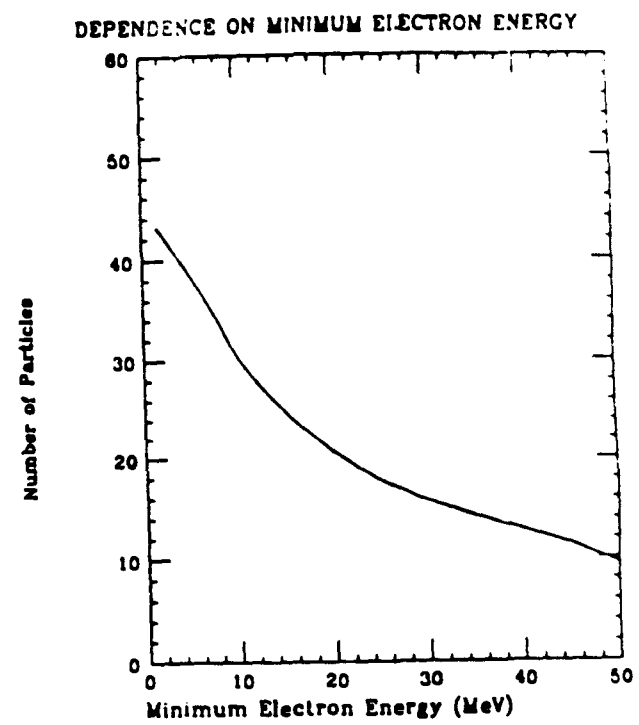

Figure 6: The number of electrons at shower maximum with energies in excess of the minimum electron energy.

Figure 1: Contributions of several processes to the average energy loss of a muon in 5 m of iron as a function of muon energy. The processes are (p) direct e^+e^- pair production, (b) bremsstrahlung, (n) photonuclear interactions, and (i) ionization; t marks the total loss.

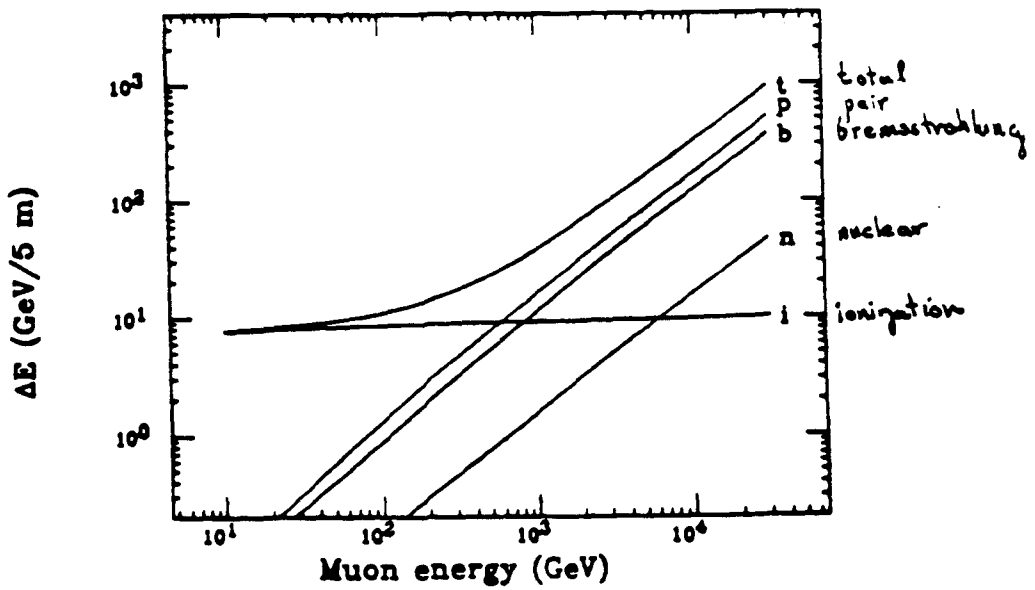

Figure 2: A 1 TeV muon traverses a model detector used in the study. Five thin chambers alternate with five 1-meter slabs of iron. The muon (entering from the left) has undergone four substantial pair-production events and a number of smaller interactions in the iron. All charged particle paths are shown.

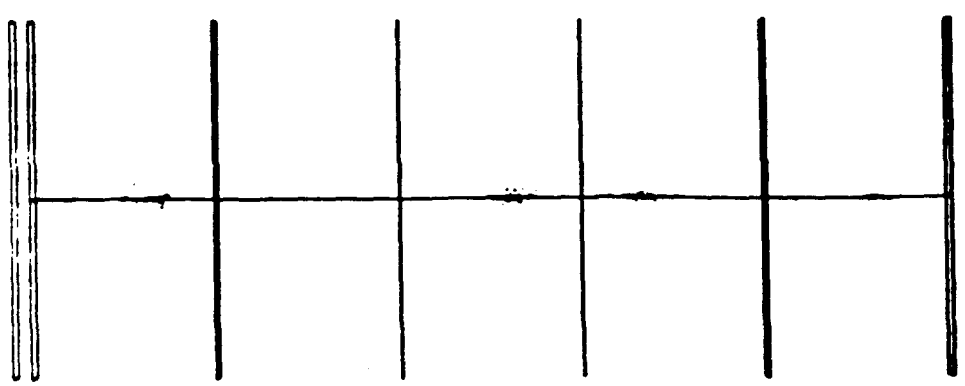

MAGNETIZED IRON

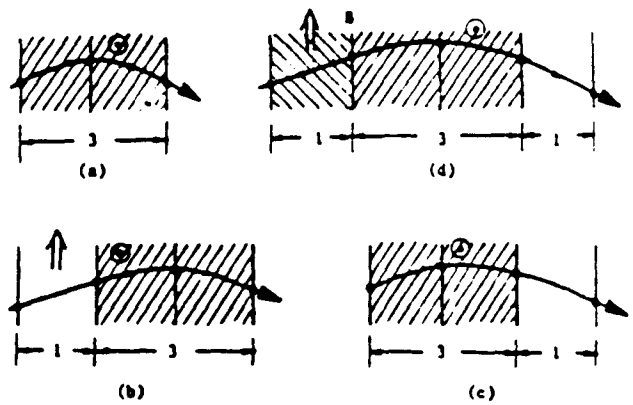

Figure 8: Muon momentum measurement schemes for various magnetized-iron geometries as described in the text.

Table 2
Relative Measurement Precision for Outside Fe Spectrometer
1. Iron only 2. 1 angle (in Fe) 3. 1 angle (in air) 4. 2 angles

Momentum	1.	2	3	4
200 GeV	12.4%	14.1%	12.3%	11.0%
400 GeV	13.9%	15.2%	13.6%	11.7%
700 GeV	17.3%	18.0%	16.6%	13.3%
1 TeV	21.7%	21.6%	20.4%	15.6%
2 TeV	38.2%	36.0%	35.3%	24.8%

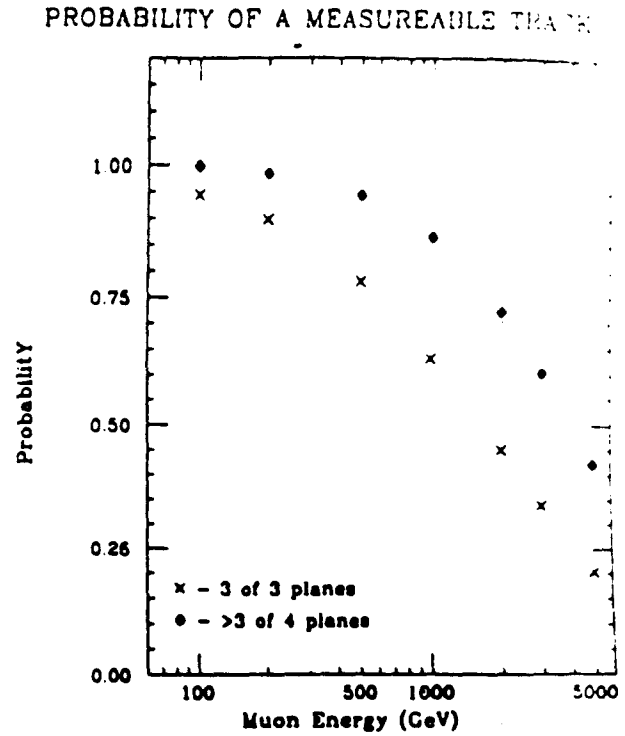

Figure 7: The probability that a muon of energy E_μ can be measured: i) requiring three unobscured planes in a three plane configuration, and ii) requiring at least three unobscured planes in a four plane configuration.

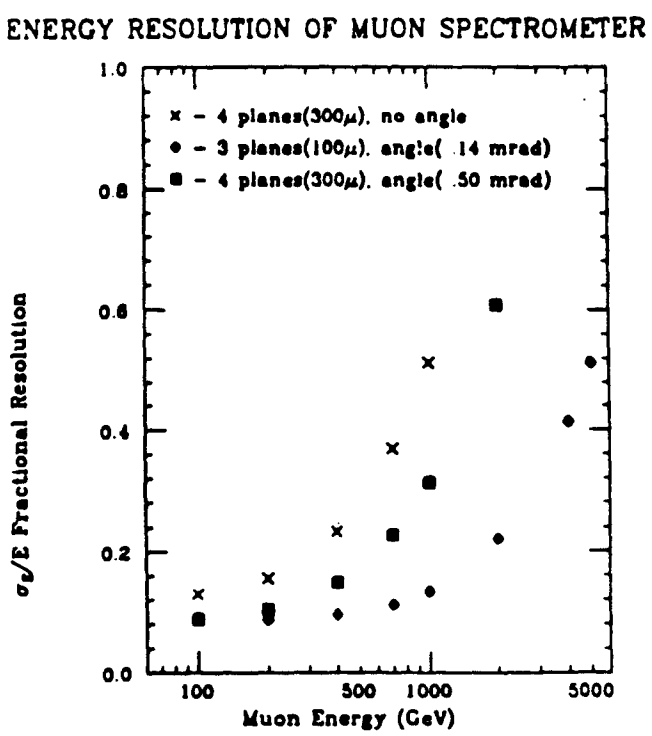

Figure 9: The resolution of the muon energy for various measurement strategies *i.e.* number of planes and the initial angle. (the resolution of the initial angle uses the point resolution in a plane for two planes separated by 1 m of air).

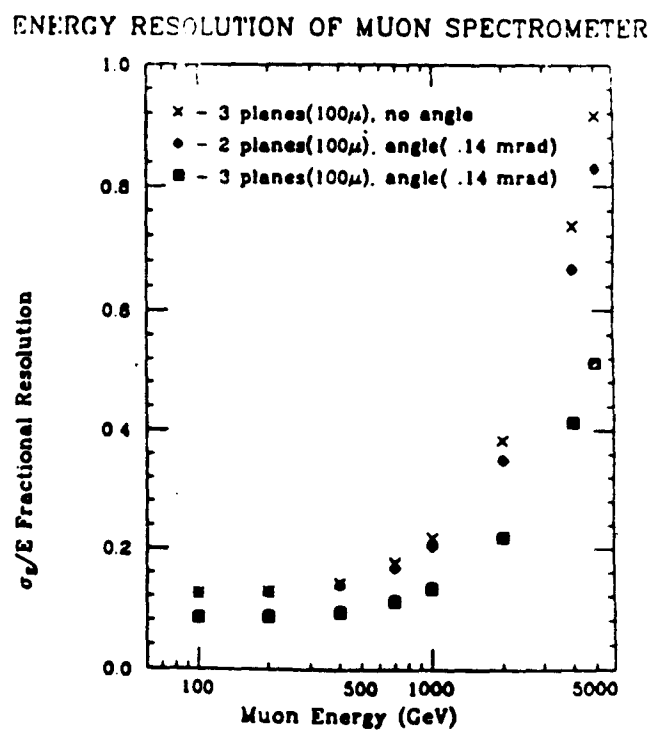

Figure 10: The resolution of the muon energy for various measurement strategies and point resolution.